

# Data-driven Fuzzy Multiple Criteria Decision Making and its Potential Applications

Lead Guest Editor: Zaoli Yang

Guest Editors: Yi Su, Harish Garg, Xue-Mei Xie, and Shaomin Wu





---

# **Data-driven Fuzzy Multiple Criteria Decision Making and its Potential Applications**

Mathematical Problems in Engineering

---

# **Data-driven Fuzzy Multiple Criteria Decision Making and its Potential Applications**

Lead Guest Editor: Zaoli Yang

Guest Editors: Yi Su, Harish Garg, Xue-Mei Xie,  
and Shaomin Wu




Copyright © 2020 Hindawi Limited. All rights reserved.

This is a special issue published in “Mathematical Problems in Engineering.” All articles are open access articles distributed under the Creative Commons Attribution License, which permits unrestricted use, distribution, and reproduction in any medium, provided the original work is properly cited.



# Chief Editor

Guangming Xie , China

## Academic Editors

Kumaravel A , India  
Waqas Abbasi, Pakistan  
Mohamed Abd El Aziz , Egypt  
Mahmoud Abdel-Aty , Egypt  
Mohammed S. Abdo, Yemen  
Mohammad Yaghoub Abdollahzadeh  
Jamalabadi , Republic of Korea  
Rahib Abiyev , Turkey  
Leonardo Acho , Spain  
Daniela Addessi , Italy  
Arooj Adeel , Pakistan  
Waleed Adel , Egypt  
Ramesh Agarwal , USA  
Francesco Aggogeri , Italy  
Ricardo Aguilar-Lopez , Mexico  
Afaq Ahmad , Pakistan  
Naveed Ahmed , Pakistan  
Elias Aifantis , USA  
Akif Akgul , Turkey  
Tareq Al-shami , Yemen  
Guido Ala, Italy  
Andrea Alaimo , Italy  
Reza Alam, USA  
Osamah Albahri , Malaysia  
Nicholas Alexander , United Kingdom  
Salvatore Alfonzetti, Italy  
Ghous Ali , Pakistan  
Nouman Ali , Pakistan  
Mohammad D. Aliyu , Canada  
Juan A. Almendral , Spain  
A.K. Alomari, Jordan  
José Domingo Álvarez , Spain  
Cláudio Alves , Portugal  
Juan P. Amezcua-Sanchez, Mexico  
Mukherjee Amitava, India  
Lionel Amodeo, France  
Sebastian Anita, Romania  
Costanza Arico , Italy  
Sabri Arik, Turkey  
Fausto Arpino , Italy  
Rashad Asharabi , Saudi Arabia  
Farhad Aslani , Australia  
Mohsen Asle Zaeem , USA

Andrea Avanzini , Italy  
Richard I. Avery , USA  
Viktor Avrutin , Germany  
Mohammed A. Awadallah , Malaysia  
Francesco Aymerich , Italy  
Sajad Azizi , Belgium  
Michele Baccocchi , Italy  
Seungik Baek , USA  
Khaled Bahlali, France  
M.V.A Raju Bahubalendruni, India  
Pedro Balaguer , Spain  
P. Balasubramaniam, India  
Stefan Balint , Romania  
Ines Tejado Balsera , Spain  
Alfonso Banos , Spain  
Jerzy Baranowski , Poland  
Tudor Barbu , Romania  
Andrzej Bartoszewicz , Poland  
Sergio Baselga , Spain  
S. Caglar Baslamisli , Turkey  
David Bassir , France  
Chiara Bedon , Italy  
Azeddine Beghdadi, France  
Andriette Bekker , South Africa  
Francisco Beltran-Carbajal , Mexico  
Abdellatif Ben Makhlof , Saudi Arabia  
Denis Benasciutti , Italy  
Ivano Benedetti , Italy  
Rosa M. Benito , Spain  
Elena Benvenuti , Italy  
Giovanni Berselli, Italy  
Michele Betti , Italy  
Pietro Bia , Italy  
Carlo Bianca , France  
Simone Bianco , Italy  
Vincenzo Bianco, Italy  
Vittorio Bianco, Italy  
David Bigaud , France  
Sardar Muhammad Bilal , Pakistan  
Antonio Bilotta , Italy  
Sylvio R. Bistafa, Brazil  
Chiara Boccaletti , Italy  
Rodolfo Bontempo , Italy  
Alberto Borboni , Italy  
Marco Bortolini, Italy

Paolo Boscariol, Italy  
Daniela Boso , Italy  
Guillermo Botella-Juan, Spain  
Abdesselem Boulkroune , Algeria  
Boulaïd Boulkroune, Belgium  
Fabio Bovenga , Italy  
Francesco Braghin , Italy  
Ricardo Branco, Portugal  
Julien Bruchon , France  
Matteo Bruggi , Italy  
Michele Brun , Italy  
Maria Elena Bruni, Italy  
Maria Angela Butturi , Italy  
Bartłomiej Błachowski , Poland  
Dhanamjayulu C , India  
Raquel Caballero-Águila , Spain  
Filippo Cacace , Italy  
Salvatore Caddemi , Italy  
Zuowei Cai , China  
Roberto Caldelli , Italy  
Francesco Cannizzaro , Italy  
Maosen Cao , China  
Ana Carpio, Spain  
Rodrigo Carvajal , Chile  
Caterina Casavola, Italy  
Sara Casciati, Italy  
Federica Caselli , Italy  
Carmen Castillo , Spain  
Inmaculada T. Castro , Spain  
Miguel Castro , Portugal  
Giuseppe Catalanotti , United Kingdom  
Alberto Cavallo , Italy  
Gabriele Cazzulani , Italy  
Fatih Vehbi Celebi, Turkey  
Miguel Cerrolaza , Venezuela  
Gregory Chagnon , France  
Ching-Ter Chang , Taiwan  
Kuei-Lun Chang , Taiwan  
Qing Chang , USA  
Xiaoheng Chang , China  
Prasenjit Chatterjee , Lithuania  
Kacem Chehdi, France  
Peter N. Cheimets, USA  
Chih-Chiang Chen , Taiwan  
He Chen , China

Kebing Chen , China  
Mengxin Chen , China  
Shyi-Ming Chen , Taiwan  
Xizhong Chen , Ireland  
Xue-Bo Chen , China  
Zhiwen Chen , China  
Qiang Cheng, USA  
Zeyang Cheng, China  
Luca Chiapponi , Italy  
Francisco Chicano , Spain  
Tirivanhu Chinyoka , South Africa  
Adrian Chmielewski , Poland  
Seongim Choi , USA  
Gautam Choubey , India  
Hung-Yuan Chung , Taiwan  
Yusheng Ci, China  
Simone Cinquemani , Italy  
Roberto G. Citarella , Italy  
Joaquim Ciurana , Spain  
John D. Clayton , USA  
Piero Colajanni , Italy  
Giuseppina Colicchio, Italy  
Vassilios Constantoudis , Greece  
Enrico Conte, Italy  
Alessandro Contento , USA  
Mario Cools , Belgium  
Gino Cortellessa, Italy  
Carlo Cosentino , Italy  
Paolo Crippa , Italy  
Erik Cuevas , Mexico  
Guozeng Cui , China  
Mehmet Cunkas , Turkey  
Giuseppe D'Aniello , Italy  
Peter Dabnichki, Australia  
Weizhong Dai , USA  
Zhifeng Dai , China  
Purushothaman Damodaran , USA  
Sergey Dashkovskiy, Germany  
Adiel T. De Almeida-Filho , Brazil  
Fabio De Angelis , Italy  
Samuele De Bartolo , Italy  
Stefano De Miranda , Italy  
Filippo De Monte , Italy

José António Fonseca De Oliveira  
Correia , Portugal  
Jose Renato De Sousa , Brazil  
Michael Defoort, France  
Alessandro Della Corte, Italy  
Laurent Dewasme , Belgium  
Sanku Dey , India  
Gianpaolo Di Bona , Italy  
Roberta Di Pace , Italy  
Francesca Di Puccio , Italy  
Ramón I. Diego , Spain  
Yannis Dimakopoulos , Greece  
Hasan Dinçer , Turkey  
José M. Domínguez , Spain  
Georgios Dounias, Greece  
Bo Du , China  
Emil Dumić, Croatia  
Madalina Dumitriu , United Kingdom  
Premraj Durairaj , India  
Saeed Eftekhari Azam, USA  
Said El Kafhali , Morocco  
Antonio Elipse , Spain  
R. Emre Erkmen, Canada  
John Escobar , Colombia  
Leandro F. F. Miguel , Brazil  
FRANCESCO FOTI , Italy  
Andrea L. Facci , Italy  
Shahla Faisal , Pakistan  
Giovanni Falsone , Italy  
Hua Fan, China  
Jianguang Fang, Australia  
Nicholas Fantuzzi , Italy  
Muhammad Shahid Farid , Pakistan  
Hamed Farooqi, Iran  
Yann Favennec, France  
Fiorenzo A. Fazzolari , United Kingdom  
Giuseppe Fedele , Italy  
Roberto Fedele , Italy  
Baowei Feng , China  
Mohammad Ferdows , Bangladesh  
Arturo J. Fernández , Spain  
Jesus M. Fernandez Oro, Spain  
Francesco Ferrise, Italy  
Eric Feulvarch , France  
Thierry Floquet, France

Eric Florentin , France  
Gerardo Flores, Mexico  
Antonio Forcina , Italy  
Alessandro Formisano, Italy  
Francesco Franco , Italy  
Elisa Francomano , Italy  
Juan Frausto-Solis, Mexico  
Shujun Fu , China  
Juan C. G. Prada , Spain  
HECTOR GOMEZ , Chile  
Matteo Gaeta , Italy  
Mauro Gaggero , Italy  
Zoran Gajic , USA  
Jaime Gallardo-Alvarado , Mexico  
Mosè Gallo , Italy  
Akemi Gálvez , Spain  
Maria L. Gandarias , Spain  
Hao Gao , Hong Kong  
Xingbao Gao , China  
Yan Gao , China  
Zhiwei Gao , United Kingdom  
Giovanni Garcea , Italy  
José García , Chile  
Harish Garg , India  
Alessandro Gasparetto , Italy  
Stylianios Georgantzinis, Greece  
Fotios Georgiades , India  
Parviz Ghadimi , Iran  
Ştefan Cristian Gherghina , Romania  
Georgios I. Giannopoulos , Greece  
Agathoklis Giaralis , United Kingdom  
Anna M. Gil-Lafuente , Spain  
Ivan Giorgio , Italy  
Gaetano Giunta , Luxembourg  
Jefferson L.M.A. Gomes , United Kingdom  
Emilio Gómez-Déniz , Spain  
Antonio M. Gonçalves de Lima , Brazil  
Qunxi Gong , China  
Chris Goodrich, USA  
Rama S. R. Gorla, USA  
Veena Goswami , India  
Xunjie Gou , Spain  
Jakub Grabski , Poland

Antoine Grall , France  
George A. Gravvanis , Greece  
Fabrizio Greco , Italy  
David Greiner , Spain  
Jason Gu , Canada  
Federico Guarracino , Italy  
Michele Guida , Italy  
Muhammet Gul , Turkey  
Dong-Sheng Guo , China  
Hu Guo , China  
Zhaoxia Guo, China  
Yusuf Gurefe, Turkey  
Salim HEDDAM , Algeria  
ABID HUSSANAN, China  
Quang Phuc Ha, Australia  
Li Haitao , China  
Petr Hájek , Czech Republic  
Mohamed Hamdy , Egypt  
Muhammad Hamid , United Kingdom  
Renke Han , United Kingdom  
Weimin Han , USA  
Xingsi Han, China  
Zhen-Lai Han , China  
Thomas Hanne , Switzerland  
Xinan Hao , China  
Mohammad A. Hariri-Ardebili , USA  
Khalid Hattaf , Morocco  
Defeng He , China  
Xiao-Qiao He, China  
Yanchao He, China  
Yu-Ling He , China  
Ramdane Hedjar , Saudi Arabia  
Jude Hemanth , India  
Reza Hemmati, Iran  
Nicolae Herisanu , Romania  
Alfredo G. Hernández-Díaz , Spain  
M.I. Herreros , Spain  
Eckhard Hitzer , Japan  
Paul Honeine , France  
Jaromir Horacek , Czech Republic  
Lei Hou , China  
Yingkun Hou , China  
Yu-Chen Hu , Taiwan  
Yunfeng Hu, China

Can Huang , China  
Gordon Huang , Canada  
Linsheng Huo , China  
Sajid Hussain, Canada  
Asier Ibeas , Spain  
Orest V. Iftime , The Netherlands  
Przemyslaw Ignaciuk , Poland  
Giacomo Innocenti , Italy  
Emilio Insfran Pelozo , Spain  
Azeem Irshad, Pakistan  
Alessio Ishizaka, France  
Benjamin Ivorra , Spain  
Breno Jacob , Brazil  
Reema Jain , India  
Tushar Jain , India  
Amin Jajarmi , Iran  
Chiranjibe Jana , India  
Łukasz Jankowski , Poland  
Samuel N. Jator , USA  
Juan Carlos Jáuregui-Correa , Mexico  
Kandasamy Jayakrishna, India  
Reza Jazar, Australia  
Khalide Jbilou, France  
Isabel S. Jesus , Portugal  
Chao Ji , China  
Qing-Chao Jiang , China  
Peng-fei Jiao , China  
Ricardo Fabricio Escobar Jiménez , Mexico  
Emilio Jiménez Macías , Spain  
Maolin Jin, Republic of Korea  
Zhuo Jin, Australia  
Ramash Kumar K , India  
BHABEN KALITA , USA  
MOHAMMAD REZA KHEDMATI , Iran  
Viacheslav Kalashnikov , Mexico  
Mathiyalagan Kalidass , India  
Tamas Kalmar-Nagy , Hungary  
Rajesh Kaluri , India  
Jyotheeswara Reddy Kalvakurthi, India  
Zhao Kang , China  
Ramani Kannan , Malaysia  
Tomasz Kapitaniak , Poland  
Julius Kaplunov, United Kingdom  
Konstantinos Karamanos, Belgium  
Michal Kawulok, Poland

Irfan Kaymaz , Turkey  
Vahid Kayvanfar , Qatar  
Krzysztof Kecik , Poland  
Mohamed Khader , Egypt  
Chaudry M. Khalique , South Africa  
Mukhtaj Khan , Pakistan  
Shahid Khan , Pakistan  
Nam-Il Kim, Republic of Korea  
Philipp V. Kiryukhantsev-Korneev ,  
Russia  
P.V.V Kishore , India  
Jan Koci , Czech Republic  
Ioannis Kostavelis , Greece  
Sotiris B. Kotsiantis , Greece  
Frederic Kratz , France  
Vamsi Krishna , India  
Edyta Kucharska, Poland  
Krzysztof S. Kulpa , Poland  
Kamal Kumar, India  
Prof. Ashwani Kumar , India  
Michal Kunicki , Poland  
Cedrick A. K. Kwuimy , USA  
Kyandoghere Kyamakya, Austria  
Ivan Kyrchei , Ukraine  
Márcio J. Lacerda , Brazil  
Eduardo Lalla , The Netherlands  
Giovanni Lancioni , Italy  
Jaroslaw Latalski , Poland  
Hervé Laurent , France  
Agostino Lauria , Italy  
Aimé Lay-Ekuakille , Italy  
Nicolas J. Leconte , France  
Kun-Chou Lee , Taiwan  
Dimitri Lefebvre , France  
Eric Lefevre , France  
Marek Lefik, Poland  
Yaguo Lei , China  
Kauko Leiviskä , Finland  
Ervin Lenzi , Brazil  
ChenFeng Li , China  
Jian Li , USA  
Jun Li , China  
Yueyang Li , China  
Zhao Li , China

Zhen Li , China  
En-Qiang Lin, USA  
Jian Lin , China  
Qibin Lin, China  
Yao-Jin Lin, China  
Zhiyun Lin , China  
Bin Liu , China  
Bo Liu , China  
Heng Liu , China  
Jianxu Liu , Thailand  
Lei Liu , China  
Sixin Liu , China  
Wanquan Liu , China  
Yu Liu , China  
Yuanchang Liu , United Kingdom  
Bonifacio Llamazares , Spain  
Alessandro Lo Schiavo , Italy  
Jean Jacques Loiseau , France  
Francesco Lolli , Italy  
Paolo Lonetti , Italy  
António M. Lopes , Portugal  
Sebastian López, Spain  
Luis M. López-Ochoa , Spain  
Vassilios C. Loukopoulos, Greece  
Gabriele Maria Lozito , Italy  
Zhiguo Luo , China  
Gabriel Luque , Spain  
Valentin Lychagin, Norway  
YUE MEI, China  
Junwei Ma , China  
Xuanlong Ma , China  
Antonio Madeo , Italy  
Alessandro Magnani , Belgium  
Toqeer Mahmood , Pakistan  
Fazal M. Mahomed , South Africa  
Arunava Majumder , India  
Sarfraz Nawaz Malik, Pakistan  
Paolo Manfredi , Italy  
Adnan Maqsood , Pakistan  
Muazzam Maqsood, Pakistan  
Giuseppe Carlo Marano , Italy  
Damijan Markovic, France  
Filipe J. Marques , Portugal  
Luca Martinelli , Italy  
Denizar Cruz Martins, Brazil

Francisco J. Martos , Spain  
Elio Masciari , Italy  
Paolo Massioni , France  
Alessandro Mauro , Italy  
Jonathan Mayo-Maldonado , Mexico  
Pier Luigi Mazzeo , Italy  
Laura Mazzola, Italy  
Driss Mehdi , France  
Zahid Mehmood , Pakistan  
Roderick Melnik , Canada  
Xiangyu Meng , USA  
Jose Merodio , Spain  
Alessio Merola , Italy  
Mahmoud Mesbah , Iran  
Luciano Mescia , Italy  
Laurent Mevel , France  
Constantine Michailides , Cyprus  
Mariusz Michta , Poland  
Prankul Middha, Norway  
Aki Mikkola , Finland  
Giovanni Minafò , Italy  
Edmondo Minisci , United Kingdom  
Hiroyuki Mino , Japan  
Dimitrios Mitsotakis , New Zealand  
Ardashir Mohammadzadeh , Iran  
Francisco J. Montáns , Spain  
Francesco Montefusco , Italy  
Gisele Mophou , France  
Rafael Morales , Spain  
Marco Morandini , Italy  
Javier Moreno-Valenzuela , Mexico  
Simone Morganti , Italy  
Caroline Mota , Brazil  
Aziz Moukrim , France  
Shen Mouquan , China  
Dimitris Mourtzis , Greece  
Emiliano Mucchi , Italy  
Taseer Muhammad, Saudi Arabia  
Ghulam Muhiuddin, Saudi Arabia  
Amitava Mukherjee , India  
Josefa Mula , Spain  
Jose J. Muñoz , Spain  
Giuseppe Muscolino, Italy  
Marco Mussetta , Italy

Hariharan Muthusamy, India  
Alessandro Naddeo , Italy  
Raj Nandkeolyar, India  
Keivan Navaie , United Kingdom  
Soumya Nayak, India  
Adrian Neagu , USA  
Erivelton Geraldo Nepomuceno , Brazil  
AMA Neves, Portugal  
Ha Quang Thinh Ngo , Vietnam  
Nhon Nguyen-Thanh, Singapore  
Papakostas Nikolaos , Ireland  
Jelena Nikolic , Serbia  
Tatsushi Nishi, Japan  
Shanzhou Niu , China  
Ben T. Nohara , Japan  
Mohammed Nouari , France  
Mustapha Nourelfath, Canada  
Kazem Nouri , Iran  
Ciro Núñez-Gutiérrez , Mexico  
Włodzimierz Ogryczak, Poland  
Roger Ohayon, France  
Krzysztof Okarma , Poland  
Mitsuhiro Okayasu, Japan  
Murat Olgun , Turkey  
Diego Oliva, Mexico  
Alberto Olivares , Spain  
Enrique Onieva , Spain  
Calogero Orlando , Italy  
Susana Ortega-Cisneros , Mexico  
Sergio Ortobelli, Italy  
Naohisa Otsuka , Japan  
Sid Ahmed Ould Ahmed Mahmoud , Saudi Arabia  
Taoreed Owolabi , Nigeria  
EUGENIA PETROPOULOU , Greece  
Arturo Pagano, Italy  
Madhumangal Pal, India  
Pasquale Palumbo , Italy  
Dragan Pamučar, Serbia  
Weifeng Pan , China  
Chandan Pandey, India  
Rui Pang, United Kingdom  
Jürgen Pannek , Germany  
Elena Panteley, France  
Achille Paolone, Italy

George A. Papakostas , Greece  
Xosé M. Pardo , Spain  
You-Jin Park, Taiwan  
Manuel Pastor, Spain  
Pubudu N. Pathirana , Australia  
Surajit Kumar Paul , India  
Luis Payá , Spain  
Igor Pažanin , Croatia  
Libor Pekař , Czech Republic  
Francesco Pellicano , Italy  
Marcello Pellicciari , Italy  
Jian Peng , China  
Mingshu Peng, China  
Xiang Peng , China  
Xindong Peng, China  
Yuxing Peng, China  
Marzio Pennisi , Italy  
Maria Patrizia Pera , Italy  
Matjaz Perc , Slovenia  
A. M. Bastos Pereira , Portugal  
Wesley Peres, Brazil  
F. Javier Pérez-Pinal , Mexico  
Michele Perrella, Italy  
Francesco Pesavento , Italy  
Francesco Petrini , Italy  
Hoang Vu Phan, Republic of Korea  
Lukasz Pieczonka , Poland  
Dario Piga , Switzerland  
Marco Pizzarelli , Italy  
Javier Plaza , Spain  
Goutam Pohit , India  
Dragan Poljak , Croatia  
Jorge Pomares , Spain  
Hiram Ponce , Mexico  
Sébastien Poncet , Canada  
Volodymyr Ponomaryov , Mexico  
Jean-Christophe Ponsart , France  
Mauro Pontani , Italy  
Sivakumar Poruran, India  
Francesc Pozo , Spain  
Aditya Rio Prabowo , Indonesia  
Anchasa Pramuanjaroenkij , Thailand  
Leonardo Primavera , Italy  
B Rajanarayan Prusty, India

Krzysztof Puszynski , Poland  
Chuan Qin , China  
Dongdong Qin, China  
Jianlong Qiu , China  
Giuseppe Quaranta , Italy  
DR. RITU RAJ , India  
Vitomir Racic , Italy  
Carlo Rainieri , Italy  
Kumbakonam Ramamani Rajagopal, USA  
Ali Ramazani , USA  
Angel Manuel Ramos , Spain  
Higinio Ramos , Spain  
Muhammad Afzal Rana , Pakistan  
Muhammad Rashid, Saudi Arabia  
Manoj Rastogi, India  
Alessandro Rasulo , Italy  
S.S. Ravindran , USA  
Abdolrahman Razani , Iran  
Alessandro Reali , Italy  
Jose A. Reinoso , Spain  
Oscar Reinoso , Spain  
Haijun Ren , China  
Carlo Renno , Italy  
Fabrizio Renno , Italy  
Shahram Rezapour , Iran  
Ricardo Riaza , Spain  
Francesco Riganti-Fulginei , Italy  
Gerasimos Rigatos , Greece  
Francesco Ripamonti , Italy  
Jorge Rivera , Mexico  
Eugenio Roanes-Lozano , Spain  
Ana Maria A. C. Rocha , Portugal  
Luigi Rodino , Italy  
Francisco Rodríguez , Spain  
Rosana Rodríguez López, Spain  
Francisco Rossomando , Argentina  
Jose de Jesus Rubio , Mexico  
Weiguo Rui , China  
Rubén Ruiz , Spain  
Ivan D. Rukhlenko , Australia  
Dr. Eswaramoorthi S. , India  
Weichao SHI , United Kingdom  
Chaman Lal Sabharwal , USA  
Andrés Sáez , Spain



Bekir Sahin, Turkey  
Laxminarayan Sahoo , India  
John S. Sakellariou , Greece  
Michael Sakellariou , Greece  
Salvatore Salamone, USA  
Jose Vicente Salcedo , Spain  
Alejandro Salcido , Mexico  
Alejandro Salcido, Mexico  
Nunzio Salerno , Italy  
Rohit Salgotra , India  
Miguel A. Salido , Spain  
Sinan Salih , Iraq  
Alessandro Salvini , Italy  
Abdus Samad , India  
Sovan Samanta, India  
Nikolaos Samaras , Greece  
Ramon Sancibrian , Spain  
Giuseppe Sanfilippo , Italy  
Omar-Jacobo Santos, Mexico  
J Santos-Reyes , Mexico  
José A. Sanz-Herrera , Spain  
Musavarah Sarwar, Pakistan  
Shahzad Sarwar, Saudi Arabia  
Marcelo A. Savi , Brazil  
Andrey V. Savkin, Australia  
Tadeusz Sawik , Poland  
Roberta Sburlati, Italy  
Gustavo Scaglia , Argentina  
Thomas Schuster , Germany  
Hamid M. Sedighi , Iran  
Mijanur Rahaman Seikh, India  
Tapan Senapati , China  
Lotfi Senhadji , France  
Junwon Seo, USA  
Michele Serpilli, Italy  
Silvestar Šesnić , Croatia  
Gerardo Severino, Italy  
Ruben Sevilla , United Kingdom  
Stefano Sfarra , Italy  
Dr. Ismail Shah , Pakistan  
Leonid Shaikhet , Israel  
Vimal Shanmuganathan , India  
Prayas Sharma, India  
Bo Shen , Germany  
Hang Shen, China

Xin Pu Shen, China  
Dimitri O. Shepelsky, Ukraine  
Jian Shi , China  
Amin Shokrollahi, Australia  
Suzanne M. Shontz , USA  
Babak Shotorban , USA  
Zhan Shu , Canada  
Angelo Sifaleras , Greece  
Nuno Simões , Portugal  
Mehakpreet Singh , Ireland  
Piyush Pratap Singh , India  
Rajiv Singh, India  
Seralathan Sivamani , India  
S. Sivasankaran , Malaysia  
Christos H. Skiadas, Greece  
Konstantina Skouri , Greece  
Neale R. Smith , Mexico  
Bogdan Smolka, Poland  
Delfim Soares Jr. , Brazil  
Alba Sofi , Italy  
Francesco Soldovieri , Italy  
Raffaele Solimene , Italy  
Yang Song , Norway  
Jussi Sopanen , Finland  
Marco Spadini , Italy  
Paolo Spagnolo , Italy  
Ruben Specogna , Italy  
Vasilios Spitas , Greece  
Ivanka Stamova , USA  
Rafał Stanisławski , Poland  
Miladin Stefanović , Serbia  
Salvatore Strano , Italy  
Yakov Strelniker, Israel  
Kangkang Sun , China  
Qiuqin Sun , China  
Shuaishuai Sun, Australia  
Yanchao Sun , China  
Zong-Yao Sun , China  
Kumarasamy Suresh , India  
Sergey A. Suslov , Australia  
D.L. Suthar, Ethiopia  
D.L. Suthar , Ethiopia  
Andrzej Swierniak, Poland  
Andras Szekrenyes , Hungary  
Kumar K. Tamma, USA





Yong (Aaron) Tan, United Kingdom  
Marco Antonio Taneco-Hernández , Mexico  
Lu Tang , China  
Tianyou Tao, China  
Hafez Tari , USA  
Alessandro Tasora , Italy  
Sergio Teggi , Italy  
Adriana del Carmen Téllez-Anguiano , Mexico  
Ana C. Teodoro , Portugal  
Efsthios E. Theotokoglou , Greece  
Jing-Feng Tian, China  
Alexander Timokha , Norway  
Stefania Tomasiello , Italy  
Gisella Tomasini , Italy  
Isabella Torcicollo , Italy  
Francesco Tornabene , Italy  
Mariano Torrisi , Italy  
Thang nguyen Trung, Vietnam  
George Tsiatas , Greece  
Le Anh Tuan , Vietnam  
Nerio Tullini , Italy  
Emilio Turco , Italy  
Ilhan Tuzcu , USA  
Efstratios Tzirtzilakis , Greece  
FRANCISCO UREÑA , Spain  
Filippo Ubertini , Italy  
Mohammad Uddin , Australia  
Mohammad Safi Ullah , Bangladesh  
Serdar Ulubeyli , Turkey  
Mati Ur Rahman , Pakistan  
Panayiotis Vafeas , Greece  
Giuseppe Vairo , Italy  
Jesus Valdez-Resendiz , Mexico  
Eusebio Valero, Spain  
Stefano Valvano , Italy  
Carlos-Renato Vázquez , Mexico  
Martin Velasco Villa , Mexico  
Franck J. Vernerey, USA  
Georgios Veronis , USA  
Vincenzo Vespri , Italy  
Renato Vidoni , Italy  
Venkatesh Vijayaraghavan, Australia

Anna Vila, Spain  
Francisco R. Villatoro , Spain  
Francesca Vipiana , Italy  
Stanislav Vitek , Czech Republic  
Jan Vorel , Czech Republic  
Michael Vynnycky , Sweden  
Mohammad W. Alomari, Jordan  
Roman Wan-Wendner , Austria  
Bingchang Wang, China  
C. H. Wang , Taiwan  
Dagang Wang, China  
Guoqiang Wang , China  
Huaiyu Wang, China  
Hui Wang , China  
J.G. Wang, China  
Ji Wang , China  
Kang-Jia Wang , China  
Lei Wang , China  
Qiang Wang, China  
Qingling Wang , China  
Weiwei Wang , China  
Xinyu Wang , China  
Yong Wang , China  
Yung-Chung Wang , Taiwan  
Zhenbo Wang , USA  
Zhibo Wang, China  
Waldemar T. Wójcik, Poland  
Chi Wu , Australia  
QiuHong Wu, China  
Yuqiang Wu, China  
Zhibin Wu , China  
Zhizheng Wu , China  
Michalis Xenos , Greece  
Hao Xiao , China  
Xiao Ping Xie , China  
Qingzheng Xu , China  
Binghan Xue , China  
Yi Xue , China  
Joseph J. Yame , France  
Chuanliang Yan , China  
Xinggang Yan , United Kingdom  
Hongtai Yang , China  
Jixiang Yang , China  
Mijia Yang, USA  
Ray-Yeng Yang, Taiwan

Zaoli Yang , China  
Jun Ye , China  
Min Ye , China  
Luis J. Yebra , Spain  
Peng-Yeng Yin , Taiwan  
Muhammad Haroon Yousaf , Pakistan  
Yuan Yuan, United Kingdom  
Qin Yuming, China  
Elena Zaitseva , Slovakia  
Arkadiusz Zak , Poland  
Mohammad Zakwan , India  
Ernesto Zambrano-Serrano , Mexico  
Francesco Zammori , Italy  
Jessica Zangari , Italy  
Rafal Zdunek , Poland  
Ibrahim Zeid, USA  
Nianyin Zeng , China  
Junyong Zhai , China  
Hao Zhang , China  
Haopeng Zhang , USA  
Jian Zhang , China  
Kai Zhang, China  
Lingfan Zhang , China  
Mingjie Zhang , Norway  
Qian Zhang , China  
Tianwei Zhang , China  
Tongqian Zhang , China  
Wenyu Zhang , China  
Xianming Zhang , Australia  
Xuping Zhang , Denmark  
Yinyan Zhang, China  
Yifan Zhao , United Kingdom  
Debao Zhou, USA  
Heng Zhou , China  
Jian G. Zhou , United Kingdom  
Junyong Zhou , China  
Xueqian Zhou , United Kingdom  
Zhe Zhou , China  
Wu-Le Zhu, China  
Gaetano Zizzo , Italy  
Mingcheng Zuo, China


# Contents

## **Evolution of High-Value Patents in Reverse Innovation: Focus on Chinese Local Enterprises**

Tie Wei  and Tingting Liu 

Research Article (13 pages), Article ID 8127096, Volume 2020 (2020)

## **CEO Media Exposure and Green Technological Innovation Decision: Evidence from Chinese Polluting Firms**

Chen Wang, Yuanlin Hu, Jianhua Zhang , and Chenglin Miao


Research Article (14 pages), Article ID 8271621, Volume 2020 (2020)

## **Evaluation of Multimodal Transport in China Based on Hesitation Fuzzy Multiattribute Decision-Making**

Bing Han , Min Wan , and Yu Zhou



Research Article (9 pages), Article ID 1823068, Volume 2020 (2020)

## **Application of Multiattribute Decision-Making for Evaluating Regional Innovation Capacity**

Yi Su , Dezhi Liang, and Wen Guo


Research Article (20 pages), Article ID 2851840, Volume 2020 (2020)

## **Self-Organized Criticality and Trend Analysis in Time Series of Blackouts for the China Power Grid**

Qun Yu , Na Cao, Qilin Liu, Yuqing Qu, and Yumin Zhang 


Research Article (8 pages), Article ID 3075935, Volume 2020 (2020)

## **Nonlinear Finite Volume Scheme Preserving Positivity for 2D Convection-Diffusion Equations on Polygonal Meshes**

Bin Lan  and Jianqiang Dong


Research Article (11 pages), Article ID 7343716, Volume 2020 (2020)

## **New Tseng-Degree Gradient Method in Variational Inequality Problem**

Zhuang Shan, Lijun Zhu , Long He, Danfeng Wu, and Haicheng Wei

Research Article (7 pages), Article ID 9832579, Volume 2020 (2020)

## **An Approach to Selection of Agricultural Product Supplier Using Pythagorean Fuzzy Sets**

Lina Dai  and Shizhen Bai

Research Article (7 pages), Article ID 1816028, Volume 2020 (2020)

## **Fuzzy Covering-Based Three-Way Clustering**

Dandan Yang 

Research Article (10 pages), Article ID 2901210, Volume 2020 (2020)

## **Research on Evaluating Algorithms for the Service Quality of Wireless Sensor Networks Based on Interval-Valued Intuitionistic Fuzzy EDAS and CRITIC Methods**

Shihui Li  and Bo Wang

Research Article (12 pages), Article ID 5391940, Volume 2020 (2020)

**Interval-Valued Complex Fuzzy Geometric Aggregation Operators and Their Application to Decision Making**

Songsong Dai , Lvqing Bi, and Bo Hu

Research Article (10 pages), Article ID 9410143, Volume 2020 (2020)

**An Approach for Resilient-Green Supplier Selection Based on WASPAS, BWM, and TOPSIS under Intuitionistic Fuzzy Sets**

Lei Xiong, Shuqi Zhong, Sen Liu , Xiao Zhang, and Yanfeng Li 

Research Article (18 pages), Article ID 1761893, Volume 2020 (2020)

**Multiple Attribute Group Decision Making Based on Simplified Neutrosophic Integrated Weighted Distance Measure and Entropy Method**

Haibo Zhang , Zhimin Mu, and Shouzhen Zeng 



Research Article (10 pages), Article ID 9075845, Volume 2020 (2020)

**Research on Probability Mean-Lower Semivariance-Entropy Portfolio Model with Background Risk**

Qi Wu, Yuelin Gao , and Ying Sun 

Research Article (13 pages), Article ID 2769617, Volume 2020 (2020)

**A Neutrosophic-Based Approach in Data Envelopment Analysis with Undesirable Outputs**

Xinna Mao, Zhao Guoxi , Mohammad Fallah, and S. A. Edalatpanah 



Research Article (8 pages), Article ID 7626102, Volume 2020 (2020)

**A Novel Ensemble Credit Scoring Model Based on Extreme Learning Machine and Generalized Fuzzy Soft Sets**

Dayu Xu , Xuyao Zhang , Junguo Hu, and Jiahao Chen

Research Article (12 pages), Article ID 7504764, Volume 2020 (2020)

**Some T-Spherical Fuzzy Einstein Interactive Aggregation Operators and Their Application to Selection of Photovoltaic Cells**

Shouzhen Zeng , Muhammad Munir, Tahir Mahmood , and Muhammad Naeem

Research Article (16 pages), Article ID 1904362, Volume 2020 (2020)

**A Model of High-Dimensional Feature Reduction Based on Variable Precision Rough Set and Genetic Algorithm in Medical Image**

Zhou Tao , Lu Huiling , Fuyuan Hu , Shi Qiu , and Wu Cuiying

Research Article (18 pages), Article ID 7653946, Volume 2020 (2020)

**Reactive Strategies in the Multiproject Scheduling with Multifactor Disruptions**

Weixin Wang , Jiafu Su , Jin Xu , and Xianlong Ge 

Research Article (11 pages), Article ID 3154047, Volume 2020 (2020)

## Contents


---

### **Restoration Methods Selection for Wood Components of Chinese Ancient Architectures Based on TODIM with Single-Valued Neutrosophic Sets**

Xiaolu. Long, Lizhi. Liu, Can. Xiao , Pengfei. Cheng , and Chengxun. Fu

Research Article (14 pages), Article ID 5049360, Volume 2020 (2020)

### **Decision Support Methodology Based on Covering-Based Interval-Valued Pythagorean Fuzzy Rough Set Model and Its Application to Hospital Open-Source EHRs System Selection**

Fang Liu, Ju Wu, Lianming Mou, and Yi Liu 

Research Article (13 pages), Article ID 6928532, Volume 2020 (2020)

## Research Article

# Evolution of High-Value Patents in Reverse Innovation: Focus on Chinese Local Enterprises

Tie Wei  and Tingting Liu 

*Business School of Guangxi University, Guangxi, Nanning 530000, China*

Correspondence should be addressed to Tie Wei; [weitie@gxu.edu.cn](mailto:weitie@gxu.edu.cn)

Received 26 April 2020; Revised 14 October 2020; Accepted 20 October 2020; Published 11 November 2020

Academic Editor: Yi Su

Copyright © 2020 Tie Wei and Tingting Liu. This is an open access article distributed under the Creative Commons Attribution License, which permits unrestricted use, distribution, and reproduction in any medium, provided the original work is properly cited.

The lack of high-value patents constraints the reverse innovation of developing countries' local enterprises. To explore how high-value patents evolve within reverse innovation in these enterprises, this paper proposes a theoretical framework to analyze the relationships among technology, law, and market values for high-value patents and builds a three-dimensional Lotka–Volterra model of high-value patents under this framework. Using this model, this study explores the evolution path and the optimal conditions for the formation high-value patents. We take a local Chinese company, Huawei, as a case to test the theoretical analysis and make some managerial suggestions accordingly. Our research provides a theoretical basis for cultivating high-value patents in reverse innovation in local enterprises in China and other developing countries.

## 1. Introduction

Since the 21st century, a phenomenon has existed in which innovative products or technologies originating in developing countries or emerging markets spread back to developed countries. This situation is quite different than the traditional innovation model, in which new products or technologies are always created in developed countries and then spread to developing countries. The direction of this innovation's diffusion is "reverse," and Immelt [1] et al. call it "reverse innovation."

On the one hand, reverse innovation is not an accident for multinational companies of developed countries; it is an important innovation strategy to integrate global resources to gain a competitive advantage [2]. On the other hand, reverse innovation also brings new opportunities to local enterprises in developing countries. In recent years, reverse innovation led by local enterprises has greatly increased, for example, Huawei's 5G technology and India's Tata car [3, 4].

For most local enterprises in developing countries, the lack of high-value patents imposes constraints on their long-term competitiveness in reverse innovation [5]. However,

existing research has not paid enough attention to the issue of high-value patents in reverse innovation in local enterprises.

A high-value patent is a concept that has been developed at the strategic level of an enterprise. This type of patent guarantees enterprises long-term and sustainable competitiveness in innovation competition [6]. The formation of high-value patents is not easy in reverse innovation in local enterprises. It is possible with the accumulation of technology and management experience for local enterprises to be competitive in the long-term and catch up with technology, which is a process of complex evolution.

A patent's value as an asset is usually reflected in three dimensions, i.e., technology, law, and market [7]. In reverse innovation, the value of the local enterprises' patents in these three dimensions changes frequently since their formation is restricted by the capital, technical ability, and market environment of local enterprises. For example, in the initial stage of reverse innovation, patents applied by local enterprises with the usual technology disadvantage do not necessarily have a very high value in the technology dimension. However, these patents may have a higher value in the market dimension since they can meet the needs of local consumers,

with the large advantages of lower cost and huge demand. However, if the technology value of a patent is kept low, it is difficult for local enterprises to obtain a sustainable competitive advantage in the long term, especially when their new products flow reversely to developed countries and face global competition in the overseas market. At the same time, the intellectual property protection in developed countries is stricter than in developing countries. If the legal claims of a local enterprise's patent are not clear and stable enough overseas, then it faces the risk of infringement litigation, which would likely result in an invalid patent. Therefore, improving the law value of patents is inevitable for local enterprises when they enter developed countries' markets.

In the process of reverse innovation, the situation and capability of the local enterprises are changing with time, which is reflected in the changes in patents' value in the three dimensions. As a result, a high-value patent may be formed in this complex process. How does this process happen? How does the value of each of the three dimensions affect the others in this process? These are key issues in the cultivation of a high-value patent for local enterprises. However, there is still a gap in research in this area.

This process is similar to the evolution of an ecosystem [8, 9]. The value of a patent in the three dimensions affects each other dimension and is influenced by the change in the situation during different phases of the reverse innovation, which is similar to the evolution of an ecosystem in which the relationships among populations change their influence on the external environment [10, 11]. Therefore, this paper constructs a theoretical analysis framework of the value relationship of high-value patents in the following three dimensions, i.e., technology, law, and market. In this framework, we propose a three-dimensional Lotka–Volterra model to analyze high-value patents' evolution path and the optimal conditions for their formation in reverse innovation in local enterprises, and finally, we use a Chinese company, Huawei, as a case in the practical analysis.

The main contributions of this paper are as follows:

- (1) It proposes a new theoretical analysis framework to discuss the issue of the formation of high-value patents. From the perspective of ecology, we explain high-value patents' relationships among the three dimensions of technology, law, and market. This study forms a new theoretical analysis framework that may help us explore more about how high-value patents are formed.
- (2) It builds a novel three-dimensional Lotka–Volterra model to explore the evolution of high-value patents in reverse innovation in local enterprises. This model is a new extension of the classic Lotka–Volterra model that can specifically simulate the evolution and formation conditions of high-value patents in a complex situation.
- (3) It analyzes the evolution of Huawei's high-value patent in reverse innovation and suggests some relative management policies. This study will help the developing countries' local enterprises cultivate their high-value patents in reverse innovation.

## 2. Literature Review

**2.1. Reverse Innovation.** In the beginning, research in this area focused on the issue of reverse innovation from the perspective of developed countries, including the degree of independence of multinational subsidiaries [12], the internal resistance to reverse innovation [13], etc. This research was mainly concerned with the phenomenon of reverse innovation that happened in emerging markets and was generally carried out by the transnational subsidiaries of developed countries [4]. This research discussed the obstacles and influencing factors encountered by subsidiaries when implementing reverse innovation in developing countries, including the independence, internal resistance, resource integration ability, strategic positioning, and intellectual property environment.

With the rise of local enterprises, reverse innovation led by developing countries has attracted the attention of researchers. This research is more concerned with case studies of local enterprises and discusses the factors that affect reverse innovation in local enterprises from different perspectives. For example, Nan [14] analyzed the case of the electronic information industry, identified the influencing factors of the local enterprise's reverse innovation, and proposed some strategies from the organizational and project levels. Xu et al. [15] and Yun [16] analyzed cases of some local technology service companies and proposed that organizational learning, industrial chain, technology chain construction, and international access are all important factors that affect the implementation of reverse innovation. In addition, Simone [13], Xu et al. [15], and Xu and Peng [17] discussed the impact of innovation networks, technological capabilities, and other factors on the implementation of reverse innovation led by local enterprises in developing countries, etc.

However, there is still little focus on the issue of the lack of high-value patents in reverse innovation in local enterprises. Some research has noted that the issue of whether to control superior intellectual property rights is a large difference between developed countries and developing countries in carrying out reverse innovation. However, there is still a lack of further in-depth discussion in this regard.

**2.2. High-Value Patents.** A high-value patent is a strategic concept that has been proposed to reflect the control of patents as a competitive strategy [18]. The high value is mainly embodied in the following three aspects: technology characters [19], claims in law [20], and market competition [21]. Wei et al. [7] and others believe that high-value patents mainly refer to patents with a high level of technological innovation, stable legal rights, and good market prospects. Li et al. [18] and others believe that high-value patents should reflect the strategic layout of enterprises. These are patents that enable enterprises to have high product competitiveness, market share and profit creativity. Ma and Zhao [21] also believe that high-value patents should highlight the high strategic value and market value.



Therefore, high-value patents can be seen as having high value in these three aspects. First, these patents have a high value in technology, which means that the technology that is contained in the patents is a relatively high level, ensuring that the owners of the patents can use them to maintain a high control of the technology in the long term [19]. Second, high-value patents have a high legal value, which means that they have great legal stability, keeping them from being involved in infringement issues [20]. Third, high-value patents have a high market value, which means that they have a high strategic position that can control the market trend [22].

The value of a patent is ultimately reflected in its market performance, i.e., making an economic profit [22]. This is a result of the market monopoly that is given by law as a patent's unique technology innovation. Therefore, a patent's value in technology and law ultimately influences its market value. A patent is usually a kind of technical solution and is presented in some claims in law. A patent also has some important technical and legal characteristics. As a technical solution, the technology value of a patent is the basis for its final market value. Patents with high technology often help enterprises gain a long-term market monopoly position due to their technology advantages [19]. At the same time, patents enjoy exclusive rights according to the law. The stability of a patent's claims in the law also affects its market and technology value, that is, whether a patent makes it easy to infringe on others' patent rights or to be infringed upon by others also affects the realization of its technology value and the final market value [20].

Therefore, for high-value patents, their technology, market, and law values affect each other. Especially in the complex situation of reverse innovation, the interaction of these values in these three dimensions will lead to complex evolution, as in an ecosystem. However, how this complex evolution happens is still unknown.

### 3. Theory and Model

*3.1. Value Relationship of High-Value Patents in the Three Dimensions.* High-value patents can help support and guarantee that enterprises maintain a long-term advantage in competition. The values of high-value patents are mainly reflected in the three dimensions of technology, market, and law, which interact with each other.

First, we discuss the impact of the technology value on the market value. In general, the technology value determines the final market value of a patent since technology advantages can guarantee a monopoly in the market [23]. However, the advantage of the technology value transforming into the market value requires good external market opportunities. If the external market opportunities are not mature or available, then patents with high technology value may not bring a high market value. For example, Japanese companies first invented the two-dimensional code technology, but these patents did not obtain a good market value [24]. In contrast, Chinese companies with a technical disadvantage have had great success with this technology by developing it for mobile payment [25]. Patents should not

only have excellent technical value but also have market opportunities to generate the market value. Some examples show that the pursuit of high technology value generates a high cost, and ultimately, the market value is restrained. For example, Kodak, which produces film, first developed digital camera technology but did not use it. Additionally, Xerox first developed the graphic operating system, etc. [25, 26]. Therefore, the technology value may promote or inhibit the market value under different market conditions.

Second, we discuss the impact of the market value on the technology value. In a specific environment, patents with low technology value may also achieve high market value when there are good market opportunities. Some patented technologies in developing countries do not necessarily have high technology content; however, due to huge market demand, they can also achieve a high market value. For example, Huawei did not have an advantage in technology in the 3G and 4G eras, but its patents had high market value because of the great market demand in developing countries [27]. Usually, these kinds of patents would not maintain a long-term advantage in competition as they lack a high technology value. However, if the enterprises can use the profits gained from the short-term advantage in the market to invest in technology research and development, then it will eventually improve their patent's technology value. Therefore, patents with a high market value do not necessarily need to have a high technology value when they initially enter the market. However, in the long term, when facing fierce market competition, enterprises could invest more in technology to improve their patent's technology value [6]. Otherwise, a short-term advantage in the market could deceive enterprises and ultimately keep them out of competition since they lack a technology advantage. Therefore, the market value may promote or inhibit the technology value in different situations [28].

Third, we discuss the impact of the law value on the technology and market values. The law value is an important precursor to guarantee the technology value and market value. The law value lies in whether the patent has stable legal protection and depends on whether it is easy for others to infringe upon [29]. If the text of the patent application is written well and the technical scheme is obviously different from others, then its legal claims are stable and its law value is high. This is an important precursor for the realization of the technology value and market value. Patents with a low law value, even if they have high technology and market values, are easy to invalidate by a lawsuit or to be infringed upon by competitors. Therefore, a high law value is an important piece that is necessary to realize technical and market value. The law value of a patent can also promote or inhibit the technical and market value [30].

Fourth, we discuss how patents' technology and market values can also affect their law value. The legal protection of a patent is regional. In some regions, patents with a low law value may also obtain certain technology and market advantages. However, these advantages are unstable since enterprises may face troubles in the law area. If enterprises can use these advantages to improve their patent's law value, then the patent's law value will be promoted. Therefore, the



patent's technology and market value can also promote or inhibit their law value.

Therefore, the relationships among technology, law, and market value are complex. Sometimes these relationships restrain each other, and sometimes, they promote each other. The relationships often change based on the enterprise's situation. Therefore, the formation of high-value patents is a long-term and continuous evolution process. In this process, the technology value is the important foundation of the market value, and the law value is the necessary guarantee for the market value so that they are finally embodied in a high market value through good market opportunities, as shown in Figure 1. This process is similar to an ecosystem, which evolves due to interactions among its inner factors and is affected by outer change [31].

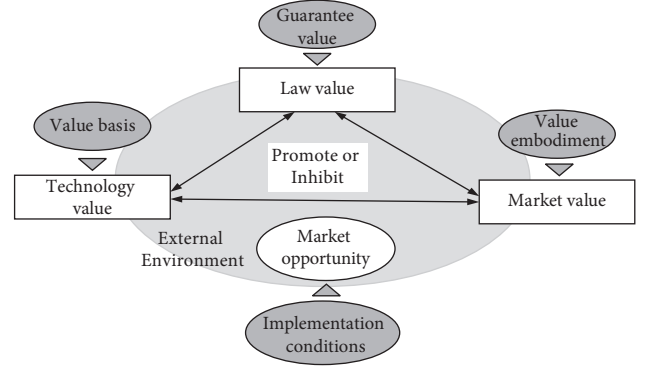


FIGURE 1: Value relationships of high-value patents.

**3.2. Formation Path of High-Value Patents in Reverse Innovation of Local Enterprises.** In reverse innovation, the formation of high-value patents in local enterprises is a complex, evolving process. Initially, a local enterprise's patents may have low technology values as they always follow the technology of developed countries. Additionally, their patent's law value may be low because developing countries usually have poor technology protection and local enterprises pay little attention to the protection of their intellectual property rights. Local enterprises mainly gain profits through low prices, cost advantage, and huge market demands. However, these advantages are limited in a local market and will not last when the market competition becomes more fierce. It is easy to be replaced by latecomers that have more advanced technology or lower costs. The low law value of the patent also makes local enterprises vulnerable to legal disputes and decreases their market advantage. Therefore, local enterprises that are thinking long term capitalize on the short-term and regional market advantage and increase their innovation investment to improve their patents' technology and law values, which may successfully turn the short-term advantage in a regional market into a long-term advantage in the international market, where reverse innovation in local enterprises occurs [6]. Therefore, we propose the formation path for high-value patents in reverse innovation in local enterprises, as shown in Figure 2.

### 3.3. Model

**3.3.1. Lotka–Volterra Model.** The Lotka–Volterra model was first used in nature for the analysis of competition and symbiosis among species and was later introduced into social science research [32, 33]. Since the Lotka–Volterra model explains the evolution of complex ecosystems well [34, 35], we used it in our research to analyze the evolution process of high-value patents in reverse innovation in local enterprises. The Lotka–Volterra model is usually composed of a logistic growth function, which is used to express two species with a mutually influential relationship, and is expressed as follows [34]:

$$\begin{cases} \dot{X} = \frac{dX}{dt} = X(a_1 - b_1X - c_1Y), \\ \dot{Y} = \frac{dY}{dt} = Y(a_1 - b_1Y - c_1X), \end{cases} \quad (1)$$

where  $X$  and  $Y$  represent the total resources owned by two species  $X$  and  $Y$ , respectively.  $a_i$  and  $b_i$  are the coefficients of the independent growth of the two species ( $i = 1, 2$ , where  $b_i$  is the limiting coefficient of species growth to resource consumption and to itself).  $c_i$  is the growth coefficient of interaction among the species. The greater the absolute value of  $c_i$  is the greater the influence between the two species.

The Lotka–Volterra model is a continuous time model. We transformed it into a discrete-time model as follows:

$$\begin{cases} X(t+1) = \frac{\alpha_1 X(t)}{1 + \beta_1 X(t) + \lambda_1 Y(t)}, \\ Y(t+1) = \frac{\alpha_1 Y(t)}{1 + \beta_1 Y(t) + \lambda_1 X(t)}, \end{cases} \quad (2)$$

$X(t+1)$  and  $Y(t+1)$  represent the total number of species  $X$  and  $Y$  in  $t+1$  time, respectively.  $X(t)$  and  $Y(t)$  represent the total number of species in  $t$  time.

(2) Equilibrium conditions and equilibrium points of the model:

#### 3.3.2. Lotka–Volterra Model of High-Value Patent Evolution in Reverse Innovation in Local Enterprises

(1) Model construction and parameter determination:

In the three dimensions of technology, law, and market, the value of high-value patents is  $V_i$ , ( $i = 1, 2, 3$ ). The rate of change with time is  $\dot{V}_i = dV_i/dt$ .  $a_i$  and  $b_i$  represent the independent development coefficients of value in each dimension.  $c_i$  and  $d_i$  represent the mutual influence coefficients between the values of each dimension. The value changes of high-value patents in the three dimensions can be expressed as follows:

$$\begin{cases} \dot{V}_1 = \frac{dV_1}{dt} = V_1(a_1 - b_1V_1 - c_1V_2 - d_1V_3), \\ \dot{V}_2 = \frac{dV_2}{dt} = V_2(a_2 - b_2V_2 - c_2V_1 - d_2V_3), \\ \dot{V}_3 = \frac{dV_3}{dt} = V_3(a_3 - b_3V_3 - c_3V_1 - d_3V_2). \end{cases} \quad (3)$$

Here, we convert the above equation into a discrete-time equation:

$$\begin{cases} V_1(t+1) = \frac{\alpha_1 V_1(t)}{1 + \beta_1 V_1(t) + \gamma_1 V_2(t) + \delta_1 V_3(t)}, \\ V_2(t+1) = \frac{\alpha_2 V_2(t)}{1 + \beta_2 V_2(t) + \gamma_2 V_1(t) + \delta_2 V_3(t)}, \\ V_3(t+1) = \frac{\alpha_3 V_3(t)}{1 + \beta_3 V_3(t) + \gamma_3 V_1(t) + \delta_3 V_2(t)}. \end{cases} \quad (4)$$

By using the nonlinear least square estimation, we calculated the value independent development coefficient and mutual influence coefficient of each dimension. The specific values of the parameters are as follows:

$$\begin{aligned} a_i &= \ln \alpha_i, \\ b_i &= \frac{\beta_i \ln \alpha_i}{\alpha_i - 1}, \\ c_i &= \frac{\gamma_i \ln \alpha_i}{\alpha_i - 1}, \\ d_i &= \frac{\delta_i \ln \alpha_i}{\alpha_i - 1}. \end{aligned} \quad (5)$$

Positive and negative signs of  $c_i$  and  $d_i$  can reflect the interaction between the values. A positive sign indicates a relationship of promotion, a negative sign indicates inhibition, and zero indicates no correlation. Therefore, when the coefficients are all positive, it means that they exhibit mutual promotion, and vice versa. When the coefficients are positive and negative, it means that the promotion and inhibition are opposite to each other. When the mutual influence coefficients are zero and nonzero, it means that there is a one-way influence relationship.

According to the previous analysis, we list the positive and negative signs of  $c_i$  and  $d_i$  in the domestic and international market environment in Table 1.

When all of the equations in (3) are equal to zero, the maximum values in all three dimensions are obtained at the same time. This situation can be regarded as the optimal equilibrium condition for the formation of high-value patents. That is, under the condition of mutual promotion or restriction of the three dimension values, patents form the best high-value patents. The equilibrium conditions can be expressed as follows:

$$\begin{cases} \dot{V}_1 = \frac{dV_1}{dt} = V_1(a_1 - b_1V_1 - c_1V_2 - d_1V_3) = 0, \\ \dot{V}_2 = \frac{dV_2}{dt} = V_2(a_2 - b_2V_2 - c_2V_1 - d_2V_3) = 0, \\ \dot{V}_3 = \frac{dV_3}{dt} = V_3(a_3 - b_3V_3 - c_3V_1 - d_3V_2) = 0. \end{cases} \quad (6)$$

The boundary conditions converging to an equilibrium state are as follows:

$$\begin{cases} \text{if } V_1 > \frac{a_1 - c_1V_2 - d_1V_3}{b_1}, \text{ then } \frac{dV_1}{dt} < 0, \\ \text{if } V_2 > \frac{a_2 - c_2V_1 - d_2V_3}{b_2}, \text{ then } \frac{dV_2}{dt} < 0, \\ \text{if } V_3 > \frac{a_3 - c_3V_1 - d_3V_2}{b_3}, \text{ then } \frac{dV_3}{dt} < 0. \end{cases} \quad (7)$$

By reducing the dimension of (7), we obtain

$$\begin{cases} \frac{dV_2/dt}{dV_1/dt} = \frac{dV_2}{dV_1} = \frac{V_2(a_2 - b_2V_2 - c_2V_1 - d_2V_3)}{V_1(a_1 - b_1V_1 - c_1V_2 - d_1V_3)} = 0, \\ \frac{dV_3/dt}{dV_1/dt} = \frac{dV_3}{dV_1} = \frac{V_3(a_3 - b_3V_3 - c_3V_1 - d_3V_2)}{V_1(a_1 - b_1V_1 - c_1V_2 - d_1V_3)} = 0, \\ \frac{dV_3/dt}{dV_2/dt} = \frac{dV_3}{dV_2} = \frac{V_3(a_3 - b_3V_3 - c_3V_1 - d_3V_2)}{V_2(a_2 - b_2V_2 - c_2V_1 - d_2V_3)} = 0. \end{cases} \quad (8)$$

For the above equation to hold, the results of all three equations must be zero. Since  $V_i \neq 0$ , then

$$\begin{cases} a_2 - b_2V_2 - c_2V_1 - d_2V_3 = 0, \\ a_3 - b_3V_3 - c_3V_1 - d_3V_2 = 0, \\ a_3 - b_3V_3 - c_3V_1 - d_3V_2 = 0. \end{cases} \quad (9)$$

In the three-dimensional coordinate diagram (Figure 3), each of the above three equations represents a plane. They represent the maximum value degree of high-value patents in technology, law, and market. If there is an intersection point, then it is the equilibrium point, which is where we obtain the best high-value patents in the three dimensions, as shown in Figures 3(a) and 3(b) which shows that the three

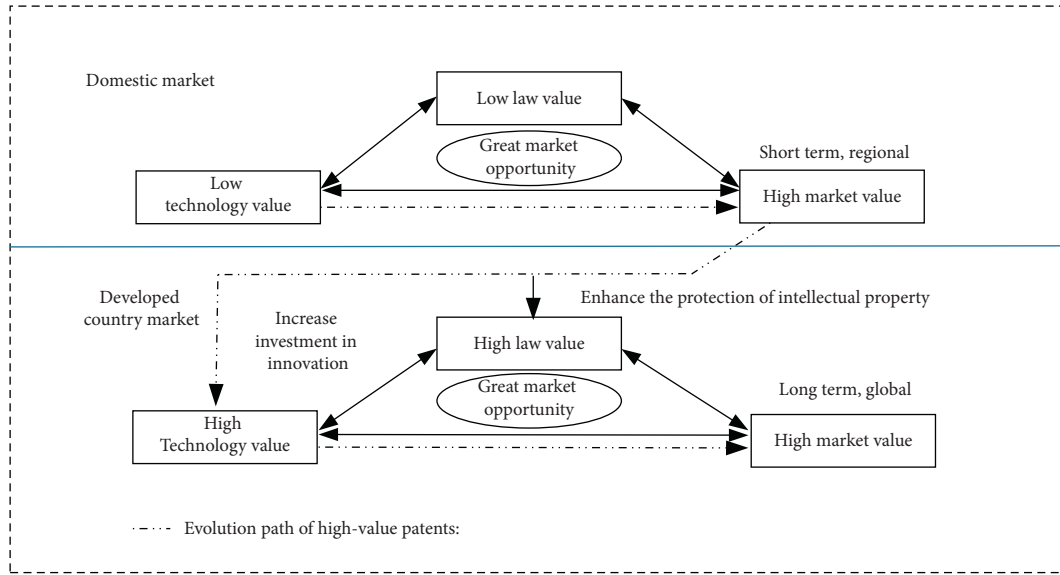


FIGURE 2: Formation path of high-value patents in reverse innovation in local enterprises.

TABLE 1: Relationships of the mutual influence coefficient.

Market environment	$c_1$	$c_2$	$c_3$	$d_1$	$d_2$	$d_3$	Route	Relationship	Result
Domestic	-	-	+	0	0	+	Low technical value, low law value, and high market value	$V_1$ and $V_2$ indicate a reciprocal inhibition, $V_1$ and $V_3$ indicate a partial interest relationship, and $V_2$ and $V_3$ indicate a partial interest relationship	Short term and regional high-value patents
International	+	-	-	-	-	-	High technical value, high law value, and high market value	$V_1$ and $V_2$ indicate a mutual promotion, $V_1$ and $V_3$ indicate a mutual promotion, and $V_2$ and $V_3$ indicate a interrelationship	Long term and global high-value patents

Note: the partial interest relationship is a kind of one-way relationship that is beneficial to one party and has no obvious impact on the other.

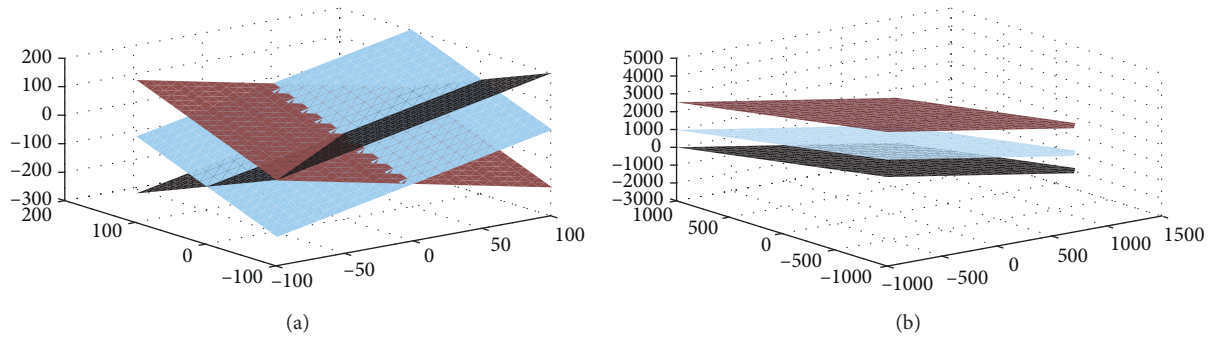


FIGURE 3: Equilibrium point of the three-dimensional coordinate diagram.

planes are parallel, and there is no intersection point, which indicates that there is no equilibrium point.

#### 4. Case Analysis

**4.1. Case Enterprise Selection and Data Collection.** In this paper, we chose Huawei as the representative of local enterprises in reverse innovation. Huawei has been successful in reverse innovation in recent years. Its new products have made great progress in developing markets in developed

countries, and it has obtained superiority in regard to technology and market competition. In the first quarter of 2019 global mobile market share report, Huawei's mobile market share was 15.7%, which surpassed Apple [36, 37]. Particularly, in the field of next generation 5G technology, Huawei has achieved successful reverse innovation. Its 5G patents are at the leading level in the world, as shown in Figure 4.

In this paper, we used the *Innography* database to collect Huawei's data; we only selected invention patents to reflect

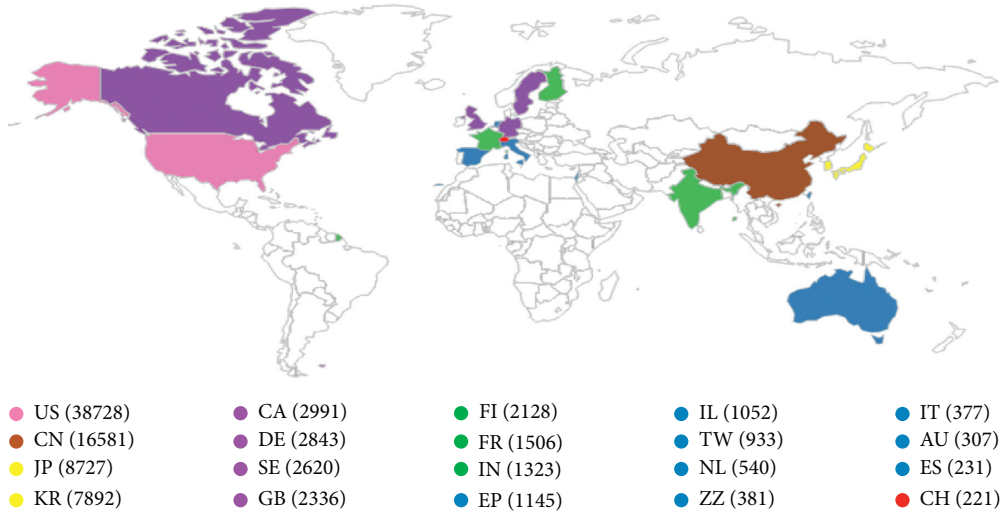


FIGURE 4: Global distribution of Huawei's 5G patents from 2001 to 2018 (data from the Innography database (<https://app.innography.com/>)).

the technical value (the scope of patent granting varies from country to country). However, these patents generally include invention patents belonging to technical solutions for new products (methods) with greater innovation. Therefore, the patents mentioned in this paper mainly refer to invention patents with greater technological content, excluding general utility model and design patents). Some studies show that Huawei has increased its R&D efforts since 2001. Since the time of 2G, there has been a focus on imitation innovation, and Huawei has been able to break the technology monopoly. The development of 5G has been a great breakthrough, and Huawei has gradually taken the leading position in the market. Therefore, we divided Huawei's reverse innovation into two stages since 2001. The first stage focused on the domestic market (2001–2011). In this stage, Huawei focused on technology introduction and imitation innovation and gained a competitive advantage in the domestic market. The second stage focused on developed countries (since 2011 to now). The strategic focus for this stage was on innovation ability and bringing the independently developed products to the developed country's market to obtain stable competitiveness.

With its development path, we collected Huawei's patents from January 1, 2001, to December 31, 2018, and selected patents with high values (according to the comprehensive scores of patent claims, patents of the same family, cite and cited, whether involved in the case, patent protection period, etc. A patent with a patent strength of more than 3 is a patent with high value). Finally, we collected 125,369 patents as a sample.

**4.2. Measurement of Patent Value.** We calculated the patents' values in technology, law, and market (see Appendix), as shown in Table 2.

From the data, all of the values in the three dimensions are rising, as shown in Figure 5.

TABLE 2: Patent technology, law, and market values.

Year	Technology value	Law value	Market value
2001	33	43	28
2002	1711	2221	1522
2003	3875	5037	3443
2004	10993	14307	9669
2005	12438	16191	10959
2006	22653	29501	19894
2007	25062	32647	22001
2008	32557	42423	28509
2009	38060	49615	33222
2010	42230	55023	37053
2011	48585	63338	42409
2012	53519	69731	47009
2013	50132	65314	44067
2014	128747	167982	111483
2015	128399	298139	196893
2016	238772	311640	206124
2017	272376	355563	234759
2018	268331	350298	231193

#### 4.3. Analysis of the Lotka–Volterra Model Based on the Evolution of High-Value Patents in Reverse Innovation in Local Enterprises

**4.3.1. Model Parameter Calculation.** We estimated the parameters of equations (1) and (2). The stability tests are shown in Tables 3–5.

The parameters were introduced into the discrete-time equation (2), and we calculated the estimated parameters of the influence coefficients in each of the three dimensions, as shown in Table 6.

We transformed the parameters of the discrete-time equations and calculated the parameters of the continuous equations (1), as shown in Table 7.

Then, we created a Lotka–Volterra model in the three dimensions to explain the evolution of the high-value patents of Huawei as follows:

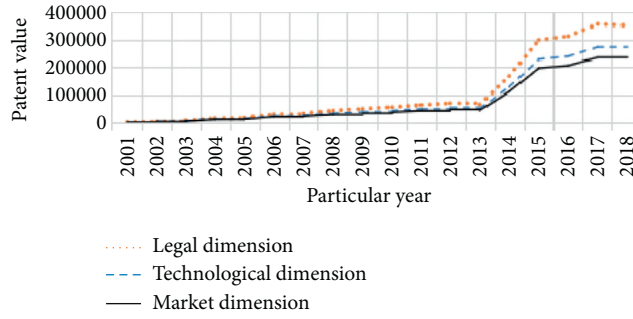


FIGURE 5: Value change of Huawei patents in the technology, law, and market dimensions (2001–2018).

TABLE 3: Stability test of parameter estimation of the technology dimension.

	Coefficient	Std. error	t-statistic	Prob
$\alpha_1$	1.008853	0.263892	3.822980	0.0021
$\beta_1$	-0.011480	0.013619	-0.842924	0.4145
$\gamma_1$	0.008296	0.009485	0.874628	0.3976
$\xi_1$	0.000754	0.001442	0.523118	0.6067
R-squared	0.955112	Mean dependent var		86967.03
Adjusted R-squared	0.944754	S.D. dependent var		99005.39
S.E. of regression	23270.73	Akaike info criterion		23.15010
Sum squared resid	7.04 E + 09	Schwarz criterion		23.34615
Log likelihood	-192.7759	Hannan–Quinn criterion		23.16959
Durbin–Watson stat	1.734431			

$$\begin{cases} \dot{V}_1 = \frac{dV_1}{dt} = V_1(0.00876 - 0.01145V_1 + 0.00826V_2 + 0.00075V_3), \\ \dot{V}_2 = \frac{dV_2}{dt} = V_2(0.00886 + 0.00826V_2 - 0.01141V_1 + 0.00075V_3), \\ \dot{V}_3 = \frac{dV_3}{dt} = V_3(0.00856 + 0.00077V_3 + 0.00834V_1 - 0.01155V_2). \end{cases} \quad (10)$$

**4.3.2. Value Degree of the Best High-Value Patents in the Three Dimensions.** We obtained the equilibrium conditions when all of the equations in the equation group (10) were equal to zero. When the equilibrium conditions were reached, the company obtained an optimal position for their high-value patents. The equilibrium conditions were obtained as follows:

$$\begin{cases} \dot{V}_1 = \frac{dV_1}{dt} = V_1(0.00876 - 0.01145V_1 + 0.00826V_2 + 0.00075V_3) = 0, \\ \dot{V}_2 = \frac{dV_2}{dt} = V_2(0.00886 + 0.00826V_2 - 0.01141V_1 + 0.00075V_3) = 0, \\ \dot{V}_3 = \frac{dV_3}{dt} = V_3(0.00856 + 0.00077V_3 + 0.00834V_1 - 0.01155V_2) = 0. \end{cases} \quad (11)$$

According to the convergence conditions of the above model, Huawei's high-value patents met the conditions of equation (7), which means that the values of Huawei's high-value patents in technology, law, and market can reach the highest point at the same time. This point can be seen as an

optimal position for evolution of the high-value patents. The value degree of each dimension of the optimal point can be calculated as follows.

By reducing the dimension, we obtained equation (12) from (11):



TABLE 4: Stability test of parameter estimation of the law dimension.

	Coefficient	Std. error	<i>t</i> -statistic	Prob
$\alpha_2$	1.008929	0.264049	3.820399	0.0021
$\beta_2$	0.008289	0.009490	0.873487	0.3982
$\gamma_2$	-0.011469	0.013626	-0.841753	0.4151
$\xi_2$	0.000753	0.001443	0.521677	0.6107
R-squared	0.955099	Mean dependent var		113468.8
Adjusted R-squared	0.944738	S.D. dependent var		129262.9
S.E. of regression	30387.03	Akaike info criterion		23.68374
Sum squared resid	1.20 E + 10	Schwarz criterion		23.87979
Log likelihood	-197.3118	Hannan-Quinn criterion		23.70323
Durbin-Watson stat	1.733973			

$$\begin{cases} \frac{dV_2/dt}{dV_1/dt} = \frac{dV_2}{dV_1} = \frac{V_2(0.00886 + 0.00826V_2 - 0.01141V_1 + 0.00075V_3)}{V_1(0.00876 - 0.01145V_1 + 0.00826V_2 + 0.00075V_3)} = 0, \\ \frac{dV_3/dt}{dV_1/dt} = \frac{dV_3}{dV_1} = \frac{V_3(0.00856 + 0.00077V_3 + 0.00834V_1 - 0.01155V_2)}{V_1(0.00876 - 0.01145V_1 + 0.00826V_2 + 0.00075V_3)} = 0, \\ \frac{dV_3/dt}{dV_2/dt} = \frac{dV_3}{dV_2} = \frac{V_3(0.00856 + 0.00077V_3 + 0.00834V_1 - 0.01155V_2)}{V_2(0.00886 + 0.00826V_2 - 0.01141V_1 + 0.00075V_3)} = 0. \end{cases} \quad (12)$$

By solving the equations, we obtained the value degree of Huawei's optimal high-value patents in the three dimensions, as shown in Table 8:

We drew the optimal point on a three-dimensional coordinate diagram (Figure 6). The intersection of the three planes is the optimal point: the optimal value point of Huawei's high-value patents in the three dimensions.

**4.3.3. Evolution Path Analysis.** We used the Runge-Kutta fourth-order method to perform a numerical simulation to show the evolution path of the high-value patents in reverse innovation, as shown in Figure 7.

The circles in the figure represent the actual calculated year data, and the asterisks represent the predicted year data. The scatter points in the figure represent the value degree of Huawei's annual patent collection in terms of technology, law, and market. When the scatter distribution is relatively dense, the value degree changes slightly, and when the scatter distribution is sparse, the value degree changes greatly. The line between the scatter points is shown in the figure. The blue line represents the evolution path of the patent value, the black arrow represents the trajectory, and the red arrow represents the predicted trajectory of the model.

Compared with the theoretical analysis of the formation path of high-value patents in reverse innovation in local enterprises, we found that the evolution path of Huawei's high-value patents is basically consistent with the theoretical analysis (see Figure 2). In the domestic market stage from 2001 to 2011, the value degree of Huawei's patents in the three dimensions of technology, law, and market was relatively low, and development was slow. In the early stage of

reverse innovation, Huawei's high-value patent evolution followed the general development law of local enterprises, that is, it began to rely on the huge market demand of the region (domestic or developing countries) to obtain a competitive advantage. From 2012 to 2018, that is, from Huawei's reverse innovation to entry in the overseas markets, the value degree of its high-value patents in both the technical and legal dimensions significantly increased, and the growth of the technological value was greater than the legal value. At the same time, at this stage, the market value of its patents also showed a substantial increase, indicating that, with the deepening of Huawei's reverse innovation strategy, when its new products and technologies are successfully reversed to the market in developed countries, the technical value and legal value of its patents are greatly improved compared with those in China. The significant improvement of the technical value indicates that Huawei has made outstanding achievements in technological catch-up. In fact, Huawei has successfully achieved certain leading advantages in some key core technology fields (such as 5G communication). At the same time, the market value of its patents has also increased rapidly, which shows that Huawei has not only achieved obvious advantages in technology but also made considerable achievements in developing markets in developed countries and meeting the needs of local consumers.

From the data, Huawei's optimal high-value patent collection appeared in 2017 and 2018 and will now decline according to the data forecast. We speculate that the reason for this decline may be that Huawei had more patent layouts in the 5G field with high technology value around 2017 and 2018. Of course, the period after 2018 is the forecasted value of the data. Since the forecasted

TABLE 5: Stability test of parameter estimation of the market dimension.

	Coefficient	Std. error	t-statistic	Prob
$\alpha_3$	1.008668	0.262033	3.849388	0.0020
$\beta_3$	0.000775	0.001434	0.540429	0.5980
$\gamma_3$	0.008385	0.009432	0.889013	0.3902
$\xi_3$	-0.011614	0.013542	-0.857598	0.4066
R-squared	0.955354	Mean dependent var		75306.76
Adjusted R-squared	0.945051	S.D. dependent var		85214.13
S.E. of regression	19975.13	Akaike info criterion		22.84469
Sum squared resid	5.19 E + 09	Schwarz criterion		23.04074
Log likelihood	-190.1798	Hannan-Quinn criterion		22.86418
Durbin-Watson stat	1.739413			

TABLE 6: Parameter estimation of discrete-time equation (2).

Dimension	Parameter				$R^2$	DW
	$\alpha_i$	$\beta_i$	$\gamma_i$	$\xi_i$		
Technology	1.008853	-0.011480	0.008296	0.000754	0.955112	1.734431
Law	1.008929	0.008289	-0.011469	0.000753	0.955099	1.733973
Market	1.008668	0.000759	0.008385	-0.011614	0.955354	1.739413

TABLE 7: Parameter estimation of continuous equation (1).

Dimension	Parameter			
	$a_i$	$b_i$	$c_i$	$d_i$
Technology	0.008761506	-0.011449695	0.008263693	0.000746719
Law	0.008860628	0.008263283	-0.011409304	0.000746682
Market	0.008563231	0.000766708	0.008344171	-0.011550404

TABLE 8: Values of Huawei's optimal high-value patents in the three dimensions.

	Technology value	Law value	Market value
Optimal point (V1, V2, V3)	3.628934612	3.641341302	3.612820702

value is based on the long-term smooth growth rate of the data, it cannot reflect the momentum after the rapid growth of 5G technology in 2017 and 2018. Therefore, more data are needed to test whether the optimal value was reached in 2017 and 2018. However, according to the actual data, the actual evolution path of Huawei's high-value patents is more consistent with the theoretical and practical analyzes.

**4.4. Management Suggestions.** According to the above analysis, we present some management suggestions as follows:

- (1) In reverse innovation, the cultivation of high-value patents in local enterprises should consider the value development of technology, law, and the market. However, this does not mean the enterprises should develop the values in these three dimensions at the same time. Local enterprises can choose whether to develop their technology or market value according to the market conditions and their capabilities. For example, in the initial phase of reverse innovation, when the local enterprises are weak in the technology area but have

advantages in costs and demands in emerging markets, they can capitalize on these advantages in the short term to increase their technology investment and accumulate their technology capabilities, thereby grasping opportunities to reverse their new products and technologies to developed countries. In this process, the local enterprises should follow the newest technologies' development and survey the global patents when they obtain some success in technology innovation, especially in the key technologies of industrial development. When they successfully reverse new products and technologies to developed countries, they need to continuously improve their technology and quality of new products to establish and maintain a long-term advantage in the global market.

- (2) In reverse innovation, a patent's law value is often ignored by local enterprises. Since the intellectual property protection system is fragile in developing countries, local enterprises usually do not pay enough attention to intellectual property protection, which leads to the low law value of their patents and a difficulty reversing their new products to developed countries where strict intellectual property protection is required.

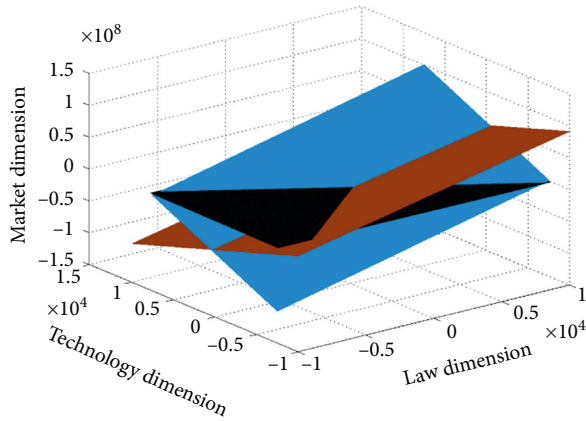


FIGURE 6: Formation of the optimal point of Huawei's high-value patents in the three dimensions.

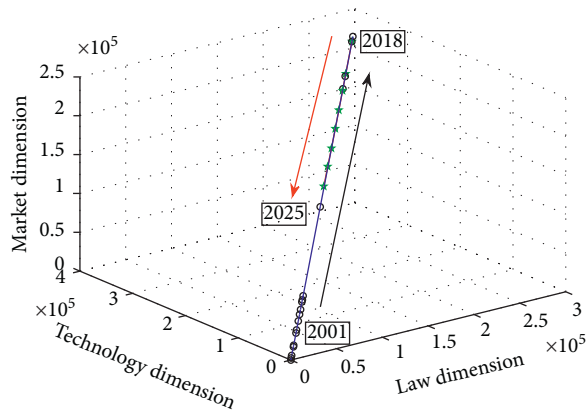


FIGURE 7: Evolution path of Huawei's high-value patents.

Even if some new products were successfully reversed to developed countries, it would be hard to maintain this situation for the long term due to the low law value of the patents and the probability of intellectual property disputes. Therefore, in the process of reverse innovation, local enterprises must pay attention to cultivate high law value in their patents, improving the written quality of the patent applications, enhancing the stability and clearance of their legal claims, etc. Especially, in the markets of developed countries, a patent's law value is sometimes a decisive factor in the successful reverse innovation in local enterprises.

- (3) The formation of high-value patents in reverse innovation in local enterprises is a long-term and complex evolution process, especially with the optimal high-value patents that can be formed after a long period of technology catch-up in developing countries. To obtain successful inverse innovation, local enterprises must make efforts to improve the value of their patents according to the changes in their external situation and their inner capability and balance the relationships among the technology, law, and market values. Especially, when local enterprises

gain an advantage in certain technologies, they must enhance their strategies in the global layout of their high-value patents and increasingly improve the whole quality of their patents.

## 5. Conclusion

This paper discussed the evolution of high-value patents in reverse innovation in local enterprises based on the ecological perspective. We draw the following conclusions.

- (1) High-value patents show their value in three dimensions, i.e., technology, law, and market. These values affect each other as the situation changes. The formation of high-value patents is a long-term evolving process resulting from the interaction among the values of these three dimensions with changes in the external situation.
- (2) For reverse innovation in local enterprises, the formation of high-value patents reflects a long-term technology catch-up process of developing countries. We built a Lotka–Volterra model of the three dimensions to explain this complex process and simulated the evolution path of high-value patents in reverse innovation in local enterprises.
- (3) We used Huawei's data to analyze the evolution path of its high-value patents in reverse innovation and found that the results were consistent with our theoretical model analysis. Therefore, through this model, we proposed some management strategies for cultivating high-value patents in reverse innovation in local enterprises.

There are some limitations in our study. For example, there may be some other paths in the formation of high-value patents that we have not discussed, and more cases should be analyzed to test the model. These limitations also provide interesting issues for future studies [38–43].

## Appendix

Patent value calculation formula (operation manual of patent value analysis index system)

Technology value = (Advanced \* 15% + Industry development trend \* 10% + Alternative \* 20%) (Precited patents, 45%) + (Applicable \* 20% + Supporting technology dependency \* 15%) (Family patents, 35%) + (Maturity \* 20%) (Not involving infringement patents, 20%)

Law value = (Judgment of patent infringement \* 20% + Noncircumvention \* 30% + Patent licensing \* 5%) (No infringement patent, 55%) + (Multinational application \* 15%) (Patent of the same family, 15%) + (Dependency \* 15% + Validity \* 15%) (Front citation patent, 30%)

Market value = (Market application \* 25% + Market share \* 20%) (Family patent, 45%) + (Market scale prospect \* 20% + Competition \* 20%) (Front cited patent, 40%) + (Policy adaptability \* 15%) (No infringement patent, 15%)



## Data Availability

The structural data used to support the findings of this study are included within the supplementary information files. The data used to support the findings of this study were supplied by INNOGRAPHY under license and so cannot be made freely available. Requests for access to these data should be made to pay.

The data of this paper is to search all patent information of INNOGRAPHY Huawei company and get the number of patents by screening invention patents and patent intensity. The number of references, the number of families, and the number of infringements are selected. The data provided in the supplementary materials are the number of patents sorted out by the author.

## Conflicts of Interest

The authors declare that they have no conflicts of interest.

## Acknowledgments

The project was supported by the National Natural Science Foundation of China (nos. 71562001 and 72062002).

## Supplementary Materials

The data provided in the supplementary materials are the number of patents sorted out by the author. (*Supplementary Materials*)

## References

- [1] J. R. Immelt, V. Govindarajan, and C. Trimble, "How GE is disrupting itself," *Harvard Business Review*, vol. 35, no. 10, 2009.
- [2] V. Govindarajan and R. Ramamurti, "Reverse innovation, emerging markets, and global strategy," *Global Strategy Journal*, vol. 1, no. 3-4, pp. 191-205, 2011.
- [3] H. Luo and Q. Zhang, "Research on the breakthrough technological innovation process of new and technological small enterprises from the perspective of knowledge management," *Science of Science and Management of S.&T.* vol. 3, pp. 143-151, 2015.
- [4] P. Cao and Y. Zeng, "Research dynamics and analysis model construction of reverse innovation," *Science and technology progress and countermeasures*, vol. 32, no. 17, pp. 22-26, 2015.
- [5] Y. Cao and L. Zhao, "Research on the mechanism of patent acquisition, patent protection, patent commercialization and technological innovation performance," *Scientific Research Management*, vol. 34, no. 8, pp. 42-52, 2013.
- [6] T. Dong, "High value patents provide inexhaustible new impetus for enterprise transformation and upgrading," *China Science and Technology Industry*, vol. 7, pp. 78-80, 2018.
- [7] B. Wei, L. Liu, and G. Rao, "Giving full play to the advantages of examination Resources to help cultivate high-value patents," *Chinese Invention and Patent*, vol. 15, no. 4, pp. 25-29, 2018.
- [8] Y. Su and W. Sun, "Analyzing a closed-loop supply chain considering environmental pollution using the NSGA-II," *IEEE Transactions on Fuzzy Systems*, vol. 27, no. 5, pp. 1066-1074, 2019.
- [9] Y. Su and W. Sun, "Sustainability evaluation of the supply chain with undesired outputs and dual-role factors based on double frontier network DEA," *Soft Computing*, vol. 22, no. 16, pp. 5525-5533, 2018.
- [10] Y. Su and T. C. Li, "Simulation analysis of knowledge transfer in a knowledge alliance based on a circular surface radiator model," *Complexity*, vol. 2020, Article ID 4301489, 27 pages, 2020.
- [11] Z. Yang, T. Ouyang, X. Fu, and X. Peng, "A decision-making algorithm for online shopping using deep-learning-based opinion pairs mining and q-rung orthopair fuzzy interaction Heronian mean operators," *International Journal of Intelligent Systems*, vol. 35, no. 5, pp. 783-825, 2020.
- [12] N. Wang, *Research on the Impact of Reverse Innovation Transfer of Subsidiaries of Multinational Companies: Theoretical and Empirical Research*, University of Foreign Economic and Trade, Beijing, China, 2016.
- [13] C. Simone, D. M. Alberto, and P. Andrea, "Reverse innovation at spere: a case study in China," *Research Technology Management*, vol. 57, no. 4, pp. 28-34, 2014.
- [14] M. Nan, *Research on Key Success Factors of Reverse Innovation in Electronic Information Industry*, Dalian University of Technology, Dalian, China, 2016.
- [15] Y. Xu, X. Wang, N. Xu, and S. Zheng, "The process and key factors of reverse innovation in late development engineering technology service enterprises," *Scientific Research Management*, vol. 38, no. 6, pp. 9-17, 2017.
- [16] Y. Yu, *Research on Key Influencing Factors of Reverse Innovation in China's Engineering Technology Service Enterprises*, Dalian University of technology, Dalian, China, 2014.
- [17] N. Xu and Z. Peng, "Case study on local product development capability, innovation network and reverse innovation of latecomers," *Research and Development Management*, vol. 29, no. 5, pp. 99-112, 2017.
- [18] R. Li, W. Zhou, J. Rong, and Z. Kong, "Analysis of cited characteristics of high value enterprise patents-taking the world's top 500 enterprise patents as an example," *Journal of the China Society for Scientific and Technical Information*, vol. 34, no. 9, pp. 899-911, 2015.
- [19] Q. Zhang, "Invention patent: the weapon of enterprise core competitiveness," *China Invention and Patent*, vol. 6, pp. 40-41, 2014.
- [20] T. Zhang and G. Li, "Research on enterprise intellectual property value and its evaluation," *Reformation and Strategy*, vol. 8, pp. 23-26, 2006.
- [21] T. Ma and X. Zhao, "The connotation of high-value patent and its restricted factors," *Chinese Invention and Patent*, vol. 15, no. 3, pp. 24-28, 2018.
- [22] X. Wan and X. Zhu, "Evaluation index system and fuzzy comprehensive evaluation of patent value," *Scientific Research Management*, vol. 2, pp. 185-191, 2008.
- [23] J. Ji and L. Dong, "Development and application of QR code technology," *Management & Technology of SME*, vol. 27, pp. 290-291, 2013.
- [24] Q. Zhu, *Research on Key Factors Influencing Technology Source Acquisition in the Process of Reverse Innovation*, Dalian University of Technology, Dalian, China, 2013.
- [25] D. Wang, "Research on core rigidity in strategic change-taking Kodak as an example," *Science of Science and Management of S.&T.* vol. 34, no. 5, pp. 97-105, 2013.
- [26] X. Zhang, "Will dinosaurs die out?—how American famous enterprises get out of the trough," *Manager Journal*, vol. 2, pp. 41-42, 1995.

- [27] Y. Hou, W. Liu, and Y. Liu, "Research on the international development path and influence mechanism of independent innovation system of China's communication industry-taking Huawei as an example," *Science and Technology for Development*, vol. 11, pp. 32–40, 2011.
- [28] Z. Xing, G. Ma, Y. Sun, and G. Liu, "Construction and promotion of high value patent cultivation system," *Chinese Universities Science and Technology*, vol. Z1, pp. 50–53, 2019.
- [29] J. Zhang and X. Zhang, "Experience sharing of claims interpretation in patent infringement determination," *Chinese Invention and Patent*, vol. 16, no. 10, pp. 98–103, 2019.
- [30] S. Yang, Y. Wang, H. Chen, L. Zhou, B. Li, and L. Dai, "Research on patent legal value evaluation," *High Tech Communication*, vol. 26, no. z1, pp. 815–823, 2016.
- [31] D. Zeng, "High value patent screening," *Science and Technology Innovation and Application*, vol. 14, pp. 4–6, 2019.
- [32] G. Giancarlo, "Giuseppe palomba and the lotka-volterra equations," *Rendiconti Lincei*, vol. 19, no. 4, pp. 347–357, 2008.
- [33] J. F. Moore, "Predators and prey: a new ecology of competition," *Harvard Business Review*, vol. 71, no. 3, pp. 75–86, 1993.
- [34] Y. Chen and F. Xie, "Bionics research on the evolution path of photovoltaic industry ecological innovation system based on Lotka voterra model," *Research and Development Management*, vol. 24, no. 3, pp. 74–84, 2012.
- [35] H.-T. Wang and T.-C. Wang, "Application of the grey Lotka-Volterra model to forecast the diffusion and competition analysis of the TV and smartphone industries," *Technological Forecasting and Social Change*, vol. 106, pp. 37–44, 2016.
- [36] J. Dan and G. Dong, "Research on reverse innovation path of emerging market latecomers: case study from Huawei," *Science & Technology Progress and Policy*, vol. 34, no. 2, pp. 87–93, 2017.
- [37] X. Fan, *Research on Marketing Strategy of JL Company*, Dalian University of Technology, Dalian, China, 2017.
- [38] M. B. Felipe, M. O. Moacir de, F. S. Franciane, and O. C. Ronald de, "The reverse transfer of innovation of foreign subsidiaries of Brazilian multinationals," *European Management Journal*, vol. 30, no. 3, pp. 219–231, 2012.
- [39] F. S. Franciane, S. Roberto, L.-V. Henry, and T. Fredrik, "Determinants of reverse knowledge transfer for emerging market multinationals: the role of complexity, autonomy and embeddedness," *Revista de Administração*, vol. 52, no. 2, pp. 176–188, 2017.
- [40] X. Han and Y. Lei, "Theoretical and practical analysis of cultivating high value patents," *Chinese Invention and Patent*, vol. 14, no. 12, pp. 8–14, 2017.
- [41] V. Rowthorn, A. J. Plum, and J. Zervos, "Legal and regulatory barriers to reverse innovation," *Annals of Global Health*, vol. 82, no. 6, pp. 991–1000, 2016.
- [42] J. Wang, L. Xue, and Z. Liang, "Multinational R&D in China: from home-country-based to host-country-based," *Innovation*, vol. 14, no. 2, pp. 192–202, 2012.
- [43] J. Zhang and J. Sun, "Research on technology catching up mode and path of communication enterprises from the perspective of standard essential patents," *Forum on Science and Technology in China*, vol. 4, pp. 112–121, 2018.

## Research Article

# CEO Media Exposure and Green Technological Innovation Decision: Evidence from Chinese Polluting Firms

Chen Wang,<sup>1</sup> Yuanlin Hu,<sup>1</sup> Jianhua Zhang ,<sup>2</sup> and Chenglin Miao<sup>3</sup>

<sup>1</sup>School of Business and Economics, Kunming University of Science and Technology, Kunming 650093, China

<sup>2</sup>School of Economics and Management Northeast Petroleum University, Daqing 163318, China

<sup>3</sup>School of Management Shandong Technology and Business University, Yantai 264003, China

Correspondence should be addressed to Jianhua Zhang; dqzhangjianhua@126.com

Received 9 June 2020; Revised 12 August 2020; Accepted 17 September 2020; Published 1 October 2020

Academic Editor: Yi Su

Copyright © 2020 Chen Wang et al. This is an open access article distributed under the Creative Commons Attribution License, which permits unrestricted use, distribution, and reproduction in any medium, provided the original work is properly cited.

The upper echelons theory is utilized to establish how CEO's attributes affect firm's technological innovation decisions. The extant literature has largely ignored the impacts of CEO media exposure. An unbalanced panel data analysis is used to examine the effects of CEO media exposure on Chinese polluting firm's green technological innovation. It is illustrated that CEO media exposure generally enhances Chinese polluting firms' green technological innovation decisions. In addition, we find that firms with state ownership and environmental regulations all moderate positively the relationship between CEO media exposure and green technological innovation. The research suggests that CEO media exposure appears to be a stimulus to firm's green technological innovation decisions.

## 1. Introduction

From an upper echelons perspective, chief executive officers' (CEOs) behaviors influence corporate policy and play an important role in driving firm's behaviors [1]. Prior studies have examined that corporate governance (i.e., board of directors and independent directors) or external normative values (i.e., institutional environment) affect green technological innovation decision [2–6]. Although some studies have investigated CEO media exposure impacts on firm's performance [7–9], few studies explore that CEO media exposure is another important factor on green innovation decision behavior. In fact, under the hierarchical organizational structure of modern enterprises, the investment decision-making behavior of enterprises is greatly influenced by CEO's will [10] and the firm's green technological innovation decision-making behavior is pronounced to a great extent by top management, especially CEO [11]. It is CEO who embeds his will into the enterprises that makes the enterprise show distinctive characteristics. To fill the gap in the literature, this study sheds light on how CEO media exposure affects green technological innovation decision.

By disclosing the relevant information and imposing public pressure on firm behaviors [8], CEO media exposure may influence firm's green technological innovation decisions. This is typically the case especially in Chinese firms, which are under unsound financial and legal environment and with more governmental interventions. In recent decades, China's environmental situation has been deteriorating because of its rapid economic growth [12]. Air pollution, water pollution, soil salinization, and man-made natural disasters do not only bring serious economic losses to China, but also aggravate social conflicts and endanger public health [13]. Will Chinese polluting enterprises consider green technological innovation while pursuing firm value? The relatively more complicated market environment in these economies also provides us with valuable opportunity to examine fully the relationship of CEO media coverage and the green technological innovation of the polluting firms. The exploration of the effects of the CEO media exposure on the firms' green technological innovation decisions will enrich the relevant literatures.

Besides, we also explore the previous researches by identifying the boundary conditions of institutional factors,

such as the company's ownership structure and legal environments. We are curious to see if the significance and strength of impact between CEO media exposure and green technological innovation for Chinese firms are universally valid or subject to certain institutional environmental factors. Additionally, as for their special status in the Chinese economic system, state-owned enterprises (SOEs) attract much more attention. In February 2016, Information Office of the State Council held a press conference with Chinese and foreign media which were aimed at promoting air pollution control and the implementation of the Environmental Protection Law of the People's Republic of China. During the conference, some reporters expressed whether the special characteristic of SOEs hindered the enforcement of laws by the China Ministry of Environmental Protection, which led to the environmental control of SOEs lag behind that of non-SOEs. Thus, is it true that SOEs, which play a leading role in the national economic system, lag behind non-SOEs in fulfilling their environmental protection responsibilities because of government protection?

And considering the pressure of CEO media exposure on firm's green technological innovation, the current situation of environmental regulation in the formal system should not be ignored. At present, China is improving various legal systems gradually, and the external environment for enterprises to fulfill their environmental protection responsibilities is being established step by step. Particularly, the exposure of Chinese media increases the possibility for administrative agencies to intervene in illegal enterprises. Media supervision should be an effective supplement to the legal supervision system. The effect of environmental regulation is full of uncertainty. Its solution to environmental pollution problem is not exogenous and is restricted by other rules, laws, regulations, customs, and other systems. Therefore, it is meaningful to explore the role of environmental governance by combining the interaction between environmental regulation and CEO media exposure.

Our finding contributes in the following aspects. First, a thorough empirical investigation has been conducted by using 2597 firm-year observations; we find that CEO media exposure indeed has promoted firm's green technological innovation. Second, in order to identify the influence of specific institutional factors on the relationship of CEO media exposure and the firm's green technological innovation, we divide the full sample into subsamples according to a firms' ownership structure and the local legal environment of the firms. The subsample analysis allows us to examine the main research questions under different institutional conditions. Finally, our empirical findings provide more insight into the emerging Chinese polluting firms, which are closely related to economy and ecology. Such information is important for investors diversifying their portfolios and also for policy makers in China when regulating the balance between economic development and ecological protection. Findings from our empirical tests have the following implications. Considering long-term sustainable development of Chinese firms, well-known firms with more media exposure are expected to have more motivation and pressure for green technological innovation.

And this impact is largely strengthened for firms which are SOEs and with a better legal environment.

The remainder of the paper is organized as follows. We introduce the background and develop hypotheses in Section 2. The data and methodology are described in Section 3. Empirical results are presented in Section 4. And Section 5 concludes the paper.

## 2. Literature Review and Hypothesis Development

*2.1. CEO Media Exposure and Green Technological Innovation Decision.* CEO media exposure has an important impact on business activities, environmental governance, and corporate value [8, 14, 15]. CEO media exposure has a positive effect on firm's green technological innovation decision in the following ways.

First, CEO media exposure corrects managers' agency behavior and promotes green technological innovation by playing the role of external governor [16, 17]. China's corporate governance and legal framework are not perfect enough to provide good guiding principles for companies, while CEO media coverage is shown to be effective in monitoring CEOs' behaviors [7]. Within the enterprise, the characteristic of managers' concentration on short-term benefit makes them more tend to avoid risks than shareholders. Thus, they are more likely to invest in projects with low risk, quick results but low returns [18]. High risk and lagging return, which are the characteristics of green technological innovation, cause managers to worry about the investment and result in their unwillingness to promote green technological innovation. CEO media exposure can expose the problems of investment decision-making and improve the probability of being discovered by investors and regulatory authorities, thus arousing investors' high attention, and even the involvement of administrative and regulatory authorities, avoiding manager's investment decision deviation from the track of maximizing enterprise value [17]. The strong market pressure brought by media supervision compels executives to make rational decision on environmental protection innovation.

Second, CEO media exposure promotes enterprises' green technological innovation by diminishing harmful information asymmetries between enterprises and the outside, reducing the financial constraints of investment in green technological innovation. The media exposure is the intermediary which disseminates enterprise information to the public, reduces the information asymmetries between enterprises and stakeholders [19], and helps the public to collect and access enterprise information, hence improving information transparency [20]. Media may act as sort of governance control mechanism because media coverage plays the role of a watchdog to reduce information asymmetry between management and external constituents [21]. Information dissemination mechanism holds that, because information asymmetry, banks, and other financial institutions cannot grasp fully the true information of enterprises. However, media reporters can improve the information transparency to diminish information



asymmetry between enterprise and stakeholders [22]. Through CEO media coverage, firms might become more credible, more familiar to investors, and thus more valuable [23]. This can help enterprises reduce the cost of debt financing and the difficulty of raising capital for innovative investments. The monitoring effect of media coverage is likely to reduce hidden news at the firm, forcing CEOs to take corrective action to reduce default risk [7]. Thus, media exposure has positive effect on promoting green technological innovation.

Third, CEO media also plays a significant part in social constructions, which affects the public how to evaluate the enterprises concerned and how their behavior meets the public's expectations [24]. In the context of increasingly transparent information disclosure and increasingly developed social media, companies with environmental accidents are more likely to receive media attention and then suffer from customer boycott, social condemnation, and government punishment, which seriously threaten the survival and development of enterprises [25]. A study indicates that CEOs who engage in social media are perceived to be more transparent and trustworthy [26]. According to legitimacy theory, legitimacy is a generalized perception or assumption that the actions of an entity are desirable, proper, or appropriate within some socially constructed system of norms, values, beliefs, and definitions [27]. The media's attention is not only the way for enterprises to obtain legitimacy, but also the source of crisis for enterprises' legitimacy [21]. With the attention of society to environmental issues, the investment of enterprises in green technological innovation has become an important aspect of the legitimacy of enterprises. In order to establish a good image, enterprises will carry out the legitimacy management of green technological innovation, so as to influence the public's understanding of environmental pollution and improve their level of environmental legitimacy.

Meanwhile, investors begin to focus on the environmental information of listed companies, especially when the enterprises carry out significant green technological innovation. It enhances not only the image and reputation of enterprises but also the capital market which will quickly respond positively to enterprises. Thus, with the enhancement of public awareness of environmental protection, CEO media exposure will force enterprises to consider the reputation effect of environmental protection innovation, which will further affect the profitability of enterprises. In this case, enterprises have the motivation to carry out green technological innovation.

Based on the above analysis, we propose the following hypothesis:

H1: CEO media exposure can enhance firm green technological innovation decision.

**2.2. Moderating Effect of State Ownership.** Ownership structure affects significantly corporate cognitive logic, leading to firms' heterogeneous responses via green technological innovation [5, 28]. According to whether the ultimate controller is a government or other agency, Chinese

enterprises are divided into SOEs and non-SOEs. There are great differences in responsibility burden, corporate governance, and market function between SOEs and non-SOEs in China [4]. Since the launch of the reform and the opening up policy in 1978, Chinese industrialization has simultaneously led to fast economic growth and increasing environmental pollution [28]. In the aspect of environmental governance, SOEs, as the pillar of national economy, play an essential role in the development of national economy. The public pays close attention to the image of these SOEs and has high expectations for their environmental responsibility performance. And the government's influence is critical environmental governance and environmental protection investment in China.

Moreover, reputation can stimulate and restrain the behavior of management. Media research has emphasized that positive press coverage can act as a valuable firm resource, in large part because it reduces the inherent uncertainty about firm and leader quality [29]. Therefore, the companies whose CEOs receive more positive media sentiment will have stronger firm performance [4]. One popular explanation for China's environmental problems is that political promotion mainly relies on GDP growth assessment and hence prompts local officials to engage in fierce competition over economic growth or the so-called political promotion tournament [30]. Fiscal decentralization provided sufficient incentives to local officials [31]. The good environmental reputation of enterprise improves the environmental performance of government.

Some research has shown that enterprises affiliated with higher levels of the government have initiated more innovation programs and received more public funding and policy support [32]. Thus, the goal and decision of enterprises' green technological innovation investment are also different. CEO will consciously arouse public praise through various actions and disseminate the correctness of enterprise decision-making to the society. With the enhancement of environmental control in various places, SOEs have shown more prominent performance in terms of environmental control constraints [33]. Due to the government's greater intervention and protection to SOEs [34], the cost of investment in green technological innovation will be guaranteed by the government's "umbrella." Under the premise of guaranteeing economic benefits, the managers of SOEs will not pay too much attention to environmental cost. In economic, social, and environmental benefits, more consideration should be given to environmental benefits and more green technological innovation should be made in enterprises. This can not only improve their reputation in the competitive market, but also meet their own political needs. However, private enterprises will pay more attention to the cost and benefit of environmental protection investment and their own interests [28]. Therefore, under the same production efficiency, CEOs have different awareness of environmental protection and make different decisions. It can be expected that SOEs have stronger motivation for environmental protection innovation than non-SOEs.

Hence, we propose the following hypothesis:

H2: state ownership positively moderates the relationship between CEO media exposure and green technological innovation.

**2.3. Moderating Effect of Environmental Regulations.** Legitimacy theory holds that an organization cannot succeed or even survive unless it believes in the goals, methods, and results recognized by society [27]. Environmental legitimacy refers to the public's overall recognition and evaluation of enterprises' environmental performance which is satisfactory and appropriate [35]. Environmental regulation is a rigid legitimacy requirement for enterprises, which plays a role in guiding enterprises' environmental behavior and is dominated by government administrative departments. It can reduce the probability of enterprises' illegal emission by improving the intensity of environmental pollution [6]. With the increase of intensity, the probability of punishment for illegal discharge will be increased, and the expected income of polluters will be reduced, forcing enterprises to increase investment in environmental facilities and technologies. In order to gain legitimacy recognition, enterprises can only increase investment in environmental protection innovation [36].

"Potter Hypothesis" holds that proper government management of the environment will stimulate enterprises to break the inherent mode of production and operation and product structure. Government's environmental supervision is the biggest source of pressure faced by enterprises when considering environmental problems. Enterprises will be forced to take certain measures to avoid punishment caused by noncompliance with environmental laws and regulations. On the one hand, enterprises should choose energy saving, emission reduction, and cleaner production; on the other hand, enterprises should accumulate business experiences through product innovation and process change and seek new and unique core competitiveness from them [37]. The goal of the government's environmental regulation policy is to limit the polluting production and operation of enterprises, so as to reduce pollution emissions and play a part in environmental protection. However, for the regulated target enterprises, environmental regulation will inevitably increase the cost of environmental compliance. To offset the "extra expenditure," enterprises usually choose environmental and technological innovation. The former solves the environmental pollution problem of enterprises from pollution sources and reduces the environmental cost of enterprises, while the latter expects to offset the environmental cost by improving the competitiveness of enterprises' products and their performance. The results show that the stricter environmental regulation is what the more capital enterprises will invest in cleaner production and technological innovation [2, 38, 39].

Thus, we propose the following hypothesis:

H3: environmental regulations positively moderate the relationship between CEO media exposure and green technological innovation.

### 3. Methodology and Data

**3.1. Methodology.** We use an unbalanced panel data regression analysis to analyze the effects of CEO media exposure on the green technological innovation decision. Our model is expressed as follows:

$$\begin{aligned} \text{Green\_Inn}_{it} = & \beta_0 + \beta_1 \text{CEO media}_{it} + \sum_{k=2}^{10} \beta_k \text{CV}_{it} \\ & + \sum_{m=1}^{16} \varphi_m \text{Industry}_{ikt} + \sum_{n=1}^{10} \delta_n \text{Year}_{nit} + \varepsilon_{it}. \end{aligned} \quad (1)$$

In previous studies, green technological innovation has been measured by indicators, such as green R&D [40] ecolabelling in environmental product certification [26], and green patents [41]. Considering the availability of data in China, green patents were employed as the indicator of green technological innovation [42]. Because there are three types of patents, actual invention refers to new products or improvement from the proposed new technical solutions, and utility patent refers to the practical new technology solutions of the product's shape, structure, or their combination. Design appearance is a new design for a product's shape, pattern, or the combination of color and shape, which create a richer aesthetic experience. It seems that the technical content of actual invention is higher and the technical content of utility model and design appearance are relatively lower. Thus, the dependent variable,  $\text{Green\_Inn}_{it}$ , is represented by two variables: green inventions, and green utility applications. First, we explicitly use green invention (Green Invention), which is the number of applications for green inventions. Second, we use green utility (Green Utility) to measure enterprise's applications for green utility patents. Our measure is more accurate than those used in the extant literature. Patents containing the keywords "green," "low-carbon," "environmental," "energy-saving," "emissions reduction," "clean," "cycling," "saving," "sustainable," "ecology," "environmental pollution," and "environmental protection" are regarded as green patents [4, 43]. We have searched the applications for green patents and transformed the data in logarithm.

The independent variable  $\text{CEO media}_{it}$  measures the extent of CEO media exposure. Following prior studies, CEO media is computed by using the natural log of one plus the number of CEOs news reports (i.e., [7, 8]). Moreover, we included control variables ( $\text{CV}_{it}$ ) at four levels: characteristics of individual top manager, firm, industry, and year. First, we included some firm characteristics: firm size is measured as the natural logarithm of total assets at the end of the year. Leverage, a proxy for firm risk, is total liabilities over total assets. ROA (return on assets) is the net income over total assets. Cash holding is the ending balance of cash and cash equivalents over sales. R&D is the natural logarithm of enterprise investment in research and development (R&D), which affects patents. Subsidy is the natural logarithm of government green subsidies, which is the government subsidies for enterprises' green technological

innovation. Top hold is the proportion of shares held by the largest shareholder. Second, TMT size is measured by the number of top management team (TMT) members. Duality equals 1 if the CEO also serves as chairman and 0 otherwise. Finally, dummies for the industry and year are included in the regressions.

Ten yearly dummies ( $I = 10$ ) and 16 industry dummies ( $K = 16$ ) are included in (1);  $\beta_0$  is the intercept,  $\varepsilon_{it}$  is residuals,  $\beta_k$  represents the regression coefficients of the control variables, and  $\varphi_m$  and  $\delta_n$  represent the regression coefficients of the industry and year dummy variables, respectively;  $i$  represents the enterprises listed.

$$\begin{aligned} \text{Green\_inn}_{it} = & \beta_0 + \beta_1 \text{CEO media}_{it} + \beta_2 \text{State}_{it} + \beta_3 \text{State}_{it} * \text{CEO media}_{it} \\ & + \sum_{k=2}^{10} \beta_k \text{CV}_{it} + \sum_{m=1}^{16} \varphi_m \text{Industry}_{ikt} + \sum_{n=1}^{10} \delta_n \text{Year}_{nit} + \varepsilon_{it}. \end{aligned} \quad (2)$$

$$\begin{aligned} \text{Green\_inn}_{it} = & \beta_0 + \beta_1 \text{CEO media}_{it} + \beta_2 \text{Rule} + \beta_3 \text{Rule}_{it} * \text{CEO media}_{it} \\ & + \sum_{k=2}^{10} \beta_k \text{CV}_{it} + \sum_{m=1}^{16} \varphi_m \text{Industry}_{ikt} + \sum_{n=1}^{10} \delta_n \text{Year}_{nit} + \varepsilon_{it}. \end{aligned} \quad (3)$$

**3.2. Data and Sample.** Our initial dataset includes all Chinese firms listed on Shanghai and Shenzhen Stock Exchanges over the period of 2010–2016. Zhang et al. [42] defined highly polluting industries as industries that discharge large-scale industrial waste. We follow the definition of highly polluting industries used by the Guidelines on Environmental Information Disclosure of Listed Companies, published by the Ministry of Ecology and Environment of People's Republic of China in 2010.

Our final sample consists of 2,597 firm-year observations, covering 16 highly polluting industries at the two-digit SIC level: nonmetallic mineral products; power, thermal production and supply; metal products; petroleum processing, coking, and nuclear fuel processing; nonferrous metal smelting and calendaring processing; pharmaceutical manufacturing; chemical raw materials and chemical products manufacturing; rubber and plastic products; ferrous metal mining; chemical fiber manufacturing; gas production and supply; paper and paper products; coal mining and washing; ferrous metal smelting and rolling; nonferrous metals mine mining; ecological protection and environmental governance; and petroleum and natural gas mining.

Firms listed for less than one year are excluded. To minimize the impact of outliers, we follow common practice in the literature and winsorize all variables at the 1st and 99th percentiles (i.e., [1, 23]). Our final sample consists of 2,597 firm-year observations.

The CEO media exposure information is extracted from Baidu, which is the leading online search engine in China. Following the method in Nguyen [23], we use the CEO's name and his firm's name to quantify CEO media exposure. We wrote a Python-based application to collect the number

of news reports on CEOs from the Baidu news website (<http://www.news.baidu.com>). State ownership may moderate the relationship, which is important to see how effective they are in promoting innovations. And environmental regulations are targets set by the government with which firms must comply. Thus, we attempt to examine the impacts of state ownership and environmental regulations on innovations at the most highly polluting firms. Following Javorcik and Wei [44], environmental regulation (rule) variable is the number of environmental regulations issued by the national government. Variable definitions are shown in Table 1. To this end, we construct the following two regressions:

of news reports on CEOs from the Baidu news website (<http://www.news.baidu.com>).

Data on R&D, government subsidies, age, the size of the TMT, duality, firm size, leverage, ownership, ROA, cash holdings, and others in highly polluting industries come from the China Stock Market and Accounting Research (CSMAR) database for the Chinese firms listed on the Shanghai and Shenzhen Stock Exchanges from 2010 to 2016. Prior studies have defined highly polluting industries as industries that discharge large-scale industrial waste [42]. We follow the definition of highly polluting industries used by the Ministry of Environmental Information Disclosure of Listed Companies in 2010.

We collected manually personal profiles of chairs and CEOs for each company. The data come primarily from the relevant securities financial websites (e.g., eastmoney.com, which is part of the stock exchanges' official website), the companies' annual reports for 2010–2016, and Baidu.com, Google, and related search engines. We also manually collected data on the ownership structure of each company from the CSMAR. The patent data on enterprises comes from the NIPA (National Intellectual Property Administration). The rule data come from the China Statistical Yearbook on the Environment.

We excluded “special treatment” companies (i.e., firms classified as failing by the stock exchanges) and companies listed on the exchange for less than two years.

## 4. Analysis and Results

**4.1. Descriptive Statistics.** Table 2 presents descriptive statistics for the characteristics of CEO media exposure and green technological innovation decision. The mean of CEO



TABLE 1: Variable definitions.

<i>Dependent variables: green technological innovation decision</i>	
Green invention	The number of applications for environmental inventions
Green utility	The number of applications for environmental utility patents
<i>Independent variables: CEO media exposure</i>	
CEO media	The natural log of one plus the number of CEOs news reports
<i>Moderating variables</i>	
State	If the firm is an SOE, which is controlled by the government or its various entities, it equals 1 and 0 otherwise
Rule	The number of environmental regulations issued by the national government
<i>Control variables</i>	
Firm size	The natural logarithm of total assets at the end of the year
Leverage	Total liabilities over total assets
ROA	Net income over total assets
Cash holding	The ending balance of cash and cash equivalents over sales
R&D	The natural logarithm of enterprise investment in research and development, which affects patents
Subsidy	The natural logarithm of government subsidies
TMT	The number of top management team members
Duality	Equals 1 if the CEO also serves as chairman and 0 otherwise

TABLE 2: Characteristics of CEO media and green technological innovation.

Year	CEO media exposure		Green invention			Green utility		
	Mean	Std. dev.	Mean	Std. dev.	%	Mean	Std. dev.	%
2010	2.995	1.471	0.765	3.133	22.41	0.615	2.968	15.91
2011	2.981	1.442	0.776	2.174	28.83	0.625	1.922	23.71
2012	2.894	1.466	0.908	2.596	29.92	0.693	2.557	20.84
2013	3.035	1.544	0.960	2.436	32.86	0.679	2.037	21.33
2014	3.029	1.569	1.197	3.922	32.14	0.825	2.980	22.92
2015	2.919	1.475	1.043	3.204	32.33	0.803	2.852	20.51
2016	3.206	1.590	1.140	3.280	32.64	1.089	4.576	22.44
2010–2016	3.008	1.510	0.970	3.015	30.15	0.761	2.956	21.06

media exposure fluctuates between 2.995 in 2010 and 3.206 in 2016, which implies that the growth of CEO media exposure is not significant. The mean of environmental invention increases from 0.765 in 2010 to 1.140 in 2016, and the mean of environmental utility increases from 0.615 in 2010 to 1.089 in 2016, which signifies that the enterprises pay more and more attention to environmental protection.

Table 3 presents the summary statistics for the variables used in our analysis. Several points are worth noting here. First, the mean is 0.97 for green invention and 0.76 for green utility. And the standard deviation is 3.02 for environmental invention and 2.96 for environmental utility, indicating that there are great differences in green technological innovation among enterprises. Second, the mean value for media exposure is 3.01 and the 50th percentile is 2.77, that is, less than 50% companies with the extent of CEO media exposure above average, which shows that CEO media exposure is not a universal phenomenon. Third, 25% of state is 1, showing that 25% of the sample companies are SOEs. R&D shows the investment in research and development. The 10th percentile is 15.66 and the mean is 17.48, which indicate that the investment in R&D of most sample companies is above average.

Table 4 presents descriptive correlations for all the variables. To ensure no strong bivariate correlation between these variables, we computed the variance inflation factor (VIF). The VIF is below 10 for all regression models, the cut-off point. The result indicates that no serious multicollinearity issues are present in our regression analyses. As expected, CEO media exposure is significantly related to the green technological innovation variables (green invention and green utility), a result consistent with H1.

**4.2. Preliminary Results.** Table 5 provides a univariate analysis of green invention and green utility for firms with different levels of CEO media exposure and environmental regulations. And we also divide the sample into SOEs and non-SOEs. Among sample firms, firms with high level CEO exposure have a higher number of green inventions than low level peers (0.431 vs. 0.35;  $p < 0.05$  for the difference); firms with high level rule have more green inventions than firms with low level (0.666 vs. 0.338;  $p < 0.01$ ); non-SOEs have fewer green inventions than SOEs (0.587 vs. 0.283;  $p < 0.01$ ). The results of green utility models are similar to

TABLE 3: Descriptive statistics per firm.

Variable	Mean	Std. dev.	Min	P10	p25	p50	p75	P90	Max
Green invention	0.97	3.02	0	0	0	0	1	3	59
Green utility	0.76	2.96	0	0	0	0	0	2	55
Media exposure	3.01	1.51	0	1.10	1.95	2.77	4.29	4.98	7.21
State	0.37	0.48	0	0	0	0	1	1	1
Rule	1.40	0.70	0	0	0.69	1.79	1.79	2.08	2.20
Firm size	22.17	1.22	19.06	20.82	21.31	21.95	22.88	23.9	26.43
Leverage	0.44	0.22	0.04	0.14	0.25	0.43	0.61	0.73	1.21
ROA	0.04	0.06	-0.26	0	0.01	0.04	0.07	0.1	0.23
Cash holding	0.31	0.40	0.01	0.05	0.09	0.17	0.36	0.73	2.67
R&D	17.48	1.54	0	15.66	16.65	17.58	18.37	19.3	22.08
Subsidy	16.27	1.85	0	14.4	15.4	16.3	17.31	18.25	21.79
Top hold	0.36	0.15	0.04	0.18	0.24	0.34	0.47	0.56	0.89
TMT size	7.37	2.40	3	5	6	7	9	10	15
CEO duality	0.23	0.42	0	0	0	0	0	1	1

those of green invention, which are consistent with our hypothesis.

**4.3. Regression Analysis and Results.** We have examined the effect of CEO media exposure on green technological innovation (green invention and green utility). As we know, the dependent variable is counted data with zero entries, and the typical approach is to use the negative binomial (NB) model. The distribution of green invention (mean value = 0.97 and sd = 3.02) and green utility counts (mean value = 0.76 and sd = 2.96) shows a large dispersion in Table 3 with large standard deviation as compared to the mean [45]. NB model might not be able to handle the presence of excess zero counts in green technological innovation data. Thus, following Fung et al. [46], we adopt the zero-inflated negative binomial (ZINB) method for our analysis by Stata 15.0 and choosing option vce (robust) which produces robust standard error estimates for our linear panel models.

Table 6 presents ZINB regression results of CEO media exposure on green innovation variables in different institutional situations using (1)–(3). In models 1 and 4 for the full sample, the coefficient of CEO media is significantly and positively correlated with green invention and green utility ( $p < 0.01$ ), suggesting that firms with high level CEO exposure are able to increase firms green innovation ability, supporting H1.

Model 2 and model 5 show, respectively, the interaction effect of CEO media exposure and state on green invention and green utility, with the inclusion of the dummy variables industry and year as control variables. CEO media exposure has a positive and significant coefficient ( $\beta = 0.165$ ,  $p < 0.01$ ); state does not have a significant coefficient ( $\beta = -0.271$ ,  $p > 0.1$ ). The coefficient of the interaction of CEO media exposure and state is also positive and significant ( $\beta = 0.128$ ,  $p < 0.01$ ). An average marginal effect (AME) of state on green invention is 0.212. Model 5 examines the interaction effect of CEO media exposure and state on green utility. CEO media exposure also has a positive and significant coefficient ( $\beta = 0.203$ ,  $p < 0.01$ ), the coefficient of CEO media  $\times$  state on green utility is also positive and significant ( $\beta = 0.267$ ,  $p < 0.1$ ), and an average marginal effect (AME) of

state on green utility is 0.302, which indicates that state enhances the positive effect of CEO media exposure on green innovation; H2 is thus supported.

Model 3 tests the moderating effect of environmental regulations on the relationship between CEO media exposure and green invention. The effect of CEO media exposure on green invention is insignificant ( $\beta = 0.094$ ,  $p > 0.1$ ); the effect of rule is negative and significant ( $\beta = -1.406$ ,  $p < 0.01$ ). The moderating effect of the interaction term is positive and significant ( $\beta = 0.085$ ,  $p < 0.05$ ). An average marginal effect (AME) of rule on green invention is 0.213. The results indicate that environmental regulation can increase the investment in environmental innovation. Similarly, model 6 presents the moderating effect of environmental regulation on the relationship between CEO media exposure and green utility. The effect of CEO media exposure on green utility is positive and significant ( $\beta = 0.159$ ,  $p < 0.1$ ); the effect of rule is negative and insignificant ( $\beta = -0.433$ ,  $p > 0.1$ ); and the effect of the interaction term CEO media  $\times$  rule is also positive and significant ( $\beta = 0.098$ ,  $p < 0.05$ ); an average marginal effect (AME) of rule on green utility is 0.296, implying results similar to those for model 3. The results of models 3 and model 4 clearly show that the effect of CEO media on green innovation is more pronounced at firms with high environmental regulation than that at firms with low environmental regulation, further supporting H3.

**4.4. Robustness Check.** First, the positive relation between CEO media exposure and green technological innovation may be driven by the current patents of the firm. Consequently, the direction of causality may run from green technological innovation to CEO media exposure. To address this potential endogeneity, we modify our CEO media exposure by using dependent variable forward two periods. This has the effect of ensuring that the measure of CEO media exposure is unrelated to the period in which green invention or green utility is released or measured.

Table 7 reports parameters estimates after controlling for endogeneity. These results largely are consistent with results reported in Table 6. The coefficient of CEO media is positive and significant. The coefficients of CEO media  $\times$  state and CEO media  $\times$  rule are only significant on green utility,

TABLE 4: Descriptive correlations.

Variable	1	2	3	4	5	6	7	8	9	10	11	12	13
Green invention	1												
Green utility	0.590***	1											
CEO exposure	0.092***	0.087***	1										
State	0.071***	0.138***	-0.225***	1									
Rule	0.020	0.029	0.036*	0	1								
Firm size	0.271***	0.258***	0.030	0.213***	0.126***	1							
Leverage	0.102***	0.101***	-0.152***	0.262***	0.007	0.477***	1						
ROA	-0.048**	-0.042**	0.164***	-0.180***	-0.046**	-0.128***	-0.478***	1					
Cash holding	-0.087**	-0.077**	0.142***	-0.206***	-0.078***	-0.231***	-0.478***	0.177***	1				
R&D	0.224***	0.198***	0.147***	0.022	0.131***	0.511***	0.082***	0.060***	-0.156***	1			
Subsidy	0.185***	0.141***	0.037*	0.081***	0.098***	0.542***	0.279***	-0.018	-0.176***	0.320***	1		
Top hold	0.058***	0.097***	-0.115***	0.101***	-0.050**	0.257***	0.062***	-0.0030	-0.0080	0.124***	0.081***	1	
TMT size	0.093***	0.061***	0.067***	0.093***	0.057***	0.251***	0.142***	-0.056***	-0.038*	0.125***	0.184***	-0.046**	1
CEO duality	-0.081**	-0.073**	0.345***	-0.214***	-0.018	-0.186***	-0.138***	0.042**	0.169***	-0.027	-0.093***	-0.105***	-0.041**

\*  $p < 0.1$ ; \*\*  $p < 0.05$ ; \*\*\*  $p < 0.01$ .

TABLE 5: The univariate analysis of green invention and green utility.

Type	Level	Number of observations	Green invention	Green utility	<i>t</i> -test for green invention	<i>t</i> -test for green utility
CEO media exposure	High	1554	0.431	0.308	0.081**	0.068***
	Low	1421	0.35	0.239		
State	With	1067	0.587	0.391	0.304***	0.181***
	Without	1908	0.283	0.21		
Rule	High	490	0.666	0.418	0.328***	0.171***
	Low	2485	0.338	0.247		

\*  $p < 0.1$ ; \*\*  $p < 0.05$ ; \*\*\*  $p < 0.01$ .

TABLE 6: Zero-inflated negative binomial regression of CEO media exposure on green invention and green utility.

Variables	Green invention <sub>t</sub>			Green utility <sub>t</sub>		
	(1)	(2)	(3)	(4)	(5)	(6)
CEO media	0.222*** (0.033)	0.165*** (0.044)	0.094 (0.070)	0.309*** (0.043)	0.203*** (0.056)	0.159* (0.096)
State		-0.271 (0.209)			0.139 (0.269)	
CEO media × state		0.128** (0.063)			0.267*** (0.078)	
Rule			-1.406*** (0.386)			-0.433 (0.279)
CEO media × rule			0.085** (0.042)			0.098* (0.057)
Firm size	-0.263*** (0.042)	-0.263*** (0.043)	-0.222*** (0.044)	-0.260*** (0.047)	-0.282*** (0.048)	-0.238*** (0.048)
Leverage	0.328 (0.309)	0.379 (0.308)	0.264 (0.308)	0.955** (0.421)	0.792* (0.410)	0.871** (0.424)
ROA	-0.513 (1.099)	-0.237 (1.108)	-0.538 (1.091)	0.575 (1.482)	0.468 (1.481)	0.379 (1.487)
Cash holding	-0.423*** (0.162)	-0.362** (0.164)	-0.348** (0.162)	-0.371** (0.189)	-0.049 (0.189)	-0.342* (0.190)
R&D	0.227*** (0.039)	0.230*** (0.039)	0.232*** (0.039)	0.203*** (0.047)	0.196*** (0.046)	0.205*** (0.047)
Subsidy	0.121*** (0.031)	0.121*** (0.031)	0.124*** (0.031)	0.065** (0.031)	0.084*** (0.032)	0.065** (0.031)
Top hold	-0.227 (0.335)	-0.273 (0.337)	-0.167 (0.335)	-0.120 (0.439)	0.008 (0.430)	-0.133 (0.441)
TMT size	0.073*** (0.020)	0.070*** (0.020)	0.074*** (0.020)	0.073*** (0.025)	0.067*** (0.024)	0.075*** (0.025)
Duality	-0.601*** (0.121)	-0.547*** (0.123)	-0.578*** (0.121)	-0.542*** (0.161)	-0.403** (0.158)	-0.519*** (0.161)
Constant	1.095*** (0.239)	1.135*** (0.250)	1.095*** (0.247)	1.729*** (0.066)	1.632*** (0.068)	1.723*** (0.066)
Year	Yes	Yes	Yes	Yes	Yes	Yes
Industry	Yes	Yes	Yes	Yes	Yes	Yes
N	2597	2597	2597	2597	2597	2597
Chi <sup>2</sup>	366.274	366.062	379.864	332.946	391.544	337.586

Note that standard errors are in parentheses: \*  $p < 0.1$ ; \*\*  $p < 0.05$ ; \*\*\*  $p < 0.01$ .

indicating that the moderating effect of state ownership and environmental regulation mainly acts on green utility. These results support our hypotheses.

Second, in an attempt to strictly control for observed selection bias, a propensity score matching (PSM) identification strategy is conducted. In the first stage of this estimation strategy, if firms with high level CEO media exposure are fundamentally different from those with low level, then the control variables employed in the main specification that capture linear relations may be

inadequate. To alleviate concerns over such functional form misspecification biases, we use the methodology of <https://onlinelibrary.wiley.com/doi/full/10.1111/j.1540-6288.2011.00305.x> [47]; we implement a commonly used matching algorithm: nearest neighbor matching. And we create two data samples that are comparable across all the control variables but differ only on the level of media exposure. For the PSM analysis, we match a firm with low CEO media exposure to the firm with high CEO media exposure using the closest propensity score estimated from the first stage.

TABLE 7: Dependent variable forward two periods.

Variables	Green invention <sub>t+2</sub>			Green utility <sub>t+2</sub>		
	(1)	(2)	(3)	(4)	(5)	(6)
CEO media	0.223*** (0.036)	0.185*** (0.049)	0.133** (0.064)	0.327*** (0.053)	0.151** (0.068)	0.180** (0.089)
State		-0.105 (0.233)			-0.215 (0.317)	
CEO media × state		0.084 (0.070)			0.376*** (0.093)	
Rule			-1.136*** (0.404)			-0.931** (0.396)
CEO media × rule			0.071 (0.044)			0.117** (0.059)
Firm size	-0.198*** (0.045)	-0.205*** (0.046)	-0.163*** (0.047)	-0.224*** (0.056)	-0.223*** (0.056)	-0.200*** (0.057)
Leverage	0.499 (0.367)	0.529 (0.366)	0.461 (0.366)	0.887* (0.512)	0.658 (0.495)	0.788 (0.515)
ROA	-1.201 (1.269)	-0.980 (1.278)	-0.986 (1.266)	1.448 (1.693)	0.622 (1.712)	1.526 (1.689)
Cash holding	-0.117 (0.164)	-0.046 (0.169)	-0.092 (0.163)	-0.282 (0.235)	0.103 (0.231)	-0.238 (0.236)
R&D	0.193*** (0.045)	0.199*** (0.045)	0.190*** (0.045)	0.172*** (0.055)	0.171*** (0.054)	0.181*** (0.055)
Subsidy	0.086*** (0.031)	0.088*** (0.031)	0.086*** (0.031)	0.049 (0.035)	0.064* (0.036)	0.049 (0.036)
Top hold	-0.537 (0.387)	-0.541 (0.387)	-0.476 (0.385)	-0.352 (0.503)	-0.244 (0.491)	-0.370 (0.505)
TMT size	0.032 (0.024)	0.031 (0.024)	0.035 (0.024)	0.114*** (0.031)	0.073** (0.030)	0.120*** (0.031)
Duality	-0.637*** (0.138)	-0.592*** (0.141)	-0.612*** (0.138)	-0.781*** (0.192)	-0.639*** (0.186)	-0.789*** (0.192)
Constant	1.135*** (0.280)	1.161*** (0.301)	1.143*** (0.292)	1.767*** (0.074)	1.650*** (0.082)	1.758*** (0.073)
Year	Yes	Yes	Yes	Yes	Yes	Yes
Industry	Yes	Yes	Yes	Yes	Yes	Yes
N	1855	1855	1855	1855	1855	1855
Chi <sup>2</sup>	243.554	243.661	252.839	212.109	257.527	227.563

Note that standard errors are in parentheses: \* $p < 0.1$ ; \*\* $p < 0.05$ ; \*\*\* $p < 0.01$ .

TABLE 8: Comparison of differences before and after variable matching.

Variable	Unmatched	Mean		$t$ -test	
	Matched	Treated	Control	T	$p > t$
Firm size	U	22.153	22.166	-0.280	0.782
	M	22.153	22.102	1.040	0.300
Leverage	U	0.402	0.466	-7.480	0.000
	M	0.402	0.402	-0.010	0.991
ROA	U	0.049	0.032	7.720	0.000
	M	0.049	0.049	0.120	0.901
Cash holding	U	0.371	0.256	7.330	0.000
	M	0.371	0.353	1.010	0.311
R&D	U	17.670	17.325	5.720	0.000
	M	17.670	17.662	0.150	0.885
Subsidy	U	16.279	16.254	0.340	0.736
	M	16.279	16.091	2.320	0.020
Top hold	U	0.349	0.375	-4.400	0.000
	M	0.349	0.338	1.830	0.068
TMT size	U	7.453	7.267	1.980	0.048
	M	7.453	7.387	0.670	0.500
Duality	U	0.361	0.115	15.450	0.000
	M	0.361	0.362	-0.040	0.967

TABLE 9: Robust check for the effects of CEO media on green invention and green utility.

<i>Panel A: propensity score analysis for environmental innovation</i>						
Variable	Sample	Treated	Controls	Difference	SE	<i>t</i> -test
Green invention	Unmatched	1.176	0.789	0.387	0.119	3.26***
	ATT	1.176	0.827	0.350	0.166	2.11**
Green utility	Unmatched	0.919	0.623	0.296	0.117	2.54**
	ATT	0.919	0.616	0.303	0.165	1.83*
<i>Panel B: zero-inflated negative binomial regression on matched CEO media exposure subsample</i>						
Variables		Green invention <sub><i>t</i></sub>			Green utility <sub><i>t</i></sub>	
	(1)	(2)	(3)	(4)	(5)	(6)
CEO media	0.220*** (0.046)	0.080 (0.060)	0.092 (0.104)	0.369*** (0.065)	0.195** (0.078)	0.147 (0.151)
State		−1.201*** (0.355)			−0.463 (0.451)	
CEO media × state		0.324*** (0.091)			0.387*** (0.113)	
Rule			−1.501*** (0.529)			−0.177 (0.407)
CEO media × rule			0.082 (0.061)			0.147* (0.088)
Firm size	−0.271*** (0.055)	−0.250*** (0.055)	−0.224*** (0.057)	−0.314*** (0.061)	−0.318*** (0.061)	−0.300*** (0.065)
Leverage	0.525 (0.401)	0.655* (0.396)	0.455 (0.399)	0.945* (0.560)	0.861 (0.540)	0.951* (0.571)
ROA	0.864 (1.413)	1.372 (1.423)	1.011 (1.402)	1.622 (1.913)	1.597 (1.930)	1.532 (1.913)
Cash holding	−0.476** (0.191)	−0.385** (0.194)	−0.403** (0.191)	−0.406* (0.220)	−0.066 (0.219)	−0.361 (0.222)
R&D	0.222*** (0.052)	0.221*** (0.052)	0.228*** (0.052)	0.260*** (0.063)	0.250*** (0.061)	0.264*** (0.063)
Subsidy	0.111*** (0.037)	0.104*** (0.037)	0.109*** (0.037)	0.053 (0.033)	0.067** (0.034)	0.054 (0.033)
Top hold	0.557 (0.430)	0.337 (0.435)	0.528 (0.429)	0.163 (0.575)	−0.141 (0.569)	0.252 (0.584)
TMT size	0.066*** (0.025)	0.062** (0.024)	0.064*** (0.024)	0.077** (0.031)	0.065** (0.030)	0.083*** (0.031)
Duality	−0.720*** (0.138)	−0.644*** (0.142)	−0.690*** (0.138)	−1.014*** (0.191)	−0.819*** (0.188)	−0.983*** (0.192)
Constant	1.048*** (0.284)	1.038*** (0.286)	1.074*** (0.236)	1.624*** (0.080)	1.509*** (0.086)	1.615*** (0.081)
Year	Yes	Yes	Yes	Yes	Yes	Yes
Industry	Yes	Yes	Yes	Yes	Yes	Yes
N	1568	1568	1568	1568	1568	1568
Chi <sup>2</sup>	252.846	262.193	261.407	226.921	262.613	230.509

Note that standard errors are in parentheses: \*  $p < 0.1$ ; \*\*  $p < 0.05$ ; \*\*\*  $p < 0.01$ .

The balance improvements after matching are summarized in Table 8. Panel A of Table 9 shows the propensity score analysis for green innovation; the results show that there is significant and positive relation between high level CEO exposure and green invention ( $p < 0.05$ ), suggesting that firms with high level CEO exposure are able to increase firm innovation ability. Then, we use ZINB model to estimate the relationship between CEO media and green innovation on the corresponding matched sample. Panel B of Table 9 reports the results; the results remain robust reaffirming the CEO media exposure effect.

## 5. Concluding Remarks

In this study, we examine with yearly data the impact of firm CEO's media exposure on the firm green technological innovation. Our sample consists of 2,597 firm-year observations for Chinese companies listed on the Shanghai and Shenzhen Stock Exchanges over the period of 2010–2016. We apply ZINB models to test whether the CEO's media coverage influences the patent application data, which reflects the level of firm green technological innovation. Given the specific market environment in the Chinese economy,



we consider the effect under different institutional situations. In particular, we investigate the moderating effect of the firm's ownership structure (i.e., state-owned vs. non-state-owned) and the environmental regulations (i.e., stronger vs. weaker). We also conduct a thorough robustness check for additional validity of our methodology and main findings.

In summary, the empirical test results are generally consistent with our hypotheses. First, CEO media coverage has a positive influence over firm green technological innovation, implying that news reports facilitate the investment in green innovation. Second, the interaction term of CEO media coverage and ownership has a positive impact on firm green innovation for the full sample data, which proves that if the firm is a SOE, the positive influence of CEO media coverage on the firm green innovation will be increased. And the interaction term of CEO media coverage and environmental regulations also has the same influence on firm green innovation, implying that firms with stronger environmental rules will invest more on green innovation. It is apparent that the firm green innovation is exposed to a stronger influence of CEO media coverage when firms are state-owned and operate in stronger environmental regulations.

Our research also provides some important practical implications. Firstly, more attention should be paid to informal systems such as media, which play an important governance role in firm's green technological innovation. As an important aspect of external governance, the external regulatory pressure of media attention has a positive effect on firm's environmental protection innovation behavior. Therefore, we should promote the role of media supervision and reputation mechanism, make it an important external mechanism of corporate environmental governance, promote companies to fulfill actively their social responsibilities, and enhance the level of environmental innovation of enterprises.

Secondly, we ought to strengthen the level of environmental regulation and promote information disclosure and public participation. The effect of CEO media exposure on firm green innovation under the different intensity of environmental regulation not only reflects the quality of regulation and the effect of implementation, but also shows that the strengthening of moderate environmental regulation plays its supervisory part and promotes firm green innovation decision. Media participation in environmental governance under environmental regulation has played a greater role, indicating that public opinion has restrictive and supervisory function. Therefore, the future institutional arrangement of environmental regulation should also consider social regulation and improve the information disclosure system. Join Ministry of Industry and Information Technology and the various regulatory bodies of the Securities Regulatory Commission to give full play to the mechanism of public participation in the supervision of firm green innovation behavior. We should promote enterprises to fulfill their environmental responsibility through stakeholder environmental pressure and form market supervision beyond government supervision.

Thirdly, the support for non-SOE's green innovation should be increased. The result of our study shows that media attention has a more significant impact on firm green innovation of SOE. The essential reason is that the investment cost of environmental protection innovation of state-owned enterprises is guaranteed by the government's "umbrella," while the investment cost of environmental innovation of non-SOEs is mostly borne by themselves. Therefore, we should formulate corresponding environmental regulations and encourage non-SOEs to invest in environment. At the same time, enterprises investing in environmental protection should be given certain tax subsidies or preferential treatment to improve the motivation of non-SOEs investing in environmental protection.

Our study still has some limitations on which further research will be explored. First, there is no distinction between positive or negative media coverage of CEOs. We will further explore the effect of the media exposure distinction on green innovation in the future. Second, there is no specific distinction between media types, such as traditional media and new media and official media and nonofficial media. Future research can further distinguish different types of media and the differences of their attention effects. Third, we did not consider the impact of public perception and mentality (including stock investors) and the intrinsic effect of media ecology (such as media corruption) on green innovation of enterprises from social culture level. Future research may benefit from these works in these directions.

## Data Availability

The data required to reproduce these findings cannot be shared at this time as the data also form part of an ongoing study.

## Disclosure

The co-authors confirm that this work was original research that has not been published previously and was not under consideration for publication elsewhere, in whole or in part.

## Conflicts of Interest

The authors declare that there are no conflicts of interest regarding the submission of this article.

## Authors' Contributions

All the authors have read and approved the final manuscript for publication.

## Acknowledgments

The authors acknowledge the financial support from the National Natural Science Foundation of China (Grant nos. 71702084, 71762020, and 72002029), the Humanity and Social Science Foundation of the Ministry of Education of China (17YJC630112 and 20YJA840022), the Heilongjiang Province Postdoctoral Science Foundation (LBH-Q19086), the Humanity and Social Science Foundation of the Ministry



of NEPU (WKJD2020001), and the Northeast Petroleum University Innovation Foundation for Postgraduate (YJSCX2017-033NEPU).

## References

- [1] P. Qiao, A. Fung, J. Miao, and H.-G. Fung, "Powerful Chief executive Officers and firm performance: integrating agency and stewardship theory," *China & World Economy*, vol. 25, no. 6, pp. 100–119, 2017.
- [2] Y. Rubashkina, M. Galeotti, and E. Verdolini, "Environmental regulation and competitiveness: empirical evidence on the Porter Hypothesis from European manufacturing sectors," *Energy Policy*, vol. 83, pp. 288–300, 2015.
- [3] Y. Su and X. L. An, "Application of threshold regression analysis to study the impact of regional technological innovation level on sustainable development," *Renewable & Sustainable Energy Reviews*, vol. 89, pp. 27–32, 2018.
- [4] Y. Bai, S. Song, J. Jiao, and R. Yang, "The impacts of government R&D subsidies on green innovation: Evidence from Chinese energy-intensive firms," *Journal of Cleaner Production*, vol. 233, pp. 819–829, 2019.
- [5] J. Zhang, W. Zhang, Q. Song et al., "Can energy saving policies drive firm innovation behaviors? - Evidence from China," *Technological Forecasting and Social Change*, vol. 154, Article ID 119953, 2020.
- [6] Y. Liu, J. Zhu, E. Y. Li, Z. Meng, and Y. Song, "Environmental regulation, green technological innovation, and eco-efficiency: the case of Yangtze river economic belt in China," *Technological Forecasting and Social Change*, vol. 155, 2020.
- [7] P.-h. Qiao, H.-G. Fung, and W. Wang, "Chinese firms' crash risk and CEO media exposure," *Applied Economics Letters*, vol. 25, no. 14, pp. 1034–1037, 2018.
- [8] X. Li, P. Qiao, and L. Zhao, "CEO media exposure, political connection and Chinese firms' stock price synchronicity," *International Review of Economics & Finance*, vol. 63, pp. 61–75, 2019.
- [9] J. Godosdiz, L. Cabezagarcia, R. Fernandezgago, and M. Nietoantolin, "Does CEO media exposure affect corporate social responsibility?" *Corporate Social Responsibility and Environmental Management*, vol. 27, no. 2, pp. 825–840, 2020.
- [10] C. H. Donald and A. M. Phyllis, "Upper echelons: the organization as a reflection of its top managers," *Academy of Management Review*, vol. 9, no. 2, pp. 193–206, 1984.
- [11] L. E. Ginzel, R. M. Kramer, and R. I. Sutton, "Organizational impression management as a reciprocal influence process: the neglected role of the organizational audience," in *Organizational Identity*, pp. 223–261, Oxford University Press, Oxford, UK, 2004.
- [12] Y. Su and Y.-Q. Yu, "Spatial agglomeration of new energy industries on the performance of regional pollution control through spatial econometric analysis," *Science of The Total Environment*, vol. 704, Article ID 135261, 2020.
- [13] D. Li, M. Zheng, C. Cao, X. Chen, S. Ren, and M. Huang, "The impact of legitimacy pressure and corporate profitability on green innovation: evidence from China top 100," *Journal of Cleaner Production*, vol. 141, pp. 41–49, 2017.
- [14] C. E. Carroll and M. McCombs, "Agenda-setting effects of business news on the public's images and opinions about major corporations," *Journalism & Communication Review*, vol. 6, no. 1, pp. 36–46, 2005.
- [15] A. Dyck, N. Volchkova, and L. Zingales, "The corporate governance role of the media: evidence from Russia," *The Journal of Finance*, vol. 63, no. 3, pp. 1093–1135, 2008.
- [16] O. Guldiken, C. Tupper, A. Nair, and H. Yu, "The impact of media coverage on ipo stock performance," *Journal of Business Research*, vol. 72, pp. 24–32, 2017.
- [17] Z. Guo, K. C. Chan, and J. Huang, "Can media coverage restrain executive empire building and pursuit of a quiet life? evidence from China," *International Review of Economics & Finance*, vol. 56, pp. 547–563, 2018.
- [18] M. Bertrand and S. Mullainathan, "Enjoying the quiet life? Corporate governance and managerial preferences," *Journal of Political Economy*, vol. 111, no. 5, pp. 1043–1075, 2003.
- [19] G. D. Saxton and A. E. Anker, "The aggregate effects of decentralized knowledge production: financial bloggers and information asymmetries in the stock market," *Journal of Communication*, vol. 63, no. 6, pp. 1054–1069, 2013.
- [20] P. C. Tetlock and C. Paul, "Does public financial news resolve asymmetric information?" *Review of Financial Studies*, vol. 23, no. 9, pp. 3520–3557, 2010.
- [21] M. K. Bednar, "Watchdog or lapdog? A behavioral view of the media as a corporate governance mechanism," *Academy of Management Journal*, vol. 55, no. 1, pp. 131–150, 2012.
- [22] S. F. Cahan, C. Chen, L. Chen, and N. H. Nguyen, "Corporate social responsibility and media coverage," *Journal of Banking & Finance*, vol. 59, pp. 409–422, 2015.
- [23] B. D. Nguyen, "Is more news good news? Media coverage of CEOs, firm value, and rent extraction," *Quarterly Journal of Finance*, vol. 5, no. 4, pp. 1–38, 2015.
- [24] S. K. Byun and J.-M. Oh, "Local corporate social responsibility, media coverage, and shareholder value," *Journal of Banking & Finance*, vol. 87, pp. 68–86, 2018.
- [25] C. Pellegrino and S. Lodhia, "Climate change accounting and the Australian mining industry: exploring the links between corporate disclosure and the generation of legitimacy," *Journal of Cleaner Production*, vol. 36, pp. 68–82, 2012.
- [26] Gusenburg, L. 2014. CEOs: You Can't Afford to Ignore Social Media Anymore. <https://blog.hubspot.com/marketing/ceos-you-cant-afford-to-ignore-social-media-anymore>.
- [27] M. C. Suchman, "Managing legitimacy: strategic and institutional approaches," *The Academy of Management Review*, vol. 20, no. 3, pp. 571–610, 1995.
- [28] Z. Liu, X. Li, X. Peng, and S. Lee, "Green or nongreen innovation? Different strategic preferences among subsidized enterprises with different ownership types," *Journal of Cleaner Production*, vol. 245, Article ID 118786, 2019.
- [29] T. G. Pollock and V. P. Rindova, "Media legitimization effects in the market for initial public offerings," *Academy of Management Journal*, vol. 46, no. 5, pp. 631–642, 2003.
- [30] G. Jin, K. Shen, and J. Li, "Interjurisdiction political competition and green total factor productivity in China: an inverted-U relationship," *China Economic Review*, vol. 61, Article ID 101224, 2020.
- [31] H. Jin, Y. Qian, and B. R. Weingast, "Regional decentralization and fiscal incentives: federalism, Chinese style," *Journal of Public Economics*, vol. 89, no. 9–10, pp. 1719–1742, 2005.
- [32] J. Guan and R. C. M. Yam, "Effects of government financial incentives on firms' innovation performance in China: evidences from Beijing in the 1990s," *Research Policy*, vol. 44, no. 1, pp. 273–282, 2015.
- [33] A. M. Leiter, A. Parolini, and H. Winner, "Environmental regulation and investment: evidence from European industry data," *Ecological Economics*, vol. 70, no. 4, pp. 759–770, 2011.
- [34] A. Shleifer and R. W. Vishny, "Politicians and firms," *The Quarterly Journal of Economics*, vol. 109, no. 4, pp. 995–1025, 1994.

- [35] P. Bansal and I. Clelland, "Talking trash: legitimacy, impression management, and unsystematic risk in the context of the natural environment," *Academy of Management Journal*, vol. 47, no. 1, pp. 93–103, 2004.
- [36] E. Kesidou and P. Demirel, "On the drivers of eco-innovations: empirical evidence from the UK," *Research Policy*, vol. 41, no. 5, pp. 862–870, 2012.
- [37] M. E. Porter and C. V. D. Linde, "Toward a new conception of the environment-competitiveness relationship," *Journal of Economic Perspectives*, vol. 9, no. 4, pp. 97–118, 1995.
- [38] P. Lanoie, J. Laurent-Lucchetti, N. Johnstone, and S. Ambec, "Environmental policy, innovation and performance: new insights on the porter hypothesis," *Journal of Economics & Management Strategy*, vol. 20, no. 3, pp. 803–842, 2011.
- [39] M. Saygili and Meryem, "Pollution abatement costs and productivity: does the type of cost matter?" *Letters in Spatial and Resource Sciences*, vol. 9, no. 1, pp. 1–7, 2016.
- [40] K. H. Lee and B. Min, "Green R&D for eco-innovation and its impact on carbon emissions and firm performance," *Journal of Cleaner Production*, vol. 108, pp. 534–542, 2015.
- [41] P. Berrone, A. Fosfuri, L. Gelabert, and L. R. Gomez-Mejia, "Necessity as the mother of "green" inventions: Institutional pressures and environmental innovations," *Strategic Management Journal*, vol. 34, no. 8, pp. 891–909, 2013.
- [42] J. Zhang, X. Li, H. G. Fung, and P. Qiao, "Do political connections promote innovation in environmentally polluting enterprises?" *China & World Economy*, vol. 27, no. 3, pp. 76–101, 2019.
- [43] D. Li, M. Zheng, C. Cao, X. Chen, S. Ren, and M. Huang, "The impact of legitimacy pressure and corporate profitability on green innovation: Evidence from China top 100," *Journal of Cleaner Production*, vol. 141, pp. 41–49, 2017.
- [44] B. S. Javorcik and S. J. Wei, "Pollution havens and foreign direct investment: dirty secret or popular myth?" *The BE Journal of Economic Analysis & Policy*, vol. 3, no. 2, pp. 76–101, 2003.
- [45] W. H. Greene, *Econometric Analysis*, Prentice-Hall, Upper Saddle River, NJ, USA, 5th edition, 2003.
- [46] H.-G. Fung, P. Qiao, J. Yau, and Y. Zeng, "Leader narcissism and outward foreign direct investment: evidence from Chinese firms," *International Business Review*, vol. 29, no. 1, Article ID 101632, 2020.
- [47] R. H. Dehejia and S. Wahba, "Propensity score-matching methods for nonexperimental causal studies," *Review of Economics and statistics*, vol. 84, no. 1, pp. 151–161, 2002.

## Research Article

# Evaluation of Multimodal Transport in China Based on Hesitation Fuzzy Multiattribute Decision-Making

Bing Han <sup>1,2</sup>, Min Wan <sup>1,2</sup> and Yu Zhou<sup>1,2</sup>

<sup>1</sup>School of Maritime Economics and Management, Dalian Maritime University, Dalian 116000, China

<sup>2</sup>Collaborative Innovation Center for Transport Studies, Dalian Maritime University, Dalian 116000, China

Correspondence should be addressed to Bing Han; hanbing0610@163.com and Min Wan; wanmin051810@163.com

Received 10 June 2020; Revised 7 September 2020; Accepted 15 September 2020; Published 29 September 2020

Academic Editor: Yi Su

Copyright © 2020 Bing Han et al. This is an open access article distributed under the Creative Commons Attribution License, which permits unrestricted use, distribution, and reproduction in any medium, provided the original work is properly cited.

Intermodal transportation, as an efficient form of transport organization, is a key technology and means for the logistics industry to balance transport costs and efficiency. How to deeply analyze the key factors constraining the level of development of multimodal transportation in China, building multimodal transportation development evaluation index system and evaluation model, evaluating comprehensively the multimodal transportation development level in China, and putting forward targeted countermeasures is of great practical significance. Based on the hesitant fuzzy multiattribute decision-making method, this paper analyzes the key factors influencing the level of multimodal transportation development from the perspective of sea-rail intermodal transport and further uses the interval number discretization and likelihood deviation maximization multiattribute decision-making method to construct a mixed-data index evaluation model, which is combined with data from 11 provinces (cities) in China. The study shows that there is a big gap among different provinces (cities) in China concerning the level of multimodal transportation development. Besides, the volume of intermodal container transportation and railway mileage are the core factors affecting the level of multimodal transportation development, and the results of the evaluation model can objectively reflect the level of multimodal transportation development and problems in each province (city). The research results further enrich the theoretical system of intermodal transportation development and provide a reference for the relevant management departments in formulating intermodal transportation plans and policies by putting forward pertinent suggestions in the field of management. In the future, the research direction should include the ecological environment, economic benefits, and other indicators into the evaluation system, expand the research scope of the modes of combined transportation such as public rail transport and public air transport, and improve the applicable scope of the evaluation model and the evaluation capability of specific scenarios.

## 1. Introduction

International Multimodal Transport means the carriage of goods by at least two different modes of transport on the basis of a multimodal transport contract from a place in one country in which the goods are taken in charge by the multimodal transport operator to a place designated for delivery in a different country that was defined by the United Nations Convention in 1980 [1]. According to the technical and economic advantages of the various modes of transportation, logistics transport can be intermodal to improve efficiency and reduce energy consumption and greenhouse gas emissions. The experience of European and American

countries shows that intermodal transportation can improve transport efficiency by 30 percent or more, decrease cargo losses and cargo discrepancies by up to 10 percent, reduce the cost of transporting goods, and decrease road traffic congestion by 20 percent or more of transportation costs and up to 50 percent. With the rapid development and continuous improvement of the regional comprehensive transportation network in China, the range of cargo transport options continue to expand, and the multimodal transportation system will be the key direction of future transport logistics development in China. Although certain progress and achievements have been made in the development of multimodal transportation in China, the overall

level of development is still not high, and there is a large gap compared with Europe and the United States. Therefore, how to deeply analyze the key factors influencing the level of development of intermodal transportation in China and seize the main contradictions in the process of multimodal transportation development has become an important issue in the field of intermodal transportation research in China.

At present, domestic and foreign scholars have carried out researches on the evaluation of the development level of multimodal transport according to different research perspectives and methods, including qualitative, modal transport, stakeholder, and comprehensive evaluation perspectives, etc. Xu et al. [2–4] made qualitative studies on the development level of comprehensive transportation, container multimodal transport synergies, and multimodal transport channels from an overall qualitative perspective. With the development of multimodal transport, the scope of its definition has not been limited to the transnational, gradually formed in accordance with the combination of different modes of transport. Du and Shi and Fang et al. [5, 6] evaluated the circulation process and path advantages and disadvantages of container sea-rail combined transport from the perspective of sea-rail combined transport. Berli et al. and Han et al. [7, 8] studied the advantages and disadvantages of sea-land coordinated development and sea-land combined transport network paths from the perspective of sea-land combined transport, respectively. From the perspective of land bridge multimodal transport, several researchers [9–11] studied the operation mechanism and development level of long rail and short truck multimodal transport. From the perspective of sea-air transport, Lu et al. [12] studied the development level of sea-air transport network with airports as transit nodes and international routes from the Far East to Europe and the Far East to Central and South America. The multimodal logistics network formed by different methods is a complex network. They include transportation nodes, transportation connection edges, transit nodes, and transit connection edges [13], which are mainly composed of “service network” (local service network) and “internal operation network” (linehaul operations network) [14]. The complex network involves many stakeholders, decision makers, operations, and planning activities [15], of which freight shippers, carriers, and logistics authorities (planners) are the three main stakeholders [16]. From the perspective of different stakeholders such as shippers, carriers, and governments, the development level evaluation of multimodal transport has different focuses on transportation cost, transportation time, pollutant emission, and transportation emission [17–22]. With the development of the multimodal transport network trend, comprehensive evaluation research on the multimodal transport has also gradually emerged. The evaluation mainly involves in the degree of collaboration between multimodal transport participants and links, system behavior, service quality, evaluation standards, line performance evaluation, etc., as well as environmental costs, operating costs, transportation costs, infrastructure costs, transportation duration, door-to-door transportation,

duration of transshipment operations, comfort, safety, reliability, stability, and other indicators [18, 23–27].

It is necessary to face a situation where an attribute may have different evaluation values in the aspect of multimodal transport evaluation. However, neither the expert review method nor the analytic hierarchy process can meet this realistic requirement. Hesitant fuzzy sets allow more than one value for the membership of an element [28], which can effectively deal with the situation where experts are hesitant and difficult to make decisions in the decision-making process. Therefore, it is conducive to building a model to improve the accuracy of the results by introducing hesitant fuzzy multiattribute decision-making to the level of multimodal transport development during the evaluation process. At present, the multiattribute decision-making method is gradually applied in many fields. How to accurately analyze the uncertain information in the decision-making process to make a scientific and reasonable decision is the key to the current research. The fuzzy multiattribute decision-making method is used to solve the problem that, when under environmental data, each decision-making individual in the decision-making group calculates the preference value according to the attributes of the decision-making object with their own preferences and existing knowledge, and then sorts and selects the best. The scientific nature and applicability of the hesitant fuzzy multiattribute decision-making method have been generally proved [29–33].

Therefore, it is of theoretical and practical significance to establish an evaluation index system for the development level of multimodal transport in China, to evaluate the development level of multimodal transport in China objectively and accurately through the actual data, to analyze the key factors restricting the development level of multimodal transport in China in depth, and to propose corresponding countermeasures. As intermodal transportation requires the entire transport process as a whole, combining different modes of transport to form a continuous, optimal, integrated transport network of goods, necessarily involving a certain spatial range by a variety of transport elements, resource integration features, we will introduce the hesitation fuzzy multiattribute decision evaluation method, and on the basis of determining the alternatives and attribute sets for the multimodal transportation level evaluation problem, we will use the Delphi method to obtain the hesitation fuzzy matrix and further use the constructed evaluation model to obtain the comprehensive similarity of each alternative and conduct a comprehensive decision analysis according to the final results to provide countermeasures and suggestions for improving the level of multimodal transportation development.

## 2. Research Design

In view of the above problems, this paper intends to explore and study the evaluation and practice of the development level of multimodal transport from a new perspective and thinking, specifically as follows: (1) study the optimization of multimodal transport network from the perspective of comprehensive development level evaluation; (2) deeply



analyze and examine the factors affecting the development of multimodal transport and build an evaluation index system; (3) study the mixed multiattribute index decision-making based on the combination of accurate data and interval type data; (4) the evaluation model is constructed, and the objective data of the development status of multimodal transport is used to analyze and verify the feasibility of the algorithm and give the targeted countermeasures for the development of multimodal transport.

**2.1. Index Construction.** The design of the evaluation index system should follow the principles of scientificity, feasibility, and objectivity. That is to say, index construction should be based on scientific and reasonable analysis, be operable and easy to operate, and reflect objective facts as much as possible. Combining and analyzing relevant literature, Yang [34] used the system engineering method to build a multimodal transport performance evaluation index system including mobility and reliability, safety, environmental management, cost efficiency, and economic development. Zhu et al. [35] set up the evaluation index system of container multimodal transport efficiency level from three aspects of system efficiency, technical efficiency, and operation efficiency. Combined with the development mission of China's multimodal transport, based on the analysis of references, following the principles of science, feasibility, and objectivity, the evaluation indexes of regional multimodal transport including production capacity, policy strength, and service quality are selected. According to the data types of precise and interval indexes, the indexes can be divided into quantitative indexes and qualitative indexes. According to the changing trend of index data value and the performance trend of the evaluation object in this aspect, the index can be divided into benefit index and cost index [36]. The evaluation index system of regional multimodal transport development level is obtained as shown in Table 1.

For the fuzziness index, the scoring method of 1–10 points is used for measurement, and the following nine intervals are used for the division of 1–10 points with reference to the scoring method of the Likert scale. The corresponding descriptions of different interval standards are shown in Table 2.

**2.2. Model Construction.** To evaluate the development level of multimodal transport in province (city), this paper not only considers the quantitative indicators such as the volume of container sea-rail transport, the proportion of container throughput, railway operating mileage, the amount of government investment, and the number of multimodal transport demonstration projects but also considers the qualitative indicators such as the business level, service state, and technical level that reflect the service quality of multimodal transport. Therefore, it is necessary to analyze the mixed data composed of precise data and interval data. Therefore, this paper uses the method of maximizing the deviation between interval separation degree and scheme

attribute, finds the optimal objective weight vector and the comprehensive index value of each scheme through the decision matrix, establishes the mixed possibility complementary judgment matrix, and obtains the sorting vector and sorts according to the scheme of component size to get the optimal scheme.

(1) Building decision matrix

Set  $X = \{x_1, x_2, \dots, x_n\}$  as the evaluation object set,  $U = \{u_1, u_2, \dots, u_m\}$  as the evaluation index set,  $W = \{w_1, w_2, \dots, w_m\}^T$  as the weight vector of the evaluation index,  $w_i \geq 0$ ,  $w_i \in [w_i^l, w_i^u]$ ,  $\sum_{i=1}^m w_i = 1$ . This paper uses an evaluation index  $u_j \in U$  to evaluate evaluation object  $x_i \in X$  and get the accurate evaluation value  $m_1$  and interval evaluation value  $m_2$  ( $m_1 + m_2 = m$ ). Furthermore, the decision matrix  $A = (a_{ij})_{n \times m} = [(a_{ij})_{n \times m_1}, (a_{ij}^l, a_{ij}^u)_{n \times m_2}]$  can be obtained by applying all the evaluation indexes to evaluate all the evaluation objects.

(2) Normalization of decision matrix

As mentioned above, indicators can be divided into accurate type (Quantitative) and interval type (Qualitative) according to the type of indicator data value. At the same time, indicators can be divided into cost type and benefit type according to the change of indicator value and the changing trend of evaluation results under the indicator. Therefore, indicator types can be divided into four types: quantitative cost type, quantitative benefit type, qualitative cost type, and qualitative benefit type. On the basis of references [37], different types of data are standardized as follows.

The standardized formula of quantitative cost index data:

$$r_{ij} = \frac{\min_j a_{ij}}{a_{ij}}, \quad j \in N. \quad (1)$$

The standardized formula of quantitative benefit index data:

$$r_{ij} = \frac{a_{ij}}{\max_j a_{ij}}, \quad j \in N. \quad (2)$$

The standardized formula of qualitative cost index data:

$$\left\{ \begin{array}{l} r_{ij}^l = \frac{(1/a_{ij}^u)}{\sqrt{\sum_{j=1}^n (1/a_{ij}^l)^2}}, \\ r_{ij}^u = \frac{(1/a_{ij}^l)}{\sqrt{\sum_{j=1}^n (1/a_{ij}^u)^2}}, \end{array} \right. \quad j \in N. \quad (3)$$

The standardized formula of qualitative benefit index data:

TABLE 1: Evaluation index system of regional multimodal transport development level.

First level indicators	Secondary index	Three-level indicators	Type
The development level of multimodal transport	Throughput	Sea-rail intermodal container volume/TEU (X1)	Quantitative index of benefit type
		Proportion of intermodal container throughput (X2)	Quantitative index of benefit type
		Total mileage of railway operation/kilometre (X3)	Quantitative index of benefit type
	Policy strength	Government investment/100 million yuan (X4)	Quantitative index of benefit type
		Number of multimodal transport demonstration projects/unit (X5)	Quantitative index of benefit type
		Business level (X6)	Qualitative index of benefit type
	Service quality	Service attitude (X7)	Qualitative index of benefit type
		Technical level (X8)	Qualitative index of benefit type

TABLE 2: Fuzzy interval division standard and description.

Interval standard	Description of qualitative index interval standard		
	Business level	Service attitude	Technical level
[1, 2]	Terrible	Terrible	Terrible
[2, 3]	Very poor	Very poor	Very poor
[3, 4]	Quite poor	Quite poor	Quite poor
[4, 5]	Poor	Poor	Poor
[5, 6]	General	General	General
[6, 7]	Good	Good	Good
[7, 8]	Quite good	Quite good	Quite good
[8, 9]	Very good	Very good	Very good
[9, 10]	Great	Great	Great

$$\left\{ \begin{array}{l} r_{ij}^l = \frac{a_{ij}^l}{\sqrt{\sum_{j=1}^n (a_{ij}^u)^2}}, \\ r_{ij}^u = \frac{a_{ij}^u}{\sqrt{\sum_{j=1}^n (a_{ij}^l)^2}}, \end{array} \right. \quad j \in N. \quad (4)$$

Here,  $N = \{1, 2, \dots, n\}$ . Based on formulas (1)–(4), the decision matrix  $A = (a_{ij})_{n \times m} = [(a_{ij})_{n \times m_1}, (a_{ij}^l, a_{ij}^u)_{n \times m_2}]$  can be transformed into a normalized matrix  $R = (r_{ij})_{n \times m} = [(r_{ij})_{n \times m_1}, (r_{ij}^l, r_{ij}^u)_{n \times m_2}]$ .

### (3) Weight vector solution

The weight vector  $W$  solution follows the idea of maximizing the overall deviation value of the evaluation object under the evaluation index set. According to the definition of interval distance in

literature [38], we can set interval number  $a = [a^l, a^u]$ ,  $b = [b^l, b^u]$  and regard  $D(a, b) = \|a - b\| = |b^l - a^l| + |b^u - a^u|$  as the distance degree of interval number  $a, b$ . Under a certain index  $u_j \in U$ , the deviation value of evaluation object  $x_i$  and other evaluation objects are expressed by  $L_{ij}(w)$ , while  $L_i(w)$  represents the sum of deviation values of all the evaluation objects:

$$L_{ij}(w) = \sum_{k=1}^n \left( |r_{ij}^l - r_{kj}^l| + |r_{ij}^u - r_{kj}^u| \right) w_j, \quad i \in N, j \in M, \quad (5)$$

$$L_i(w) = \sum_{j=1}^n L_{ij}(w) = \sum_{j=1}^n \sum_{k=1}^n \left( |r_{ij}^l - r_{kj}^l| + |r_{ij}^u - r_{kj}^u| \right) w_j, \quad i \in N. \quad (6)$$

Furthermore, build the overall deviation function of the evaluation object under all indexes:

$$L(w) = \sum_{j=1}^m L_i(w) = \sum_{j=1}^m \sum_{i=1}^n \sum_{k=1}^n \left( |r_{ij}^l - r_{kj}^l| + |r_{ij}^u - r_{kj}^u| \right) w_j. \quad (7)$$

To solve the weight vector  $W$  is to solve the maximum  $L(w)$  value problem under certain constraints. The solution equation is as follows:

$$\begin{aligned} \max L(w) &= \sum_{j=1}^m \sum_{i=1}^n \sum_{k=1}^n \left( |r_{ij}^l - r_{kj}^l| + |r_{ij}^u - r_{kj}^u| \right) w_i \\ \text{s.t. } w &= (w_1, w_2, \dots, w_m)^T, \\ w_j &\in [w_j^l, w_j^u], w_j \geq 0, \sum_{j=1}^m w_j = 1. \end{aligned} \quad (8)$$

## (4) Solution of the comprehensive index value

The comprehensive index value  $z_i$  is the sum of the evaluation values of each province (city) in the evaluation system of the multimodal transport development level index. The calculation formula is as follows:

$$z_i = \sum_{j=1}^m r_{ij} w_j, \quad j \in M, \quad (9)$$

where  $w_j$  is the weight of the  $j$ th index,  $r_{ij}$  is the evaluation value in the normalized matrix  $R = (r_{ij})_{n \times m} = [(r_{ij})_{n \times m_1}, (r_{ij}^L, r_{ij}^U)_{n \times m_2}]$ .

## (5) Constructing the complementary matrix of possibility degree

According to formula (9), the comprehensive index of each province (city) is interval data. It is necessary to introduce the concept of interval comparison possibility to compare interval numbers. The definition of interregional probability in the cited references is as follows [39]:

Let  $a = [a^L, a^U]$ ,  $b = [b^L, b^U]$ , and  $S(a) = a^U - a^L$ ,  $S(b) = b^U - b^L$ ; then,

$$P(a \geq b) = \frac{\max\{0, S(a) + S(b) - \max(a^U - b^L, 0)\}}{S(a) + S(b)}. \quad (10)$$

Define the possibility that  $P(a \geq b)$  is  $a \geq b$ . In this definition,  $P(a \geq b)$  has the following properties:

- (a)  $P(a \geq b) + P(b \geq a) = 1$
- (b) If  $P(a \geq b) = P(b \geq a)$ , then  $P(a \geq b) = P(b \geq a) = (1/2)$
- (c) If  $a^U \leq b^L$ , then  $P(a \geq b) = 0$ ; if  $a^L \geq b^U$ , then  $P(a \geq b) = 1$

- (d) For three interval numbers  $a, b, c$ , if  $a \geq b$ , then  $P(a \geq c) \geq P(b \geq c)$

Based on formula (10), we can get the complementary judgment matrix of possibility degree  $P = (P_{ij})_{n \times n}$ .

## (6) Sorting vector solution

On the basis of the complementary judgment matrix of the possibility degree of each province (city), the calculation formula of the sequence vector  $h = (h_1, h_2, \dots, h_n)^T$  of the fuzzy complementary judgment matrix is obtained [38]:

$$h_i = \frac{\left(\sum_{j=1}^n P_{ij} + (n/2) - 1\right)}{n(n-1)}. \quad (11)$$

The ranking vector of probability matrix  $P$  is obtained, and the development level of multimodal transport in each province is ranked according to the component size of the ranking vector.

### 3. Empirical Analysis

From five aspects of production, policy, and service, this paper makes an empirical analysis on the development level of rail sea intermodal transport in 18 provinces (cities) in China, obtains the original data through the port Yearbook, provincial Yearbook, annual report, and other documents, and constructs the decision matrix as shown in Table 3 by applying the evaluation index system in Table 1.

According to step 2, the benefit and cost indicators as well as formulas (1)–(6), the decision matrix  $A$  can be transformed into a normalization matrix as shown in Table 4.

The single objective optimization model is established by using the idea of interval distance and a maximum deviation of the scheme index:

$$\begin{aligned} \max D(w) &= 16.6w_1 + 20.98w_2 + 20.46w_3 + 11.89w_4 + 17w_5 + 3.36w_6 + 2.94w_7 + 2.90w_8 \\ \text{s.t. } &0.12 \leq w_1 \leq 0.18, 0.10 \leq w_2 \leq 0.16, 0.10 \leq w_3 \leq 0.18, 1.12 \leq w_4 \leq 0.16, 0.08 \leq w_5 \leq 0.14, \\ &0.08 \leq w_6 \leq 0.14, 0.08 \leq w_7 \leq 0.14, 0.06 \leq w_8 \leq 0.12, \\ &\sum_{i=1}^8 w_i = 1, \quad w_i \geq 0, \quad i \in (1, 2, 3, \dots, 8). \end{aligned} \quad (12)$$

Using Python 2.7 software to solve the model, the optimal weight vector is  $W = (0.18, 0.16, 0.18, 0.12, 0.14, 0.08, 0.08, 0.06)$ .

According to formula (9), the comprehensive index value  $z_j(w) (j \in N)$  is as follows:



TABLE 3: Decision matrix.

	(X1)	(X2) (%)	(X3)	(X4)	(X5)	(X6)	(X7)	(X8)
Shanghai (A)	15.56	0.39	465.10	170.00	1	[8, 9]	[8, 9]	[7, 8]
Shandong (B)	63.81	2.49	5726.40	118.00	2	[7, 8]	[8, 9]	[8, 9]
Jiangsu (C)	25.17	1.46	2816.40	89.24	3	[7, 8]	[7, 8]	[8, 9]
Liaoning (D)	111.92	5.74	5914.70	45.90	4	[8, 9]	[7, 8]	[8, 9]
Fujian (E)	16.87	1.08	3191.40	106.20	1	[6, 7]	[7, 8]	[7, 8]
Guangdong (F)	43.26	0.69	4200.70	85.20	3	[7, 8]	[8, 9]	[7, 8]
Guangxi (G)	29.76	4.91	5191.40	40.63	1	[7, 8]	[6, 7]	[7, 8]
Hainan (H)	0.86	0.41	1033.40	181.00	1	[6, 7]	[7, 8]	[6, 7]
Hebei (I)	20.60	5.50	7162.00	70.70	3	[7, 8]	[7, 8]	[7, 8]
Tianjin (J)	34.93	2.32	1148.90	9.25	1	[7, 8]	[8, 9]	[7, 8]
Zhejiang (K)	42.64	1.55	2624.00	124.00	2	[8, 9]	[7, 8]	[7, 8]

TABLE 4: Standardized decision matrix.

	(X1)	(X2)	(X3)	(X4)	(X5)	(X6)	(X7)	(X8)
Shanghai (A)	0.14	0.07	0.06	0.05	0.25	[0.30, 0.38]	[0.29, 0.37]	[0.26, 0.33]
Shandong (B)	0.57	0.43	0.80	0.08	0.50	[0.26, 0.34]	[0.29, 0.37]	[0.29, 0.38]
Jiangsu (C)	0.22	0.25	0.39	0.10	0.75	[0.26, 0.34]	[0.25, 0.33]	[0.29, 0.38]
Liaoning (D)	1.00	1.00	0.83	0.20	1.00	[0.30, 0.38]	[0.25, 0.33]	[0.29, 0.38]
Fujian (E)	0.15	0.19	0.45	0.09	0.25	[0.22, 0.30]	[0.25, 0.33]	[0.26, 0.33]
Guangdong (F)	0.39	0.12	0.59	0.11	0.75	[0.26, 0.34]	[0.29, 0.37]	[0.26, 0.33]
Guangxi (G)	0.27	0.86	0.72	0.23	0.25	[0.26, 0.34]	[0.22, 0.29]	[0.26, 0.33]
Hainan (H)	0.01	0.07	0.14	0.05	0.25	[0.22, 0.30]	[0.25, 0.33]	[0.22, 0.29]
Hebei (I)	0.18	0.96	1.00	0.13	0.75	[0.26, 0.34]	[0.25, 0.33]	[0.26, 0.33]
Tianjin (J)	0.31	0.40	0.16	1.00	0.25	[0.26, 0.34]	[0.29, 0.37]	[0.26, 0.33]
Zhejiang (K)	0.38	0.27	0.37	0.07	0.50	[0.30, 0.38]	[0.25, 0.33]	[0.26, 0.33]

$$Z_A(w) = [0.2687, 0.2839],$$

$$Z_B(w) = [0.4568, 0.4750],$$

$$z_C(w) = [0.3252, 0.3458],$$

$$z_D(w) = [0.7118, 0.7324],$$

$$z_E(w) = [0.2355, 0.2531],$$

$$z_F(w) = [0.3738, 0.3890],$$

$$z_G(w) = [0.4291, 0.4477],$$

$$z_H(w) = [0.1325, 0.1477],$$

$$z_I(w) = [0.5429, 0.5605],$$

$$z_J(w) = [0.3661, 0.3813],$$

$$z_K(w) = [0.3157, 0.3333].$$

(13)

$$p = \begin{bmatrix} 0.5 & 0 & 0 & 0 & 1 & 0 & 0 & 1 & 0 & 0 & 0 \\ 1 & 0.5 & 1 & 0 & 1 & 1 & 1 & 1 & 0 & 1 & 1 \\ 1 & 0 & 0.5 & 0 & 1 & 0 & 0 & 1 & 0 & 0 & 1 \\ 1 & 1 & 1 & 0.5 & 1 & 1 & 1 & 1 & 1 & 1 & 1 \\ 0 & 0 & 0 & 0 & 0.5 & 0 & 0 & 1 & 0 & 0 & 0 \\ 1 & 0 & 1 & 0 & 1 & 0.5 & 0 & 1 & 0 & 0.5 & 1 \\ 1 & 0 & 1 & 0 & 1 & 1 & 0.5 & 1 & 0 & 1 & 1 \\ 0 & 0 & 0 & 0 & 0 & 0 & 0 & 0.5 & 0 & 0 & 0 \\ 1 & 1 & 1 & 0 & 1 & 1 & 1 & 1 & 0.5 & 1 & 1 \\ 1 & 0 & 1 & 0 & 1 & 0.5 & 0 & 1 & 0 & 0.5 & 1 \\ 1 & 0 & 0 & 0 & 1 & 0 & 0 & 1 & 0 & 0 & 0.5 \end{bmatrix}. \quad (14)$$

Calculate the possibility of the comparison of the comprehensive index values of multimodal transport in different regions and establish the possibility matrix:

According to formula (11), the order vector of probability  $p$  is  $W = (0.0636, 0.1182, 0.0818, 0.1364, 0.0545, 0.0955, 0.1091, 0.0455, 0.1273, 0.0955, 0.0727)$ .

The right ordering vector  $w$  and the possibility degree in proof P are obtained, and the ordering of interval number  $z_j(w)$  is as follows:

$$Z_D(w) \underset{1}{\geq} Z_I(w) \underset{1}{\geq} Z_B(w) \underset{1}{\geq} Z_G(w) \underset{1}{\geq} Z_J(w) \underset{0.5}{\geq} Z_F(w) \underset{1}{\geq} Z_C(w) \underset{1}{\geq} Z_K(w) \underset{1}{\geq} Z_A(w) \underset{1}{\geq} Z_E(w) \underset{1}{\geq} Z_H(w). \quad (15)$$

According to the size of  $z_j(w)$  ( $i = 1, 2, 3, \dots, 8$ ) value, the provinces (municipalities) are ranked as follows:

$$D \underset{1}{\succ} I \underset{1}{\succ} B \underset{1}{\succ} G \underset{1}{\succ} J \underset{0.5}{\succ} F \underset{1}{\succ} C \underset{1}{\succ} K \underset{1}{\succ} A \underset{1}{\succ} E \underset{1}{\succ} H. \quad (16)$$

It shows that Liaoning is the province with the highest level of multimodal transport development, followed by Hebei, Shandong, and Guangxi, with the advantage probability of 100%. Tianjin is ranked fifth with a 50% advantage over Guangdong, followed by Guangdong, Jiangsu, Zhejiang, Shanghai, Fujian, and Hainan, with the advantage probability of 100%. According to the weight of the indexes in the model, we can see sea-rail transport capacity, intermodal container throughput ratio, and railway mileage are the main influence factors affecting the development of regional sea-rail transport, Liaoning with good infrastructure foundation, a higher rate of cargo containers, and high proportion therefore ranked first, but in the aspect of government investment and personnel service attitude in Liaoning is yet to be promoted. Hebei, Shandong, Guangxi, and Tianjin all have a good logistics network foundation and container freight volume, and at the same time, have different degrees of problems in the proportion of container combined transportation, multimodal transportation demonstration project, business level, and so on. Guangdong, Jiangsu, Zhejiang, Shanghai, Fujian, and Hainan are at a disadvantage compared with the northern provinces in sea-rail combined transport due to the developed sea transport and water systems around them. Meanwhile, the above provinces should fully recognize their own advantages and disadvantages and develop sea-rail, sea-land, water-to-water, and other combined transport modes in an integrated manner.

#### 4. Conclusion

Based on the perspective of sea-rail intermodal transportation, this paper deeply analyzes the key indicators that influence the level of intermodal transport development, constructs a mixed multievaluation index system which includes precise and interval data, and evaluates the level of multimodal transport development in 11 provinces (cities) in China by using the fuzzy multiattribute decision method model.

The following conclusions are drawn: (1) The evaluation method of regional multimodal transportation development level is studied from the perspective of sea-rail multimodal transportation, and the intermodal transportation development level evaluation index system based on sea-rail multimodal transport is constructed through the analysis of

relevant literature and a questionnaire survey of experts and industry insiders. (2) The application of the multiattribute decision model solves the problem of unifying data standards for multiple indicators of intermodal transportation and provides new ideas for obtaining more objective and comprehensive evaluation results. (3) Based on the perspective of sea-rail intermodal transportation, we solve the weights of mixed evaluation indexes and obtain the key factors for the development of intermodal transportation in each province (city) as cargo containerization, containerized sea-rail intermodal transportation volume, and railway mileage, which provide the development direction for each region to improve the level of intermodal transport. (4) According to objective and real data, qualitative and quantitative index data will be comprehensively evaluated, and it is found that the development level of multimodal transportation in each province (city) of China. It is uneven and problematic, and more targeted responses need to be developed.

Based on the research results, the following suggestions are proposed: First, for government departments, it is necessary to coordinate the development and construction of multimodal transport in various regions, increase investment in multimodal transport infrastructure, guide the standardized development of industry regulations and technical standards, and break information barriers to promote efficient information transmission. Second, multimodal transport operators should fully understand the key factors affecting the development of their own transport capacity and concentrate limited resources to strengthen the core competitiveness. Third, for shippers, when choosing the route of multimodal transport service, it is necessary to give full consideration to the hard targets of the carrier in terms of containerization of goods, intermodal transport, intermodal transport operating mileage, etc., so as to ensure the efficient and safe delivery of goods. The research in this paper also needs to further improve the evaluation index system, such as increasing the evaluation indexes of ecological environment and economic benefits, so as to be able to more objectively and comprehensively evaluate the level of intermodal transportation development. Future research should expand intermodal transportation modes, such as intermodal road-rail and road-air so that the model can be adapted to more regional scales and enhance the applicability of the model.

#### Data Availability

The data used to support the findings of this study are available from the corresponding author upon request.

## Conflicts of Interest

The authors declare no conflicts of interest.

## Acknowledgments

This work was supported by the National Key Research and Development Project (Grant No. 2019YFB1600401), Youth Program of National Natural Science Foundation of China (Grant no. 71503029), and the State Key Program of National Natural Science of China (Grant no. 71831002).

## References

- [1] Kam, B. Liu, and Tanlin, "The development trend of international multimodal transport and China's countermeasures," *China's Circulation Economy*, vol. 4, no. 12, pp. 17–20, 2019.
- [2] Y. Xu, B. Su, L. Zhang et al., "Study on comprehensive evaluation and adaptability of regional economy and transportation system development in Shaanxi Province," *Eco-logical Economy*, vol. 32, no. 3, pp. 108–112, 2016.
- [3] H. Park, H. Liu, and B. Zhang, "Comprehensive evaluation of container multimodal transport coordination capability," *China Navigation*, vol. 36, no. 4, pp. 125–129, 2013.
- [4] Z. Jin, Q. Xu, and M. Chen, "Evaluation and empirical study of intermodal container transport channels," *China Science and Technology Paper Online*, vol. 6, no. 5, pp. 390–394, 2011.
- [5] Q. Du and X. Shi, *Sea-Rail Combined Transport Model Based on Queuing Theory*, IEEE, Piscataway, NJ, USA, 2016.
- [6] X. Fang, C. Cao, Z. Chen et al., "Using mixed methods to design service quality evaluation indicator system of railway container multimodal transport," *Science Progress*, vol. 103, no. 1, Article ID 003685041989049, 2019.
- [7] J. Berli, M. Bunel, and C. Ducruet, "Sea-land interdependence in the global maritime network: the case of Australian port cities," *Networks and Spatial Economics*, vol. 18, no. 3, pp. 447–471, 2018.
- [8] X. Han, Y. Wang, and Z. Jin, "Study on the optimization of land sea intermodal transportation path of containers around the Bohai Sea considering multi tasks," *Logistics Engineering and Management*, vol. 41, no. 3, pp. 79–82, 2019.
- [9] Y. Wiseman and Y. Giat, "Red sea and Mediterranean Sea land bridge via Eilat," *World Review of Intermodal Transportation Research*, vol. 5, no. 4, pp. 353–368, 2015.
- [10] V. N. Filina, "Russian market of transport services in international container transportation," *Studies on Russian Economic Development*, vol. 23, no. 2, pp. 153–161, 2012.
- [11] R. Pomfret, "The Eurasian land bridge: linking regional value chains along the new silk road," *Cambridge Journal of Regions, Economy and Society*, vol. 12, no. 1, pp. 45–56, 2019.
- [12] M. Lu, Y. Chen, R. Morphet et al., "The spatial competition between containerised rail and sea transport in Eurasia," *Palgrave Communications*, vol. 5, no. 1, Article ID 122, 2019.
- [13] Z. He, J.-N. Guo, and J.-X. Xu, "Cascade failure model in multimodal transport network risk propagation," *Mathematical Problems in Engineering*, vol. 2019, no. 2, 7 pages, Article ID 3615903, 2019.
- [14] G. Wang, "Study on international logistics operation mode based on multimodal transport," *China Circulation Economy*, vol. 2003, no. 5, pp. 20–22, 2003.
- [15] T. G. Crainic, G. Perboli, and M. Rosano, "Simulation of intermodal freight transportation systems: a taxonomy," *European Journal of Operational Research*, vol. 270, no. 2, pp. 401–418, 2018.
- [16] D. Sheng, X. C. Li, and X. D. Fu, "Modeling the effects of unilateral and uniform emission regulations under shipping company and port competition," *Transportation Research Part E: Logistics and Transportation Review*, vol. 101, no. 5, pp. 99–114, 2017.
- [17] A. Gillen, J. Yee, and B. Golden, "Scheduling players in team competitions: theory and computational results," *American Journal of Mathematical and Management Sciences*, vol. 3, no. 2, pp. 89–119, 1983.
- [18] Y. Su and T. Li, "Simulation analysis of knowledge transfer in a knowledge alliance based on a circular surface radiator model," *Complexity*, vol. 2020, no. 8, 27 pages, Article ID 4301489, 2020.
- [19] G. Lanza, T. G. Crainic, W. Rei, and N. Ricciardi, "A study on travel time stochasticity in service network design with quality targets," in *Proceedings of the 9th International Conference on Computational Logistics, ICCL 2018*, Vietri sul Mare, Italy, October 2018.
- [20] J. E. Holler Branco, D. H. Branco, E. M. De Aguiar, J. V. Caixeta Filho, and L. Rodrigues, "Study of optimal locations for new sugarcane mills in Brazil: application of a MINLP network equilibrium model," *Biomass & Bioenergy*, vol. 127, no. 8, pp. 105241–105249, 2019.
- [21] Y. Sun, X. Li, X. Liang, and C. Zhang, "A bi-objective fuzzy credibilistic chance-constrained programming approach for the hazardous materials road-rail multimodal routing problem under uncertainty and sustainability," *Sustainability*, vol. 11, no. 9, Article ID 2577, 2019.
- [22] J. Wan and S. Wei, "Multi-objective multimodal transportation path selection based on hybrid algorithm," *Journal of Tianjin University*, vol. 2019, no. 3, pp. 285–292, 2019.
- [23] X. Fang, Z. Ji, Z. Chen, and W. Chen, "Synergy degree evaluation of container multimodal transport system," *Sustainability*, vol. 12, no. 4, Article ID 1487, 2020.
- [24] M. Friedrich, "Evaluating the service quality in multimodal transport networks," *Transportation Research Procedia*, vol. 15, pp. 100–112, 2016.
- [25] S. Stoilova and L. Kunchev, "Study of criteria for evaluation of transportation with intermodal transport," "Study of criteria for evaluation of transportation with intermodal transport," in *Proceedings of the 16th International Scientific Conference: Engineering for Rural Development*, L. Malinowska and V. Osadcuks, Eds., Latvia Univ Agriculture, Faculty Engineering, Inst Mechanics, Jelgava, Latvia, pp. 349–357, May 2017.
- [26] B. Di Pierro, G. Iacobellis, B. Turchiano et al., *Performance Assessment for Intermodal Transportation Systems: A Case Study*, IEEE, New York, NY, USA, 2017.
- [27] Q. Wang, J. Chen, M. Tseng, H. M. Luan, and M. H. Ali, "Modelling green multimodal transport route performance with witness simulation software," *Journal of Cleaner Production*, vol. 248, Article ID 119245, 2020.
- [28] C. Cui, X. Zhu, Y. Ren et al., "Evaluation of agricultural modernization level based on hesitant fuzzy multi-attribute decision-making method," *Management Review*, vol. 31, no. 11, pp. 195–201, 2019.
- [29] J. Mao, Q. Sun, and K. Gui, "Study on hesitant fuzzy multi-attribute quality evaluation based on surface defect information of autobody panels," *Mathematical Problems in Engineering*, vol. 2020, Article ID 8203254, 10 pages, 2020.
- [30] L. Xu, Y. Liu, and H. Liu, "Some improved  $q$ -Rung orthopair fuzzy aggregation operators and their applications to

- multiattribute group decision-making," *Mathematical Problems in Engineering*, vol. 2019, no. 2, 18 pages, Article ID 2036728, 2019.
- [31] Y. Liu, J. Liu, and Y. Qin, "Dynamic intuitionistic fuzzy multiattribute decision making based on evidential reasoning and MDIFWG operator," *Journal of Intelligent & Fuzzy Systems*, vol. 36, no. 6, pp. 5973–5987, 2019.
- [32] S.-M. Chen and W.-H. Han, "Multiattribute decision making based on nonlinear programming methodology, particle swarm optimization techniques and interval-valued intuitionistic fuzzy values," *Information Sciences*, vol. 471, pp. 252–268, 2019.
- [33] Z. Yang, H. Garg, J. Li, G. Srivastava, and Z. Cao, "Investigation of multiple heterogeneous relationships using a q-Rung orthopair fuzzy multi-criteria decision algorithm," *Neural Computing and Applications*, pp. 1–22, 2020.
- [34] L. Yang, "Research on development strategies of China's container multimodal transport," *Railway Transport and Economy*, vol. 38, no. 7, pp. 7–10, 2016.
- [35] H. Zhu, H. Yao, and B. Liu, "Study on the construction of evaluation index system of container multimodal transport efficiency," *Railway Transport and Economy*, vol. 40, no. 5, pp. 8–14, 2018.
- [36] Z. Xu and Z. Sun, "The ranking method for a class of uncertain multi-attribute decision-making problems," *Journal of Management Science*, vol. 2002, no. 3, pp. 35–39, 2002.
- [37] H. Lin and P. Shao, "Evaluation and application of online advertising media based on mixed multi-attribute decision," *Management Review*, vol. 24, no. 12, pp. 53–63, 2012.
- [38] Z. Xu, "Multi attribute decision making method based on deviation maximization of degree of separation and possibility," *Control and Decision*, vol. 16, no. z1, pp. 818–821, 2001.
- [39] Z. Xu, "An algorithm for ranking fuzzy complementary judgment matrix," *Journal of Systems Engineering*, vol. 16, no. 4, pp. 311–314, 2001.

## Research Article

# Application of Multiattribute Decision-Making for Evaluating Regional Innovation Capacity

Yi Su <sup>1,2</sup>, Dezhi Liang,<sup>1</sup> and Wen Guo<sup>1</sup>

<sup>1</sup>*School of Economics and Management, Harbin Engineering University, Harbin 150001, China*

<sup>2</sup>*School of Management, Zhejiang University, Hangzhou, Zhejiang 310012, China*

Correspondence should be addressed to Yi Su; 13527715@qq.com

Received 23 May 2020; Revised 22 July 2020; Accepted 10 September 2020; Published 17 September 2020

Academic Editor: Yang Li

Copyright © 2020 Yi Su et al. This is an open access article distributed under the Creative Commons Attribution License, which permits unrestricted use, distribution, and reproduction in any medium, provided the original work is properly cited.

The growing imbalance in regional innovation development has become an urgent issue in China's strategy to build an innovative country. To enrich the regional innovation capacity evaluation system, scientifically assess regional innovation capacity, and explore available pathways to improve regional innovation capacity, this paper introduces a multiattribute decision-making method for evaluating regional innovation capacity. First, a random forest model and the DEMATEL-based analytic network process (DANP) method are applied to calculate the weights of the evaluation attributes. Second, the multiobjective optimization by the ratio analysis method based on the maximum and minimum (MOORA-min-max method) is used to calculate the evaluation attribute gap ratios and regional innovation capacity of each region. Finally, the limitations of regional innovation development are identified based on the evaluation attribute gap ratios and the critical influence strength roadmap (CISR) to explore the regional innovation capacity improvement pathways. The results show that "output capacity of R&D personnel in universities and research institutes" is the most fundamental evaluation attribute in the regional innovation capacity evaluation, while "output efficiency of R&D funds in universities and research institutes" is the most influential evaluation attribute. Research in Sichuan and Inner Mongolia reveals that regions need to identify critical constraints in four aspects: knowledge creation, knowledge acquisition, enterprise innovation, and innovation environment, to improve regional innovation capacity.

## 1. Introduction

Persistent imbalance in the development of regional innovation capacity constitutes a substantial bottleneck constraining the effort to upgrade countries' integrated innovation capacity. China's regional innovation development is influenced by its history, economy, and geography and thus varies significantly [1–3]. To better promote the role of regional innovation in high-quality economic development, Chinese policymakers have placed innovation at the centre of overall national development. The 19th National Congress of the Communist Party of China proposed that "innovation is the first impetus for leading development" and issued a strategic plan to accelerate the construction of an innovation-oriented country.

Regional innovation capacity is an essential indicator of an innovation-oriented country, and many scholars have focused on regional innovation capacity in recent years

[4, 5]. Scholars have thoroughly studied the conceptual definition of regional innovation capacity, including its differences, indicators, influencing factors, and formation mechanisms [6–10]. For example, Shan constructed a system for evaluating regional innovation capacity based on four aspects: input capacity, innovation environment, management capacity, and innovation output [11]. Hamidi et al. examined the relationship between regional compactness and regional innovation capacity in the United States [12]. Tang et al. studied the spatial effect of absorptive capacity on regional innovation capacity from the perspective of knowledge spillover theory [13]. Many organizations have also published reports on the evaluation of innovation. The World Intellectual Property Organization and others cofounded the Global Innovation Index (GII), which ranks countries according to their innovation capacity and economic performance. Similarly, the National Research Group on S&T Development Strategy released the China Regional



Innovation Capability report, which provides an objective, dynamic, and comprehensive assessment of China's innovation capacity in each region.

With the advent of the Fourth Industrial Revolution, the ability to innovate has once again become a vital capacity for countries to compete for the right to global value distribution. For China, which displays significant differences in regional innovation development, improving regional innovation is an urgent issue. An accurate evaluation of regional innovation capacity is the basis for monitoring the current state of regional innovation development, identifying constraints on regional innovation development, and exploring pathways for improving regional innovation capacity. Accordingly, this paper selects evaluation indicators from four aspects, namely, knowledge creation, knowledge acquisition, enterprise innovation, and innovation environment and then applies the multiattribute decision-making method to evaluate the innovation capacity of all 31 provinces in China and to explore pathways for improving regional innovation capacity. The main contributions of this paper are as follows: (1) The random forest model and the decision-making trial and evaluation laboratory- (DEMATEL-) based analytic network process (DANP) method are introduced to innovation capacity evaluation research, thereby enriching the method for calculating objective weights; moreover, a multiattribute decision-making evaluation model of regional innovation capacity provides a new method to evaluate regional innovation objectively. (2) The multiobjective optimization by ratio analysis (MOORA) method and the critical influence strength roadmap (CISR) are introduced into the field of innovation research to provide a new approach to scientifically identify the factors limiting regional innovation capacity.

## 2. Literature Review

To date, scholars have not reached a consensus on how to evaluate regional innovation [14]. In the existing literature, innovation capacity evaluation research is divided into two aspects: evaluation indexes and evaluation methods. In terms of research on evaluation indexes, common indicators for evaluating regional innovation capacity include innovation resource inputs, innovation outputs, and innovation environments [15–17]. Other scholars have proposed patents as an essential indicator of regional innovation capacity [18–21]. For example, Hamidi et al. used the number of patents as one indicator of regional innovation capacity [12]. In addition, scholars have assessed the selection of indicators for evaluating regional innovation capacity in terms of system structure and green innovation. For example, Han et al. used the innovation participant framework [17] to classify innovation participants into eight categories, including government departments, research institutes, colleges and universities, enterprises, and technology intermediaries. They selected 63 innovation participant indexes to analyse the innovation capacity of 16 cities in Korea [22]. Chen et al. established regional innovation capabilities based on knowledge management from 6 aspects: knowledge base, knowledge creation, knowledge

dissemination, knowledge sharing, knowledge application, and innovation environment [23]. Wang et al. constructed a system of regional innovation evaluation indicators from green innovation inputs, green innovation outputs, and green innovation environments [24].

The research on evaluation methods for innovation capacity is divided into the calculation of evaluation index weights and the comprehensive evaluation of innovation capacity. The subjective weighting method and objective weighting method are the most common approaches for calculating the weights of evaluation indexes [25]. The former refers to weights determined subjectively through people's experience; for example, Shan developed a hierarchical analysis model of regional innovation capacity and used the analytic hierarchy process to calculate the weight of each evaluation indicator [11]. The latter refers to the analysis of the relationships between indicators based on objective data; for example, Yan et al. determined the indicator weights of regional technological innovation capacity by using the entropy method and empirically analysed the technological innovation capacity of 80 regions in Hubei Province, China [26]. Scholars have also proposed to comprehensively determine the weights of index combinations. For example, Xu et al. used the cloud model method and the entropy method to determine the initial weight of an index. Then, the cloud model was combined with the DEMATEL method to determine the final comprehensive weight of the indicator [27]. In terms of the comprehensive evaluation of innovation capacity, Sheng et al. used grey system theory and the Delphi method to establish a system of indicators for evaluating regional S&T innovation capacity. They then applied a new grey cluster model based on a mixed centre-point triangular whitenization weight function to evaluate the regional S&T innovation capacity of five cities in Jiangsu Province, China [28]. Yang et al. proposed a method based on uncertain linguistic variables for evaluating enterprise innovation capacity and analysed the innovation capacity of five firms [29]. Similarly, Zhen introduced the induced 2-tuple linguistic Choquet ordered harmonic average (I-2TCOHA) operator to aggregate the 2-tuple linguistic information corresponding to each alternative and rank the alternatives to evaluate the technological innovation capacity of a firm [30]. Li et al. proposed a multidimensional grey fuzzy decision-making method with feedback based on the weight vector and weight matrix and applied the method to evaluate regional financial innovation capacity [31]. Wang et al. used the fuzzy analytic hierarchy process to evaluate regional green innovation capacity [24].

In summary, the subjective evaluation method (represented by the analytic hierarchy process) determines evaluation indicator weights based on subjective ideas, while ignoring the information provided by data, resulting in the lack of an objective scientific basis for the resulting weights. In contrast, the objective evaluation method can effectively avoid subjective problems but suffers from certain deficiencies; for example, the entropy method ignores the lack of a horizontal comparison between indicators. The random forest model can calculate the influence strength among indicators, thereby avoiding the problem of subjectivity, and

thus can make comparisons between evaluation indicators. Existing scholars have performed a considerable amount of work on methods to evaluate innovation capacity and have proposed a series of policy recommendations; however, these suggestions are generally universal. Due to the differences among individual entities, the pathways to improving innovation capacity also vary. The MOORA method and critical influence strength roadmap (CISR) are introduced to evaluate innovation capacity; the former identifies the maximum gap ratio among the evaluation indicators, while the latter is a diagram showing the influence pathways among the evaluation indicators. The combination of these two can effectively identify the factors that restrict the development of individual innovation capacity and enables improvements in innovation capacity with individual differences.

### 3. Establishing the Indicator System and Building the Model

This section briefly introduces the construction of the indicators and models for evaluating regional innovation capacity. First, the main participants of the regional innovation system are universities, research institutes, companies, government agencies, and intermediaries [7, 17, 32], which are responsible for different roles: universities and research institutions with excellent researchers and sufficient innovation resources assume the role of knowledge creation; enterprises, as core participants in regional innovation systems, take on a greater role in transferring innovation knowledge; and government and intermediaries are responsible for providing a suitable environment for regional innovation. Second, the evaluation model uses the “drop-column importance” concept proposed by Terence et al. to measure the influence strength between evaluation indicators [33, 34]. The calculated influence strength is used as the raw data for the DANP approach, replacing the expert scoring approach. The DANP method is used to obtain a diagram of the influence strength network and the weight of each evaluation indicator. The MOORA method is then combined with maximum or minimum values to develop the MOORA-max-min method, which can calculate the gap ratio between the current level of an evaluation indicator and its maximum or minimum value. The regional innovation capacity is then calculated according to the weights of the evaluation indicators and the gap ratios. The model construction process is shown in Figure 1.

**3.1. Establishing the Indicator System.** The concept of the regional innovation system was first proposed by the British scholar Cooke in 1992. A regional innovation system is a regional organizational system formed by the division of labour, interconnected enterprises, universities, research institutions, intermediary services, and local governments within a specific geographical area [35]. Evaluation

indicators should consider the generation and application of knowledge and the underlying environment of regional innovation [36–39]. After analysing the characteristics and linkages of China’s regional innovation system, this paper constructs an evaluation indicator system from four aspects: knowledge creation, knowledge acquisition, enterprise innovation, and innovation environment. (1) Knowledge creation: knowledge creation is a source of regional innovation and refers to the process involving universities and research institutes, research funding, and inputs from researchers, including the inputs and outputs of innovation, measured mainly as research inputs, patents, and thesis outputs. (2) Knowledge acquisition: knowledge acquisition refers to the flow and utilization of knowledge within a region, measured mainly by thesis cooperation, corporate financial support, and the use of foreign investment. (3) Enterprise innovation: the translation of innovation results into products by firms is an important part of regional innovation. Corporate innovation is measured by corporate research inputs, patent outputs, and new product development. (4) Innovation environment: a good innovation environment can promote regional innovation. The innovation environment is measured mainly in terms of regional development, quality of intermediary services, and sustainability capacity. The resulting system of indicators for the evaluation of regional innovation capacity is shown in Table 1.

To guarantee the reproducibility of this study, the data in this paper come from publicly published statistical yearbooks and government reports, mainly including the China Statistical Yearbook, China Statistical Yearbook of Science and Technology, China Statistical Yearbook of High-Tech Industry, China Industry Economy Statistical Yearbook, China Torch Statistical Yearbook, statistical and analytical reports on Chinese science and technology papers, and related data released by the Ministry of Science and Technology, State Intellectual Property Office, State Administration for Industry and Commerce, and the Technology Innovation Fund for Science and Technology-based Small and Mid-Size Enterprises (SMEs).

### 3.2. Building the Multiattribute Decision-Making Evaluation Model of Regional Innovation Capacity

#### 3.2.1. Using a Random Forest Model to Construct an Initial Influence Strength Matrix

Step 1: discretize the data for all evaluation attributes through a three-level interval discretization method comprising the top third (marked “H”), the middle third (marked “M”), and the bottom third (marked “L”) of the value range for each evaluation attribute [40].

Step 2: divide the  $n$  evaluation attributes  $(x_1, x_2, \dots, x_n)$  into  $n$  groups according to the individual evaluation attributes (called decision evaluation



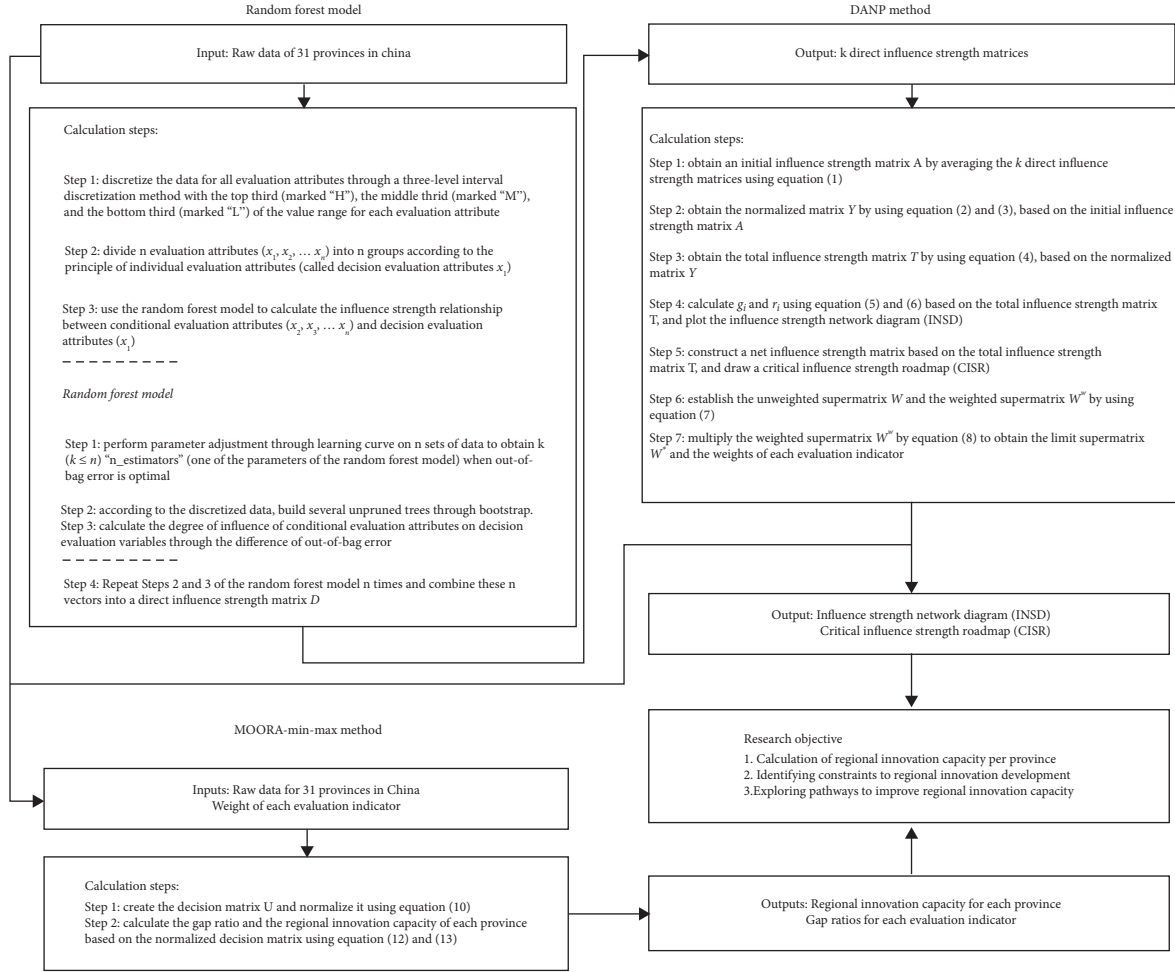


FIGURE 1: Procedure of constructing the multiattribute decision-making evaluation model.

attributes  $x_1$ ) and  $n-1$  evaluation attributes (called conditional evaluation attributes  $x_2, x_3, \dots, x_n$ ).

Step 3: use the random forest model to calculate the influence strength relationship among conditional evaluation attributes ( $x_2, x_3, \dots, x_n$ ) and decision evaluation attributes ( $x_1$ ); the calculated influence vector of conditional evaluation attributes  $x_2, \dots, x_n$  on  $x_1$  is  $(a_{11}, a_{21}, \dots, a_{n1})$ , where  $a_{11} = 0$ . Steps 2 and 3 are repeated  $n$  times for each decision variable  $x_i$  ( $i = 1, 2, \dots, n$ ) to obtain  $n$  combinations of vectors. Furthermore, these  $n$  combinations of vectors are combined into an  $n$ -dimensional matrix  $D = [d_{ij}]_{n \times n}$ , where matrix  $D$  is called the direct influence strength matrix and  $d_{ij}$  represents the degree of influence of the  $i^{\text{th}}$  evaluation attribute on the  $j^{\text{th}}$  evaluation attribute when  $i = j$ ,  $d_{ij} = 0$ . Steps 2 to 4 are repeated  $k$  times ( $k$ , one of the parameters of the random forest model, is the number of  $n$  estimators obtained through the

learning curve) to obtain  $k$  direct influence strength matrices  $D$ .

### 3.2.2. Applying the DANP Method to Draw the Influence Strength Network Diagram and Calculate the Evaluation Attribute Weights

Step 1: calculate the initial influence strength matrix. The  $k$  direct influence strength matrices  $D$  are measured by averaging them using the following equation to obtain the initial influence strength matrix  $A$ :

$$A = [a_{ij}]_{n \times n} = \left[ \frac{\sum_{s=1}^k d_{ij}}{k} \right]_{n \times n}. \quad (1)$$

Step 2: normalize the initial influence strength matrix. The initial influence strength matrix  $A$  is converted by

TABLE 1: Regional innovation capacity evaluation indicator system

Primary indicators	Secondary indicators	Tertiary indicators	Description
Regional innovation capacity	Knowledge creation	Regional technology manpower investment (C1)	Average full-time personnel equivalent of research and experimental development per 10,000 population (person-years per 10,000 population)
		Regional government R&D investment (C2)	Government investment in R&D as a percentage of GDP (%)
		Output capacity of R&D personnel in universities and research institutes (C3)	Number of invention patent applications per 100 million yuan of internal expenditure on R&D (cases/billion yuan)
		Output efficiency of R&D personnel in universities and research institutes (C4)	Number of patents granted per 10,000 R&D personnel for inventions (pieces per 10,000)
		Output efficiency of R&D funds in universities and research institutes (C5)	Number of invention patents granted per 100 million yuan of internal expenditure on R&D activities (cases/billion)
		Publication of journal papers at home and abroad (C6)	Average number of papers published per 100,000 R&D personnel (per 100,000)
		Regional knowledge cooperation (C7)	Number of coauthored scientific and technical papers per 100,000 R&D staff (per 100,000)
		Cooperation between enterprises and universities and research institutes (C8)	The proportion of internal expenditure on research and development at universities and research institutes from corporate funds (%)
	Knowledge acquisition	Technology flow (C9)	Technical market transaction amount (by flow) (10,000 yuan)
		Enterprise acquisition of technical capabilities (C10)	Expenditure on the purchase/introduction of technology by industrial enterprises above scale (10,000 yuan)
		Regional ability to use foreign capital (C11)	Foreign share of registered capital of foreign-invested enterprises per capita at the end of the year (10,000 dollars)
		Enterprise R&D personnel input capability (C12)	Share of R&D personnel employed in industrial enterprises above scale (%)
	Enterprise innovation	Enterprise R&D funding investment capacity (C13)	Total internal expenditure on R&D activities of industrial enterprises above scale as a proportion of sales revenue (%)
		Enterprise R&D output capacity (C14)	Average number of invention patent applications per 10,000 R&D personnel in industrial enterprises above scale (pieces per 10,000)
		Enterprise core technology level (C15)	Average number of useful invention patents per 10,000 industrial enterprises above scale (pieces per 10,000 units)
		Enterprise new product development capability (C16)	Share of sales revenue from new products in sales revenue of industrial enterprises above scale (%)
		Regional market openness (C17)	Total exports and imports by destination and source of goods as a share of GDP (%)
		Regional talent training (C18)	Expenditure on education as a percentage of GDP (%)
	Innovation environment	Quality of local workers (C19)	Proportion of the population aged six years and above with tertiary education (%)
		Financial institution support (C20)	Loans obtained from financial institutions out of the amount of internal expenditure on research and development of industrial enterprises above scale (RMB 10,000)
		The proportion of high-tech enterprises (C21)	Number of high-technology enterprises as a proportion of the number of industrial enterprises above scale (%)
		Incubation capacity of technology business incubators (C22)	Number of technology business incubators graduating in a year (number of enterprises)
		Regional economic development level (C23)	Number of technology business incubators graduating in a year (number of enterprises) GDP level per capita (yuan/person)
		Regional sustainability (C24)	Integrated value of regional energy consumption and sewage emissions <sup>1</sup>

<sup>1</sup>The integrated value is obtained after the dimensionless treatment of the energy consumption (equivalent value) of the regional GDP, the total power consumption, the total discharge of industrial sewage, and the discharge of major pollutants in the exhaust gas.

means of the following equations to obtain the normalized initial influence strength matrix  $Y$ :

$$Y = \Delta \times A, \quad (2)$$

$$\Delta = \min \left\{ \frac{1}{\max_i \sum_{j=1}^n a_{ij}}, \frac{1}{\max_j \sum_{i=1}^n a_{ij}} \right\}, \quad (3)$$

where  $\Delta$  is the reciprocal of the maximum value of the sum of the rows or the columns of the initial influence strength matrix and is used to normalize the initial influence strength matrix.

Step 3: solve the total influence strength matrix. Based on the initial influence strength matrix  $D$  and the Markov chain matrix, the total influence strength matrix  $T$  is calculated using the following equation:

$$T = Y + Y^2 + \dots + Y^\infty = Y(E - Y)^{-1}, \quad (4)$$

where  $E$  is the  $n$ -dimensional identity matrix.

Step 4: draw the influence strength network diagram. The following equations are used to obtain  $g_i$  and  $r_i$ , and then the influence strength network diagram is plotted:

$$g_i = (g_i)_{n \times 1} = \left[ \sum_{j=1}^n t_{ij} \right]_{n \times 1}, \quad (5)$$

$$r_i = (r_i)_{n \times 1} = (r_j)_{1 \times n}' = \left[ \sum_{i=1}^n t_{ij} \right]_{1 \times n}', \quad (6)$$

where  $'$  represents the matrix transposition and  $g_i$  represents the total influence strength of the  $i^{\text{th}}$  evaluation attribute on the other evaluation attributes, called the degree of influence of the  $i^{\text{th}}$  evaluation attribute.  $r_i$  represents the total influence strength of the other evaluation attributes on the  $i^{\text{th}}$  evaluation attribute and is called the degree of influence of the  $i^{\text{th}}$  evaluation attribute. The centrality degree  $c_i = g_i + r_i$  reflects the importance of the  $i^{\text{th}}$  evaluation attribute in the system. The causality degree  $h_i = g_i - r_i$ , when  $h_i > 0$ , indicates that the  $i^{\text{th}}$  evaluation attribute is the causality attribute and influences the other evaluation attributes; if  $h_i < 0$ , then the  $i^{\text{th}}$  evaluation attribute is the result attribute and is influenced by the other evaluation attributes.

Step 5: build the unweighted supermatrix  $W$  and the weighted supermatrix  $W^w$ . The unweighted supermatrix  $W$  is calculated using the total influence strength

matrix  $T$  and equation (7). In addition, the unweighted supermatrix  $W$  is the weighted supermatrix  $W^w$  because all the evaluation attributes in this paper are of the same level:

$$W = W^w = (T^\Phi)' = \begin{bmatrix} \frac{t_{11}}{o_1} & \dots & \frac{t_{1j}}{o_1} & \dots & \frac{t_{1n}}{o_1} \\ \vdots & & \vdots & & \vdots \\ \frac{t_{i1}}{o_i} & \dots & \frac{t_{ij}}{o_i} & \dots & \frac{t_{in}}{o_i} \\ \vdots & & \vdots & & \vdots \\ \frac{t_{n1}}{o_n} & \dots & \frac{t_{nj}}{o_n} & \dots & \frac{t_{nn}}{o_n} \end{bmatrix}, \quad o_i = \sum_{j=1}^n t_{ij}. \quad (7)$$

Step 6: calculate the weights for each evaluation attribute. Equation (8) is iterated until the results converge to a stable limit supermatrix  $W^*$  to obtain the weights:

$$W^* = \lim_{\alpha \rightarrow \infty} (W^w)^\alpha. \quad (8)$$

### 3.2.3. Calculating Regional Innovation Capacity Using the MOORA-Min-Max Method

Step 1: establish a decision matrix. The decision matrix  $U = [u_{xy}]_{m \times n}$ ,  $x \in \{1, 2, \dots, m\}$ ,  $y \in \{1, 2, \dots, n\}$ , where  $m$  represents the number of regions,  $n$  represents the number of evaluation attributes, and  $u_{xy}$  represents the value of the  $y^{\text{th}}$  evaluation attribute in province  $x$  consisting of actual data from the 31 provinces in China.

Step 2: normalize the decision matrix. Given the quantitative variation among the indicators for the evaluation of regional innovation capacity, the decision matrix must be normalized. Equation (9) is rewritten as equation (10) based on the concept of range normalization:

$$u_{xy}^* = \frac{u_{xy}}{\sqrt{\sum_{x=1}^m u_{xy}^2}}, \quad (9)$$

$$u_{xy}^* = \frac{|u_y^{\max} - u_{xy}|}{(|u_y^{\max} - u_y^{\min}|)}. \quad (10)$$

Step 3: determine the gap ratio for each province. The gap ratio equation (11) is rewritten as equation (12) based on the normative decision matrix, and equation (13) is used to calculate the regional innovation capacity for each province:

$$Z_x^* = \sum_{y=1}^q w_y u_{xy}^* - \sum_{y=q+1}^n w_y u_{xy}^*, \quad (11)$$

$$Z_x^* = \sum_{y=1}^n w_y \cdot u_{xy}^*, \quad (12)$$

$$\text{RIC}_x = 1 - Z_x^*, \quad (13)$$

where  $w_y$  represents the weight of the  $y^{\text{th}}$  evaluation attribute,  $Z_x^*$  represents the gap ratio of regional innovation capacity in province  $x$ , and  $\text{RIC}_x$  represents the regional innovation capacity in province  $x$ .

#### 4. Empirical Study

This paper applies the constructed multiattribute decision-making evaluation model of regional innovation capacity to assess the regional innovation capacity of the 31 provinces in China and to explore ways to improve regional innovation capacity.

**4.1. Calculating the Direct Influence Strength between Evaluation Attributes Based on a Random Forest Model.** After the three-level interval discretization of the original data, the evaluation attributes are divided into 24 groups according to the individual evaluation attributes (called decision attributes  $x_1$ ) and 23 attributes (called conditional attributes  $x_2, x_3, \dots, x_{24}$ ). Then, learning curves are used to train random forest models. For example, “regional technology manpower investment (C1)” is set as a decision attribute, C2 to C24 are set as the conditional attributes, and a learning curve is used for parameter tuning. These steps are repeated to determine that the value of  $k$  is 20. After  $k$  is determined, the direct influence strength between the evaluation attributes is calculated using a random forest model to obtain 20 direct influence strength matrices; then, the initial influence strength matrix  $A$  is obtained via equation (1), as shown in Table 2.

**4.2. Drawing an Influence Strength Network Diagram and Calculating the Evaluation Attribute Weights Based on the DANP Method.** The DANP method uses DEMATEL to calculate the total influence strength matrix of the evaluation attributes and then solves the evaluation attribute weights, and the method is used to draw an influence strength network diagram.

This paper calculates the accuracy of the random forest model and verifies the consistency of the 20 direct influence strength matrices before calculating the total influence strength matrix to ensure the reliability of the evaluation results. The former step tests the accuracy of the influence strength calculated by the random forest models, and the latter step tests the consensus among the 20 direct influence strength matrices. The random forest model typically uses the out-of-bag error (OOB error) rate to measure the model quality. As shown in Table 3, the average OOB error is between 0.01 and 0.26, with the evaluation attribute “cooperation between enterprises and universities and research institutes (C8)” having the worst quality and an average OOB error of 0.26 with an average accuracy of 74.20%. The evaluation attribute “regional technology manpower investment (C1)” has the highest quality with an average accuracy of 99%. A consistency test among the 20 direct influence strength matrices yields an average consistency gap ratio of 3.129% (less than 5%), as shown in Table 4, indicating that the 20 direct influence strength matrices have a high degree of consensus and that the results are reliable.

The initial influence strength matrix  $A$  is transformed by using equations (2) and (3) to obtain the normalized initial influence strength matrix  $Y$ . Then, matrix  $Y$  is calculated according to (4) to obtain the total influence strength matrix  $T$  (Table 5). Finally, the degree of influence ( $g_i$ ), degree of being influenced ( $r_i$ ), centrality degree ( $c_i$ ), and causality degree ( $h_i$ ) for each evaluation attribute are calculated using equations (5) and (6) (Table 6). Table 6 shows that evaluation attributes C1, C2, C3, C6, C10, C11, C17, C19, C20, C21, C22, and C23 are the cause attributes and C4, C5, C7, C8, C9, C12, C13, C14, C15, C16, C18, and C24 are the result attributes. The influence strength network diagram is then drawn according to the calculated centrality and causality of each evaluation attribute (Figure 2).

The influence strength network diagram visualizes the importance and grouping of each evaluation attribute (cause or result attribute), but it remains challenging to demonstrate the complex associations among each attribute. This paper introduces the concept of the net influence strength  $\zeta$  to reflect the relation between each pair of attributes. The net influence strength  $\zeta$  is the relative magnitude of  $t_{ij}$  and  $t_{ji}$  in the total influence strength matrix  $T$ ,  $\zeta_{ij} = t_{ij} - t_{ji}$ . When  $\zeta_{ij} > 0$ , the  $i^{\text{th}}$  evaluation attribute greatly influences the  $j^{\text{th}}$  evaluation attribute, and  $C_i$  influences  $C_j$ ; when  $\zeta_{ij} < 0$ ,  $C_j$  influences  $C_i$ . For example,  $t_{13} = 0.013$  and  $t_{31} = 0.042$  in the total influence strength matrix  $T$ ,  $\zeta_{13} < 0$ , C3 influences C1, and thus,  $\zeta_{13} = 0$ ,  $\zeta_{13} = 1$  in the net influence strength matrix  $\zeta$ . Additionally, given that influence strength exists between two or more evaluation attributes,  $\zeta_{ij}$  is null when  $i = j$ . Similar calculations are repeated to obtain the net influence strength matrix  $\zeta$  (Table 7). For the  $i^{\text{th}}$  evaluation attribute,  $\zeta_{ij} = 1$  is grouped to obtain a net influence grouping for each evaluation attribute (Table 8). The number of net influence groupings indicates the net influence strength level of the

TABLE 2: Initial influence strength matrix.

A	C1	C2	C3	C4	C5	C6	C7	C8	C9	C10	C11	C12	C13	C14	C15	C16	C17	C18	C19	C20	C21	C22	C23	C24
C1	—	8.468	0.403	16.129	16.532	10.484	23.79	14.92	13.307	12.097	9.678	17.339	12.5	12.903	14.92	16.936	21.371	10.484	4.032	16.936	12.903	7.662	10.484	13.71
C2	8.871	—	0.403	18.952	12.097	10.887	28.629	17.339	10.887	11.291	7.662	15.323	14.516	14.516	14.113	8.871	7.661	10.081	6.855	10.887	5.242	6.452	10.081	10.484
C3	7.258	8.065	—	14.516	12.903	22.581	28.629	10.484	16.533	10.081	5.645	13.307	16.129	18.549	15.323	19.758	8.871	15.323	6.049	10.887	10.484	10.484	12.903	14.92
C4	9.678	8.468	3.629	—	111.694	9.678	31.855	27.42	14.92	4.839	6.452	8.871	13.307	18.145	15.726	19.758	14.516	8.065	5.645	10.081	9.678	7.662	10.484	16.533
C5	10.484	10.081	14.113	80.242	—	8.871	12.097	18.549	19.758	10.484	4.033	27.42	14.113	20.162	21.774	29.032	22.178	9.275	3.226	10.081	11.694	8.871	10.484	12.097
C6	11.291	10.081	3.629	15.726	14.92	—	41.129	25.807	9.275	8.871	6.049	15.323	27.823	10.887	14.92	19.758	11.694	60.081	4.839	10.887	16.129	8.065	18.145	38.71
C7	11.29	10.081	4.839	18.549	12.097	14.516	—	20.968	9.275	9.274	3.629	15.726	18.145	39.113	17.742	8.065	11.694	33.468	4.032	8.065	13.307	8.065	10.484	12.5
C8	13.307	7.258	3.629	14.516	22.178	13.307	14.516	—	14.516	8.871	5.242	22.178	23.387	9.678	8.871	18.952	4.839	32.662	2.823	10.081	10.081	17.339	10.484	30.645
C9	10.081	8.065	2.823	15.323	18.549	9.274	6.452	22.178	—	8.468	7.662	12.097	22.178	7.662	13.307	23.79	13.71	11.694	5.242	13.307	8.871	22.984	7.258	8.871
C10	14.92	8.065	2.419	13.307	17.339	14.92	9.274	20.161	9.678	—	7.662	16.532	31.855	12.903	20.161	18.952	11.694	14.92	5.645	11.291	16.129	4.839	6.452	23.387
C11	11.291	12.097	2.016	11.694	18.952	8.871	7.258	23.387	6.855	11.694	—	18.549	33.065	18.146	8.871	14.516	5.645	14.517	4.839	12.097	7.258	8.468	9.678	31.855
C12	8.871	7.662	2.016	17.742	17.339	10.081	11.694	12.5	9.678	11.694	6.049	—	37.097	20.565	14.113	35.081	8.871	18.145	5.645	11.291	14.516	6.855	8.468	14.516
C13	10.081	7.662	0.807	12.5	13.307	16.936	10.484	44.355	15.323	13.71	6.049	16.936	—	19.758	16.129	26.21	6.452	9.678	9.678	18.549	16.129	8.468	12.904	14.92
C14	8.468	7.258	2.823	16.936	44.758	18.549	38.71	14.92	8.871	11.694	8.871	13.307	10.081	—	13.71	16.533	11.291	27.016	5.242	8.065	8.065	7.258	10.081	6.452
C15	7.662	6.452	2.823	18.145	14.516	10.484	8.468	25	25	8.468	6.049	17.742	19.758	11.694	—	16.936	10.484	9.678	6.452	10.484	7.258	13.307	8.065	14.516
C16	5.242	6.452	6.452	13.307	44.758	10.484	30.242	28.226	17.742	7.258	4.839	20.161	29.839	15.726	11.694	—	14.516	12.097	5.242	10.081	10.484	13.71	14.92	14.516
C17	14.92	4.033	3.629	12.097	18.952	10.081	19.355	29.839	17.339	16.936	8.468	14.113	19.758	19.355	22.581	10.887	—	11.694	4.033	10.081	10.081	8.468	7.258	10.887
C18	6.452	11.291	4.032	12.097	16.533	31.855	14.113	12.097	14.113	5.645	5.242	14.92	11.291	16.936	22.178	16.936	8.468	—	7.662	12.5	8.871	12.5	10.081	23.387
C19	6.452	4.032	5.242	11.694	8.468	12.097	17.339	17.339	16.936	5.242	10.484	31.855	11.291	25.403	13.71	16.532	12.097	7.258	—	21.371	6.049	9.678	12.903	15.323
C20	8.871	8.065	4.839	12.903	13.71	16.936	17.742	27.016	14.113	5.645	9.678	27.823	20.565	20.565	12.904	11.694	5.242	7.258	4.032	—	12.5	8.065	17.742	11.291
C21	6.855	11.291	2.42	23.387	26.21	14.92	21.774	12.097	14.516	5.242	8.871	23.791	19.355	22.581	16.129	12.097	9.274	8.871	4.436	18.952	—	18.549	9.274	24.194
C22	7.258	8.871	3.629	14.517	17.742	16.533	12.5	19.355	12.5	5.645	7.662	20.565	12.5	20.565	20.968	11.694	4.839	10.484	1.613	10.887	13.71	—	8.871	21.774
C23	6.452	8.468	4.033	12.097	14.516	20.565	11.291	19.355	12.5	7.258	8.468	15.726	18.952	15.323	26.613	13.71	6.452	5.645	6.452	14.516	13.71	12.097	—	16.936
C24	7.258	11.694	2.419	14.113	8.065	15.323	24.194	23.387	10.484	7.258	7.258	10.484	18.549	16.533	25.403	22.581	7.258	22.178	13.307	16.129	17.742	12.5	9.678	—

TABLE 3: Average OOB error for each decision evaluation attribute.

Evaluation attribute	C1	C2	C3	C4	C5	C6	C7	C8	C9	C10	C11	C12	C13	C14	C15	C16	C17	C18	C19	C20	C21	C22	C23	C24
Average OOB	0.01	0.02	0.04	0.12	0.21	0.23	0.16	0.26	0.06	0.04	0.04	0.22	0.21	0.2	0.07	0.14	0.04	0.11	0.07	0.08	0.07	0.11	0.1	0.25
Accuracy (%)	99	98	95.7	88.1	78.6	77	84.5	74.2	93.8	95.6	96.1	78	79.3	80.5	93.1	85.9	95.7	88.6	93.1	91.6	93.1	89.3	90.2	74.7

oob\_ave $_{C_n} = \sum_{s=1}^k \text{oob}_{C_{n^k}}/k$ , where  $\text{oob}_{C_{n^k}}$  represents the out-of-bag error (OOB error) rate of the evaluation attribute  $C_n$  as the decision evaluation attribute in the  $k^{\text{th}}$  random forest model, where  $k = 20$ .



TABLE 4: Consistency test results for the 20 direct influence matrices.

Number of matrices	No. 1	No. 2	No. 3	No. 4	No. 5	No. 6	No. 7	No. 8	No. 9	No. 10	No. 11	No. 12	No. 13	No. 14	No. 15	No. 16	No. 17	No. 18	No. 19	No. 20	Average
$p$	0.07345	0.062409	0.043803	0.037418	0.038652	0.036685	0.031286	0.031428	0.032798	0.031113	0.031761	0.027984	0.027597	0.027436	0.027384	0.027191	0.028	0.027765	0.029973	0.031675	0.03529
$p$ (%)	7.345	6.241	4.38	3.742	3.865	3.668	3.129	3.143	3.28	3.111	3.176	2.798	2.76	2.744	2.738	2.719	2.8	2.777	2.997	3.167	3.529

$p = 1/n(n-1) \sum_{i=1}^n \sum_{j=1}^n |(f_{ij}^k - f_{ij}^{k-1}) / f_{ij}^k| < 5\%$ , where  $f_{ij}^k$  represents the elements of the average influence strength matrix derived from  $k$  direct influence strength matrices.

TABLE 5: Total influence strength matrix

T	C1	C2	C3	C4	C5	C6	C7	C8	C9	C10	C11	C12	C13	C14	C15	C16	C17	C18	C19	C20	C21	C22	C23	C24
C1	0.028	0.041	0.013	0.087	0.101	0.06	0.099	0.091	0.065	0.05	0.038	0.083	0.081	0.076	0.076	0.085	0.071	0.069	0.024	0.067	0.058	0.046	0.051	0.075
C2	0.041	0.022	0.011	0.085	0.086	0.056	0.102	0.088	0.056	0.045	0.032	0.073	0.078	0.073	0.069	0.064	0.042	0.064	0.028	0.051	0.04	0.04	0.047	0.064
C3	0.042	0.041	0.012	0.085	0.097	0.085	0.112	0.085	0.073	0.047	0.031	0.077	0.09	0.089	0.079	0.092	0.049	0.082	0.029	0.057	0.055	0.052	0.057	0.08
C4	0.056	0.05	0.026	0.096	0.3	0.071	0.131	0.134	0.084	0.045	0.037	0.088	0.099	0.104	0.095	0.111	0.073	0.08	0.032	0.065	0.063	0.056	0.062	0.095
C5	0.056	0.052	0.042	0.223	0.114	0.069	0.099	0.119	0.091	0.054	0.034	0.116	0.101	0.105	0.104	0.126	0.084	0.08	0.028	0.065	0.066	0.058	0.061	0.087
C6	0.058	0.053	0.022	0.103	0.118	0.058	0.149	0.131	0.071	0.052	0.037	0.096	0.127	0.091	0.094	0.108	0.063	0.179	0.032	0.068	0.076	0.058	0.076	0.14
C7	0.05	0.046	0.021	0.093	0.099	0.072	0.06	0.104	0.06	0.046	0.028	0.082	0.092	0.126	0.084	0.072	0.055	0.116	0.025	0.052	0.06	0.048	0.053	0.076
C8	0.054	0.041	0.019	0.088	0.115	0.07	0.086	0.067	0.07	0.045	0.031	0.095	0.104	0.073	0.07	0.094	0.043	0.113	0.024	0.057	0.056	0.066	0.054	0.111
C9	0.045	0.039	0.017	0.082	0.102	0.056	0.064	0.101	0.038	0.041	0.033	0.071	0.095	0.062	0.07	0.095	0.055	0.067	0.025	0.058	0.049	0.073	0.044	0.064
C10	0.057	0.042	0.017	0.084	0.105	0.071	0.075	0.105	0.061	0.028	0.035	0.085	0.12	0.078	0.088	0.093	0.055	0.08	0.029	0.059	0.066	0.043	0.046	0.096
C11	0.049	0.048	0.015	0.079	0.105	0.059	0.07	0.108	0.054	0.049	0.02	0.086	0.119	0.085	0.066	0.083	0.042	0.077	0.027	0.059	0.049	0.048	0.05	0.11
C12	0.045	0.041	0.016	0.092	0.109	0.062	0.081	0.091	0.061	0.05	0.032	0.054	0.129	0.092	0.077	0.122	0.05	0.084	0.028	0.059	0.063	0.046	0.05	0.079
C13	0.049	0.042	0.014	0.084	0.102	0.076	0.081	0.15	0.073	0.054	0.033	0.089	0.064	0.092	0.082	0.108	0.046	0.074	0.036	0.074	0.067	0.051	0.059	0.084
C14	0.046	0.041	0.019	0.099	0.16	0.079	0.131	0.095	0.061	0.051	0.037	0.081	0.08	0.057	0.079	0.089	0.057	0.105	0.027	0.053	0.052	0.047	0.053	0.067
C15	0.04	0.036	0.016	0.087	0.095	0.058	0.067	0.106	0.085	0.041	0.03	0.081	0.091	0.069	0.045	0.083	0.049	0.064	0.028	0.053	0.046	0.055	0.045	0.074
C16	0.043	0.042	0.027	0.097	0.164	0.068	0.119	0.126	0.081	0.045	0.032	0.098	0.122	0.091	0.079	0.064	0.065	0.081	0.029	0.06	0.06	0.063	0.065	0.085
C17	0.057	0.033	0.019	0.081	0.106	0.061	0.091	0.119	0.074	0.059	0.036	0.079	0.095	0.088	0.091	0.076	0.032	0.073	0.024	0.055	0.054	0.048	0.045	0.072
C18	0.04	0.047	0.019	0.08	0.1	0.101	0.084	0.086	0.067	0.037	0.03	0.079	0.079	0.083	0.09	0.086	0.048	0.053	0.031	0.059	0.051	0.055	0.051	0.095
C19	0.04	0.032	0.021	0.076	0.085	0.063	0.087	0.094	0.071	0.037	0.04	0.11	0.079	0.099	0.073	0.085	0.053	0.064	0.016	0.075	0.045	0.049	0.056	0.078
C20	0.044	0.04	0.021	0.08	0.096	0.073	0.088	0.113	0.066	0.038	0.038	0.103	0.097	0.09	0.072	0.077	0.041	0.065	0.024	0.035	0.058	0.047	0.065	0.072
C21	0.044	0.05	0.018	0.109	0.13	0.074	0.103	0.094	0.073	0.04	0.039	0.102	0.1	0.101	0.085	0.084	0.053	0.073	0.027	0.075	0.038	0.07	0.053	0.1
C22	0.04	0.041	0.018	0.082	0.101	0.07	0.077	0.096	0.062	0.036	0.033	0.087	0.079	0.087	0.085	0.074	0.039	0.068	0.019	0.054	0.058	0.03	0.047	0.089
C23	0.039	0.041	0.019	0.078	0.095	0.078	0.075	0.098	0.063	0.04	0.035	0.08	0.092	0.078	0.096	0.079	0.042	0.06	0.029	0.062	0.059	0.054	0.031	0.081
C24	0.043	0.049	0.017	0.085	0.09	0.074	0.105	0.111	0.064	0.042	0.035	0.075	0.096	0.087	0.099	0.099	0.047	0.095	0.043	0.069	0.069	0.058	0.053	0.054

TABLE 6: Regional innovation capacity evaluation attributes of centrality and causality.

Evaluation attribute	C1	C2	C3	C4	C5	C6	C7	C8	C9	C10	C11	C12	C13	C14	C15	C16	C17	C18	C19	C20	C21	C22	C23	C24
Degree of influence ( $g_i$ )	1.535	1.355	1.6	2.052	2.036	2.062	1.621	1.649	1.447	1.616	1.557	1.614	1.685	1.67	1.443	1.805	1.567	1.553	1.531	1.544	1.734	1.475	1.503	1.658
Degree of being influenced	1.106	1.009	0.461	2.236	2.776	1.665	2.236	2.515	1.625	1.07	0.807	2.07	2.309	2.075	1.949	2.15	1.255	1.967	0.665	1.443	1.361	1.263	1.272	2.026
( $r_i$ )																								
Centrality degree ( $c_i$ )	2.641	2.364	2.062	4.287	4.811	3.726	3.858	4.164	3.072	2.687	2.364	3.683	3.994	3.746	3.393	3.955	2.823	3.52	2.196	2.987	3.095	2.738	2.775	3.684
Ranking	20	22	24	2	1	8	6	3	14	19	21	10	4	7	12	5	16	11	23	15	13	18	17	9
Causality degree ( $h_i$ )	0.43	0.346	1.139	-0.184	-0.74	0.397	-0.615	-0.866	-0.178	0.546	0.75	-0.456	-0.624	-0.405	-0.506	-0.345	0.312	-0.414	0.865	0.101	0.373	0.212	0.231	-0.368
Group	Cause	Cause	Cause	Result	Result	Cause	Result	Result	Result	Cause	Cause	Result	Result	Result	Result	Result	Cause	Result	Cause	Cause	Cause	Cause	Cause	Result

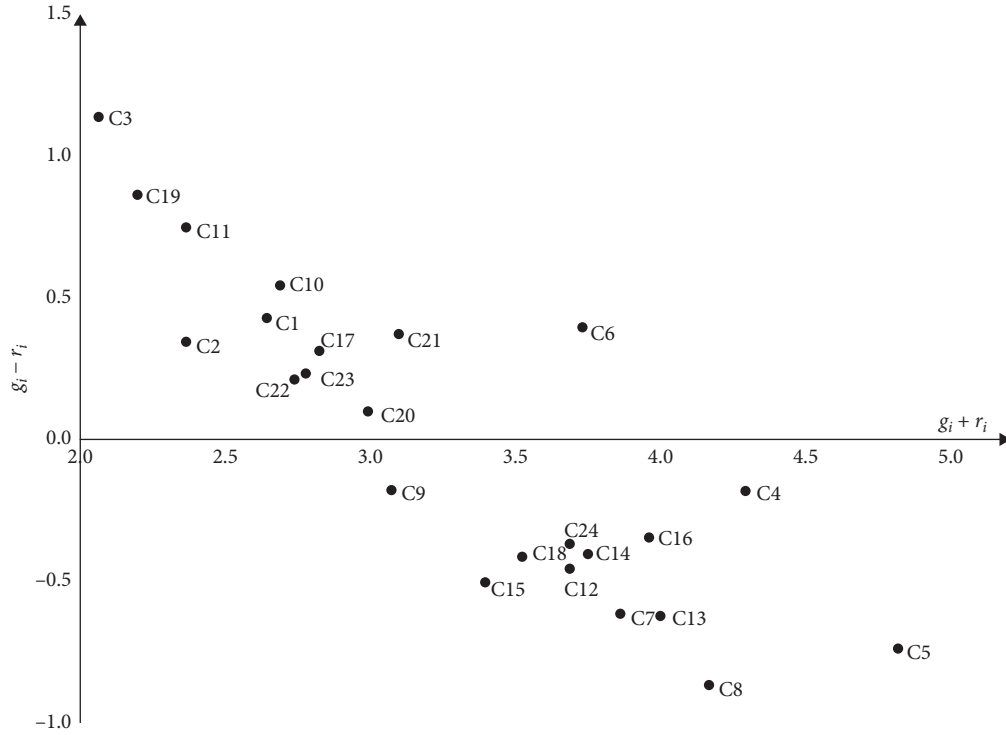


FIGURE 2: Influence strength network diagram.

TABLE 7: Net influence strength matrix

$\zeta$	C1	C2	C3	C4	C5	C6	C7	C8	C9	C10	C11	C12	C13	C14	C15	C16	C17	C18	C19	C20	C21	C22	C23	C24
C1	—	0	0	1	1	1	1	1	1	0	0	1	1	1	1	1	1	1	0	1	1	1	1	1
C2	1	—	0	1	1	1	1	1	1	1	0	1	1	1	1	1	1	1	0	1	0	0	1	1
C3	1	1	—	1	1	1	1	1	1	1	1	1	1	1	1	1	1	1	1	1	1	1	1	1
C4	0	0	0	—	1	0	1	1	1	0	0	0	1	1	1	1	0	0	0	0	0	0	0	1
C5	0	0	0	0	—	0	0	1	0	0	0	1	0	0	1	0	0	0	0	0	0	0	0	0
C6	0	0	0	1	1	—	1	1	1	0	0	1	1	1	1	1	1	1	0	0	1	0	0	1
C7	0	0	0	0	1	0	—	1	0	0	0	1	1	0	1	0	0	1	0	0	0	0	0	0
C8	0	0	0	0	0	0	0	—	0	0	0	1	0	0	0	0	0	1	0	0	0	0	0	0
C9	0	0	0	0	1	0	1	1	—	0	0	1	1	1	0	1	0	0	0	0	0	1	0	1
C10	1	0	0	1	1	1	1	1	1	—	0	1	1	1	1	1	0	1	0	1	1	1	1	1
C11	1	1	0	1	1	1	1	1	1	1	—	1	1	1	1	1	1	1	0	1	1	1	1	1
C12	0	0	0	1	0	0	0	0	0	0	0	—	1	1	0	1	0	1	0	0	0	0	0	1
C13	0	0	0	0	1	0	0	1	0	0	0	0	—	1	0	0	0	0	0	0	0	0	0	0
C14	0	0	0	0	1	0	1	1	0	0	0	0	0	—	1	0	0	1	0	0	0	0	0	0
C15	0	0	0	0	0	0	0	1	1	0	0	1	1	0	—	1	0	0	0	0	0	0	0	0
C16	0	0	0	0	1	0	1	1	0	0	0	0	1	1	0	—	0	0	0	0	0	0	0	0
C17	0	0	0	1	1	0	1	1	1	1	0	1	1	1	1	1	—	1	0	1	1	1	1	1
C18	0	0	0	1	1	0	0	0	1	0	0	0	1	0	1	1	0	—	0	0	0	0	0	0
C19	1	1	0	1	1	1	1	1	1	1	1	1	1	1	1	1	1	1	—	1	1	1	1	1
C20	0	0	0	1	1	1	1	1	1	0	0	1	1	1	1	1	0	1	0	—	0	0	1	1
C21	0	1	0	1	1	0	1	1	1	0	0	1	1	1	1	1	0	1	0	1	—	1	0	1
C22	0	1	0	1	1	1	1	1	0	0	0	1	1	1	1	1	0	1	0	1	0	—	0	1
C23	0	0	0	1	1	1	1	1	1	0	0	1	1	1	1	1	0	1	0	0	1	1	—	1
C24	0	0	0	0	1	0	1	1	0	0	0	0	1	1	1	1	0	1	0	0	0	0	0	—

evaluation attributes. When the number of net influence groupings is equal, further analysis of the net influence strength among these evaluation attributes is needed. For example, for the evaluation attributes C1, C2, and C10, the

net influence grouping is 18; in Table 8, C2 influences C1, and C10 and C10 influence C1. The relations between the evaluation attributes are clarified through net influence groupings, and the CISR is finally drawn (Figure 3).

TABLE 8: Net influence groupings.

Evaluation attribute	Net influence groupings	Number
C1	C4, C5, C6, C7, C8, C9, C12, C13, C14, C15, C16, C17, C18, C20, C21, C22, C23, C24	18
C2	C1, C4, C5, C6, C7, C8, C9, C10, C12, C13, C14, C15, C16, C17, C18, C20, C23, C24	18
C3	C1, C2, C4, C5, C6, C7, C8, C9, C10, C11, C12, C13, C14, C15, C16, C17, C18, C19, C20, C21, C22, C23, C24	23
C4	C5, C7, C8, C9, C13, C14, C15, C16, C24	9
C5	C8, C12, C15	3
C6	C4, C5, C7, C8, C9, C12, C13, C14, C15, C16, C17, C18, C21, C24	14
C7	C5, C8, C12, C13, C15, C18	6
C8	C12, C18	2
C9	C5, C7, C8, C12, C13, C14, C16, C22, C24	9
C10	C1, C4, C5, C6, C7, C8, C9, C12, C13, C14, C15, C16, C18, C20, C21, C22, C23, C24	18
C11	C1, C2, C4, C5, C6, C7, C8, C9, C10, C12, C13, C14, C15, C16, C17, C18, C20, C21, C22, C23, C24	21
C12	C4, C13, C14, C16, C18, C24	6
C13	C5, C8, C14	3
C14	C5, C7, C8, C15, C18	5
C15	C8, C9, C12, C13, C16	5
C16	C5, C7, C8, C13, C14	5
C17	C4, C5, C7, C8, C9, C10, C12, C13, C14, C15, C16, C18, C20, C21, C22, C23, C24	17
C18	C4, C5, C9, C13, C15, C16	6
C19	C1, C2, C4, C5, C6, C7, C8, C9, C10, C11, C12, C13, C14, C15, C16, C17, C18, C20, C21, C22, C23, C24	22
C20	C4, C5, C6, C7, C8, C9, C12, C13, C14, C15, C16, C18, C23, C24	14
C21	C2, C4, C5, C7, C8, C9, C12, C13, C14, C15, C16, C18, C20, C22, C24	15
C22	C2, C4, C5, C6, C7, C8, C12, C13, C14, C15, C16, C18, C20, C24	14
C23	C4, C5, C6, C7, C8, C9, C12, C13, C14, C15, C16, C18, C21, C22, C24	15
C24	C5, C7, C8, C13, C14, C15, C16, C18	8

The CISR illustrates that the “output capacity of R&D personnel in universities and research institutes (C3)” is the most prominent evaluation attribute of net influence strength and can be considered the most fundamental evaluation attribute, while the “cooperation between enterprises and universities and research institutes (C8)” is at the end of the CISR with the smallest net influence strength.

The unweighted supermatrix  $W$  and the weighted supermatrix  $W^w$  are obtained from equations (7) and (8), and multiplicative operations are performed on the weighted supermatrix  $W^w$  until the resultant convergent stable limit supermatrix  $W^*$  is obtained. Then, the weights for each evaluation attribute can be determined (Table 9).

**4.3. Calculating Regional Innovation Capacity Based on the MOORA-Min-Max Method.** This paper normalizes the data from the 31 provinces in China for 2017 using equations (10) and (12) and calculates the gap ratio, and the results are shown in Table 10. Finally, the regional innovation capacity and ranking of each province are calculated using equation (13), as shown in Table 11.

**4.4. Exploring Regional Innovation Capacity Improvement Pathways Based on CISR.** Table 11 illustrates the differences in regional innovation capacity among the 31

provinces in China. This paper explores regional innovation capacity improvement pathways to improve the imbalance in regional innovation capacity. Due to page limitations, the following presents an analysis of both the possible pathways for improving regional innovation capacity based on the CISR and the regional innovation capacity gap ratio using Sichuan and Inner Mongolia as examples.

As shown in Figure 4, Sichuan’s largest gap ratio is “enterprise new product development capability (C16),” which is influenced by “regional knowledge cooperation (C7),” “enterprise R&D personnel input capability (C12),” “enterprise R&D output capacity (C14),” “enterprise core technology level (C15),” and “regional talent training (C18)”: among these five evaluation attributes, C7 has the largest gap ratio. Therefore, regional knowledge cooperation could be enhanced to improve Sichuan’s regional innovation capacity. Inner Mongolia’s largest gap ratio is “output efficiency of R&D funds in universities and research institutes (C5),” which is influenced by “Enterprise R&D funding investment capacity (C13),” “enterprise R&D output capacity (C14),” “enterprise core technology level (C15),” and “enterprise new product development capability (C16)”: C16 has the largest gap ratio among these five attributes. Thus, Inner Mongolia should improve enterprises’ new product development capacity.

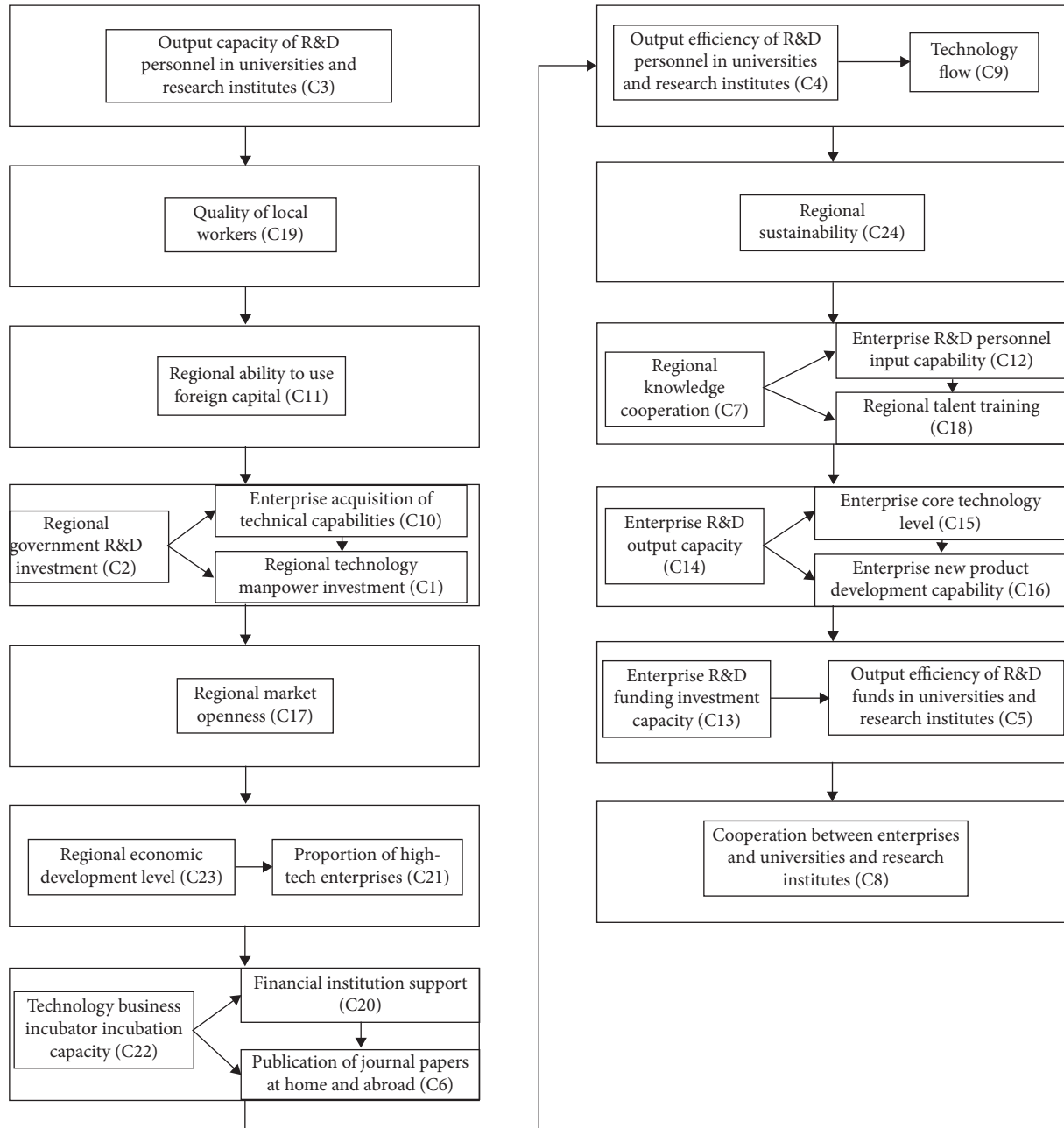


FIGURE 3: Critical influence strength roadmap (CISR).

**4.5. Management Implications of the Multiattribute Decision-Making Evaluation Model.** Regional innovation capacity provides a comprehensive description of regional innovation development. Improving regional innovation capacity does not involve only a single area of improvement but instead requires four main areas. (1) Knowledge creation: innovation resources are fundamental to knowledge creation. Regions need to increase investment in both human and material innovation

resources to increase innovation knowledge output. In addition, each region should improve the output efficiency of R&D personnel and R&D funding through measures such as optimizing the allocation of innovative resources. (2) Knowledge acquisition: cooperation is a meaningful way to fill resource gaps and achieve complementary strengths. Regional enterprises should strengthen financial support for universities and research institutes and actively introduce advanced technologies



TABLE 9: Regional innovation capacity evaluation attribute weights.

Evaluation attributes	C1	C2	C3	C4	C5	C6	C7	C8	C9	C10	C11	C12	C13	C14	C15	C16	C17	C18	C19	C20	C21	C22	C23	C24
Weights	0.0282	0.0257	0.0121	0.0581	0.0717	0.0423	0.0559	0.064	0.0414	0.0273	0.0202	0.052	0.0582	0.0524	0.0493	0.0552	0.0321	0.0504	0.0171	0.0362	0.0348	0.0325	0.0322	0.0507

Gap ratio	C1	C2	C3	C4	C5	C6	C7	C8	C9	C10	C11	C12	C13	C14	C15	C16	C17	C18	C19	C20	C21	C22	C23	C24
Beijing	0	0	0.0097	0	0.0118	0	0.0285	0.0487	0	0.0213	0.0086	0.0083	0.011	0.0037	0	0.0241	0.0228	0.0439	0	0.0193	0	0.0207	0	0.0035
Tianjin	0.0136	0.0216	0.0103	0.0472	0.0551	0.0278	0.0421	0.0291	0.0326	0.0259	0.0108	0	0.0033	0.0391	0.0267	0.0134	0.0179	0.05	0.008	0.0329	0.0184	0.0293	0.0032	0.0029
Hebei	0.0255	0.0249	0.0115	0.0524	0.0598	0.0341	0.045	0.0516	0.0352	0.0249	0.02	0.0352	0.0297	0.0494	0.0473	0.0413	0.0271	0.0443	0.0161	0.0316	0.0308	0.0274	0.0268	0.0359
Shanxi	0.026	0.0255	0.0105	0.05	0.0462	0.0291	0.0435	0.0368	0.0364	0.0262	0.0201	0.0438	0.0382	0.0519	0.0438	0.0462	0.0295	0.0401	0.014	0.0336	0.032	0.0296	0.0279	0.0243
Inner Mongolia	0.026	0.0257	0.0121	0.0577	0.0717	0.0345	0.0429	0.0546	0.0384	0.0266	0.0199	0.0368	0.0325	0.042	0.0454	0.0474	0.0303	0.0418	0.0126	0.0334	0.0314	0.0287	0.0209	0.0247
Liaoning	0.0243	0.0224	0.0107	0.0371	0.0415	0.0162	0.039	0.0165	0.0355	0.0238	0.0167	0.0336	0.0163	0.0382	0.0381	0.0322	0.0218	0.0454	0.013	0.0336	0.0268	0.0273	0.0242	0.0243
Jilin	0.0251	0.0238	0.0099	0.0465	0.0257	0.0184	0.0415	0.0492	0.0375	0.0262	0.0201	0.0398	0.0488	0.0524	0.0493	0.0364	0.0295	0.0437	0.014	0.0354	0.0261	0.0289	0.0238	0.007
Heilongjiang	0.0261	0.0236	0.0094	0.0273	0	0.0022	0.0323	0	0.0394	0.0267	0.0201	0.0398	0.0252	0.0547	0.0446	0.0476	0.0301	0.0423	0.0147	0.0355	0.0302	0.0296	0.0279	0.0137
Shanghai	0.0113	0.014	0.0107	0.0218	0.0433	0.0154	0.0434	0.0486	0.0261	0.0041	0	0.0197	0.0061	0.02	0.026	0.011	0	0.0466	0.0058	0.0315	0.0188	0.0281	0.0008	0.0089
Jiangsu	0.0128	0.0247	0.0093	0.0357	0.0402	0.034	0.0515	0.0323	0.0215	0.0191	0.0141	0.0205	0.0138	0.0315	0.037	0.0255	0.016	0.0504	0.013	0.0203	0.0206	0	0.007	0.0434
Zhejiang	0.0126	0.0251	0.0094	0.0378	0.0289	0.0407	0.0554	0.0089	0.0315	0.023	0.0168	0.0137	0	0.0446	0.0461	0	0.016	0.0466	0.0137	0.0205	0.0274	0.0172	0.0118	0.0284
Anhui	0.0238	0.0236	0.0064	0.036	0.0307	0.0361	0.0528	0.0484	0.0359	0.0258	0.0199	0.0227	0.0228	0	0.0393	0.0229	0.0283	0.0425	0.0163	0.0317	0.0261	0.0276	0.0274	0.0168
Fujian	0.0207	0.025	0.0109	0.0433	0.0462	0.0394	0.0552	0.0361	0.0379	0.0215	0.017	0.0371	0.024	0.0394	0.0453	0.0439	0.0219	0.0484	0.0139	0.0271	0.0298	0.0275	0.0148	0.0142
Jiangxi	0.0259	0.0254	0.011	0.0547	0.0656	0.0347	0.0493	0.0347	0.0375	0.025	0.0194	0.0439	0.037	0.0408	0.0473	0.0407	0.0284	0.0396	0.0168	0.0326	0.0225	0.0283	0.0274	0.0119
Henan	0.0219	0.0252	0.0114	0.0455	0.0598	0.0388	0.0521	0.0371	0.0269	0.0199	0.0189	0.0284	0.0187	0.0333	0.045									

Gap ratio	C1	C2	C3	C4	C5	C6	C7	C8	C9	C10	C11	C12	C13	C14	C15	C16	C17	C18	C19	C20	C21	C22	C23	C24
Beijing	0	0	0.0097	0	0.0118	0	0.0285	0.0487	0	0.0213	0.0086	0.0083	0.011	0.0037	0	0.0241	0.0228	0.0439	0	0.0193	0	0.0207	0	0.0035
Tianjin	0.0136	0.0216	0.0103	0.0472	0.0551	0.0278	0.0421	0.0291	0.0326	0.0259	0.0108	0	0.0033	0.0391	0.0267	0.0134	0.0179	0.05	0.008	0.0329	0.0184	0.0293	0.0032	0.0029
Hebei	0.0255	0.0249	0.0115	0.0524	0.0598	0.0341	0.045	0.0516	0.0352	0.0249	0.02	0.0352	0.0297	0.0494	0.0473	0.0413	0.0271	0.0443	0.0161	0.0316	0.0308	0.0274	0.0268	0.0359
Shanxi	0.026	0.0255	0.0105	0.05	0.0462	0.0291	0.0435	0.0368	0.0364	0.0262	0.0201	0.0438	0.0382	0.0519	0.0438	0.0462	0.0295	0.0401	0.014	0.0336	0.032	0.0296	0.0279	0.0243
Inner Mongolia	0.026	0.0257	0.0121	0.0577	0.0717	0.0345	0.0429	0.0546	0.0384	0.0266	0.0199	0.0368	0.0325	0.042	0.0454	0.0474	0.0303	0.0418	0.0126	0.0334	0.0314	0.0287	0.0209	0.0247
Liaoning	0.0243	0.0224	0.0107	0.0371	0.0415	0.0162	0.039	0.0165	0.0355	0.0238	0.0167	0.0336	0.0163	0.0382	0.0381	0.0322	0.0218	0.0454	0.013	0.0336	0.0268	0.0273	0.0242	0.0243
Jilin	0.0251	0.0238	0.0099	0.0465	0.0257	0.0184	0.0415	0.0492	0.0375	0.0262	0.0201	0.0398	0.0488	0.0524	0.0493	0.0364	0.0295	0.0437	0.014	0.0354	0.0261	0.0289	0.0238	0.007
Heilongjiang	0.0261	0.0236	0.0094	0.0273	0	0.0022	0.0323	0	0.0394	0.0267	0.0201	0.0398	0.0252	0.0547	0.0446	0.0476	0.0301	0.0423	0.0147	0.0355	0.0302	0.0296	0.0279	0.0137
Shanghai	0.0113	0.014	0.0107	0.0218	0.0433	0.0154	0.0434	0.0486	0.0261	0.0041	0	0.0197	0.0061	0.02	0.026	0.011	0	0.0466	0.0058	0.0315	0.0188	0.0281	0.0008	0.0089
Jiangsu	0.0128	0.0247	0.0093	0.0357	0.0402	0.034	0.0515	0.0323	0.0215	0.0191	0.0141	0.0205	0.0138	0.0315	0.037	0.0255	0.016	0.0504	0.013	0.0203	0.0206	0	0.007	0.0434
Zhejiang	0.0126	0.0251	0.0094	0.0378	0.0289	0.0407	0.0554	0.0089	0.0315	0.023	0.0168	0.0137	0	0.0446	0.0461	0	0.016	0.0466	0.0137	0.0205	0.0274	0.0172	0.0118	0.0284
Anhui	0.0238	0.0236	0.0064	0.036	0.0307	0.0361	0.0528	0.0484	0.0359	0.0258	0.0199	0.0227	0.0228	0	0.0393	0.0229	0.0283	0.0425	0.0163	0.0317	0.0261	0.0276	0.0274	0.0168
Fujian	0.0207	0.025	0.0109	0.0433	0.0462	0.0394	0.0552	0.0361	0.0379	0.0215	0.017	0.0371	0.024	0.0394	0.0453	0.0439	0.0219	0.0484	0.0139	0.0271	0.0298	0.0275	0.0148	0.0142
Jiangxi	0.0259	0.0254	0.011	0.0547	0.0656	0.0347	0.0493	0.0347	0.0375	0.025	0.0194	0.0439	0.037	0.0408	0.0473	0.0407	0.0284	0.0396	0.0168	0.0326	0.0225	0.0283	0.0274	0.0119
Henan	0.0219	0.0252	0.0114	0.0455	0.0598	0.0388	0.0521	0.0371	0.0269	0.0199	0.0189	0.0284	0.0187	0.0333	0.045	0.0379	0.0228	0.0491	0.0147	0	0.0285	0.0158	0.018	0.047
Hubei	0.0251	0.0256	0.0101	0.0505	0.0528	0.0365	0.049	0.0408	0.0374	0.0259	0.02	0.0413	0.0399	0.0489	0.0478	0.0457	0.0284	0.044	0.0167	0.0279	0.0286	0.0216	0.0264	0.028
Hunan	0.0235	0.0232	0.0095	0.0409	0.0478	0.0212	0.0418	0.0305	0.0269	0.0235	0.0196	0.0264	0.0195	0.0371	0.0439	0.029	0.0296	0.0465	0.0134	0.0278	0.0266	0.0198	0.022	0.017
Guangdong	0.0246	0.0248	0.0105	0.0453	0.0572	0.0307	0.0487	0.0242	0.038	0.0255	0.0196	0.0326	0.0155	0.0363	0.0436	0.0198	0.0305	0.0447	0.0153	0.0324	0.027	0.0277	0.0255	0.0168
Guangxi	0.0172	0.0243	0.0104	0.0375	0.0373	0.0423	0.0559	0.0338	0.0097	0	0.0154	0.0265	0.0073	0.0099	0.0222	0.012	0.0049	0.0462	0.0144	0.0275	0.0162	0.0058	0.0154	0.0507
Guangxi	0.0273	0.0248	0	0.0308	0.0045	0.003	0.0411	0.0545	0.0097	0.0265	0.0199	0.0501	0.048	0.0265	0.0465	0.0446	0.0262	0.0367	0.0171	0.0358	0.0288	0.0308	0.0291	0.013
Hainan	0.0271	0.0241	0.0095	0.0517	0.0462	0.0129	0.0162	0.064	0.0401	0.0272	0.0134	0.0341	0.0468	0.0353	0.028	0.0489	0.0257	0.0323	0.0148	0.0362	0.0138	0.0313	0.0258	0
Chungking	0.0231	0.0244	0.0105	0.0407	0.0444	0.0281	0.0469	0.0214	0.0367	0.0194	0.0188	0.0261	0.0089	0.04	0.043	0.0128	0.026	0.0426	0.0145	0.0309	0.0219	0.0296	0.021	0.0108
Sichuan	0.025	0.0207	0.0082	0.0403	0.0417	0.0267	0.0445	0.0408	0.03	0.0253	0.0199	0.0338	0.0346	0.0288	0.0407	0.0458	0.0285	0.0417	0.0158	0.0279	0.0252	0.0258	0.027	0.0234
Guizhou	0.0272	0.025	0.0066	0.0471	0.037	0.0314	0.0333	0.0454	0.0376	0.0259	0.0201	0.0365	0.0391	0.0313	0.0459	0.052	0.0311	0.029	0.0163	0.0332	0.0279	0.0313	0.0292	0.018
Yunnan	0.0268	0.0244	0.0106	0.0509	0.0509	0.032	0.0399	0.0518	0.038	0.0262	0.0201	0.0352	0.033	0.041	0.0445	0.0496	0.0296	0.0306	0.0167	0.0354	0.0296	0.0298	0.0304	0.0158
Tibet	0.0282	0.0252	0.0079	0.0581	0.0499	0.0324	0.0437	0.0618	0.0414	0.0273	0.02	0.052	0.0582	0.0474	0.0481	0.0546	0.0314	0	0.0168	0.0362	0.026	0.0325	0.0288	0.0018
Shaanxi	0.0231	0.0171	0.0078	0.0338	0.0386	0.0003	0.0264	0.0534	0.0303	0.0262	0.0194	0.0319	0.0293	0.0414	0.0406	0.0486	0.0284	0.0424	0.0138	0.0344	0.0246	0.0273	0.023	0.0134
Gansu	0.027	0.0226	0.0098	0.0488	0.0486	0.0064	0.0221	0.0429	0.0387	0.0272	0.0198	0.0384	0.0415	0.0394	0.045	0.0551	0.031	0.0229	0.0144	0.0353	0.0276	0.0296	0.0322	0.0105
Qinghai	0.0268	0.0246	0.0106	0.0534	0.0533	0.0248	0.0283	0.0555	0.0402	0.0273	0.0202	0.0471	0.0476	0.0487	0.0534	0.0321	0.0263	0.0154	0.0362	0.0252	0.0322	0.0272	0.0105	
Ningxia	0.0257	0.0238	0.0104	0.0456	0.0441	0.0329	0.0346	0.0625	0.0402	0.0271	0.0174	0.0362	0.0346	0.0266	0.0456	0.047	0.0297	0.0361	0.0137	0.0362	0.0333	0.0318	0.0251	0.0168
Sinkiang	0.0276	0.0255	0.0105	0.0486	0.0446	0.0069	0	0.0598	0.0397	0.0272	0.0202	0.0507	0.0472	0.0275	0.0479	0.0552	0.0263	0.0309	0.0126	0.0361	0.0348	0.0305	0.0269	0.0244

TABLE 11: Regional innovation capacity and ranking of China's 31 provinces.

Region	RIC	Ranking
Beijing	0.7141	1
Shanghai	0.538	2
Guangdong	0.4572	3
Tianjin	0.4388	4
Zhejiang	0.4239	5
Jiangsu	0.4059	6
Heilongjiang	0.3704	7
Chungking	0.3575	8
Liaoning	0.3416	9
Anhui	0.3363	10
Hubei	0.333	11
Shaanxi	0.3243	12
Hainan	0.2947	13
Hunan	0.2883	14
Shandong	0.2835	15
Sichuan	0.2779	16
Guangxi	0.2672	17
Gansu	0.2633	18
Fujian	0.2595	19
Guizhou	0.2427	20
Jilin	0.2409	21
Sinkiang	0.2381	22
Ningxia	0.2232	23
Yunnan	0.2092	24
Jiangxi	0.1996	25
Qinghai	0.1984	26
Shanxi	0.1947	27
Henan	0.181	28
Hebei	0.1721	29
Tibet	0.1704	30
Inner Mongolia	0.1619	31

both domestically and abroad. Regional R&D personnel should develop cooperation between science, technology, and innovation research to improve the output of scientific and technological papers and other results. Local governments should develop regionally appropriate policies to encourage foreign funding for regional innovation development. (3) Enterprise innovation: as essential participants in innovation transformation, enterprises must increase the output of their innovation results by increasing resource investment and conducting research on core technology. Additionally, enterprises should improve their new product development capabilities to achieve economic benefits. (4) Innovation environment: a good innovation environment is an important prerequisite for regional innovation development. Regions need to improve their talent training systems by increasing spending on education. Innovation intermediaries should fully play their role in supporting regional innovation by providing financial and facility resources for regional innovation. Finally, regional innovation should consider energy consumption, environmental pollution, and other issues to achieve sustainable innovation.

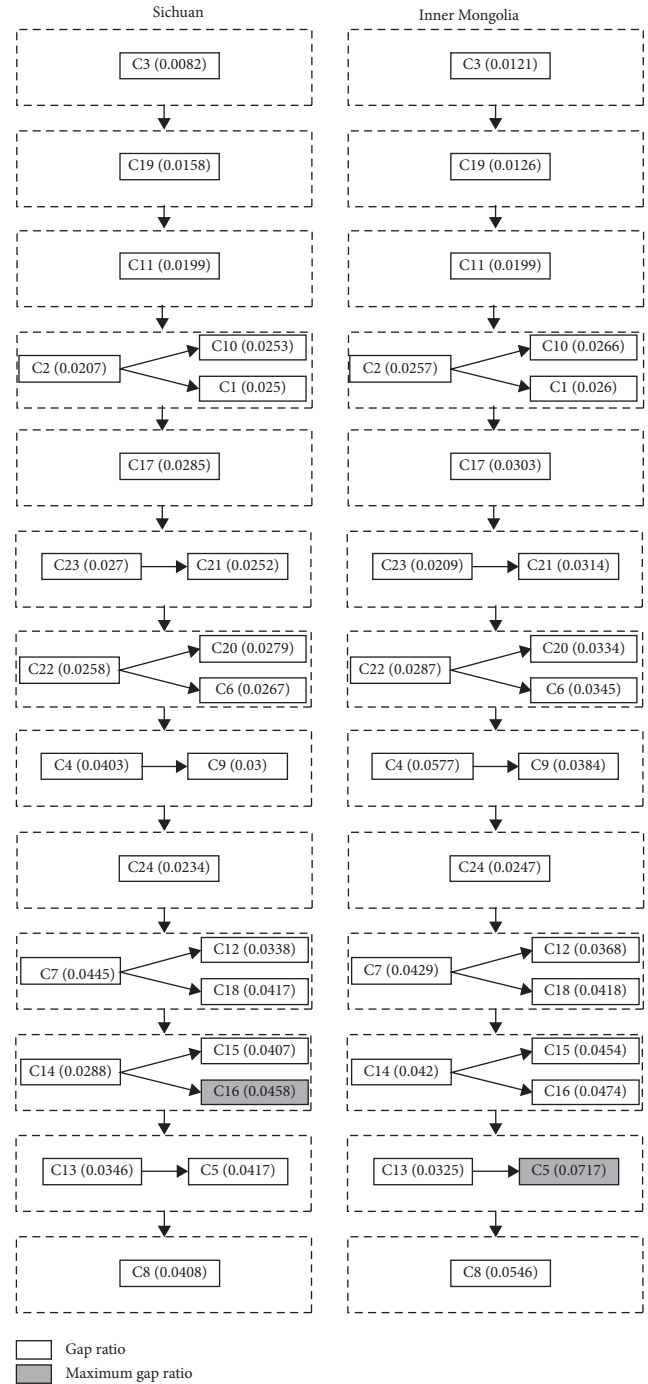


FIGURE 4: Regional innovation capacity improvement route.

## 5. Conclusion

This paper builds a multiattribute decision-making evaluation model of regional innovation capacity. The model uses a random forest model to determine the influence strength between evaluation attributes and obtains the objective weights of the evaluation attributes using the DANP method. Finally, the MOORA-min-max method is employed to calculate the

regional innovation capacity in each of China's 31 provinces and to explore regional innovation capacity improvement pathways. The empirical results suggest the following: (1) "Output capacity of R&D personnel in universities and research institutes (C3)" is the most fundamental evaluation attribute; this may be due to China's growing emphasis on industry-university-research as innovation-driven development strategies are proposed. Colleges and research institutes are essential subjects of industry-university-research. Therefore, C3 is the most fundamental evaluation attribute. (2) "Output efficiency of R&D funds in universities and research institutes (C5)" is the evaluation attribute with the largest weight. Given the emphasis on resource efficiency in regional innovation, C5 carries the greatest weight in regional innovation capacity evaluations. (3) Regional innovation capacity is an integrated reflection of innovation development, and enhancing regional innovation capacity involves identifying and addressing critical constraints.

Despite our efforts, two limitations provide ideas for future research. First, the evaluation indicator system constructed by different methods and innovation evaluation indicators (e.g., innovation policy) that are more difficult to monitor can affect the evaluation results, and future research needs to explore a more efficient evaluation indicator system. Second, the multiattribute decision-making evaluation model for regional innovation capacity proposed in this paper is a data-driven approach, and the parameters of the evaluation model ignore the subjective preferences of decision-makers, which should be considered in the future.

## Data Availability

The readers can access the data from publicly published statistical yearbooks and government reports via the following links: <http://www.istic.ac.cn/tabid/640/default.aspx>, <http://www.most.gov.cn/>, <http://www.cnipa.gov.cn/tjxx/index.htm>, <http://www.saic.gov.cn/>, <http://www.stats.gov.cn/tjsj/ndsj/>, <http://tongji.cnki.net/kns55/navi/HomePage.aspx?id=N2019030267&name=YBVCX&floor=1>, <http://data.cnki.net/area/Yearbook/Single/N2018050242?z=D18>, <http://tongji.cnki.net/kns55/navi/HomePage.aspx?id=N2012110073&name=YZGJN>, <http://data.cnki.net/trade/Yearbook/Single/N201901Z0258?z=018>, <https://bbs.pinggu.org/thread-7955189-1-1.html>, <https://www.istic.ac.cn/tabid/640/default.aspx>, <http://www.most.gov.cn/>, <http://www.cnipa.gov.cn/tjxx/index.htm>, <http://www.saic.gov.cn/>, and <http://www.innofund.gov.cn/>.

## Conflicts of Interest

The authors declare that they have no conflicts of interest.

## Acknowledgments

This work was supported by the National Natural Science Foundation of China (71774036), Natural Science Foundation of Heilongjiang Province (QC2018088), and the Special Foundation of Central Universities Basic Research Fee (3072020CFW0904 and 3072020CFW0907).

## References

- [1] Y. Su and X. L. An, "Application of threshold regression analysis to study the impact of regional technological innovation level on sustainable development," *Renewable & Sustainable Energy Reviews*, vol. 89, pp. 27–32, 2018.
- [2] X. Tian and J. Wang, "Research on the disequilibrium development of output of regional innovation based on R&D personnel," *Sustainability*, vol. 10, no. 8, p. 2708, 2018.
- [3] K. Xu, L. Loh, and Q. Chen, "Sustainable innovation governance: an analysis of regional innovation with a super efficiency slack-based measure model," *Sustainability*, vol. 12, no. 7, p. 3008, 2020.
- [4] M. Piazza, E. Mazzola, L. Abbate, and G. Perrone, "Network position and innovation capability in the regional innovation network," *European Planning Studies*, vol. 27, no. 9, pp. 1857–1878, 2019.
- [5] L. Sleuwaegen and P. Boiardi, "Creativity and regional innovation: evidence from EU regions," *Research Policy*, vol. 43, no. 9, pp. 1508–1522, 2014.
- [6] J. Chen, L. Wang, and Y. Li, "Natural resources, urbanization and regional innovation capabilities," *Resources Policy*, vol. 66, p. 101643, 2020.
- [7] A.-B. Heindl and I. Liefner, "The Analytic Hierarchy Process as a methodological contribution to improve regional innovation system research: explored through comparative research in China," *Technology in Society*, vol. 59, Article ID 101197, 2019.
- [8] X. Pan, Y. Ming, M. Li, S. Guo, and C. Han, "Inter-regional innovation correlation effects and influencing factors in China," *Business Process Management Journal*, vol. 26, no. 4, 2019.
- [9] Y. Su and Y.-q. Yu, "Spatial agglomeration of new energy industries on the performance of regional pollution control through spatial econometric analysis," *Science of the Total Environment*, vol. 704, Article ID 135261, 2020.
- [10] H. A. R. M. van den Heiligenberg, G. J. Heimeriks, M. P. Hekkert, and F. G. van Oort, "A habitat for sustainability experiments: success factors for innovations in their local and regional contexts," *Journal of Cleaner Production*, vol. 169, pp. 204–215, 2017.
- [11] D. Shan, "Research of the construction of regional innovation capability evaluation system: based on indicator analysis of hangzhou and ningbo," *Procedia Engineering*, vol. 174, pp. 1244–1251, 2017.
- [12] S. Hamidi, A. Zandiatashbar, and A. Bonakdar, "The relationship between regional compactness and regional innovation capacity (RIC): empirical evidence from a national study," *Technological Forecasting and Social Change*, vol. 142, pp. 394–402, 2019.
- [13] Y. Tang, Y. Chen, K. Wang, H. Xu, and X. Yi, "An analysis on the spatial effect of absorptive capacity on regional innovation ability based on empirical research in China," *Sustainability*, vol. 12, no. 7, p. 3021, 2020.
- [14] C. Hauser, M. Siller, T. Schatzer, J. Walde, and G. Tappeiner, "Measuring regional innovation: a critical inspection of the ability of single indicators to shape technological change," *Technological Forecasting and Social Change*, vol. 129, pp. 43–55, 2018.
- [15] Y. Su and T. Li, "Simulation analysis of knowledge transfer in a knowledge alliance based on a circular surface radiator model," *Complexity*, vol. 2020, Article ID 4301489, 27 pages, 2020.

- [16] J. M. Zabala-Iturriagoitia, P. Voigt, A. Gutiérrez-Gracia, and F. Jiménez-Sáez, "Regional innovation systems: how to assess performance," *Regional Studies*, vol. 41, no. 5, pp. 661–672, 2007.
- [17] S. L. Zhao, L. Cacciolatti, S. H. Lee, and W. Song, "Regional collaborations and indigenous innovation capabilities in China: a multivariate method for the analysis of regional innovation systems," *Technological Forecasting and Social Change*, vol. 94, pp. 202–220, 2015.
- [18] Z. J. Acs, L. Anselin, and A. Varga, "Patents and innovation counts as measures of regional production of new knowledge," *Research Policy*, vol. 31, no. 7, pp. 1069–1085, 2002.
- [19] P. Fan, "Innovation in China," *Journal of Economic Surveys*, vol. 28, no. 4, pp. 725–745, 2014.
- [20] F. Quatraro, "Diffusion of regional innovation capabilities: evidence from Italian patent data," *Regional Studies*, vol. 43, no. 10, pp. 1333–1348, 2009.
- [21] C.-H. Yang, C.-M. Lee, and C.-H. A. Lin, "Why does regional innovative capability vary so substantially in China? The role of regional innovation systems," *Asian Journal of Technology Innovation*, vol. 20, no. 2, pp. 239–255, 2012.
- [22] S. Han, G. M. Yoo, and S. Kwak, "A comparative analysis of regional innovation characteristics using an innovation actor framework," *Science, Technology and Society*, vol. 23, no. 1, pp. 137–162, 2018.
- [23] W.-l. Chen and C.-j. Wang, "Study of the construction of assessment system on regional innovation capacity in knowledge management," *Procedia Engineering*, vol. 29, pp. 1830–1834, 2012.
- [24] H. Wang, L. An, and X. Zhang, "Evaluation of regional innovation ability based on green and low-carbon perspective," *Bulgarian Chemical Communications*, vol. 49, pp. 55–58, 2017.
- [25] X. Liu, T. Gao, and X. Wang, "The measure of regional innovation capability," in *Regional Innovation Index of China: 2017: How Frontier Regions Innovate*, pp. 3–13, Springer, Singapore, 2018.
- [26] Q. Yan and R. Y. Hou, "Evaluation of regional scientific and technological innovation capability and empirical research," *Agro Food Industry Hi-Tech*, vol. 28, no. 1, pp. 3179–3181, 2017.
- [27] J. Xu and J. Zhai, "Research on the evaluation of green innovation capability of manufacturing enterprises in innovation network," *Sustainability*, vol. 12, no. 3, p. 807, 2020.
- [28] K. Q. Sheng and S. F. Liu, "On evaluation system for regional scientific and technical innovation ability and a positive study of 5 cities in south of Jiangsu," *Journal of Grey System*, vol. 27, no. 4, pp. 92–103, 2015.
- [29] C. Yang, Q. Zhang, and S. Ding, "An evaluation method for innovation capability based on uncertain linguistic variables," *Applied Mathematics and Computation*, vol. 256, pp. 160–174, 2015.
- [30] Z. Zhen, "A novel model for enterprise technological innovation capability evaluation with 2-tuple linguistic information," *Journal of Intelligent & Fuzzy Systems*, vol. 31, no. 1, pp. 541–546, 2016.
- [31] L. Li, R. Wang, and X. Li, "Grey fuzzy comprehensive evaluation of regional financial innovation ability based on two types weights," *Grey Systems: Theory and Application*, vol. 6, no. 2, pp. 187–202, 2016.
- [32] Y. Su and W. Sun, "Analyzing a closed-loop supply chain considering environmental pollution using the NSGA-II," *Ieee Transactions on Fuzzy Systems*, vol. 27, no. 5, pp. 1066–1074, 2019.
- [33] L. Breiman, "Random forests," *Machine Learning*, vol. 45, no. 1, pp. 5–32, 2001.
- [34] T. Parr, K. Turgutlu, C. Csiszar, and J. Howard, "Beware default random forest importances," *March*, vol. 26, 2018.
- [35] P. Cooke, M. G. Uranga, and G. Etxebarria, "Regional systems of innovation: an evolutionary perspective," *Environment and Planning A: Economy and Space*, vol. 30, no. 9, pp. 1563–1584, 1998.
- [36] H. Jiao, J. Zhou, T. Gao, and X. Liu, "The more interactions the better? The moderating effect of the interaction between local producers and users of knowledge on the relationship between R&D investment and regional innovation systems," *Technological Forecasting and Social Change*, vol. 110, pp. 13–20, 2016.
- [37] Z. Wang, Q. He, S. Xia, D. Sarpong, A. Xiong, and G. Maas, "Capacities of business incubator and regional innovation performance," *Technological Forecasting and Social Change*, vol. 158, Article ID 120125, 2020.
- [38] Z. Yang, T. Ouyang, X. Fu, and X. Peng, "A decision-making algorithm for online shopping using deep-learning-based opinion pairs mining and q-rung orthopair fuzzy interaction Heronian mean operators," *International Journal of Intelligent Systems*, vol. 35, no. 5, pp. 783–825, 2020.
- [39] S. L. Zhao, W. Song, D. Y. Zhu, X. B. Peng, and W. Cai, "Evaluating China's regional collaboration innovation capability from the innovation actors perspective-An AHP and cluster analytical approach," *Technology in Society*, vol. 35, no. 3, pp. 182–190, 2013.
- [40] J. J. H. Liou, Y.-C. Chuang, E. K. Zavadskas, and G.-H. Tzeng, "Data-driven hybrid multiple attribute decision-making model for green supplier evaluation and performance improvement," *Journal of Cleaner Production*, vol. 241, Article ID 118321, 2019.

## Research Article

# Self-Organized Criticality and Trend Analysis in Time Series of Blackouts for the China Power Grid

Qun Yu <sup>1</sup>, Na Cao,<sup>1</sup> Qilin Liu,<sup>1</sup> Yuqing Qu,<sup>2</sup> and Yumin Zhang <sup>1</sup>

<sup>1</sup>School of Electrical Engineering and Automation, Shandong University of Science and Technology, Qingdao 266590, China

<sup>2</sup>Key Laboratory of the Ministry of Education on Smart Power Grids, Tianjin University, Tianjin 300072, China

Correspondence should be addressed to Qun Yu; [yuqun\\_70@163.com](mailto:yuqun_70@163.com)

Received 6 June 2020; Revised 4 August 2020; Accepted 10 August 2020; Published 29 August 2020

Guest Editor: Zaoli Yang

Copyright © 2020 Qun Yu et al. This is an open access article distributed under the Creative Commons Attribution License, which permits unrestricted use, distribution, and reproduction in any medium, provided the original work is properly cited.

This paper proposes effective evidence on the correlation between trend and self-organized criticality (SOC) of the power outage sequence in China. Taking the data series of blackouts from 1981 to 2014 in the China power grid as the research object, the method of V/S is introduced into the analysis of the power system blackout sequence to demonstrate their prominent long-time correlations. It also verifies the probability distribution of load loss about blackout size in the China power grid has a tail feature, which shows that the time series of blackouts in the China power grid is consistent with SOC. Meanwhile, a kind of mathematical statistics analysis is presented to prove that there is a seasonal trend of blackouts, and the blackout frequency and blackout size have not decreased over time but have an upward trend in the China power grid, thereby indicating that blackout risk may be increasing with time. The last 34 years' data samples of power failure accidents in the China power grid are used to test the proposed method, and the numerical results show that the proposed self-organized criticality and trend analysis method can pave the way for further exploration of the mechanism of power failure in the China power grid.

## 1. Introduction

In contemporary society, electricity has become an essential energy for the development of all countries in the world, and the safe operation of the power grid is very important. However, domestic and foreign power grid blackouts occur frequently, which brought great impact to all countries. For example, in 2003, the large blackout in the east and Canada of the United States caused 61.8 GW load damage and \$30 billion loss. In 2009, the large blackout in Brazil resulted in 24 GW load loss. In 2011, the large blackout in Japan brought about 22 GW load loss. In 2012, the large blackout in India led to 50 GW load damage. These large blackouts often begin from a single component failure in the system, causing cascading failure in turn. To study the internal dynamic mechanism of blackouts for preventing the occurrence of large blackouts and to reduce the adverse effects and losses caused by blackouts, domestic and foreign scholars have done a lot of research and analysis on power system blackouts.

Twenty years of blackout data in the China power grid from 1981 to 2000 inclusive were analyzed by Guo et al. [1–3]. They used mathematical statistics to analyze the blackouts in the China power grid and obtained some conclusions. They observed an upward trend in blackout size and a downward trend in blackout frequency. Besides, it has been found that due to natural disasters, the number of blackouts caused by mechanical failures and human error is on the rise. Twenty-two years' data from 1981 to 2002 were analyzed by Yu and Guo [4–7]. They found that blackout size follows a power-law probability distribution in the China power grid. Duan and Su [8] analyzed the long-term correlation and power-law distribution of grid faults and revealed the self-organized criticality of fault time series of transmission systems or distribution systems. Chao et al. [9] analyzed a time series of blackouts in the Puyang power grid and calculated the Hurst exponent [10]. They found that the probability distribution of the number of faults per day follows the power law, and the Hurst exponent values were around 0.67, indicating long-term correlation, so the faults



occurred in Puyang distribution network possessed SOC. Xu et al. [11] analyzed the distribution of times between faults in the Guangdong power grid from 2000 to 2013 inclusive. They found that the probability distribution of time between faults has a power-law tail. They used rescaled range analysis and scaled windowed variance to calculate the Hurst exponent and found values close to 1.0, indicating long-term correlation and self-similarity. Yu et al. [12] combined the method of relative value and the method of  $R/S$  to analyze the correlation of the load loss sequence of the China power grid from 1981 to 2014, pointing out that the positive correlation of the loss load of the China power grid blackout is getting stronger. From a macro point of view, the number of loss of the China power grid in the next few years will increase, but the relative value of the loss load will decrease. The time interval series of blackout accidents in the China power grid also have long-range positive correlation and statistical self-similarity, which were obtained by Yu et al. [13] using the method of  $V/S$ .

Carreras et al. [14] analyzed the four-year data of North American power systems from 1994 to 1997 and calculated that the Hurst exponent of blackout size was greater than 0.5, indicating long-range correlation and self-similarity. Subsequently, Carreras et al. [15] analyzed the 15-year data from 1984 to 1998. They found that the probability distribution of blackout size has a power-law tail and has a long-term correlation. They also found that the results from a sand pile model, known to be SOC, agree with the disturbance data, following the work of Bak et al. [16]. Thus, they considered that the blackout data seem consistent with SOC. They also raised that there may be seasonal periodicities in blackout data, but no evidence was found. Simonoff et al. [17] analyzed 14 years of blackout data from 1990 to 2004 of the North American power system. They used statistical hypothesis testing to enhance the credibility of conclusions. They found some new conclusions that the number of blackouts in summer is higher than that in winter, and the number of blackouts tends to increase by 14% of the year. They also found that, as weather events became more common, equipment failures will be less. Possible trends or changes in blackouts over time were analyzed by Amin and Hines et al. [18, 19]. Hines et al. [19] analyzed 23 years' data of North American power system blackouts from 1984 to 2006 inclusive. They described several patterns that appear in the data. These included the observation that the number of large blackouts has not decreased, blackouts show seasonal trends and time-of-day trends, and there is no apparent positive correlation between blackout size and restoration time. Seasonal variations were analyzed in [20, 21]. Cornforth [21] found the long-tail distribution of the 23-year electrical disturbance data. They also found a seasonal trend in disturbances, with an increasing number of disturbances and severity of disturbances measured by load loss and by customers affected. Carreras et al. [22] analyzed 22 years' data of North American electric power system blackouts from 1984 to 2006. They validated the power law and long-term correlation of the East-West interconnection blackouts in North American power grid and analyzed the waiting time distribution. Besides, they found that the

annual mean blackout size is highly variable, and the risk of large blackouts is greater than that of medium size.

The work reported here is based on the 34-year blackout data in the China power grid from 1981 to 2014. Based on this relatively complete dataset, we analyze the SOC and possible trends of blackouts in the China power grid. The results observed in this paper can provide reference for effective blackout-risk assessment, and it is of great significance to guide the planning and construction of the power system.

The major contributions of this paper are summarized as follows:

- (1) This paper proposes effective evidence on the correlation between trend and self-organized criticality (SOC) of the power outage sequence in China
- (2) The  $V/S$  method is proposed to demonstrate that the trend and self-organized criticality (SOC) of the power outage sequence have prominent long-time correlations
- (3) A kind of mathematical statistics analysis is presented to prove the law of power blackouts in the China power grid, which will have an important implication for the investment in the electricity industry

The rest of this paper is organized as follows. Section 2 introduces the dataset and research analysis method. Section 3 investigates the time series of blackouts based on self-organized criticality (SOC). Section 4 analyzes the trends of time series of blackouts. The conclusions are drawn in Section 5.

## 2. The Blackout Data in China from 1981 to 2014 and the Methodology

**2.1. The Dataset.** We analyzed the 34-year blackout data in the China power grid from 1981 to 2014, which are available publicly from [23–32]. Some blackouts have the record of load loss, and some do not have. To make the analysis results reliable and accurate, we selected the 277 blackouts with load loss record as the research object, and other blackouts without load loss record were filtered out. On average, 8.15 blackouts occurred in a year, indicating that a blackout occurred every 44.6 days. The average load loss of blackout size per year was 3518.2 MW, and the average load loss per blackout per year was 431.7 MW. Besides, we conducted a statistical analysis of blackouts with the load loss greater than 300 MW. Figure 1 shows a time series of blackouts in the China power grid.

**2.2. The Methodology.** The blackout data were imported to Excel; manually record and review each record repeatedly to ensure accuracy. In order to investigate SOC of time series of blackouts, we used  $V/S$  to analyze the correlation of the time series of blackouts in the China power grid and used Clauset's method suggested by Clauset et al. [33] to analyze the power law of load loss about blackout size in the China power grid. To test the upward trend in blackout frequency

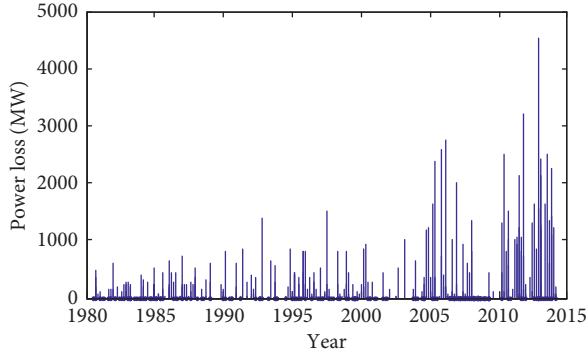


FIGURE 1: Time series of blackouts in the China power grid from 1981 to 2014.

and blackout size, we divided the data into 34 groups yearly, corresponding to the year in which they were reported. The number and load loss maps of annual blackout were plotted. To test the seasonal trends in the blackout data, we divided the data into 12 groups every month, corresponding to the months they were reported. From the data of the 34-year blackout event, the seasonal trend is obvious. However, to test this result, we compared the summer data with the data from the entire dataset and calculated the 95% confidence interval to assess the importance of this difference.

### 3. SOC of Time Series of Blackouts in the China Power Grid

**3.1. Long-Time Correlation.** If a power-law curve progressively attenuates the autocorrelation function of a time series, the time series can be considered to have a long-time correlation [15].  $V/S$  is used to calculate the Hurst exponent [34] to determine the long-range positive correlation of blackouts in the China power grid. The  $V/S$  method can be explained as follows [35].

$\bar{x}$  is the sample mean  $(1/n) \sum_{t=1}^n x_t$ , and  $S_{n,q}^2$  is an estimator of  $\sigma^2 = \sum_t \text{Cov}(x_t, x_0)$  defined as

$$S_{n,q}^2 = \frac{1}{n} \sum_{t=1}^n (x_t - \bar{x})^2 + 2 \sum_{t=1}^q w_t(q) \gamma_t, \quad (1)$$

where  $n$  is the number of the time series.

In (1),

$$w_t(q) = 1 - \frac{t}{q+1}, \quad q < n, \quad (2)$$

$w_t(q)$  are the Bartlett weights, and  $\gamma_t$  are the sample covariance:

$$\gamma_t = \frac{\sum_{i=1}^{n-t} (x_i - \bar{x})(x_{i+t} - \bar{x})}{n}, \quad 0 \leq t < n. \quad (3)$$

Then, the statistic  $V_s(n)$  is defined as follows:

$$V_s(n) = \frac{\left[ \sum_{k=1}^n \left( \sum_{t=1}^k (x_t - \bar{x}) \right)^2 - (1/n) \left( \sum_{k=1}^n \sum_{t=1}^k (x_t - \bar{x}) \right)^2 \right]}{n^2 S_{n,q}^2}. \quad (4)$$

The above process is repeated for every scale,  $n, 2n, 3n, \dots, k \cdot n$ . The scaling relationship is

$$V_s(n) \approx c \cdot n^{2H}. \quad (5)$$

Taking the logarithm of both ends of equation (5),

$$\lg[V_s(n)] = \lg c + 2H \lg n, \quad (6)$$

where  $c$  is the statistical constant and  $H$  is the Hurst exponent.

The correlation can be judged based on the Hurst exponent of the time series. When  $H=0.5$ , it indicates that the time series is uncorrelated and random. When  $0.5 < H < 1.0$ , it indicates that the time series has long-range time correlations. When  $0 < H < 0.5$ , it indicates that the time series has long-range anticorrelations.

We used the  $V/S$  method to analyze the long-range correlation of time series about blackouts in the China power grid. The statistical results are shown in Figure 2. From Figure 2, we can see that the  $V_s(n)$  statistics of the China power grid fit well with the fit line. The Hurst exponent of the load loss of blackout size in the China power grid is 0.7, which indicates that there is a significant long-range time correlation in time series of blackouts in the China power grid.

**3.2. Probability Distribution.** In order to make the analysis result reasonable and effective and to avoid the least square fitting method to analyze the data power-law deviation, we used the method described in [34] to analyze and test the power law of blackouts in the China power grid. Its power-law model parameters are shown in Table 1, and its cumulative probability distribution is shown in Figure 3.

It is known from Table 2 that  $p > 0.1$ , according to which it can be considered that the power-law distribution of load loss about blackout size in the China power grid is reasonable. Also, it is possible to exclude the hypothesis that other distributions, such as Poisson or exponential distribution, are more suitable than power-law distributions. The logarithmic likelihood ratios (LR) of the power-law distribution to the Poisson distribution and the power-law distribution to the exponential distribution are calculated by likelihood ratio test. The results are shown in Table 2.

From Table 2, we can see that the LR of the power-law distribution and Poisson distribution and exponential distribution are both greater than 0, indicating that the power-law distribution is more suitable, and the Poisson distribution and the exponential distribution have  $p$  less than 0.1, which can reject the hypothesis that the load loss about blackout size in the China power grid follows the Poisson distribution or exponential distribution.

Based on the above analysis, it can be seen that the load loss about blackout size in the China power grid does not satisfy the Poisson distribution or the exponential distribution but approximates the power-law distribution, which strongly indicates that the time series of blackouts in the China power grid has the characteristic of SOC.

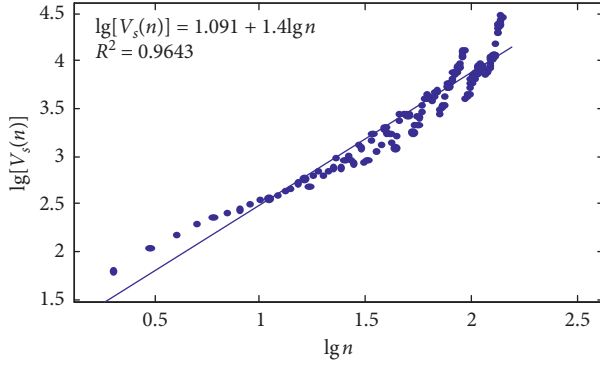


FIGURE 2: Log-log plot of  $V_s(n)$  and  $n$  of blackouts in the China power grid.

TABLE 1: Power-law model parameters of load loss about blackout size in the China power grid.

$n^1$	$x_{\min}^2$	$\alpha^3$	$n_{\text{tail}}^4$	$p^5$
277	737	2.86	52	0.15

<sup>1</sup> $n$  is the number of samples. <sup>2</sup> $x_{\min}$  is the lower bound of the power-law behavior. <sup>3</sup> $\alpha$  is the estimated value of the power exponent. <sup>4</sup> $n_{\text{tail}}$  is the standard deviation of the uncertainty of the fitting parameter. <sup>5</sup> $p$  is the rationality of the quantified power-law hypothesis; when  $p > 0.1$ , indicating that the power-law hypothesis is reasonable, there is a reason to believe that the data satisfy the power-law distribution. When  $p \leq 0.1$ , the power-law hypothesis is rejected, and the data do not satisfy the power-law distribution.

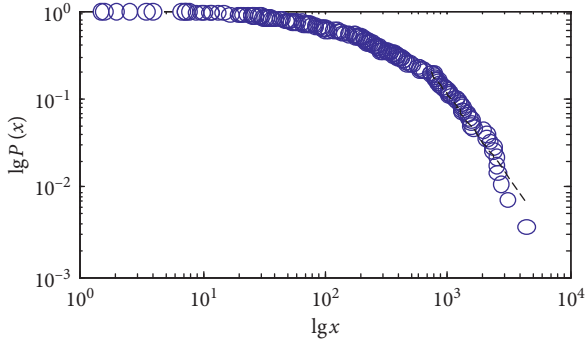


FIGURE 3: Log-log plot of load loss about blackout size in the China power grid.

TABLE 2: Log-likelihood ratio test of the power-law distribution to the Poisson distribution and exponential distribution.

Power law		Poisson		Exponential	
LR	$p$	LR	$p$	LR	$p$
5.29	0.15	6.31	0.04	4.26	0.08

#### 4. Trends in the Blackout in the China Power Grid

**4.1. The Trend of Blackout Frequency and Blackout Size.** Figure 4 shows the number of blackouts per year in the China power grid, and the magnitude of these blackouts varies in size (measured in MW). The number of blackouts

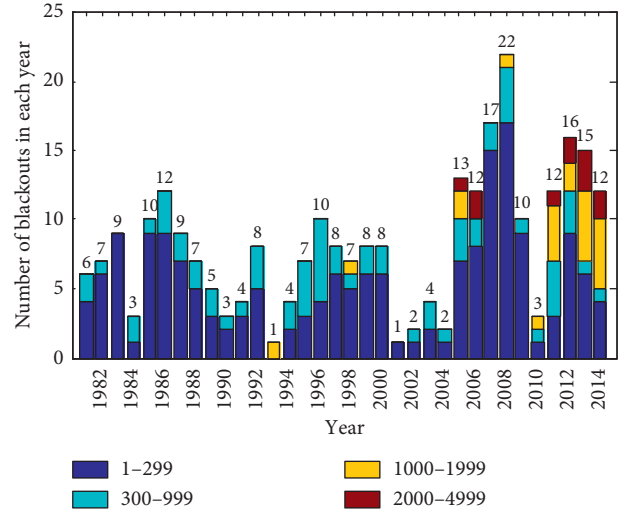


FIGURE 4: The number of blackouts per year in the China power grid.

per year in the China power grid has no obvious periodicity and has no clear increase or decrease trend. However, beginning in 2005, except for 2010, the number of blackouts per year is greater than the average number of 8.15 of blackouts per year, which indicates that the blackout frequency has not decreased and has the possibility of an upward trend over time in the China power grid. Besides, 22 blackouts occurred in 2008, related to the extremely rainy and snowy weather in the South China power grid for a long time.

Figure 5 shows the load loss of blackout size per year for all 277 event records. The year with the greatest load loss of blackout size is 2013, which is related to a major cascading failure. The large blackouts of 2005, 2006, 2007, 2011, 2012, and 2014 are also apparent. Beginning in 2005, except for 2009 and 2010, the load loss of blackout size per year is greater than the average of 3,517.3 MW, which indicates that the load loss of blackout size has not decreased over time in the China power grid and has the possibility of an upward trend.

Figures 4 and 5 show that the number of blackouts and the load loss of blackout size per year in the China power grid have not decreased over time and have the possibility of an upward trend. To test our conclusions, we divided the 34 years' data into six periods. Table 3 shows some descriptive statistics for these data.

Figure 6 shows the number of blackouts between the same time interval for the 34 years' data. This shows a large increase in the number of blackouts from 1988 to 2009, which indicates that the number of blackouts in the China power grid has an upward trend.

Figure 7 shows the load loss of the time interval of blackout size for the 34 years' data. This shows a large increase in the load loss of the time interval of blackout size from 1981 to 2009, which indicates that the load loss of the time interval of blackout size in the China power grid has an upward trend.

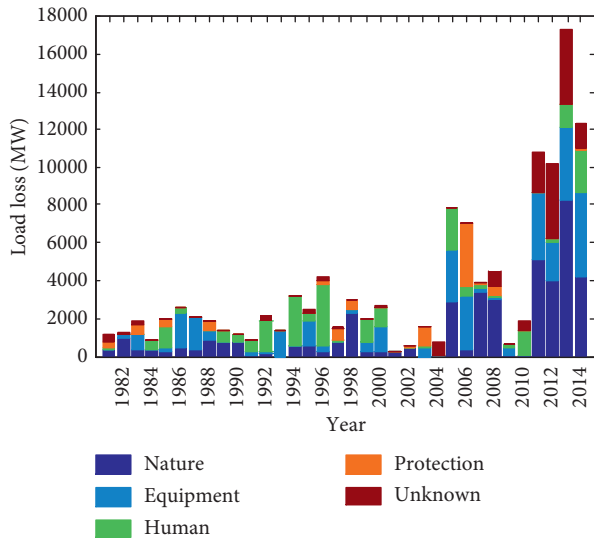


FIGURE 5: The load loss of blackout size per year in the China power grid.

TABLE 3: Statistics of the time interval of blackout data in the China power grid.

Time interval	Blackout frequency	Load loss (MW)	Mean size in each blackout (MW)
1981–1987	56	11,833.5	211.3
1988–1994	32	12,065.9	377.1
1995–2001	49	16,169.2	330.0
2002–2008	72	26,412	366.9
2009–2014	68	53,108	781.0

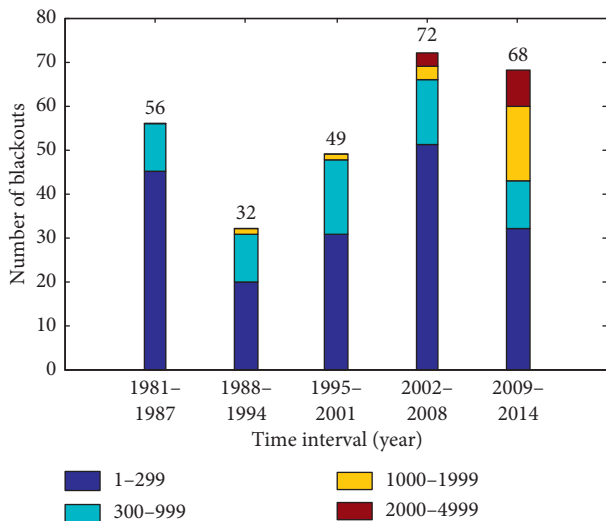


FIGURE 6: The number of blackouts between the same time interval in the China power grid.

Figures 6 and 7 show that, in recent years, the number of blackouts and load loss of the time interval of blackout size in the China power grid show an upward trend but have not

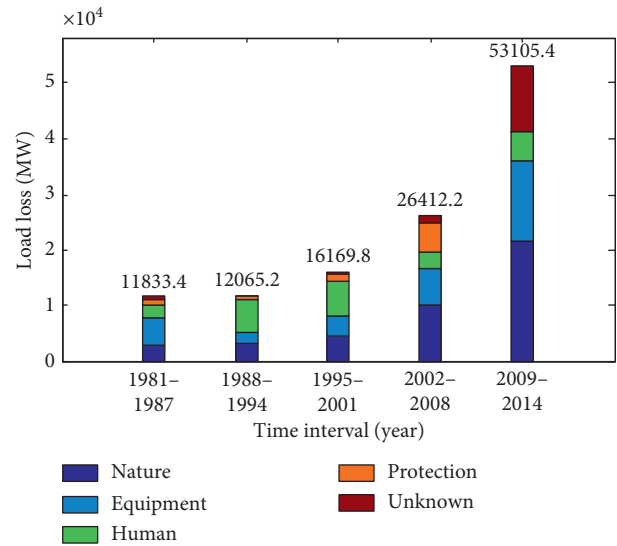


FIGURE 7: The load loss of blackouts between the same time interval in the China power grid.

decreased with time; this confirms our analysis that blackout frequency and blackout size in the China power grid have not decreased over time during the years from 1981 to 2014, and in fact, they have an upward trend.

**4.2. Seasonal Trends of the Blackout.** Figures 8 and 9 show the seasonal trend of blackout frequency. The peak value of summer months is obvious, and statistical analysis supports this view. The average number of monthly blackouts is 23.08 times, and the 95% confidence interval is 19.15 to 27.01. Blackouts in July and August are 32 and 31, respectively, well beyond these ranges, indicating that the monthly data do not match the same distribution, so the seasonal trend of the number of blackouts is present. In addition, we also find the highest number of blackouts in summer followed by spring, and the highest number of blackouts occurred in July followed by August.

Figures 10 and 11 show the seasonal trend of blackout size. The peak value of summer months is obvious, and statistical analysis supports this view. The average load loss of monthly blackouts is 9,965.8 MW, and the 95% confidence interval is 6,977 MW to 12,955 MW. The load loss of blackout size in July and May is 19,816.9 MW and 15,552.3 MW, respectively, well beyond these ranges, indicating that the monthly data did not match the same distribution, so the seasonal trend of the load loss of blackout size is present. In addition, we also find the highest load loss of blackout size in summer followed by spring, and the highest number of blackouts occurred in July followed by May.

By statistical analysis, we find that blackout frequency and blackout size show an obvious seasonal trend. As can be seen from Figures 8–11, blackout frequency and blackout size increase significantly during the summer and spring months, so we can reject this hypothesis and conclude that

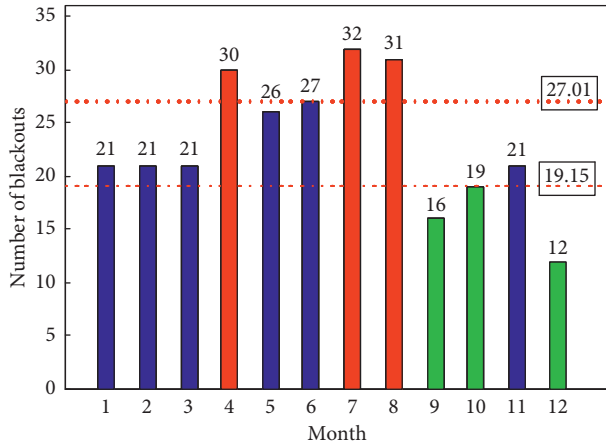


FIGURE 8: The number of blackouts every month in the China power grid.

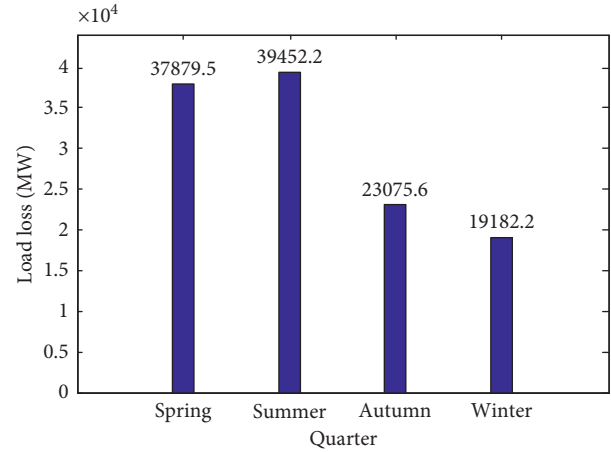


FIGURE 11: The load loss of blackout size in each quarter in the China power grid.

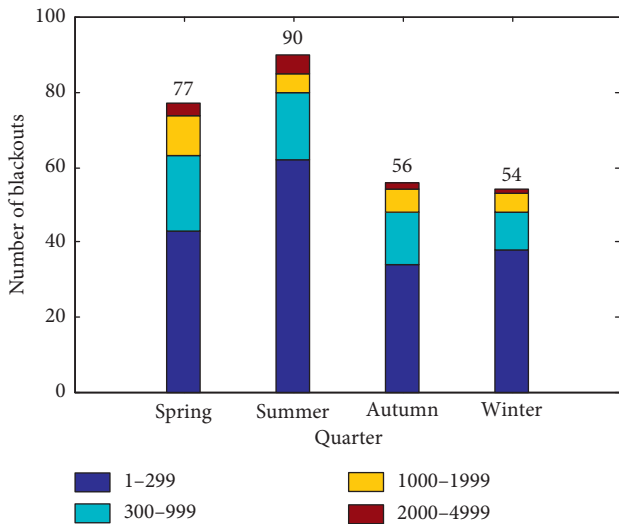


FIGURE 9: The number of blackouts in each quarter in the China power grid.

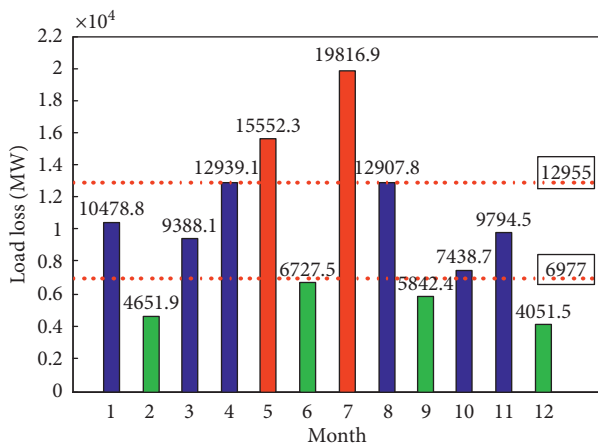


FIGURE 10: The load loss of blackout size every month in the China power grid.

the risk of blackouts does change over time. Besides, we also find that blackout frequency and blackout size which occurred in summer are the largest followed by spring. In July, blackout frequency and blackout size are the largest.

## 5. Conclusion

This paper presents the method of V/S to calculate the long-range correlation of blackouts in the China power grid. This paper also proposed a rigorous method to analyze the power-law distribution of blackouts. The simulation results verify that the time series of blackouts in the China power grid has obvious self-organized criticality. In addition, we use mathematical statistics to analyze the possible trend of blackout data in the China power grid and provide more rigorous analysis by using appropriate statistical tests. The conclusions can be summarized as follows:

- (1) The SOC of blackouts in the China power grid indicates that blackouts may be inevitable, and large blackouts are rare but expected to occur occasionally. The blackout frequency and blackout size in the China power grid have not decreased over time, and they have the possibility of an upward trend, indicating that blackout risk does not decrease over time. This is true, although power companies have put a lot of effort in improving the security and reliability of their power systems.
- (2) The seasonal trend of blackouts in the China power grid indicates that the risk of blackouts does change over time. This conclusion may guide the electricity industry to formulate a time maintenance plan to improve grid reliability. For example, in summer of the highest risk, we can increase the number of operator staff on duty and the number of overhauls of the power grid, thus reducing the risk of blackouts.

## Data Availability

The data, provided in the article, were collected from a report on the safety generation accident of National Power Grid



Corp and China Electric Power Press. They are available in the public domain, so the authors have no restriction on the data.

## Conflicts of Interest

The authors declare that they have no conflicts of interest.

## Acknowledgments

This work was supported by the Science and Technology Project of SGCC in 2018 (Multisand Pile Theory of Inter-connection Power Grid Blackouts Early Warning Technology and System Development, no. XTB17201800166).

## References

- [1] J. B. Guo, Y. H. Yin, and G. C. Yao, "Statistic and analysis for instability incidents in the bulk of power systems in 1998–1991," *Power System Technology*, vol. 18, no. 2, pp. 58–61, 1994.
- [2] J. B. Guo, "Statistics and analysis of incidents in bulk power system from 1991 to 1995," *Power System Technology*, vol. 22, no. 2, pp. 72–74, 1998.
- [3] J. Qu and J. B. Guo, "Statistics and analysis of faults in main domestic power system from 1996 to 2000," *Power System Technology*, vol. 28, no. 21, pp. 60–63, 2004.
- [4] Q. Yu and J. B. Guo, "Self-organized criticality and its application in power system collapse prevention," in *Proceedings of the 2006 International Conference on Power System Technology*, pp. 1–3, IEEE Computer Society, New York, NY, USA, 2006.
- [5] Q. Yu and J. B. Guo, "Statistics and self-organized criticality characters of blackouts in China Electric Power Systems," *Automation of Electric Power Systems*, vol. 30, no. 2, pp. 16–21, 2006.
- [6] Q. Yu and J. B. Guo, "Study on self-organized criticality of power system blackouts in China," *Power System Technology*, vol. 30, no. 6, pp. 1–5, 2006.
- [7] Q. Yu and J. B. Guo, "Self-organized criticality and extreme statistics analysis of electric power system blackouts," *Automation of Electric Power Systems*, vol. 31, no. 3, pp. 1–3, 2007.
- [8] X. Duan and S. Su, "Self-organized criticality in time series of power systems fault, its mechanism, and potential application," *IEEE Transactions on Power Systems*, vol. 25, no. 4, pp. 1857–1864, 2010.
- [9] D. F. Chao, J. X. Yang, S. Su, and D. Y. Shi, "Self-organized criticality and its cause of faults in Puyang distribution system," *Power System Technology*, vol. 35, no. 1, pp. 72–75, 2011.
- [10] B. B. Mandelbrot and J. R. Wallis, "Noah, joseph, and operational hydrology," *Water Resources Research*, vol. 4, no. 5, pp. 909–918, 1968.
- [11] L. X. Xu, J. M. Yang, Z. Chao, and M. B. Liu, "Statistical distribution and nonlinear characteristic analysis of fault time intervals in power grids," *Power System Technology*, vol. 37, no. 12, pp. 3482–3488, 2013.
- [12] Q. Yu, Y. Q. Qu, and L. Shi, "Self-correlation analysis of power grid blackouts based on relative value method and Hurst exponent," *Automation of Electric Power Systems*, vol. 42, no. 1, pp. 55–60, 2018.
- [13] Q. Yu, Y. Q. Qu, N. Cao, and J. Yi, "Statistics and distribution characteristics analysis of time interval of blackout in Chinese power grid," *SCIENTIA SINICA Technologica*, vol. 49, no. 1, pp. 55–62, 2018.
- [14] B. A. Carreras, D. E. Newman, I. Dobson, and A. B. Poole, "Initial evidence for self-organized criticality in electric power system blackouts," in *Proceedings of the the 33rd Annual Hawaii International Conference on System Sciences*, IEEE Computer Society, New York, NY, USA, pp. 1–6, 2000.
- [15] B. A. Carreras, D. E. Newman, I. Dobson, and A. B. Poole, "Evidence for self-organized criticality in a time series of electric power system blackouts," *IEEE Transactions on Circuits and Systems I: Regular Papers*, vol. 51, no. 9, pp. 1733–1740, 2004.
- [16] P. Bak, C. Tang, and K. Wiesenfeld, "Self-organized criticality: an explanation of  $1/f$  noise," *Physical Review Letters*, vol. 59, no. 4, pp. 381–384, 1988.
- [17] J. S. Simonoff, C. E. Restrepo, and R. Zimmerman, "Risk-management and risk-analysis-based decision tools for attacks on electric power," *Risk Analysis*, vol. 27, no. 3, pp. 547–570, 2007.
- [18] M. Amin, "Energy infrastructure defense systems," *Proceedings of the IEEE*, vol. 93, no. 5, pp. 861–875, 2007.
- [19] P. Hines, J. Apt, and S. Talukdar, "Large blackouts in North America: historical trends and policy implications," *Energy Policy*, vol. 37, no. 12, pp. 5249–5259, 2009.
- [20] R. Weron and I. Simonsen, "Blackouts, risk, and fat-tailed distributions," in *Proceedings of the Third Nikkei Econophysics Symposium*, Springer Science and Technology, Tokyo, Japan, pp. 215–219, 2004.
- [21] D. Cornforth, "Long tails from the distribution of 23 years of electrical disturbance data," in *Proceedings of the 2009 IEEE/PES Power Systems Conference and Exposition*, pp. 1–8, IEEE Computer Society, New York, NY, USA, 2009.
- [22] B. A. Carreras, D. E. Newman, and I. Dobson, "North American blackout time series statistics and implications for blackout risk," *IEEE Transactions on Power Systems*, vol. 31, no. 6, pp. 4406–4414, 2016.
- [23] Q. Yu, "Research on self-organized critical characteristics of power system blackouts," Doctoral dissertation, China Electric Power Research Institute, Beijing, China, 2010.
- [24] National Electric Power Dispatching and Communication Center, *Analysis of Typical Accidents of National Power Grid (1988–1998)*, China Electric Power Press, Beijing, China, 2000.
- [25] National Electric Power Dispatching and Communication Center, *Analysis of Typical Accidents of National Power Grid (1999–2007)*, China Electric Power Press, Beijing, China, 2008.
- [26] National Power Grid Corp Security Supervision Department, *Report on the Safety Generation Accident of the National Power Grid Corp in 2008*, China Electric Power Press, Beijing, China, 2009.
- [27] National Power Grid Corp Security Supervision department, *Report on the Safety Generation Accident of the National Power Grid Corp in 2009*, China Electric Power Press, Beijing, China, 2010.
- [28] National Power Grid Corp security supervision department, *Report on the Safety Generation Accident of the National Power Grid Corp in 2010*, China Electric Power Press, Beijing, 2011.
- [29] National Power Grid Corp Security Supervision department, *Report on the Safety Generation Accident of the National Power Grid Corp in 2011*, China Electric Power Press, Beijing, China, 2012.
- [30] National Power Grid Corp Security Supervision Department, *Report on the Safety Generation Accident of the National Power Grid Corp in 2012*, China Electric Power Press, Beijing, China, 2013.



- [31] National Power Grid Corp Security Supervision Department, *Report on the Safety Generation Accident of the National Power Grid Corp in 2013*, China Electric Power Press, Beijing, 2014.
- [32] National Power Grid Corp Security Supervision Department, *Report on the Safety Generation Accident of the National Power Grid Corp in 2014*, China Electric Power Press, Beijing, China, 2015.
- [33] A. Clauset, C. R. Shalizi, and M. E. J. Newman, "Power-law distributions in empirical data," *Siam Review*, vol. 51, no. 4, pp. 661–703, 2009.
- [34] H. E. Hurst, "Long-term storage capacity of reservoirs," *American Society of Civil Engineers*, vol. 116, no. 12, pp. 770–799, 1951.
- [35] L. Giraitis, P. Kokoszka, R. Leipus, and G. Teyssière, "Rescaled variance and related tests for long memory in volatility and levels," *Journal of Econometrics*, vol. 112, no. 2, pp. 265–294, 2003.

## Research Article

# Nonlinear Finite Volume Scheme Preserving Positivity for 2D Convection-Diffusion Equations on Polygonal Meshes

Bin Lan <sup>1,2</sup> and Jianqiang Dong<sup>3</sup>

<sup>1</sup>*School of Mathematics and Information Science, North Minzu University, Yinchuan 750021, China*

<sup>2</sup>*The Key Laboratory of Intelligent Information and Big Data Processing of Ningxia Province, North Minzu University, Yinchuan 750021, China*

<sup>3</sup>*College of Civil Engineering, Hefei University of Technology, Hefei 230009, China*

Correspondence should be addressed to Bin Lan; [lanbin@nun.edu.cn](mailto:lanbin@nun.edu.cn)

Received 12 May 2020; Revised 20 July 2020; Accepted 29 July 2020; Published 21 August 2020

Guest Editor: Zaoli Yang

Copyright © 2020 Bin Lan and Jianqiang Dong. This is an open access article distributed under the Creative Commons Attribution License, which permits unrestricted use, distribution, and reproduction in any medium, provided the original work is properly cited.

In this paper, a nonlinear finite volume scheme preserving positivity for solving 2D steady convection-diffusion equation on arbitrary convex polygonal meshes is proposed. First, the nonlinear positivity-preserving finite volume scheme is developed. Then, in order to avoid the computed solution beyond the upper bound, the cell-centered unknowns and auxiliary unknowns on the cell-edge are corrected. We prove that the present scheme can avoid the numerical solution beyond the upper bound. Our scheme is locally conservative and has only cell-centered unknowns. Numerical results show that our scheme preserves the above conclusion and has second-order accuracy for solution.

## 1. Introduction

Convection-diffusion equations are widely used in the fields of solid mechanics, material science, image processing, and so on. So, it is both theoretically and practically important to investigate numerical methods for such equations. An accurate numerical method must maintain the fundamental properties of practical problems. The extremum principle is an important property of solutions for the convection-diffusion equation. It includes minimum principle and maximum principle. The authors of [1, 2] pointed out that the discrete maximum principle (DMP) plays an important role in proving the existence and uniqueness of discrete solution, enforcing numerical stability, and deriving convergence for a sequence of approximate solutions [3]. Pert [4] pointed out that a scheme violating extremum principle can lead to two problems: fully implicit discretization with large time-steps has relatively poor accuracy, and spurious negative values are generated. Moreover, it is proved that a linear operator, resulting from the discretization of diffusion equations,

satisfies extremum principle if and only if it is both differential and nonnegativity maintaining.

In general cases, the discrete extremum principle (DEP) is more restrictive than monotonicity (positivity-preserving). However, it is difficult to construct a reliable discretization method that satisfies the DEP on arbitrary convex polygonal meshes. Hence, positivity-preserving is one of the key requirements to discrete schemes for the convection-diffusion equation, which says that it can only guarantee nonnegative bound of the numerical solution. Sheng and Yuan [2] pointed out that the scheme without positivity-preserving can lead to the violation of the entropy constraints of the second law of thermodynamics, causing heat to flow from regions of lower temperature to higher temperature. In regions of large temperature variations, this can cause the temperature to become negative.

The finite volume methods (FVM) guarantee the local conservation. But many classical schemes fail to maintain positivity for strong anisotropic diffusion tensors or on distorted meshes [5–8]. Some nonlinear methods have been developed [9–21] for general diffusion or convection-

diffusion equations, which guarantee the positivity on general or distorted meshes for general tensor coefficients.

Bertolazzi and Manzini [22] proposed a MUSCL-like cell-centered finite volume method, where the discretization of advective fluxes is based on a least-square reconstruction of the vertex values from cell averages. Lipnikov et al. [23] proposed a new slope limiting technique based on a specially minimal nonlinear correction, which follows the ideas of the monotonic upstream-centered scheme for conservation laws (MUSCL). Then, in the studies by Wang et al. and Zhang et al. [16, 24], the limiting technique is used to avoid nonphysical oscillation. In the study by Lan et al. [21], a new upwind scheme is used to discretize the convective flux, and the method did not introduce any slope limiting technique.

In this paper, we develop a nonlinear FV scheme, which satisfies DEP for convection-diffusion problems on arbitrary convex polygonal meshes. Following the idea of the discretization for diffusive flux [18] and convective flux [21], the adaptive approach of choosing stencil is applied. Positivity-preserving scheme can only guarantee nonnegative bound of the numerical solution. Considering that the computation of value on the cell edge and the value of cell-centered unknowns may be out of bound, a correcting technique is introduced. Our scheme is constructed by a nonlinear combination technique and has second-order accuracy for the solution and first-order for the flux.

The article is organized as follows. The model problem is described, and some notations are introduced in Section 2. The main process of construction for the 2D steady convection-diffusion equation is given in Section 3. In Section 4, several numerical tests are exhibited to illustrate the features of our scheme. At last, some conclusions are given in Section 5.

## 2. The Problem and Notation

Consider the following stationary convection-diffusion problem for unknown function  $u = u(x)$ :

$$-\nabla \cdot (\kappa \nabla u - \vec{v} u) = f, \quad \text{in } \Omega, \quad (1)$$

$$u = g, \quad \text{on } \partial\Omega, \quad (2)$$

where  $\Omega$  is a bounded polygonal domain in  $\mathbb{R} \times \mathbb{R}$  with boundary  $\partial\Omega$ ,  $\kappa = \kappa(x)$  is a known diffusive coefficient, and  $\vec{v} = \vec{v}(x)$  is a velocity vector field.

Assume that the functions  $\vec{v}(x)$ ,  $f(x)$ , and  $g(x)$  satisfy the constraints listed as follows:

$$\begin{aligned} \nabla \cdot \vec{v} &\geq 0, \quad \vec{v} \in C^1(\bar{\Omega})^2, \\ f &\in L^2(\Omega), \\ g &\in H^{1/2}(\partial\Omega) \cap C(\partial\Omega), \end{aligned} \quad (3)$$

and there are two positive constants  $\lambda_1$  and  $\lambda_2$  such that

$$\lambda_1 |\xi|^2 \leq \kappa(x) \xi \cdot \xi \leq \lambda_2 |\xi|^2, \quad \forall \xi \in \mathbb{R} \times \mathbb{R}. \quad (4)$$

The solvability of the problem (1)-(2) has been given, and the maximum and minimum principle can be found in the study by Gilbarg and Trudinger [25].

We use a mesh on  $\Omega$  made up of arbitrary convex polygon cells. The set of all cells, edges, and nodes are denoted by  $\mathcal{T}$ ,  $\mathcal{E}$ , and  $\mathcal{N}$ , respectively.

We denote the cell by  $K, L, \dots$ , and the cell center is also denoted by  $K, L, \dots$ . In addition, the common edge of two cells  $K$  and  $L$  is denoted by  $\sigma$ , i.e.,  $\sigma = K|L \in \mathcal{E}$ . The cell-edge  $\sigma$  is also denoted by  $AB$ , and the midpoint of  $\sigma$  is denoted by  $M$ . Moreover, we denote  $P_1$  and  $P_2$  are two adjacent midpoints of cell  $K$  (Figure 1).

Let  $\vec{n}_{K,\sigma}$  (or  $\vec{n}_{L,\sigma}$ ) be the unit outer normal vector on the cell-edge  $\sigma$  of cell  $K$  (or  $L$ ),  $\kappa^T$  be the transpose of matrix  $\kappa$ , and  $\mathcal{E}_K$  be the set of all edges of cell  $K$ . Denote  $\varepsilon_{\text{int}} = \varepsilon \cap \Omega$  and  $\varepsilon_{\text{ext}} = \varepsilon \cap \partial\Omega$ . Denote  $h = (\sup_{K \in \mathcal{T}} m(K))^{1/2}$ , where  $m(K)$  is the area of cell  $K$ .

Integrating (1) over the cell  $K$ , we obtain

$$\sum_{\sigma \in \mathcal{E}_K} (\mathcal{F}_{K,\sigma} + \mathcal{G}_{K,\sigma}) = \int_K f(x) dx, \quad (5)$$

where the diffusive and convective flux are defined as

$$\mathcal{F}_{K,\sigma} = - \int_{\sigma} \nabla u(x) \cdot \kappa^T(x) \vec{n}_{K,\sigma} dl, \quad (6)$$

$$\mathcal{G}_{K,\sigma} = \int_{\sigma} \vec{v} u(x) \cdot \vec{n}_{K,\sigma} dl. \quad (7)$$

## 3. Construction of the Scheme

**3.1. The Diffusive Flux.** Following the idea in the study by Sheng and Yuan [18], the adaptive approach of choosing stencil is applied for the approximation of the diffusive flux (equation (6)) together with a nonlinear combination technique. In the method, the two nonnegative parameters are introduced to define a nonlinear two-point flux. Then, the continuity of normal flux on the cell edge is used to give the final discretization of the diffusive flux. At last, the continuity of normal flux is used to obtain the value of  $u_M$ . First, we give a brief review of the construction.

Figure 1 shows that a ray originating at the point  $K$  along the direction  $\kappa^T \vec{n}_{K,\sigma}$  must intersect one segment connecting two neighboring midpoints of edge of cell  $K$ , where the two midpoints are denoted by  $P_1$  and  $P_2$ , and the cross point is denoted by  $O_1$ . Similarly, a ray originating at the midpoint  $M$  along the direction  $-\kappa^T \vec{n}_{K,\sigma}$  must intersect one certain  $KP_4$ , where  $P_4$  must be one vertex of  $\sigma$ , and the cross point is denoted by  $O_2$ .

Let  $\vec{t}_{KP_1}$ ,  $\vec{t}_{KP_2}$ ,  $\vec{t}_{MK}$ , and  $\vec{t}_{MP_4}$  be some unit tangential vectors along their corresponding directions, respectively.  $\theta_i (i = 1, \dots, 4)$  are some corresponding angles. Hence, we established the following relations:

$$\frac{\kappa^T \vec{n}_{K,\sigma}}{|\kappa^T \vec{n}_{K,\sigma}|} = \frac{\sin \theta_2}{\sin(\theta_1 + \theta_2)} \vec{t}_{KP_1} + \frac{\sin \theta_1}{\sin(\theta_1 + \theta_2)} \vec{t}_{KP_2}, \quad (8)$$

$$\frac{\kappa^T \vec{n}_{K,\sigma}}{|\kappa^T \vec{n}_{K,\sigma}|} = \frac{\sin \theta_4}{\sin(\theta_3 + \theta_4)} \vec{t}_{MK} + \frac{\sin \theta_3}{\sin(\theta_3 + \theta_4)} \vec{t}_{MP_4}. \quad (9)$$

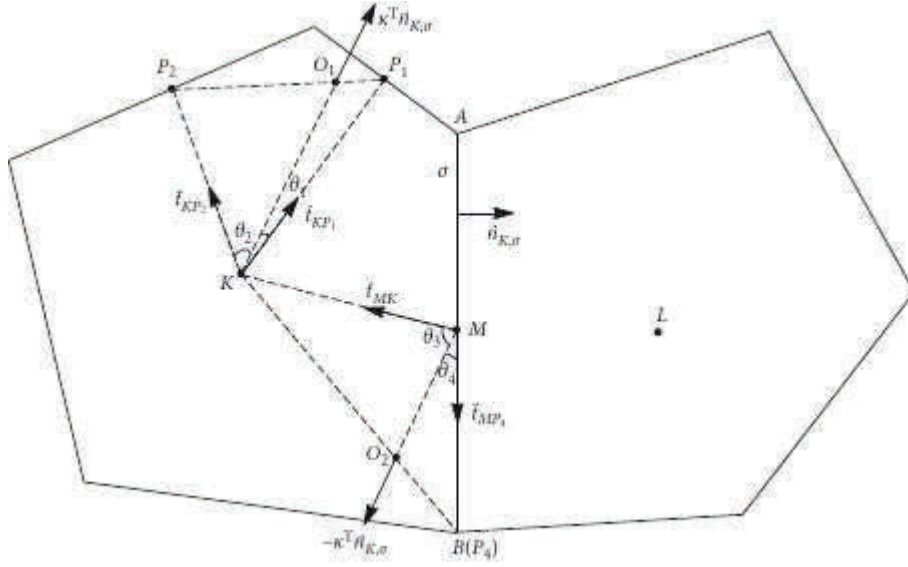


FIGURE 1: Local stencil 1.

Substituting equation (8) into equation (6) and neglecting the high-order terms, we have

$$\begin{aligned} \bar{F}_1 &= -|\kappa_K^T \vec{n}_{K,\sigma}| \left( \frac{\sin \theta_2}{\sin(\theta_1 + \theta_2)} \frac{u_{P_1} - u_K}{|KP_1|} + \frac{\sin \theta_1}{\sin(\theta_1 + \theta_2)} \frac{u_{P_2} - u_K}{|KP_2|} \right) \\ &= a_1(u_K - u_{P_1}) + a_2(u_K - u_{P_2}), \end{aligned} \quad (10)$$

where

$$\begin{aligned} a_1 &= \frac{|\kappa_K^T \vec{n}_{K,\sigma}|}{|KP_1|} \frac{\sin \theta_2}{\sin(\theta_1 + \theta_2)}, \\ a_2 &= \frac{|\kappa_K^T \vec{n}_{K,\sigma}|}{|KP_2|} \frac{\sin \theta_1}{\sin(\theta_1 + \theta_2)}. \end{aligned} \quad (11)$$

Similarly, substituting equation (9) into equation (6), we have

$$\begin{aligned} \bar{F}_2 &= |\kappa_K^T \vec{n}_{K,\sigma}| \left( \frac{\sin \theta_4}{\sin(\theta_3 + \theta_4)} \frac{u_K - u_M}{|MK|} + \frac{\sin \theta_3}{\sin(\theta_3 + \theta_4)} \frac{u_{P_4} - u_M}{|MP_4|} \right) \\ &= a_3(u_K - u_M) + a_4(u_{P_4} - u_M), \end{aligned} \quad (12)$$

where

$$\begin{aligned} a_3 &= \frac{|\kappa_K^T \vec{n}_{K,\sigma}|}{|MK|} \frac{\sin \theta_4}{\sin(\theta_3 + \theta_4)}, \\ a_4 &= \frac{|\kappa_K^T \vec{n}_{K,\sigma}|}{|MP_4|} \frac{\sin \theta_3}{\sin(\theta_3 + \theta_4)}. \end{aligned} \quad (13)$$

Combined with equations (10)–(12), the discrete normal flux on  $\sigma$  can be defined as follows:

$$\begin{aligned} F_{K,\sigma} &= \mu_1 \bar{F}_1 + \mu_2 \bar{F}_2 = \mu_1 a_1(u_K - u_{P_1}) + \mu_1 a_2(u_K - u_{P_2}) \\ &\quad + \mu_2 a_3(u_K - u_M) + \mu_2 a_4(u_{P_4} - u_M), \end{aligned} \quad (14)$$

where  $\mu_1$  and  $\mu_2$  are some nonlinear coefficients with  $\mu_1 + \mu_2 = 1$ , which will be given later.

In order to assure  $\mu_1$  and  $\mu_2$  are positive, two additional parameters  $\omega_1$  and  $\omega_2$  are introduced later. According to the different positions of  $P_1$  and  $P_2$ , three cases exist.

We assume that  $u_{P_1} \neq u_M$  and  $u_{P_2} \neq u_M$ , the normal flux (14) can be rewritten as

$$\begin{aligned} F_{K,\sigma} &= (\mu_1(a_1 + a_2) + \mu_2 a_3)u_K - \mu_2(a_3 + a_4)u_M \\ &\quad - \mu_1(a_1 u_{P_1} + a_2 u_{P_2}) + \mu_2 a_4 u_{P_4} \\ &= (\mu_1(a_1 + a_2)(1 + \omega_1) + \mu_2 a_3)u_K \\ &\quad - \mu_2(a_3 + a_4(1 + \omega_2))u_M \\ &\quad - \mu_1(a_1(u_{P_1} + \omega_1 u_K) + a_2(u_{P_2} + \omega_1 u_K)) \\ &\quad + \mu_2 a_4(u_{P_4} + \omega_2 u_M). \end{aligned} \quad (15)$$

In order to obtain the two-point flux approximation, the last two terms of the above expression should vanish; hence,  $\mu_1$  and  $\mu_2$  are given as follows:

$$\begin{aligned} \mu_1 &= \frac{a_4(u_{P_4} + \omega_2 u_M)}{a_1(u_{P_1} + \omega_1 u_K) + a_2(u_{P_2} + \omega_1 u_K) + a_4(u_{P_4} + \omega_2 u_M)}, \\ \mu_2 &= \frac{a_1(u_{P_1} + \omega_1 u_K) + a_2(u_{P_2} + \omega_1 u_K)}{a_1(u_{P_1} + \omega_1 u_K) + a_2(u_{P_2} + \omega_1 u_K) + a_4(u_{P_4} + \omega_2 u_M)}. \end{aligned} \quad (16)$$

Hence, (15) can be expressed as follows:

$$F_{K,\sigma} = A_{K,\sigma,1} u_K - A_{K,\sigma,2} u_M, \quad (17)$$

where

$$\begin{aligned} A_{K,\sigma,1} &= \mu_1 (a_1 + a_2) (1 + \omega_1) + \mu_2 a_3, \\ A_{K,\sigma,2} &= \mu_2 (a_3 + a_4 (1 + \omega_2)). \end{aligned} \quad (18)$$

In order to assure  $\mu_1 > 0$  and  $\mu_2 > 0$ , two parameters  $\omega_1$  and  $\omega_2$  can be chosen such that

$$\begin{aligned} a_1(u_{P_1} + \omega_1 u_K) + a_2(u_{P_2} + \omega_1 u_K) &\geq 0, \\ a_4(u_{P_4} + \omega_2 u_M) &\geq 0. \end{aligned} \quad (19)$$

If

$$\begin{aligned} a_1((u_{P_1} + \omega_1 u_K) + a_2(u_{P_2} + \omega_1 u_K)) \\ = a_4(u_{P_4} + \omega_2 u_M) = 0. \end{aligned} \quad (20)$$

We let  $\mu_1 = \mu_2 = (1/2)$ .

If  $u_{P_1} = u_M$  or  $u_{P_2} = u_M$ , equation (14) can be expressed in the similar form (17) by using the above method.

Similarly, on the edge  $\sigma$  of the cell  $L$ , we have

$$F_{L,\sigma} = A_{L,\sigma,1} u_L - A_{L,\sigma,2} u_M. \quad (21)$$

Using the continuity of normal flux  $F_{K,\sigma} + F_{L,\sigma} = 0$  on edge  $\sigma$ , we obtain

$$u_M = \frac{A_{K,\sigma,1} u_K + A_{L,\sigma,1} u_L}{A_{K,\sigma,2} + A_{L,\sigma,2}}. \quad (22)$$

Substitute equation (22) into equation (17) to obtain the nonlinear two-point diffusive flux on  $\sigma = K|L$ :

$$F_{K,\sigma} = A_{K,\sigma} u_K - A_{L,\sigma} u_L, \quad (23)$$

where  $A_{K,\sigma} = A_{K,\sigma,1} A_{L,\sigma,2} / (A_{K,\sigma,2} + A_{L,\sigma,2})$ , and  $A_{L,\sigma} = A_{K,\sigma,2} A_{L,\sigma,1} / (A_{K,\sigma,2} + A_{L,\sigma,2})$ .

From the computation of vertex unknowns, a method with second-order accuracy has been proposed in the study by Sheng and Yuan [26]. We know that  $u_M > 0$  as long as  $u_K > 0$  and  $u_L > 0$  in equation (22).

**3.2. The Convective Flux.** We focus on the expression of convective flux in equation (7) for  $\forall \sigma = K|L \in \mathcal{E}_{\text{int}}$  and obtain

$$\begin{aligned} \mathcal{G}_{K,\sigma} &= u_M \int_{\sigma} \vec{v} \cdot \vec{n}_{K,\sigma} dl + O(h^2) \\ &= u_M (v_{K,\sigma}^+ - v_{K,\sigma}^-) + O(h^2), \end{aligned} \quad (24)$$

where  $u_M$  is the value of midpoint  $M$  on the cell-edge  $\sigma$ , and

$$\begin{aligned} v_{K,\sigma}^+ &= \frac{1}{2} (|v_{K,\sigma}| + v_{K,\sigma}), \\ v_{K,\sigma}^- &= \frac{1}{2} (|v_{K,\sigma}| - v_{K,\sigma}), \\ v_{K,\sigma} &= \int_{\sigma} v \cdot \vec{n}_{K,\sigma} dl. \end{aligned} \quad (25)$$

In order to ensure that the discretization of equation (24) has the same structure as the scheme (23), we divide the

integral term into positive part ( $v_{K,\sigma}^+$ ) and negative part ( $v_{K,\sigma}^-$ ). Moreover, the property of upwind is also considered.

Neglecting the high-order terms, we have the following approximate expression of the upwind formula [27]:

$$\mathcal{G}_{K,\sigma} \approx u_M (v_{K,\sigma}^+ - v_{K,\sigma}^-). \quad (26)$$

In order to approximate the continuous flux  $\mathcal{G}_{K,\sigma}$  on the cell-edge  $\sigma$  with second-order accuracy, we propose the following method.

A local stencil is given in Figure 2. For the cell  $K$ ,  $M$  is the midpoint of an arbitrary edge and  $M_1$ ,  $M_2$  are the other two midpoints adjacent to it. We denote  $S_{\Delta MM_1 K}$  be the area of triangle  $MM_1 K$  and define

$$\bar{u}_K = \sum_{M \in \sigma, \sigma \in \mathcal{E}_K} \omega_M u_M, \quad (27)$$

where  $\omega_M = ((S_{\Delta MM_1 K} + S_{\Delta KM_2 M})^{-1} / \sum_{M \in \sigma, \sigma \in \mathcal{E}_K} (S_{\Delta MM_1 K} + S_{\Delta KM_2 M})^{-1})$ . For a special case (Figure 3), we set the cell  $K$  as a triangle and define  $\bar{u}_K = \omega_M u_M + \omega_{M_1} u_{M_1} + \omega_{M_2} u_{M_2}$ , where

$$\begin{aligned} \omega_M &= \frac{s_1}{s}, \\ \omega_{M_1} &= \frac{s_2}{s}, \\ \omega_{M_2} &= \frac{s_3}{s}, \\ s &= s_1 + s_2 + s_3, \\ s_1 &= (S_{\Delta MM_1 K} + S_{\Delta KM_2 M})^{-1}, \\ s_2 &= (S_{\Delta MM_1 K} + S_{\Delta KM_1 M_2})^{-1}, \\ s_3 &= (S_{\Delta KM_1 M_2} + S_{\Delta MKM_2})^{-1}. \end{aligned} \quad (28)$$

It is obvious that  $\bar{u}_K$  is a second-order approximation to  $u_K$ , i.e.,  $|u(K) - \sum_{M \in \sigma, \sigma \in \mathcal{E}_K} \omega_M u(M)| = O(h^2)$  if the solution  $u \in C^2(K)$ .

Then, the approximation of  $\mathcal{G}_{K,\sigma}$  on cell-edge  $\sigma$  can be defined as follows.

For  $\sigma \in \mathcal{E}_{\text{int}}$ , we define

$$G_{K,\sigma} = B_{K,\sigma} u_K - B_{L,\sigma} u_L, \quad (29)$$

where

$$\begin{aligned} B_{K,\sigma} &= \frac{v_{K,\sigma}^+ u_M}{\bar{u}_K} \geq 0, \\ B_{L,\sigma} &= \frac{v_{L,\sigma}^+ u_M}{\bar{u}_L} \geq 0. \end{aligned} \quad (30)$$

For  $\sigma \in \mathcal{E}_{\text{ext}}$ , we define

$$G_{K,\sigma} = B_{K,\sigma} u_K - b_{K,\sigma}, \quad (31)$$

where

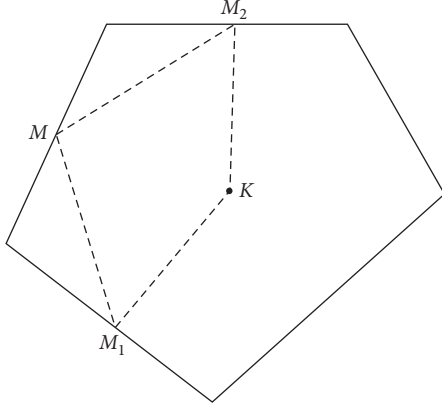


FIGURE 2: Local stencil 2.

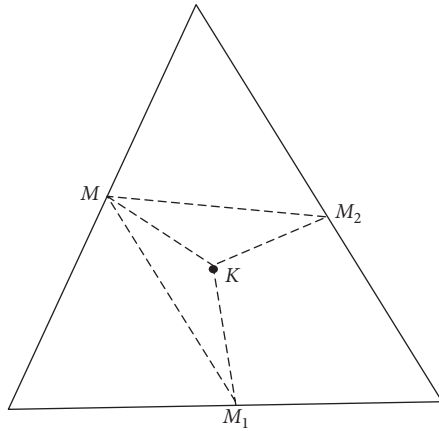


FIGURE 3: Local stencil of triangle.

$$B_{K,\sigma} = \frac{v_{K,\sigma}^+ u_M}{\bar{u}_K} \geq 0, \quad (32)$$

$$b_{K,\sigma} = v_{K,\sigma}^- g_M.$$

**3.3. The Finite Volume Scheme and Picard Iteration.** By using the definition of discretization of diffusive and convective flux, the finite volume scheme can be constructed as follows:

$$\sum_{\sigma \in \mathcal{E}_K} (F_{K,\sigma} + G_{K,\sigma}) = |K|F_K + \sum_{\sigma \in \mathcal{E}_K \cap \mathcal{E}_{\text{ext}}} (A_{K,\sigma,2} u_M + b_{K,\sigma}), \quad K \in \mathcal{T}. \quad (33)$$

$$u_{M_i} = g_{M_i}, \quad \forall M_i \in \partial\Omega, \quad (34)$$

where  $f_K = f(K)$  and  $g_{M_i} = g(x_{M_i})$ .

Let  $U$  be the discrete unknown vector and  $A(U)$  be the coefficient matrix. A nonlinear algebraic system of the schemes (33) and (34) can be formed:  $A(U)U = F$ . The  $A(U)$  is assembled by the coefficients of diffusive term  $F_{K,\sigma}$  and convective term  $G_{K,\sigma}$ . We use the Picard nonlinear iteration method to solve the system: choose a small value  $\mathcal{E}_{\text{non}} > 0$  and initial vector  $U^0 > 0$  and repeat for nonlinear iteration index  $s = 1, 2, \dots$ :

- (1) Solve  $A(U^{(s-1)})U^{(s)} = F$
- (2) Stop if  $\|A(U^{(s)})U^{(s)} - F\|_2 \leq \mathcal{E}_{\text{non}} \|A(U^{(0)})U^{(0)} - F\|_2$

The linear algebraic system with coefficient matrix  $A(U^{(s-1)})$  is solved by the biconjugate gradient stabilized (BiCGSTab) method, and the linear iterations are terminated when relative norm of the initial residual becomes smaller than  $\varepsilon_{\text{lin}}$ .

**3.4. The Algorithm.** In this subsection, we describe the detailed algorithm.

Step 1. Initialize  $U^{(0)} > 0$ ,  $\varepsilon_{\text{non}}$ , and  $\varepsilon_{\text{lin}}$ .

Step 2. When  $s = 0$ ,

- (a) compute  $A_{K,\sigma}^{(0)}$  and  $B_{K,\sigma}^{(0)}$ ;
- (b) compute initial residual  $\|A(U^{(0)})U^{(0)} - F\|_2$ .

Step 3. When  $s = 1, 2, \dots$ ,

- (a) solve  $A(U^{(s-1)})U^{(s)} = F$ ;
- (b) correct  $U^{(s)}$ , see Remark 1;
- (c) compute  $u_p^{(s)}$  and correct  $u_M^{(s)}$ ,  $\forall M \in \sigma, \sigma \in \mathcal{E}, P \in \mathcal{N}$ , see Remark 2;
- (d) compute  $A_{K,\sigma}^{(s)}$  and  $B_{K,\sigma}^{(s)}$ ;
- (e) compute residual  $\|A(U^{(s)})U^{(s)} - F\|_2$ ;
- (f) whether  $\|A(U^{(s)})U^{(s)} - F\|_2 \leq \varepsilon_{\text{non}} \|A(U^{(0)})U^{(0)} - F\|_2$ , if true, then go to (Step 4), otherwise, go to (Step 3).

Step 4. Stop.

**Remark 1.** For  $\forall u_K^{(s)}$ , if  $u_K^{(s)} > \max\{u_M^{(s-1)}, M \in \sigma, \sigma \in \mathcal{E}_K\}$ , let  $u_K^{(s)} = \bar{u}_K^{(s-1)}$ .

**Remark 2.** The value of  $\forall u_M^{(s)}$  can be obtained by equation (22). If  $\forall u_M^{(s)} > \max\{u_K^{(s)}, u_L^{(s)}, u_A^{(s)}, u_B^{(s)}\}$ , where the common edge  $\sigma$  of two cells  $K$  and  $L$  is also denoted by  $AB$  (Figure 1). Let  $u_M^{(s)} = u_M^{(s-1)}$ .

It should be noted that the algorithm in Remark 1 is important to avoid the numerical solution beyond the upper bound where the numerical results need to depend on nonnegative initial values of nonlinear iteration.

**Theorem 1.** Let  $F \geq 0$ ,  $U^{(0)} \geq 0$ , and linear systems in Picard iterations are solved exactly. Then,

$$U^{(s)} \geq 0, \quad (s = 1, 2, 3, \dots). \quad (35)$$

The detailed proof of positivity is given in the study by Yuan and Sheng [11].

Now, we state our conclusion, which says that our scheme can avoid the numerical solution beyond the upper bound. Denote  $u_{\text{max}} = \max\{0, u_K, u_M, \forall K \in \mathcal{T}, \forall M \in \mathcal{E}\}$ .

We assume  $u_{K_0} = u_{\text{max}}$ . Using Remark 1, we know that  $u_{K_0} \leq \max\{u_M, M \in \sigma, \sigma \in \mathcal{E}_{K_0}\}$ .

## 4. Numerical Experiments

In order to demonstrate the accuracy and robustness of the scheme, we test several problems and take  $\varepsilon_{\text{non}} = 1.0e^{-6}$  and



$\varepsilon_{\text{lin}} = 1.0e^{-10}$ . The convergence order can be obtained by the following formula:

$$\text{Order} = \frac{\log(\text{Error}(N_1)/\text{Error}(N_2))}{\log(N_2/N_1)}, \quad (36)$$

where  $N_1$  and  $N_2$  represent different number of cells, and  $\text{Error}(N_1)$  and  $\text{Error}(N_2)$  are the corresponding  $L_2$  errors.

**4.1. The Problem with Anisotropic Diffusion Tensor.** Consider the problems (1) and (2) with Dirichlet boundary condition on  $\Omega = [0, 1] \times [0, 1]$ , and take  $\nu = (-1, 1)^T$ . The exact solution is

$$u(x, y) = \cos\left(\frac{\pi x}{2}\right)e^y, \quad (37)$$

and the diffusion coefficient is

$$\kappa = \begin{pmatrix} 100\varepsilon & 0 \\ 0 & \varepsilon \end{pmatrix}. \quad (38)$$

First, we test the accuracy of our scheme on random quadrilateral meshes shown in Figure 4. Table 1 gives the corresponding  $L_2$  error and the numbers of nonlinear iteration numbers  $it_{\text{non}}^\#$  with a different parameter  $\varepsilon$ . We can see that our scheme obtains second-order accuracy for the solution and at least first-order accuracy for the flux. The average number of nonlinear iterations is 36.8 when  $\varepsilon = 10^{-6}$ . However, for  $\varepsilon = 1.0$ , the corresponding number increases while the number of cell increases.

**4.2. The Problem with Discontinuous Coefficient.** Consider the problems (1) and (2) with Dirichlet boundary condition on  $\Omega = [0, 1] \times [0, 1]$ , and take  $\nu = (1, 1)^T$ . The exact solution is

$$u(x, y) = \begin{cases} \sin \frac{\pi}{2}x + \sin \frac{\pi}{2}y, & x < \frac{1}{2}, \\ \frac{\sqrt{2}c\pi(x - (1/2))}{4} + \sin \frac{\pi}{2}y + \frac{\sqrt{2}}{2}, & x \geq \frac{1}{2}, \end{cases} \quad (39)$$

and the diffusion coefficient is

$$\kappa = \begin{cases} c_0 \times \varepsilon, & x < \frac{1}{2}, \\ \varepsilon, & x \geq \frac{1}{2}, \end{cases} \quad (40)$$

where  $c_0 = 40$ .

We test this problem on random triangle meshes shown in Figure 5. The numerical results with a different parameter  $\varepsilon = 1.0, 10^{-6}$  are given in Table 2. We can see that our scheme almost obtain second-order accuracy for the solution and at least first-order accuracy for the flux. The average numbers of nonlinear iterations are 25 and 23 for  $\varepsilon = 1.0$  and  $\varepsilon = 1.0, 10^{-6}$ , respectively.

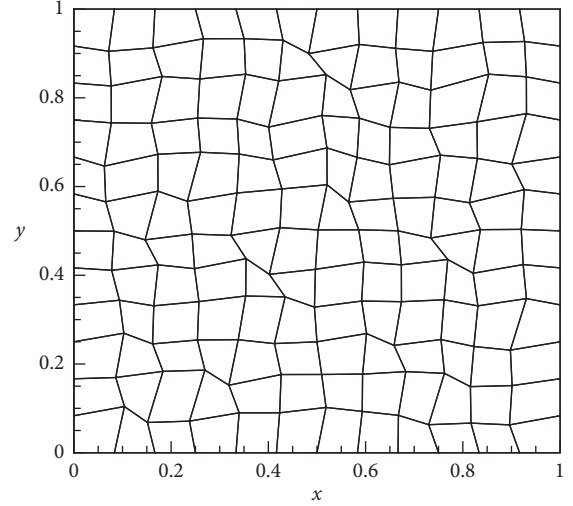


FIGURE 4: The random quadrilateral meshes.

Then, in order to illustrate the efficiency of our scheme, the comparison of accuracy between the studies by Lan et al. and Zhang et al. [19, 24] and present scheme is given in Table 3. As can be seen from the table, the accuracy is 1.5 in the study by Zhang et al. [24] and more than 2.0 in the study by Lan et al. [19] and our new scheme. However, the computed results in our scheme can approximate the exact solution more well.

**4.3. Positivity of Numerical Solutions.** Now, we consider the problem (1)-(2) in the unit square  $\Omega = [0, 1]^2$  with homogeneous Dirichlet boundary conditions. Take  $\vec{\nu} = (1, 1)^T$ , and set

$$\kappa = \begin{pmatrix} \cos \theta & \sin \theta \\ -\sin \theta & \cos \theta \end{pmatrix} \begin{pmatrix} k_1 & 0 \\ 0 & k_2 \end{pmatrix} \begin{pmatrix} \cos \theta & -\sin \theta \\ \sin \theta & \cos \theta \end{pmatrix}, \quad (41)$$

$$f = \begin{cases} 1, & \text{if } (x, y) \in \left[\frac{3}{8}, \frac{5}{8}\right]^2, \\ 0, & \text{otherwise.} \end{cases}$$

We take  $k_1 = 1$ ,  $k_2 = 100$ , and  $\theta = 5\pi/6$ .

The analytical solution  $u(x, y)$  is unknown, but the minimum principle states that it is nonnegative. It is a challenging task to solve it accurately because they can result in significant violation of the positivity and even produce a numerical solution with nonphysical oscillations. We will show that our new nonlinear scheme can also obtain the nonnegative solution.

First, we test the new scheme on the random quadrilateral meshes with  $128 \times 128$  cells. The corresponding distribution is similarly shown in Figure 6), and the numerical solution is given in Figure 7. The minimum value is  $u_{\min} = 0$  and the maximum value is  $u_{\max} = 6.7603 \times 10^{-4}$ , which show that our scheme preserves the positivity of the solution and does not produce any nonphysical oscillations. Then, we test it on the random triangular meshes. The computed results show that  $u_{\min} = 0$  and  $u_{\max} = 6.7582 \times 10^{-4}$ .

TABLE 1: Accuracy for the problem with anisotropic coefficient.

	Cells	144	576	2304	9216	36864
$\varepsilon = 1.0$	$\varepsilon_2^u$	$3.11E-3$	$7.50E-4$	$2.09E-4$	$5.46E-5$	$1.42E-5$
	Order	—	2.05	1.84	1.94	1.94
	$\varepsilon_2^F$	$1.06E+0$	$3.94E-1$	$1.76E-1$	$8.28E-2$	$3.96E-2$
	Order	—	2.07	1.54	2.03	0.99
	$it_{\text{non}}^{\#}$	55	85	116	126	153
$\varepsilon = 10^{-6}$	$\varepsilon_2^u$	$5.28E-3$	$1.24E-3$	$3.18E-4$	$8.06E-5$	$2.13E-5$
	Order	—	2.09	1.96	1.98	1.92
	$\varepsilon_2^F$	$7.93E-3$	$1.99E-3$	$5.31E-4$	$1.34E-4$	$3.57E-5$
	Order	—	2.07	1.54	2.03	0.99
	$it_{\text{non}}^{\#}$	36	40	36	33	39

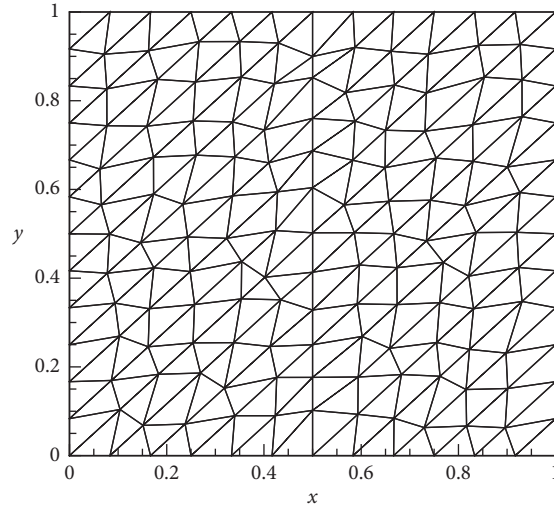


FIGURE 5: The random triangle meshes.

TABLE 2: Accuracy for the problem with discontinuous coefficient.

$\varepsilon$	Cells	288	1152	4608	18432	73728
1.0	$\varepsilon_2^u$	$4.87E-4$	$1.39E-4$	$3.82E-5$	$8.68E-6$	$2.13E-6$
	Order	—	1.81	1.86	2.14	2.03
	$\varepsilon_2^F$	$7.83E-2$	$3.04E-2$	$1.39E-2$	$5.51E-3$	$2.50E-3$
	Order	—	2.07	1.54	2.03	0.99
	$it_{\text{non}}^{\#}$	23	24	26	26	26
$10^{-6}$	$\varepsilon_2^u$	$4.54E-4$	$1.18E-4$	$3.13E-5$	$7.93E-6$	$2.01E-6$
	Order	—	1.94	1.91	1.98	1.98
	$\varepsilon_2^F$	$6.60E-4$	$1.63E-4$	$4.15E-5$	$1.04E-5$	$2.63E-6$
	Order	—	2.07	1.54	2.03	0.99
	$it_{\text{non}}^{\#}$	23	24	23	23	23

These computed results illustrate that our new scheme preserves the positivity of numerical solutions and satisfies the discrete minimum principle.

**4.4. Nonphysical Oscillations.** We also consider the last nonsmooth anisotropic solution and compute it on the random quadrilateral meshes. Here, we reset  $f = 0$ . The computational domain is a unit square with a hole,  $\Omega = [0, 1]^2 \setminus [4/9, 5/9]^2$ , so that the boundary  $\partial\Omega$  is composed of two disjoint parts  $\Gamma_0$  and  $\Gamma_1$  as shown in Figure 8 where the number of cell is  $72 \times 72$ .  $\Gamma_0$  is the exterior boundary, and  $\Gamma_1$  is the interior boundary. We set  $g = 0$  on  $\Gamma_0$  and  $g = 2$  on  $\Gamma_1$ .

The numerical solutions on the random quadrilateral meshes are shown in Figure 9. The computed results show that  $u_{\min} = 6.94E-13$  and  $u_{\max} = 1.98$ . It means that the minimum 0 is attained on the  $\Gamma_0$ , and the maximum 2 is attained on the  $\Gamma_1$ . So, these computed results illustrate that our scheme can avoid the numerical solution beyond the upper bound and does not produce any nonphysical oscillations.

Then, the computed results without the correct method in Remarks 1 and 2 are shown in Figure 10, and  $u_{\min} = 3.87E-6$  and  $u_{\max} = 1.91$ . However, the numerical oscillations are produced in the computational domain.

TABLE 3: Comparison of accuracy with discontinuous coefficient ( $\varepsilon = 10^{-5}$ ).

Method	Mesh	Cells	256	1024	4096	16384
Zhang et al. [24]	Uniform	$\varepsilon_2^u$	$1.10E-1$	$3.98E-2$	$1.42E-2$	$5.02E-3$
		Order	—	1.47	1.49	1.50
	Random	$\varepsilon_2^u$	$1.10E-1$	$3.95E-2$	$1.38E-2$	$5.11E-3$
		Order	—	1.48	1.52	1.43
Lan et al. [19]	Uniform	$\varepsilon_2^u$	$4.23E-3$	$9.77E-4$	$2.31E-4$	$5.50E-5$
		Order	—	2.12	2.08	2.07
	Random	$\varepsilon_2^u$	$6.87E-3$	$1.57E-3$	$3.78E-4$	$8.96E-5$
		Order	—	2.13	2.05	2.08
Present	Uniform	$\varepsilon_2^u$	$9.34E-4$	$1.82E-4$	$3.63E-5$	$8.43E-6$
		Order	—	2.36	2.32	2.11
	Random	$\varepsilon_2^u$	$9.16E-4$	$1.89E-4$	$4.04E-5$	$9.85E-6$
		Order	—	2.28	2.23	2.04

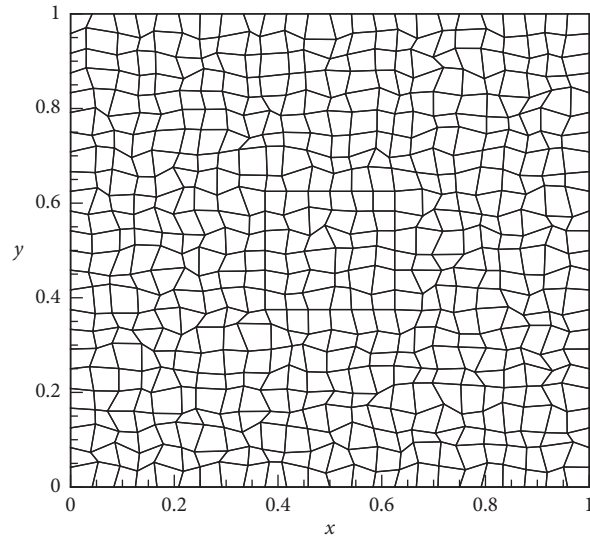
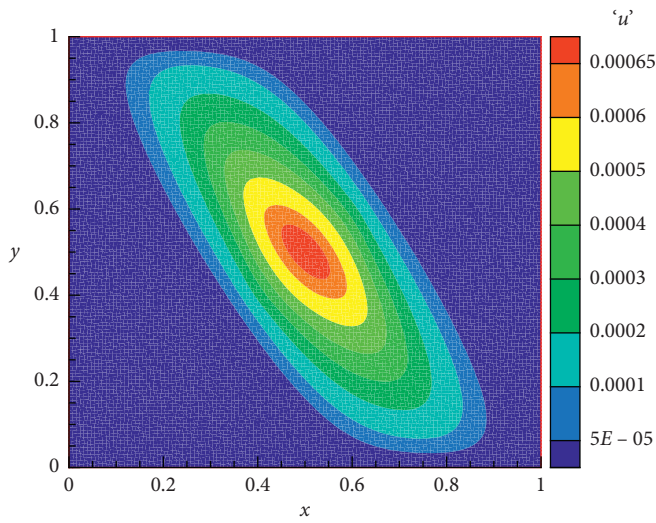
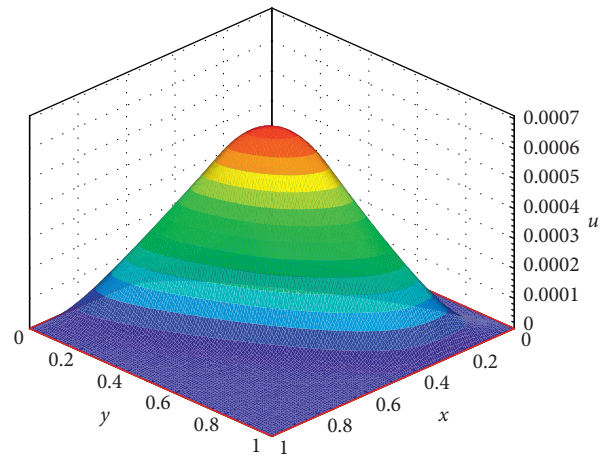


FIGURE 6: The random quadrilateral meshes.



(a)



(b)

FIGURE 7: The numerical solutions on the random quadrilateral meshes.

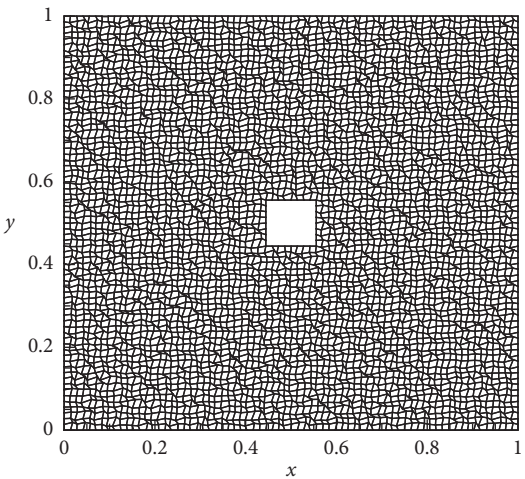


FIGURE 8: The random quadrilateral meshes with a hole.

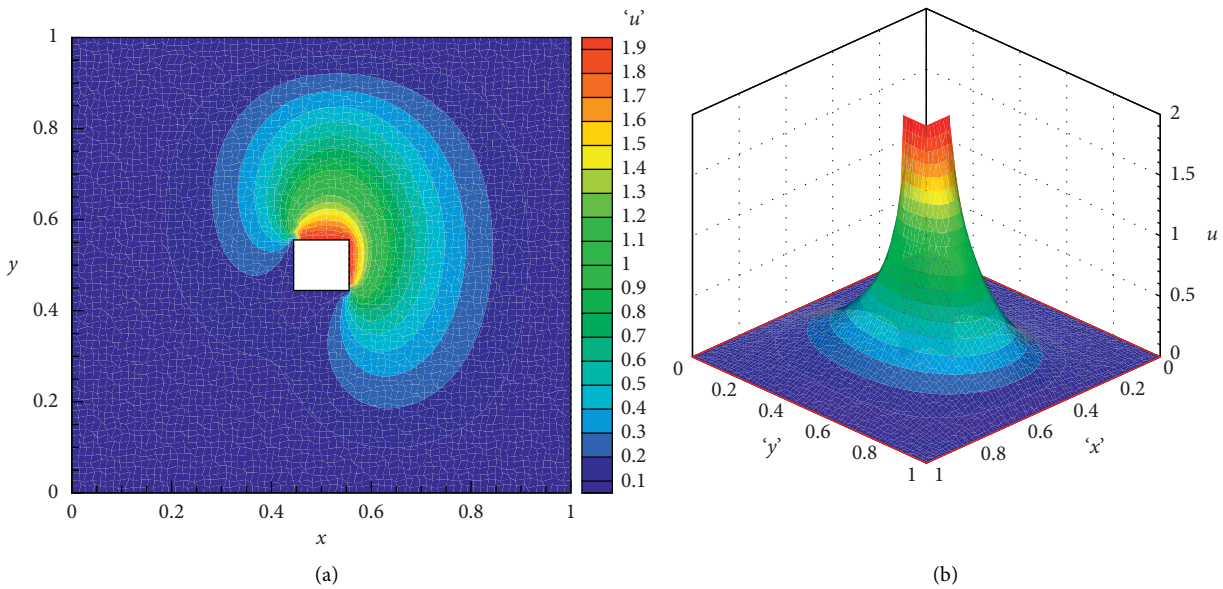


FIGURE 9: The numerical results on the random quadrilateral meshes.

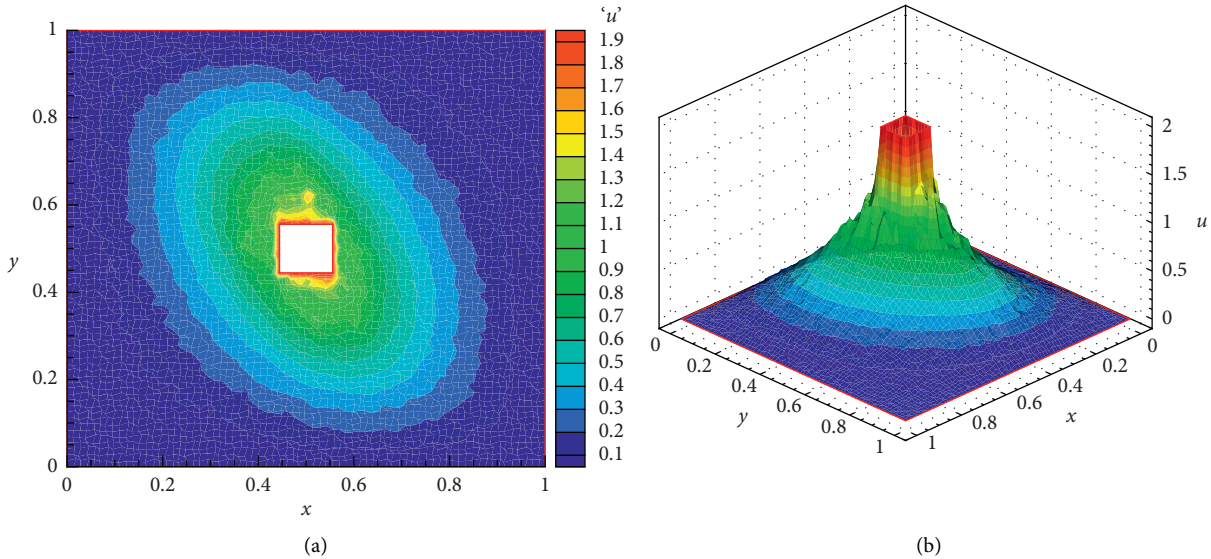


FIGURE 10: The numerical results without corrections on the random quadrilateral meshes.

## 5. Conclusion

The aim of this paper is to build a nonlinear finite volume scheme preserving positivity for solving the 2D convection-diffusion equation on arbitrary convex polygonal meshes. We first develop the nonlinear positive finite volume scheme. Then, a corrected method is proposed, and the numerical solution beyond the upper bound can be avoided.

Our scheme includes only cell-centered unknowns. Numerical results show that our new scheme obtains second-order accuracy for the solution and first-order accuracy for the flux. In addition, it can not only keep the positivity but also do not produce any oscillation.

## Data Availability

The authors confirm that the data supporting the findings of this study are available within the article (No. 7343716).

## Conflicts of Interest

The authors declare that they have no conflicts of interest.

## Acknowledgments

This work was partially supported by the Natural Science Foundation of Ningxia (2020AAC03235); General School Level Project (12020000153); National Natural Science Foundation of China (11601013 and 11772165); First-Class Disciplines Foundation of Ningxia (NXYLXK2017B09); and Natural Science Foundation of Ningxia (2020AAC03233).

## References

- [1] M. G. Edwards and H. Zheng, "A quasi-positive family of continuous Darcy-flux finite-volume schemes with full pressure support," *Journal of Computational Physics*, vol. 227, no. 22, pp. 9333–9364, 2008.
- [2] Z. Sheng and G. Yuan, "The finite volume scheme preserving extremum principle for diffusion equations on polygonal meshes," *Journal of Computational Physics*, vol. 230, no. 7, pp. 2588–2604, 2011.
- [3] K. Morton, *Numerical Solution of Convection-Diffusion Problems*, Chapman & Hall, London, UK, 1996.
- [4] G. J. Pert, "Physical constraints in numerical calculations of diffusion," *Journal of Computational Physics*, vol. 42, no. 1, pp. 20–52, 1981.
- [5] J. M. Nordbotten and I. Aavatsmark, "Monotonicity conditions for control volume methods on uniform parallelogram grids in homogeneous media," *Computational Geosciences*, vol. 9, no. 1, pp. 61–72, 2005.
- [6] A. Lapin, "Mixed hybrid finite element method for a variational inequality with a quasi-linear operator," *Computational Methods in Applied Mathematics*, vol. 9, no. 4, pp. 354–367, 2009.
- [7] H. A. Friis and M. G. Edwards, "A family of MPFA finite-volume schemes with full pressure support for the general tensor pressure equation on cell-centered triangular grids," *Journal of Computational Physics*, vol. 230, no. 1, pp. 205–231, 2011.
- [8] K. Lipnikov, G. Manzini, and D. Svyatskiy, "Analysis of the monotonicity conditions in the mimetic finite difference method for elliptic problems," *Journal of Computational Physics*, vol. 230, no. 7, pp. 2620–2642, 2011.
- [9] C. Le Potier, "Schéma volumes finis monotone pour des opérateurs de diffusion fortement anisotropes sur des mailages de triangles non structurés," *Comptes Rendus Mathématique*, vol. 341, no. 12, pp. 787–792, 2005.
- [10] K. Lipnikov, M. Shashkov, D. Svyatskiy, and Y. Vassilevski, "Monotone finite volume schemes for diffusion equations on unstructured triangular and shape-regular polygonal meshes," *Journal of Computational Physics*, vol. 227, no. 1, pp. 492–512, 2007.
- [11] G. Yuan and Z. Sheng, "Monotone finite volume schemes for diffusion equations on polygonal meshes," *Journal of Computational Physics*, vol. 227, no. 12, pp. 6288–6312, 2008.
- [12] A. Danilov and Y. Vassilevski, "A monotone nonlinear finite volume method for diffusion equations on conformal polyhedral meshes," *Russian Journal of Numerical Analysis and Mathematical Modelling*, vol. 24, pp. 207–227, 2009.
- [13] K. Lipnikov, D. Svyatskiy, and Y. Vassilevski, "Interpolation-free monotone finite volume method for diffusion equations on polygonal meshes," *Journal of Computational Physics*, vol. 228, no. 3, pp. 703–716, 2009.
- [14] Z. Sheng, J. Yue, and G. Yuan, "Monotone finite volume schemes of nonequilibrium radiation diffusion equations on distorted meshes," *SIAM Journal on Scientific Computing*, vol. 31, no. 4, pp. 2915–2934, 2009.
- [15] Z. Sheng and G. Yuan, "An improved monotone finite volume scheme for diffusion equation on polygonal meshes," *Journal of Computational Physics*, vol. 231, no. 9, pp. 3739–3754, 2012.
- [16] S. Wang, G. Yuan, Y. Li, and Z. Sheng, "A monotone finite volume scheme for advection-diffusion equations on distorted meshes," *International Journal for Numerical Methods in Fluids*, vol. 69, no. 7, pp. 1283–1298, 2012.
- [17] Z. Sheng and G. Yuan, "A cell-centered nonlinear finite volume scheme preserving fully positivity for diffusion equation," *Journal of Scientific Computing*, vol. 68, no. 2, pp. 521–545, 2016.
- [18] Z. Sheng and G. Yuan, "A new nonlinear finite volume scheme preserving positivity for diffusion equations," *Journal of Computational Physics*, vol. 315, pp. 182–193, 2016.
- [19] B. Lan, Z. Sheng, and G. Yuan, "A monotone finite volume scheme with second order accuracy for convection-diffusion equations on deformed meshes," *Computer Physics Communication*, vol. 24, pp. 1455–1476, 2018.
- [20] B. Lan, Z. Sheng, and G. Yuan, "A new finite volume scheme preserving positivity for radionuclide transport calculations in radioactive waste repository," *International Journal of Heat and Mass Transfer*, vol. 121, pp. 736–746, 2018.
- [21] B. Lan, Z. Sheng, and G. Yuan, "A new positive scheme for 2D convection-diffusion equation," *ZAMM-Journal of Applied Mathematics and Mechanics*, vol. 99, pp. 1–13, 2019.
- [22] E. Bertolazzi and G. Manzini, "A cell-centered second-order accurate finite volume method for convection-diffusion problems on unstructured meshes," *Mathematical Models and Methods in Applied Sciences*, vol. 14, no. 8, pp. 1235–1260, 2004.
- [23] K. Lipnikov, D. Svyatskiy, and Y. Vassilevski, "A monotone finite volume method for advection-diffusion equations on unstructured polygonal meshes," *Journal of Computational Physics*, vol. 229, no. 11, pp. 4017–4032, 2010.
- [24] Q. Zhang, Z. Sheng, and G. Yuan, "A finite volume scheme preserving extremum principle for convection-diffusion



- equations on polygonal meshes,” *International Journal for Numerical Methods in Fluids*, vol. 84, no. 10, pp. 616–632, 2017.
- [25] D. Gilbarg and N. Trudinger, *Elliptic Partial Differential Equations of Second Order*, Springer-Verlag, Berlin, Germany, 2001.
- [26] Z. Sheng and G. Yuan, “A nine point scheme for the approximation of diffusion operators on distorted quadrilateral meshes,” *SIAM Journal on Scientific Computing*, vol. 30, no. 3, pp. 1341–1361, 2008.
- [27] B. van Lee, “Towards the ultimate conservative difference scheme. V.A second-order sequel to Godunov’s method,” *Journal of Computational Physics*, vol. 32, pp. 101–136, 1979.



## Research Article

# New Tseng-Degree Gradient Method in Variational Inequality Problem

Zhuang Shan,<sup>1</sup> Lijun Zhu ,<sup>2,3</sup> Long He,<sup>1</sup> Danfeng Wu,<sup>1</sup> and Haicheng Wei<sup>4</sup>

<sup>1</sup>School of Mathematics and Information Science, North Minzu University, Yinchuan 750021, China

<sup>2</sup>The Key Laboratory of Intelligent Information and Data Processing of NingXia Province, North Minzu University, Yinchuan 750021, China

<sup>3</sup>Health Big Data Research Institute of North Minzu University, Yinchuan 750021, China

<sup>4</sup>Advanced Intelligent Perception Control Technology Innovative Team of NingXia, Minzu University, Yinchuan 750021, China

Correspondence should be addressed to Lijun Zhu; zhulijun1995@yahoo.com

Received 17 May 2020; Accepted 27 June 2020; Published 5 August 2020

Guest Editor: Zaoli Yang

Copyright © 2020 Zhuang Shan et al. This is an open access article distributed under the Creative Commons Attribution License, which permits unrestricted use, distribution, and reproduction in any medium, provided the original work is properly cited.

This paper focuses on the problem of variational inequalities with monotone operators in real Hilbert space. The Tseng algorithm constructed by Thong replaced a high-precision step. Thus, a new Tseng-like gradient method is constructed, and the convergence of the algorithm is proved, and the convergence performance is higher.

## 1. Introduction

Let  $H$  be the real Hilbert space, and  $\langle \cdot, \cdot \rangle$  and  $\|\cdot\|$  are respectively defined as the inner product and norm of space  $H$ . Let  $C$  be a nonempty closed convex subset of space  $H$ . Let  $\mathfrak{T}: H \rightarrow H$  be an operator on the set  $C$ . The variational inequality problem (VIP) means to find a point  $x^*$  on  $C$  such that

$$\langle \mathfrak{T}x^*, x - x^* \rangle \geq 0, \quad \forall x \in C. \quad (1)$$

We use  $VI(\mathfrak{T}, C)$  to denote the solution set of problem (1). At present, the regular method and the projection method are the two main methods to solve the problem of variational inequality. Variational inequalities can also solve other problems such as equilibrium, fixed points, and optimization. In addition, it is also widely used in the industry, especially supply chain management and transportation. Supply chain management is a new type of management concept, which emphasizes the rapid market demand response, combat readiness management, high flexibility, low risk, cost-effectiveness, and other goals, attracting many theoretical and practical industry people to study and practice it. Some well-known international companies, such

as Hewlett-Packard and Dell, have made great achievements in the practice of supply chain management. Therefore, the supply chain is an effective way for enterprises to adapt to global competition in the 21st century (see eg., [1–11]).

At present, the theoretical support of the variational inequality problem is gradually maturing, and people are gradually changing from the theoretical research of the problem to the construction of the variational inequality algorithm. In recent years, the variational inequality algorithm has developed rapidly, but the use conditions are harsh. The use of the Tseng algorithm does not require too harsh conditions, such as the strongly monotone or inverse strongly monotone of the problem and only one projection equation is used to approximate the solution of the problem. The specific method is as follows:

$$\begin{cases} y_n = P_C(x_n - \rho \mathfrak{T}x_n), \\ x_{n+1} = y_n - \rho(\mathfrak{T}y_n - \mathfrak{T}x_n). \end{cases} \quad (2)$$

There  $\rho \in (0, 1/L)$  and  $P_C$  is a projection operator in set  $C$  of Hilbert space  $H$ . In recent years, the Tseng algorithm has been widely recognized. Subsequently, Duong Viet and others improved the Tseng method. For the specific method, please see Lemma 7 [12].

Although the Tseng algorithm constructed by Duong Viet et al. has many advantages, the shortcoming is that the step size is too simple. The work of this paper is to improve the convergence of the algorithm by optimizing the step size, making it more precise and practical on the basis of convergence. The step size adopted in this article is currently commonly used, and it has high accuracy itself, which can effectively improve the convergence speed of the algorithm. In addition, this paper popularizes the application field of the algorithm to make it more applicable.

The structure of this paper is as follows: In Section 2, we give some necessary definitions and lemmas. In Section 3, we give an algorithm for construction. We analyze and prove that the algorithm weakly converges to a certain point in  $VI(C, \mathfrak{T})$  and give some inferences.

## 2. Preliminaries

Let  $H$  be a real Hilbert space and  $C$  be a nonempty closed convex subset of  $H$ . As we all know, the following equation can be directly proved in Hilbert space.

When  $\forall x \in H, y \in H$ , and  $\alpha \in R$ , we can get

$$\begin{aligned} \|x + y\|^2 &= \|x\|^2 + 2\langle x, y \rangle + \|y\|^2; \\ \|\alpha x + (1 - \alpha)y\|^2 &= \alpha\|x\|^2 + (1 - \alpha)\|y\|^2 - \alpha(1 - \alpha)\|x - y\|^2. \end{aligned} \quad (3)$$

**Definition 1.** Let  $\mathfrak{T}$  be a operator on a Hilbert space, and then the operator  $\mathfrak{T}$  is a nonexpansive operator, if the operator  $\mathfrak{T}$  has the property

$$\|\mathfrak{T}x - \mathfrak{T}y\| \leq c\|x - y\|, \quad \text{for all } x, y \in C, \quad (4)$$

and for some constant  $c \in [0, 1]$ .

Let  $P_C$  be a projection operator in set  $C$  of Hilbert space  $H$ , then  $\forall x \in H$ . There is only one point  $P_C x$  such that  $\|P_C x - y\| \leq \|x - y\|, \forall y \in C$ . It is easy to prove that  $P_C$  is a nonexpansive operator.

**Lemma 1** (see [13]). Let  $H$  be a real Hilbert space and  $C$  be a nonempty closed convex subset of  $H$ . For a given  $x \in H, z \in C$ . Then,  $\forall y \in C$  has the following relationship:

$$z = P_C x \iff \langle x - z, z - y \rangle \geq 0. \quad (5)$$

**Lemma 2** (see [13]). Let  $H$  be a real Hilbert space and  $C$  be a nonempty closed convex subset of  $H, x \in H$ , then  $\forall y \in C$ . The following equation holds

$$\begin{aligned} (i) \quad & \|P_C x - P_C y\|^2 \leq \langle P_C x - P_C y, x - y \rangle, \\ (ii) \quad & |\langle P_C x - y, x - y \rangle|^2 \leq \|x - y\|^2 + \|P_C x - x\|^2. \end{aligned}$$

If the reader wants to know more about the nature of projections, please refer to part 3 in [13].

**Definition 2.** Let  $\mathfrak{T}: H \longrightarrow H$ , if  $\forall x, y \in H$  satisfies

$$\|\mathfrak{T}x - \mathfrak{T}y\| \leq S\|x - y\|, \quad S > 0. \quad (6)$$

Then, the operator  $\mathfrak{T}$  is called  $S$ -Lipschitz continuous;

$$\langle \mathfrak{T}x - \mathfrak{T}y, x - y \rangle \geq 0, \quad (7)$$

Then, the operator  $\mathfrak{T}$  is called monotonic.

**Lemma 3** (see [14]). Let  $\{\varphi_n\}$ ,  $\{\delta_n\}$ , and  $\{\alpha_n\}$  be sequences in  $[0, +\infty)$  such that

$$\varphi_{n+1} \leq \varphi_n + \alpha_n(\varphi_n - \varphi_{n-1}), \quad \forall n \geq 1, \quad \sum_{n=1}^{+\infty} \delta_n < +\infty, \quad (8)$$

and there is a real number  $\alpha$ , for any  $n \in N$ , such that  $0 \leq \alpha_n \leq \alpha < 1$ . Then,

$$(i) \quad \sum_{n=1}^{+\infty} [\varphi_n - \varphi_{n-1}]_+ < +\infty,$$

where  $[\varphi_n - \varphi_{n-1}]_+ = \max\{\varphi_n - \varphi_{n-1}, 0\}$ .

$$(i) \quad \text{There is a point } \varphi^* \in [0, +\infty) \text{ such that } \lim_{n \rightarrow +\infty} \varphi_n = \varphi^*.$$

**Lemma 4** (Opial 1967). Let  $\emptyset \neq C \subset H$  and  $\{x_n\}$  be the sequence in  $H$  such that the following two conditions hold:

$$\begin{aligned} (i) \quad & \forall x \in C, \lim_{n \rightarrow +\infty} \|x_n - x\| \text{ exist}; \\ (ii) \quad & \text{Every point of weakly gathering in the sequence } \{x_n\} \text{ is in } C. \end{aligned}$$

Then,  $x_n$  weakly converges to a point  $x$  in  $C$ .

**Lemma 5** (minty, please refer to reference [15], Lemma 7.1.7). Let  $\mathfrak{T}: C \longrightarrow H$  be a monotone continuous operator. Then,  $x^*$  is the solution to problem (1) if and only if  $x^*$  is a solution to the following problem:

$$\text{find } x \in C \text{ such that } \langle \mathfrak{T}y, y - x \rangle \geq 0, \quad \forall y \in C. \quad (9)$$

**Remark 1.** The solution set  $VI(C, \mathfrak{T})$  of variational inequality (1) is closed and convex.

**Lemma 6** (see [15]). Let  $\mathfrak{T}: H \longrightarrow H$  be monotone and Lipschitz continuous on  $H$  with the constant  $S$  and  $VI(C, \mathfrak{T}) \neq \emptyset, \rho$  be a positive obtained real number such that  $\rho \in (0, (1/S))$ . If  $\{\eta_n\}$  is a nonincreasing sequence, make  $0 \leq \eta_n \leq \eta$  and

$$\eta < \frac{\sqrt{1 + 8\mathfrak{K}} - 1 - 2\mathfrak{K}}{2(1 - 2\mathfrak{K})}, \quad (10)$$

where  $\mathfrak{K} := ((1 - \rho S)/(1 + \rho S))$ , then the sequence  $\{x_n\}$  obtained by next algorithm weakly converges to  $VI(C, \mathfrak{T})$ .

(i) Step 0: given  $\rho > 0$ ; Let  $x_0, x_1 \in H$  be arbitrary

(ii) Step 1: set  $\omega_n = x_n + \eta_n(x_n - x_{n-1})$  and compute

$$y_n = P_C(\omega_n - \rho \mathfrak{T}\omega_n). \quad (11)$$

When  $y_n = \omega_n$ , then stop iteration, and  $y_n$  is the solution to the (VIP) problem; otherwise,

(iii) Step 2: compute

$$x_{n+1} = y_n - \rho(\mathfrak{T}y_n - \mathfrak{T}\omega_n). \quad (12)$$

Set  $n = n + 1$  and go to Step 1.

**Lemma 7** (see [15]). Suppose that  $\rho \in (0, (1/S))$ . Let  $\{x_n\}$  be a sequence in  $H$  defined by

$$\begin{cases} x_0 \in H, \\ y_n = P_C(x_n - \rho \mathfrak{T}x_n), \\ x_{n+1} = y_n - P_C(\rho \mathfrak{T}y_n - \rho \mathfrak{T}x_n). \end{cases} \quad (13)$$

Then, the sequence  $\{x_n\}$  converges weakly to an element of  $VI(C, \mathfrak{T})$ .

### 3. Main Results

Let  $\mathfrak{T}: H \longrightarrow H$  be monotone and Lipschitz continuous on  $H$  with the constant  $S$  and  $VI(C, \mathfrak{T}) \neq \emptyset$ . First, we introduce Algorithm 1.

**Lemma 8.** Let  $\{\rho_n\}$  be a sequence obtained by Algorithm 1, then the sequence  $\{x_n\}$  decreases monotonically and its lower bound is  $\min\{(\mu/S), \rho_0\}$ , where  $S > 0$  is the Lipschitz condition constant.

*Proof.* According to the definition, the sequence  $\{\rho_n\}$  is monotonically nonincreasing, because  $\mathfrak{T}$  is a Lipschitz condition function. At that time,  $\mathfrak{T}y_n - \mathfrak{T}\omega_n \neq 0$ , and we have

$$\frac{\mu \|y_n - \omega_n\|}{\|\mathfrak{T}y_n - \mathfrak{T}\omega_n\|} \geq \frac{\mu \|y_n - \omega_n\|}{S \|y_n - \omega_n\|} = \frac{\mu}{S}. \quad (14)$$

Obviously, the sequence  $\{\rho_n\}$  has a lower bound  $\min\{(\mu/S), \rho_0\}$ .

**Theorem 1.** Let the sequence  $\{x_n\}$  be obtained by Algorithm 1, then  $\forall p \in VI(C, \mathfrak{T})$  have

$$\|x_{n+1} - p\|^2 \leq \|\omega_n - p\|^2 - \left(1 - \rho_n^2 \frac{\mu^2}{\rho_{n+1}^2}\right) \|y_n - \omega_n\|^2. \quad (15)$$

*Proof*

$$\begin{aligned} \|x_{n+1} - p\|^2 &= \|y_n - \rho_n(\mathfrak{T}y_n - \mathfrak{T}\omega_n) - p\|^2 \\ &= \|y_n - p\|^2 + \rho_n^2 \|\mathfrak{T}y_n - \mathfrak{T}\omega_n\|^2 - 2\rho_n \langle y_n - p, \mathfrak{T}y_n - \mathfrak{T}\omega_n \rangle \\ &= \|\omega_n - p\|^2 + \|\omega_n - y_n\|^2 + 2\langle y_n - p, \mathfrak{T}y_n - \mathfrak{T}\omega_n \rangle + \rho_n^2 \|\mathfrak{T}y_n - \mathfrak{T}\omega_n\|^2 - 2\rho_n \langle y_n - p, \mathfrak{T}y_n - \mathfrak{T}\omega_n \rangle \\ &= \|\omega_n - p\|^2 + \|\omega_n - y_n\|^2 - 2\langle y_n - \omega_n, y_n - \omega_n \rangle + 2\langle y_n - \omega_n, y_n - p \rangle + \rho_n^2 \|\mathfrak{T}y_n - \mathfrak{T}\omega_n\|^2 \\ &\quad - 2\rho_n \langle y_n - p, \mathfrak{T}y_n - \mathfrak{T}\omega_n \rangle \\ &= \|\omega_n - p\|^2 - \|\omega_n - y_n\|^2 + 2\langle y_n - \omega_n, y_n - p \rangle + \rho_n^2 \|\mathfrak{T}y_n - \mathfrak{T}\omega_n\|^2 - 2\rho_n \langle y_n - p, \mathfrak{T}y_n - \mathfrak{T}\omega_n \rangle. \end{aligned} \quad (16)$$

Since  $y_n = P_C(\omega_n - \rho_n \mathfrak{T}\omega_n)$ , so

$$\langle y_n - \omega_n + \rho_n \mathfrak{T}\omega_n, y_n - p \rangle \leq 0, \quad (17) \quad \langle y_n - \omega_n, y_n - p \rangle \leq -\rho_n \langle \mathfrak{T}\omega_n, y_n - p \rangle, \quad (18)$$

or

can be obtained from (16) and (18):

$$\begin{aligned} \|x_{n+1} - p\|^2 &\leq \|\omega_n - p\|^2 - \|\omega_n - y_n\|^2 - 2\rho_n \langle \mathfrak{T}\omega_n, y_n - p \rangle \\ &\quad + \rho_n^2 \|\mathfrak{T}y_n - \mathfrak{T}\omega_n\|^2 - 2\rho_n \langle y_n - p, \mathfrak{T}y_n - \mathfrak{T}\omega_n \rangle \\ &= \|\omega_n - p\|^2 - \|\omega_n - y_n\|^2 + \rho_n^2 \|\mathfrak{T}y_n - \mathfrak{T}\omega_n\|^2 - 2\rho_n \langle y_n - p, \mathfrak{T}y_n \rangle \\ &\leq \|\omega_n - p\|^2 - \|\omega_n - y_n\|^2 + \rho_n^2 \frac{\mu^2}{\rho_{n+1}^2} \|y_n - \omega_n\|^2 \\ &\quad - 2\rho_n \langle y_n - p, \mathfrak{T}y_n - \mathfrak{T}p \rangle - 2\rho_n \langle y_n - p, \mathfrak{T}p \rangle \\ &\leq \|\omega_n - p\|^2 - \left(1 - \rho_n^2 \frac{\mu^2}{\rho_{n+1}^2}\right) \|y_n - \omega_n\|^2. \end{aligned} \quad (19)$$

- (i) Step 0: given  $\rho_0 > 0$ . Let  $x_0, x_1 \in H$  be arbitrary and  $\mu \in ((1/\sqrt{2}), 1)$
- (ii) Step 1: set  $\omega_n = x_n + \eta_n(x_n - x_{n-1})$  and compute  $y_n = P_C(\omega_n - \rho_n \mathfrak{T}\omega_n)$
- (iii) When  $y_n = \omega_n$ , then stop iteration, and  $y_n$  is the solution to the (VIP) problem; otherwise,
- (iv) Step 2: compute  $x_{n+1} = y_n - \rho_n(\mathfrak{T}y_n - \mathfrak{T}\omega_n)$
- (v) and  $\rho_{n+1} = \begin{cases} \min\{(\mu\|y_n - \omega_n\|/\|\mathfrak{T}y_n - \mathfrak{T}\omega_n\|), \rho_n\}, & \mathfrak{T}y_n - \mathfrak{T}\omega_n \neq 0, \\ \rho_n, & \text{other} \end{cases}$
- (vi) Set  $n = n + 1$  and go to Step 1

ALGORITHM 1: New Tseng-degree gradient algorithm.

**Theorem 2.** Let  $\{\rho_n\}$  be a sequence generated by Algorithm 1. If  $\{\eta_n\}$  is a nonincreasing sequence, make  $0 \leq \eta_n \leq \eta$  and

$$\eta < \frac{\sqrt{1+8\mathfrak{K}}-1-2\mathfrak{K}}{2(1-2\mathfrak{K})}, \quad (20)$$

where  $\mathfrak{K} := 1 - \mu^2$ , then the sequence  $\{x_n\}$  obtained by Algorithm 1 weakly converges to  $VI(C, \mathfrak{T})$ .

*Proof.* The first step.

Let  $\mathfrak{K}_n := (1 - \rho_n^2(\mu^2/\rho_{n+1}^2))/1 + \rho_n^2(\mu^2/\rho_{n+1}^2) \leq 1 - \rho_n^2(\mu^2/\rho_{n+1}^2) \leq 1 - \mu^2 = \mathfrak{K}$ .

Since  $(\sqrt{1+8\mathfrak{K}_n}-1-2\mathfrak{K}_n)/(2(1-2\mathfrak{K}_n))$  monotonically increases in  $(0, (1/2))$ ;  $\{\rho_n\}$  monotonically decreases, so  $(\rho_n^2/\rho_{n+1}^2) \geq 1$ , and then there  $\eta < ((\sqrt{1+8\mathfrak{K}_n}-1-2\mathfrak{K}_n)/2(1-2\mathfrak{K}_n)) < ((\sqrt{1+8\mathfrak{K}}-1-2\mathfrak{K})/2(1-2\mathfrak{K}))$ .

From the second step, through the construction of  $x_{n+1}$ , we can get

$$\begin{aligned} \|x_{n+1} - y_n\| &= \|y_n - \rho_n(\mathfrak{T}y_n - \mathfrak{T}\omega_n) - y_n\| \\ &\leq \rho_n \|\mathfrak{T}y_n - \mathfrak{T}\omega_n\| \\ &\leq \rho_n \frac{\mu}{\rho_{n+1}} \|y_n - \omega_n\|. \end{aligned} \quad (21)$$

So,

$$\|x_{n+1} - \omega_n\| \leq \|x_{n+1} - y_n\| + \|y_n - \omega_n\| \leq \left(1 + \rho_n \frac{\mu}{\rho_{n+1}}\right) \|y_n - \omega_n\|, \quad (22)$$

thus having

$$\|y_n - \omega_n\| \geq \frac{1}{(1 + \rho_n(\mu/\rho_{n+1}))} \|x_{n+1} - \omega_n\|. \quad (23)$$

Let  $p \in VI(C, \mathfrak{T})$ , through Theorem 1, and we can get

$$\|x_{n+1} - p\|^2 \leq \|\omega_n - p\|^2 - \left(1 - \rho_n^2 \frac{\mu^2}{\rho_{n+1}^2}\right) \|y_n - \omega_n\|^2. \quad (24)$$

From (23) and (24), we can get

$$\begin{aligned} \|x_{n+1} - p\|^2 &\leq \|\omega_n - p\|^2 - \frac{1 - \rho_n^2(\mu^2/\rho_{n+1}^2)}{1 + \rho_n^2(\mu^2/\rho_{n+1}^2)} \|x_{n+1} - \omega_n\|^2 \\ &= \|\omega_n - p\|^2 - \frac{1 - \rho_n(\mu/\rho_{n+1})}{1 + \rho_n(\mu/\rho_{n+1})} \|x_{n+1} - \omega_n\| \\ &\leq \|\omega_n - p\|^2 - \mathfrak{K} \|x_{n+1} - \omega_n\|^2. \end{aligned} \quad (25)$$

Through the construction of  $\omega_n$ , we can get

$$\begin{aligned} \|\omega_n - p\|^2 &= \|x_n + \eta_n(x_n - x_{n-1}) - p\|^2 \\ &= \|(1 + \eta_n)(x_n - p) - \eta_n(x_{n-1} - p)\|^2 \\ &\leq (1 + \eta_n) \|x_n - p\|^2 - \eta_n \|x_{n-1} - p\|^2 \\ &\quad + \eta_n(1 + \eta_n) \|x_n - x_{n-1}\|^2. \end{aligned} \quad (26)$$

From (25) and (26), we can get

$$\begin{aligned} \|x_{n+1} - p\|^2 &\leq (1 + \eta_n) \|x_n - p\|^2 - \eta_n \|x_{n-1} - p\|^2 + \eta_n(1 + \eta_n) \|x_n - x_{n-1}\|^2 \\ &\leq (1 + \eta_n) \|x_n - p\|^2 - \eta_n \|x_{n-1} - p\|^2 + 2\eta \|x_n - x_{n-1}\|^2. \end{aligned} \quad (27)$$

On the other hand,

$$\begin{aligned} \|x_{n+1} - \omega_n\|^2 &= \|x_{n+1} - x_n - \eta_n(x_n - x_{n-1})\|^2 \\ &= \|x_{n+1} - x_n\|^2 + \eta_n^2 \|x_n - x_{n-1}\|^2 - 2\eta_n \langle x_{n+1} - x_n, x_n - x_{n-1} \rangle \\ &\geq \|x_{n+1} - x_n\|^2 + \eta_n^2 \|x_n - x_{n-1}\|^2 - 2\eta_n \|x_{n+1} - x_n\| \|x_n - x_{n-1}\| \\ &\geq (1 - \eta_n) \|x_{n+1} - x_n\|^2 + (\eta_n^2 - \eta_n) \|x_n - x_{n-1}\|^2. \end{aligned} \quad (28)$$

From (25), (26), and (28), we get

$$\begin{aligned}
 \|x_{n+1} - p\|^2 &\leq (1 + \eta_n)\|x_n - p\|^2 - \eta_n\|x_{n-1} - p\|^2 + \eta_n(1 + \eta_n)\|x_n - x_{n-1}\|^2 \\
 &\quad - \mathfrak{K}(1 + \eta_n)\|x_{n+1} - x_n\|^2 - \mathfrak{K}(\eta_n^2 - \eta_n)\|x_n - x_{n-1}\|^2 \\
 &= (1 + \eta_n)\|x_n - p\|^2 - \eta_n\|x_{n-1} - p\|^2 - \mathfrak{K}(1 - \eta_n)\|x_{n+1} - x_n\|^2 \\
 &\quad + [\eta_n(1 + \eta_n) - \mathfrak{K}(\eta_n^2 - \eta_n)]\|x_n - x_{n-1}\|^2 \\
 &= (1 + \eta_n)\|x_n - p\|^2 - \eta_n\|x_{n-1} - p\|^2 - \gamma_n\|x_{n+1} - x_n\|^2 + \mu_n\|x_n - x_{n-1}\|^2,
 \end{aligned} \tag{29}$$

where  $\gamma_n := \mathfrak{K}(1 - \eta_n)$  and  $\mu_n := \eta_n(1 + \eta_n) - \mathfrak{K}(\eta_n^2 - \eta_n) \geq 0$ .

Let  $\Gamma_n := \|x_n - p\|^2 - \eta_n\|x_{n-1} - p\|^2 + \mu_n\|x_n - x_{n-1}\|^2$ . From (29), we can obtain

$$\begin{aligned}
 \Gamma_{n+1} - \Gamma_n &= \|x_{n+1} - p\|^2 - (1 + \eta_{n+1})\|x_n - p\|^2 + \eta_n\|x_{n-1} - p\|^2 \\
 &\quad + \mu_{n+1}\|x_{n+1} - x_n\|^2 - \mu_n\|x_n - x_{n-1}\|^2 \\
 &\leq \|x_{n+1} - p\|^2 - (1 + \eta_n)\|x_n - p\|^2 + \eta_n\|x_{n-1} - p\|^2 \\
 &\quad + \mu_{n+1}\|x_{n+1} - x_n\|^2 - \mu_n\|x_n - x_{n-1}\|^2 \\
 &\leq -(\gamma_n - \mu_{n+1})\|x_{n+1} - x_n\|^2.
 \end{aligned} \tag{30}$$

Because  $0 \leq \eta_n \leq \eta_{n+1} \leq \eta$ , so

$$\begin{aligned}
 \gamma_n - \mu_{n+1} &= \mathfrak{K}(1 - \eta_n) - \eta_{n+1}(1 + \eta_{n+1}) + \mathfrak{K}(\eta_{n+1}^2 - \eta_{n+1}) \\
 &\geq \mathfrak{K}(1 + \eta_{n+1}) - \eta_{n+1}(1 + \eta_{n+1}) + \mathfrak{K}(\eta_{n+1}^2 - \eta_{n+1}) \\
 &\geq \mathfrak{K}(1 - \eta_n) - \eta(1 + \eta) + \mathfrak{K}(\eta^2 - \eta) \\
 &\geq -(1 - \mathfrak{K})\eta^2 - (1 + 2\mathfrak{K})\eta + \mathfrak{K}.
 \end{aligned} \tag{31}$$

Combining (30) and (31), we get

$$\Gamma_{n+1} - \Gamma_n \leq -\delta\|x_{n+1} - x_n\|^2, \tag{32}$$

where  $\delta := -(1 - \mathfrak{K})\eta^2 - (1 + 2\mathfrak{K})\eta + \mathfrak{K}$ ,  $\delta > 0$  can be obtained from (20).

Easy to prove

$$\Gamma_{n+1} - \Gamma_n \leq 0. \tag{33}$$

Therefore, the sequence  $\{\Gamma_n\}$  is nonincreasing.

On the other hand, due to  $\mu_n \geq 0$ , there is

$$\begin{aligned}
 \Gamma_n &= \|x_n - p\|^2 - \eta_n\|x_{n-1} - p\|^2 + \mu_n\|x_n - x_{n-1}\|^2 \\
 &\geq \|x_n - p\|^2 - \eta_n\|x_{n-1} - p\|^2.
 \end{aligned} \tag{34}$$

This means

$$\|x_n - p\|^2 \leq \eta_n\|x_{n-1} - p\|^2 + \Gamma_n \leq \eta\|x_{n-1} - p\|^2 + \Gamma_1 \leq \dots \leq \eta^n\|x_0 - p\|^2 + \Gamma_1(1 + \dots + \eta^{n-1}) \leq \eta^n\|x_0 - p\|^2 + \frac{\Gamma_1}{1 - \eta}. \tag{35}$$

Similarly,

$$\begin{aligned}
 \Gamma_{n+1} &= \|x_{n+1} - p\|^2 - \eta_{n+1}\|x_n - p\|^2 + \mu_{n+1}\|x_{n+1} - x_n\|^2 \\
 &\geq \|x_{n+1} - p\|^2 - \eta_{n+1}\|x_n - p\|^2 \geq -\eta_{n+1}\|x_n - p\|^2.
 \end{aligned} \tag{36}$$

From (35) and (36), we can see that

$$-\Gamma_{n+1} \leq \eta_{n+1}\|x_n - p\|^2 \leq \eta\|x_n - p\|^2 \leq \eta^{n+1}\|x_0 - p\|^2 + \frac{\eta\Gamma_1}{1 - \eta}. \tag{37}$$

According to (32), we get the following inequality:

$$\begin{aligned}
 \delta \sum_{n=1}^k \|x_{n+1} - x_n\|^2 &\leq \Gamma_1 - \Gamma_{k+1} \leq \eta^{k+1}\|x_0 - p\|^2 + \frac{\Gamma_1}{1 - \eta} \\
 &\leq \|x_0 - p\|^2 + \frac{\Gamma_1}{1 - \eta}.
 \end{aligned} \tag{38}$$

In other words,  $\sum_{n=1}^{\infty} \|x_{n+1} - x_n\|^2 < +\infty$ ,  $\|x_{n+1} - x_n\|^2 \rightarrow 0$  can be obtained from the convergence series property, that is,  $\|x_{n+1} - x_n\| \rightarrow 0$ . So,

$$\begin{aligned}
 \|x_{n+1} - \omega_n\|^2 &= \|x_{n+1} - x_n\|^2 + \eta_n^2\|x_n - x_{n-1}\|^2 \\
 &\quad - 2\eta_n\langle x_{n+1} - x_n, x_n - x_{n-1} \rangle.
 \end{aligned} \tag{39}$$

So,  $\|x_{n+1} - \omega_n\| \rightarrow 0$ . By (27) and Lemma 3, we have

$$\lim_{n \rightarrow +\infty} \|x_n - p\|^2 = l, \quad (40)$$

and from (26), we can get

$$\begin{aligned} \|\omega_n - p\|^2 &= \|x_n - p\|^2 + \eta_n (\|x_n - p\|^2 - \|x_{n-1} - p\|^2) \\ &\quad + \eta_n (1 + \eta_n) \|x_n - x_{n-1}\|^2. \end{aligned} \quad (41)$$

According to the sequence,  $\{\eta_n\}$  is bounded, so

$$\lim_{n \rightarrow +\infty} \|\omega_n - p\|^2 = l. \quad (42)$$

From this, we get that  $\{x_n\}$ ,  $\{\omega_n\}$ , and  $\{z_n\}$  are all bounded sequences, and then there

$$0 \leq \|x_n - \omega_n\| \leq \|x_n - x_{n+1}\| + \|x_{n+1} - \omega_n\| \longrightarrow 0, n \longrightarrow +\infty. \quad (43)$$

Now, we prove that the sequence  $\{x_n\}$  weakly converges to  $p \in VI(C, \mathfrak{T})$ . In fact, because the sequence  $\{x_n\}$  is bounded, we assume that there is a subset of the sequence  $\{x_n\}$ , which makes it weakly converge to  $z \in H$ . Without loss of generality, we still use  $\{x_n\}$  below to represent the subset. That is,  $x_n \rightharpoonup z$ , where “ $\rightharpoonup$ ” represents weak convergence.

Because of  $\|x_n - \omega_n\| \longrightarrow 0$ , there is a subset to make it weakly converge to  $z$ . We still use  $\{\omega_n\}$  below to represent the sequence, which is  $\omega_n \rightharpoonup z$ . Similarly, the following uses  $\{y_n\}$  to represent the subset of the original number sequence  $\{y_n\}$ . Since  $\mathfrak{T}$  is a monotone operator and  $y_n = P_C(\omega_n - \rho_n \mathfrak{T}\omega_n)$ ,  $\forall x \in C$ , there is

$$\begin{aligned} 0 &\leq \langle y_n - \omega_n + \rho_n \mathfrak{T}\omega_n, x - y_n \rangle \\ &= \langle y_n - \omega_n, x - y_n \rangle + \rho_n \langle \mathfrak{T}\omega_n, x - y_n \rangle \\ &= \langle y_n - \omega_n, x - y_n \rangle + \rho_n \langle \mathfrak{T}\omega_n, x - \omega_n \rangle + \rho_n \langle \mathfrak{T}\omega_n, \omega_n - y_n \rangle \\ &\leq \langle y_n - \omega_n, x - y_n \rangle + \rho_n \langle \mathfrak{T}\omega_n, x - \omega_n \rangle + \rho_n \langle \mathfrak{T}x, \omega_n - y_n \rangle. \end{aligned} \quad (44)$$

Let  $n \longrightarrow +\infty$ , then  $\forall x \in C$  has

$$\langle \mathfrak{T}x, x - z \rangle \geq 0. \quad (45)$$

By Lemma 4, we can get  $z \in VI(C, \mathfrak{T})$ , so we have proved the following:

- (a)  $\forall p \in VI(C, \mathfrak{T})$ , then  $\lim_{n \rightarrow \infty} \|x_n - p\|^2$  limits exist;
- (b) Each weak convergence point of the logarithmic sequence  $\{x_n\}$  is in  $VI(C, \mathfrak{T})$ .

From Lemma 3, we know that the sequence  $\{x_n\}$  weakly converges to  $p \in VI(C, \mathfrak{T})$ .

**Corollary 1.** Given  $\rho_0 > 0$ , suppose that  $\{x_n\}$  be a sequence in  $H$  defined by

$$\begin{cases} x_0, x_1 \in H, \mu \in \left(\frac{1}{\sqrt{2}}, 1\right), \\ y_n = P_C(x_n - \rho_n \mathfrak{T}x_n), \\ x_{n+1} = y_n - P_C(\rho_n \mathfrak{T}y_n - \rho_n \mathfrak{T}x_n), \end{cases} \quad (46)$$

where

$$\rho_{n+1} = \begin{cases} \min \left\{ \frac{\mu \|y_n - \omega_n\|}{\|\mathfrak{T}y_n - \mathfrak{T}\omega_n\|}, \rho_n \right\}, & \mathfrak{T}y_n - \mathfrak{T}\omega_n \neq 0, \\ \rho_n, & \text{other.} \end{cases} \quad (47)$$

Then, the sequence  $\{x_n\}$  converges weakly to an element of  $\in VI(C, \mathfrak{T})$ .

**Lemma 9.** Let  $\pi > 0$ . A point  $x \in C$  is a solution of  $VI(C, \mathfrak{T})$  if and only if  $x \in \text{Fix}P_C(I d - \pi \mathfrak{T})$  (see [16]).

According to Theorem 2 and Lemma 9, we get the following two inferences.

**Corollary 2.** Let  $\{\rho_n\}$  be a sequence obtained by Algorithm 1, and  $\pi > 0$  and  $\text{Fix}P_C(I d - \pi \mathfrak{T}) \neq \emptyset$ . If  $\{\eta_n\}$  is a nonincreasing sequence, make  $0 \leq \eta_n \leq \eta$  and  $\eta < (\sqrt{1 + 8\mathfrak{K}} - 1 - 2\mathfrak{K}) / (2(1 - 2\mathfrak{K}))$ , where  $\mathfrak{K} := 1 - \mu^2$ , then the sequence  $\{x_n\}$  obtained by Algorithm 1 weakly converges to  $\text{Fix}P_C(I d - \pi \mathfrak{T})$ .

**Corollary 3.** Given  $\rho_0 > 0$ , suppose that  $\{x_n\}$  be a sequence in  $H$  defined by

$$\begin{cases} x_0, x_1 \in H, \mu \in \left(\frac{1}{\sqrt{2}}, 1\right), \\ y_n = P_C(x_n - \rho_n \mathfrak{T}x_n), \\ x_{n+1} = y_n - P_C(\rho_n \mathfrak{T}y_n - \rho_n \mathfrak{T}x_n), \end{cases} \quad (48)$$

where

$$\rho_{n+1} = \begin{cases} \min \left\{ \frac{\mu \|y_n - \omega_n\|}{\|\mathfrak{T}y_n - \mathfrak{T}\omega_n\|}, \rho_n \right\}, & \mathfrak{T}y_n - \mathfrak{T}\omega_n \neq 0, \\ \rho_n, & \text{other.} \end{cases} \quad (49)$$

Then, the sequence  $\{x_n\}$  converges weakly to an element of  $\text{Fix}P_C(I d - \pi \mathfrak{T})$ .

The new Tseng-like gradient method is convergent. It is known that the algorithm has good accuracy due to the selection of step size. Finally, it also can be known that the algorithm has good applicability through inference.



## Data Availability

The data used to support the findings of this study are available from the corresponding author upon request.

## Conflicts of Interest

The authors declare that they have no conflicts of interest.

## Acknowledgments

This work was supported by the grants study on numerical simulation of soil solute transport based on lattice Boltzmann method project of the National Natural Science Foundation of China 11861003. Professor Hefang Jing is the project host and the project funding is 400,000 RMB.

## References

- [1] Y. I. Alber and A. N. Iusem, "Extension of subgradient techniques for nonsmooth optimization in Banach spaces," *Set-Valued Analysis*, vol. 9, no. 4, pp. 315–335, 2001.
- [2] F. Alvarez, "Weak convergence of a relaxed and inertial hybrid projection-proximal point Algorithm for maximal monotone operators in Hilbert space," *SIAM Journal on Optimization*, vol. 14, no. 3, pp. 773–782, 2004.
- [3] H. Attouch, X. Goudou, and P. Redont, "The heavy ball with friction method, I. The continuous dynamical system: global exploration of the local minima of a real-valued function by asymptotic analysis of a dissipative dynamical system," *Communications in Contemporary Mathematics*, vol. 2, no. 1, pp. 1–34, 2000.
- [4] H. Attouch and M.-O. Czarnecki, "Asymptotic control and stabilization of nonlinear oscillators with non-isolated equilibria," *Journal of Differential Equations*, vol. 179, no. 1, pp. 278–310, 2002.
- [5] H. H. Bauschke and P. L. Combettes, *Convex Analysis and Monotone Operator Theory in Hilbert Spaces*, Springer, New York, NY, USA, 2011.
- [6] R. I. Bot, E. R. Csetnek, and S. C. Laszlo, "An inertial forward-backward algorithm for the minimization of the sum of two nonconvex functions," *EURO Journal on Computational Optimization*, vol. 4, pp. 3–25, 2016.
- [7] R. I. Bot and E. R. Csetnek, "An inertial Tsengs type proximal algorithm for nonsmooth and nonconvex optimization problems," *Journal of Optimization Theory and Applications*, vol. 171, pp. 600–616, 2015.
- [8] R. I. Bot, E. R. Csetnek, and C. Hendrich, "Inertial Douglas-Rachford splitting for monotone inclusion problems," *Applied Mathematics and Computation*, vol. 256, pp. 472–487, 2015.
- [9] R. I. Bot and E. R. Csetnek, "An inertial alternating direction method of multipliers," *Minimax Theory and Applications*, vol. 1, pp. 29–49, Springer, Dordrecht, Netherlands, 2016.
- [10] R. I. Bot and E. R. Csetnek, "A hybrid proximal-extragradient algorithm with inertial effects?" *Numerical Functional Analysis and Optimization*, vol. 36, no. 8, pp. 951–963, 2015.
- [11] Y. Censor, A. Gibali, and S. Reich, "Algorithms for the split variational inequality problem," *Numerical Algorithms*, vol. 59, no. 2, pp. 301–323, 2012.
- [12] D. V. Thong and D. V. Hieu, "Modified Tseng's extragradient algorithms for variation inequality problems," *Journal of Fixed Point Theory and Applications*, vol. 20, no. 4, 2018.
- [13] R. I. Bot and E. R. Csetnek, "An inertial forward-backward-forward primal-dual splitting algorithm for solving monotone inclusion problems," *Numerical Algorithms*, vol. 71, pp. 519–540, 2016.
- [14] F. Alvarez and H. Attouch, "An inertial proximal method for maximal monotone operators via discretization of a nonlinear oscillator with damping," *Set-Valued Analysis*, vol. 9, no. 1-2, pp. 3–11, 2001.
- [15] W. Takahashi, *Nonlinear Functional Analysis; Fixed Point Theory and its Applications*, Yokohama Publishers, vol. 152, 18 pages, Yokohama, Tokyo, Japan, 2000.
- [16] L. J. Zhu, Y. Yao, and M. Postolache, "Projection methods with linesearch technique for pseudomonotone equilibrium problems and fixed point problems," *UPB Scientific Bulletin, Series A*, In press.



## Research Article

# An Approach to Selection of Agricultural Product Supplier Using Pythagorean Fuzzy Sets

Lina Dai  and Shizhen Bai

*Management School, Harbin University of Commerce, Harbin 150028, Heilongjiang, China*

Correspondence should be addressed to Lina Dai; [dailinahrb1984@hotmail.com](mailto:dailinahrb1984@hotmail.com)

Received 5 June 2020; Accepted 17 July 2020; Published 4 August 2020

Guest Editor: Zaoli Yang

Copyright © 2020 Lina Dai and Shizhen Bai. This is an open access article distributed under the Creative Commons Attribution License, which permits unrestricted use, distribution, and reproduction in any medium, provided the original work is properly cited.

The selection of agricultural product supplier is an important link to optimize the supply chain management of agricultural products. Due to the uncertainty factors and the lack of decision-makers' cognition, the selection of agricultural products suppliers has become a very complex and difficult work. Therefore, in order to effectively deal with these problems, this study proposes an agricultural product supplier selection algorithm based on the Pythagorean fuzzy power Bonferroni mean operator under Pythagorean fuzzy environment. In this method, first, the power operator and Bonferroni mean operator are combined and embedded in the Pythagorean fuzzy sets to build a Pythagorean fuzzy power Bonferroni mean operator. Then, a multiattribute decision-making method based on the operator proposed in this paper is proposed. Finally, an analysis of examples of agricultural product supplier selection is given to verify the rationality and effectiveness of this method.

## 1. Introduction

The sources of safety problems of agricultural products mainly include excessive use of pesticides and chemical fertilizers in agricultural production, environmental pollution caused by “three wastes” in the processing of agricultural products, environmental degradation caused by water loss and soil erosion in the ecological environment, excessive use of additives in food production and processing, and food packaging materials that do not meet the requirements. In addition, primary agricultural and livestock products, such as fruits, vegetables, meat, eggs, and aquatic products, are perishable and obviously affected by geography and seasons, and there is a certain degree of time-space separation between supply and demand, which will also cause safety problems of agricultural products. Therefore, the supply of agricultural products is closely related to people's life and production and has been concerned by various countries for a long time [1, 2]. At present, a large number of enterprises, such as supermarkets, catering enterprises, and agricultural products processing enterprises, faced with the problem of selection of agricultural products suppliers [3]. The purchase

of agricultural products is the starting point and key link of the supply chain of agricultural products. The price, cold-chain transportation, distance, production standards, and other aspects of agricultural products will ultimately affect the market competitiveness of terminal products of fresh agricultural products supply chain [4]. How to select a reasonable supplier has become one of the concerns of many agricultural products-related enterprises.

Many internal and external uncertainty factors of enterprise need to be considered in the selection process of agricultural products suppliers, which is also affected by the subjective preferences of decision-makers. Therefore, the selection of agricultural products suppliers is essentially a fuzzy multiattribute decision-making problem. Fuzzy multiattribute decision-making problem has always been a hot topic in the field of decision-making and has attracted the attention of many scholars [5–10]. The fuzzy set theory proposed by Zadeh [11] lays the foundation for practical operation of fuzzy multiattribute decision-making problems. With the continuous research of fuzzy set theory, Atanassov put forward the intuitionistic fuzzy set theory [12]. After that, many scholars have extended the

intuitionistic fuzzy set [13–19]. Among them, Yager proposed that the Pythagorean fuzzy set is one of the important research studies [18, 19]. Compared with the intuitionistic fuzzy set, the Pythagorean fuzzy set has stronger information representation ability and is more close to the practical problems. Once the Pythagorean fuzzy set is put forward, it has gained widespread attention in academic circles.

Many scholars mainly focus on the study of the extended form of the Pythagorean fuzzy set, including the study of the information integration operator of the Pythagorean fuzzy set and the fuzzy multiattribute decision-making based on Pythagoras. For example, Garg [20] improved the score function, which can better compare the sizes of Pythagorean fuzzy numbers. He et al. [21] studied the Pythagorean hesitant fuzzy integration operator and its decision-making application. In view of the important role of the integration operator in the Pythagorean hesitant fuzzy multiattribute decision-making and the imperfection of the integration operator, He et al. [21] systematically studied the Pythagorean hesitant fuzzy integration operator. Gou et al. studied the continuity and differentiation of Pythagorean fuzzy numbers. Peng et al. [22] combined the properties of Pythagorean fuzzy set and parameterization of the soft set, constructed the Pythagorean fuzzy soft set, introduced the properties of the Pythagorean fuzzy soft set and discussed its decision-making application, and then discussed its DeMorgan's law. Zhao and Wang [23] proposed a multiattribute decision-making method based on the Hamacher operator in view of the multiattribute decision-making problem of dual hesitant Pythagorean fuzzy uncertain linguistic information. Then, based on the Hamacher operator, Zhao and Wang [23] defined the operation rule between dual hesitant Pythagorean fuzzy uncertain linguistic variables. He et al. [24] applied the power average operator to the Pythagorean fuzzy decision-making environment, defined the average operator of the Pythagorean fuzzy power, orderly weighted the average operator of Pythagorean fuzzy power, geometric operator of Pythagorean fuzzy power and orderly weighted geometric operator of Pythagorean fuzzy power, and then studied their properties, respectively. In the latest research progress, Chen [25] published a paper on proposing a new Pythagorean Chebyshev distance measure and established a practical method for eliminating and selecting the conversion based on Chebyshev distance measure. Shakeel et al. [26] defined the Einstein operator on the Pythagorean trapezoid fuzzy set and expanded it into two average aggregation operators. Ullah et al. [27] proposed the concept of the complex Pythagorean fuzzy set (CPFS) in view of the limitation of the complex fuzzy set and complex intuitionistic fuzzy set. Yang and Chang [28] defined the new concept of the interval-valued Pythagorean normal fuzzy set and developed a series of aggregation operators for addressing the interval-valued Pythagorean normal fuzzy information. Harish [29] presented a Pythagorean fuzzy neutrality aggregation operator. Han et al. [30] developed an interval-valued Pythagorean prioritized operator from the perspective of game theory.

It can be seen from the above literature that up to now, the research of the Pythagorean fuzzy set has made some

achievements, but it still has room to expand in the field of the information aggregation operator and its application. Therefore, this study proposes the average operator of Pythagorean fuzzy power Bonferroni, which will be applied to the study of agricultural product supplier selection, so as to build a decision-making support framework for agricultural product supplier selection based on the Pythagoras power Bonferroni average operator. The main contributions of this study are as follows:

- (1) The average operator of Pythagorean fuzzy power Bonferroni was proposed.
- (2) A decision-making algorithm for agricultural product supplier selection was proposed based on the Pythagorean fuzzy power Bonferroni average (PFPBA) operator.

The other contents of this paper are as follows: part 2 reviews the basic concepts, algorithms, and distance measures of Pythagorean fuzzy. Part 3 puts forward the Pythagorean fuzzy power Bonferroni mean operator and analyzes its properties. Part 4 constructs a multiattribute decision-making method based on the average operator of the Pythagorean fuzzy power Bonferroni mean operator. Part 5 gives an example to verify the validity and rationality of the method. Part 6 summarizes some conclusions.

## 2. Pythagorean Fuzzy Sets

*Definition 1* (see [18, 19]). Assuming that  $X$  is a nonempty general set, the expression of the Pythagorean fuzzy set  $A$  defined on  $X$  is

$$A = \{ \langle x, u_A(x), v_A(x) \rangle \mid x \in X \}, \quad (1)$$

where  $u_A(x): X \rightarrow [0, 1]$  and  $v_A(x): X \rightarrow [0, 1]$  represent the membership function and nonmembership function of  $A$  and  $\forall x \in X, u_A(x)^2 + v_A(x)^2 \leq 1$ . In addition, the hesitancy degree is defined as  $\pi(x) = \sqrt{1 - u_A(x)^2 - v_A(x)^2}$ .

For simplicity,  $p_A(x) = (u_A(x), v_A(x))$  is called a Pythagorean fuzzy number. Assuming that  $p_i = (u_i, v_i) (i = 1, 2)$ ,  $p = (u_p, v_p)$  is three Pythagorean fuzzy numbers, and  $\lambda$  is any real number greater than or equal to 0, then the following operation rules are specified:

- (1)  $p_1 \oplus p_2 = (\sqrt{u_1^2 + u_2^2 - u_1^2 u_2^2}, v_1 v_2)$
- (2)  $p_1 \otimes p_2 = (u_1 u_2, \sqrt{v_1^2 + v_2^2 - v_1^2 v_2^2})$
- (3)  $\lambda p = (\sqrt{1 - (1 - u^2)^\lambda}, v^\lambda)$
- (4)  $p^\lambda = (\sqrt{1 - (1 - v^2)^\lambda}, v^\lambda)$

Therefore, the following conclusions can be drawn:

- (1)  $\alpha_1 \oplus \alpha_2 = \alpha_2 \oplus \alpha_1$
- (2)  $\alpha_1 \otimes \alpha_2 = \alpha_2 \otimes \alpha_1$
- (3)  $\lambda(\alpha_1 \oplus \alpha_2) = \lambda \alpha_1 \oplus \lambda \alpha_2$
- (4)  $(\alpha_1 \otimes \alpha_2)^\lambda = \alpha_1^\lambda \otimes \alpha_2^\lambda$
- (5)  $\lambda_1 \alpha + \lambda_2 \alpha = (\lambda_1 + \lambda_2) \alpha$
- (6)  $\alpha^{\lambda_1} \otimes \alpha^{\lambda_2} = \alpha^{\lambda_1 + \lambda_2}$

**Definition 2** (see [18-19]). Assuming  $p = (u, v)$  is a Pythagorean fuzzy number, the score function of  $p$  is defined as  $S_{(p)} = u^2 - v^2$ , and the exact function of  $p$  is defined as  $H_{(p)} = u^2 + v^2$ . For any two Pythagorean fuzzy numbers  $p_1 = (u_1, v_1)$  and  $p_2 = (u_2, v_2)$ , the definitions are as follows:

- (1) If  $S_{(p_1)} > S_{(p_2)}$ , then  $p_1 > p_2$
- (2) If  $S_{(p_1)} > S_{(p_2)}$ , then  $p_1 = p_2$  when  $H_{(p_1)} = H_{(p_2)}$ ;  
 $p_1 < p_2$  when  $H_{(p_1)} > H_{(p_2)}$

**Definition 3** (see [18, 19]). Assuming that  $p_1 < p_2$ ,  $\alpha_1 = (u_1, v_1)$  and  $\alpha_2 = (u_2, v_2)$  are any two Pythagorean

fuzzy numbers, then the standard hamming distance  $d(\alpha_1, \alpha_2)$  of  $\alpha_1$  and  $\alpha_2$  can be defined as

$$d(\alpha_1, \alpha_2) = \frac{|u_1^2 - u_2^2| + |v_1^2 - v_2^2| + |\pi_1^2 - \pi_2^2|}{2}, \quad (2)$$

where  $\pi_1 = \sqrt{1 - u_1^2 - v_1^2}$  and  $\pi_2 = \sqrt{1 - u_2^2 - v_2^2}$ .

### 3. PFPBA Operator

**Definition 4** (see [31]). Assuming  $s$  and  $t$  are nonnegative real numbers that are not both zero and  $\alpha_i$  ( $i = 1, 2, \dots, n$ ) is a series of nonnegative real numbers, if

$$PBM^{s,t}(a_1, a_2, a_3, \dots, a_n) = \left[ \frac{1}{n(n-1)} \sum_{i,j=1, i \neq j}^n \left\{ \left( \frac{n(1+T(a_i))}{\sum_{i=1}^n (1+T(a_i))} a_i \right)^s \cdot \left( \frac{n(1+T(a_j))}{\sum_{j=1}^n (1+T(a_j))} a_j \right)^t \right\} \right]^{(1/s+t)}. \quad (3)$$

Then,  $PBM^{s,t}$  is the average operator of power Bonferroni, in which  $T(a_i) = \sum_{j=1, j \neq i}^n \text{Sup}(a_i, a_j)$  ( $i = 1, 2, \dots, n$ ), and  $\text{Sup}(a_i, a_j)$  represents the supporting degree of  $a_i$  and  $a_j$  and meets the following conditions:

- (1)  $\text{Sup}(a_i, a_j) \in [0, 1]$
- (2)  $\text{Sup}(a_i, a_j) = \text{Sup}(a_j, a_i)$
- (3)  $\text{Sup}(a, b) \geq \text{Sup}(c, d)$  if and only if  $|a - b| \geq |c - d|$
- (4) If  $d(a_i, a_j) \leq d(a_i, a_k)$ , then  $\text{Sup}(a_i, a_j) \geq \text{Sup}(a_i, a_k)$ , in which  $d$  is the standard hamming distance of  $a_i$  and  $a_j$ .

**Definition 5.** Assuming that  $s$  and  $t$  are nonnegative real numbers that are not both zero,  $a_i$  ( $i = 1, 2, \dots, n$ ) is the set of a group of Pythagorean fuzzy numbers, and  $a_i = (u_i, v_i)$  ( $i = 1, 2, \dots, n$ ), and  $q \geq 1$ . Then, the Pythagorean fuzzy power Bonferroni mean (PFPBA) operator can be defined as

$$PFPBM(a_1, a_2, a_3, \dots, a_n) = \left[ \frac{1}{n(n-1)} \oplus \sum_{i,j=1, i \neq j}^n \left\{ \left( \frac{n(1+T(a_i))}{\sum_{i=1}^n (1+T(a_i))} a_i \right)^s \otimes \left( \frac{n(1+T(a_j))}{\sum_{j=1}^n (1+T(a_j))} a_j \right)^t \right\} \right]^{(1/s+t)}, \quad (4)$$

where  $T(a_i) = \sum_{j=1, j \neq i}^n \text{Sup}(a_i, a_j)$  ( $i = 1, 2, \dots, n$ ), and  $\text{Sup}(a_i, a_j)$  indicates the supporting degree of  $a_i$  and  $a_j$  and meets the following conditions:

- (1)  $\text{Sup}(a_i, a_j) \in [0, 1]$
- (2)  $\text{Sup}(a_i, a_j) = \text{Sup}(a_j, a_i)$
- (3)  $\text{Sup}(a, b) \geq \text{Sup}(c, d)$  if and only if  $|a - b| \geq |c - d|$

- (4) If  $d(a_i, a_j) \leq d(a_i, a_k)$ , then  $\text{Sup}(a_i, a_j) \geq \text{Sup}(a_i, a_k)$ , in which  $d$  is the standard hamming distance of the two Pythagorean fuzzy numbers.

**Definition 6.** Assuming that  $\alpha_i = (u_i, v_i)$  ( $i = 1, 2, \dots, n$ ) is the Pythagorean fuzzy number and  $s$  and  $t$  are nonnegative real numbers that are not both zero, then the integration value of these Pythagorean fuzzy numbers obtained by using the PFPBA operator is still a Pythagorean fuzzy number, and

$$\text{PFPBA}(a_1, a_2, \dots, a_n) = \left( \sqrt[1/n(n-1)]{\left\{ 1 - \left[ \prod_{\substack{i,j=1 \\ i \neq j}}^n \left( 1 - (1 - (1 - u_i^2))^s \right) \left( 1 - \left( 1 - (1 - u_i^2)^{\frac{n(1+T(a_j))}{\sum_{i=1}^n (1+T(a_j))}} \right)^t \right) \right] \right\}^{(1/n(n-1))} \right)^{(1/s+t)} \right)^{1/2}, \quad (5)$$

$$\sqrt[1/n(n-1)]{\left\{ 1 - \left[ \prod_{\substack{i,j=1 \\ i \neq j}}^n \left( 1 - (1 - v_i)^{\frac{2n(1+T(a_j))}{\sum_{i=1}^n (1+T(a_j))}} \right) \left( (1 - v_j)^{\frac{2n(1+T(a_j))}{\sum_{j=1}^n (1+T(a_j))}} \right)^t \right] \right\}^{(1/n(n-1))} \right)^{(1/s+t)} \right)^{1/2}.$$

According to the Definition 3, it is easy to prove that the above formula is true by mathematical induction.

Some basic properties of the average operators of Pythagorean fuzzy power Bonferroni are discussed as follows:

- (1) (Power equitability) Assuming that  $\alpha_i = (u_i, v_i)$  ( $i = 1, 2, \dots, n$ ) is the Pythagorean fuzzy number and  $\alpha_1 = \alpha_2 = \dots = \alpha_n = \alpha$ , then

$$\text{PFPBA}(a_1, a_2, a_3, \dots, a_n) = \alpha. \quad (6)$$

- (2) (Permutation invariance) Assuming that  $\alpha_i = (u_i, v_i)$  ( $i = 1, 2, \dots, n$ ) is the  $\alpha_i = (u_i, v_i)$  ( $i = 1, 2, \dots, n$ ) number and  $\beta_1, \beta_2, \beta_3, \dots, \beta_n$  is any permutation and combination of  $\alpha_1, \alpha_2, \alpha_3, \dots, \alpha_n$ , then

$$\text{PFPBA}(a_1, a_2, a_3, \dots, a_n) = \text{PFPBA}(\beta_1, \beta_2, \beta_3, \dots, \beta_n). \quad (7)$$

- (3) (Boundedness) Assuming that  $\alpha_i = (u_i, v_i)$  ( $i = 1, 2, \dots, n$ ) is the Pythagorean fuzzy number,  $\beta_i = (n(1+T(a_j))/\sum_{j=1}^n (1+T(a_j)))a_i$ ,  $\beta^+ = \max(\beta_i)$ , and  $\beta^- = \min(\beta_i)$ , then

$$\beta^- \leq \text{PFPBA}(a_1, a_2, a_3, \dots, a_n) \leq \beta^+. \quad (8)$$

#### 4. Multiattribute Decision-Making Model Based on the PFPBA Operator

In the problem of Pythagorean fuzzy information multiattribute decision-making, assume that there are  $n$  alternative schemes  $X = (x_1, x_2, x_3, \dots, x_n)$  and  $m$  decision attributes  $C = (c_1, c_2, c_3, \dots, c_m)$ . The experts provide the evaluation information of Pythagorean fuzzy and set the attribute value of the scheme  $x_i$  under the attribute of  $c_j$  to be  $a_{ij}$ . In which  $a_{ij}$  is the Pythagorean fuzzy number, and then, the decision matrix of Pythagorean fuzzy  $M = (a_{ij})_{nm}$  can be obtained.  $u_{ij}$  and  $v_{ij}$  represent the value of membership degree and nonmembership degree of the attribute  $j$  of the alternative scheme  $i$ . A decision

method based on Pythagorean fuzzy information is proposed as follows in combination with the Pythagorean fuzzy power Bonferroni operator, and the specific steps are illustrated in Figure 1:

- Step 1: use the PFPBA operator to integrate the attribute values of schemes  
 Step 2: calculate the score function of each scheme according to Definition 2  
 Step 3: sort the schemes according to the score function  
 Step 4: select the best scheme according to the scheme ranking

#### 5. Example Analysis of Agricultural Product Supplier Selection

**5.1. Calculation Process.** The safety of agricultural products is a major livelihood issue. Countries have raised their standards for the production and processing of agricultural products, and ordinary people have also raised their awareness of consumption of agricultural products. In order to adapt to the rapidly changing market demand of agricultural products, reduce the operating costs of agricultural production enterprises, and improve the core competitiveness of the company, enterprises need to select appropriate agricultural products suppliers for cooperation. When selecting suppliers, enterprises often need to define their own needs and select appropriate suppliers according to their own needs. In addition, as the concept of green agricultural products has been strongly advocated and gradually gained popularity in recent years, enterprises should also consider environmental protection and implement the strategy of sustainable development when selecting suppliers for cooperation. An agricultural product enterprise in a city intends to select a supplier as a stable source of supply for agricultural products. After preliminary market research, it selects suppliers from multiple perspectives and selects four suppliers with core competitiveness, which are represented with  $X = (x_1, x_2, x_3, x_4)$ , respectively. The decision-maker evaluates four suppliers from 4 aspects:  $C_1$  green technology level (including pollution control level and environmental planning ability),  $C_2$  product advantage (including product

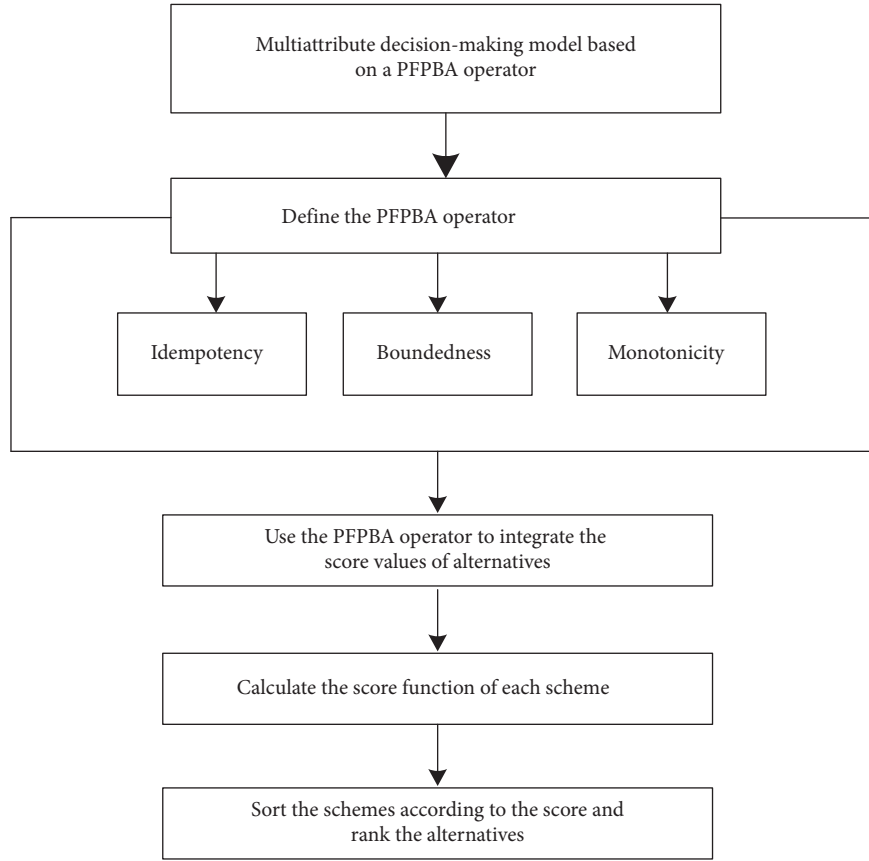


FIGURE 1: The framework of the proposed method.

TABLE 1: Pythagorean fuzzy decision matrix.

	$C_1$	$C_2$	$C_3$	$C_4$
$x_1$	$\langle 0.899, 0.301 \rangle$	$\langle 0.703, 0.601 \rangle$	$\langle 0.497, 0.796 \rangle$	$\langle 0.602, 0.299 \rangle$
$x_2$	$\langle 0.402, 0.698 \rangle$	$\langle 0.893, 0.202 \rangle$	$\langle 0.802, 0.106 \rangle$	$\langle 0.503, 0.302 \rangle$
$x_3$	$\langle 0.801, 0.402 \rangle$	$\langle 0.703, 0.491 \rangle$	$\langle 0.6, 0.202 \rangle$	$\langle 0.693, 0.401 \rangle$
$x_4$	$\langle 0.697, 0.205 \rangle$	$\langle 0.807, 0.200 \rangle$	$\langle 0.8, 0.401 \rangle$	$\langle 0.605, 0.602 \rangle$

price, product quality, and the product warranty period),  $C_3$  risk bearing capacity (including the company's capital scale and enterprise prospect), and  $C_4$  enterprise production ability (including the company's equipment quantity and production efficiency) to select the best supplier. After consultation, the expert group gives the following decision matrix as shown in Table 1:

Step 1: according to the actual situation, establish the Pythagorean fuzzy decision matrix, as shown in Table 1

Step 2: use the integration operator PFPBA to calculate the comprehensive attribute value of each scheme, and meanwhile, we take  $s = t = 1$ , and the comprehensive attribute value of each scheme is calculated as follows:

$$\begin{aligned}
 x_1 &= (0.6872, 0.5181), \\
 x_2 &= (0.5141, 0.3327), \\
 x_3 &= (0.7035, 0.3813), \\
 x_4 &= (0.7302, 0.3598)
 \end{aligned} \tag{9}$$

Step 3: the score of each scheme is calculated as  $s_{x_1} = 0.2038$ ,  $s_{x_2} = 0.1536$ ,  $s_{x_3} = 0.3495$ ,  $s_{x_4} = 0.4038$ , respectively

Step 4: after comparison of score values, it can be known according to  $s_{x_4} > s_{x_3} > s_{x_1} > s_{x_2}$  that the scheme  $s_{x_4}$  is the best one

## 5.2. Comparison with Different Methods

- (1) When the Pythagorean fuzzy power average operator is used to integrate these attribute values:



Step 1: Establish the Pythagorean fuzzy decision matrix according to actual situation, as shown in Table 1.

Step 2: Use the Pythagorean fuzzy power average operator to calculate the comprehensive attribute value of each scheme. Then, the comprehensive attribute value of each scheme can be calculated:

$$\begin{aligned}x_1 &= (0.9856, 0.0264), \\x_2 &= (0.9529, 0.0019), \\x_3 &= (0.9816, 0.0079), \\x_4 &= (0.9878, 0.0042).\end{aligned}\quad (10)$$

$$\begin{aligned}x_1 &= (0.2206, 0.8464), \\x_2 &= (0.0673, 0.6122), \\x_3 &= (0.2439, 0.6877), \\x_4 &= (0.2832, 0.6525)\end{aligned}\quad (11)$$

Step 3: The score value of each scheme can be calculated as  $s_{x_1} = 0.9707, s_{x_2} = 0.9080, s_{x_3} = 0.9634, s_{x_4} = 0.9758$ , respectively.

Step 4: After comparison of score values, it can be known according to  $s_{x_4} > s_{x_1} > s_{x_3} > s_{x_2}$  that the scheme  $s_{x_4}$  is the best one.

- (2) When the average operator of Pythagorean fuzzy Bonferroni mean is used to integrate these attribute values:

Step 1: establish the Pythagorean fuzzy decision matrix according to actual situation, as shown in Table 1

Step 2: use the Pythagorean fuzzy Bonferroni mean operator to calculate the comprehensive attribute value of each scheme with  $s = t = 1$  as follows:

Step 3: the score value of each scheme can be calculated as  $s_{x_1} = -0.6677, s_{x_2} = -0.3703, s_{x_3} = -0.4134, s_{x_4} = -0.3456$ , respectively

Step 4: after comparison of score values, it can be known that the scheme  $s_{x_2}$  is the best one

From the above results, it can be known that the results of the method proposed in this paper are the same as the optimal scheme based on the Pythagorean fuzzy power average operator, but their total order is not the same, and it is also different from the sorting results based on the Pythagorean fuzzy Bonferroni mean operator. The reason for this difference is that the two methods do not consider the heterogeneity between attributes and their impact on the evaluation results. Therefore, the method proposed in this paper has strong advantages.

## 6. Conclusion

Considering the uncertain information faced in the selection of agricultural product suppliers, this study proposes a multiattribute decision-making method based on the

Pythagorean fuzzy power Bonferroni mean operator. In this method, the heterogeneous relationship between attributes and the abnormal value of evaluation information are fully considered, and the power operator and Bonferroni average operator are integrated and introduced into the Pythagorean fuzzy information environment to construct an agricultural product supplier selection algorithm based on the Pythagorean fuzzy power Bonferroni mean operator. This algorithm has a strong ability in dealing with uncertain information, and at the same time, it considers the influence of the internal relationship between attributes on the decision results and avoids the adverse effect of the extreme value in the evaluation information on the ranking results through the PA operator. In the future, this study can be combined with other operators, such as Muirhead mean operator and Hamy mean operator, to propose more extensive Pythagorean fuzzy information aggregation operators. At the same time, the operators proposed in this paper can also be applied in other practical decision-making fields, such as traffic route selection, enterprise performance evaluation, and human resource management.

## Data Availability

The data used to support the findings of this study are included within the article.

## Conflicts of Interest

The authors declare that they have no conflicts of interest.

## Acknowledgments

The authors acknowledge that this work was supported by the Natural Science Foundation of China (No. 71671054) and Heilongjiang Social Science Foundation of China (No. 18JYB147).

## References

- [1] Y. L. Liu and T. T. Jin, "Application of Raman spectroscopy technique to agricultural products quality and safety determination," *Spectroscopy and Special Analysis*, vol. 35, no. 9, pp. 2567–2572, 2015.
- [2] C. Ma, D. Wang, D. Wang et al., "Considerations of constructing quality, health and safety management system for agricultural products sold via e-commerce," *International Journal of Agricultural and Biological Engineering*, vol. 11, no. 1, pp. 31–39, 2018.
- [3] B. Yan, C. Yan, C. Ke, and X. Tan, "Information sharing in supply chain of agricultural products based on the internet of things," *Industrial Management & Data Systems*, vol. 116, no. 7, pp. 1397–1416, 2016.
- [4] G. Chen, "Production decision of agricultural products: A game model based on negative exponential utility function," *Journal of Intelligent & Fuzzy Systems*, vol. 37, no. 5, pp. 6139–6149, 2019.
- [5] Z. Yang, T. Ouyang, X. Fu, and X. Peng, "A decision-making algorithm for online shopping using deep-learning-based opinion pairs mining and q-rung orthopair fuzzy interaction



- Heronian mean operators," *International Journal of Intelligent Systems*, vol. 35, no. 5, pp. 783–825, 2020.
- [6] Z. L. Yang, H. Garg, J. Li, G. Srivastava, and Z. Cao, "Investigation of multiple heterogeneous relationships using a q-rung orthopair fuzzy multi-criteria decision algorithm," *Neural Computing and Applications*, pp. 1–22, 2020.
  - [7] X. Zhang and Z. Xu, "A new method for ranking intuitionistic fuzzy values and its application in multi-attribute decision making," *Fuzzy Optimization and Decision Making*, vol. 11, no. 2, pp. 135–146, 2012.
  - [8] G. Yu, "An algorithm for multi-attribute decision making based on soft rough sets," *Journal of Computational Analysis and Applications*, vol. 20, no. 7, pp. 1248–1258, 2016.
  - [9] Z. Yang, X. Li, H. Garg, and M. Qi, "Decision support algorithm for selecting an antivirus mask over COVID-19 pandemic under spherical normal fuzzy environment," *International Journal of Environmental Research and Public Health*, vol. 17, no. 10, p. 3407, 2020.
  - [10] Z. L. Yang, X. Li, Z. H. Cao, and J. Q. Li, "Q-rung orthopair normal fuzzy aggregation operators and their application in multi-attribute decision-making," *Mathematics*, vol. 7, no. 12, Article ID 1142, 2019.
  - [11] L. A. Zadeh, "Fuzzy sets," *Information and Control*, vol. 8, no. 3, pp. 338–353, 1965.
  - [12] K. T. Atanassov, "Intuitionistic fuzzy sets," *Fuzzy Sets and Systems*, vol. 20, no. 1, pp. 87–96, 1986.
  - [13] K. Atanassov and G. Gargov, "Interval valued intuitionistic fuzzy sets," *Fuzzy Sets and Systems*, vol. 31, no. 3, pp. 343–349, 1989.
  - [14] P. Liu and S.-M. Chen, "Multiattribute group decision making based on intuitionistic 2-tuple linguistic information," *Information Sciences*, vol. 430–431, pp. 599–619, 2018.
  - [15] Z. Yang, G. Xiong, Z. Cao, Y. Li, and L. Huang, "A decision method for online purchases considering dynamic information preference based on sentiment orientation classification and discrete DIFWA operators," *IEEE Access*, vol. 7, pp. 77008–77026, 2019.
  - [16] H. M. Nehi, "A new ranking method for intuitionistic fuzzy numbers," *International Journal of Fuzzy Systems*, vol. 12, no. 1, pp. 80–86, 2010.
  - [17] Z. Yang, J. Li, L. Huang, and Y. Shi, "Developing dynamic intuitionistic normal fuzzy aggregation operators for multi-attribute decision-making with time sequence preference," *Expert Systems with Applications*, vol. 82, pp. 344–356, 2017.
  - [18] R. R. Yager, "Pythagorean membership grades in multicriteria decision making," *IEEE Transactions on Fuzzy Systems*, vol. 22, no. 4, pp. 958–965, 2014.
  - [19] R. R. Yager and A. M. Abbasov, "Pythagorean membership grades, complex numbers, and decision making," *International Journal of Intelligent Systems*, vol. 28, no. 5, pp. 436–452, 2013.
  - [20] H. Garg, "New logarithmic operational laws and their aggregation operators for Pythagorean fuzzy set and their applications," *International Journal of Intelligent Systems*, vol. 34, no. 1, pp. 82–106, 2019.
  - [21] X. He, W. F. Liu, and X. Y. Du, "Pythagorean hesitant fuzzy aggregation operators and their applications in decision making," *Application Research of Computers*, vol. 37, no. 8, pp. 1–7, 2019.
  - [22] X. Peng, Y. Yang, J. P. Song et al., "Pythagorean fuzzy soft set and its application," *Computer Engineering*, vol. 7, pp. 224–229, 2015.
  - [23] X. D. Zhao and F. Wang, "Dual hesitant Pythagorean fuzzy uncertain linguistic Hamacher aggregation operators in multiple attribute decision making," *Fuzzy Systems and Mathematics*, vol. 33, no. 5, pp. 89–106, 2019.
  - [24] X. He, Y. X. Du, and W. F. Liu, "Pythagorean fuzzy power average operators," *Fuzzy Systems and Mathematics*, vol. 30, no. 6, pp. 116–124, 2016.
  - [25] T.-Y. Chen, "New Chebyshev distance measures for Pythagorean fuzzy sets with applications to multiple criteria decision analysis using an extended ELECTRE approach," *Expert Systems With Applications*, vol. 147, Article ID 113164, 2020.
  - [26] M. Shakeel, S. Abdullah, M. Aslam, and M. Jamil, "Ranking methodology of induced Pythagorean trapezoidal fuzzy aggregation operators based on Einstein operations in group decision making," *Soft Computing*, vol. 24, no. 10, pp. 7319–7334, 2020.
  - [27] K. Ullah, T. Mahmood, Z. Ali, and N. Jan, "On some distance measures of complex Pythagorean fuzzy sets and their applications in pattern recognition," *Complex & Intelligent Systems*, vol. 6, no. 1, pp. 15–27, 2020.
  - [28] Z. Yang and J. Chang, "Interval-valued Pythagorean normal fuzzy information aggregation operators for multi-attribute decision making," *IEEE Access*, vol. 8, pp. 51295–51314, 2020.
  - [29] G. Harish, "Neutrality operations-based Pythagorean fuzzy aggregation operators and its applications to multiple attribute group decision-making process," *Journal of Ambient Intelligence and Humanized Computing*, vol. 11, no. 7, pp. 3021–3041, 2020.
  - [30] Y. Han, Y. Deng, Z. Cao, and C.-T. Lin, "An interval-valued Pythagorean prioritized operator-based game theoretical framework with its applications in multicriteria group decision making," *Neural Computing and Applications*, vol. 32, no. 12, pp. 7641–7659, 2020.
  - [31] P. Liu and X. Liu, "Multiattribute group decision making methods based on linguistic Intuitionistic fuzzy power Bonferroni mean operators," *Complexity*, vol. 2017, Article ID 3571459, 15 pages, 2017.

## Research Article

# Fuzzy Covering-Based Three-Way Clustering

**Dandan Yang** 

*College of Mathematics and Physics, Inner Mongolia University for Nationalities, Tongliao 028000, China*

Correspondence should be addressed to Dandan Yang; [yangdandan@hrbeu.edu.cn](mailto:yangdandan@hrbeu.edu.cn)

Received 17 April 2020; Revised 28 June 2020; Accepted 11 July 2020; Published 31 July 2020

Guest Editor: Yi Su

Copyright © 2020 Dandan Yang. This is an open access article distributed under the Creative Commons Attribution License, which permits unrestricted use, distribution, and reproduction in any medium, provided the original work is properly cited.

This paper investigates the three-way clustering involving fuzzy covering, thresholds acquisition, and boundary region processing. First of all, a valid fuzzy covering of the universe is constructed on the basis of an appropriate fuzzy similarity relation, which helps capture the structural information and the internal connections of the dataset from the global perspective. Due to the advantages of valid fuzzy covering, we explore the valid fuzzy covering instead of the raw dataset for RFCM algorithm-based three-way clustering. Subsequently, from the perspective of semantic interpretation of balancing the uncertainty changes in fuzzy sets, a method of partition thresholds acquisition combining linear and nonlinear fuzzy entropy theory is proposed. Furthermore, boundary regions in three-way clustering correspond to the abstaining decisions and generate uncertain rules. In order to improve the classification accuracy, the  $k$ -nearest neighbor (kNN) algorithm is utilized to reduce the objects in the boundary regions. The experimental results show that the performance of the proposed three-way clustering based on fuzzy covering and kNN-FRFCM algorithm is better than the compared algorithms in most cases.

## 1. Introduction

Three-way decisions (3WD) proposed by Yao [1, 2] is a hot topic in various fields in recent years. Since it was put forward, the idea of tripartition has attracted many scholars to do research. Especially recently, great progress has been made in the theoretical research and model building of three-way decisions based on rough sets. For example, Liang and Liu et al. [3–6] proposed fuzzy three-way decision models and stochastic three-way decision models to deal with real-valued or linguistic-valued decision-making problems. Qian et al. [7] established multigranulation decision-theoretic rough set model based on granular computing theory. Hu [8, 9] introduced the concept of three-way decision space and established a three-way decision model based on partially ordered sets. Qi et al. [10] investigated the 3WD model in the framework of lattice theory. Li et al. [11] have constructed a cost-sensitive sequential three-way decision model to simulate the decision-making process from coarse granularity (high cost) to fine granularity (low cost) and please refer [12–14] for further generalizations and applications of this model. Yao et al. [15] construct an

optimization-based framework for three-way approximations of fuzzy sets. In the meanwhile, for dynamic objects and attributes, some algorithms and incremental 3WD models are designed for classification of dynamic data [16, 17]. From the viewpoint of application, three-way decisions have been widely used in research fields such as pattern recognition [18, 19], artificial intelligence [20–22], engineering, managements [23], and social communities [24].

Based on the above backgrounds and work in three-way decisions, a novel method for three-way clustering based on fuzzy covering is discussed. First, the fuzzy covering of the dataset according to the reasonable fuzzy similarity relation is constructed. The fuzzy covering of the universe requires that the more similar the objects in the universe are, the more similar the corresponding fuzzy classes are. The fuzzy covering established in this way can better reflect the intrinsic relationship between objects in the universe. Therefore, clustering results will have more accuracy with valid fuzzy covering. One of the inevitable problems of clustering is threshold calculation. As is well known, for most of the three-way decision models mentioned above, we

first need to obtain the pair of partition thresholds  $\alpha$  and  $\beta$ . Different thresholds lead to different decision results. The appropriate partition thresholds make the decision more accurate, whereas the inappropriate thresholds distort the decision. Traditionally, the partition thresholds are usually selected according to the experts experience in advance [25–27]. According to the loss function, Yao et al. [1] proposed a method to determine the thresholds by Bayesian risk decision theory. By using Shannon entropy as a measure of uncertainty, Deng et al. [28] present an information-theoretic approach to explain and calculate the thresholds. Zhou et al. [29] explore the shadowed set to automatically obtain the partition thresholds of the three-way decisions but cannot theoretically give a reasonable semantic explanation. To address this issue, inspired by the idea of balancing the uncertainty change of fuzzy sets, a threshold calculation method combining linear fuzzy entropy with nonlinear fuzzy entropy is proposed. This method provides a new scientific explanation for the generation of thresholds. And then, the boundary regions of three-way clustering are processed by the kNN algorithm to reduce uncertainty and improve decision accuracy.

The structure of the rest of this paper is as follows: Section 2 briefly introduces the necessary notions of three-way decisions. Section 3 focuses on constructing the fuzzy covering of the raw dataset according to the fuzzy similarity relation and some necessary conditions and discusses its related properties. In Section 4, a novel rough fuzzy C-means (FRFCM) algorithm based on valid fuzzy covering is established. Then, we investigate the partition thresholds by combining the linear and nonlinear fuzzy entropy. Furthermore, the framework for processing the boundary region of three-way clustering using the kNN algorithm is introduced. In Section 5, the validity and practicability of the algorithm are evaluated by experiment. Concluding remarks are given in Section 6.

## 2. Preliminaries

The basic concepts on three-way decisions are briefly reviewed in this section.

An information system is defined as a 4-tuple  $S = (U, At = C \cup D, V, f)$ , where  $U = \{x_1, x_2, \dots, x_n\}$  denotes a finite nonempty universe,  $C$  is a nonempty finite of condition attributes,  $D$  is a nonempty finite of decision attributes, and  $V = \cup_{a \in At} V_a$ , where  $V_a$  is a domain of attribute  $a$ ;  $f: U \times C \rightarrow V$  is an information function such that  $f(x, a) \in V_a$  for every  $x \in U, a \in At$ . If  $V_a$  is a membership function value, then the value of object  $x$  under attribute  $a$  can be expressed as  $\mu_a(x) \in [0, 1]$ .

The trisecting-and-acting framework of three-way decisions is an extension of binary decision in order to overcome some shortcomings of binary decision. The traditional binary decision model only has acceptance and rejection options, which can easily lead to errors when the information available is insufficient to make an accurate judgment. Sometimes, the cost of wrong decisions is very high. Therefore, deferment decision is necessary, which allows decision makers to collect more information and

make more accurate judgment. This is a strategy that people often adopt in the decision-making process, and deferment decision is consistent with human cognition. A three-way decision model based on the evaluation function and a pair of thresholds is shown as follows.

*Definition 1* (see [30]). Let  $U$  be a finite nonempty universe,  $v$  be an evaluation function, and  $(\alpha, \beta)$  a pair of thresholds,  $0 \leq \beta < \alpha \leq 1$ , then the positive, negative, and boundary regions of any subset  $A \subseteq U$  are defined as follows:

$$\begin{aligned} \text{POS}_{(\alpha, \beta)}(A) &= \{x \in U \mid v_A(x) \geq \alpha\}, \\ \text{NEG}_{(\alpha, \beta)}(A) &= \{x \in U \mid v_A(x) \leq \beta\}, \\ \text{BND}_{(\alpha, \beta)}(A) &= \{x \in U \mid \beta < v_A(x) < \alpha\}. \end{aligned} \quad (1)$$

Evaluation function is the key of decision. The result of decision-making is different with different evaluation functions. There are various evaluation functions that can be adopted. If a fuzzy membership function  $\mu_A$  is used as an evaluation function, then the induced three regions are defined by the following equations [31]:

$$\begin{aligned} \text{POS}_{(\alpha, \beta)}(\mu_A) &= \{x \in U \mid \mu_A(x) \geq \alpha\}, \\ \text{NEG}_{(\alpha, \beta)}(\mu_A) &= \{x \in U \mid \mu_A(x) \leq \beta\}, \\ \text{BND}_{(\alpha, \beta)}(\mu_A) &= \{x \in U \mid \beta < \mu_A(x) < \alpha\}. \end{aligned} \quad (2)$$

The three-valued approximations of a fuzzy set is described by Zadeh [32] as follows: (1)  $x$  belongs to  $A$ , if  $\mu_A(x) \geq \alpha$ ; (2)  $x$  does not belong to  $A$ , if  $\mu_A(x) \leq \beta$ ; (3) and  $x$  has an indeterminate status relative to  $A$ , if  $\beta < \mu_A(x) < \alpha$ . These three cases correspond to the three-way decisions of the above fuzzy set. When  $\alpha = 1$  and  $\beta = 0$ , we obtain the qualitative three-way decisions of a fuzzy set. However, the qualitative decision model of fuzzy set is very restrictive, and we generally do not select these two thresholds.

## 3. Fuzzy Covering and Its Validity

The focus of this section is on the method of constructing valid fuzzy covering of raw data and discusses the properties of the fuzzy covering. Let us first recall some concepts that help us to better understand fuzzy covering.

*Definition 2* (see [33, 34]). Let  $U = \{x_1, x_2, \dots, x_N\}$  be a finite universe and  $F(U)$  be the fuzzy power set of  $U$ . For each  $\gamma \in (0, 1]$ , we call  $P = (P_1, P_2, \dots, P_m)$  with  $P_i \in F(U) (i = 1, 2, \dots, m)$ , a fuzzy  $\gamma$ -covering of  $U$ , if  $(\cup_{i=1}^m P_i)(x) \geq \gamma$  for each  $x \in U$ .  $(U, P)$  is called a fuzzy  $\gamma$ -covering approximation space. If  $\sum_{i=1}^m P_i(x) \geq 1$  for each  $x \in U$ , then  $P$  is called a fuzzy covering of  $U$ .  $(U, P)$  is called a fuzzy covering approximation space.  $\sum_{i=1}^m P_i(x) = 1$  for each  $x \in U$ , then  $P$  is called a fuzzy partition of  $U$ . We call  $(U, P)$  a fuzzy partition approximation space.

*Definition 3* (see [35]). Let  $\sigma$  be a mapping  $\sigma: F(U) \times F(U) \rightarrow [0, 1]$ .  $\sigma(A, B)$  is called the degree of similarity between fuzzy sets  $A$  and  $B$ , if  $\sigma(A, B)$  satisfies the following properties:

- (1)  $\sigma(A, A) = 1, \forall A \in F(U)$
- (2)  $\sigma(A, B) = \sigma(B, A)$
- (3) if  $A \subseteq B \subseteq C$ , then  $\sigma(A, C) \leq \sigma(A, B) \wedge \sigma(B, C)$

Some similarity measures are listed as follows:

$$\begin{aligned}\sigma_1(A, B) &= \frac{\sum_{i=1}^N (\mu_A(x_i) \wedge \mu_B(x_i))}{\sum_{i=1}^N (\mu_A(x_i) \vee \mu_B(x_i))}, \\ \sigma_2(A, B) &= \frac{2 \sum_{i=1}^N (\mu_A(x_i) \wedge \mu_B(x_i))}{\sum_{i=1}^N (\mu_A(x_i) + \mu_B(x_i))}, \\ \sigma_3(A, B) &= 1 - \frac{1}{N} \sum_{i=1}^N |\mu_A(x_i) - \mu_B(x_i)|.\end{aligned}\quad (3)$$

The fuzzy set in this paper is constructed by fuzzy similarity relation  $R$  which satisfies the following properties. For any  $x, y \in U$ ,

- (1)  $0 \leq R(x, y) \leq 1$
- (2)  $R(x, y) = R(y, x)$

For a fuzzy similarity relation  $R \in F(U \times U)$ ,  $\forall x_i \in U$ , and  $[x_i]_R \in F(U)$ , the membership of  $x_j$  belonging to fuzzy set  $[x_i]_R$  is denoted as

$$[x_i]_R(x_j) = R(x_i, x_j), \quad x_j \in U. \quad (4)$$

Obviously, if  $R(x_i, x_j) = 1$ , it means that  $x_j$  certainly belongs to  $[x_i]_R$ . Conversely, if  $R(x_i, x_j) = 0$ , it indicates that  $x_j$  certainly does not belong to  $[x_i]_R$ .  $[x_i]_R$  is also called a fuzzy similarity class associated with  $R$  on  $U$ . Therefore, the set of fuzzy similarity classes  $\{[x_i]_R: i = 1, 2, \dots, |U|\}$  constructed by relation  $R$  is a fuzzy covering of universe  $U$ .

In the following, we investigate the validity and related properties of the fuzzy covering of the raw dataset.

**Definition 4.** Let  $U = \{x_1, x_2, \dots, x_N\}$  be a universe.  $R$  is the fuzzy similarity relation on  $U$ , and  $\sigma$  is the similarity relation on  $F(U)$ .  $\mathbf{P} = \{[x_1], [x_2], \dots, [x_N]\}$  is a fuzzy covering of  $U$  constructed by fuzzy similarity relation  $R$ . For any  $x_i \in U$ ,  $M_i = \{x_j | R(\sigma([x_i], [x_j]), R(x_i, x_j)) \geq \varphi, x_j \in U, j \geq i, \varphi \in (0.5, 1]\}$  is the set of similarity objects with  $x_i$ .  $\mathbf{P}$  is defined as a valid fuzzy covering of  $U$  with respect to  $\theta$ , if the following condition holds:

$$I(\mathbf{P}) = \frac{2 \cdot \sum_{i=1}^N \text{card}(M_i)}{N(N+1)} \geq \theta, \quad (5)$$

where  $\theta \in (0.5, 1]$ .

It is easy to know that the value of  $I(\mathbf{P})$  depends on  $\sigma$  and  $R$  and the choice of  $\varphi$ .  $\varphi$  is generally assigned no less than 0.8. The closer the  $I(\mathbf{P})$  is to 1, the more relation the  $R$  expresses the structure of sample space. If  $\theta$  is less than 0.5, the fuzzy covering of the universe is invalid. The fuzzy covering  $\mathbf{P} = \{[x_1], [x_2], \dots, [x_N]\}$  satisfies that similar objects in  $U$  have corresponding similar fuzzy classes, so the fuzzy covering  $\mathbf{P}$  more fully reflects the original distribution of objects in  $U$ .

**Proposition 1.** Let  $\varphi_1 < \varphi_2$ , then  $I_{\varphi_1}(C) \geq I_{\varphi_2}(C)$ .

*Proof.* It can be easily verified by the definition.  $\square$

**Remark 1.** Let  $\mathbf{P}_1$  and  $\mathbf{P}_2$  be two valid fuzzy coverings of  $U$  with respect to the same  $\theta$ . We choose fuzzy covering with a larger validity index  $I(\cdot)$  as research data.

## 4. Three-Way Clustering

**4.1. Rough Fuzzy C-Means Algorithm Based on Fuzzy Covering.** In this section, we discuss the rough fuzzy C-means algorithm with fuzzy covering. The reason for clustering with fuzzy covering is that each fuzzy similarity class can reflect the relationship with the whole dataset, avoiding the disadvantage of excessive loss of clustering information with raw data.

The combination of fuzzy set and rough set provides an important direction for uncertain reasoning. Lingras [36] developed rough C-means (RCM) by combining the C-means clustering algorithm with rough set theory. The new clustering center is only related to the positive region and the boundary region, unlike fuzzy C-means (FCM) [37], which is related to all objects. Since there is no membership involved, rough C-means (RCM) cannot effectively deal with the uncertainty caused by overlapping boundaries. In such circumstances, Mitra et al. [25] proposed a rough fuzzy C-means (RFCM) algorithm in which it combines the advantages of both fuzzy set and rough set into the framework of the C-means clustering algorithm. When dividing objects into approximation regions, replacing the absolute distance with a fuzzy membership is the innovation of the rough fuzzy C-means. This adjustment enhances the robustness of the clustering to deal with overlapping situations. Maji et al. [26] modified the calculation of the new clustering center in the RFCM model by assuming that the objects in the lower approximation have definite weights and the objects in the boundary have fuzzy weights. In what follows, we discuss the rough fuzzy C-means of fuzzy covering (FRFCM) algorithm, which is an RFCM algorithm based on fuzzy covering of the universe.

Suppose  $S_A = [[x]_1, [x]_2, \dots, [x]_N]^T$  is a valid fuzzy covering of  $U = \{x_1, x_2, \dots, x_N\}$ . The cluster centers are denoted as  $V = \{v_1, v_2, \dots, v_C\} \subset \mathfrak{R}^N$ . In the FRFCM algorithm,  $S_A$  is divided into  $C$  clusters  $Q_1, Q_2, \dots, Q_C$ . The membership of  $[x_j]$  to the cluster  $i$  is

$$\mu_{ij} = \frac{1}{\sum_{k=1}^C (d_{ij}/d_{kj})^{2/(m-1)}}, \quad (6)$$

where  $d_{ij}$  is the distance between  $[x_j]$  and  $v_i$ ,  $\mu_{ij} \in [0, 1]$ , and  $\sum_{i=1}^C \mu_{ij} = 1$ . The parameter  $m$  is the fuzzifier greater than 1.

A two-category dataset is taken to explain the influence of different parameters  $m$  on classification. The membership degree of each object belonging to each cluster can be considered as a function which is related to relative distances and the fuzzifier parameter. Then, formula (6) translates to the following form:



$$\mu(a, m) = \begin{cases} \frac{1}{1 + (a/(1-a))^{2/(m-1)}}, & a \in [0, 1), \\ 0, & a = 1, \end{cases} \quad (7)$$

where  $a$  denotes the relative distance of an object with respect to one of the clusters.

The uncertainty caused by different fuzzifier parameter  $m$  can be illustrated in Figure 1.

It is easily to obtain that if the value of  $m$  tends to 1, the memberships are most crisp, as well as the uncertainty of the system is reduced which is suitable for three-way clustering. In this circumstance, only objects that are approximately the same distance from each cluster center are divided into boundary regions. In addition, the parameter  $m$  cannot be assigned with a very large value because as the value increases, the memberships of objects around the center of the cluster will be assigned to 1 and most objects are divided into boundary region which will increase the uncertainty of the system and the error rate of decision-making. Furthermore, the positive region of cluster may become empty.

The center vectors  $v_1, v_2, \dots, v_C$  are updated as follows:

$$v_i = \begin{cases} w_{il}A_i + w_{ib}B_i, & \text{if } \underline{R}Q_i \neq \emptyset \wedge R_bQ_i \neq \emptyset, \\ B_i, & \text{if } \underline{R}Q_i = \emptyset \wedge R_bQ_i \neq \emptyset, \\ A_i, & \text{if } \underline{R}Q_i \neq \emptyset \wedge R_bQ_i = \emptyset, \end{cases} \quad (8)$$

where  $A_i = \sum_{[x_j] \in \underline{R}Q_i} \mu_{ij}^m [x_j] / \sum_{[x_j] \in \underline{R}Q_i} \mu_{ij}^m$  and  $B_i = \sum_{[x_j] \in R_bQ_i} \mu_{ij}^m [x_j] / \sum_{[x_j] \in R_bQ_i} \mu_{ij}^m$  can be considered as the contributions to the center  $v_i$  by the fuzzy lower region and fuzzy boundary region, respectively.  $R_bQ_i = \overline{R}Q_i - \underline{R}Q_i$  denotes the boundary region of cluster  $G_i$ , where  $\overline{R}Q_i$  and  $\underline{R}Q_i$  are the lower and upper approximations of cluster  $Q_i$  with respect to relation  $R$ , respectively. The weighted values  $w_{il}$  and  $w_{ib}$  usually satisfy  $w_{il} + w_{ib} = 1$  and  $w_{il} > w_{ib}$ . In this paper, we take  $w_{il} = (\text{card}(\underline{R}Q_i)) / (\text{card}(\underline{R}Q_i) + \text{card}(R_bQ_i))$  and  $w_{ib} = (\text{card}(R_bQ_i)) / (\text{card}(\underline{R}Q_i) + \text{card}(R_bQ_i))$ .

The approximation regions are determined by the FRFCM algorithm with the following principles: if  $\mu_{pj} - \mu_{qj} \leq \delta$ , where  $p = \min_l d(v_l, [x_j])$  and  $q = \min_{l \neq p} d(v_l, [x_j])$ , then  $[x_j]_j \in \overline{R}Q_p$  and  $[x_j]_j \in \overline{R}Q_q$ . It also means  $x_j \in \overline{R}Q_p$  and  $x_j \in \overline{R}Q_q$ . In this case,  $x_j$  cannot be divided into the positive region of any clusters. Otherwise,  $[x_j]_j \in \underline{R}Q_p$  and  $x_j \in \underline{R}Q_p$ . Due to the particularity structure of the fuzzy covering of  $U$ , the results of fuzzy covering clustering can well reflect the clustering results of the raw dataset through the above FRFCM algorithm.

#### 4.2. Acquisition of Thresholds for Three-Way Clustering.

In this section, we firstly review the shadowed set model for computing thresholds. Then, a novel method of calculating thresholds is proposed by combining the linear and non-linear fuzzy entropy.

The FRFCM algorithm is an important tool to deal with imprecise, incomplete, and inconsistent data. The thresholds in FRFCM which determines the formation of approximation regions should be carefully selected. The

unreasonable thresholds may cause the partition of approximate regions to be distorted, and clustering centers may deviate from the expected locations. Therefore, we should compute the partition thresholds scientifically according to some principles.

There are many methods to obtain the thresholds, and the most popular method is the shadowed set [38]. In fact, the shadowed set adopts the method of elevating and reducing membership degree, which divides the domain of fuzzy set into three regions. The corresponding membership function is as follows:

$$S_A(x) = \begin{cases} 1, & \mu_A(x) \geq \alpha, \\ 0, & \mu_A(x) \leq \beta, \\ [0, 1], & \beta < \mu_A(x) < \alpha, \end{cases} \quad (9)$$

where  $\mu_A$  is the membership function of fuzzy set  $A$ .

In the following study, only discrete fuzzy systems are considered, and similar models and conclusions can be obtained for continuous fuzzy systems. According to shadowed sets theory, the following formula is proposed to calculate the minimum  $V$  value to obtain the optimal thresholds  $\alpha$  and  $\beta$ :

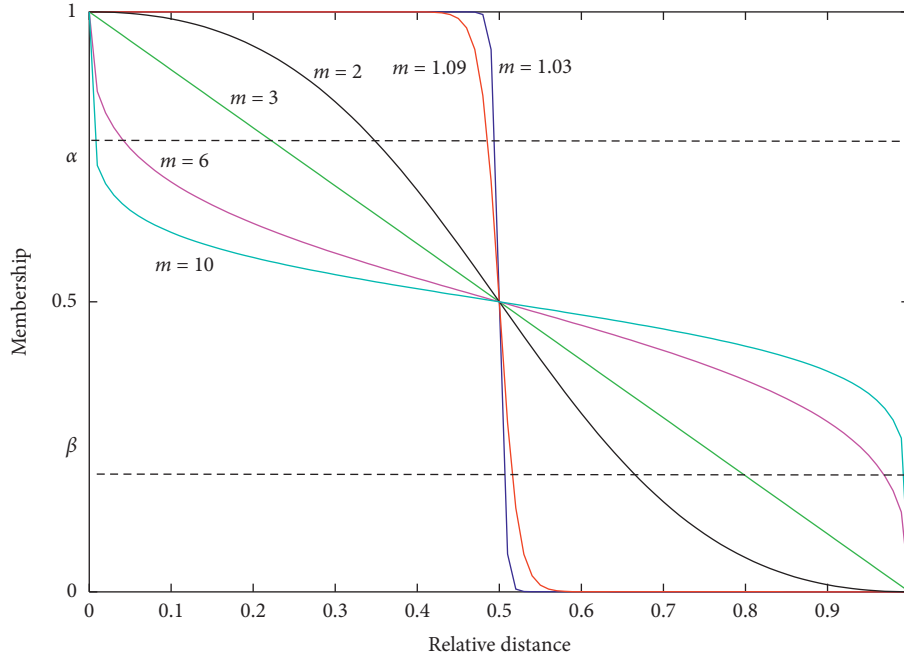
$$V = \left| \sum_{\mu_A(x) \leq \beta} \mu_A(x) dx + \sum_{\mu_A(x) \geq \alpha} (1 - \mu_A(x)) dx - \text{card}\{x \mid \beta < \mu_A(x) < \alpha\} \right|. \quad (10)$$

However, the semantic interpretation of obtaining threshold pairs by using the above method is not very clear. Because the shadowed set model can not reasonably explain the relationship between the obtained shadowed set and the fuzziness of the raw fuzzy set, further research is needed. Various methods for measuring uncertainty are described in the literature [39]. Fuzzy entropy is an important tool to measure the uncertainty of fuzzy set and meets the following requirements.

**Definition 5** (see [40]). Let  $A = \{(x_i, \mu_A(x_i)), x_i \in U\}$  be a fuzzy set on the universe of discourse  $U = \{x_1, x_2, \dots, x_N\}$ . The fuzzy entropy of fuzzy set  $A$  is the mapping  $E: F(U) \rightarrow R^+$ , which satisfies the following four conditions:

- (1)  $E(A) = 0$  if  $A \in P(U)$
- (2)  $E([1/2]_U) = \max_{A \in F(U)} E(A)$
- (3)  $\forall A, B \in F(U)$ , if  $\mu_B \geq \mu_A \geq 1/2$  or  $\mu_B \leq \mu_A \leq 1/2$ , then  $E(A) \geq E(B)$
- (4)  $E(A^c) = E(A)$ ,  $\forall A \in F(U)$

It is easy to verify that, for any  $x_i \in U$ ,  $\mu_A(x_i) = 0$  or  $\mu_A(x_i) = 1$ , the value of corresponding entropy function is 0, then the fuzzy entropy of the fuzzy set equals 0; i.e., the uncertainty of the fuzzy set is the minimum. When  $\mu_A(x_i) = 1/2$  holds for any  $x_i \in U$ , the value of corresponding entropy function is 1, then the fuzzy set has maximum uncertainty. The commonly used linear and nonlinear fuzzy entropy functions are listed as follows [41–43]:

FIGURE 1: The approximate regions with different values of  $m$ .

$$\begin{aligned}
 E_A^1(x) &= 1 - |2\mu_A(x) - 1|, \quad x \in U, \\
 E_A^2(x) &= \sin \pi \mu_A(x), \quad x \in U, \\
 E_A^3(x) &= 2 \min(\mu_A(x), 1 - \mu_A(x)), \quad x \in U, \\
 E_A^4(x) &= -\frac{1}{\log 2} (\mu_A(x) \log \mu_A(x) + (1 - \mu_A(x)) \log (1 - \mu_A(x))), \quad x \in U.
 \end{aligned} \tag{11}$$

With the above fuzzy entropy functions of fuzzy measure, the corresponding fuzzy entropy of the fuzzy set  $A$  can be easily obtained as follows:

$$E_j(A) = \sum_{x \in U} E_A^j(x), \quad j = 1, 2, 3, 4. \tag{12}$$

The basic idea of calculating the thresholds by fuzzy entropy is to reduce the uncertainty of the membership of the objects which are the elevating or reducing operation in

the shadowed set to 0, while the membership of objects corresponding to the middle part in the shadowed set is adjusted to the maximal uncertainty; i.e., the fuzzy degree increases to 1. In what follows, we propose a flexible fuzzy entropy method which combines the linear fuzzy entropy function  $E_A^1(x_i)$  and nonlinear fuzzy entropy function  $E_A^2(x_i)$  to obtain the clustering thresholds. Then, the calculation model is as follows:

$$\begin{aligned}
 (\alpha_{\text{opt}}, \beta_{\text{opt}}) &= \arg \min_{(\alpha, \beta)} \left| \lambda \left( \sum_{\substack{x_i \in U \\ \mu_A(x_i) \geq \alpha \\ \mu_A(x_i) \leq \beta}} E_A^1(x_i) - \sum_{\substack{x_i \in U \\ \beta < \mu_A(x_i) < \alpha}} (1 - E_A^1(x_i)) \right) \right. \\
 &\quad \left. + (1 - \lambda) \left( \sum_{\substack{x_i \in U \\ \mu_A(x_i) \geq \alpha \\ \mu_A(x_i) \leq \beta}} E_A^2(x_i) - \sum_{\substack{x_i \in U \\ \beta < \mu_A(x_i) < \alpha}} (1 - E_A^2(x_i)) \right) \right|,
 \end{aligned} \tag{13}$$



where  $\lambda \in [0, 1]$  is a parameter adjusting the impacts of linear entropy and nonlinear entropy.

In equation (13), when  $\lambda = 1$ , only linear fuzzy entropy function  $E_A^1(x_i)$  is used to calculate the thresholds. If  $\lambda = 0$ , only nonlinear fuzzy entropy function  $E_A^2(x_i)$  is used to calculate the thresholds. The smaller the value of  $\lambda$ , the more the influence brought from the linear fuzzy entropy, and vice versa. In the subsequent experiments of this study, we assign  $\lambda = 0.5$ .

Figure 2 illustrates the increase and decrease in fuzzy degree of the fuzzy entropy function by taking the linear fuzzy entropy function  $E_A^1(x)$ , the nonlinear fuzzy entropy function  $E_A^2(x)$ , and the fuzzy entropy function  $E_A^C(x)$  which is combined by  $E_A^1(x)$  and  $E_A^2(x)$  with equal weight as examples.

It can be seen from Figure 2 that the curve of flexible fuzzy entropy function lies between the curve of linear and nonlinear entropy functions. The method of using flexible fuzzy entropy to obtain the thresholds can prevent the uncertainty of fuzzy set measured by linear or nonlinear fuzzy entropy from being too small or too large, which leads to the partition thresholds unreasonable.

Thresholds used in RFCM and its related algorithms are usually user-defined. However, the threshold calculated by the above model can not only be interpreted from the change in fuzzy degree of fuzzy set but also be adjusted and optimized automatically.

According to  $\alpha_{\text{opt}}$  and  $\beta_{\text{opt}}$ , the positive, boundary, and negative regions of each cluster  $Q_i$  can be expressed as

$$\begin{aligned} \text{POS}(Q_i) &= \{x_j \mid \mu_{ij} \geq \alpha_{\text{opt}}\}, \\ \text{BND}(Q_i) &= \{x_j \mid \beta_{\text{opt}} < \mu_{ij} < \alpha_{\text{opt}}\}, \\ \text{NEG}(Q_i) &= U - \text{POS}(Q_i) - \text{BND}(Q_i) = \{x_j \mid \mu_{ij} \leq \beta_{\text{opt}}\}, \end{aligned} \quad (14)$$

where  $\mu_{ij}$  is the membership degree of the  $j$ th object belonging to the  $i$ th class.

**4.3. Boundary Region Processing of Three-Way Clustering Based on kNN Algorithm.** Following the above discussion on automatically selecting the optimal partition thresholds based on fuzzy entropy theory, this section will present the object processing in the boundary regions of three-way clustering.

In the three-way clustering, the boundary region objects are rarely further processed.  $k$ -nearest neighbor (kNN) algorithm [44] is a well-known nonparametric classifier, which is considered as one of the simplest methods in data mining and pattern recognition. The principle of the kNN algorithm is to find  $k$  nearest neighbors of a query in dataset and then predicts the query with the major class in the  $k$  nearest neighbors. In this paper, the kNN algorithm will be utilized to process the objects in the boundary regions. If the object does not find a positive region, it is still classified to the boundary region. Therefore, the uncertainty of the boundary region decreases with the decrease in the number

of objects in the boundary region, and reclassifying the objects in the boundary region can improve the accuracy of the three-way clustering.

The details of updating the boundary region with the kNN algorithm are as follows.

Because the kNN algorithm mainly relies on limited adjacent objects for classification, it is more suitable than other methods for the overlap of class domain or the object set to be classified at the boundary region. Therefore, Algorithm 1 can handle the uncertain arising from the boundary region. Of course, dealing with the boundary region with the  $k$ -nearest neighbor algorithm will add extra computing burden and may also face the risk of misclassification of objects.

In what follows, based on valid fuzzy covering, FRFCM and kNN algorithms, we proposed a three-way clustering algorithm, which is called the kNN-FRFCM algorithm, and it can be formed, as shown in Algorithm 2.

Thus, according to Algorithm 2, we obtain three-way clustering results of the original dataset by using the valid fuzzy covering.

## 5. Experiment Analysis

Three-way clustering method based on fuzzy covering proposed in this paper is suitable for dataset with less data and dimension or data with similar amount of data and dimension. Otherwise, clustering with the fuzzy covering constructing by the data with a large amount of data and few dimension will cause the curse of dimensionality. In this paper, six datasets include Iris, Breast Cancer Wisconsin (Original) (BCWO) which eliminates the missing data, New thyroid, Seeds, Forest-type mapping (FTM), and CT from UCI Machine Learning Repository [45] for empirical study. On these datasets and their corresponding fuzzy covering, the results of clustering methods including FCM, RCM, RFCM, kNN-RCM, and kNN-RFCM are compared. In order to distinguish the results of the raw dataset and the fuzzy covering with the same algorithm, the clustering algorithms of the fuzzy covering are expressed as FFCM, FRCM, FRFCM, kNN-FRCM, and kNN-FRFCM, respectively. Details of the six datasets are described in Table 1.

The partition threshold related to RCM and its related algorithms is set as 0.001.  $\varphi$  and  $\theta$  involved in fuzzy covering are set as 0.8 and 0.9, respectively. The value of  $k$  in the kNN algorithm is assigned as 7, and the evaluation indexes such as the normalized mutual information (NMI) [47], ACC [48], and rand index (RI) [49] are utilized to investigate the validity of the algorithm. Furthermore, the reasonable values of fuzzifier  $m$  involved in all comparison algorithms are greater than 1.  $m = 1.03$  and  $m = 1.1$  are selected, and the experimental comparison results are listed in Tables 2–7.

From Tables 2–7, it can be easily concluded that the selected fuzzy parameters have a significant impact on the performance of all comparison algorithms when dealing with the same dataset. Since the boundary region is the main cause of system uncertainty, thus, too large boundary regions are not required for three-way clustering and we need to pay attention to the uncertainty caused by the fuzzifier  $m$

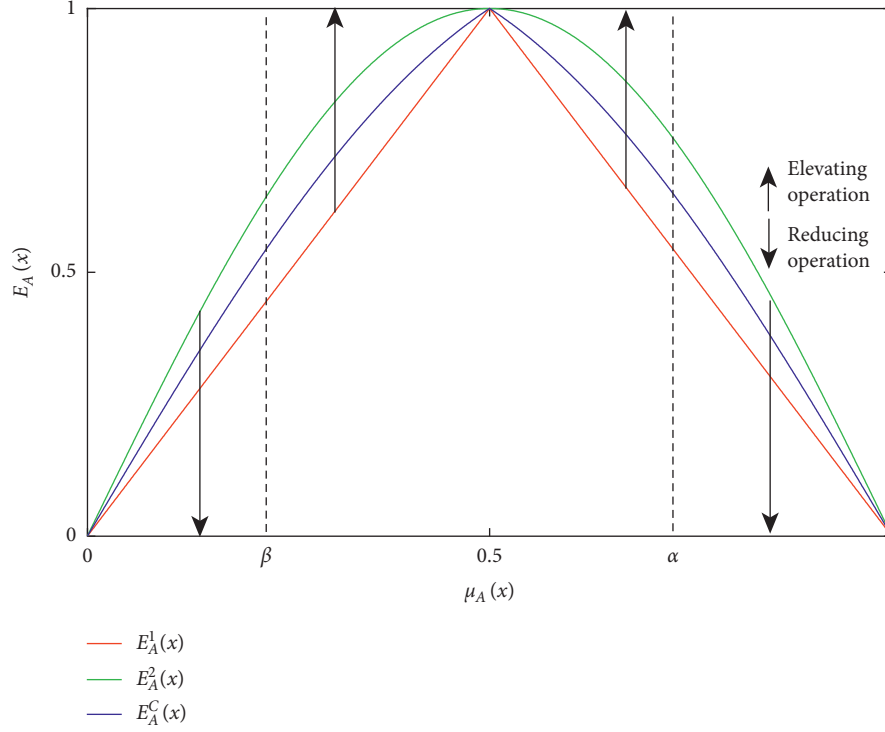


FIGURE 2: The operations of fuzzy entropy functions  $E_A^1(x)$ ,  $E_A^2(x)$ , and  $E_A^C(x)$ .

**Input:** a set of objects  $U = \{x_1, x_2, \dots, x_N\}$ , the cluster centers  $V = \{v_1, v_2, \dots, v_C\}$ , the positive region  $POS = \cup_{i=1}^C POS(Q_i)$ , boundary region  $BND = \cup_{i=1}^C BND(Q_i)$ , and the optimal value of  $k$ .

**Output:** the updated positive region  $POS(X)$  and boundary region  $BND(X)$

**Step 1:** calculate the distance between  $x_i$  and other objects, where  $x_i \in BND$ ;

**Step 2:** find the region where the  $k$  points with the smallest distance are located;

**Step 3:**  $n_{Q_i}$  is the number of  $k$  objects in the positive region of class  $Q_i$ , where  $i = 1, 2, \dots, C$ .  $n_{Q_{C+1}}$  is the number of  $k$  objects in the boundary region, and  $n_{Q_1} + n_{Q_2} + \dots + n_{Q_C} + n_{Q_{C+1}} = k$ . If there is only one cluster  $Q_j$ , such that  $n_{Q_j} = \max_{i \in \{1, 2, \dots, C+1\}} n_{Q_i}$ , then  $POS(Q_j) = POS(Q_j) \cup \{x_i\}$  and  $BND = BND - \{x_i\}$  else  $x_i \in BND$

**Step 4:** repeat Steps 1–3 until all boundary objects have been computed.

ALGORITHM 1: Processing the boundary regions of three-way clustering based on the kNN algorithm.

**Input:** the valid fuzzy covering of universe  $[x_i] (i = 1, 2, \dots, N)$ , the cluster centers  $v_i (i = 1, 2, \dots, C)$ , and the initial fuzzy membership degrees  $\mu_{ij} (i = 1, 2, \dots, C, j = 1, 2, \dots, N)$ ;

**Output:** the positive, boundary, and negative regions of each cluster, respectively.

**Step 1:** compute the optimal partition thresholds  $\alpha_{iopt}$  and  $\beta_{iopt}$  for each cluster  $Q_i$  using formula (13);

**Step 2:** according to formula (14), determine the positive region  $POS(Q_i)$ , boundary region  $BND(Q_i)$ , and  $NEG(Q_i)$  for each cluster  $Q_i$  by  $\alpha_{iopt}$ ,  $\beta_{iopt}$ , and fuzzy partition matrix  $(\mu_{ij})_{C \times N}$ ;

**Step 3:** update each clustering region by Algorithm 1;

**Step 4:** update the membership partition matrix  $(\mu_{ij})_{N \times N}$  by formula (6);

**Step 5:** update the cluster center  $v_i (i = 1, 2, \dots, C)$  with formula (8);

**Step 6:** repeat Step 1 to Step 5 until convergence is reached;

**Step 7:** the results of fuzzy covering clustering are replaced by the corresponding objects in the universe.

ALGORITHM 2: kNN-FRFCM algorithm-based three-way clustering.

TABLE 1: Description of datasets.

No.	Datasets	# objects	# attributes	# classes
1	Iris	150	4	3
2	BCWO	683	10	2
3	New thyroid	215	5	3
4	Seeds	210	7	3
5	FTM	326	27	4
6	CT	221	36	2

TABLE 2: The comparative validity results ( $m = 1.03$ ).

	Iris			Seeds		
	NMI	ACC	RI	NMI	ACC	RI
FCM	0.7419	0.8867	0.8737	0.6949	0.8952	0.8744
RCM	0.7328	0.8400	0.8891	0.6670	0.8857	0.8666
RFCM	0.7419	0.8867	0.8737	0.6670	0.8857	0.8666
kNN-RCM	0.7777	0.9000	0.8859	0.6743	0.8905	0.8693
kNN-RFCM	0.7419	0.8867	0.8737	0.6743	0.8905	0.8693
FFCM	<b>0.8226</b>	<b>0.9333</b>	<b>0.9195</b>	0.6748	0.8952	0.8713
FRCM	0.7767	0.9133	0.9124	0.6748	0.8952	0.8713
FRFCM	0.8112	0.9267	0.9160	0.6777	0.8952	0.8742
kNN-FRCM	0.7919	0.9267	0.9124	0.6748	0.8952	0.8713
kNN-FRFCM	<b>0.8226</b>	<b>0.9333</b>	<b>0.9195</b>	<b>0.6852</b>	<b>0.9000</b>	<b>0.8770</b>

TABLE 3: The comparative validity results ( $m = 1.03$ ).

	BCWO			New thyroid		
	NMI	ACC	RI	NMI	ACC	RI
FCM	0.7478	0.9605	0.9240	0.4945	0.8605	0.7908
RCM	0.7368	0.9502	0.9277	0.5585	0.8744	0.8203
RFCM	0.7585	0.9605	0.9312	0.5966	0.8884	0.8180
kNN-RCM	0.7368	0.9590	0.9277	0.5563	0.9023	0.7913
kNN-RFCM	0.7546	0.9619	0.9267	0.5966	0.8884	0.8180
FFCM	<b>0.7759</b>	<b>0.9649</b>	<b>0.9321</b>	0.6245	0.8977	0.8329
FRCM	<b>0.7759</b>	<b>0.9649</b>	<b>0.9321</b>	0.6501	0.9070	0.8531
FRFCM	<b>0.7759</b>	<b>0.9649</b>	<b>0.9321</b>	0.6448	0.9023	0.8523
kNN-FRCM	<b>0.7759</b>	<b>0.9649</b>	<b>0.9321</b>	<b>0.6583</b>	<b>0.9116</b>	<b>0.8540</b>
kNN-FRFCM	<b>0.7759</b>	<b>0.9649</b>	<b>0.9321</b>	<b>0.6583</b>	<b>0.9116</b>	<b>0.8540</b>

TABLE 4: The comparative validity results ( $m = 1.03$ ).

	FTM			CT		
	NMI	ACC	RI	NMI	ACC	RI
FCM	0.7271	0.8939	0.9031	0.3118	0.8145	0.6964
RCM	0.7475	0.8990	0.9039	0.3296	0.8235	0.7080
RFCM	0.7411	0.8990	0.9018	0.3309	0.8190	0.7133
kNN-RCM	0.7475	0.8990	0.9039	0.3296	0.8235	0.7080
kNN-RFCM	0.7411	0.8990	0.9018	0.3550	0.8326	0.7234
FFCM	<b>0.7823</b>	<b>0.9091</b>	<b>0.9153</b>	<b>0.4327</b>	<b>0.8371</b>	<b>0.7260</b>
FRCM	0.7823	0.9091	0.9153	<b>0.4327</b>	<b>0.8371</b>	<b>0.7260</b>
FRFCM	0.7677	0.8990	0.9128	0.4267	0.8281	0.7234
kNN-FRCM	0.7823	0.9091	0.9153	<b>0.4327</b>	<b>0.8371</b>	<b>0.7260</b>
kNN-FRFCM	<b>0.7906</b>	<b>0.9141</b>	<b>0.9200</b>	0.4244	0.8326	0.7200

in the implementation of the algorithms. Moreover, the clustering results show that kNN-FRFCM algorithm has better performance than the other algorithms in most of

TABLE 5: The comparative validity results ( $m = 1.1$ ).

	Iris			Seeds		
	NMI	ACC	RI	NMI	ACC	RI
FCM	0.7582	0.8933	0.8797	<b>0.6949</b>	<b>0.8952</b>	0.8744
RCM	0.7328	0.8400	0.8891	0.6670	0.8857	0.8666
RFCM	0.7360	0.8733	0.8714	0.6769	0.8857	<b>0.8746</b>
kNN-RCM	0.7777	0.9000	0.8859	0.6743	0.8905	0.8693
kNN-RFCM	0.7582	0.8933	0.8797	0.6728	0.8905	0.8740
FFCM	0.8024	0.9267	0.9124	0.6629	0.8905	0.8694
FRCM	0.7767	0.9133	0.9124	0.6748	<b>0.8952</b>	0.8713
FRFCM	0.7991	0.9200	0.9197	0.6345	0.8762	0.8643
kNN-FRCM	0.7919	0.9267	0.9124	0.6748	<b>0.8952</b>	0.8713
kNN-FRFCM	<b>0.8136</b>	<b>0.9333</b>	<b>0.9197</b>	0.6480	0.8857	0.8622

TABLE 6: The comparative validity results ( $m = 1.1$ ).

	BCWO			New thyroid		
	NMI	ACC	RI	NMI	ACC	RI
FCM	0.7478	0.9605	0.9240	0.4945	0.8605	0.7908
RCM	0.7368	0.9502	0.9277	0.5585	0.8744	0.8203
RFCM	0.7391	0.9517	0.9268	0.6058	0.8884	0.8250
kNN-RCM	0.7368	0.9590	0.9277	0.5563	0.9023	0.7913
kNN-RFCM	0.7347	0.9575	0.9186	0.6058	0.8884	0.8250
FFCM	0.7759	0.9649	0.9321	0.6245	0.8977	0.8329
FRCM	0.7759	0.9649	0.9321	0.6501	0.9070	0.8531
FRFCM	0.7778	0.9649	0.9340	0.6448	0.9023	0.8523
kNN-FRCM	0.7759	0.9649	0.9321	<b>0.6583</b>	<b>0.9116</b>	<b>0.8540</b>
kNN-FRFCM	<b>0.7889</b>	<b>0.9678</b>	<b>0.9376</b>	<b>0.6583</b>	<b>0.9116</b>	<b>0.8540</b>

TABLE 7: The comparative validity results ( $m = 1.1$ ).

	FTM			CT		
	NMI	ACC	RI	NMI	ACC	RI
FCM	0.7271	0.8939	0.9031	0.3118	0.8145	0.6964
RCM	0.7475	0.8990	0.9039	0.3296	0.8235	0.7080
RFCM	0.7411	0.8990	0.9018	0.3023	0.7919	0.6954
kNN-RCM	0.7475	0.8990	0.9039	0.3296	0.8235	0.7080
kNN-RFCM	0.7411	0.8990	0.9018	0.3274	0.8190	0.7055
FFCM	<b>0.7746</b>	<b>0.9040</b>	<b>0.9107</b>	0.4327	0.8371	0.7260
FRCM	0.7823	0.9091	0.9153	0.4327	0.8371	0.7260
FRFCM	0.7632	0.8838	0.9110	0.4338	0.8100	<b>0.7374</b>
kNN-FRCM	0.7823	0.9091	0.9153	0.4327	0.8371	0.7260
kNN-FRFCM	<b>0.8074</b>	<b>0.9192</b>	<b>0.9246</b>	<b>0.4725</b>	<b>0.8416</b>	0.7350

cases. This is mainly because it can reduce the uncertainty of the system by reprocessing the objects in the boundary regions. From the clustering results, we can also obtain that the results of clustering based on fuzzy covering are mostly better than the results of clustering with raw data. Therefore, the valid fuzzy covering can replace the raw dataset for clustering, and the clustering results are better than the raw dataset. The premise that fuzzy covering can replace the raw dataset for clustering is to select the appropriate fuzzy similarity relation [46].

## 6. Conclusions

In this paper, a valid fuzzy covering of the raw dataset is constructed by some principles. Because the similarity between fuzzy similarity classes in the valid fuzzy covering can be used to measure the similarity between objects in the raw dataset, each fuzzy similarity class reflects the connection with the whole dataset, so valid fuzzy covering instead of the raw data for clustering can improve the precision of clustering. From the perspective of semantic explanation of uncertainty change in fuzzy sets, we investigate the method of combining linear fuzzy entropy with nonlinear fuzzy entropy to obtain decision threshold pairs. The advantage of calculating thresholds method in this paper not only objectively obtains the classification thresholds based on the objects intrinsic relations but also the formula is simple and easy to understand, as well as the method of calculating the thresholds avoids the inappropriate subjective assignment. Additionally, the objects in the boundary region obtained by the FRFCM algorithm are reprocessed by the kNN algorithm to reduce the uncertainty of the system.

Furthermore, we will continue to investigate the method of thresholds acquisition and the processing method of boundary region for three-way clustering following the idea of this paper. The three-way clustering in incremental information system is one of the future research directions too.

## Data Availability

The experimental data supporting the findings of this study are available on the website provided in this article.

## Conflicts of Interest

The author declares that there are no conflicts of interest.

## Acknowledgments

This work was supported by the Science Research Project of Inner Mongolia University for Nationalities with the title “Research on three-way clustering methods of preference linguistic data” (no. NMDYB18030) and Natural Science Foundation of Inner Mongolia Autonomous Region (nos. 2018MS01008 and 2020MS07008).

## References

- [1] Y. Yao, “Three-way decisions with probabilistic rough sets,” *Information Sciences*, vol. 180, no. 3, pp. 341–353, 2010.
- [2] Y. Y. Yao, “An outline of a theory of three-way decisions,” in *RSTC 2012, LNCS (LNAI)*, Springer, Berlin, Germany, 2012.
- [3] D. Liang, D. Liu, W. Pedrycz, and P. Hu, “Triangular fuzzy decision-theoretic rough sets,” *International Journal of Approximate Reasoning*, vol. 54, no. 8, pp. 1087–1106, 2013.
- [4] D. Liang and D. Liu, “Deriving three-way decisions from intuitionistic fuzzy decision-theoretic rough sets,” *Information Sciences*, vol. 300, pp. 28–48, 2015.
- [5] D. Liang, W. Pedrycz, D. Liu, and P. Hu, “Three-way decisions based on decision-theoretic rough sets under linguistic assessment with the aid of group decision making,” *Applied Soft Computing*, vol. 29, pp. 256–269, 2015.
- [6] D. Liu, T. R. Li, and D. C. Liang, “Three-way decisions in stochastic decision-theoretic rough sets,” in *Transactions on Rough Sets XVIII*, Springer, Berlin, Germany, 2014.
- [7] Y. Qian, H. Zhang, Y. Sang, and J. Liang, “Multigranulation decision-theoretic rough sets,” *International Journal of Approximate Reasoning*, vol. 55, no. 1, pp. 225–237, 2014.
- [8] B. Q. Hu, “Three-way decisions space and three-way decisions,” *Information Sciences*, vol. 281, pp. 21–52, 2014.
- [9] B. Q. Hu, “Three-way decision spaces based on partially ordered sets and three-way decisions based on hesitant fuzzy sets,” *Knowledge-Based Systems*, vol. 91, pp. 16–31, 2016.
- [10] J. Qi, T. Qian, and L. Wei, “The connections between three-way and classical concept lattices,” *Knowledge-Based Systems*, vol. 91, pp. 143–151, 2016.
- [11] H. X. Li, X. Z. Zhou, B. Huang, and D. Liu, “Cost-sensitive three-way decision: a sequential strategy,” in *Proceedings of the International Conference on Rough Sets and Knowledge Technology*, Halifax, NS, Canada, October 2013.
- [12] J. Yang, G. Wang, Q. Zhang, Y. Chen, and T. Xu, “Optimal granularity selection based on cost-sensitive sequential three-way decisions with rough fuzzy sets,” *Knowledge-Based Systems*, vol. 163, pp. 131–144, 2019.
- [13] H. Ju, W. Pedrycz, H. Li, W. Ding, X. Yang, and X. Zhou, “Sequential three-way classifier with justifiable granularity,” *Knowledge-Based Systems*, vol. 163, pp. 103–119, 2019.
- [14] Y. Fang, C. Gao, and Y. Yao, “Granularity-driven sequential three-way decisions: a cost-sensitive approach to classification,” *Information Sciences*, vol. 507, pp. 644–664, 2020.
- [15] Y. Yao, S. Wang, and X. Deng, “Constructing shadowed sets and three-way approximations of fuzzy sets,” *Information Sciences*, vol. 412–413, pp. 132–153, 2017.
- [16] X. Yang, T. Li, D. Liu, H. Chen, and C. Luo, “A unified framework of dynamic three-way probabilistic rough sets,” *Information Sciences*, vol. 420, pp. 126–147, 2017.
- [17] Q. Zhang, G. Lv, Y. Chen, and G. Wang, “A dynamic three-way decision model based on the updating of attribute values,” *Knowledge-Based Systems*, vol. 142, pp. 71–84, 2018.
- [18] H. Li, L. Zhang, B. Huang, and X. Zhou, “Sequential three-way decision and granulation for cost-sensitive face recognition,” *Knowledge-Based Systems*, vol. 91, pp. 241–251, 2016.
- [19] A. V. Savchenko, “Sequential three-way decisions in multi-category image recognition with deep features based on distance factor,” *Information Sciences*, vol. 489, pp. 18–36, 2019.
- [20] Y. Zhang, Z. Zhang, D. Miao, and J. Wang, “Three-way enhanced convolutional neural networks for sentence-level sentiment classification,” *Information Sciences*, vol. 477, pp. 55–64, 2019.
- [21] A. Campagner and D. Ciucci, “Three-way and semisupervised decision tree learning based on orthopartitions,” in *Proceedings of the International Conference on Information Processing and Management of Uncertainty in Knowledge-Based Systems*, Cádiz, Spain, June 2018.
- [22] H.-R. Zhang and F. Min, “Three-way recommender systems based on random forests,” *Knowledge-Based Systems*, vol. 91, pp. 275–286, 2016.
- [23] D. Liu, T. Li, and D. Liang, “Three-way government decision analysis with decision-theoretic rough sets,” *International Journal of Uncertainty, Fuzziness and Knowledge-Based Systems*, vol. 20, no. 1, pp. 119–132, 2012.
- [24] Y. L. Liu, L. Pan, X. Y. Jia, C. J. Wang, and J. Y. Xie, “Three-way decision based overlapping community detection,” in *Proceedings of the International Conference on Rough Sets and Knowledge Technology*, Halifax, NS, Canada, October 2013.



- [25] S. Mitra, H. Banka, and W. Pedrycz, "Rough-fuzzy collaborative clustering," *IEEE Transactions on Systems, Man and Cybernetics, Part B (Cybernetics)*, vol. 36, no. 4, pp. 795–805, 2006.
- [26] P. Maji and S. Pal, "RFCM: A hybrid clustering algorithm using rough and fuzzy sets," *Fundamenta Informaticae*, vol. 80, no. 4, pp. 475–496, 2007.
- [27] P. Maji and S. K. Pal, "Rough set based generalized fuzzy C-means algorithm and quantitative indices," *IEEE Transactions on Systems, Man, and Cybernetics, Part B (Cybernetics)*, vol. 37, no. 6, pp. 1529–1540, 2007.
- [28] X. Deng and Y. Yao, "An information-theoretic interpretation of thresholds in probabilistic rough sets," in *Proceedings of the International Conference on Rough Sets and Knowledge Technology*, Chengdu, China, August 2012.
- [29] J. Zhou, W. Pedrycz, and D. Miao, "Shadowed sets in the characterization of rough-fuzzy clustering," *Pattern Recognition*, vol. 44, no. 8, pp. 1738–1749, 2011.
- [30] Y. Yao, "Three-way decisions and cognitive computing," *Cognitive Computation*, vol. 8, no. 4, pp. 543–554, 2016.
- [31] X. Deng and Y. Yao, "Decision-theoretic three-way approximations of fuzzy sets," *Information Sciences*, vol. 279, pp. 702–715, 2014.
- [32] L. A. Zadeh, "Fuzzy sets," *Information and Control*, vol. 8, no. 3, pp. 338–353, 1965.
- [33] L. Ma, "Two fuzzy covering rough set models and their generalizations over fuzzy lattices," *Fuzzy Sets and Systems*, vol. 294, pp. 1–17, 2016.
- [34] C. Wang, D. Chen, and Q. Hu, "Fuzzy information systems and their homomorphisms," *Fuzzy Sets and Systems*, vol. 249, pp. 128–138, 2014.
- [35] G. Deng, Y. Jiang, and J. Fu, "Monotonic similarity measures between fuzzy sets and their relationship with entropy and inclusion measure," *Fuzzy Sets and Systems*, vol. 287, pp. 97–118, 2016.
- [36] P. Lingras and C. West, "Interval set clustering of web users with rough  $k$ -means," *Journal of Intelligent Information Systems*, vol. 23, no. 1, pp. 5–16, 2004.
- [37] J. C. Bezdek, *Pattern Recognition with Fuzzy Objective Function Algorithms*, Plenum Press, New York, NY, USA, 1981.
- [38] W. Pedrycz, "Interpretation of clusters in the framework of shadowed sets," *Pattern Recognition Letters*, vol. 26, no. 15, pp. 2439–2449, 2005.
- [39] G. J. Klir and T. A. Folger, *Fuzzy Sets, Uncertainty, and Information*, Prentice-Hall, Englewood Cliffs, NJ, USA, 1988.
- [40] X. C. Liu, "Entropy, distance measure and similarity measure of fuzzy sets and their relations," *Fuzzy Sets and Systems*, vol. 52, no. 3, pp. 305–318, 1992.
- [41] N. R. Pal and J. C. Bezdek, "Measuring fuzzy uncertainty," *IEEE Transactions on Fuzzy Systems*, vol. 2, no. 2, pp. 107–118, 1994.
- [42] G. J. Klir, U. H. St. Clair, and B. Yuan, *Fuzzy Set Theory: Foundations and Applications*, Prentice-Hall, Englewood Cliffs, NJ, USA, 1997.
- [43] K. Yao, "Sine entropy of uncertain set and its applications," *Applied Soft Computing*, vol. 22, pp. 432–442, 2014.
- [44] A. Mucherino, P. J. Papajorgji, and P. M. Pardalos, "K-nearest neighbor classification," *Data Mining in Agriculture*, pp. 83–106, Springer, Berlin, Germany, 2009.
- [45] D. Dua and C. Graff, *UCI Machine Learning Repository*, University of California, School of Information and Computer Science, Irvine, CA, USA, 2020, <http://archive.ics.uci.edu/ml>.
- [46] Q. Q. Gu, C. Ding, and J. W. Han, "On trivial solution and scale transfer problems in graph regularized NMF," in *Proceedings of the Twenty-Second International Joint Conference on Artificial Intelligence*, pp. 1288–1293, Barcelona, Catalonia, Spain, July 2011.
- [47] Y. Lei, J. C. Bezdek, J. Chan, N. X. Vinh, S. Romano, and J. Bailey, "Extending information-theoretic validity indices for fuzzy clustering," *IEEE Transactions on Fuzzy Systems*, vol. 25, no. 4, pp. 1013–1018, 2017.
- [48] W. Xu, X. Liu, and Y. Gong, "Document clustering based on non-negative matrix factorization," in *Proceedings of the 26th Annual International ACM SIGIR Conference on Research and Development in Information Retrieval*, pp. 267–273, Toronto Canada, July 2003.
- [49] R. J. G. B. Campello, "A fuzzy extension of the rand index and other related indexes for clustering and classification assessment," *Pattern Recognition Letters*, vol. 28, no. 7, pp. 833–841, 2007.

## Research Article

# Research on Evaluating Algorithms for the Service Quality of Wireless Sensor Networks Based on Interval-Valued Intuitionistic Fuzzy EDAS and CRITIC Methods

Shihui Li  and Bo Wang

*School of Electro-Mechanical and Informaiton, Yiwu Industrial & Commercial College, Yiwu 322000, China*

Correspondence should be addressed to Shihui Li; 2003010164@ywicc.edu.cn

Received 28 March 2020; Revised 17 June 2020; Accepted 30 June 2020; Published 22 July 2020

Academic Editor: Harish Garg

Copyright © 2020 Shihui Li and Bo Wang. This is an open access article distributed under the Creative Commons Attribution License, which permits unrestricted use, distribution, and reproduction in any medium, provided the original work is properly cited.

Wireless sensor networks play an important role in economic production and social life. However, in recent years, the number of wireless sensor network vulnerabilities has been increasing rapidly, which makes wireless sensor networks face more and more severe challenges. It is of great significance to realize the quantitative evaluation of wireless sensor networks in order to maintain the service quality of wireless sensor networks more effectively. The evaluating problem of the service quality of wireless sensor networks is a kind of multiple attribute group decision-making (MAGDM) problem. In this paper, depending on the classical EDAS method, the EDAS method will be extended to interval-valued intuitionistic fuzzy sets (IVIFSs) to address some MAGDM issues. At first, some essential concepts of IVIFSs are briefly reviewed. Subsequently, relying on the CRITIC method, the attributes' weights are decided. Furthermore, integrating the EDAS method with IVIFSs, IVIF-EDAS method is established, and all calculating procedures are depicted. Finally, an empirical application for evaluating the service quality of wireless sensor networks is given to demonstrate this novel algorithm, and some comparative analyses are made to confirm the merits of the designed method.

## 1. Introduction

In order to improve the accuracy of real-life decision-making, Zadeh [1] initially designed the fuzzy sets (FSs). Atanassov [2] designed the intuitionistic fuzzy sets (IFSs), which could be a generalization of FSs. In IFSs, there are three mathematical functions expressing the degrees of membership, nonmembership, and hesitancy. And they must satisfy the only condition that their sum of three degrees cannot exceed one. Gou et al. [3] pointed out a novel exponential operational law about IFNs and offered a method which was utilized to aggregate intuitionistic fuzzy information. He et al. [4] integrated the power averaging operators with IFSs and defined several intuitionistic fuzzy power interaction aggregation operators. Zhang and He [5] defined the extensions of intuitionistic fuzzy geometric interaction operators by using the  $t$ -norm and the corresponding  $t$ -conorm means. Li and Wu [6] presented the

intuitionistic fuzzy cross-entropy distance and the GRA. Liang et al. [7] extended the MABAC method to IFSs by utilizing the novel distance measures. Khan and Lohani [8] put forward a novel similarity measure about IFNs depending on the distance measure of the double sequence of bounded variation. Chen et al. [9] developed the novel MCDM method based on the TOPSIS method and similarity measures in the context of IFSs. Li et al. [10] developed a grey target decision-making method in the form of IFNs on the basis of grey relational analysis [11]. Garg [12] developed some intuitionistic fuzzy averaging operators by taking the degrees of hesitation between the membership mathematical functions into consideration. Gupta et al. [13] extended the fuzzy entropy [14] to IFSs with axiomatic justification and proposed the importance of parameter alpha. Bao et al. [15] put forward the prospect theory and the evidential reasoning method under IFSs. Gan and Luo [16] employed a hybrid method on the basis of DEMATEL and IFSs. Gupta et al. [17]



modified the superiority and inferiority ranking (SIR) method and combined it under IFSs. Krishankumar et al. [18] developed IFSP (intuitionistic fuzzy set-based PROMETHEE) which was a novel ranking method. Luo and Wang [19] combined IFSs with the VIKOR method relying on a novel distance measure by taking the IFSs into consideration. Hao et al. [20] presented the novel intuitionistic fuzzy MADM method depending on the decision theory. Zhang et al. [21] defined the intuitionistic fuzzy TOPSIS method based on CVPIFRS models with an application to biomedical problems. Garg [22] developed the generalized intuitionistic fuzzy entropy-based approach for solving multiattribute decision-making problems with unknown attribute weights. Liu et al. [23] presented some novel intuitionistic fuzzy operators by extending the BM operator on the basis of the Dombi operations [24] and designed some MAGDM methods. Jin et al. [25] developed two group decision-making (GDM) methods which could obtain the normalized intuitionistic fuzzy priority weights from the designed IFPRs on the basis of the order consistency and the multiplicative consistency. Wu et al. [26] gave VIKOR algorithms for assessing the financing risk about rural tourism projects under IVIFSs. Wu et al. [27] designed the algorithms for evaluating the competitiveness of tourist destination with some IVIF Hamy mean operators. Wu et al. [28] proposed some IVIF Dombi Heronian mean operators for evaluating the ecological tourism value. Chen and Kuo [29] presented the novel MADM method using the nonlinear programming (NLP) model with hyperbolic tangent function and IVIFSs. Lu and Wei [30] proposed the TODIM method for social-integration-based rural performance appraisal under IVIFSs and integrated the ELECTRE method with IFSs to tackle some MCDM issues. Garg and Kumar [31] defined the group decision-making approach based on possibility degree measures and the linguistic intuitionistic fuzzy aggregation operators using Einstein norm operations. Garg and Arora [32] proposed the generalized intuitionistic fuzzy soft power aggregation operator based on the  $t$ -norm and its application in multicriteria decision-making.

Keshavarz Ghorabae et al. [33] designed the evaluation based on distance from average solution (EDAS) to solve multicriteria inventory classification (MCIC) issues. In recent years, this method was enriched by the related extensions. For example, Ghorabae et al. [34] modified such an EDAS method to tackle supplier selection issues. Keshavarz Ghorabae et al. [35] presented the EDAS method with normal distribution to tackle stochastic issues. Peng and Liu [36] designed the neutrosophic soft MADM algorithms on the basis of EDAS and defined the similarity measure. Kahraman et al. [37] integrated the EDAS method with IFSs to select the solid waste disposal site. He et al. [38] designed the EDAS model for MAGDM with PULTSs. Keshavarz Ghorabae et al. [39] made some comparative analyses about the phenomenon of order reversal depending on EDAS and TOPSIS. Wang et al. [40] proposed the EDAS model for MAGDM under the 2-tuple linguistic neutrosophic environment. Li et al. [41] defined the EDAS for MAGDM issues under the q-rung

orthopair fuzzy environment. Feng et al. [42] integrated the EDAS with the extended hesitant fuzzy linguistic environment. Karasan and Kahraman [43] designed the interval-valued neutrosophic EDAS to decision-making issues.

Unfortunately, we failed to find the work of the EDAS method based on the CRITIC method with IVIFSs in the existing literature. So, investigating the EDAS method with IVIFSs is essential. The fundamental objective of our research is to develop an original method which can be more effectively to address some MAGDM issues in the context of the EDAS method and IVIFSs. Hence, the highlights of this work are illustrated subsequently. Above all, the EDAS method is extended to the IVIFSs. In addition, because the DMs are restrained by their knowledge, it is tricky to assign the criteria weights directly. Hence, the CRITIC method is utilized to decide each attribute's weight. Last but not the least, an empirical application is offered to demonstrate this novel approach, and several comparative analyses are offered to demonstrate some merits of the novel approach.

However, there are no studies on the EDAS method for MAGDM under IVIFSs in the existing literature. Therefore, it is necessary to pay attention to this issue. The innovativeness of the paper can be summarized as follows: (1) the EDAS method is modified by IVIFSs; (2) the interval-valued intuitionistic fuzzy EDAS (IVIF-EDAS) method is designed to solve the MAGDM issues with IVIFSs; (3) a case study for evaluating the service quality of wireless sensor networks is designed to prove the developed method; and (4) some comparative studies are given to verify the rationality of the IVIF-EDAS method.

The reminder of our essay proceeds as follows. Some fundamental knowledge of IVIFSs is concisely reviewed in Section 2. The extended EDAS method is integrated with IVIFSs, and the calculating procedures are simply depicted in Section 3. An empirical application for assessing the service quality of wireless sensor networks is given to show the superiority of this approach, and some comparative analyses are offered to prove some merits of such a method in Section 4. At last, we make an overall conclusion of such a work in Section 5.

## 2. Preliminaries

*Definition 1* (see [2]). The interval-valued IFSs (IVIFSs) on  $X$  are the object of the form

$$I = \{ \langle x, \tilde{\mu}_I(x), \tilde{\nu}_I(x) \rangle \mid x \in X \}, \quad (1)$$

where  $\tilde{\mu}_I(x) \subset [0, 1]$  is the “membership degree of  $I$ ” and  $\tilde{\nu}_I(x) \subset [0, 1]$  is named the “nonmembership degree of  $I$ ,” and  $\tilde{\mu}_I(x)$  and  $\tilde{\nu}_I(x)$  meet the mathematical condition:  $0 \leq \sup \tilde{\mu}_I(x) + \sup \tilde{\nu}_I(x) \leq 1, \forall x \in X$ . For convenience, we call  $I = ([\mu^L, \mu^R], [\nu^L, \nu^R])$  as an IVIFN.

*Definition 2* (see [44]). Let  $I_1 = ([\mu_1^L, \mu_1^R], [\nu_1^L, \nu_1^R])$  and  $I_2 = ([\mu_2^L, \mu_2^R], [\nu_2^L, \nu_2^R])$  be two IVIFNs; the operation formula of them can be defined as follows:

$$I_1 \oplus I_2 = ([\mu_1^L + \mu_2^L - \mu_1^L \mu_2^L, \mu_1^R + \mu_2^R - \mu_1^R \mu_2^R], [\nu_1^L \nu_2^L, \nu_1^R \nu_2^R]), \quad (2)$$

$$I_1 \otimes I_2 = ([\mu_1^L \mu_2^L, \mu_1^R \mu_2^R], [\nu_1^L + \nu_2^L - \nu_1^L \nu_2^L, \nu_1^R + \nu_2^R - \nu_1^R \nu_2^R]), \quad (3)$$

$$\lambda I_1 = ([1 - (1 - \mu_1^L)^\lambda, 1 - (1 - \mu_1^R)^\lambda], [(\nu_1^L)^\lambda, (\nu_1^R)^\lambda]), \quad \lambda > 0, \quad (4)$$

$$I_1^\lambda = ([(\mu_1^L)^\lambda, (\mu_1^R)^\lambda], [1 - (1 - \lambda_1^L)^\lambda, 1 - (1 - \lambda_1^R)^\lambda]), \quad \lambda > 0. \quad (5)$$

Derived from Definition 2, the following properties of the operation laws can be obtained:

- (1)  $I_1 \oplus I_2 = I_2 \oplus I_1$ ,  $I_1 \otimes I_2 = I_2 \otimes I_1$ ,  $((I_1)^{\lambda_1})^{\lambda_2} = (I_1)^{\lambda_1 \lambda_2}$
- (2)  $\lambda(I_1 \oplus I_2) = \lambda I_1 \oplus \lambda I_2$ ,  $(I_1 \otimes I_2)^\lambda = (I_1)^\lambda \otimes (I_2)^\lambda$
- (3)  $\lambda_1 I_1 \otimes \lambda_2 I_1 = (\lambda_1 + \lambda_2) I_1$ ,  $(I_1)^{\lambda_1} \otimes (I_1)^{\lambda_2} = (I_1)^{(\lambda_1 + \lambda_2)}$

**Definition 3** (see [45]). Let  $I_1 = ([\mu_1^L, \mu_1^R], [\nu_1^L, \nu_1^R])$  and  $I_2 = ([\mu_2^L, \mu_2^R], [\nu_2^L, \nu_2^R])$  be IVIFNs; the score and accuracy values of  $I_1$  and  $I_2$  can be defined as follows:

$$S(I_1) = \frac{\mu_1^L + \mu_1^R(1 - \mu_1^L - \nu_1^L) + \mu_1^R + \mu_1^R(1 - \mu_1^R - \nu_1^R)}{2},$$

$$S(I_2) = \frac{\mu_2^L + \mu_2^R(1 - \mu_2^L - \nu_2^L) + \mu_2^R + \mu_2^R(1 - \mu_2^R - \nu_2^R)}{2}, \quad (6)$$

$$H(I_1) = \frac{\mu_1^L + \nu_1^L + \mu_1^R + \nu_1^R}{2},$$

$$H(I_2) = \frac{\mu_2^L + \nu_2^L + \mu_2^R + \nu_2^R}{2}. \quad (7)$$

For two IFNs  $I_1$  and  $I_2$ , regarding Definition 3,

- (1) If  $s(I_1) < s(I_2)$ , then  $I_1 < I_2$
- (2) If  $s(I_1) > s(I_2)$ , then  $I_1 > I_2$
- (3) If  $s(I_1) = s(I_2)$  and  $h(I_1) < h(I_2)$ , then  $I_1 < I_2$
- (4) If  $s(I_1) = s(I_2)$  and  $h(I_1) > h(I_2)$ , then  $I_1 > I_2$
- (5) If  $s(I_1) = s(I_2)$  and  $h(I_1) = h(I_2)$ , then  $I_1 = I_2$

Under the context of the IVIFNs, some aggregation operators will be introduced in this chapter, including the interval-valued intuitionistic fuzzy WA (IVIFWA) operator and the interval-valued intuitionistic fuzzy WG (IVIFWG) operator.

**Definition 4** (see [44]). Let  $I_j = (\mu_{I_j}, \nu_{I_j})$  ( $j = 1, 2, \dots, n$ ) be a set of IVIFNs; the IVIFWA operator is defined as

$$\text{IVIFWA}_\omega(I_1, I_2, \dots, I_n) = \oplus_{j=1}^n (\omega_j I_j), \quad (8)$$

where  $\omega = (\omega_1, \omega_2, \dots, \omega_n)^T$  is the weight vector of  $I_j$  ( $j = 1, 2, \dots, n$ ) and  $\omega_j > 0$ ,  $\sum_{j=1}^n \omega_j = 1$ .

Derived from Definition 4, the subsequent result can be obtained:

**Theorem 1.** The fused value by the IVIFWA operator could also be an IVIFN, where

$$\text{IVIFWA}_\omega(I_1, I_2, \dots, I_n) = \oplus_{j=1}^n (\omega_j I_j)$$

$$= \left( \left[ 1 - \prod_{j=1}^n (1 - \mu_{I_j}^L)^{\omega_j}, 1 - \prod_{j=1}^n (1 - \mu_{I_j}^R)^{\omega_j} \right], \left[ \prod_{j=1}^n (\nu_{I_j}^L)^{\omega_j}, \prod_{j=1}^n (\nu_{I_j}^R)^{\omega_j} \right] \right), \quad (9)$$

where  $\omega = (\omega_1, \omega_2, \dots, \omega_n)^T$  is the weight vector of  $I_j$  ( $j = 1, 2, \dots, n$ ) and  $\omega_j > 0$ ,  $\sum_{j=1}^n \omega_j = 1$ .

**Definition 5** (see [44]). Let  $I_j$  ( $j = 1, 2, \dots, n$ ) be a set of IVIFNs; the IVIFWG operator can be given as

$$\text{IVIFWG}_\omega(I_1, I_2, \dots, I_n) = \otimes_{j=1}^n (I_j)^{\omega_j}, \quad (10)$$

where  $\omega = (\omega_1, \omega_2, \dots, \omega_n)^T$  is the weight vector of  $I_j$  ( $j = 1, 2, \dots, n$ ) and  $\omega_j > 0$ ,  $\sum_{j=1}^n \omega_j = 1$ .

Derived from Definition 5, the detailed result can be obtained.

**Theorem 2.** The fused value by using the IVIFWG operator could also be an IVIFN, where

$$\text{IVIFWG}_\omega(I_1, I_2, \dots, I_n) = \bigotimes_{j=1}^n (I_j)^{\omega_j} \\ = \left( \left[ \prod_{j=1}^n (\mu_{I_j}^L)^{\omega_j}, \prod_{j=1}^n (\mu_{I_j}^R)^{\omega_j} \right], \left[ 1 - \prod_{j=1}^n (1 - \nu_{I_j}^L)^{\omega_j}, 1 - \prod_{j=1}^n (1 - \nu_{I_j}^R)^{\omega_j} \right] \right), \quad (11)$$

where  $\omega = (\omega_1, \omega_2, \dots, \omega_n)^T$  is the weight vector of  $I_j$  ( $j = 1, 2, \dots, n$ ) and  $\omega_j > 0$ ,  $\sum_{j=1}^n \omega_j = 1$ .

### 3. The EDAS Method with IVIFNs

Integrating the EDAS method with IVIFSs, we build the IVIF-EDAS method in which the assessment values are given by IVIFNs. The calculating procedures of the developed method can be described subsequently.

Let  $Z = \{Z_1, Z_2, \dots, Z_n\}$  be the attribute set and  $z = \{z_1, z_2, \dots, z_n\}$  be the attribute weight  $Z_j$ , where  $z_j \in [0, 1]$ ,  $j = 1, 2, \dots, n$ ,  $\sum_{j=1}^n z_j = 1$ . Assume  $D = \{D_1, D_2, \dots, D_l\}$  is a set of decision makers that have a significant degree of  $d = \{d_1, d_2, \dots, d_l\}$ , where  $d_k \in [0, 1]$ ,  $k = 1, 2, \dots, l$ ,  $\sum_{k=1}^l d_k = 1$ . Let  $Y = \{Y_1, Y_2, \dots, Y_m\}$  be a discrete collection of alternatives. And  $Q = (q_{ij})_{m \times n}$  is the overall IVIFN decision matrix;  $q_{ij}$  means the value of alternative  $Y_i$  regarding attribute  $Z_j$ . Subsequently, the specific calculating procedures will be depicted.

Step 1: set up each decision maker's IVIFN decision matrix  $Q^{(k)} = (q_{ij}^k)_{m \times n}$ , and calculate the overall IVIFN decision matrix  $Q = (q_{ij})_{m \times n}$ :

$$Q^{(k)} = [q_{ij}^k]_{m \times n} = \begin{bmatrix} q_{11}^k & q_{12}^k & \cdots & q_{1n}^k \\ q_{21}^k & q_{22}^k & \cdots & q_{2n}^k \\ \vdots & \vdots & \ddots & \vdots \\ q_{m1}^k & q_{m2}^k & \cdots & q_{mn}^k \end{bmatrix}, \quad (12)$$

$$Q = [q_{ij}]_{m \times n} = \begin{bmatrix} q_{11} & q_{12} & \cdots & q_{1n} \\ q_{21} & q_{22} & \cdots & q_{2n} \\ \vdots & \vdots & \ddots & \vdots \\ q_{m1} & q_{m2} & \cdots & q_{mn} \end{bmatrix}, \quad (13)$$

$$q_{ij} = \left( \left[ 1 - \prod_{k=1}^l (1 - \mu_{q_{ij}^k}^L)^{d_k}, 1 - \prod_{k=1}^l (1 - \mu_{q_{ij}^k}^R)^{d_k} \right], \right. \\ \left. \cdot \left[ \prod_{k=1}^l (\nu_{q_{ij}^k}^L)^{d_k}, \prod_{k=1}^l (\nu_{q_{ij}^k}^R)^{d_k} \right] \right), \quad (14)$$

where  $q_{ij}^k$  is the assessment value of alternative  $Y_i$  ( $i = 1, 2, \dots, m$ ) on the basis of the attribute  $Z_j$  ( $j = 1, 2, \dots, n$ ) and the decision maker  $D_k$  ( $k = 1, 2, \dots, l$ ).

Step 2: normalize the overall IVIFN decision matrix  $Q = (q_{ij})_{m \times n}$  to  $Q^N = [q_{ij}^N]_{m \times n}$ :

$$q_{ij}^N = \begin{cases} ([\mu_{ij}^L, \mu_{ij}^R], [\nu_{ij}^L, \nu_{ij}^R]), & Z_j \text{ is a benefit criterion,} \\ ([\nu_{ij}^L, \nu_{ij}^R], [\mu_{ij}^L, \mu_{ij}^R]), & Z_j \text{ is a cost criterion.} \end{cases} \quad (15)$$

Step 3: utilize the CRITIC method to determine the weighting matrix of attributes.

Criteria Importance through Intercriteria Correlation (CRITIC) method will be designed in this part which is utilized to decide attributes' weights. This method was initially put forward by Diakoulaki et al. [46] which took the correlations between attributes into consideration. Subsequently, the calculating procedures of this method will be presented:

- (1) Depending on the normalized overall IVIFN decision matrix  $Q^N = (q_{ij}^N)_{m \times n}$ , the correlation coefficient between attributes can be calculated:

$$IC_{jt} = \frac{\sum_{i=1}^m (S(q_{ij}^N) - S(q_j^N))(S(q_{it}^N) - S(q_t^N))}{\sqrt{\sum_{i=1}^m (S(q_{ij}^N) - S(q_j^N))^2} \sqrt{\sum_{i=1}^m (S(q_{it}^N) - S(q_t^N))^2}}, \\ j, t = 1, 2, \dots, n, \quad (16)$$

where  $q_j^N = 1/m \sum_{i=1}^m S(q_{ij}^N)$  and  $q_t^N = 1/m \sum_{i=1}^m S(q_{it}^N)$ .

- (2) Calculate attributes' standard deviation:

$$IS_j = \sqrt{\frac{1}{m-1} \sum_{i=1}^m (S(q_{ij}^N) - S(q_j^N))^2}, \quad j = 1, 2, \dots, n, \quad (17)$$

where  $q_j^N = 1/m \sum_{i=1}^m S(q_{ij}^N)$ .

- (3) Calculate the attributes' weights:

$$z_j = \frac{IS_j \sum_{t=1}^n (1 - IC_{jt})}{\sum_{j=1}^n (IS_j \sum_{t=1}^n (1 - IC_{jt}))}, \quad j = 1, 2, \dots, n, \quad (18)$$

where  $z_j \in [0, 1]$  and  $\sum_{j=1}^n z_j = 1$ .

Step 4: calculate the average solution (AV) regarding all designed attributes:

$$AV = [AV_j]_{1 \times n} = \left[ \frac{\sum_{i=1}^m \hat{q}_{ij}^N}{m} \right]_{1 \times n}, \quad (19)$$

$$[AV_j]_{1 \times n} = \left[ \frac{\sum_{i=1}^m \hat{q}_{ij}^N}{m} \right]_{1 \times n} = \left( \begin{bmatrix} 1 - \prod_{i=1}^m \left( 1 - (\mu_{ij}^N)^L \right)^{1/m}, 1 - \prod_{i=1}^m \left( 1 - (\mu_{ij}^N)^R \right)^{1/m} \\ \left[ \prod_{i=1}^m \left( (\nu_{ij}^N)^L \right)^{1/m}, \prod_{i=1}^m \left( (\nu_{ij}^N)^R \right)^{1/m} \right] \end{bmatrix} \right)_{1 \times n} \quad (20)$$

Step 5: depending on the AV's results, the positive distance from average (PDA) and negative distance from average (NDA) can be defined:

$$PDA_{ij} = [PDA_{ij}]_{m \times n} = \frac{\max(0, (s(q_{ij}^N) - s(AV_j)))}{s(AV_j)}, \quad (21)$$

$$NDA_{ij} = [NDA_{ij}]_{m \times n} = \frac{\max(0, (s(AV_j) - s(q_{ij}^N)))}{s(AV_j)}. \quad (22)$$

Step 6: calculate  $SP_i$  and  $SN_i$  which express the weighted sum of PDA and NDA:

$$SP_i = \sum_{j=1}^n z_j \cdot PDA_{ij}, NP_i = \sum_{j=1}^n z_j \cdot NDA_{ij}. \quad (23)$$

Step 7: depending on the above calculated results,  $SP_i$  and  $SN_i$  can be normalized as

$$\begin{aligned} NSP_i &= \frac{SP_i}{\max_i (SP_i)}, \\ NSN_i &= 1 - \frac{SN_i}{\max_i (SN_i)}. \end{aligned} \quad (24)$$

Step 8: calculate the appraisal score  $AS_i$  regarding every alternative's  $NSP_i$  and  $NSN_i$ :

$$AS_i = \frac{1}{2} (NSP_i + NSN_i). \quad (25)$$

Step 9: according to  $AS_i$ , all the alternatives can be ranked. The higher the value of  $AS_i$  is, the optimal alternative will be selected.

## 4. The Empirical Example and Comparative Analysis

**4.1. An Empirical Example.** With the development of research on wireless technique and other related techniques, wireless sensor networks (WSNs) have been widely used in various applications which involve diverse working environments, monitoring objects, and data conditions. Different applications require different quality of service (QoS) for data collection and data transmission. Thus, it is essential to provide QoS

guarantee mechanisms in WSNs to achieve good performance in various applications. Accordingly, it is of great significance to study the QoS guarantee mechanisms in WSNs. In general terms, the QoS of WSNs focuses on timeliness and reliability of data transmission, as well as coverage and connectivity of the network topology for data collection. The QoS guarantee implementation relies on different mechanisms in WSNs. Although many methods and techniques have been proposed in the existing literature, the QoS guarantee mechanism is still faced with the following challenges in complex applications: (1) there exist several types of data traffic which have different QoS requirements. Therefore, a multiple-level QoS guarantee mechanism is in great demand. (2) There could be multiple QoS requirements for one data traffic. Thus, it is necessary to provide multiple-QoS guarantee mechanisms for these traffics. (3) Since the traffic distributes are nonuniform in space and time, a method for the efficient transmission in a dynamic traffic is required. (4) There exists nonuniform replacement of the nodes as well as dynamic and changeful topology in many applications of the WSN. It is necessary to provide an efficient deployment method to satisfy the requirement of effectively covering. In this chapter, an empirical example for evaluating the service quality of wireless sensor networks which considered the complex MAGDM issues [47–54] will be provided by making use of the IVIF-EDAS method. Thus, in such a section, we present a numerical example to assess computer network systems with IVIFNs in order to show the designed method. There are five wireless sensor networks  $A_i (i = 1, 2, 3, 4, 5)$  to select. The expert group selects four attributes to evaluate these five wireless sensor networks: ①  $G_1$  is the product quality factor; ②  $G_2$  is the technology factor; ③  $G_3$  is the delivery factor; and ④  $G_4$  is the price factor. Taking its own business development into consideration, a company wants to choose a wireless sensor network. There are five potential wireless sensor networks  $Y_i (i = 1, 2, 3, 4, 5)$ . In order to select the optimal wireless sensor network, the expert group invites five experts  $D = \{D_1, D_2, D_3, D_4, D_5\}$  (expert's weight  $d = (1/5, 1/5, 1/5, 1/5, 1/5)$ ) to assess these wireless sensor networks. All experts give their assessment information depending on the four subsequently attributes: ①  $Z_1$  is the traffic convenience; ②  $Z_2$  is the product price; ③  $Z_3$  is the green environmental protection ability; and ④  $Z_4$  is the service quality. Evidently,  $Z_2$  is the  $g$  cost attribute, while  $Z_1, Z_3$ , and  $Z_4$  are the benefit attributes. To obtain the optimal wireless sensor network, the calculating procedures are involved:

Step 1: set up each decision maker's IVIFN evaluation matrix  $Q^{(k)} = (q_{ij}^k)_{m \times n} (i = 1, 2, \dots, m, j = 1, 2, \dots, n)$  as in Tables 1–5. Derived from these tables and equations (12)–(14), the overall IVIFN decision matrix could be calculated. The results are recorded in Table 6.

Step 2: normalize the evaluation matrix  $Q = [q_{ij}]_{m \times n}$  to  $Q^N = [q_{ij}^N]_{m \times n}$  (see Table 7).

TABLE 1: IVIFN evaluation information by  $D_1$ .

	$Z_1$	$Z_2$	$Z_3$	$Z_4$
$Y_1$	[[0.35, 0.38], [0.58, 0.62]]	[[0.21, 0.31], [0.33, 0.69]]	[[0.24, 0.33], [0.41, 0.66]]	[[0.32, 0.43], [0.45, 0.57]]
$Y_2$	[[0.29, 0.39], [0.44, 0.61]]	[[0.28, 0.34], [0.46, 0.64]]	[[0.11, 0.25], [0.32, 0.75]]	[[0.39, 0.44], [0.52, 0.61]]
$Y_3$	[[0.40, 0.49], [0.51, 0.60]]	[[0.33, 0.51], [0.53, 0.67]]	[[0.44, 0.50], [0.52, 0.56]]	[[0.28, 0.39], [0.61, 0.72]]
$Y_4$	[[0.33, 0.48], [0.54, 0.67]]	[[0.42, 0.49], [0.51, 0.58]]	[[0.41, 0.44], [0.46, 0.59]]	[[0.41, 0.46], [0.49, 0.53]]
$Y_5$	[[0.26, 0.48], [0.61, 0.74]]	[[0.42, 0.47], [0.52, 0.58]]	[[0.41, 0.48], [0.51, 0.59]]	[[0.38, 0.53], [0.55, 0.62]]

TABLE 2: IVIFN evaluation information by  $D_2$ .

	$Z_1$	$Z_2$	$Z_3$	$Z_4$
$Y_1$	[[0.38, 0.42], [0.55, 0.62]]	[[0.43, 0.49], [0.51, 0.57]]	[[0.29, 0.39], [0.59, 0.71]]	[[0.45, 0.48], [0.50, 0.55]]
$Y_2$	[[0.37, 0.48], [0.56, 0.63]]	[[0.34, 0.44], [0.51, 0.66]]	[[0.46, 0.50], [0.52, 0.54]]	[[0.39, 0.48], [0.50, 0.61]]
$Y_3$	[[0.37, 0.50], [0.54, 0.63]]	[[0.27, 0.39], [0.67, 0.73]]	[[0.41, 0.52], [0.54, 0.59]]	[[0.16, 0.33], [0.72, 0.84]]
$Y_4$	[[0.46, 0.49], [0.52, 0.54]]	[[0.32, 0.38], [0.56, 0.68]]	[[0.37, 0.43], [0.47, 0.63]]	[[0.29, 0.34], [0.68, 0.71]]
$Y_5$	[[0.40, 0.48], [0.52, 0.60]]	[[0.46, 0.49], [0.51, 0.54]]	[[0.42, 0.47], [0.55, 0.58]]	[[0.33, 0.38], [0.62, 0.67]]

TABLE 3: IVIFN evaluation information by  $D_3$ .

	$Z_1$	$Z_2$	$Z_3$	$Z_4$
$Y_1$	[[0.44, 0.48], [0.52, 0.56]]	[[0.38, 0.42], [0.48, 0.62]]	[[0.31, 0.42], [0.59, 0.69]]	[[0.40, 0.49], [0.58, 0.60]]
$Y_2$	[[0.38, 0.42], [0.59, 0.62]]	[[0.35, 0.43], [0.58, 0.65]]	[[0.42, 0.48], [0.52, 0.58]]	[[0.26, 0.33], [0.59, 0.74]]
$Y_3$	[[0.35, 0.42], [0.59, 0.65]]	[[0.48, 0.50], [0.51, 0.52]]	[[0.18, 0.36], [0.64, 0.82]]	[[0.38, 0.43], [0.56, 0.62]]
$Y_4$	[[0.27, 0.34], [0.59, 0.73]]	[[0.26, 0.43], [0.62, 0.74]]	[[0.38, 0.46], [0.52, 0.62]]	[[0.31, 0.45], [0.62, 0.69]]
$Y_5$	[[0.46, 0.51], [0.52, 0.54]]	[[0.44, 0.51], [0.52, 0.56]]	[[0.34, 0.45], [0.62, 0.66]]	[[0.35, 0.45], [0.55, 0.65]]

TABLE 4: IVIFN evaluation information by  $D_4$ .

	$Z_1$	$Z_2$	$Z_3$	$Z_4$
$Y_1$	[[0.42, 0.48], [0.51, 0.58]]	[[0.37, 0.44], [0.59, 0.63]]	[[0.25, 0.37], [0.68, 0.75]]	[[0.22, 0.35], [0.67, 0.78]]
$Y_2$	[[0.41, 0.49], [0.52, 0.59]]	[[0.36, 0.39], [0.49, 0.64]]	[[0.27, 0.43], [0.65, 0.73]]	[[0.42, 0.45], [0.52, 0.58]]
$Y_3$	[[0.43, 0.48], [0.52, 0.57]]	[[0.42, 0.48], [0.52, 0.58]]	[[0.41, 0.48], [0.54, 0.59]]	[[0.34, 0.49], [0.58, 0.66]]
$Y_4$	[[0.32, 0.43], [0.64, 0.67]]	[[0.32, 0.43], [0.59, 0.68]]	[[0.36, 0.39], [0.58, 0.64]]	[[0.15, 0.39], [0.64, 0.85]]
$Y_5$	[[0.37, 0.45], [0.56, 0.63]]	[[0.36, 0.45], [0.55, 0.64]]	[[0.42, 0.50], [0.52, 0.58]]	[[0.27, 0.45], [0.65, 0.73]]

TABLE 5: IVIFN evaluation information by  $D_5$ .

	$Z_1$	$Z_2$	$Z_3$	$Z_4$
$Y_1$	[[0.63, 0.66], [0.69, 0.37]]	[[0.45, 0.46], [0.48, 0.55]]	[[0.39, 0.45], [0.59, 0.61]]	[[0.43, 0.47], [0.54, 0.57]]
$Y_2$	[[0.43, 0.47], [0.52, 0.57]]	[[0.37, 0.43], [0.59, 0.63]]	[[0.40, 0.50], [0.52, 0.60]]	[[0.41, 0.48], [0.52, 0.59]]
$Y_3$	[[0.47, 0.49], [0.51, 0.53]]	[[0.29, 0.35], [0.65, 0.71]]	[[0.42, 0.48], [0.53, 0.58]]	[[0.27, 0.43], [0.67, 0.73]]
$Y_4$	[[0.41, 0.49], [0.52, 0.59]]	[[0.43, 0.47], [0.52, 0.57]]	[[0.46, 0.48], [0.52, 0.54]]	[[0.19, 0.38], [0.67, 0.81]]
$Y_5$	[[0.33, 0.45], [0.64, 0.67]]	[[0.48, 0.50], [0.51, 0.52]]	[[0.44, 0.46], [0.53, 0.56]]	[[0.21, 0.37], [0.68, 0.79]]

Step 3: decide the attribute weights  $z_j$  ( $j = 1, 2, \dots, n$ ) by making use of the CRITIC method as recorded in Table 8.

Step 4: depending on the calculated results of Table 8, the value of average solution (AV) can be obtained on the basis of all proposed attributes by equations (19) and (20) (see Table 9).

Step 5: relying on the results of AV, the PDA and NDA can be calculated by utilizing equations (21) and (22) (see Tables 10 and 11).

Step 6: on the basis of equation (23) and attribute weighting vector  $\omega = (0.1311, 0.2162, 0.2233, 0.4094)$ , the values of  $SP_i$  and  $SN_i$  can be calculated:

$$SP_1 = 0.0018, SP_2 = 0.2063, SP_3 = 0.0375, SP_4 = 0.0659, SP_5 = 0.0000,$$

$$SN_1 = 0.1379, SN_2 = 0.0356, SN_3 = 0.0689, SN_4 = 0.1052, SN_5 = 0.0338.$$

(26)

TABLE 6: Overall IVIFN evaluation information.

	$Z_1$	$Z_2$	$Z_3$	$Z_4$
$Y_1$	([0.4341, 0.4442], [0.5051, 0.5233])	([0.4722, 0.4833], [0.4901, 0.5189])	([0.2798, 0.2980], [0.6087, 0.6455])	([0.4376, 0.4521], [0.5475, 0.5499])
$Y_2$	([0.5341, 0.5365], [0.4152, 0.42532])	([0.5502, 0.5708], [0.4209, 0.4429])	([0.6432, 0.6679], [0.3807, 0.3988])	([0.5908, 0.6213], [0.3216, 0.4453])
$Y_3$	([0.4325, 0.4365], [0.5472, 0.5711])	([0.4029, 0.4233], [0.5120, 0.5431])	([0.4458, 0.4687], [0.4897, 0.4988])	([0.3246, 0.4362], [0.2109, 0.4907])
$Y_4$	([0.5231, 0.5433], [0.4761, 0.4866])	([0.4877, 0.4902], [0.4211, 0.4766])	([0.5765, 0.5870], [0.4211, 0.4465])	([0.3287, 0.4309], [0.4870, 0.4998])
$Y_5$	([0.4168, 0.4561], [0.5232, 0.5690])	([0.4907, 0.5142], [0.4606, 0.4980])	([0.4755, 0.5219], [0.4658, 0.4785])	([0.4598, 0.4622], [0.1121, 0.2366])



TABLE 7: The normalized IVIFN evaluation information.

	$Z_1$	$Z_2$	$Z_3$	$Z_4$
$Y_1$	([0.4341, 0.4442], [0.5051, 0.5233])	([0.4901, 0.5189], [0.4722, 0.4833])	([0.2798, 0.2980], [0.6087, 0.6455])	([0.4376, 0.4521], [0.5475, 0.5499])
$Y_2$	([0.5341, 0.5365], [0.4152, 0.42532])	([0.4209, 0.4429], [0.5502, 0.5708])	([0.6432, 0.6679], [0.3807, 0.3988])	([0.5908, 0.6213], [0.3216, 0.4453])
$Y_3$	([0.4325, 0.4365], [0.5472, 0.5711])	([0.5120, 0.5431], [0.4029, 0.4233])	([0.4458, 0.4687], [0.4897, 0.4988])	([0.3246, 0.4362], [0.2109, 0.4907])
$Y_4$	([0.5231, 0.5433], [0.4761, 0.4866])	([0.4211, 0.4766], [0.4877, 0.4902])	([0.5765, 0.5870], [0.4211, 0.4465])	([0.3287, 0.4309], [0.4870, 0.4998])
$Y_5$	([0.4168, 0.4561], [0.5232, 0.5690])	([0.4606, 0.4980], [0.4907, 0.5142])	([0.4755, 0.5219], [0.4658, 0.4785])	([0.4598, 0.4622], [0.1121, 0.2366])

TABLE 8: The attribute weights  $z_j$ .

	$Z_1$	$Z_2$	$Z_3$	$Z_4$
$Z_j$	0.1311	0.2162	0.2233	0.4094

TABLE 9: The value of average solution.

	Average solution
$Z_1$	$([0.4286, 0.4782], [0.4784, 0.5231])$
$Z_2$	$([0.5219, 0.5690], [0.4221, 0.4410])$
$Z_3$	$([0.4522, 0.4897], [0.4588, 0.5099])$
$Z_4$	$([0.4308, 0.4906], [0.3265, 0.4128])$

TABLE 10: The results of  $PDA_{ij}$ .

	$Z_1$	$Z_2$	$Z_3$	$Z_4$
$Y_1$	0.0000	0.0054	0.0000	0.0000
$Y_2$	0.1236	0.0000	0.2833	0.3164
$Y_3$	0.0000	0.1436	0.0000	0.0000
$Y_4$	0.0929	0.0000	0.1565	0.0000
$Y_5$	0.0000	0.0000	0.0000	0.0000

TABLE 11: The results of  $NDA_{ij}$ .

	$Z_1$	$Z_2$	$Z_3$	$Z_4$
$Y_1$	0.0084	0.0000	0.3875	0.0288
$Y_2$	0.0000	0.1477	0.0000	0.0000
$Y_3$	0.0938	0.0000	0.1252	0.0245
$Y_4$	0.0000	0.0038	0.0000	0.3567
$Y_5$	0.1293	0.0368	0.0359	0.0046

Step 7: the results of Step 6 could be normalized by equation (24):

$$\begin{aligned}
 NSP_1 &= 0.0063, NSP_2 = 1.0000, NSP_3 = 0.1200, NSP_4 \\
 &= 0.3037, NSP_5 = 0.0000, \\
 NSN_1 &= 0.0000, NSN_2 = 0.7528, NSN_3 = 0.5462, NSN_4 \\
 &= 0.1982, NSN_5 = 0.7361.
 \end{aligned} \quad (27)$$

Step 8: on the basis of each alternative's  $NSP_i$  and  $NSN_i$ , the values of AS are calculated:

$$\begin{aligned}
 AS_1 &= 0.0038, AS_2 = 0.8715, AS_3 = 0.3581, AS_4 \\
 &= 0.2613, AS_5 = 0.3732.
 \end{aligned} \quad (28)$$

Step 9: according to the AS, all the alternatives can be ranked; the higher the value of AS is, the optimal alternative will be selected. Evidently, the rank of these five alternatives is  $Y_2 > Y_5 > Y_3 > Y_4 > Y_1$ , and  $Y_2$  is the best wireless sensor network.

4.2. *Comparative Analysis.* In this part, our developed method is compared with some other methods to illustrate its superiority.

First of all, our presented method is compared with IVIFWA and IVIFWG operators [44]. For the IVIFWA operator, the calculated result is  $S(Y_1) = 0.4364$ ,  $S(Y_2) = 0.5806$ ,  $S(Y_3) = 0.4852$ ,  $S(Y_4) = 0.4941$ , and  $S(Y_5) = 0.4752$ . Thus, the ranking order is  $Y_2 > Y_4 > Y_3 > Y_5 > Y_1$ . For the IVIFWG operator, the calculated result is  $S(Y_1) = 0.4197$ ,  $S(Y_2) = 0.5708$ ,  $S(Y_3) = 0.4762$ ,  $S(Y_4) = 0.4673$ , and  $S(Y_5) = 0.4733$ . So, the ranking order is  $Y_2 > Y_3 > Y_5 > Y_4 > Y_1$ .

Furthermore, our presented method is compared with the modified VIKOR method with IVIFSs [55]. Then, we can obtain the calculation result. The closest ideal score values are determined as  $CI^+(Y_1) = 1.0000$ ,  $CI^+(Y_2) = 0.1705$ ,  $CI^+(Y_3) = 0.3404$ ,  $CI^+(Y_4) = 0.6723$ , and  $CI^+(Y_5) = 0.4065$ . And the farthest worst score values are determined as  $CI^-(Y_1) = 0.0000$ ,  $CI^-(Y_2) = 0.5103$ ,  $CI^-(Y_3) = 0.7247$ ,  $CI^-(Y_4) = 0.1856$ , and  $CI^-(Y_5) = 0.1139$ . Then, each alternative's relative closeness is calculated as  $DRC_1 = 1.0000$ ,  $DRC_2 = 0.2652$ ,  $DRC_3 = 0.3265$ ,  $DRC_4 = 0.7982$ , and  $DRC_5 = 0.8077$ . Hence, the ranking order of alternatives is  $Y_2 > Y_3 > Y_4 > Y_5 > Y_1$ .

In the end, our presented method is compared with GRA-based IVIFSs [56]. Then, we can obtain the calculation result. The grey relational grades of each alternative are calculated as  $\gamma_1 = 0.8398$ ,  $\gamma_2 = 1.0000$ ,  $\gamma_3 = 0.8307$ ,  $\gamma_4 = 0.8821$ , and  $\gamma_5 = 0.8672$ . Therefore, the ranking order of alternatives is  $Y_2 > Y_4 > Y_5 > Y_1 > Y_3$ .

Eventually, the results of dissimilar methods are recorded in Table 12.

Derived from Table 12, it is evident that the optimal wireless sensor network is  $Y_2$  in the mentioned methods, while the worst choice is  $Y_1$  in most situations. In other words, these methods' ranking results are slightly different. Different methods could effectively tackle MAGDM issues from different kinds of angles. IVIFWA and IVIFWG operators emphasize to aggregate evaluation information. The modified VIKOR method with IVIFSs emphasizes the closest to the ideal solution and the farthest to the worst solution. The GRA-based IVIFSs emphasize the degree of similarity or difference between two sequences on the basis of the relation. However, our developed method emphasizes to calculate the expected function from the average solution. Compared with the aforementioned methods, it is more practical and effective since the procedures of calculation are simpler, and it is more convenient to apply to the practical situations.

TABLE 12: Evaluation results of dissimilar methods.

Methods	Ranking order	The optimal alternative	The worst alternative
IVIFWA	$Y_2 > Y_4 > Y_3 > Y_5 > Y_1$	$Y_2$	$Y_1$
IVIFWG	$Y_2 > Y_3 > Y_5 > Y_4 > Y_1$	$Y_2$	$Y_1$
The modified VIKOR	$Y_2 > Y_3 > Y_4 > Y_5 > Y_1$	$Y_2$	$Y_1$
The GRA method	$Y_2 > Y_4 > Y_5 > Y_1 > Y_3$	$Y_2$	$Y_3$
The developed method	$Y_2 > Y_5 > Y_3 > Y_4 > Y_1$	$Y_2$	$Y_1$

## 5. Conclusion

In this paper, IVIF-EDAS method is developed to tackle the MAGDM issues based on the description of the EDAS method and some fundamental notions of IVIFSs. To begin with, the fundamental information of IVIFSs is simply introduced. After that, the IVIFWA and IVIFWG operators are utilized to integrate the IVIFNs. Subsequently, relying on the CRITIC method, the attributes' weights are decided. In addition, applying the EDAS method to the IVIFSs, a new method is designed, and the calculating procedures are listed in detail. Finally, an application for assessing the service quality of wireless sensor networks has been given to show the superiority of this novel method, and comparative analysis between the IVIF-EDAS method and some other methods could also be made to further verify some merits of such a method. In our future works, the EDAS method and the CRITIC method will be extensively applied in different uncertain and ambiguous environments [57–67].

## Data Availability

The data used to support the findings of this study are included within the article.

## Conflicts of Interest

The authors declare no conflicts of interest.

## References

- [1] L. A. Zadeh, "Fuzzy sets," *Information and Control*, vol. 8, no. 3, pp. 338–353, 1965.
- [2] K. T. Atanassov, "Intuitionistic fuzzy sets," *Fuzzy Sets and Systems*, vol. 20, no. 1, pp. 87–96, 1986.
- [3] X. J. Gou, Z. S. Xu, and Q. Lei, "New operational laws and aggregation method of intuitionistic fuzzy information," *Journal of Intelligent & Fuzzy Systems*, vol. 30, pp. 129–141, 2016.
- [4] Y. He, Z. He, and H. Huang, "Decision making with the generalized intuitionistic fuzzy power interaction averaging operators," *Soft Computing*, vol. 21, no. 5, pp. 1129–1144, 2017.
- [5] L. Zhang and Y. He, "Extensions of intuitionistic fuzzy geometric interaction operators and their application to cognitive microcredit origination," *Cognitive Computation*, vol. 11, no. 5, pp. 748–760, 2019.
- [6] M. Li and C. Wu, "A distance model of intuitionistic fuzzy cross entropy to solve preference problem on alternatives," *Mathematical Problems in Engineering*, vol. 2016, Article ID 8324124, 9 pages, 2016.
- [7] R. X. Liang, S. S. He, J. Q. Wang, K. Chen, and L. Li, "An extended mabac method for multi-criteria group decision-making problems based on correlative inputs of intuitionistic fuzzy information," *Computational & Applied Mathematics*, vol. 38, p. 28, 2019.
- [8] M. S. Khan and Q. M. D. Lohani, "IEEE, a similarity measure for atanassov intuitionistic fuzzy sets and its application to clustering," in *In Proceedings of the 2016 International Workshop on Computational Intelligence (IWCi)*, Dhaka, Bangladesh, Decembr 2016.
- [9] S.-M. Chen, S.-H. Cheng, and T.-C. Lan, "Multicriteria decision making based on the topsis method and similarity measures between intuitionistic fuzzy values," *Information Sciences*, vol. 367–368, pp. 279–295, 2016.
- [10] P. Li, J. Liu, S. F. Liu, X. Su, and J. Wu, "Grey target method for intuitionistic fuzzy decision making based on grey incidence analysis," *Journal of Grey System*, vol. 28, pp. 96–109, 2016.
- [11] F. Lei, G. W. Wei, J. P. Lu, C. Wei, and J. Wu, "Gra method for probabilistic linguistic multiple attribute group decision making with incomplete weight information and its application to waste incineration plants location problem," *International Journal of Computational Intelligence Systems*, vol. 12, pp. 1547–1556, 2019.
- [12] H. Garg, "Novel intuitionistic fuzzy decision making method based on an improved operation laws and its application," *Engineering Applications of Artificial Intelligence*, vol. 60, pp. 164–174, 2017.
- [13] P. Gupta, H. D. Arora, and P. Tiwari, "Generalized entropy for intuitionistic fuzzy sets," *Malaysian Journal of Mathematical Sciences*, vol. 10, pp. 209–220, 2016.
- [14] J. Lu, C. Wei, J. Wu, and G. Wei, "Topsis method for probabilistic linguistic magdm with entropy weight and its application to supplier selection of new agricultural machinery products," *Entropy*, vol. 21, no. 10, p. 953, 2019.
- [15] T. Bao, X. Xie, P. Long, and Z. Wei, "Madm method based on prospect theory and evidential reasoning approach with unknown attribute weights under intuitionistic fuzzy environment," *Expert Systems with Applications*, vol. 88, pp. 305–317, 2017.
- [16] J. W. Gan and L. Luo, "Using dematel and intuitionistic fuzzy sets to identify critical factors influencing the recycling rate of end-of-life vehicles in China," *Sustainability*, vol. 9, no. 10, 2017.
- [17] P. Gupta, M. K. Mehlawat, N. Grover, and W. Chen, "Modified intuitionistic fuzzy sir approach with an application to supplier selection," *Journal of Intelligent & Fuzzy Systems*, vol. 32, no. 6, pp. 4431–4441, 2017.
- [18] R. Krishankumar, K. S. Ravichandran, and A. B. Saeid, "A new extension to promethee under intuitionistic fuzzy environment for solving supplier selection problem with linguistic preferences," *Applied Soft Computing*, vol. 60, pp. 564–576, 2017.
- [19] X. Luo and X. Z. Wang, "Extended vikor method for intuitionistic fuzzy multiattribute decision-making based on a new distance measure," *Mathematical Problems in Engineering*, vol. 2017, Article ID 4072486, 16 pages, 2017.

- [20] Z. Hao, Z. Xu, H. Zhao, and R. Zhang, "Novel intuitionistic fuzzy decision making models in the framework of decision field theory," *Information Fusion*, vol. 33, pp. 57–70, 2017.
- [21] L. Zhang, J. Zhan, and Y. Yao, "Intuitionistic fuzzy topsis method based on cvpifrs models: an application to biomedical problems," *Information Sciences*, vol. 517, pp. 315–339, 2020.
- [22] H. Garg, "Generalized intuitionistic fuzzy entropy-based approach for solving multi-attribute decision-making problems with unknown attribute weights," *Proceedings of the National Academy of Sciences, India Section A: Physical Sciences*, vol. 89, no. 1, pp. 129–139, 2019.
- [23] P. Liu, J. Liu, and S.-M. Chen, "Some intuitionistic fuzzy dombi bonferroni mean operators and their application to multi-attribute group decision making," *Journal of the Operational Research Society*, vol. 69, no. 1, pp. 1–24, 2018.
- [24] G. Wei, J. Wu, C. Wei, J. Wang, and J. Lu, "Models for madm with 2-tuple linguistic neutrosophic dombi bonferroni mean operators," *IEEE Access*, vol. 7, pp. 108878–108905, 2019.
- [25] F. Jin, Z. Ni, H. Chen, and Y. Li, "Approaches to group decision making with intuitionistic fuzzy preference relations based on multiplicative consistency," *Knowledge-Based Systems*, vol. 97, pp. 48–59, 2016.
- [26] L. Wu, H. Gao, and C. Wei, "Vikor method for financing risk assessment of rural tourism projects under interval-valued intuitionistic fuzzy environment," *Journal of Intelligent & Fuzzy Systems*, vol. 37, no. 2, pp. 2001–2008, 2019.
- [27] L. Wu, J. Wang, and H. Gao, "Models for competitiveness evaluation of tourist destination with some interval-valued intuitionistic fuzzy hamy mean operators," *Journal of Intelligent & Fuzzy Systems*, vol. 36, no. 6, pp. 5693–5709, 2019.
- [28] L. Wu, G. Wei, J. Wu, and C. Wei, "Some interval-valued intuitionistic fuzzy dombi heronian mean operators and their application for evaluating the ecological value of forest ecological tourism demonstration areas," *International Journal of Environmental Research and Public Health*, vol. 17, no. 3, p. 829, 2020.
- [29] S.-M. Chen and L.-W. Kuo, "Multiattribute decision making based on non-linear programming methodology with hyperbolic function and interval-valued intuitionistic fuzzy values," *Information Sciences*, vol. 453, pp. 379–388, 2018.
- [30] J. Lu and C. Wei, "Todim method for performance appraisal on social-integration-based rural reconstruction with interval-valued intuitionistic fuzzy information," *Journal of Intelligent & Fuzzy Systems*, vol. 37, no. 2, pp. 1731–1740, 2019.
- [31] H. Garg and K. Kumar, "Group decision making approach based on possibility degree measures and the linguistic intuitionistic fuzzy aggregation operators using einstein norm operations," *Journal of Multiple-Valued Logic and Soft Computing*, vol. 31, pp. 175–209, 2018.
- [32] H. Garg and R. Arora, "Generalized intuitionistic fuzzy soft power aggregation operator based on  $t$  norm and their application in multicriteria decision-making," *International Journal of Intelligent Systems*, vol. 34, no. 2, pp. 215–246, 2019.
- [33] M. Keshavarz Ghorabae, E. K. Zavadskas, L. Olfat, and Z. Turskis, "Multi-criteria inventory classification using a new method of evaluation based on distance from average solution (edas)," *Informatica*, vol. 26, no. 3, pp. 435–451, 2015.
- [34] M. K. Ghorabae, E. K. Zavadskas, M. Amiri, and Z. Turskis, "Extended edas method for fuzzy multi-criteria decision-making: an application to supplier selection," *International Journal of Computers Communications & Control*, vol. 11, no. 3, pp. 358–371, 2016.
- [35] M. Keshavarz Ghorabae, M. Amiri, E. K. Zavadskas, Z. Turskis, and J. Antucheviciene, "Stochastic edas method for multi-criteria decision-making with normally distributed data," *Journal of Intelligent & Fuzzy Systems*, vol. 33, no. 3, pp. 1627–1638, 2017.
- [36] X. Peng and C. Liu, "Algorithms for neutrosophic soft decision making based on edas, new similarity measure and level soft set," *Journal of Intelligent & Fuzzy Systems*, vol. 32, no. 1, pp. 955–968, 2017.
- [37] C. Kahraman, M. Keshavarz Ghorabae, E. K. Zavadskas, S. Cevik Onar, M. Yazdani, and B. Oztaysi, "Intuitionistic fuzzy edas method: an application to solid waste disposal site selection," *Journal of Environmental Engineering and Landscape Management*, vol. 25, no. 1, pp. 1–12, 2017.
- [38] Y. He, F. Lei, G. W. Wei, R. Wang, J. Wu, and C. Wei, "Edas method for multiple attribute group decision making with probabilistic uncertain linguistic information and its application to green supplier selection," *International Journal of Computational Intelligence Systems*, vol. 12, no. 2, pp. 1361–1370, 2019.
- [39] M. Keshavarz-Ghorabae, M. Amiri, E. K. Zavadskas, Z. Turskis, and J. Antucheviciene, "A comparative analysis of the rank reversal phenomenon in the edas and topsis methods," *Economic Computation and Economic Cybernetics Studies and Research*, vol. 52, pp. 121–134, 2018.
- [40] P. Wang, J. Wang, and G. Wei, "Edas method for multiple criteria group decision making under 2-tuple linguistic neutrosophic environment," *Journal of Intelligent & Fuzzy Systems*, vol. 37, no. 2, pp. 1597–1608, 2019.
- [41] Z. X. Li, G. W. Wei, R. Wang, J. Wu, C. Wei, and Y. Wei, "Edas method for multiple attribute group decision making under  $q$  rung orthopair fuzzy environment," *Technological and Economic Development of Economy*, vol. 26, no. 1, pp. 86–102, 2020.
- [42] X. Feng, C. Wei, and Q. Liu, "Edas method for extended hesitant fuzzy linguistic multi-criteria decision making," *International Journal of Fuzzy Systems*, vol. 20, no. 8, pp. 2470–2483, 2018.
- [43] A. Karasan and C. Kahraman, "A novel interval-valued neutrosophic edas method: prioritization of the united nations national sustainable development goals," *Soft Computing*, vol. 22, no. 15, pp. 4891–4906, 2018.
- [44] Z. Xu and R. R. Yager, "Some geometric aggregation operators based on intuitionistic fuzzy sets," *International Journal of General Systems*, vol. 35, no. 4, pp. 417–433, 2006.
- [45] H.-W. Liu and G.-J. Wang, "Multi-criteria decision-making methods based on intuitionistic fuzzy sets," *European Journal of Operational Research*, vol. 179, no. 1, pp. 220–233, 2007.
- [46] D. Diakoulaki, G. Mavrotas, and L. Papayannakis, "Determining objective weights in multiple criteria problems: the critic method," *Computers & Operations Research*, vol. 22, no. 7, pp. 763–770, 1995.
- [47] X. Deng, J. Wang, and G. Wei, "Some 2-tuple linguistic pythagorean heronian mean operators and their application to multiple attribute decision-making," *Journal of Experimental & Theoretical Artificial Intelligence*, vol. 31, no. 4, pp. 555–574, 2019.
- [48] X. Y. Tang and G. W. Wei, "Dual hesitant pythagorean fuzzy bonferroni mean operators in multi-attribute decision making," *Archives of Control Sciences*, vol. 29, pp. 339–386, 2019.
- [49] G. Wei, S. Zhang, J. Lu, J. Wu, and C. Wei, "An extended bidirectional projection method for picture fuzzy magdm and its application to safety assessment of construction project," *IEEE Access*, vol. 7, pp. 166138–166147, 2019.
- [50] X. Deng and H. Gao, "Todim method for multiple attribute decision making with 2-tuple linguistic pythagorean fuzzy information," *Journal of Intelligent & Fuzzy Systems*, vol. 37, no. 2, pp. 1769–1780, 2019.

- [51] H. Gao, M. Lu, and Y. Wei, "Dual hesitant bipolar fuzzy hamacher aggregation operators and their applications to multiple attribute decision making," *Journal of Intelligent & Fuzzy Systems*, vol. 37, no. 4, pp. 5755–5766, 2019.
- [52] Z. Li and M. Lu, "Some novel similarity and distance measures of pythagorean fuzzy sets and their applications," *Journal of Intelligent & Fuzzy Systems*, vol. 37, no. 2, pp. 1781–1799, 2019.
- [53] J. Wang, H. Gao, and M. Lu, "Approaches to strategic supplier selection under interval neutrosophic environment," *Journal of Intelligent & Fuzzy Systems*, vol. 37, no. 2, pp. 1707–1730, 2019.
- [54] R. Wang, "Research on the application of the financial investment risk appraisal models with some interval number muirhead mean operators," *Journal of Intelligent & Fuzzy Systems*, vol. 37, no. 2, pp. 1741–1752, 2019.
- [55] S. Zeng, S.-M. Chen, and L.-W. Kuo, "Multiattribute decision making based on novel score function of intuitionistic fuzzy values and modified vikor method," *Information Sciences*, vol. 488, pp. 76–92, 2019.
- [56] S.-F. Zhang and S.-Y. Liu, "A gra-based intuitionistic fuzzy multi-criteria group decision making method for personnel selection," *Expert Systems with Applications*, vol. 38, no. 9, pp. 11401–11405, 2011.
- [57] E. K. Zavadskas, J. Antucheviciene, and P. Chatterjee, "Multiple-criteria decision-making (mcdm) techniques for business processes information management," *Information*, vol. 10, no. 1, 2019.
- [58] E. K. Zavadskas, J. Antucheviciene, and S. Kar, "Multi-objective and multi-attribute optimization for sustainable development decision aiding," *Sustainability*, vol. 11, 2019.
- [59] G. Wei, Y. Tang, M. Zhao, R. Lin, and J. Wu, "Selecting the low-carbon tourism destination: based on pythagorean fuzzy taxonomy method," *Mathematics*, vol. 8, no. 5, p. 832, 2020.
- [60] P. Liu and H. Li, "Interval-valued intuitionistic fuzzy power bonferroni aggregation operators and their application to group decision making," *Cognitive Computation*, vol. 9, no. 4, pp. 494–512, 2017.
- [61] S. Zeng, C. Llopis-Albert, and Y. Zhang, "A novel induced aggregation method for intuitionistic fuzzy set and its application in multiple attribute group decision making," *International Journal of Intelligent Systems*, vol. 33, no. 11, pp. 2175–2188, 2018.
- [62] X. Gou and Z. Xu, "Novel basic operational laws for linguistic terms, hesitant fuzzy linguistic term sets and probabilistic linguistic term sets," *Information Sciences*, vol. 372, pp. 407–427, 2016.
- [63] G. Wei, J. Lu, C. Wei, and J. Wu, "Probabilistic linguistic gra method for multiple attribute group decision making," *Journal of Intelligent & Fuzzy Systems*, vol. 38, no. 4, pp. 4721–4732, 2020.
- [64] H. Jiang, J. Zhan, B. Sun, and J. C. R. Alcantud, "An madm approach to covering-based variable precision fuzzy rough sets: an application to medical diagnosis," *International Journal of Machine Learning and Cybernetics*, 2020.
- [65] X. Ma, J. Zhan, B. Sun, and J. C. R. Alcantud, "Novel classes of coverings based multigranulation fuzzy rough sets and corresponding applications to multiple attribute group decision-making," *Artificial Intelligence Review*, 2020.
- [66] J. Zhan, B. Sun, and X. Zhang, "Pf-topsis method based on cpfrs models: an application to unconventional emergency events," *Computers & Industrial Engineering*, vol. 139, Article ID 106192, 2020.
- [67] L. Wang and N. Li, "Pythagorean fuzzy interaction power bonferroni mean aggregation operators in multiple attribute decision making," *International Journal of Intelligent Systems*, vol. 35, no. 1, pp. 150–183, 2020.

## Research Article

# Interval-Valued Complex Fuzzy Geometric Aggregation Operators and Their Application to Decision Making

Songsong Dai<sup>1</sup>, Lvqing Bi<sup>2</sup>, and Bo Hu<sup>3</sup>

<sup>1</sup>School of Electronics and Information Engineering, Taizhou University, Taizhou 318000, China

<sup>2</sup>School of Electronics and Communication Engineering,  
Guangxi Colleges and Universities Key Laboratory of Complex System Optimization and Big Data Processing,  
Yulin Normal University, Yulin 537000, China

<sup>3</sup>School of Big Data and Computer Science, Guizhou Normal University, Guiyang 550025, China

Correspondence should be addressed to Songsong Dai; ssdai@stu.xmu.edu.cn

Received 29 May 2020; Accepted 3 July 2020; Published 22 July 2020

Guest Editor: Zaoli Yang

Copyright © 2020 Songsong Dai et al. This is an open access article distributed under the Creative Commons Attribution License, which permits unrestricted use, distribution, and reproduction in any medium, provided the original work is properly cited.

This paper investigates the geometric aggregation operators for aggregating the interval-valued complex fuzzy sets (IVCFSs) whose membership grades are a special set of complex numbers. We develop some geometric aggregation operators under the interval-valued complex fuzzy environment, namely, interval-valued complex fuzzy geometric (IVCFG), interval-valued complex fuzzy weighted geometric (IVCFWG), and interval-valued complex fuzzy ordered weighted geometric (IVCFOWG) operators. Then, we investigate the rotational and reflectional invariances of these operators. Further, a decision-making approach based on these operators is presented under the interval-valued complex fuzzy environment and an example is illustrated to demonstrate the efficiency of the proposed approach.

## 1. Introduction

The aggregation operator is a powerful method for decision making, pattern recognition, and cluster analysis. In the past decades, in both theoretical and applied studies, aggregation operators have attained great advances. Many types of aggregation operators have been proposed under different environments, such as fuzzy environment [1–4], intuitionistic fuzzy environment [5–9], interval-valued intuitionistic fuzzy environment [10–14], Pythagorean fuzzy environment [15–17], neutrosophic fuzzy environment [18–20], and hesitant fuzzy environment [21–25].

In the above fuzzy environments, membership degrees are the subsets of real numbers. As a generalization of traditional fuzzy set [26], Ramot et al. [27] introduced the concept of complex fuzzy set (CFS), which is characterized by a complex-valued membership function. In many practical situations, complex fuzzy sets are useful [28–40]. Moreover, many researchers extended the concept of CFS to interval-valued complex fuzzy set (IVCFS) [41, 42] and

complex intuitionistic fuzzy set (CIFS) [43]. Therefore, many researchers discussed how to aggregate CFSs. Ramot et al. [32] introduced the concept of complex fuzzy aggregation. Ma et al. [38] proposed a product-sum aggregation operator under complex fuzzy environment. Bi et al. [39, 40] proposed several aggregation operators under complex fuzzy environment. Garg and Rani [44, 45] investigated the aggregation operators under complex intuitionistic fuzzy environment.

However, we still have the key question: why complex fuzzy aggregation? Moreover, why complex fuzzy sets? As mentioned in [46], from mathematical and practical viewpoints, complex fuzzy sets are natural and useful. But complex fuzzy sets (CFSs) remain a puzzle from the intuitive viewpoint. Fuzzy sets and other extensions give intuitively clear way to describe how humans deal with different types of uncertainty. So before we start to examine the information aggregation issue under interval-valued complex fuzzy environment, we first discuss some phenomena which maybe ignored in real life. When we ask the way, two persons may



give the answers “it is about 1 km away,” and then we think that 1 km is a reasonable result. However, if their answers are not exclusively same about direction, as shown in Figure 1, 0.95 km also is a reasonable result since  $C = (A + B)/2$ .

How does this phenomenon affect human decision making? For example, there are two hospitals  $H_1$  and  $H_2$ ; which one is the nearest hospital? Then, we get data about distance and direction from strangers. It is a very interesting case; two strangers both agree that hospital  $H_1$  is nearer than hospital  $H_2$ , but after data aggregation, the result that  $H_2$  is nearer than hospital  $H_1$  is also reasonable, as shown in Figure 2. The order only relying on the distance is reasonable since we want to go to the nearest hospital. The method based on complex fuzzy aggregation is reasonable since it is a center-based method.

Complex fuzzy aggregation operator can perfectly describe above phenomenon in human decision making since it does not satisfy the property of amplitude monotonicity [40]. Monotonicity is a basic property, which holds in many types of aggregation operators under different fuzzy environments [1–25]. Complex fuzzy aggregation operator as a nonmonotone average is very natural and gives an intuitive way to describe how humans deal with such type of uncertainty.

In this paper, we focus on the aggregation operator under interval-valued complex fuzzy environment. IVCFSs also are very appropriate for some applications in real life. For example, when we get lost, we often ask strangers for directions in our daily life. Then, we get some answers, such as “0.5–0.6 km, east” and “0.5–0.7 km, northeast.” These answers can be represented in terms of IVCFSs. We present the theory of the weighted geometric aggregation operators among the IVCFSs. First we review necessary concepts and some basic properties related to this paper in Section 2. In Section 3, we present an interval-valued complex fuzzy weighted geometric (IVCFWG) operator on CFSs. In Section 4, we present an interval-valued complex fuzzy ordered weighted geometric (IVCFOWG) operator. In Section 5, we present a decision-making approach based on the proposed operator under IVCFS environment. Finally, conclusions are given in Section 6.

## 2. Preliminaries

In this paper, our discussion is based on interval-valued complex fuzzy set theory. Some basic concepts are recalled below, whereas for other concepts, refer to reports from Ref. [27, 28, 41, 42, 47].

Let  $D$  be the set of complex numbers on complex unit disk, i.e.,  $D = \{a \in \mathbb{C} \mid |a| \leq 1\}$ . Let  $U$  be a fixed universe, and a mapping  $A: U \rightarrow D$  is called a complex fuzzy set on  $U$ .

Let  $\mathcal{J}^{[0,1]}$  be the set of all closed subintervals of  $[0, 1]$ , i.e.,  $\mathcal{J}^{[0,1]} = \{[a, b] \mid 0 \leq a \leq b \leq 1\}$ . Let  $\dot{D}$  be the boundary set of  $D$  i.e.,  $\dot{D} = \{a \in \mathbb{C} \mid |a| = 1\}$ . A mapping  $A: U \rightarrow \mathcal{J}^{[0,1]} \cdot \dot{D}$  is called an IVCFS on  $U$ . For any  $x \in U$ , its membership degree  $\mu_A(x)$  is

$$[r_A(x), \overline{r_A(x)}] \cdot e^{j\nu_A(x)}, \quad (1)$$

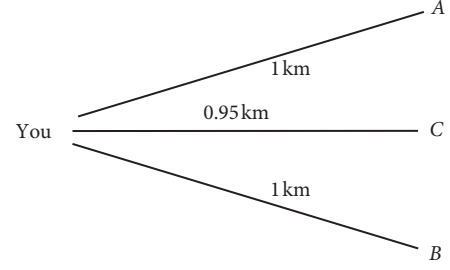


FIGURE 1: A target location example.

where  $j = \sqrt{-1}$ ,  $\mathcal{J}^{[0,1]} \cdot \dot{D}$  is the dot product set of  $\mathcal{J}^{[0,1]}$  and  $\dot{D}$ ,  $[r_A(x), \overline{r_A(x)}] \in \mathcal{J}^{[0,1]}$  is the interval-valued amplitude part, and  $\nu_A(x) \in \mathbb{R}$  is the phase part.

For convenience, we only consider the values on  $\mathcal{J}^{[0,1]} \cdot \dot{D}$ , which are called interval-valued complex fuzzy values (IVCFVs). Let  $a = [r_a, \overline{r_a}] \cdot e^{j\nu_a}$  be an IVCVF, where the interval-valued amplitude part is  $[r_a, \overline{r_a}] \in \mathcal{J}^{[0,1]}$  and the phase part is  $\nu_a \in \mathbb{R}$ . The modulus of  $a$  is the interval-valued amplitude part  $[r_a, \overline{r_a}]$ , denoted by  $|a|$ . An order of IVCFVs is defined by the interval-valued amplitude part, i.e.,

$$|a| \leq |b| \text{ if } r_a \leq r_b \text{ and } \overline{r_a} \leq \overline{r_b}. \quad (2)$$

Let  $a = [r_a, \overline{r_a}] \cdot e^{j\nu_a}$  and  $b = [r_b, \overline{r_b}] \cdot e^{j\nu_b}$  be two IVCFVs and let the parameters be  $\lambda > 0$  and  $\theta \in \mathbb{R}$ ; four operators of IVCFVs include multiplication, power, rotation, and reflection which are defined as follows.

(i) Multiplication of two IVCFVs  $a, b \in \mathcal{J}^{[0,1]} \cdot \dot{D}$ :

$$a \otimes b = [r_a \cdot r_b, \overline{r_a} \cdot \overline{r_b}] \cdot e^{j(\nu_a + \nu_b)}. \quad (3)$$

(ii) Power of an IVCVF  $a \in \mathcal{J}^{[0,1]} \cdot \dot{D}$ :

$$a^\lambda = \left[ r_a^\lambda, \overline{r_a}^\lambda \right] \cdot e^{j\lambda\nu_a}. \quad (4)$$

(iii) Rotation of an IVCVF  $a \in \mathcal{J}^{[0,1]} \cdot \dot{D}$ :

$$\text{Rot}_\theta(a) = [r_a, \overline{r_a}] \cdot e^{j(\nu_a + \theta)}. \quad (5)$$

(iv) Reflection of an IVCVF  $a \in \mathcal{J}^{[0,1]} \cdot \dot{D}$ :

$$\text{Ref}(a) = [r_a, \overline{r_a}] \cdot e^{-j\nu_a}. \quad (6)$$

When  $a, b \in D$ ,  $\otimes$  is a complex intersection defined by Ramot et al. [27]. When  $a, b \in [0, 1]$ ,  $\otimes$  is a t-norm [48].

**Theorem 1.** Suppose that  $a, b, c$  are three IVCFVs, and the parameters are  $\lambda_1 > 0, \lambda_2 > 0$ , and  $\theta_1, \theta_2 \in \mathbb{R}$ . Then, we have

- (1)  $a \otimes b = b \otimes a$
- (2)  $(a \otimes b) \otimes c = a \otimes (b \otimes c)$
- (3)  $(a \otimes b)^{\lambda_1} = a^{\lambda_1} \otimes b^{\lambda_1}$

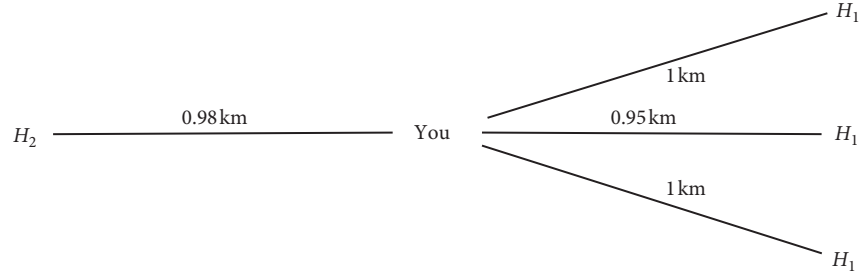


FIGURE 2: A decision-making example.

$$(4) a^{\lambda_1 + \lambda_2} = a^{\lambda_1} \otimes a^{\lambda_2}$$

$$(5) \text{Ref}(\text{Ref}(a)) = a$$

$$(6) \text{Rot}_{\theta_1}(\text{Rot}_{\theta_2}(a)) = \text{Rot}_{\theta_1 + \theta_2}(a)$$

$$(7) \text{Ref}(a^{\lambda_1}) = \text{Ref}(a)^{\lambda_1}$$

$$(8) \text{Ref}(a \otimes b) = \text{Ref}(a) \otimes \text{Ref}(b)$$

*Proof.* Let  $a = [\underline{r}_a, \overline{r}_a] \cdot e^{j\nu_a}$ ,  $b = [\underline{r}_b, \overline{r}_b] \cdot e^{j\nu_b}$ , and  $c = [\underline{r}_c, \overline{r}_c] \cdot e^{j\nu_c}$ .

(1) By the definition of multiplication of two IVCfVs, we have

$$\begin{aligned} a \otimes b &= [\underline{r}_a \cdot \underline{r}_b, \overline{r}_a \cdot \overline{r}_b] \cdot e^{j(\nu_a + \nu_b)} \\ &= [\underline{r}_b \cdot \underline{r}_a, \overline{r}_b \cdot \overline{r}_a] \cdot e^{j(\nu_b + \nu_a)} \\ &= b \otimes a. \end{aligned} \quad (7)$$

(2) And

$$\begin{aligned} (a \otimes b) \otimes c &= [\underline{r}_a \cdot \underline{r}_b, \overline{r}_a \cdot \overline{r}_b] \cdot e^{j(\nu_a + \nu_b)} \otimes [\underline{r}_c, \overline{r}_c] \cdot e^{j\nu_c} \\ &= [\underline{r}_a, \overline{r}_a] \cdot e^{j\nu_a} \otimes [\underline{r}_b \cdot \underline{r}_c, \overline{r}_b \cdot \overline{r}_c] \cdot e^{j(\nu_b + \nu_c)} \\ &= a \otimes (b \otimes c). \end{aligned} \quad (8)$$

(3) By the definition of power of two IVCfVs, we have

$$\begin{aligned} (a \otimes b)^{\lambda_1} &= \left[ [\underline{r}_a \cdot \underline{r}_b, \overline{r}_a \cdot \overline{r}_b] \cdot e^{j(\nu_a + \nu_b)} \right]^{\lambda_1} \\ &= \left[ (\underline{r}_a \cdot \underline{r}_b)^{\lambda_1}, (\overline{r}_a \cdot \overline{r}_b)^{\lambda_1} \right] \cdot e^{j\lambda_1(\nu_a + \nu_b)} \\ &= [\underline{r}_a^{\lambda_1} \cdot \underline{r}_b^{\lambda_1}, \overline{r}_a^{\lambda_1} \cdot \overline{r}_b^{\lambda_1}] \cdot e^{j(\lambda_1\nu_a + \lambda_1\nu_b)} \\ &= a^{\lambda_1} \otimes b^{\lambda_1}. \end{aligned} \quad (9)$$

(4) And

$$\begin{aligned} a^{\lambda_1 + \lambda_2} &= [\underline{r}_a^{\lambda_1 + \lambda_2}, \overline{r}_a^{\lambda_1 + \lambda_2}] \cdot e^{j(\lambda_1 + \lambda_2)\nu_a} \\ &= [\underline{r}_a^{\lambda_1} \cdot \underline{r}_a^{\lambda_2}, \overline{r}_a^{\lambda_1} \cdot \overline{r}_a^{\lambda_2}] \cdot e^{j(\lambda_1\nu_a + \lambda_2\nu_a)} \\ &= a^{\lambda_1 + \lambda_2}. \end{aligned} \quad (10)$$

(5) By the definition of reflection of two IVCfVs, we have

$$\begin{aligned} \text{Ref}(\text{Ref}(a)) &= \text{Ref}\left([\underline{r}_a, \overline{r}_a] \cdot e^{-j\nu_a}\right) \\ &= [\underline{r}_a, \overline{r}_a] \cdot e^{-(-j\nu_a)} \\ &= [\underline{r}_a, \overline{r}_a] \cdot e^{j\nu_a} \\ &= a. \end{aligned} \quad (11)$$

(6) By the definition of rotation of two IVCfVs, we have

$$\begin{aligned} \text{Rot}_{\theta_1}(\text{Rot}_{\theta_2}(a)) &= \text{Rot}_{\theta_1}\left([\underline{r}_a, \overline{r}_a] \cdot e^{j(\nu_a + \theta_2)}\right) \\ &= [\underline{r}_a, \overline{r}_a] \cdot e^{j(\nu_a + \theta_2 + \theta_1)} \\ &= \text{Rot}_{\theta_1 + \theta_2}(a). \end{aligned} \quad (12)$$

(7) For any two IVCfVs  $a, b$  and real value  $\lambda > 0$ , we have

$$\begin{aligned} \text{Ref}(a)^\lambda &= \left[ [\underline{r}_a, \overline{r}_a] \cdot e^{-j\nu_a} \right]^\lambda \\ &= [\underline{r}_a^\lambda, \overline{r}_a^\lambda] \cdot e^{j(-\lambda\nu_a)} \\ &= \text{Ref}(a^\lambda). \end{aligned} \quad (13)$$

(8) For any two IVCfVs  $a, b$ , we have

$$\begin{aligned} \text{Ref}(a) \otimes \text{Ref}(b) &= [\underline{r}_a, \overline{r}_a] \cdot e^{-j\nu_a} \otimes [\underline{r}_b, \overline{r}_b] \cdot e^{-j\nu_b} \\ &= [\underline{r}_a \cdot \underline{r}_b, \overline{r}_a \cdot \overline{r}_b] \cdot e^{j(-\nu_a - \nu_b)} \\ &= [\underline{r}_a \cdot \underline{r}_b, \overline{r}_a \cdot \overline{r}_b] \cdot e^{-j(\nu_a + \nu_b)} \\ &= \text{Ref}(a \otimes b). \end{aligned} \quad (14)$$

Moreover, the multiplication and power operators have the following properties.  $\square$

**Theorem 2.** Suppose that  $a = [\underline{r}_a, \overline{r}_a] \cdot e^{j\nu_a}$ ,  $b = [\underline{r}_b, \overline{r}_b] \cdot e^{j\nu_b}$ ,  $c = [\underline{r}_c, \overline{r}_c] \cdot e^{j\nu_c}$ , and  $d = [\underline{r}_d, \overline{r}_d] \cdot e^{j\nu_d}$  are four IVCfVs; the parameters are  $\lambda_1 > 0, \lambda_2 > 0$ , and  $\theta \in \mathbb{R}$ . Then we have

(1) (Amplitude monotonicity) If  $|a| \leq |b|, |c| \leq |d|$ , then  $|a \otimes c| \leq |b \otimes d|$

- (2) (Amplitude boundedness)  $[r_a \wedge r_b, \overline{r_a} \wedge \overline{r_b}] \leq |a \otimes b| \leq 1$   
 (3) If  $\lambda_1 \leq \lambda_2$ , then  $|a^{\lambda_2}| \leq |a^{\lambda_1}|$   
 (4) If  $|a| \leq |b|$ , then  $|a^{\lambda_1}| \leq |b^{\lambda_1}|$ ,  $|\text{Ref}(a)| \leq |\text{Ref}(b)|$ ,  
 $|\text{Rot}_\theta(a)| \leq |\text{Rot}_\theta(b)|$

*Proof.* Since the amplitude terms of IVCFVs are interval values, we can obtain the above results from the properties of multiplication operator of interval values.

Rotational invariance and reflectional invariance are two important geometric properties of complex fuzzy operators [28, 29, 39]. They show that a complex fuzzy operator is invariant under a rotation and a reflection, respectively. We define the following two similar properties for interval-valued complex fuzzy operators as follows.

- (i) An interval-valued complex fuzzy operator  $v: (\mathcal{J}^{[0,1]} \cdot \dot{D})^n \longrightarrow \mathcal{J}^{[0,1]} \cdot \dot{D}$  is rotationally invariant if and only if, for any  $\theta$ ,

$$v(\text{Rot}_\theta(a_1), \dots, \text{Rot}_\theta(a_n)) = \text{Rot}_\theta(v(a_1, \dots, a_n)). \quad (15)$$

- (ii) An interval-valued complex fuzzy operator  $v: (\mathcal{J}^{[0,1]} \cdot \dot{D})^n \longrightarrow \mathcal{J}^{[0,1]} \cdot \dot{D}$  is reflectionally invariant if and only if

$$v(\text{Ref}(a_1), \dots, \text{Ref}(a_n)) = \text{Ref}(v(a_1, \dots, a_n)). \quad (16)$$

Then, for the multiplication operator of IVCFVs, we have the following results.  $\square$

**Theorem 3.** The multiplication operator of IVCFVs is reflectionally invariant.

*Proof.* Trivial from Theorem 1 (16).  $\square$

**Theorem 4.** The multiplication operator of IVCFVs is not rotationally invariant.

*Proof.* For any two IVCFVs  $a = [r_a, \overline{r_a}] \cdot e^{j\nu_a}$ ,  $b = [r_b, \overline{r_b}] \cdot e^{j\nu_b}$  and real value  $\theta$ , we have

$$\begin{aligned} & \text{Rot}_\theta(a) \otimes \text{Rot}_\theta(b) \\ &= [r_a, \overline{r_a}] \cdot e^{j(\nu_a + \theta)} \otimes [r_b, \overline{r_b}] \cdot e^{j(\nu_b + \theta)} \\ &= [r_a \cdot r_b, \overline{r_a} \cdot \overline{r_b}] \cdot e^{j(\nu_a + \nu_b + 2\theta)}, \\ & \text{Rot}_\theta(a \otimes b) = [r_a \cdot r_b, \overline{r_a} \cdot \overline{r_b}] \cdot e^{j(\nu_a + \nu_b + \theta)}. \end{aligned} \quad (17)$$

Since  $\nu_a + \nu_b + 2\theta \neq \nu_a + \nu_b + \theta$ , the multiplication operator is not rotationally invariant.  $\square$

### 3. Interval-Valued Complex Fuzzy Weighted Geometric Operators

In this section, we introduce the weighted geometric operators in an interval-valued complex fuzzy environment and discuss their fundamental characteristics.

**Definition 1.** Let  $a_i (i = 1, 2, \dots, n)$  be a collection of IVCFVs; an interval-valued complex fuzzy weighted geometric (IVCFWG) operator is defined as

$$\text{IVCFWG}(a_1, a_2, \dots, a_n) = \otimes_{i=1}^n a_i^{w_i}, \quad (18)$$

where  $w_i \in [0, 1]$  for all  $i$  and  $\sum_{i=1}^n w_i = 1$ .

When  $w_i = 1/n (i = 1, 2, \dots, n)$ , then the IVCFWG operator is denoted by interval-valued complex fuzzy geometric (IVCFA) operator, i.e.,

$$\text{IVCFWG}(a_1, a_2, \dots, a_n) = \otimes_{i=1}^n a_i^{1/n}. \quad (19)$$

When  $a_i \in \mathcal{J}^{[0,1]} (i = 1, 2, \dots, n)$ , the IVCFWG operator can reduce to a traditional interval-valued fuzzy weighted geometric operator of values on unit interval  $\mathcal{J}^{[0,1]}$ .

When  $a_i \in [0, 1] (i = 1, 2, \dots, n)$ , the IVCFWG operator can reduce to a traditional weighted geometric operator [49] of real numbers on unit interval  $[0, 1]$ .

When  $a_i \in [0, 1]$  and  $w_i = 1/n (i = 1, 2, \dots, n)$ , the CFWP operator can reduce to a traditional geometric mean operator [50] of real numbers on unit interval  $[0, 1]$ .

**Theorem 5.** Let  $a_i (i = 1, 2, \dots, n)$  be a collection of IVCFVs; then, the aggregated value  $\text{IVCFWG}(a_1, a_2, \dots, a_n)$  is also an IVCFV and

$$\begin{aligned} & \text{IVCFWG}(a_1, a_2, \dots, a_n) \\ &= \left[ \prod_{i=1}^n r_{a_i}^{w_i}, \prod_{i=1}^n \overline{r_{a_i}}^{w_i} \right] \cdot e^{j(\sum_{i=1}^n w_i \nu_{a_i})}, \end{aligned} \quad (20)$$

where  $w_i \in [0, 1]$  for all  $i$  and  $\sum_{i=1}^n w_i = 1$ .

*Proof.* It is easy to check that the aggregated value is also an IVCFV. Now, we prove equation (20) by mathematical induction method.

For  $n = 2$ , we have  $a_1^{w_1} = [r_{a_1}^{w_1}, \overline{r_{a_1}}^{w_1}] \cdot e^{jw_1 \nu_{a_1}}$ ,  $a_2^{w_2} = [r_{a_2}^{w_2}, \overline{r_{a_2}}^{w_2}] \cdot e^{jw_2 \nu_{a_2}}$ ; then,

$$\begin{aligned} & \text{IVCFWG}(a_1, a_2) \\ &= a_1^{w_1} \otimes a_2^{w_2} \\ &= \left[ r_{a_1}^{w_1} r_{a_2}^{w_2}, \overline{r_{a_1}}^{w_1} \overline{r_{a_2}}^{w_2} \right] \cdot e^{j(w_1 \nu_{a_1} + w_2 \nu_{a_2})} \\ &= \left[ \prod_{i=1}^2 r_{a_i}^{w_i}, \prod_{i=1}^2 \overline{r_{a_i}}^{w_i} \right] \cdot e^{j(\sum_{i=1}^2 w_i \nu_{a_i})}. \end{aligned} \quad (21)$$

If equation (20) holds for  $n = k$ , i.e.,

$$\begin{aligned} & \text{IVCFWG}(a_1, a_2, \dots, a_k) \\ &= \left[ \prod_{i=1}^k r_{a_i}^{w_i}, \prod_{i=1}^k \overline{r_{a_i}}^{w_i} \right] \cdot e^{j(\sum_{i=1}^k w_i \nu_{a_i})}, \end{aligned} \quad (22)$$

then for  $n = k + 1$ ,

$$\begin{aligned}
& \text{IVCFWG}(a_1, a_2, \dots, a_{k+1}) \\
&= \text{IVCFWG}(a_1, a_2, \dots, a_k) \otimes a_{k+1}^{w_{k+1}} \\
&= \left[ \prod_{i=1}^k \underline{r_{a_i}}^{w_i}, \prod_{i=1}^k \overline{r_{a_i}}^{w_i} \right] \cdot e^{j(\sum_{i=1}^k w_i \gamma_{a_i})} \otimes a_{k+1}^{w_{k+1}} \\
&= \left[ \left( \prod_{i=1}^k \underline{r_{a_i}}^{w_i} \right) \cdot \underline{r_{a_{k+1}}}^{w_{k+1}}, \left( \prod_{i=1}^k \overline{r_{a_i}}^{w_i} \right) \cdot \overline{r_{a_{k+1}}}^{w_{k+1}} \right] \\
&\quad \cdot e^{j(\sum_{i=1}^k w_i \gamma_{a_i} + w_{k+1} \gamma_{a_{k+1}})} \\
&= \left[ \prod_{i=1}^{k+1} \underline{r_{a_i}}^{w_i}, \prod_{i=1}^{k+1} \overline{r_{a_i}}^{w_i} \right] \cdot e^{j(\sum_{i=1}^{k+1} w_i \gamma_{a_i})}.
\end{aligned} \tag{23}$$

Therefore, equation (20) holds for all  $n$ .

The working of the proposed IVCFWG operator is explained with a numerical example as follows.  $\square$

**Example 1.** Let  $a_1 = [0.6, 0.7] \cdot e^{j0.1\pi}$ ,  $a_2 = [0.3, 0.5] \cdot e^{j0.2\pi}$ ,  $a_3 = [0.6, 0.8] \cdot e^{j0.7\pi}$ , and  $a_4 = [0.4, 0.7] \cdot e^{j0.4\pi}$  be four IVCFVs and  $w = (0.1, 0.2, 0.3, 0.4)^T$  be the associated weight vector. Then, by using equation (20),

$$\begin{aligned}
\prod_{i=1}^4 \underline{r_{a_i}}^{w_i} &= 0.6^{0.1} \cdot 0.3^{0.2} \cdot 0.6^{0.3} \cdot 0.4^{0.4} = 0.4441, \\
\prod_{i=1}^4 \overline{r_{a_i}}^{w_i} &= 0.7^{0.1} \cdot 0.5^{0.2} \cdot 0.8^{0.3} \cdot 0.7^{0.4} = 0.6812, \\
\sum_{i=1}^4 w_i \gamma_{a_i} &= 0.1 \cdot 0.1\pi + 0.2 \cdot 0.2\pi + 0.3 \cdot 0.7\pi + 0.4 \cdot 0.4\pi \\
&= 0.42\pi,
\end{aligned} \tag{24}$$

we obtain  $\text{IVCFWG}(a_1, a_2, a_3, a_4) = [0.4441, 0.6812] \cdot e^{j0.42\pi}$ .

Based on Theorem 5, the proposed IVCFWG operator satisfies the following properties.

**Theorem 6.** Let  $a_i (i = 1, 2, \dots, n)$  and  $b_i (i = 1, 2, \dots, n)$  be two collections of IVCFVs, the weights be  $w_i \in [0, 1] (i = 1, 2, \dots, n)$ , and  $\sum_{i=1}^n w_i = 1$ . Then, we have the following properties:

(1) (Idempotency) If  $a_i = a (i = 1, 2, \dots, n)$ , then

$$\text{IVCFWG}(a_1, a_2, \dots, a_n) = a. \tag{25}$$

(2) (Amplitude monotonicity) If  $|a_i| \leq |b_i| (i = 1, 2, \dots, n)$ , then

$$\begin{aligned}
& |\text{IVCFWG}(a_1, a_2, \dots, a_n)| \\
& \leq |\text{IVCFWG}(b_1, b_2, \dots, b_n)|.
\end{aligned} \tag{26}$$

(3) (Amplitude boundedness)

$$r_1 \leq |\text{IVCFWG}(a_1, a_2, \dots, a_n)| \leq r_2, \tag{27}$$

where  $r_1, r_2$  are two interval values:

$$\begin{aligned}
r_1 &= \left[ \min_i \underline{r_{a_i}}, \min_i \overline{r_{a_i}} \right], \\
r_2 &= \left[ \max_i \underline{r_{a_i}}, \max_i \overline{r_{a_i}} \right].
\end{aligned} \tag{28}$$

*Proof.*

(1) Let  $a_i = a = [\underline{r_a}, \overline{r_a}]$ , ( $i = 1, 2, \dots, n$ ); then,

$$\begin{aligned}
& \text{IVCFWG}(a_1, a_2, \dots, a_n) \\
&= \left[ \prod_{i=1}^n \underline{r_{a_i}}^{w_i}, \prod_{i=1}^n \overline{r_{a_i}}^{w_i} \right] \cdot e^{j(\sum_{i=1}^n w_i \gamma_{a_i})} \\
&= \left[ \underline{r_a}^{\sum_{i=1}^n w_i}, \overline{r_a}^{\sum_{i=1}^n w_i} \right] \cdot e^{j\gamma_a} \\
&= [\underline{r_a}, \overline{r_a}] \cdot e^{j\gamma_a} \\
&= a.
\end{aligned} \tag{29}$$

(2) The property of the amplitude monotonicity is trivial from Theorem 2 (4).

(3) The property of the amplitude boundedness is easily obtained from idempotency and amplitude monotonicity.

Note that idempotency is concerned with both the phase part and amplitude part of IVCFVs. Amplitude boundedness and amplitude monotonicity are only concerned with the amplitude part of IVCFVs.  $\square$

**Theorem 7.** The IVCFWG operator is reflectionally invariant.

*Proof.* For any collection of IVCFVs  $a_i (i = 1, 2, \dots, n)$ , from equation (20), we have

$$\begin{aligned}
& \text{IVCFWG}(\text{Ref}(a_1), \text{Ref}(a_2), \dots, \text{Ref}(a_n)) \\
&= \left[ \prod_{i=1}^n (\underline{r_{a_i}})^{w_i}, \prod_{i=1}^n (\overline{r_{a_i}})^{w_i} \right] \cdot e^{j(\sum_{i=1}^n w_i \gamma_{a_i})} \\
&= \left[ \prod_{i=1}^n (\underline{r_{a_i}})^{w_i}, \prod_{i=1}^n (\overline{r_{a_i}})^{w_i} \right] \cdot e^{-j(\sum_{i=1}^n w_i \gamma_{a_i})}, \\
& \text{Ref}(\text{IVCFWG}(a_1, a_2, \dots, a_n)) \\
&= \text{Ref}(\otimes_{i=1}^n a_i^{w_i}) \\
&= \left[ \prod_{i=1}^n (\underline{r_{a_i}})^{w_i}, \prod_{i=1}^n (\overline{r_{a_i}})^{w_i} \right] \cdot e^{-j(\sum_{i=1}^n w_i \gamma_{a_i})}.
\end{aligned} \tag{30}$$

Then,  $\text{IVCFWG}(\text{Ref}(a_1), \text{Ref}(a_2), \dots, \text{Ref}(a_n)) = \text{Ref}(\otimes_{i=1}^n w_i a_i)$  is reflectionally invariant.  $\square$

**Theorem 8.** The IVCFWG operator is rotationally invariant.

*Proof.* For any collection of IVCfVs  $a_i$  ( $i = 1, 2, \dots, n$ ) and any  $\theta \in \mathbb{R}$ , we have

$$\begin{aligned} & \text{IVCFWG}(\text{Rot}_\theta(a_1), \text{Rot}_\theta(a_2), \dots, \text{Rot}_\theta(a_n)) \\ &= \left[ \prod_{i=1}^n \left( \underline{r_{a_i}} \right)^{w_i}, \prod_{i=1}^n \left( \overline{r_{a_i}} \right)^{w_i} \right] \cdot e^{j(\sum_{i=1}^n w_i (\nu_{a_i} + \theta))} \\ &= \left[ \prod_{i=1}^n \left( \underline{r_{a_i}} \right)^{w_i}, \prod_{i=1}^n \left( \overline{r_{a_i}} \right)^{w_i} \right] \cdot e^{j((\sum_{i=1}^n w_i \nu_{a_i}) + (\sum_{i=1}^n w_i \theta))} \quad (31) \\ &= \left[ \prod_{i=1}^n \left( \underline{r_{a_i}} \right)^{w_i}, \prod_{i=1}^n \left( \overline{r_{a_i}} \right)^{w_i} \right] \cdot e^{j((\sum_{i=1}^n w_i \nu_{a_i}) + \theta)} \\ &=_{\text{Rot}\theta} (\text{IVCFWG}(a_1, a_2, \dots, a_n)). \end{aligned}$$

Then, the IVCFWG operator is rotationally invariant.  $\square$

#### 4. Interval-Valued Complex Fuzzy Ordered Weighted Geometric Operators

Based on the order of IVCfVs defined by equation (2) and the ordered weighted averaging (OWA) operator introduced by Yager [1], we define an interval-valued complex fuzzy ordered weighted geometric (IVCFOWG) operator as follows.

**Definition 2.** Let  $a_i$  ( $i = 1, 2, \dots, n$ ) be a collection of CFVs; then, an IVCFOWG operator is defined as

$$\text{IVCFOWG}(a_1, a_2, \dots, a_n) = \otimes_{i=1}^n a_{\sigma(i)}^{w_i}, \quad (32)$$

where  $w_i \in [0, 1]$  ( $i = 1, 2, \dots, n$ ) and  $\sum_{i=1}^n w_i = 1$ ,  $(\sigma(1), \sigma(2), \dots, \sigma(n))$  is a permutation of  $(1, 2, \dots, n)$  such that  $a_{\sigma(i-1)} \geq a_{\sigma(i)}$  for all  $i$ .

Especially, when  $w_i = 1/n$  ( $i = 1, 2, \dots, n$ ), the IVCFOWG operator is reduced to the IVCFWG operator.

Similar to the IVCFWG operator, the IVCFOWG operator has the following properties.

**Theorem 9.** Let  $a_i$  ( $i = 1, 2, \dots, n$ ) be a collection of IVCfVs; then, the aggregated value  $\text{IVCFOWG}(a_1, a_2, \dots, a_n)$  is also an IVCfV and

$$\begin{aligned} & \text{IVCFOWG}(a_1, a_2, \dots, a_n) \\ &= \left[ \prod_{i=1}^n \left( \underline{r_{a_{\sigma(i)}}} \right)^{w_i}, \prod_{i=1}^n \left( \overline{r_{a_{\sigma(i)}}} \right)^{w_i} \right] \cdot e^{j(\sum_{i=1}^n w_i \nu_{a_{\sigma(i)}})}, \quad (33) \end{aligned}$$

where  $w_i \in [0, 1]$  for all  $i$  and  $\sum_{i=1}^n w_i = 1$ ,  $(\sigma(1), \sigma(2), \dots, \sigma(n))$  is a permutation of  $(1, 2, \dots, n)$  such that  $a_{\sigma(i-1)} \geq a_{\sigma(i)}$  for all  $i$ .

*Proof.* The proof is similar to Theorem 5.

The working of the proposed IVCFOWG operator is explained with a numerical example as follows.  $\square$

**Example 2.** Let  $a_1 = [0.6, 0.7] \cdot e^{j0.1\pi}$ ,  $a_2 = [0.3, 0.5] \cdot e^{j0.2\pi}$ ,  $a_3 = [0.6, 0.8] \cdot e^{j0.7\pi}$ , and  $a_4 = [0.4, 0.7] \cdot e^{j0.4\pi}$  be four IVCfVs and  $w = (0.1, 0.2, 0.3, 0.4)^T$  be the associated weight vector. By the order from equation (2), we have  $a_3 \geq a_1 \geq a_4 \geq a_2$ . Then, by using equation (33),

$$\prod_{i=1}^4 \underline{r_{a_{\sigma(i)}}}^{w_i} = 0.6^{0.1} \cdot 0.6^{0.2} \cdot 0.4^{0.3} \cdot 0.3^{0.4} = 0.4026,$$

$$\prod_{i=1}^4 \overline{r_{a_{\sigma(i)}}}^{w_i} = 0.8^{0.1} \cdot 0.8^{0.2} \cdot 0.7^{0.3} \cdot 0.5^{0.4} = 0.6369,$$

$$\begin{aligned} \sum_{i=1}^4 w_i \nu_{a_i} &= 0.1 \cdot 0.7\pi + 0.2 \cdot 0.1\pi + 0.3 \cdot 0.4\pi + 0.4 \cdot 0.2\pi \\ &= 0.29\pi, \end{aligned} \quad (34)$$

we obtain  $\text{IVCFOWG}(a_1, a_2, a_3, a_4) = [0.4026, 0.6369] \cdot e^{j0.29\pi}$ . It is different from  $\text{IVCFWG}(a_1, a_2, a_3, a_4) = [0.4441, 0.6812] \cdot e^{j0.42\pi}$  (see Example 1).

**Theorem 10.** Let  $a_i$  ( $i = 1, 2, \dots, n$ ) be a collection of CFVs, CFOWP weights be  $w_i \in [0, 1]$  ( $i = 1, 2, \dots, n$ ), and  $\sum_{i=1}^n w_i = 1$ . Then, we have the following properties.

(1) (Idempotency) If  $a_i = a$  ( $i = 1, 2, \dots, n$ ), then

$$\text{IVCFOWG}(a_1, a_2, \dots, a_n) = a. \quad (35)$$

(2) (Amplitude monotonicity) If  $|a_i| \leq |b_i|$  ( $i = 1, 2, \dots, n$ ), then

$$\begin{aligned} & |\text{IVCFOWG}(a_1, a_2, \dots, a_n)| \\ & \leq |\text{IVCFOWG}(b_1, b_2, \dots, b_n)|. \end{aligned} \quad (36)$$

(3) (Amplitude boundedness)

$$r_1 \leq |\text{IVCFOWG}(a_1, a_2, \dots, a_n)| \leq r_2. \quad (37)$$

where  $r_1, r_2$  are two interval values:

$$\begin{aligned} r_1 &= \left[ \min_i \underline{r_{a_i}}, \min_i \overline{r_{a_i}} \right], \\ r_2 &= \left[ \max_i \underline{r_{a_i}}, \max_i \overline{r_{a_i}} \right]. \end{aligned} \quad (38)$$

*Proof.* The proof is similar to Theorem 6.  $\square$

**Theorem 11.** The IVCFOWG operator is reflectionally invariant and rotationally invariant.

*Proof.* The proof is similar to Theorems 7 and 8.



Note that the operator  $\otimes$  does not have the property of rotational invariance, but the IVCFWG and IVCFOWG operators defined based on  $\otimes$  operator have the property of rotational invariance.

Here, we investigate the aggregation operators based on special class of the IVCFVs, which belong to subsets of the upper-right quadrant of the complex unit disk. Let  $D_1 = \{e^{j\nu} \mid \nu \in [0, \pi/2]\}$ ; we consider the aggregation operator on  $\mathcal{J}^{[0,1]} \cdot D_1$ .

Let us consider the closeness of IVCFVs on  $\mathcal{J}^{[0,1]} \cdot D_1$  under the IVCFWG and IVCFOWG operations. For the IVCFWG operator, we have the following result.  $\square$

**Theorem 12.** Let  $z_1, z_2, \dots, z_n \in \mathcal{J}^{[0,1]} \cdot D_1$ . Then, the aggregated value

$$\text{IVCFWG}(z_1, z_2, \dots, z_n) \in \mathcal{J}^{[0,1]} \cdot D_1. \quad (39)$$

*Proof.* Denoting  $\text{IVCFWG}(z_1, z_2, \dots, z_n) = [t, \bar{t}] \cdot e^{j\nu}$ , from Theorem 5,  $[t, \bar{t}]$  is an interval value. Since  $\nu = \sum_{i=1}^n w_i \cdot \nu_{z_i}$  is a weighted arithmetic aggregation operator of real numbers on  $[0, \pi/2]$ , then we have  $\nu \in [0, \pi/2]$ . Thus,  $\text{IVCFWG}(z_1, z_2, \dots, z_n) \in \mathcal{J}^{[0,1]} \cdot D_1$ .

Similar to the above theorem, we have the following.  $\square$

**Theorem 13.** Let  $z_1, z_2, \dots, z_n \in \mathcal{J}^{[0,1]} \cdot D_1$ . Then, the aggregated value

$$\text{IVCFOWG}(z_1, z_2, \dots, z_n) \in \mathcal{J}^{[0,1]} \cdot D_1. \quad (40)$$

The above theorems show us that the IVCFWG and the IVCFOWG operators are close under values on  $\mathcal{J}^{[0,1]} \cdot D_1$ .

Consider other quadrants of the complex unit disk. Let

$$D_k = \left\{ z = e^{j\theta} \mid \theta \in \left[ \frac{(k-1)\pi}{2}, \frac{k\pi}{2} \right] \right\}, \quad (41)$$

for  $k = 1$  to 4.

Now, we discuss the closeness of the IVCFWG and the IVCFOWG operators on values of other quadrants of the complex unit disk. Plainly, we have the following.

**Theorem 14.** For any  $k \in \{1, 2, 3, 4\}$ , if  $z_1, z_2, \dots, z_n \in \mathcal{J}^{[0,1]} \cdot D_k$ , then we have

$$\begin{aligned} \text{IVCFWG}(z_1, z_2, \dots, z_n) &\in \mathcal{J}^{[0,1]} \cdot D_k, \\ \text{IVCFOWG}(z_1, z_2, \dots, z_n) &\in \mathcal{J}^{[0,1]} \cdot D_k. \end{aligned} \quad (42)$$

*Proof.* Similar to Theorem 12.  $\square$

## 5. An Approach to Decision Making with the IVCFWG Operator

In this section, we present an approach using the IVCFWG operator to a decision making with interval-valued complex fuzzy information.

We consider a target selection application of CFSs. Assume that our position is fixed, and then we can measure the distance and angle of the possible alternatives by using a

position sensor and an angular sensor (or other attributes from expert opinions). Assume that we get a measurement  $(d \pm \epsilon, q)$ . Here, we use an interval value  $[\underline{d}, \bar{d}]$  to represent  $d \pm \epsilon$  by setting  $\underline{d} = d - \epsilon$  and  $\bar{d} = d + \epsilon$ . To improve the target location accuracy, we repeatedly measure the alternatives. Then, the target is selected in the following approach according to aggregation theory.

Let  $x_i (i = 1, 2, \dots, n)$  be the possible alternatives and  $e_k (k = 1, 2, \dots, m)$  be the experts. Then, the decision maker provides a decision matrix  $A = (a_{ik})_{n \times m}$ , where  $a_{ik}$  is an interval-valued complex fuzzy value given by the expert  $e_k$  for alternative  $x_i$ . Further, assume that  $w = (w_1, w_2, \dots, w_n)^T$  is the weight vector of the different experts such that  $w_i \geq 0 (i = 1, 2, \dots, n)$  and  $\sum_{i=1}^n w_i = 1$ . The process can be summarized as follows:

*Step 1.* Transform the decision matrix  $A$  into the normalized interval-valued complex fuzzy decision matrix  $C = (c_{ik})_{n \times m}$  using  $c_{ik} = a_{ik}/d$  where  $d = \max_{ik} |a_{ik}|$ .

*Step 2.* Aggregate all the interval-valued complex fuzzy values  $a_{ik} (k = 1, 2, \dots, m)$  and get the overall interval-valued complex fuzzy value  $b_i$  corresponding to the alternative  $x_i$  by the IVCFWG operator,  $b_i = \text{IVCFWG}(a_{i1}, a_{i2}, \dots, a_{im})$ .

*Step 3.* Rank the overall IVCFVs  $b_i (i = 1, 2, \dots, n)$  using (2).

Next, we give an example to illustrate the above approach.

*Example 3.* Suppose we want to go to the nearest bank, then we often use GPS navigation system or ask strangers for directions.

Suppose that there are three alternatives  $x_i (i = 1, 2, 3)$  and three experts (GPS or stranger)  $e_i (i = 1, 2, 3)$  with the weight vector  $(0.4, 0.3, 0.3)^T$ . The three experts evaluate the three alternatives under the IVCFS environment, and their corresponding rating values are summarized in the decision matrix  $C = (c_{ik})_{3 \times 3}$  represented in Table 1, where  $c_{ik} = r_{ik} \cdot e^{j\nu_{ik}\pi}$  is an interval-valued complex fuzzy value,  $[r_{ik}, \bar{r}_{ik}]$  represents the distance between  $r_{ik}$  km and  $\bar{r}_{ik}$  km, and  $\nu_{ik}$  represents the direction for the alternative  $x_i$ .

*Step 1.* The values  $c_{ik}$  do not need normalization.

*Step 2.* Aggregate the interval-valued complex fuzzy values  $b_i$  of the alternatives  $x_i$  by using the IVCFWG operator (see equation (20)):

$$\begin{aligned} \prod_{i=1}^3 r_{a_{1i}}^{w_i} &= 0.19^{0.4} \cdot 0.11^{0.3} \cdot 0.16^{0.3} = 0.1532, \\ \prod_{i=1}^3 \bar{r}_{a_{1i}}^{w_i} &= 0.25^{0.4} \cdot 0.23^{0.3} \cdot 0.23^{0.3} = 0.2378, \\ \sum_{i=1}^3 w_i \nu_{a_{1i}} &= (0.4 \cdot 0.11 + 0.3 \cdot 0.13 + 0.3 \cdot 0.11) \cdot \pi \\ &= 0.116\pi, \end{aligned} \quad (43)$$



TABLE 1: Decision matrix.

	$e_1$	$e_2$	$e_3$
$x_1$	$[0.19, 0.25] \cdot e^{j0.11\pi}$	$[0.11, 0.23] \cdot e^{j0.13\pi}$	$[0.16, 0.23] \cdot e^{j0.11\pi}$
$x_2$	$[0.12, 0.23] \cdot e^{j0.52\pi}$	$[0.18, 0.24] \cdot e^{j0.54\pi}$	$[0.18, 0.20] \cdot e^{j0.52\pi}$
$x_3$	$[0.10, 0.16] \cdot e^{j1.11\pi}$	$[0.19, 0.23] \cdot e^{j1.12\pi}$	$[0.17, 0.19] \cdot e^{j1.14\pi}$

and we obtain  $b_1 = \text{IVCFWG}(a_{11}, a_{12}, a_{13}) = [0.1532, 0.2378] \cdot e^{j0.116\pi}$ .

$$\begin{aligned} \prod_{i=1}^3 r_{a_{2i}}^{w_i} &= 0.12^{0.4} \cdot 0.18^{0.3} \cdot 0.18^{0.3} = 0.1531, \\ \prod_{i=1}^3 \overline{r_{a_{2i}}^{w_i}} &= 0.23^{0.4} \cdot 0.24^{0.3} \cdot 0.2^{0.3} = 0.2234, \\ \sum_{i=1}^3 w_i \gamma_{a_{2i}} &= (0.4 \cdot 0.52 + 0.3 \cdot 0.54 + 0.3 \cdot 0.52) \cdot \pi \\ &= 0.526\pi, \end{aligned} \quad (44)$$

and we obtain  $b_2 = \text{IVCFWG}(a_{11}, a_{12}, a_{13}) = [0.1531, 0.2234] \cdot e^{j0.126\pi}$ .

$$\begin{aligned} \prod_{i=1}^3 r_{a_{3i}}^{w_i} &= 0.1^{0.4} \cdot 0.19^{0.3} \cdot 0.17^{0.3} = 0.1422, \\ \prod_{i=1}^3 \overline{r_{a_{3i}}^{w_i}} &= 0.16^{0.4} \cdot 0.23^{0.3} \cdot 0.19^{0.3} = 0.1878, \\ \sum_{i=1}^3 w_i \gamma_{a_{3i}} &= (0.4 \cdot 1.11 + 0.3 \cdot 1.12 + 0.3 \cdot 1.14) \cdot \pi \\ &= 1.122\pi, \end{aligned} \quad (45)$$

and we obtain  $b_3 = \text{IVCFWG}(a_{11}, a_{12}, a_{13}) = [0.1422, 0.1878] \cdot e^{j0.122\pi}$ .

*Step 3.* Rank the interval-valued complex fuzzy values  $b_i$  ( $i = 1, 2, 3$ ):  $|b_1| > |b_2| > |b_3|$ , which shows that the alternative  $x_3$  is the optimal choice, i.e., the nearest bank.

An IVCFs is a generalization of complex fuzzy sets (CFS), interval-valued fuzzy sets (IVFS), and fuzzy sets (FS). IVCFs can handle two-dimensional information in a single set. Then, IVCFs contains much more information than CFS, IVFS, and FS.

It is revealed from the present study that the aggregation operators under IVFSs and FSs [5, 6] are the special cases of the proposed aggregation operators. Thus, the proposed aggregation operators can be equivalently utilized to solve the DM problem under these existing environments by setting phase term to be zero while the existing operators [5, 6] are unable to solve the problems under the IVCFs environment considered in the present paper. Thus, interval-valued complex fuzzy aggregation operators are more general than some (interval-valued) fuzzy aggregation operators.

## 6. Conclusion

As mentioned in [50], the basic feature of aggregation operators is their monotonicity property. However, aggregation operators under the complex fuzzy environment [40] are not monotone. Interestingly, such aggregation operators can explain some phenomena in our real life.

In this paper, we discussed the geometric aggregation operators under the interval-valued complex fuzzy environment. Two interval-valued complex fuzzy aggregation operators, the IVCFWG and the IVCFOG operators, are developed and their properties are studied. It is also interesting to note that both the IVCFWG and the IVCFOG operators are rotationally invariant and reflectionally invariant. Further, based on the proposed operators, we presented a decision-making approach under interval-valued complex fuzzy information. An illustrative example is given for illustrating the proposed approach.

It was observed that the aggregation operator based on nonadditive integrals (Choquet [51] and Sugeno integrals [52]) is one of the hot topics in this field [49]. As future work, we can consider the complex fuzzy aggregation operators based on complex integrals.

## Data Availability

The data used to support the findings of this study are included in the article.

## Conflicts of Interest

The authors declare that they have no conflicts of interest.

## Acknowledgments

This research was funded by the Open Foundation of Guangxi Colleges and Universities Key Laboratory of Complex System Optimization and Big Data Processing (grant no. 2017CSOBDP0103).

## References

- [1] R. R. Yager, "On ordered weighted averaging aggregation operators in multicriteria decisionmaking," *IEEE Transactions on Systems, Man, and Cybernetics*, vol. 18, no. 1, pp. 183–190, 1988.
- [2] R. R. Yager, "The power average operator," *IEEE Transactions on Systems, Man, and Cybernetics-Part A: Systems and Humans*, vol. 31, no. 6, pp. 724–731, 2001.
- [3] Z. S. Xu and R. R. Yager, "Power geometric operators and their use in group decision making," *IEEE Transactions on Fuzzy Systems*, vol. 18, pp. 94–105, 2010.
- [4] L. Zhou, H. Chen, and J. Liu, "Generalized power aggregation operators and their applications in group decision making," *Computers & Industrial Engineering*, vol. 62, no. 4, pp. 989–999, 2012.
- [5] Z. S. Xu, "Intuitionistic fuzzy aggregation operators," *IEEE Transactions on Fuzzy Systems*, vol. 15, no. 6, pp. 1179–1187, 2007.

- [6] Z. Xu and R. R. Yager, "Some geometric aggregation operators based on intuitionistic fuzzy sets," *International Journal of General Systems*, vol. 35, no. 4, pp. 417–433, 2006.
- [7] Z. S. Xu, *Intuitionistic Fuzzy Aggregation and Clustering*, Springer, Berlin, Germany, 2013.
- [8] Z. Xu, "Approaches to multiple attribute group decision making based on intuitionistic fuzzy power aggregation operators," *Knowledge-Based Systems*, vol. 24, no. 6, pp. 749–760, 2011.
- [9] P. Liu and Y. Wang, "Multiple attribute group decision making methods based on intuitionistic linguistic power generalized aggregation operators," *Applied Soft Computing*, vol. 17, pp. 90–104, 2014.
- [10] P. Liu, "Some Hamacher aggregation operators based on the interval-valued intuitionistic fuzzy numbers and their application to group decision making," *IEEE Transactions on Fuzzy Systems*, vol. 22, no. 1, pp. 83–97, 2014.
- [11] P. Liu, "Multiple attribute decision-making methods based on normal intuitionistic fuzzy interaction aggregation operators," *Symmetry*, vol. 9, no. 11, p. 261, 2017.
- [12] D. Yu, Y. Wu, and T. Lu, "Interval-valued intuitionistic fuzzy prioritized operators and their application in group decision making," *Knowledge-Based Systems*, vol. 30, pp. 57–66, 2012.
- [13] P. Liu, "Multiple attribute group decision making method based on interval-valued intuitionistic fuzzy power Heronian aggregation operators," *Computers & Industrial Engineering*, vol. 108, pp. 199–212, 2017.
- [14] P. Liu and H. Li, "Interval-valued intuitionistic fuzzy power Bonferroni aggregation operators and their application to group decision making," *Cognitive Computation*, vol. 9, no. 4, pp. 494–512, 2017.
- [15] S. Zeng, Z. Mu, and T. Baležentis, "A novel aggregation method for Pythagorean fuzzy multiple attribute group decision making," *International Journal of Intelligent Systems*, vol. 33, no. 3, pp. 573–585, 2018.
- [16] X. Zhang, "A novel approach based on similarity measure for Pythagorean fuzzy multiple criteria group decision making," *International Journal of Intelligent Systems*, vol. 31, no. 6, pp. 593–611, 2016.
- [17] H. Garg, "A new generalized pythagorean fuzzy information aggregation using einstein operations and its application to decision making," *International Journal of Intelligent Systems*, vol. 31, no. 9, pp. 886–920, 2016.
- [18] J. Ye, "A multicriteria decision-making method using aggregation operators for simplified neutrosophic sets," *Journal of Intelligent & Fuzzy Systems*, vol. 26, no. 5, pp. 2459–2466, 2014.
- [19] A. Tu, J. Ye, and B. Wang, "Multiple attribute decision-making method using similarity measures of neutrosophic cubic sets," *Symmetry*, vol. 10, no. 6, p. 215, 2018.
- [20] A. Tu, J. Ye, and B. Wang, "Symmetry measures of simplified neutrosophic sets for multiple attribute decision-making problems," *Symmetry*, vol. 10, no. 5, p. 144, 2018.
- [21] M. Xia and Z. Xu, "Hesitant fuzzy information aggregation in decision making," *International Journal of Approximate Reasoning*, vol. 52, no. 3, pp. 395–407, 2011.
- [22] B. Zhu, Z. Xu, and M. Xia, "Hesitant fuzzy geometric Bonferroni means," *Information Sciences*, vol. 205, pp. 72–85, 2012.
- [23] C. Song, Z. Xu, and H. Zhao, "A novel comparison of probabilistic hesitant fuzzy elements in multi-criteria decision making," *Symmetry*, vol. 10, no. 177, 2018.
- [24] F. Amin, A. Fahmi, S. Abdullah, A. Ali, R. Ahmed, and F. Ghani, "Triangular cubic linguistic hesitant fuzzy aggregation operators and their application in group decision making," *Journal of Intelligent and Fuzzy System*, vol. 34, no. 4, pp. 2401–2416, 2018.
- [25] A. Fahmi, S. Abdullah, F. Amin, A. Ali, and W. A. Khan, "Some geometric operators with triangular cubic linguistic hesitant fuzzy number and their application in group decision-making," *Journal of Intelligent and Fuzzy Systems*, vol. 35, no. 2, pp. 2485–2499, 2018.
- [26] L. A. Zadeh, "Fuzzy sets," *Information and Control*, vol. 8, no. 3, pp. 338–353, 1965.
- [27] D. Ramot, R. Milo, M. Friedman, and A. Kandel, "Complex fuzzy sets," *IEEE Transactions on Fuzzy Systems*, vol. 10, no. 2, pp. 171–186, 2002.
- [28] S. Dick, "Toward complex fuzzy logic," *IEEE Transactions on Fuzzy Systems*, vol. 13, no. 3, pp. 405–414, 2005.
- [29] S. Dai, "A generalization of rotational invariance for complex fuzzy operations," *IEEE Transactions on Fuzzy Systems*, p. 1, 2020.
- [30] S. Dai, "Comment on 'toward complex fuzzy logic'," *IEEE Transactions on Fuzzy Systems*, p. 1, 2019.
- [31] S. Dai, "Complex fuzzy ordered weighted distance measures," *Iranian Journal of Fuzzy Systems*, 2020.
- [32] D. Ramot, M. Friedman, G. Langholz, and A. Kandel, "Complex fuzzy logic," *IEEE Transactions on Fuzzy Systems*, vol. 11, no. 4, pp. 450–461, 2003.
- [33] B. Hu, L. Bi, and S. Dai, "The orthogonality between complex fuzzy sets and its application to signal detection," *Symmetry*, vol. 9, no. 175, 2017.
- [34] L. Bi, B. Hu, S. Li, and S. Dai, "The parallelity of complex fuzzy sets and parallelity preserving operators," *Journal of Intelligent & Fuzzy Systems*, vol. 34, no. 6, pp. 4173–4180, 2018.
- [35] L. Bi, Z. Zeng, B. Hu, and S. Dai, "Two classes of entropy measures for complex fuzzy sets," *Mathematics*, vol. 7, no. 96, 2019.
- [36] G. Zhang, T. S. Dillon, K.-Y. Cai, J. Ma, and J. Lu, "Operation properties and," *International Journal of Approximate Reasoning*, vol. 50, no. 8, pp. 1227–1249, 2009.
- [37] A. U. M. Alkouri and A. R. Salleh, "Linguistic variables, hedges and several distances on complex fuzzy sets," *Journal of Intelligent & Fuzzy Systems*, vol. 26, no. 5, pp. 2527–2535, 2014.
- [38] J. Ma, G. Zhang, and J. Lu, "A method for multiple periodic factor prediction problems using complex fuzzy sets," *IEEE Transactions on Fuzzy Systems*, vol. 20, pp. 32–45, 2012.
- [39] L. Bi, S. Dai, and B. Hu, "Complex fuzzy geometric aggregation operators," *Symmetry*, vol. 10, p. 251, 2018.
- [40] L. Bi, S. Dai, B. Hu, and S. Li, "Complex fuzzy arithmetic aggregation operators," *Journal of Intelligent & Fuzzy Systems*, vol. 36, pp. 2765–2771, 2019.
- [41] S. Greenfield, F. Chiclana, and S. Dick, "Interval-valued complex fuzzy logic," in *Proceedings of the 2016 IEEE International Conference on Fuzzy Systems (FUZZ-IEEE)*, pp. 2014–2019, Melbourne, Australia, December 2016.
- [42] S. Greenfield, F. Chiclana, and S. Dick, "Join and meet operations for interval-valued complex fuzzy logic," in *Proceedings of the 2016 Annual Conference of the North American Fuzzy Information Processing Society (NAFIPS)*, pp. 1–5, El Paso, TX, USA, October 2016.
- [43] A. Alkouri and A. Salleh, "Complex intuitionistic fuzzy sets," in *Proceedings of the International Conference on Fundamental and Applied Sciences (ICFAS 2012)*, pp. 464–470, Kuala Lumpur, Malaysia, June 2012.
- [44] D. Rani and H. Garg, "Complex intuitionistic fuzzy power aggregation operators and their applications in multicriteria

- decision-making,” *Expert Systems*, vol. 35, no. 6, Article ID e12325, 2018.
- [45] H. Garg and D. Rani, “Some generalized complex intuitionistic fuzzy aggregation operators and their application to multicriteria decision-making process,” *Arabian Journal for Science and Engineering*, vol. 44, pp. 2679–2698, 2019.
  - [46] O. Kosheleva, V. Kreinovich, and T. Ngamsantivong, “Why complex-valued fuzzy? Why complex values in general? a computational explanation,” in *Proceedings of the 2013 Joint IFSA World Congress and NAFIPS Annual Meeting (IFSA/NAFIPS)*, pp. 1233–1236, Edmonton, Canada, June 2013.
  - [47] S. Dai, L. Bi, and B. Hu, “Distance measures between the interval-valued complex fuzzy sets,” *Mathematics*, vol. 7, p. 549, 2019.
  - [48] E. P. Klement, R. Mesiar, and E. Pap, *Triangular Norms*, Kluwer Academic Publishers, Dordrecht, Netherlands, 2000.
  - [49] M. Grabisch, J. L. Marichal, R. Mesiar, and E. Pap, *Aggregation Functions*, Cambridge University Press, Cambridge, UK, 2009.
  - [50] M. Grabisch, J. L. Marichal, R. Mesiar, and E. Pap, “Aggregation functions: means,” *Information Sciences*, vol. 181, pp. 1–22, 2011.
  - [51] G. Choquet, “Theory of capacities,” *Annales de l’institut Fourier*, vol. 5, pp. 131–295, 1954.
  - [52] M. Sugeno, *Theory of fuzzy integrals and its applications*, PhD thesis, Tokyo Institute of Technology, Tokyo, Japan, 1974.

## Research Article

# An Approach for Resilient-Green Supplier Selection Based on WASPAS, BWM, and TOPSIS under Intuitionistic Fuzzy Sets

Lei Xiong,<sup>1</sup> Shuqi Zhong,<sup>2</sup> Sen Liu ,<sup>3</sup> Xiao Zhang,<sup>4</sup> and Yanfeng Li <sup>5</sup>

<sup>1</sup>School of Economics and Management, Yunnan Normal University, Kunming 650500, Yunnan, China

<sup>2</sup>International Business School, Yunnan University of Finance and Economics, Kunming 650221, China

<sup>3</sup>School of Logistics, Yunnan University of Finance and Economics, Kunming 650221, China

<sup>4</sup>School of International Trade and Economics, University of International Business and Economic, Beijing 100029, China

<sup>5</sup>Business School, Yunnan University of Business Management, Kunming 650106, China

Correspondence should be addressed to Yanfeng Li; [lyf@ynufe.edu.cn](mailto:lyf@ynufe.edu.cn)

Received 23 February 2020; Revised 12 May 2020; Accepted 18 May 2020; Published 22 July 2020

Guest Editor: Zaoli Yang

Copyright © 2020 Lei Xiong et al. This is an open access article distributed under the Creative Commons Attribution License, which permits unrestricted use, distribution, and reproduction in any medium, provided the original work is properly cited.

The green supply chain management (GSCM) is an enterprise's effort to protect the environment and a key way to achieve sustainable environmental development. On the contrary, globalization brings more risks to the supply chain. Resilience has become a critical definition in supply chain management to help enterprises review the disruption and return to normal state. Therefore, choosing a resilient-green supplier to build a supply chain environment with flexibility and greenness under interruption becomes necessary for research works. However, the existing studies tended to focus on only one of the factors with resilience and greenness, and no comprehensive criteria system and performance value is expressed by a crisp number. Therefore, this paper proposes a hybrid method which integrates the Best-Worst method (BWM), Weighted Aggregated Sum-Product Assessment (WASPAS), and Technique for Order Preference by Similarity to Ideal Solution (TOPSIS) to solve the critical problems. Firstly, BWM is used to weigh the criteria; secondly, intuitionistic fuzzy numbers are introduced into the ranking stage. Then, the integrated WASPAS and TOPSIS are used to rank the alternatives to select the optimal resilient-green supplier. Finally, an illustrative example proves the feasibility of this method.

## 1. Introduction

With the environment adverse changes, green supply chain management (GSCM) emerged as the times when enterprises and products needed to adapt to the characteristic of resource-efficient and environment-friendly. GSCM required collaboration between the upstream and downstream enterprises in the supply chain, integrating efficient and green concepts into key nodes of product design, production, packaging, transportation, marketing, and recycling [1]. Core enterprises should be responsible not only for their own actions but also for the negative environmental impact of upstream and downstream enterprises. Therefore, the supplier selection has become the key issue of green supply chain coordination [2]. It is also a critical way for enterprises to gain competitiveness under the environment-friendly trend and policy.

Due to the globalization of the supply chain, logistics and information flow are facing the fluctuation risk brought by the disruptions, which are mainly caused by the natural disasters, man-made disasters, and technological threats. GSCM was confronted with similar problems. How to simultaneously weaken the impact of the supply chain on the environment and improve the ability to respond to disruptions has become a critical issue to be solved urgently in the supply chain management. Integrating resilient practice into the green supply chain can deal with the disaster-related uncertainty, reduce the quality fluctuation in green raw materials, and effectively avoid the logistics interruption in product transportation, marketing, and recycling.

Therefore, it is a new challenge for managers to construct the supply chain that can operate in the environment of green policy and respond to the disruptions in time when disasters occur. In the resilient-GSCM, the supplier selection

is the key way to achieve the goal. At present, the relationship between the resilience and green was established in supply chain management [3–5]. Several research studies have also discussed the resilient supplier selection [6–10] and green supplier selection [1, 11–14]. However, few studies considered both the resilience and greenness factors in supplier selection problems. Thus, a decision-making method was proposed for selecting suppliers that can take both environmental problems and disruption risks for further research studies into account.

Supplier selection is a typical multicriteria group decision-making (MCGDM) problems. The MCGDM always consists of three research fields [15, 16]: expert weighting methods, criteria weighting methods, and aggregation operators. The studies of expert weighting methods and criteria weighting methods are mainly concentrating on the computation of the weights of the experts and criteria and which are often obtained by decision makers directly based on experiences and preferences [17] or worked out by the decision matrix [18–20]. The aggregation operators are mainly focused on the conversion process of the collective decision matrix to the integrated evaluate values of alternatives with the weights of the experts and criteria in various aggregation methods [21, 22], and then rank the alternatives. Scholars usually focus on one or two fields in MCGDM, and few studies researched these all three ways simultaneously in one article due to the huge amount of work, for example, some research studies only focus on criteria weighting methods [23, 24] or aggregation operators [21, 25]. Wu et al. [26] focus on both experts and criteria weighting methods. Zavadskas et al. [27] discussed the optimization of criteria weighting and aggregation operator.

Through literature review, it was found that there were several limitations in terms of the resilient-green supplier selection. Firstly, few studies focused on the resilient-green supplier selection. According to the green manufacturing process and resilience-related characteristics, the resilience-greenness criteria system was constructed; secondly, the language terms used in many MCGDM problems were not in line with the expression habits of decision makers and reduced the accuracy of decision-making process; thirdly, the traditional weighting methods (such as AHP) of MCGDM had more steps to compare, so the calculation process was more complicated; lastly, the single MCGDM method made the alternatives' ranking inaccurate and inconsistent.

Therefore, in order to fill the research gap, a novel method, which integrated WASPAS, BWM, and TOPSIS based on intuitionistic fuzzy numbers, was proposed to select the resilient-green supplier under the supply chain environment. The reasons of why we integrate these techniques in our method are mainly based on the following three ways. (1) Compared with triangle fuzzy number and trapezoid fuzzy number (only can represent one grade of membership that is crisp in the unit interval), intuitionistic fuzzy number can reflect more grades of membership, that is, membership degree, nonmembership degree, and hesitation degree [28]. The hesitation degree represents the definition of “neither this nor that” [29]. Intuitionistic

fuzziness has more advantages in reflecting fuzziness and uncertainty in the decision matrix. Therefore, our research is conducted in the intuitionistic fuzzy environment. (2) BWM simplifies the calculation steps, and the weighting results are more consistent than the traditional AHP [30]. Therefore, BWM is selected as the method of criteria weighting in this study. The integrated WASPAS and TOPSIS methods make up for the instability of traditional WASPAS due to the change of parameter value, improving the accuracy and certainty of decision results [31]. Hence, we integrate BWM, WASPAS, and TOPSIS techniques to become a new MCGDM approach, which has advantages that a single classical approach does not. (3) As mentioned above, the research of MCGDM is mainly divided into three aspects, and few studies researched these entire three ways at the same time in one article due to the amount of work. In this study, we focus on the improvement of criteria weighting process, and the aggregation operators are not our focus. Hence, through literature review, we find that the intuitionistic Fuzzy Weighted Averaging (IFWA) and Intuitionistic Fuzzy Ordered Weighted Averaging (IFOWA) proposed by Xu [32] are applicable to different situations with intuitionistic fuzzy sets. Besides, IFWA is more appropriate for the research of the weighting methods for criteria in intuitionistic fuzzy sets [33]. Hence, we choose IFWA operator [32] as the aggregation operator to aggregate the decision information in this study, due to the advantages of logical [34, 35], easy to operate [36], and highly recognized [33, 37].

This paper consists of seven parts. Section 1 is an introduction, Section 2 presents the literature review, and the construction of the criteria system appears in Section 3. Section 4 introduces some basic definitions about the decision method. In Section 5, a hybrid MCGDM method is proposed, and the feasibility of the method is verified by an illustrative example in Section 7. Finally, the conclusion of the whole paper is presented in Section 8.

## 2. Literature Review

GSCM was part of the efforts of organizations and researchers to respond to environmental awareness and sustainable development policies [13]. The implementation of GSCM could protect the environment, save resources, and enhance the competitiveness of supply chain enterprises. Therefore, GSCM has become a more popular definition.

With the increase of public awareness and pressure from the governments, researchers paid more attention on the GSCM and much related works have been performed. For example, Handfield et al. [38] defined GSCM for the first time, incorporating environmental factors into customer orders cycle for design, procurement, manufacturing, assembly, packaging, logistics, and distribution activities. Zhu et al. [39] improved the definition and put forward that the purpose of implementing green supply chain was to help enterprises obtain profits and market share. After that scholars mainly defined the GSCM from the aspects of green practices and principles, emphasizing the integration of environmental dimension/issues into supply chain

management in order to achieve environmental performance [40–44] and involving a series of green measures throughout the product's life cycle, including product design, material selection and procurement, manufacturing process, delivery of the final products, marketing, reverse logistics, and end-of-life management [45–50]. In the past two decades, many studies have focused on the green supplier evaluation and selection. Handfield et al. [51] introduced environmental factors into the supplier evaluation criteria and calculated them with the analytic hierarchy process (AHP). Tsai and Hung [52] constructed an evaluation model from the perspective of performance to help enterprises manage and monitor green supply chain. Akman [53] clustered suppliers according to criteria-delivery, quality, cost, and service by c-means clustering method and finally used VIKOR to rank the green suppliers. Lo et al. [12] constructed the criteria system of performance, environmental protection, and risk, combining MCGDM and FMOLP to solve the problem of green supplier selection and order allocation. Peng et al. [54] established evaluation criteria from three aspects of economy, environment, and society, determined the criteria weight in the picture fuzzy environment, and selected more sustainable suppliers.

Global supply chains enabling the interrelated business activities were handled around the world in a decentralized way; thus, enterprises could reduce the production costs and achieve profits by finding competitive partners [55]. In the globalization environment, natural disasters (floods and earthquakes), man-made disasters (fires, traffic accidents, and terrorist attacks), and technological threats (technology leaks) would lead to the fluctuation and interruption in supply chains [56–58]. Increasing supply chain resilient practice and choosing more resilient suppliers were effective ways to avoid the interruption. Holling [59] first proposed the concept of resilience and pointed out it was the special ability to absorb change. With the application of resilience in the supply chain, the resilient supply chain emerged as a new concept [60]. Ponomarov and Holcomb [61] defined it as “the adaptive capability of the supply chain to prepare for unexpected events, respond to disruptions, and function.” Other definition focused on the ability of enterprises to recover normal operation after interruption [62, 63]. At present, resilience could be improved from two aspects: (1) improving the supply chain (e.g., creating redundancies, increasing flexibility, and changing the corporate culture) [64] and (2) selecting resilient supplier (before, during, and after disruption) [8]. Parkouhi and Ghadikolaei [10] used the grey VIKOR method to evaluate the rating of resilient suppliers by referring to the opinions of paper industry experts, and the criteria system was constructed from four dimensions of the benefits, opportunities, costs, and risks. Rajesh and Ravi [65] determined the criteria and its sub-criteria from five aspects: primary performance factors, responsiveness, risk deduction, technical support, and sustainability, then ranked resilient suppliers with the grey relational analysis method.

In the field of supply chain management, resilience and greenness have already been linked. Azevedo et al. [66] took the automobile enterprises and supply chain as the research

background by using the integrated assessment model to evaluate the greenness and resilience index. The results showed that enhancing resilience was conducive to improve the supply chain competitiveness, while green practice mainly affected the environment. Sonia et al. [67] designed the supply chain by integrating the ecologically sustainability and resilience based on the carbon footprint and emission, via the usage of the fuzzy AHP, TOPSIS, and multiobjective optimization method. Fahimnia and Jabbarzadeh [68] constructed a novel multiobjective optimization model and discussed the relationship between the sustainability and resilience at the level of supply chain design. Based on the research studies of drug supply chain design, Zahiri et al. [69] proposed a new stochastic fuzzy goal programming for the problem of model uncertainty and case analysis of the Truvada supply chain in the French LGBTQ community. Mohammed et al. [4] proposed a fuzzy multiobjective programming model to achieve a resilient and green supply chain design approach, which could reduce the supply chain costs and environmental impact and, moreover, extend the value of resilience. Yavari and Zaker [5] proposed a comprehensive model of the two-layered network structure to improve the design in the resilient-green closed-loop supply chain for the power network interruption to the perishable product supply chain and ultimately expected to achieve low cost and low carbon emissions in the supply chain. However, the concept of resilient green was often used for supply chain design in different industries, with only few relevant research studies for supplier selection. As the main external risk, the supplier selection with the scientific decision-making method could effectively improve the supply chain. The disruption would hinder the green development goal, and the relevant research on resilient-green supply chain is essential.

The supplier selection belonged to the category of multicriteria group decision-making (MCGDM) problem, which was usually divided into multiattribute group decision-making (MAGDM) (solution space is discrete) and multiobjective decision-making (MODM) (solution space is continuous) [70]. MAGDM as a classic solution, included TOPSIS [71], AHP [72], Analytic Network Process (ANP) [73], VIKOR [74], BWM [30], Weighted Aggregated Sum-Product Assessment (WASPAS) [75], the decision-making trial and evaluation laboratory (DEMATEL), preference ranking organization method for enrichment evaluation (PROM-ETHEE), and the elimination and choice translating reality (ELECTRE) [76].

The recent existing studies about resilient-green supplier selection methods mainly focused on three aspects. (1) MCGDM-based methods: the comprehensive ranking of suppliers was obtained by evaluating multiple criteria of several alternatives. Common MCGDM methods included TOPSIS [77, 78], VIKOR [79], AHP [80], BWM [78], WASPAS [81], and DEMATEL [82]. (2) Artificial intelligence (AI)-based methods: this method could simulate the decision-making behavior of experts accurately by analyzing a large amount of past data through computer programs, including neural network method [83], case-based reasoning, and genetic algorithm [84]. (3) Hybrid methods: these



methods supported experts to integrate any of the two methods, so as to make up for the shortcomings of the single method. For example, fuzzy BWM-VIKOR [26], fuzzy AHP-TOPSIS [85], fuzzy Entropy-TOPSIS [14], BWM-DEMATEL-TOPSIS [86], and MABAC-ELECTRE [55]. The comparison of this study with previous studies on dimensions and approaches are shown in Table 1.

Literatures review showed that there were still some limitations in the resilient-green supplier selection. (1) Resilience and greenness have been linked in the application of the supply chain. Scholars also considered that the links could promote the supply chain sustainability. However, most of the existing research studies focused on the supply chain design and lacked relevant literature to improve the resilient-green supply chain from the perspective of supplier selection. As the main source of supply chain external conflict, choosing the resilient-green supplier scientifically has become a necessary research object. (2) Decision makers' opinions were difficult to express accurately with language, which affected the accuracy of criteria weighting and alternatives ranking. (3) The single MCGDM method was difficult to improve the alternatives ranking and could not work out the consistency of result.

Therefore, a criteria system for the resilient-green supplier selection based on the literature review of the green/resilient supply chain was proposed in order to fill the research gap, which integrated BWM, WASPAS, and TOPSIS into the proposed method. BWM was used in the process of weighting the criteria weight as a foolproof method. The TOPSIS method was integrated into WASPAS with intuitionistic fuzzy sets to make the final alternative as close as possible to the positive ideal solution (PIS). Finally, the novel method's effectiveness was verified by an example.

### 3. The Criteria of Resilient-Green Supplier Selection

The number of studies on green supplier selection was increasing [1, 4, 12, 13, 81]. However, the previous research studies ignored the green supplier selection under the disruption environment. At present, the government's requirements for environmental protection continue to spread to various industries. The supply chain exhibits a global trend, and it is increasingly important to develop effective measures to prevent the disruption of natural disasters. In this case, construction of the criteria system for resilient-green supplier selection becomes a critical branch in supplier selection.

From the perspective of integrating production process and green supply chain practices [88], the green supplier selection criteria were proposed. Green products production mainly includes design, raw material procurement, manufacturing, distribution, marketing, recycling, life cycle management, and other processes. According to practices related to each process, it is believed that the following factors should be considered. Eco-design (design) was recognized by many scholars as a prerequisite with the purpose of reducing the negative impact on the environment [89–91], which could determine the trend of greenness of

products. Green procurement (raw material procurement) reflects the environmental action taken by suppliers in response to the environmental protection [77]. The pollution production and green packing (manufacturing) are two processes in manufacturing. The control of harmful substance emissions can directly affect the greenness, while green packaging is related to the recycling logistics network. Green image (marketing), as an assessment of supplier's past efforts for environmental protection, has attracted the attention of many scholars [1, 11, 13]. Life cycle management refers to the supplier's management ability and level of each process in terms of the cost, energy use, and process design.

Considering disruption from the three aspects of before, during, and after is a comprehensive view. This paper discusses the capabilities that resilient supplier should have from the two dimensions of vulnerability and recovery to build selection metrics. Vulnerability emphasized the preparation of the system before the occurrence of disasters, and recovery referred to the absorption capacity of the system during the disaster and the recovery ability after the disaster [92, 93]. The four indicators were used to select the resilient suppliers according to [8], namely, surplus inventory (vulnerability), factory segregation (vulnerability), reliability (vulnerability), and reorganization (recovery).

In the process of building the criteria system, there is an interactive part of resilience and greenness. The criteria part as coincident criteria is proposed, which acts on the resilient-green supplier selection in three aspects. Table 2 provides a detailed description of the criteria, definition, and references of resilient-green supplier selection.

## 4. Preliminaries

### 4.1. Intuitionistic Fuzzy Set

*Definition 1* (see [101]). Let  $\tilde{a}$  be a fuzzy set in the universe of discourse  $X$ , and  $\mu_{\tilde{a}}$  is a membership function  $\mu_{\tilde{a}}: X \rightarrow [0, 1]$ , where  $\mu_{\tilde{a}}(x) \leq 1 \forall x$ . Fuzzy set can be represented in the following way:

$$\tilde{a} = \{ \langle x, \mu_{\tilde{a}}(x) \rangle : x \in X \}. \quad (1)$$

*Definition 2* (see [102]). Let  $\tilde{a}$  be an fuzzy set in the universe of discourse  $X$ , where  $\mu_{\tilde{a}}$  is a membership function  $\mu_{\tilde{a}}: X \rightarrow [0, 1]$ ,  $\nu_{\tilde{a}}$  is a nonmembership function  $\nu_{\tilde{a}}: X \rightarrow [0, 1]$ , and  $0 \leq \mu_{\tilde{a}} + \nu_{\tilde{a}} \leq 1$ . Intuitionistic fuzzy set can be represented in the following way:

$$\tilde{a} = \{ \langle x, \mu_{\tilde{a}}(x), \nu_{\tilde{a}}(x) \rangle : x \in X \}. \quad (2)$$

$\pi_{\tilde{a}}(x)$  is called the hesitancy degree of  $x$  to  $\tilde{a}$ , where  $0 \leq \pi_{\tilde{a}}(x) \leq 1$ . When  $\pi_{\tilde{a}}(x) = 0$ , the intuitionistic fuzzy set should turn into a traditional fuzzy set:

$$\pi_{\tilde{a}}(x) = 1 - \mu_{\tilde{a}}(x) - \nu_{\tilde{a}}(x). \quad (3)$$

*Definition 3* (see [102]). Let  $\tilde{a}$  and  $\tilde{b}$  be IFSs of the universe  $X$ , and the addition and multiplication of  $\tilde{a}$  and  $\tilde{b}$  are as follows:

TABLE 1: Comparison of this study with previous studies.

Literature	Dimensions		Approach	Theme
	Resilience	Greenness		
Kuo et al. [83]		✓	Artificial neural network (ANN) + data envelopment analysis (DEA) + analytic network process (ANP)	The integration results of the three methods are better than two other hybrid methods, ANN-DEA and ANP-DEA
Zouggari and Benyoucef [85]		✓	Fuzzy AHP + fuzzy TOPSIS	Solving order allocation problem with fuzzy TOPSIS
Hashemi et al. [87]		✓	Grey relational analysis (GRA) + analytic network process (ANP)	ANP improves the uncertainty in GRA
Hosseini and Khaled [8]	✓		Classification and regression tree (CART) + neural network (NN) + analytic hierarchy process (AHP)	Hybrid methods with different categories have better prediction resilience than single-category methods
Parkouhi and Ghadikolaei [10]	✓		Analytic network process (ANP) + VIKOR	Application of grey number and fuzzy set in model
Amindoust [56]	✓	✓	Assurance region DEA method (AR-DEA)	Combining sustainable criteria with resilient criteria in supplier selection
Demir et al. [79]		✓	VIKOR-based sorting method (VIKORSORT)	VIKORSORT can be used to sort green suppliers into the predefined ordered classes
Proposed method	✓	✓	BWM + fuzzy WASPAS + fuzzy TOPSIS	Introducing TOPSIS into ranking stage of WASPAS can improve the accuracy and consistency

TABLE 2: Criteria for resilient-green supplier selection.

Criteria of greenness	Definition	References
$G_1$ Eco-design	Product materials are easy to recycle and reuse, using as little material and energy as possible, thus reducing the impact on the environment	[14, 94]
$G_2$ Green procurement	Purchasers are trained to purchase raw materials in accordance with green principles (environmentally friendly and harmless), and purchasers can communicate with product designers in a timely manner	[78]
$G_3$ Pollution production	Air pollution, liquid waste, solid waste, and harmful materials produced per unit of products	[13, 95]
$G_4$ Green packing	Green packaging meets the 4R1D principle: reduce, reuse, reclaim, recycle and degradable	[96]
$G_5$ Green image	Ability to produce products in accordance with green principles and the proportion of consumers accepting green products	[1, 97]
$G_6$ Life cycle management	Management (cost control, process design, and energy use) of the green products life cycle including design, material selection, manufacturing, marketing, and logistics	[1]
<i>Criteria of resilience</i>		
$S_1$ Surplus inventory	Under the disruption environment, surplus inventory can make up for production interruption, which can effectively temporarily prevent supply chain breakdown	[8]
$S_2$ Factory segregation	Enterprises has scattered and spare factory, each factory has the same technical conditions and material reserves in order to make up for production activities quickly	[56]
$S_3$ Reliability	Establish good cooperative relationship with partners with recognition; enterprises can provide materials and services in time, accounts are clear and true, and disruption cost is known	[60]
$S_4$ Reorganization	Ability to integrate resources rapidly and reconstruct corporate culture and organization	[8]
<i>Coincident criteria</i>		
$O_1$ Logistics	Greenness: planning reasonable transport routes to reduce CO <sub>2</sub> emissions; setting up recycling logistics, realizing the packaging reuse, and scientifically integrating this route into delivery route; use of new-energy vehicles Resilience: change the delivery route and implement the mode of multimodal transport rapidly when the original route is impacted	[98, 99]
$O_2$ Warehousing	Greenness: building materials are environmentally friendly, recyclable, and do not release harmful gases; classified warehousing of different products, rational layout of warehousing space, and avoiding production circuitous transportation Resilience: the warehouse is made of antiseismic and sunscreen building materials to provide physical protection for products in the natural disasters	[100]
$O_3$ Cooperation commitment	Greenness: managers actively take green initiatives; signing environmental commitment among partners to form green supply chain upstream and downstream linkages Resilience: enterprises have scheduled backup suppliers and establish contract relationship with backup suppliers in time when interrupting cooperation with other suppliers	[14, 100]

$$\begin{aligned}\tilde{a} \oplus \tilde{b} &= \{ \langle \mu_{\tilde{a}}(x) + \mu_{\tilde{b}}(x) - \mu_{\tilde{a}}(x)\mu_{\tilde{b}}(x), \nu_{\tilde{a}}(x)\nu_{\tilde{b}}(x) \rangle : x \in X \}, \\ \tilde{a} \otimes \tilde{b} &= \{ \langle \mu_{\tilde{a}}(x)\mu_{\tilde{b}}(x), \nu_{\tilde{a}}(x) + \nu_{\tilde{b}}(x) - \nu_{\tilde{a}}(x)\nu_{\tilde{b}}(x) \rangle : x \in X \}.\end{aligned}\quad (4)$$

Let  $\lambda$  be a constant, and the algorithm for  $\tilde{a}$  is as follows:

$$\begin{aligned}\lambda \tilde{a} &= \{ \langle 1 - (1 - \mu_{\tilde{a}}(x))^\lambda, (\nu_{\tilde{a}}(x))^\lambda \rangle : x \in X \}, \\ \tilde{a}^\lambda &= \{ \langle (\mu_{\tilde{a}}(x))^\lambda, 1 - (1 - \nu_{\tilde{a}}(x))^\lambda \rangle : x \in X \}.\end{aligned}\quad (5)$$

**Definition 4.** Let  $\tilde{a}$  and  $\tilde{b}$  be IFSs of the universe  $X$ ;  $d(\tilde{a}, \tilde{b})$  represents the distance measure between  $\tilde{a}$  and  $\tilde{b}$ ;  $d(\tilde{a}, \tilde{b})$  must fulfil the following properties [103]:

- (i)  $d(\tilde{a}, \tilde{b}) \geq 0$
- (ii)  $d(\tilde{a}, \tilde{b}) = d(\tilde{b}, \tilde{a})$
- (iii)  $d(\tilde{a}, \tilde{b}) = 0$ , if and only if,  $\tilde{a} = \tilde{b}$
- (iv) If  $\tilde{a} \subseteq \tilde{b} \subseteq \tilde{c}$  then  $d(\tilde{a}, \tilde{c}) \geq d(\tilde{a}, \tilde{b})$  and  $d(\tilde{a}, \tilde{c}) \geq d(\tilde{b}, \tilde{c})$

Let  $\tilde{a} = \{ \langle x, \mu_{\tilde{a}}(x), \nu_{\tilde{a}}(x) \rangle : x \in X \}$  and  $\tilde{b} = \{ \langle x, \mu_{\tilde{b}}(x), \nu_{\tilde{b}}(x) \rangle : x \in X \}$ , and the normalized Euclidean distance  $D_{NE}(\tilde{a}, \tilde{b})$  between  $\tilde{a}$  and  $\tilde{b}$  can be represented in the following way [104]:

$$D_{NE}(\tilde{a}, \tilde{b}) = \sqrt{\frac{1}{2n} \sum_{i=1}^n \left[ \left( \mu_{\tilde{a}}(x_i) - \mu_{\tilde{b}}(x_i) \right)^2 + \left( \nu_{\tilde{a}}(x_i) - \nu_{\tilde{b}}(x_i) \right)^2 + \left( \pi_{\tilde{a}}(x_i) - \pi_{\tilde{b}}(x_i) \right)^2 \right]}. \quad (6)$$

**Definition 5.** Assume there are  $k$  decision makers in the decision procedure,  $\tilde{w}^* = (\tilde{w}_1^*, \tilde{w}_2^*, \dots, \tilde{w}_k^*)$  is the weight of a group of decision makers, where  $\sum_{d=1}^k \tilde{w}_d^* = 1$ . In order to integrate all decision makers' opinion into a group decision opinion, the Intuitionistic Fuzzy Weighted Averaging (IFWA) operator can be represented in the following way [32]:

$$\begin{aligned}r_{ij} &= \text{IFWA}_{\tilde{w}^*}(r_{ij}^{(1)}, r_{ij}^{(2)}, \dots, r_{ij}^{(k)}) \\ &= \tilde{w}_1^* r_{ij}^{(1)} \oplus \tilde{w}_2^* r_{ij}^{(2)} \oplus \tilde{w}_3^* r_{ij}^{(3)} \oplus \dots \oplus \tilde{w}_k^* r_{ij}^{(k)} \\ &= \left[ 1 - \prod_{d=1}^k (1 - \mu_{ij}^d)^{\tilde{w}_d^*}, \prod_{d=1}^k (\nu_{ij}^d)^{\tilde{w}_d^*} \right].\end{aligned}\quad (7)$$

where  $r_{ij}^{(k)}$  represents an intuitionistic performance value in  $k$ th expert matrix and  $r_{ij}$  is the intuitionistic performance value aggregated by the all experts' weights.

**4.2. Best-Worst Method.** Best-worst method was proposed by Rezaei [105], which simplified the calculation process. BWB optimizes the comparison way, turning secondary comparisons into reference comparisons. Analytic Hierarchy Process (AHP), which is similar to the BWB principle, has more  $(n^2 - 5n - 6)/2$  times of comparison.

Step 1: gather experts to discuss a common set of decision criteria  $(C_1, C_2, \dots, C_m)$ .

Step 2: select the best (most important) and worst (least important) criteria, respectively.

Step 3: calculate the preference of the best criterion over all the other criteria by number 1 to 9.  $a_{ij} > 1$  represents  $i$  is more important than  $j$ , the importance of  $i$  to  $j$  increases as the number increases. The result is recorded as Best-to-Others:

$$A_B = (a_{B1}, a_{B2}, \dots, a_{Bm}). \quad (8)$$

Step 4: calculate the preference of all the criteria over the worst criterion by number 1 to 9, and the result is recorded as Others-to-Worst:

$$A_W = (a_{1W}, a_{2W}, \dots, a_{mW})^T, \quad (9)$$

where  $a_{ii} = 1$

Step 5: compute the optimal criteria weight by the following formula:

s.t.

$$\begin{aligned}\left| \frac{w_B}{w_j} - a_{Bj} \right| &\leq \xi, \quad \text{for all } j, \\ \left| \frac{w_j}{w_W} - a_{jW} \right| &\leq \xi, \quad \text{for all } j,\end{aligned}\quad (10)$$

$$\sum_j w_j = 1, w_j \geq 0, \quad \text{for all } j.$$

By solving the above inequalities, the final criteria weight  $w_j = (w_1, w_2, \dots, w_m)$  was obtained.

**4.3. WASPAS Method.** WASPAS method was proposed by Chakraborty and Zavadskas in 2004, which was a dominant MCGDM method integrating the weighted sum model (WSM) and weighted product model (WPM) [75]. Compared with WSM and WPM, WASPAS could provide more accurate results and simplify the calculation process [106], so it has become a more efficient tool for dealing with MCGDM problems. Assuming that  $w_j$  is weight of  $j$ th criterion,  $x_{ij}$  denotes the performance value of  $i$ th alternative according to the  $j$ th criterion ( $i = 1, 2, \dots, n$  and  $j = 1, 2, \dots, m$ ). The WASPAS method steps are as follows:

Step 1: calculate the linear normalization of performance values as follows:

$$\bar{x}_{ij} = \begin{cases} \frac{x_{ij}}{\max_i x_{ij}}, & \text{if } j \in C_b, \\ \frac{\min_i x_{ij}}{x_{ij}}, & \text{if } j \in C_n, \end{cases} \quad (11)$$

where  $C_b$  and  $C_n$  are the sets of the beneficial and nonbeneficial criteria.

Step 2: compute the measures of WSM ( $Q_i^{(1)}$ ) and WPM ( $Q_i^{(2)}$ ) for each alternative as follows:

$$Q_i^{(1)} = \sum_{j=1}^m w_j \bar{x}_{ij}, \quad (12)$$

$$Q_i^{(2)} = \prod_{j=1}^m (\bar{x}_{ij})^{w_j}. \quad (13)$$

Step 3: obtain the aggregated measures of the WASPAS method for each alternative as follows:

$$Q_i = \lambda Q_i^{(1)} + (1 - \lambda) Q_i^{(2)}, \quad (14)$$

where  $\lambda$  represents the parameter of the WASPAS method and  $\lambda \in [0, 1]$ . When  $\lambda = 1$ , the WASPAS method is transformed to WSM, and  $\lambda = 0$ ; it is transformed to WPM.

Step 4: rank the alternatives according to decreasing values of  $Q_i$ .

**4.4. TOPSIS Method.** TOPSIS was proposed by Hwang and Yoon [71], as a classical MCGDM problem processing method. Its principle is to make the final solution as close as possible to PIS (positive ideal solution) and away from NIS (negative ideal solution). The TOPSIS method steps are as follows:

Step 1: normalize the decision matrix as follows:

$$r_{ij} = \frac{x_{ij}}{\sqrt{\sum_{k=1}^n x_{kj}^2}}, \quad (15)$$

where  $x_{ij}$  is the performance value (crisp number) in decision matrix and  $r_{ij}$  denotes the normalized value,  $i \in \{1, 2, \dots, n\}$  and  $j \in \{1, 2, \dots, m\}$ .

Step 2: aggregate the criteria weights to the normalized matrix by the following:

$$v_{ij} = w_j r_{ij}. \quad (16)$$

Step 3: obtain the  $v_j^+$  (PIS) and  $v_j^-$  (NIS) for each criterion as follows:

$$v_j^+ = \begin{cases} \max\{v_{1j}, v_{2j}, \dots, v_{nj}\}, & \text{if } j \in C_b, \\ \min\{v_{1j}, v_{2j}, \dots, v_{nj}\}, & \text{if } j \in C_n, \end{cases} \quad (17)$$

$$v_j^- = \begin{cases} \max\{v_{1j}, v_{2j}, \dots, v_{nj}\}, & \text{if } j \in C_b, \\ \max\{v_{1j}, v_{2j}, \dots, v_{nj}\}, & \text{if } j \in C_n, \end{cases} \quad (18)$$

where  $C_b$  and  $C_n$  are the sets of the beneficial and nonbeneficial criteria.

Step 4: compute the separation measures for each alternative as follows:

$$S_i^+ = \sqrt{\sum_{j=1}^m (v_j^+ - v_{ij})^2}, \quad i = 1, 2, \dots, n, \quad (19)$$

$$S_i^- = \sqrt{\sum_{j=1}^m (v_j^- - v_{ij})^2}, \quad i = 1, 2, \dots, n.$$

Step 5: obtain the closeness coefficient of each alternative to the ideal solution as follows:

$$CC_i = \frac{S_i^-}{S_i^- + S_i^+}, \quad (20)$$

where the value of  $CC_i$  is bigger and the alternative  $A_i$  is better.

## 5. The Proposed Method

The proposed method consists of the following three steps: (1) Preparation stage: It constructs the decision-making group to determine the criteria, alternatives, and intuitionistic fuzzy set. After that each expert establishes the fuzzy decision matrix. (2) Computation stage: weigh the criteria by the BWM method after the discussion of experts. Then, aggregate the priori given expert weights into the fuzzy decision matrix by the IFWA operator. (3) Selection stage: after calculating the WASPAS measures of each alternative, the fuzzy TOPSIS is integrated into this step. Fuzzy positive/negative ideal solutions are computed; finally, the closeness coefficient of each alternatives is obtained. Figure 1 represents the conceptual framework of the proposed method.

Suppose that there are a set of  $n$  alternatives ( $A_1, A_2, \dots, A_n$ ), a set of  $m$  criteria ( $C_1, C_2, \dots, C_m$ ), and a set of  $k$  decision makers ( $D_1, D_2, \dots, D_k$ ). The proposed method is as follows:

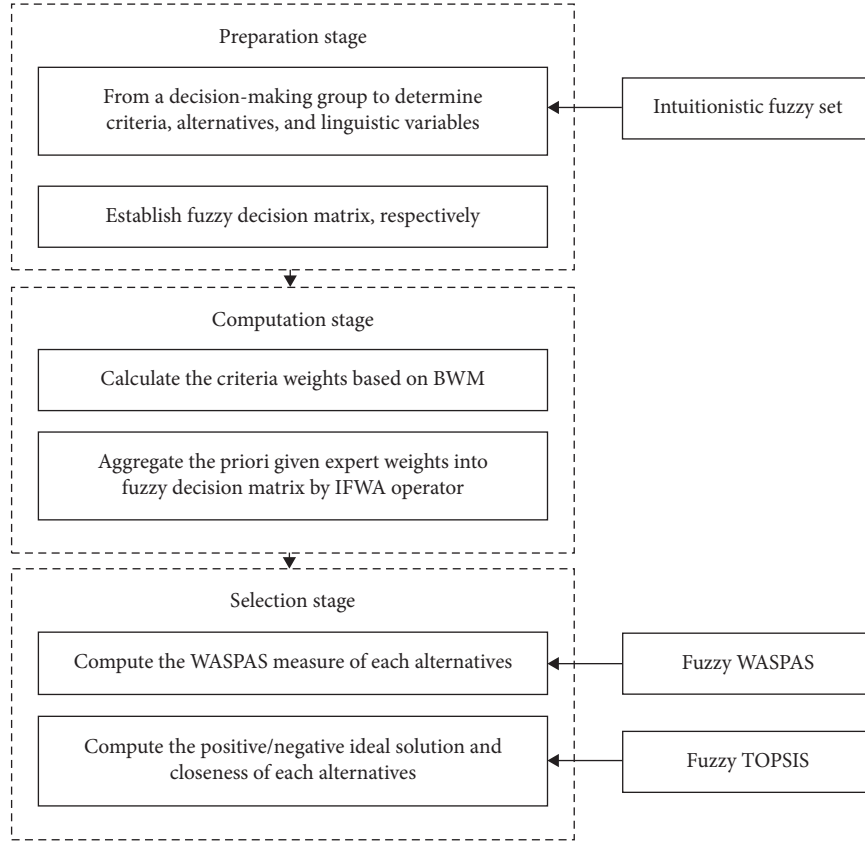


FIGURE 1: The conceptual framework of the proposed method.

Step 1: a group of decision makers select the best (most important) and worst (least important) criteria after discussion.

Step 2: calculate the Best-to-Others and Others-to-Worst by number 1 to 9:

$$\begin{aligned} A_B &= (a_{B1}, a_{B2}, \dots, a_{Bm}), \\ A_W &= (a_{1W}, a_{2W}, \dots, a_{mW})^T. \end{aligned} \quad (21)$$

Step 3: compute the optimal criteria weight by equation (10) and obtain

$$w_j^* = (w_1^*, w_2^*, \dots, w_m^*). \quad (22)$$

Step 4: construct the fuzzy decision matrix  $DM^{(d)}$  of the  $d$ th decision maker as follows:

$$DM^{(d)} = (\tilde{x}_{ij}^d)_{n \times m} = \begin{matrix} & C_1 & C_2 & \dots & C_m \\ \begin{matrix} A_1 \\ A_2 \\ \vdots \\ A_n \end{matrix} & \begin{bmatrix} \tilde{x}_{11}^d & \tilde{x}_{12}^d & \dots & \tilde{x}_{1m}^d \\ \tilde{x}_{21}^d & \tilde{x}_{22}^d & \dots & \tilde{x}_{2m}^d \\ \vdots & \vdots & \ddots & \vdots \\ \tilde{x}_{n1}^d & \tilde{x}_{n2}^d & \dots & \tilde{x}_{nm}^d \end{bmatrix} \end{matrix}, \quad d = 1, \dots, k, \quad (23)$$

where  $\tilde{x}_{ij}^d$  is an intuitionistic fuzzy set, and it denotes the performance value of the alternative  $A_i$  on the criterion  $C_j$  by decision maker  $D_d$ ,  $1 \leq i \leq n$ ,  $1 \leq j \leq m$ , and  $1 \leq d \leq k$ . In addition, experts use the linguistic terms [107] to evaluate the alternatives as shown in Table 3.

Step 5: aggregate the decision group weights  $\tilde{w}^* = (\tilde{w}_1^*, \tilde{w}_2^*, \dots, \tilde{w}_k^*)$  into the fuzzy decision matrix  $DM^{(d)}$  by the IFWA operator in equation (7) and obtain the fuzzy average decision matrix  $DM$ , where  $\sum_{d=1}^k \tilde{w}_d^* = 1$ :

$$DM = (\tilde{x}_{ij})_{n \times m} = \begin{matrix} & C_1 & C_2 & \dots & C_m \\ \begin{matrix} A_1 \\ A_2 \\ \vdots \\ A_n \end{matrix} & \begin{bmatrix} \tilde{x}_{11} & \tilde{x}_{12} & \dots & \tilde{x}_{1m} \\ \tilde{x}_{21} & \tilde{x}_{22} & \dots & \tilde{x}_{2m} \\ \vdots & \vdots & \ddots & \vdots \\ \tilde{x}_{n1} & \tilde{x}_{n2} & \dots & \tilde{x}_{nm} \end{bmatrix} \end{matrix}, \quad (24)$$

where  $\tilde{x}_{ij}$  is an intuitionistic fuzzy set, and it represents the average performance value of the alternative  $A_i$  on the criterion  $C_j$  by all decision makers,  $1 \leq i \leq n$ ,  $1 \leq j \leq m$ .

Step 6: calculate the normalized performance values by the following equation:

TABLE 3: Linguistic terms and corresponding IFNs.

Linguistic terms	Intuitionistic fuzzy numbers $(\mu, \nu)$
Extremely good (EG)	(1.00, 0.00)
Very very good (VVG)	(0.90, 0.10)
Very good (VG)	(0.80, 0.10)
Good (G)	(0.70, 0.20)
Medium good (MG)	(0.60, 0.30)
Fair (F)	(0.50, 0.40)
Medium poor (MP)	(0.40, 0.50)
Poor (P)	(0.25, 0.60)
Very poor (VP)	(0.10, 0.75)
Very very poor (VVP)	(0.10, 0.90)

$$\tilde{s}_{ij} = \begin{cases} \frac{\tilde{x}_{ij}}{\max_i \tilde{x}_{ij}} = \frac{(u_{ij}, v_{ij})}{(\max_i u_{ij}, \min_i v_{ij})}, & \text{if } j \in C_b, \\ \frac{\min_i \tilde{x}_{ij}}{\tilde{x}_{ij}} = \frac{(\min_i u_{ij}, \max_i v_{ij})}{(u_{ij}, v_{ij})}, & \text{if } j \in C_n, \end{cases} \quad (25)$$

and the normalized fuzzy decision matrix  $\overline{DM}$  can be obtained:

$$\overline{DM} = (\tilde{s}_{ij})_{n \times m} = \begin{matrix} & C_1 & C_2 & \dots & C_m \\ \begin{matrix} A_1 \\ A_2 \\ \vdots \\ A_n \end{matrix} & \begin{bmatrix} \tilde{s}_{11} & \tilde{s}_{12} & \dots & \tilde{s}_{1m} \\ \tilde{s}_{21} & \tilde{s}_{22} & \dots & \tilde{s}_{2m} \\ \vdots & \vdots & \ddots & \vdots \\ \tilde{s}_{n1} & \tilde{s}_{n2} & \dots & \tilde{s}_{nm} \end{bmatrix} \end{matrix}, \quad (26)$$

where  $\tilde{s}_{ij}$  denotes the normalized performance value and  $C_b$  and  $C_n$  are the sets of the beneficial and nonbeneficial criteria.

Step 7: compute the measures of WSM ( $\tilde{Q}_i^{(1)}$ ) for each alternative in equation (12) as follows:

$$\begin{aligned} \tilde{Q}_i^{(1)} &= \sum_{j=1}^m w_j^* \tilde{s}_{ij} = \tilde{Q}_{i1}^{(1)} \oplus \tilde{Q}_{i2}^{(1)} \oplus \dots \oplus \tilde{Q}_{im}^{(1)} \\ &= (w_1^* \otimes \tilde{s}_{i1}) \oplus (w_2^* \otimes \tilde{s}_{i2}) \oplus \dots \oplus (w_m^* \otimes \tilde{s}_{im}), \end{aligned} \quad (27)$$

where  $w_j^*$  represents average weight of the  $j$ th criterion from all decision makers.

Step 8: calculate the measures of WPM ( $\tilde{Q}_i^{(2)}$ ) for each alternative in equation (13) as follows:

$$\tilde{Q}_i^{(2)} = \prod_{j=1}^m (\tilde{s}_{ij})^{w_j^*} = \tilde{Q}_{i1}^{(2)} \otimes \tilde{Q}_{i2}^{(2)} \otimes \dots \otimes \tilde{Q}_{im}^{(2)} = (\tilde{s}_{i1})^{w_1^*} \otimes (\tilde{s}_{i2})^{w_2^*} \otimes \dots \otimes (\tilde{s}_{im})^{w_m^*}. \quad (28)$$

Step 9: obtain the WASPAS measures of each alternative by the result of steps 7 and 8:

$$\tilde{Q}_i = \lambda \tilde{Q}_i^{(1)} + (1 - \lambda) \tilde{Q}_i^{(2)}, \quad (29)$$

where criterion  $C_j$  of alternative  $A_i$  measure as follows:

$$\tilde{Q}_{ij} = \lambda \tilde{Q}_{ij}^{(1)} + (1 - \lambda) \tilde{Q}_{ij}^{(2)}, \quad (30)$$

where  $\lambda$  is the parameter of the method and  $\lambda \in [0, 1]$ .

Step 10: after constructing the decision matrix in the WASPAS method, the TOPSIS method is investigated in this step. Fuzzy positive/negative ideal solution ( $\tilde{v}_j^+/\tilde{v}_j^-$ ) are obtained based on equations (17) and (18) as follows:

$$\tilde{v}_j^+ = \begin{cases} \max\{\tilde{Q}_{1j}, \tilde{Q}_{2j}, \dots, \tilde{Q}_{nj}\} = \left( \max_j u_{ij}, \min_j v_{ij} \right) = (u_j^+, v_j^+), & \text{if } j \in C_b, \\ \min\{\tilde{Q}_{1j}, \tilde{Q}_{2j}, \dots, \tilde{Q}_{nj}\} = \left( \min_j u_{ij}, \max_j v_{ij} \right) = (u_j^+, v_j^+), & \text{if } j \in C_n, \end{cases} \quad (31)$$

$$\tilde{v}_j^- = \begin{cases} \min\{\tilde{Q}_{1j}, \tilde{Q}_{2j}, \dots, \tilde{Q}_{nj}\} = \left( \min_j u_{ij}, \max_j v_{ij} \right) = (u_j^-, v_j^-), & \text{if } j \in C_b, \\ \max\{\tilde{Q}_{1j}, \tilde{Q}_{2j}, \dots, \tilde{Q}_{nj}\} = \left( \max_j u_{ij}, \min_j v_{ij} \right) = (u_j^-, v_j^-), & \text{if } j \in C_n. \end{cases} \quad (32)$$



Step 11: compute the distance from each alternative to  $\tilde{v}_j^+/\tilde{v}_j^-$  according to equation (6) as follows:

$$D_i^+ = D(\tilde{v}_j^+, \tilde{Q}_{ij}) = \sqrt{\frac{1}{2m} \sum_{j=1}^m [(\mu_j^+ - \mu_{ij})^2 + (v_j^+ - v_{ij})^2 + (\pi_j^+ - \pi_{ij})^2]}, \quad (33)$$

$$D_i^- = D(\tilde{v}_j^-, \tilde{Q}_{ij}) = \sqrt{\frac{1}{2m} \sum_{j=1}^m [(\mu_j^- - \mu_{ij})^2 + (v_j^- - v_{ij})^2 + (\pi_j^- - \pi_{ij})^2]}, \quad (34)$$

where  $D_i^+$  denotes the distance between the alternative  $A_i$  and the positive ideal solution  $\tilde{v}_j^+$ .

Step 12: calculate the closeness coefficient of each alternative to the ideal solution as follows:

$$CC_i = \frac{D_i^-}{D_i^- + D_i^+}, \quad (35)$$

where the higher value of  $CC_i$  represents that the  $i$ th alternative is better.

## 6. Comparing the Proposed Approach with Other Methods

WASPAS, integrating the WAM and WPM model, has the advantage of higher accuracy. In addition, the WASPAS overcomes the complex multiplication calculation and becomes a convenient MCGDM method. However, through previous studies, it was found that the improved accuracy of ranking value and uncertain expression of performance value were usually ignored in the application of WASPAS and weighting the criteria was also complex. By improving some typical hybrid methods, the ranking value accuracy is increased. The hesitancy is taken into decision matrix, and a concise method to calculate criteria weight is chosen.

The main differences between the hybrid method proposed in this paper and other related methods are as follows. (1) WASPAS and TOPSIS are integrated to improve accuracy in the ranking stage so that the alternatives ranking results are closer to the decision makers' idea. (2) Intuitionistic fuzzy sets are used in the process to provide experts with freedom to express the hesitation, and it is another dimension besides the affirmation and negation.

(3) The determination of criteria weights is simpler and clearer. Compared with the classical comparison method, BWM can simplify the steps and reduce the computational difficulty.

## 7. Illustrative Examples and Discussion

**7.1. Illustrative Example.** In this paper, H company's resilient-green supplier selection in supply chain environment was taken as an example. Assuming that three decision makers ( $d_1, d_2, d_3$ ) evaluate four alternatives (suppliers) ( $A_1, A_2, A_3, A_4$ ), H company provided three decision makers' weights (0.3, 0.3, 0.4) according to different functions. Each decision matrix must contain all the indicators, including  $G_1$ -eco-design,  $G_2$ -green procurement,  $G_3$ -pollution production,  $G_4$ -green Packing,  $G_5$ -green image,  $G_6$ -life cycle management,  $S_1$ -surplus inventory,  $S_2$ -factory segregation,  $S_3$ -reliability,  $S_4$ -reorganization,  $O_1$ -logistics,  $O_2$ -warehousing, and  $O_3$ -cooperation commitment.

*Step 1.* Decision makers consult to select the most important ( $G_3$ ) and least important ( $O_2$ ) criteria, respectively.

*Step 2.* Calculate the Best-to-Others and Others-to-Worst by number 1 to 9, as shown in Tables 4 and 5:

$$\begin{aligned} A_B &= (6, 5, 1, 7, 4, 2, 3, 4, 6, 7, 2, 8, 4), \\ A_W &= (5, 4, 8, 4, 6, 7, 7, 7, 5, 6, 8, 1, 5)^T. \end{aligned} \quad (36)$$

*Step 3.* Obtain the optimal criteria weight by equation (10):

$$w_j^* = (0.085, 0.03, 0.244, 0.028, 0.063, 0.089, 0.085, 0.089, 0.041, 0.063, 0.112, 0.022, 0.049). \quad (37)$$

*Step 4.* The three experts construct the decision matrix separately. The linguistic terms used in the matrix are shown in Table 3:

TABLE 4: Pairwise comparison vector for the best criterion.

Criteria	$G_1$	$G_2$	$G_3$	$G_4$	$G_5$	$G_6$	$S_1$	$S_2$	$S_3$	$S_4$	$O_1$	$O_2$	$O_3$
Best criterion $G_3$	6	5	1	7	4	2	3	4	6	7	2	8	4

TABLE 5: Pairwise comparison vector for the worst criterion.

Criteria	$G_1$	$G_2$	$G_3$	$G_4$	$G_5$	$G_6$	$S_1$	$S_2$	$S_3$	$S_4$	$O_1$	$O_2$	$O_3$
Worst criterion $O_2$	5	4	8	4	6	7	7	7	5	6	8	1	5

$$\begin{aligned}
DM^{(1)} &= \begin{bmatrix} EG & VG & F & MP & VG & VP & VVG & VG & F & VVG & MG & G & VP \\ VG & MG & G & F & MG & P & EG & VG & VG & VVP & MP & VG & P \\ EG & EG & MP & VG & G & G & G & VVG & P & MP & F & P & VP \\ G & F & P & G & MP & F & EG & F & VVP & G & F & MP & VVP \end{bmatrix}, \\
DM^{(2)} &= \begin{bmatrix} MG & MP & P & G & F & P & VG & EG & MP & F & VP & MG & F \\ G & F & VP & MG & G & VVG & MG & F & VG & G & VVP & G & G \\ VG & F & MP & EG & VG & MP & P & VVG & F & P & F & VG & P \\ G & VG & VVP & VG & F & F & VG & MG & G & MP & G & G & VP \end{bmatrix}, \\
DM^{(3)} &= \begin{bmatrix} VP & F & MP & MG & VVG & VP & MP & EG & F & MG & F & P & MG \\ P & VG & VG & MP & EG & F & VG & VG & G & G & VVG & MP & VG \\ F & G & F & P & VG & G & F & F & G & P & MG & VVP & F \\ VVP & VVG & VP & G & F & P & VP & VVG & VG & F & EG & VP & MG \end{bmatrix},
\end{aligned} \tag{38}$$

where linguistic terms can be transferred to the intuitionistic fuzzy numbers by Table 3.

*Step 5.* Aggregate the decision group weights  $\tilde{w}^* = (0.3, 0.3, 0.4)$  into the fuzzy decision matrix

$DM^{(d)}$  by IFWA operator in equation (7), and obtain the fuzzy average decision matrix DM as follows:

$$DM = \begin{bmatrix} (1, 0) & (0.6, 0.28) & (0.39, 0.49) & (0.59, 0.31) & (0.8, 0.15) & (0.15, 0.7) & (0.75, 0.19) & (1, 0) & (0.47, 0.43) & (0.72, 0.24) & (0.44, 0.44) & (0.53, 0.35) & (0.45, 0.43) \\ (0.62, 0.25) & (0.68, 0.21) & (0.65, 0.23) & (0.5, 0.4) & (1, 0) & (0.65, 0.3) & (1, 0) & (0.74, 0.15) & (0.77, 0.13) & (0.58, 0.31) & (0.67, 0.31) & (0.65, 0.23) & (0.66, 0.21) \\ (1, 0) & (1, 0) & (0.44, 0.46) & (1, 0) & (0.77, 0.12) & (0.63, 0.26) & (0.52, 0.37) & (0.81, 0.17) & (0.54, 0.34) & (0.3, 0.57) & (0.54, 0.36) & (0.46, 0.41) & (0.33, 0.55) \\ (0.53, 0.37) & (0.8, 0.15) & (0.15, 0.74) & (0.73, 0.16) & (0.47, 0.43) & (0.41, 0.47) & (1, 0) & (0.75, 0.21) & (0.65, 0.24) & (0.55, 0.35) & (1, 0) & (0.43, 0.45) & (0.35, 0.55) \end{bmatrix}, \tag{39}$$

where

$$\begin{aligned}
\tilde{x}_{12} &= \left[ 1 - \prod_{d=1}^3 (1 - \mu_{ij}^d)^{\tilde{w}_d^*}, \prod_{d=1}^3 (\nu_{ij}^d)^{\tilde{w}_d^*} \right] \\
&= \left[ 1 - (1 - 0.8)^{0.3} * (1 - 0.4)^{0.3} * (1 - 0.5)^{0.4}, (0.1)^{0.3} \right. \\
&\quad \left. * (0.5)^{0.3} * (0.4)^{0.4} \right] \\
&= (0.6, 0.28).
\end{aligned} \tag{40}$$

*Step 6.* Normalize the performance values by equation (24), and the normalized fuzzy decision matrix  $\overline{DM}$  is

obtained. Table 6 contains performance values in the  $\overline{DM}$ .

*Step 7.* Compute the measures of WSM ( $\tilde{Q}_{ij}^{(1)}$ ) and WPM ( $\tilde{Q}_{ij}^{(2)}$ ) for each criterion  $C_j$  of alternative  $A_i$  by equations (27) and (28). Tables 7 and 8 represent the WSM and WPM measures of each performance value, respectively.

$$\tilde{Q}_{12}^{(2)} = (\tilde{x}_{12})^{w_2^*} = (0.6, 0.28)^{0.03} = (0.985, 0.01). \tag{41}$$

*Step 8.* According to equation (30), the WASPAS measures are obtained, as shown in Table 9, and  $\lambda = 0.5$  is set in this paper:

TABLE 6: The normalized performance values in the average decision matrix.

Criteria	$A_1$	$A_2$	$A_3$	$A_4$
$G_1$	(1, 0)	(0.617, 0.252)	(1, 0)	(0.534, 0.365)
$G_2$	(0.599, 0.282)	(0.676, 0.211)	(1, 0)	(0.8, 0.152)
$G_3$	(0.393, 0.494)	(0.645, 0.225)	(0.442, 0.457)	(0.148, 0.741)
$G_4$	(0.586, 0.31)	(0.497, 0.4)	(1, 0)	(0.734, 0.163)
$G_5$	(0.8, 0.152)	(1, 0)	(0.774, 0.123)	(0.472, 0.428)
$G_6$	(0.148, 0.7)	(0.652, 0.298)	(0.631, 0.26)	(0.412, 0.47)
$S_1$	(0.748, 0.19)	(1, 0)	(0.516, 0.367)	(1, 0)
$S_2$	(1, 0)	(0.737, 0.152)	(0.81, 0.174)	(0.754, 0.211)
$S_3$	(0.472, 0.428)	(0.765, 0.132)	(0.54, 0.342)	(0.645, 0.238)
$S_4$	(0.718, 0.235)	(0.583, 0.314)	(0.299, 0.568)	(0.547, 0.347)
$O_1$	(0.442, 0.443)	(0.67, 0.313)	(0.543, 0.357)	(1, 0)
$O_2$	(0.528, 0.351)	(0.65, 0.234)	(0.457, 0.412)	(0.427, 0.447)
$O_3$	(0.455, 0.431)	(0.664, 0.211)	(0.326, 0.546)	(0.35, 0.55)

$$\bar{s}_{12} = (\bar{x}_{12}/\max_1 \bar{x}_{12}) = (0.6, 0.28)/(1, 0) = (0.6, 0.28).$$

TABLE 7: The WSM measures of each performance value.

Criteria	$A_1$	$A_2$	$A_3$	$A_4$
$G_1$	(1, 0)	(0.078, 0.89)	(1, 0)	(0.063, 0.918)
$G_2$	(0.027, 0.963)	(0.033, 0.954)	(1, 0)	(0.047, 0.945)
$G_3$	(0.115, 0.842)	(0.223, 0.695)	(0.133, 0.826)	(0.038, 0.93)
$G_4$	(0.024, 0.968)	(0.019, 0.975)	(1, 0)	(0.036, 0.951)
$G_5$	(0.096, 0.888)	(1, 0)	(0.089, 0.876)	(0.039, 0.948)
$G_6$	(0.014, 0.969)	(0.09, 0.898)	(0.085, 0.887)	(0.046, 0.935)
$S_1$	(0.111, 0.868)	(1, 0)	(0.06, 0.918)	(1, 0)
$S_2$	(1, 0)	(0.112, 0.846)	(0.137, 0.856)	(0.117, 0.871)
$S_3$	(0.026, 0.966)	(0.058, 0.92)	(0.031, 0.957)	(0.042, 0.943)
$S_4$	(0.077, 0.913)	(0.054, 0.93)	(0.022, 0.965)	(0.049, 0.936)
$O_1$	(0.063, 0.913)	(0.117, 0.878)	(0.084, 0.891)	(1, 0)
$O_2$	(0.016, 0.977)	(0.023, 0.969)	(0.013, 0.981)	(0.012, 0.982)
$O_3$	(0.029, 0.96)	(0.052, 0.927)	(0.019, 0.971)	(0.021, 0.971)

TABLE 8: The WPM measures of each performance value.

Criteria	$A_1$	$A_2$	$A_3$	$A_4$
$G_1$	(1, 0)	(0.96, 0.024)	(1, 0)	(0.948, 0.038)
$G_2$	(0.985, 0.01)	(0.988, 0.007)	(1, 0)	(0.993, 0.005)
$G_3$	(0.796, 0.153)	(0.898, 0.062)	(0.819, 0.138)	(0.627, 0.281)
$G_4$	(0.985, 0.01)	(0.981, 0.014)	(1, 0)	(0.991, 0.005)
$G_5$	(0.986, 0.01)	(1, 0)	(0.984, 0.008)	(0.954, 0.035)
$G_6$	(0.844, 0.102)	(0.963, 0.031)	(0.96, 0.026)	(0.924, 0.055)
$S_1$	(0.976, 0.018)	(1, 0)	(0.945, 0.038)	(1, 0)
$S_2$	(1, 0)	(0.973, 0.015)	(0.981, 0.017)	(0.975, 0.021)
$S_3$	(0.97, 0.023)	(0.99, 0.006)	(0.975, 0.017)	(0.982, 0.011)
$S_4$	(0.979, 0.017)	(0.967, 0.024)	(0.927, 0.052)	(0.963, 0.027)
$O_1$	(0.913, 0.063)	(0.956, 0.041)	(0.934, 0.048)	(1, 0)
$O_2$	(0.986, 0.01)	(0.991, 0.006)	(0.983, 0.012)	(0.982, 0.013)
$O_3$	(0.962, 0.027)	(0.98, 0.012)	(0.947, 0.038)	(0.95, 0.038)

$$\bar{Q}_{12}^{(1)} = (w_2^* \otimes \bar{s}_{12}) = 0.03 \otimes (0.6, 0.28) = (0.027, 0.962).$$

TABLE 9: The WASPAS measures of each performance value.

Criteria	$A_1$	$A_2$	$A_3$	$A_4$
$G_1$	(1, 0)	(0.808, 0.146)	(1, 0)	(0.779, 0.187)
$G_2$	(0.879, 0.098)	(0.892, 0.082)	(1, 0)	(0.918, 0.069)
$G_3$	(0.575, 0.359)	(0.719, 0.208)	(0.604, 0.338)	(0.401, 0.511)
$G_4$	(0.879, 0.098)	(0.864, 0.117)	(1, 0)	(0.907, 0.069)
$G_5$	(0.888, 0.094)	(1, 0)	(0.879, 0.084)	(0.79, 0.182)
$G_6$	(0.608, 0.314)	(0.817, 0.167)	(0.809, 0.152)	(0.731, 0.227)
$S_1$	(0.854, 0.125)	(1, 0)	(0.773, 0.187)	(1, 0)
$S_2$	(1, 0)	(0.845, 0.113)	(0.872, 0.12)	(0.851, 0.135)
$S_3$	(0.829, 0.149)	(0.903, 0.074)	(0.844, 0.128)	(0.869, 0.102)
$S_4$	(0.861, 0.125)	(0.823, 0.15)	(0.733, 0.224)	(0.812, 0.159)
$O_1$	(0.715, 0.24)	(0.803, 0.19)	(0.754, 0.207)	(1, 0)
$O_2$	(0.883, 0.099)	(0.906, 0.076)	(0.871, 0.109)	(0.867, 0.113)
$O_3$	(0.808, 0.161)	(0.862, 0.106)	(0.772, 0.192)	(0.779, 0.192)

$$v_j^+ = \begin{cases} \max\{v_{1j}, v_{2j}, \dots, v_{nj}\}, & \text{if } j \in C_b, \\ \min\{v_{1j}, v_{2j}, \dots, v_{nj}\}, & \text{if } j \in C_n. \end{cases} \quad (42)$$

For example,

$$\begin{aligned} \tilde{Q}_{12} &= 0.5\tilde{Q}_{12}^{(1)} + (1 - 0.5)\tilde{Q}_{12}^{(2)} = 0.5 \otimes (0.027, 0.963) \oplus 0.5 \\ &\otimes (0.985, 0.01) = (0.881, 0.098). \end{aligned} \quad (43)$$

*Step 9.* Fuzzy positive/negative ideal solutions ( $\tilde{v}_j^+/\tilde{v}_j^-$ ) from Table 9 are obtained based on equations (31) and (32) as follows:

$$\begin{aligned} \tilde{v}_j^+ &= \max\{\tilde{Q}_{1j}, \tilde{Q}_{2j}, \dots, \tilde{Q}_{nj}\} = \left( \max_j u_{ij}, \min_j v_{ij} \right) \\ &= (u_j^+, v_j^+), \\ \tilde{v}_j^- &= \min\{\tilde{Q}_{1j}, \tilde{Q}_{2j}, \dots, \tilde{Q}_{nj}\} = \left( \min_j v_{ij}, \max_j u_{ij} \right) \\ &= (u_j^-, v_j^-), \end{aligned} \quad (44)$$

the  $\tilde{v}_j^+/\tilde{v}_j^-$  from four alternatives under each criterion are represented in Table 10.

*Step 10.* According to Table 10 and equations (33) and (34), the distance between each alternative to positive/negative ideal solution ( $\tilde{v}_j^+/\tilde{v}_j^-$ ) is calculated. Finally, obtain the closeness coefficient for ranking four alternatives. Relevant values are shown in Table 11.

According to Table 11, the alternatives are ranked as  $A_2 > A_3 > A_4 > A_1$ .

**7.2. Sensitivity Analysis.** In the WASPAS method,  $\lambda$  represents the parameter and  $\lambda \in [0, 1]$ . How does the value of  $\lambda$  affect the final order of suppliers? In order to solve the problems, the sensitivity analysis was provided. We assign different values to  $\lambda$ , then calculate the distance between each alternative to positive/negative ideal solution ( $\tilde{v}_j^+/\tilde{v}_j^-$ ) and closeness coefficient under different conditions, so as to better carry out sensitivity analysis. The results of each alternative with different values of  $\lambda$  are shown in Table 12.

The second supplier is always considered to be the best choice, and the first supplier performs poorly in any case. There are two special cases. when  $\lambda = 0.8$ , the third supplier is superior to the second and becomes the best. When  $\lambda = 0.9$ ,  $A_2$ ,  $A_3$ , and  $A_4$  these three suppliers are almost the same good.

**7.3. Comparative Analysis.** As a classical research field, there are many techniques for dealing with MCGDM problems, including TOPSIS [71], AHP [72], ANP [73], VIKOR [74], BWM [30], WASPAS [75], DEMATEL,

TABLE 10: The positive/negative ideal solution of each criterion.

Criteria	$\tilde{v}_j^+$	$\tilde{v}_j^-$
$G_1$	(1, 0)	(0.779, 0.187)
$G_2$	(1, 0)	(0.879, 0.099)
$G_3$	(0.719, 0.208)	(0.401, 0.501)
$G_4$	(1, 0)	(0.863, 0.117)
$G_5$	(1, 0)	(0.79, 0.182)
$G_6$	(0.817, 0.152)	(0.607, 0.316)
$S_1$	(1, 0)	(0.773, 0.187)
$S_2$	(1, 0)	(0.845, 0.135)
$S_3$	(0.903, 0.074)	(0.828, 0.15)
$S_4$	(0.861, 0.125)	(0.733, 0.224)
$O_1$	(1, 0)	(0.711, 0.244)
$O_2$	(0.906, 0.076)	(0.867, 0.113)
$O_3$	(0.862, 0.106)	(0.772, 0.192)

TABLE 11: The  $D_i^+$ ,  $D_i^-$ , and  $CC_i$  of each alternative.

	$A_1$	$A_2$	$A_3$	$A_4$
$D_i^+$	0.168	0.094	0.112	0.133
$D_i^-$	0.096	0.137	0.109	0.104
$CC_i$	0.364	0.595	0.492	0.439

$$D_1^+ = \sqrt{(1/2m) \sum_{j=1}^m [(\mu_j^+ - \mu_{ij})^2 + (v_j^+ - v_{ij})^2 + (\pi_j^+ - \pi_{ij})^2]} = 0.168.$$

PROM-ETHEE, and the ELECTRE [76]. In order to prove the feasibility and practicability of the method proposed in this paper, we compare the alternative ranking obtained in the above illustrative example with the results of the classical MCGDM methods. Through literature review, we find that AHP is one of the earliest methods to deal with MCGDM problems [108]. TOPSIS and VIKOR as two commonly used and well-known comparative methods, which has similar calculation logic [109]. WASPAS is a novel method which has been put forward in recent years, which has higher consistency and accuracy [31]. AHP, TOPSIS, VIKOR, and WASPAS are the popular and classical methods in recent years [110, 111], so we choose these four methods to compare with the proposed methods. Table 13 represents the comparison results.

In the prioritization of alternatives in Table 13, there are differences in the ranking results of various methods when the parameters change. However, most of the prioritization of alternatives prove that  $A_2$  is the best supplier and  $A_1$  is the worst supplier. Among this, the IF-TOPSIS and IF-AHP are consistent with the result of the method proposed in this paper. IF-VIKOR has the same ranking order when parameters change. The value of  $\lambda$  in IF-WASPAS greatly affects the priority. When  $\lambda \in [0.1, 0.5]$ , the result is consistent with that of this paper. When  $\lambda \geq 0.6$ , the fourth alternative becomes the best choice. With the increase of the value of  $\lambda$ , the ranking result is constantly changing. It can be concluded that the single WASPAS method is greatly influenced by the value of  $\lambda$  and has weak stability. The content of Table 12 shows that the value of  $\lambda$  has little influence on the prioritization of the proposed method, so it is concluded that hybrid method we proposed can improve the accuracy and stability of ranking results.

TABLE 12: The  $D_i^+$ ,  $D_i^-$ , and  $CC_i$  of each alternative by each  $\lambda$  value.

		$D_i^+$	$D_i^-$	$CC_i$	Prioritization of alternatives
$\lambda = 0.1$	$A_1$	0.281	0.934	0.77	$A_2 > A_3 > A_4 > A_1$
	$A_2$	0.025	0.953	0.975	
	$A_3$	0.043	0.939	0.956	
	$A_4$	0.08	0.931	0.921	
$\lambda = 0.2$	$A_1$	0.282	0.915	0.764	$A_2 > A_3 > A_4 > A_1$
	$A_2$	0.034	0.935	0.965	
	$A_3$	0.054	0.919	0.945	
	$A_4$	0.088	0.912	0.912	
$\lambda = 0.3$	$A_1$	0.285	0.068	0.192	$A_2 > A_3 > A_4 > A_1$
	$A_2$	0.048	0.107	0.692	
	$A_3$	0.068	0.08	0.54	
	$A_4$	0.098	0.064	0.397	
$\lambda = 0.4$	$A_1$	0.138	0.08	0.366	$A_2 > A_3 > A_4 > A_1$
	$A_2$	0.067	0.12	0.644	
	$A_3$	0.087	0.091	0.513	
	$A_4$	0.112	0.081	0.42	
$\lambda = 0.5$	$A_1$	0.168	0.096	0.364	$A_2 > A_3 > A_4 > A_1$
	$A_2$	0.094	0.137	0.595	
	$A_3$	0.112	0.109	0.492	
	$A_4$	0.133	0.104	0.439	
$\lambda = 0.6$	$A_1$	0.211	0.117	0.357	$A_2 > A_3 > A_4 > A_1$
	$A_2$	0.132	0.159	0.546	
	$A_3$	0.147	0.134	0.477	
	$A_4$	0.164	0.132	0.447	
$\lambda = 0.7$	$A_1$	0.364	0.152	0.365	$A_2 > A_3 > A_4 > A_1$
	$A_2$	0.189	0.189	0.5	
	$A_3$	0.195	0.172	0.468	
	$A_4$	0.211	0.168	0.442	
$\lambda = 0.8$	$A_1$	0.343	0.197	0.365	$A_3 > A_2 > A_4 > A_1$
	$A_2$	0.271	0.23	0.459	
	$A_3$	0.262	0.23	0.468	
	$A_4$	0.285	0.216	0.43	
$\lambda = 0.9$	$A_1$	0.46	0.399	0.464	$A_2 = A_3 = A_4 > A_1$
	$A_2$	0.39	0.391	0.5	
	$A_3$	0.358	0.358	0.5	
	$A_4$	0.4	0.4	0.5	

TABLE 13: Comparison of the alternative ranking with the classical MCGDM methods.

Method	Prioritization of alternatives
IF-TOPSIS	$A_2 > A_3 > A_4 > A_1$
IF-WASPAS	$\lambda \in [0.1, 0.5]$ $A_2 > A_3 > A_4 > A_1$
	$\lambda = 0.6$ $A_4 > A_1 > A_2 > A_3$
	$\lambda = 0.7$ $A_4 > A_3 > A_1 > A_2$
	$\lambda \in [0.8, 0.9]$ $A_4 > A_1 > A_3 > A_2$
IF-AHP	$A_2 > A_3 > A_4 > A_1$
IF-VIKOR	$\gamma = 0.3/\gamma = 0.5/\gamma = 0.8$ $A_2 > A_3 > A_1 > A_4$
The proposed method	$\lambda = 0.5\lambda = 0.5$ $A_2 > A_3 > A_4 > A_1$

**7.4. Discussion.** The purpose of this section is to discuss the advantages of the supplier selection method used in this paper. The method is specifically manifested in the following two aspects:

- (1) The ranking results are more accurate. WASPAS method has clear logic and simple calculation process, which makes the decision results more precise. In this paper, TOPSIS is integrated at the end of WASPAS to make the alternatives closer to the positive ideal solution (PIS) and away from the negative ideal solution (NIS). In this way, the results based on WASPAS and TOPSIS are more consistent.
- (2) Criteria weighting processes are improved. Compared with the traditional AHP, the BWM calculation process only involves integers, and the calculation steps are greatly reduced, which reduces the arithmetic difficulty for decision makers and improves the consistency of the results.

## 8. Conclusion

By considering the environmental protection and the globalization of the supply chain, resilient-green supplier selection has become a critical issue in the supply chain management. A supplier selection model integrating WASPAS and TOPSIS method based on intuitionistic fuzzy sets is provided. Firstly, the weights of each criteria are measured by the BWM method; secondly, the decision matrix is processed with the integrated WASPAS and TOPSIS, and the alternatives are ranked.

This paper makes two contributions to the research studies on the resilient-green supplier selection. (1) In the background of supply chain management, most scholars have established the relationship between the resilience and greenness from the perspective of supply chain design, but there are few studies focusing on the resilient-green supplier selection. According to the green manufacturing process, resilient-related characteristics, and their intersection, the resilient-green supplier selection criteria system is constructed. (2) In terms of the research methods, a hybrid decision-making method based on the intuitionistic fuzzy numbers is proposed, integrating the WASPAS and TOPSIS to reduce the uncertainty and inaccuracy in the decision-making process. The intuitionistic fuzzy number reflects the preferences of the decision makers more accurately and avoid the fuzziness. In addition, the decision-making system proposed can not only solve the supplier selection problem but also address the site selection, supplier segmentation, performance evaluation, and other issues.

This paper proves the validity of the decision-making model through the illustrative examples, but there are still some limitations. Firstly, the determination of criteria weight by experts was dealt with. Future research studies should mention the method of weighting experts. Secondly, the intuitionistic fuzzy numbers are only used in the ranking stage. Introduction of the fuzzy sets into the weight determination is an important work. Finally, this paper proposes a decision-making method suitable for the intuitionistic fuzzy numbers. And future research studies should be extended to the application of other fuzzy sets.

## Data Availability

All related data are included within the article.

## Conflicts of Interest

The authors declare that there are no conflicts of interest regarding the publication of this article.

## Acknowledgments

This work was supported by the National Natural Science Foundation Council of China under Project nos. 71862035 and 71502159; Yunnan Fundamental Research Project under grant no. 2019FB085; and Philosophy and Social Science Key Foundation of Yunnan Province under Project no. ZDZZD201904.

## References

- [1] J. Qin, X. Liu, and W. Pedrycz, "An extended TODIM multi-criteria group decision making method for green supplier selection in interval type-2 fuzzy environment," *European Journal of Operational Research*, vol. 258, no. 2, pp. 626–638, 2017.
- [2] C. Blome, D. Hollos, and A. Paulraj, "Green procurement and green supplier development: antecedents and effects on supplier performance," *International Journal of Production Research*, vol. 52, no. 1, pp. 32–49, 2014.
- [3] R. Ruiz-Benitez, C. López, and J. C. Real, "Environmental benefits of lean, green and resilient supply chain management: the case of the aerospace sector," *Journal of Cleaner Production*, vol. 167, pp. 850–862, 2017.
- [4] A. Mohammed, I. Harris, A. Soroka, and R. Nujoom, "A hybrid MCDM-fuzzy multi-objective programming approach for a G-resilient supply chain network design," *Computers & Industrial Engineering*, vol. 127, pp. 297–312, 2019.
- [5] M. Yavari and H. Zaker, "An integrated two-layer network model for designing a resilient green-closed loop supply chain of perishable products under disruption," *Journal of Cleaner Production*, vol. 230, pp. 198–218, 2019.
- [6] A. Haldar, A. Ray, D. Banerjee, and S. Ghosh, "Resilient supplier selection under a fuzzy environment," *International Journal of Management Science and Engineering Management*, vol. 9, no. 2, pp. 147–156, 2014.
- [7] S. A. Torabi, M. Baghersad, and S. A. Mansouri, "Resilient supplier selection and order allocation under operational and disruption risks," *Transportation Research Part E: Logistics and Transportation Review*, vol. 79, pp. 22–48, 2015.
- [8] S. Hosseini and A. A. Khaled, "A hybrid ensemble and AHP approach for resilient supplier selection," *Journal of Intelligent Manufacturing*, vol. 30, no. 1, pp. 207–228, 2019.
- [9] D. Pramanik, A. Haldar, S. C. Mondal, S. K. Naskar, and A. Ray, "Resilient supplier selection using AHP-TOPSIS-QFD under a fuzzy environment," *International Journal of Management Science and Engineering Management*, vol. 12, no. 1, pp. 45–54, 2016.
- [10] S. V. Parkouhi and A. S. Ghadikolaei, "A resilience approach for supplier selection: using fuzzy analytic network process and grey VIKOR techniques," *Journal of Cleaner Production*, vol. 161, pp. 431–451, 2017.
- [11] S. Mousakhani, S. Nazari-Shirkouhi, and A. Bozorgi-Amiri, "A novel interval type-2 fuzzy evaluation model based group decision analysis for green supplier selection problems: a case study of battery industry," *Journal of Cleaner Production*, vol. 168, pp. 205–218, 2017.
- [12] H.-W. Lo, J. J. H. Liou, H.-S. Wang, and Y.-S. Tsai, "An integrated model for solving problems in green supplier selection and order allocation," *Journal of Cleaner Production*, vol. 190, pp. 339–352, 2018.
- [13] S. A. S. Haeri and J. Rezaei, "A grey-based green supplier selection model for uncertain environments," *Journal of Cleaner Production*, vol. 221, pp. 768–784, 2019.
- [14] B. M. dos Santos, L. P. Godoy, and L. M. S. Campos, "Performance evaluation of green suppliers using entropy-TOPSIS-F," *Journal of Cleaner Production*, vol. 207, pp. 498–509, 2019.
- [15] Z. Wu and J. Xu, "Managing consistency and consensus in group decision making with hesitant fuzzy linguistic preference relations," *Omega*, vol. 65, pp. 28–40, 2016.
- [16] G. van Valkenhoef and T. Tervonen, "Entropy-optimal weight constraint elicitation with additive multi-attribute utility models," *Omega*, vol. 64, pp. 1–12, 2016.
- [17] D. Wu, "Supplier selection in a fuzzy group setting: a method using grey related analysis and Dempster-Shafer theory," *Expert Systems with Applications*, vol. 36, no. 5, pp. 8892–8899, 2009.
- [18] H. Li, W. Wang, L. Fan, Q. Li, and X. Chen, "A novel hybrid MCDM model for machine tool selection using fuzzy DEMATEL, entropy weighting and later defuzzification VIKOR," *Applied Soft Computing*, vol. 91, Article ID 106207, 2020.
- [19] H.-C. Liu, M.-Y. Quan, Z. Li, and Z.-L. Wang, "A new integrated MCDM model for sustainable supplier selection under interval-valued intuitionistic uncertain linguistic environment," *Information Sciences*, vol. 486, pp. 254–270, 2019.
- [20] D. A. Wood, "Supplier selection for development of petroleum industry facilities, applying multi-criteria decision making techniques including fuzzy and intuitionistic fuzzy TOPSIS with flexible entropy weighting," *Journal of Natural Gas Science and Engineering*, vol. 28, pp. 594–612, 2016.
- [21] G. Sirbiladze, I. Khutsishvili, and B. Midodashvili, "Associated immediate probability intuitionistic fuzzy aggregations in MCDM," *Computers & Industrial Engineering*, vol. 123, pp. 1–8, 2018.
- [22] H. Garg and R. Arora, "Novel scaled prioritized intuitionistic fuzzy soft interaction averaging aggregation operators and their application to multi criteria decision making," *Engineering Applications of Artificial Intelligence*, vol. 71, pp. 100–112, 2018.
- [23] M. O. M. Javad, M. Darvishi, and A. O. M. Javad, "Green supplier selection for the steel industry using BWM and fuzzy TOPSIS: a case study of Khouzesan steel company," *Sustainable Futures*, vol. 2, Article ID 100012, 2020.
- [24] M. Abdel-Baset, V. Chang, A. Gamal, and F. Smarandache, "An integrated neutrosophic ANP and VIKOR method for achieving sustainable supplier selection: a case study in importing field," *Computers in Industry*, vol. 106, pp. 94–110, 2019.
- [25] H. Garg, "Novel intuitionistic fuzzy decision making method based on an improved operation laws and its application," *Engineering Applications of Artificial Intelligence*, vol. 60, pp. 164–174, 2017.



- [26] Q. Wu, L. Zhou, Y. Chen, and H. Chen, "An integrated approach to green supplier selection based on the interval type-2 fuzzy best-worst and extended VIKOR methods," *Information Sciences*, vol. 502, pp. 394–417, 2019.
- [27] E. K. Zavadskas, J. Antucheviciene, S. H. R. Hajiagha, and S. S. Hashemi, "Extension of weighted aggregated sum product assessment with interval-valued intuitionistic fuzzy numbers (WASPAS-IVIF)," *Applied Soft Computing*, vol. 24, pp. 1013–1021, 2014.
- [28] Z. Xu and H. Liao, "Intuitionistic fuzzy analytic hierarchy process," *IEEE Transactions on Fuzzy Systems*, vol. 22, no. 4, pp. 749–761, 2014.
- [29] J. Yuan and X. Luo, "Approach for multi-attribute decision making based on novel intuitionistic fuzzy entropy and evidential reasoning," *Computers & Industrial Engineering*, vol. 135, pp. 643–654, 2019.
- [30] J. Rezaei, "Best-worst multi-criteria decision-making method," *Omega*, vol. 53, pp. 49–57, 2015.
- [31] M. Deveci, F. Canitez, and I. Gökaşar, "WASPAS and TOPSIS based interval type-2 fuzzy MCDM method for a selection of a car sharing station," *Sustainable Cities and Society*, vol. 41, pp. 777–791, 2018.
- [32] Z. Xu, "Intuitionistic fuzzy aggregation operators," *IEEE Transactions on Fuzzy Systems*, vol. 15, pp. 1179–1187, 2007.
- [33] Z.-X. Su, G.-P. Xia, M.-Y. Chen, and L. Wang, "Induced generalized intuitionistic fuzzy OWA operator for multi-attribute group decision making," *Expert Systems with Applications*, vol. 39, no. 2, pp. 1902–1910, 2012.
- [34] Q. Mou, Z. Xu, and H. Liao, "A graph based group decision making approach with intuitionistic fuzzy preference relations," *Computers & Industrial Engineering*, vol. 110, pp. 138–150, 2017.
- [35] G. W. Wei and J. M. Merigó, "Methods for strategic decision-making problems with immediate probabilities in intuitionistic fuzzy setting," *Scientia Iranica*, vol. 19, no. 6, pp. 1936–1946, 2012.
- [36] F. E. Boran, S. Genç, M. Kurt, and D. Akay, "A multi-criteria intuitionistic fuzzy group decision making for supplier selection with TOPSIS method," *Expert Systems with Applications*, vol. 36, no. 8, pp. 11363–11368, 2009.
- [37] S.-F. Zhang and S.-Y. Liu, "A GRA-based intuitionistic fuzzy multi-criteria group decision making method for personnel selection," *Expert Systems with Applications*, vol. 38, no. 9, pp. 11401–11405, 2011.
- [38] R. B. Handfield, S. V. Walton, L. K. Seegers, and S. A. Melnyk, "'Green' value chain practices in the furniture industry," *Journal of Operations Management*, vol. 15, no. 4, pp. 293–315, 1997.
- [39] Q. Zhu, J. Sarkis, and Y. Geng, "Green supply chain management in China: pressures, practices and performance," *International Journal of Operations & Production Management*, vol. 25, no. 5, pp. 449–468, 2005.
- [40] S. H'mida and S. Y. Lakhali, "A model for assessing the greenness effort in a product supply chain," *International Journal of Global Environmental Issues*, vol. 7, pp. 4–24, 2010.
- [41] S. Y. Lee and R. D. Klassen, "Drivers and enablers that foster environmental management capabilities in small- and medium-sized suppliers in supply chains," *Production Operations Management*, vol. 17, pp. 573–586, 2010.
- [42] H.-M. Wee, M.-C. Lee, J. C. P. Yu, and C. E. Wang, "Optimal replenishment policy for a deteriorating green product: life cycle costing analysis," *International Journal of Production Economics*, vol. 133, no. 2, pp. 603–611, 2011.
- [43] I. Gavronski, R. D. Klassen, S. Vachon, and L. F. M. D. Nascimento, "A resource-based view of green supply management," *Transportation Research Part E: Logistics and Transportation Review*, vol. 47, no. 6, pp. 872–885, 2011.
- [44] A. Parmigiani, R. D. Klassen, and M. V. Russo, "Efficiency meets accountability: performance implications of supply chain configuration, control, and capabilities," *Journal of Operations Management*, vol. 29, no. 3, pp. 212–223, 2011.
- [45] A. A. Hervani, M. M. Helms, and J. Sarkis, "Performance measurement for green supply chain management," *Benchmarking: An International Journal*, vol. 12, no. 4, pp. 330–353, 2005.
- [46] S. K. Srivastava, "Green supply-chain management: a state-of-the-art literature review," *International Journal of Management Reviews*, vol. 9, pp. 53–80, 2010.
- [47] A. E. Saadany, M. Y. Jaber, and M. Bonney, "Environmental performance measures for supply chains," *Management Research Review*, vol. 34, pp. 1202–1221, 2011.
- [48] Z. Wu and M. Pagell, "Balancing priorities: decision-making in sustainable supply chain management," *Journal of Operations Management*, vol. 29, no. 6, pp. 577–590, 2011.
- [49] J. Sarkis, Q. Zhu, and K.-H. Lai, "An organizational theoretic review of green supply chain management literature," *International Journal of Production Economics*, vol. 130, no. 1, pp. 1–15, 2011.
- [50] R. Liang and J.-Q. Wang, "A linguistic intuitionistic cloud decision support model with sentiment analysis for product selection in E-commerce," *International Journal of Fuzzy Systems*, vol. 21, no. 3, pp. 963–977, 2019.
- [51] R. Handfield, S. V. Walton, R. Sroufe, and S. A. Melnyk, "Applying environmental criteria to supplier assessment: a study in the application of the analytical hierarchy process," *European Journal of Operational Research*, vol. 141, no. 1, pp. 70–87, 2002.
- [52] W.-H. Tsai and S.-J. Hung, "A fuzzy goal programming approach for green supply chain optimisation under activity-based costing and performance evaluation with a value-chain structure," *International Journal of Production Research*, vol. 47, no. 18, pp. 4991–5017, 2009.
- [53] G. Akman, "Evaluating suppliers to include green supplier development programs via fuzzy c-means and VIKOR methods," *Computers & Industrial Engineering*, vol. 86, pp. 69–82, 2015.
- [54] J.-J. Peng, C. Tian, W.-Y. Zhang, S. Zhang, and J.-Q. Wang, "An integrated multi-criteria decision-making framework for sustainable supplier selection under picture fuzzy environment," *Technological and Economic Development of Economy*, vol. 26, no. 3, pp. 573–598, 2020.
- [55] P. Ji, H.-Y. Zhang, and J.-Q. Wang, "Selecting an outsourcing provider based on the combined MABAC-ELECTRE method using single-valued neutrosophic linguistic sets," *Computers & Industrial Engineering*, vol. 120, pp. 429–441, 2018.
- [56] A. Amindoust, "A resilient-sustainable based supplier selection model using a hybrid intelligent method," *Computers & Industrial Engineering*, vol. 126, pp. 122–135, 2018.
- [57] A. Chavooshi, A. A. Bahmani, A. Darijani, A. Mootab Saei, E. Mehrabi, and M. Gholipour, "The role of wood and paper industries management of Iran in sustainable development," *Journal of Conservation and Utilization of Natural Resources*, vol. 1, pp. 79–95, 2012.
- [58] F. Sabouhi, M. S. Pishvaei, and M. S. Jabalameli, "Resilient supply chain design under operational and disruption risks

- considering quantity discount: a case study of pharmaceutical supply chain," *Computers & Industrial Engineering*, vol. 126, pp. 657–672, 2018.
- [59] C. S. Holling, "Resilience and stability of ecological systems," *Annual Review of Ecology and Systematics*, vol. 4, no. 1, pp. 1–23, 1973.
- [60] S. Hosseini, N. Morshedlou, D. Ivanov, M. D. Sarder, K. Barker, and A. A. Khaled, "Resilient supplier selection and optimal order allocation under disruption risks," *International Journal of Production Economics*, vol. 213, pp. 124–137, 2019.
- [61] S. Y. Ponomarov and M. C. Holcomb, "Understanding the concept of supply chain resilience," *The International Journal of Logistics Management*, vol. 20, no. 1, pp. 124–143, 2009.
- [62] E. Brandon-Jones, B. Squire, C. W. Autry, and K. J. Petersen, "A contingent resource-based perspective of supply chain resilience and robustness," *Journal of Supply Chain Management*, vol. 50, pp. 55–73, 2014.
- [63] D. Ivanov and B. Sokolov, "Control and system-theoretic identification of the supply chain dynamics domain for planning, analysis and adaptation of performance under uncertainty," *European Journal of Operational Research*, vol. 224, no. 2, pp. 313–323, 2013.
- [64] Y. Sheffi and B. R. James, "A supply chain view of the resilient enterprise," *MIT Sloan Management Review*, vol. 47, pp. 41–48, 2005.
- [65] R. Rajesh and V. Ravi, "Supplier selection in resilient supply chains: a grey relational analysis approach," *Journal of Cleaner Production*, vol. 86, pp. 343–359, 2015.
- [66] S. G. Azevedo, K. Govindan, H. Carvalho, and V. Cruz-Machado, "Ecosilient index to assess the greenness and resilience of the upstream automotive supply chain," *Journal of Cleaner Production*, vol. 56, pp. 131–146, 2013.
- [67] M. Sonia, L. Young, and M. Muhammad, "Sustainable and resilient supply chain network design under disruption risks," *Sustainability*, vol. 6, pp. 6666–6686, 2014.
- [68] B. Fahimnia and A. Jabbarzadeh, "Marrying supply chain sustainability and resilience: a match made in heaven," *Transportation Research Part E: Logistics and Transportation Review*, vol. 91, pp. 306–324, 2016.
- [69] B. Zahiri, J. Zhuang, and M. Mohammadi, "Toward an integrated sustainable-resilient supply chain: a pharmaceutical case study," *Transportation Research Part E: Logistics and Transportation Review*, vol. 103, pp. 109–142, 2017.
- [70] J. J. H. Liou and G.-H. Tzeng, "Comments on 'multiple criteria decision making (MCDM) methods in economics: an overview'" *Technological and Economic Development of Economy*, vol. 18, no. 4, pp. 672–695, 2012.
- [71] C.-L. Hwang and K. Yoon, "Introduction," *Multiple Attribute Decision Making*, vol. 186, pp. 1–15, 1981.
- [72] T. L. Saaty, "A scaling method for priorities in hierarchical structures," *Journal of Mathematical Psychology*, vol. 15, no. 3, pp. 234–281, 1977.
- [73] T. L. Saaty, *Decision Making with Dependence and Feedback: The Analytic Network Process*, RWS Publications, Pittsburgh, PA, USA, 1996.
- [74] S. Opricovic, *Multicriteria Optimization of Civil Engineering System*, Faculty of Civil Engineering, Belgrade, Serbia, 1998.
- [75] E. K. Zavadskas, Z. Turskis, J. Antucheviciene, and A. Zakarevicius, "Optimization of weighted aggregated sum product assessment," *Elektron Elektrotech*, vol. 122, pp. 3–6, 2012.
- [76] B. Roy, "Classement et choix en présence de points de vue multiples," *Revue Française d'Informatique et de Recherche Opérationnelle*, vol. 2, no. 8, pp. 57–75, 1968.
- [77] D. Kannan, A. B. L. D. S. Jabbour, and C. J. C. Jabbour, "Selecting green suppliers based on GSCM practices: using fuzzy TOPSIS applied to a Brazilian electronics company," *European Journal of Operational Research*, vol. 233, no. 2, pp. 432–447, 2014.
- [78] H. Gupta and M. K. Barua, "Supplier selection among SMEs on the basis of their green innovation ability using BWM and fuzzy TOPSIS," *Journal of Cleaner Production*, vol. 152, pp. 242–258, 2017.
- [79] L. Demir, M. E. Akpınar, C. Araz, and M. A. Ilgin, "A green supplier evaluation system based on a new multi-criteria sorting method: VIKORSORT," *Expert Systems with Applications*, vol. 114, pp. 479–487, 2018.
- [80] S. Gupta, U. Soni, and G. Kumar, "Green supplier selection using multi-criterion decision making under fuzzy environment: a case study in automotive industry," *Computers & Industrial Engineering*, vol. 136, pp. 663–680, 2019.
- [81] M. Keshavarz Ghorabae, E. K. Zavadskas, M. Amiri, and A. Esmaeili, "Multi-criteria evaluation of green suppliers using an extended WASPAS method with interval type-2 fuzzy sets," *Journal of Cleaner Production*, vol. 137, pp. 213–229, 2016.
- [82] R.-J. Lin, "Using fuzzy DEMATEL to evaluate the green supply chain management practices," *Journal of Cleaner Production*, vol. 40, pp. 32–39, 2013.
- [83] R. J. Kuo, Y. C. Wang, and F. C. Tien, "Integration of artificial neural network and MADA methods for green supplier selection," *Journal of Cleaner Production*, vol. 18, no. 12, pp. 1161–1170, 2010.
- [84] J. Luan, Z. Yao, F. Zhao, and X. Song, "A novel method to solve supplier selection problem: hybrid algorithm of genetic algorithm and ant colony optimization," *Mathematics and Computers in Simulation*, vol. 156, pp. 294–309, 2019.
- [85] A. Zouggari and L. Benyoucef, "Simulation based fuzzy TOPSIS approach for group multi-criteria supplier selection problem," *Engineering Applications of Artificial Intelligence*, vol. 25, no. 3, pp. 507–519, 2012.
- [86] R.-X. Nie, Z.-P. Tian, J.-Q. Wang, H.-Y. Zhang, and T.-L. Wang, "Water security sustainability evaluation: applying a multistage decision support framework in industrial region," *Journal of Cleaner Production*, vol. 196, pp. 1681–1704, 2018.
- [87] S. H. Hashemi, A. Karimi, and M. Tavana, "An integrated green supplier selection approach with analytic network process and improved Grey relational analysis," *International Journal of Production Economics*, vol. 159, pp. 178–191, 2015.
- [88] M.-L. Tseng, M. S. Islam, N. Karia, F. A. Fauzi, and S. Afrin, "A literature review on green supply chain management: trends and future challenges," *Resources, Conservation and Recycling*, vol. 141, pp. 145–162, 2019.
- [89] S.-B. Tsai, Y.-M. Wei, K.-Y. Chen, L. Xu, P. Du, and H.-C. Lee, "Evaluating green suppliers from a green environmental perspective," *Environment and Planning B: Planning and Design*, vol. 43, no. 5, pp. 941–959, 2016.
- [90] R. M. Vanalle, G. M. D. Ganga, M. G. Filho, and W. C. Lucato, "Green supply chain management: an investigation of pressures, practices, and performance within the Brazilian automotive supply chain," *Journal of Cleaner Production*, vol. 151, pp. 250–259, 2017.

- [91] V. K. Sharma, P. Chandna, and A. Bhardwaj, "Green supply chain management related performance indicators in agro industry: a review," *Journal of Cleaner Production*, vol. 141, pp. 1194–1208, 2017.
- [92] J. Johansson, H. Hassel, and E. Zio, "Reliability and vulnerability analyses of critical infrastructures: comparing two approaches in the context of power systems," *Reliability Engineering & System Safety*, vol. 120, pp. 27–38, 2013.
- [93] J. Johansson and H. Hassel, "An approach for modelling interdependent infrastructures in the context of vulnerability analysis," *Reliability Engineering & System Safety*, vol. 95, no. 12, pp. 1335–1344, 2010.
- [94] G. Scur and M. E. Barbosa, "Green supply chain management practices: multiple case studies in the Brazilian home appliance industry," *Journal of Cleaner Production*, vol. 141, pp. 1293–1302, 2017.
- [95] H. Carvalho, K. Govindan, S. G. Azevedo, and V. Cruz-Machado, "Modelling green and lean supply chains: an eco-efficiency perspective," *Resources, Conservation and Recycling*, vol. 120, pp. 75–87, 2017.
- [96] G. Zhang and Z. Zhao, "Green packaging management of logistics enterprises," *Physics Procedia*, vol. 24, pp. 900–905, 2012.
- [97] K. Govindan, S. Rajendran, J. Sarkis, and P. Murugesan, "Multi criteria decision making approaches for green supplier evaluation and selection: a literature review," *Journal of Cleaner Production*, vol. 98, pp. 66–83, 2015.
- [98] Öy Uygün and A. Dede, "Performance evaluation of green supply chain management using integrated fuzzy multi-criteria decision making techniques," *Computers & Industrial Engineering*, vol. 102, pp. 502–511, 2016.
- [99] F. Çörmü and İ Otay, "A two-stage fuzzy approach for supplier evaluation and order allocation problem with quantity discounts and lead time," *Information Sciences*, vol. 339, pp. 143–157, 2016.
- [100] S. Hosseini and K. Barker, "A Bayesian network model for resilience-based supplier selection," *International Journal of Production Economics*, vol. 180, pp. 68–87, 2016.
- [101] L. A. Zadeh, "Fuzzy sets," *Information and Control*, vol. 8, no. 3, pp. 338–353, 1965.
- [102] K. T. Atanassov, "Intuitionistic fuzzy sets," *Fuzzy Sets and Systems*, vol. 20, no. 1, pp. 87–96, 1986.
- [103] W. Wang and X. Xin, "Distance measure between intuitionistic fuzzy sets," *Pattern Recognition Letters*, vol. 26, no. 13, pp. 2063–2069, 2005.
- [104] E. Szmidt and J. Kacprzyk, "Distances between intuitionistic fuzzy sets," *Fuzzy Sets and Systems*, vol. 114, no. 3, pp. 505–518, 2000.
- [105] J. Rezaei, "Best-worst multi-criteria decision-making method: some properties and a linear model," *Omega*, vol. 64, pp. 126–130, 2015.
- [106] K. A. Alam, R. Ahmed, F. S. Butt, S.-G. Kim, and K.-M. Ko, "An uncertainty-aware integrated fuzzy AHP-WASPAS model to evaluate public cloud computing services," *Procedia Computer Science*, vol. 130, pp. 504–509, 2018.
- [107] A. Memari, A. Dargi, M. R. A. Jokar, R. Ahmad, and A. R. A. Rahim, "Sustainable supplier selection: a multi-criteria intuitionistic fuzzy TOPSIS method," *Journal of Manufacturing Systems*, vol. 50, pp. 9–24, 2019.
- [108] J. Falak, M. Kunjan, D. Nagaraju, and S. Narayanan, "Evaluation of continuous improvement techniques using hybrid MCDM technique under fuzzy environment," *Materials Today: Proceedings*, vol. 22, pp. 1295–1305, 2020.
- [109] N. Ploskas and J. Papathanasiou, "A decision support system for multiple criteria alternative ranking using TOPSIS and VIKOR in fuzzy and nonfuzzy environments," *Fuzzy Sets and Systems*, vol. 377, pp. 1–30, 2019.
- [110] S. Bid and G. Siddique, "Human risk assessment of Panchet Dam in India using TOPSIS and WASPAS multi-criteria decision-making (MCDM) methods," *Heliyon*, vol. 5, Article ID e01956, 2019.
- [111] L. Suganthi, "Multi expert and multi criteria evaluation of sectoral investments for sustainable development: an integrated fuzzy AHP, VIKOR/DEA methodology," *Sustainable Cities and Society*, vol. 43, pp. 144–156, 2018.

## Research Article

# Multiple Attribute Group Decision Making Based on Simplified Neutrosophic Integrated Weighted Distance Measure and Entropy Method

Haibo Zhang <sup>1</sup>, Zhimin Mu,<sup>2</sup> and Shouzhen Zeng <sup>1</sup>

<sup>1</sup>School of Business, Ningbo University, Ningbo 315211, China

<sup>2</sup>Department of Basic Science, Tianjin Agricultural University, Tianjin 300384, China

Correspondence should be addressed to Haibo Zhang; [haibo12500@163.com](mailto:haibo12500@163.com) and Shouzhen Zeng; [zszzxl@163.com](mailto:zszzxl@163.com)

Received 2 June 2020; Accepted 18 June 2020; Published 20 July 2020

Guest Editor: Zaoli Yang

Copyright © 2020 Haibo Zhang et al. This is an open access article distributed under the Creative Commons Attribution License, which permits unrestricted use, distribution, and reproduction in any medium, provided the original work is properly cited.

Simplified neutrosophic set (SNS) is a popular tool in modelling potential, imprecise, and uncertain information within complex environments. In this paper, a method based on the integrated weighted distance measure and entropy weight is proposed for handling SNS multiple attribute group decision-making (MAGDM) problems. To this end, the simplified neutrosophic (SN) integrated weighted distance (SVNIWD) measure is first developed for overcoming the limitations of the existing methods. Afterward, the proposed SNIWD's several properties and particular status are studied. Moreover, a flexible and useful MAGDM approach that combines the strengths of the SNIWD and the SNS is proposed, wherein the SN entropy measure is applied to calculate the unknown weight information regarding attributes. Finally, a numerical case of investment evaluation and subsequent comparative analysis are conducted to prove the superiority of the proposed framework.

## 1. Introduction

The aim of the multiple attribute group decision-making (MAGDM) problem is to determine suitable alternatives with respect to multiple attributes according to the judgement provided by various decision makers. It is impossible for a decision maker to always express an accurate preference because of the increasing uncertainties of the assessed problems. To solve the difficulties, many effective mathematical tools are introduced during the decision process. The fuzzy set (FS) firstly developed by Zadeh [1] is widely used to model imprecise and vague information in MAGDM. An element's membership value in fuzzy theory lies in the range  $[0, 1]$ , while the value of its complement is called the nonmembership. To provide a more effective method, the conception of intuitionistic FS (IFS) was proposed by Atanassov [2] which is described by membership and nonmembership functions, and their sum cannot exceed 1. Later, Yager [3] presented the Pythagorean FS (PFS), whose special merit is that the square sum of the membership and

nonmembership shall lie in interval  $[0, 1]$ . Thus, the PFS is a more powerful tool to describe uncertainties than the IFS and FS. Up to now, the PFS has gained more and more attention and has been widely used in decision making as well as other areas [4–15].

Recently, Smarandache [16] defined the idea of the neutrosophic set (NS) utilizing three parameters: the degrees of truth, indeterminacy, and false for the first time. These three components in the NS are entirely irrelevant from each other, which help people present their preference more flexibly and accurately compared with the previous IFS and PFS. To enhance the computational efficiency of the NS, Wang et al. [17] and Ye [18] put forward the concept of simplified neutrosophic set (SNS). The SNS has gained increasing attention from researchers in these years because of its preponderance in describing uncertainties. For example, Ye [19] extended the TOPSIS method to handle simplified neutrosophic (SN) environments and studied its application in selecting suppliers. Peng et al. [20] introduced an outranking method for SN MAGDM problems. Peng et al. [21]

developed some aggregation methods for SN information. Kucuk and Sahin [22] provided a hybrid method for SN decision-making in which the weight information is unknown. Ye [23] gave a netting approach to cluster SN information based on new associated coefficients. Sahin and Liu [24] developed several SN aggregation operators utilizing the possibility information. Liu and Luo [25] proposed a power aggregation to infuse the SNS and explored its usefulness in MAGDM. Ye [26] introduced a generalized ordered weighted SN cosine similarity measure and applied it to solve MAGDM problems. Zeng et al. [27] presented a novel TOPSIS approach for SN decision-making considering the high-efficiency correlation coefficient. Peng and Dai [28] conducted a bibliometric survey of the development concerning the neutrosophic set from 1998 to 2017.

Various distance measures have been put forward and used in decision-making process for reflecting the deviations between the arguments. One of the most widely used distances is the weighted distance, including weighted Hamming and weighted Euclidean distances [29]. Motivated by the ideal of the ordered weighted method [30], Xu and Chen [31] presented the ordered weighted distance (OWD) measure considering the importance of the ordered deviations by designing weight scheme. Later, Merigó and Gil-Lafuente [32] presented the ordered weighted averaging distance (OWAD) measure, and applied it to evaluate financial products. So far, a variety extensions of the OWD and the OWAD measures have been presented in the literature. Xu and Xia [33] explored the OWD with hesitant fuzzy information and developed the hesitant fuzzy OWD and hybrid weighted similarity measures. Zeng and Su [34] adapted the OWD into the IFS situation and presented the intuitionistic fuzzy OWD (IFOWD). Zeng [37] studied the usefulness of the IFOWD using a generalized mean method. Shakeel et al. [38] developed the cubic OWD (COWD) and gave its application in decision-making. Zhou et al. [37, 38] worked on several continuous OWD measures. Some authors also extended the OWD and the OWAD using more complex variables, such as the logarithmic means [39, 40], induced aggregation [41–43], and weighted average [44–46]. More recently, considering the usefulness of the SNS, Sahin and Kucuk [47] proposed the simplified neutrosophic OWD (SNOWD) and studied its performance in the group decision-making problem.

With awareness the capabilities of the SNS which are analyzed above, the purpose of this research is to propose a new SN distance measure that can correct the shortcomings of the existing methods and apply it to MAGDM. To this end, we present the simplified neutrosophic integrated weighted distance (SNIWD) measure, which combines the significance of the existing SNOWD and SN weighted distance (SNWD) measures. Therefore, it can eliminate the limitations of the SNOWD that cannot account for the importance of attribute in MAGDM problems. Moreover, it generalizes a wide kind of existing SN distance measures, including the SNOWD and the SNWD measures. We also verify the merits of the proposed SNIWD measure by exploring its application to MAGDM problems, in which the weight information of attributes is unknown.

The reminder of this paper is carried out as follows: Section 2 gives the backgrounds of the SNS and the OWD measure. Section 3 defines the SNIWD measure and studies its main properties and various cases. Section 4 constructs a MAGDM model based on the SNIWD measure and entropy measure, and a mathematical example is provided in Section 5. Finally, Section 6 draws some valuable conclusions.

## 2. Preliminaries

### 2.1. The Simplified Neutrosophic Set (SNS)

*Definition 1* (see [16]). A neutrosophic set (NS)  $P$  in a finite set  $X$  is denoted as

$$P = \{ \langle x, T_P(x), I_P(x), F_P(x) \rangle \mid x \in X \}, \quad (1)$$

where  $T_P(x)$ ,  $I_P(x)$ , and  $F_P(x)$  are called the truth, the indeterminacy, and the falsity-membership functions, respectively. Moreover,  $T_P(x)$ ,  $I_P(x)$  and  $F_P(x)$  are the standard and nonstandard subsets of real numbers  $]0^-, 1^+[$  and satisfy

$$0^- \leq \sup T_P(x) + \sup I_P(x) + \sup F_P(x) \leq 3^+. \quad (2)$$

To extend the application of the NS in engineering and science areas, Ye [18] defined the simplified neutrosophic set (SNS).

*Definition 2* (see [18]). A simplified neutrosophic set (SNS)  $Q$  in a finite set  $X$  is described in the following form:

$$Q = \{ \langle x, T_Q(x), I_Q(x), F_Q(x) \rangle \mid x \in X \}, \quad (3)$$

where  $T_Q(x)$ ,  $I_Q(x)$ , and  $F_Q(x)$  represent the truth, the indeterminacy, and the falsity-membership functions, respectively, and satisfy

$$\begin{aligned} 0 &\leq T_Q(x), I_Q(x), F_Q(x) \leq 1, \\ 0 &\leq T_Q(x) + I_Q(x) + F_Q(x) \leq 3. \end{aligned} \quad (4)$$

For convenience, element  $q = (T_q, I_q, F_q)$  is generally named as a simplified neutrosophic number (SNN), and the complement of  $q = (T_q, I_q, F_q)$  is defined as  $q^c = (F_q, 1 - I_q, T_q)$ .

Let  $q = (T_q, I_q, F_q)$  and  $s = (T_s, I_s, F_s)$  be two SNNs; some of mathematical operations are provided by Ye [18]:

- (1)  $q \oplus s = (T_q + T_s - T_q * T_s, I_q * I_s, F_q * F_s)$
- (2)  $\lambda q = (1 - (1 - T_q)^\lambda, (I_q)^\lambda, (F_q)^\lambda) \quad (\lambda > 0)$

*Definition 3* (see [19]). Let  $x_i = (T_{x_i}, I_{x_i}, F_{x_i})$  ( $i = 1, 2$ ) be two SNNs; then, the Hamming distance measure between  $x_1$  and  $x_2$  is presented as follows:

$$d_{\text{SNN}}(x_1, x_2) = \frac{1}{3} \left( |T_{x_1} - T_{x_2}| + |I_{x_1} - I_{x_2}| + |F_{x_1} - F_{x_2}| \right). \quad (5)$$

On the basis of the distance measure defined in equation (5), Sahin and Kucuk [47] proposed a SN similar measure between  $x_1$  and  $x_2$  as follows:

$$SM_{SNN}(x_1, x_2) = \frac{d_{SNN}(x_1, x_2^c)}{d_{SNN}(x_1, x_2) + d_{SNN}(x_1, x_2^c)}. \quad (6)$$

## 2.2. The SNOWD Measure

**Definition 4** (see [47]). Let  $Q = \{q_1, q_2, \dots, q_n\}$  and  $S = \{s_1, s_2, \dots, s_n\}$  be two collections of SNNs, and  $d_{SNN}(q_i, s_i)$  is the distance between SNNs  $q_i$  and  $s_i$ ; then, the simplified neutrosophic weighted distance (SNWD) measure can be defined as follows:

$$SNWD(Q, S) = \left( \sum_{i=1}^n w_i (d_{SNN}(q_i, s_i))^k \right)^{1/k}, \quad (7)$$

where  $k > 0$  and  $\omega = (\omega_1, \omega_2, \dots, \omega_n)$  is the weighted vector of  $d_{SNN}(q_i, s_i)$  such that  $\omega_i \in [0, 1]$  and  $\sum_{i=1}^n \omega_i = 1$ .

Motivated by the OWD measure [31], Sahin and Kucuk [47] proposed the conception of the SNOWD measure, whose significance property is the ordered mechanism for the aggregated information.

**Definition 5** (see [47]). Let  $Q = \{q_1, q_2, \dots, q_n\}$  and  $S = \{s_1, s_2, \dots, s_n\}$  be two sets of SNNs, and  $d_{SNN}(q_i, s_i)$  is the distance between SNNs  $q_i$  and  $s_i$ ; then, the simplified neutrosophic ordered weighted distance (SNOWD) measure is defined as

$$SNOWD(Q, S) = \left( \sum_{i=1}^n w_i (d_{SNN}(q_{\sigma(i)}, s_{\sigma(i)}))^k \right)^{1/k}, \quad (8)$$

where  $d_{SNN}(q_{\sigma(i)}, s_{\sigma(i)})$  ( $i = 1, 2, \dots, n$ ) is the reorder values such that  $d_{SNN}(q_{\sigma(1)}, s_{\sigma(1)}) \geq d_{SNN}(q_{\sigma(2)}, s_{\sigma(2)}) \geq \dots \geq d_{SNN}(q_{\sigma(n)}, s_{\sigma(n)})$ . The associated weight vector of the SNOWD is  $w = (w_1, w_2, \dots, w_n)$  with  $\sum_{i=1}^n w_i = 1$  and  $w_i \in [0, 1]$ .

The SNOWD measure possesses some good properties that the OWD also has, including boundedness, commutativity, idempotency, and monotonicity. However, the

SNOWD can only consider the weights of ordered deviations, but fail to reflect the weights (importance) of aggregated arguments that the SNWD can. Therefore, we shall propose an integrated weighted distance measure to eliminate the existing defects in the SNOWD measure.

## 3. SN Integrated Weighted Distance (SNIWD) Measure

It is observed from Definitions 1 and 5 that the SNWD can reflect the importance of the input argument but fails to account for the positions' weights of the ordered distances that the SNOWD can, while the SNOWD cannot emphasize the importance of aggregated deviations that the SNWD can. To solve the limitations, we present the SN integrated weighted distance (SNIWD) measure that can combine both merits of the SNOWD and the SNWD measures.

**Definition 6.** Let  $Q = \{q_1, q_2, \dots, q_n\}$  and  $S = \{s_1, s_2, \dots, s_n\}$  be two collections of SNNs, and  $d_{SNN}(q_i, s_i)$  is the distance between SNNs  $q_i$  and  $s_i$ ; then, the SNIWD measure is defined as

$$SNIWD(Q, S) = \left( \sum_{i=1}^n \psi_i (d_{SNN}(q_{\sigma(i)}, s_{\sigma(i)}))^k \right)^{1/k}, \quad (9)$$

where the integrated weights  $\psi_i$  are defined as

$$\psi_i = \varepsilon w_i + (1 - \varepsilon) \omega_{\sigma(i)}, \quad (10)$$

wherein  $\omega_i$  is the weight of  $d_{SNN}(q_i, s_i)$  ( $i = 1, 2, \dots, n$ ) such that  $\omega_i \in [0, 1]$  and  $\sum_{i=1}^n \omega_i = 1$ ,  $w_i$  is the relative weight of the SNIWD satisfying  $\sum_{i=1}^n w_i = 1$  and  $w_i \in [0, 1]$ , and  $\varepsilon$  is a real parameter satisfying  $\varepsilon \in [0, 1]$ .

Obviously, when  $\varepsilon = 1$  and  $\varepsilon = 0$ , the SNIWD is generalized to the SNOWD and the SNWD measures, respectively. Therefore, the SNIWD can be viewed as a combination of the SNOWD and SNWD measures, which can be proved by the following formula:

$$SNIWD(Q, S) = \left( \sum_{i=1}^n \psi_i (d_{SNN}(q_{\sigma(i)}, s_{\sigma(i)}))^k \right)^{1/k} = \left( \varepsilon \sum_{i=1}^n w_i (d_{SNN}(q_{\sigma(i)}, s_{\sigma(i)}))^k + (1 - \varepsilon) \sum_{i=1}^n \omega_i (d_{SNN}(q_i, s_i))^k \right)^{1/k}. \quad (11)$$

**Example 1.** Let

$$\begin{aligned} Q &= \{(0.9, 0.4, 0.7), (0.6, 0.2, 0.4), (0.4, 0.8, 0.5), (0.7, 0.1, 0.6)\}, \\ S &= \{(0.5, 0.5, 0.3), (0.5, 0.4, 0.1), (0.3, 0.7, 0.4), (0.4, 0.4, 0.1)\}, \end{aligned} \quad (12)$$

be two collections of SNNs; then, the computational procedure of the SNIWD is listed as follows:

- (1) Utilize equation (5) to calculate  $d_{SNN}(q_i, s_i)$  ( $i = 1, 2, \dots, 4$ ):

$$\begin{aligned} d_{SNN}(q_1, s_1) &= 0.3, \\ d_{SNN}(q_2, s_2) &= 0.2, \\ d_{SNN}(q_3, s_3) &= 0.1, \\ d_{SNN}(q_4, s_4) &= 0.4. \end{aligned} \quad (13)$$

- (2) Rank  $d_{SNN}(q_i, s_i)$  ( $i = 1, 2, \dots, 4$ ) according to the decreasing order:



$$\begin{aligned}
d_{\text{SNN}}(q_{\sigma(1)}, s_{(1)}) &= d_{\text{SNN}}(q_4, s_4) = 0.4, \\
d_{\text{SNN}}(q_{\sigma(2)}, s_{(2)}) &= d_{\text{SNN}}(q_1, s_1) = 0.3, \\
d_{\text{SNN}}(q_{\sigma(3)}, s_{(3)}) &= d_{\text{SNN}}(q_2, s_2) = 0.2, \\
d_{\text{SNN}}(q_{\sigma(4)}, s_{(4)}) &= d_{\text{SNN}}(q_3, s_3) = 0.1.
\end{aligned} \tag{14}$$

(3) Let  $w = (0.22, 0.28, 0.36, 0.14)$  and  $\omega = (0.2, 0.4, 0.1, 0.3)$ ; then, compute the integrated weights  $\psi_i$  according to equation (10) (let  $\varepsilon = 0.6$ ):

$$\begin{aligned}
\psi_1 &= 0.6 \times 0.22 + (1 - 0.6) \times 0.3 = 0.252, \\
\psi_2 &= 0.6 \times 0.28 + (1 - 0.6) \times 0.2 = 0.248, \\
\psi_3 &= 0.6 \times 0.36 + (1 - 0.6) \times 0.4 = 0.376, \\
\psi_4 &= 0.6 \times 0.14 + (1 - 0.6) \times 0.1 = 0.124.
\end{aligned} \tag{15}$$

(4) Let  $k = 2$ ; then, calculate the distance between  $Q$  and  $S$  utilizing the SNIWD measure defined in equation (9):

$$\begin{aligned}
\text{SNIWD}(Q, S) &= \left( \sum_{i=1}^4 \psi_i (d_{\text{SNN}}(q_{\sigma(i)}, s_{\sigma(i)}))^2 \right)^{1/2} \\
&= (0.252 \times 0.4^2 + 0.248 \times 0.3^2 + 0.376 \times 0.2^2 + 0.124 \times 0.1^2)^{1/2} \\
&= 0.2809.
\end{aligned} \tag{16}$$

We can also illustrate the aggregation by applying the SNIWD measure given in equation (11):

$$\begin{aligned}
\text{SNIWD}(Q, S) &= \left( \sum_{i=1}^4 \psi_i (d_{\text{SNN}}(q_{\sigma(i)}, s_{\sigma(i)}))^2 \right)^{1/2} \\
&= \left( 0.6 \times \left( \sum_{i=1}^n w_i (d_{\text{SNN}}(q_{\sigma(i)}, s_{\sigma(i)}))^2 \right) + (1 - 0.6) \times \left( \sum_{i=1}^n \omega_i (d_{\text{SNN}}(q_i, s_i))^2 \right) \right)^{1/2} \\
&= (0.6 \times 0.0762 + (1 - 0.6) \times 0.083)^{1/2} \\
&= 0.2809.
\end{aligned} \tag{17}$$

Obviously, the same results are rendered by both methods. Following the aforementioned definitions and the example, we can see that the SNIWD possesses the dual aggregated functions by combining the ordered weighted and arithmetic weighed methods, i.e., it covers both features of the previous SNOWD and the SNWD measures as it weights both the deviations and their ordered positions. Thus, it can not only reflect the weights of the input arguments themselves but also highlight the importance of their ordered positions during aggregation process. Moreover, it provides a possibility for decision makers to select suitable parameters according to actual demands or interests.

The SNIWD measure generalizes a wide range of SN distance measures by designing different values of the weights and parameters, for example:

*Remark 1.* Let  $k = 1$ ; then, we obtain the SN integrated weighted Hamming distance (SNIWHD) measure, and the SN integrated weighted Euclidean distance (SNIWED) measure is formed when  $k = 2$ .

*Remark 2.* If  $\varepsilon = 1$ , then the SNIWD is reduced to the SNOWD measure. Thus, all particular SN distance measures of the SNOWD mentioned in the result of Sahin and Kucuk [47] are the SNIWD's special cases, for example:

- (i) The SN Hamming ordered weighted distance (SNHOWD) measure ( $k = 1$ )
- (ii) The SN Euclidean ordered weighted distance (SNEOWD) measure ( $k = 2$ )
- (iii) The SN geometric ordered weighted distance (SNGOWD) measure ( $k \rightarrow 0$ )
- (iv) Maximum SN distance measure ( $w = (1, 0, 0, \dots, 0)$ )
- (v) Minimum SN distance measure ( $w = (0, 0, \dots, 0, 1)$ )
- (vi) Normalized SN distance measure ( $w = (1/n, 1/n, \dots, 1/n)$ )

*Remark 3.* If  $\varepsilon = 0$ , then the SNIWD is reduced to the SNWD measure. Then, we can achieve various families of the

SNWD that can be seen as the SNIWD's particular status, such as:

- (i) The SN Hamming weighted distance (SNHWD) measure ( $k = 1$ )
- (ii) The SN Euclidean weighted distance (SNEWD) measure ( $k = 2$ )
- (iii) The SN geometric weighted distance (SNGWD) measure ( $k \rightarrow 0$ )
- (iv) Normalized SN distance measure ( $\omega = (1/n, t1/m, q \dots h, 1/n)$ )

**Remark 4.** By applying similar analysis introduced in the recent literature [48–53], more other cases of the SNIWD measure can be created, such as the the centered-SNIWD, median-SNIWD, and the Olympic-SNIWD measures.

The following theorems show that the SNIWD measure satisfies some desirable properties of monotonicity, boundedness, idempotency, commutativity, and reflexivity.

**Theorem 1** (monotonicity). If  $d_{\text{SNN}}(q_i, s_i) \geq d_{\text{SNN}}(q'_i, s'_i)$  for  $i = 1, 2, \dots, n$ , then

$$\text{SNIWD}((q_1, s_1), \dots, (q_n, s_n)) \geq \text{SNIWD}((q'_1, s'_1), \dots, (q'_n, s'_n)). \quad (18)$$

**Theorem 2** (idempotency). If  $d_{\text{SNN}}(q_i, s_i) = d$  for  $i = 1, 2, \dots, n$ , then

$$\text{SNIWD}((q_1, s_1), \dots, (q_n, s_n)) = d. \quad (19)$$

**Theorem 3** (boundedness). Let  $d_{\min} = \min_i (d_{\text{SNN}}(q_i, s_i))$  and  $d_{\max} = \max_i (d_{\text{SNN}}(q_i, s_i))$ ; then,

$$d_{\min} \leq \text{SNIWD}((q_1, s_1), \dots, (q_n, s_n)) \leq d_{\max}. \quad (20)$$

**Theorem 4** (commutativity). If  $((q'_1, s'_1), \dots, (q'_n, s'_n))$  is any permutation of  $((q_1, s_1), \dots, (q_n, s_n))$ , then

$$\text{SNIWD}((q_1, s_1), \dots, (q_n, s_n)) = \text{SNIWD}((q'_1, s'_1), \dots, (q'_n, s'_n)). \quad (21)$$

**Theorem 5** (reflexivity). If  $q_i = s_i$  for  $i = 1, 2, \dots, n$ , then

$$\text{SNIWD}((q_1, s_1), \dots, (q_n, s_n)) = 0. \quad (22)$$

#### 4. Application in MAGDM

As a generalization of various distance measures, the SNIWD is applicable to many fields, such as data analysis, decision-making, social management, pattern recognition, and financial investment. In this section, an application in the MAGDM problems is studied. Suppose that a MAGDM problem has  $m$  different alternatives  $B_1, B_2, \dots, B_m$ , and some experts  $E_1, E_2, \dots, E_t$  are consulted to assess  $n$  finite attributes  $C_1, C_2, \dots, C_n$ . Following the available

information, the general procedure based on the SNIWD and entropy measures for MAGDM can be summarized as follows.

**Step 1.** Construct the SN individual decision matrix  $R^l = (r_{ij}^{(l)})_{m \times n}$ , where  $r_{ij}^{(l)} = (T_{ij}^{(l)}, I_{ij}^{(l)}, F_{ij}^{(l)})$  provided by expert  $e_l$  ( $l = 1, 2, \dots, t$ ) is a SNN denoting the assessment of alternative  $B_i$  with respect to attribute  $C_j$ .

**Step 2.** Determine the weight vector of experts (or decision makers) based on the similarity measure method [47]. In some actual problems, the weights of the experts cannot be determined beforehand. Thus, we introduce a method to derive the weights' information of experts based on the similar measures between individual opinions  $R^l = (r_{ij}^{(l)})_{m \times n}$  and the overall decision matrix  $R^* = (r_{ij}^{(*)})_{m \times n}$ :

$$\text{sm}(R^{(l)}, R^*) = \sum_{i=1}^n \sum_{j=1}^m \text{sm}(r_{ij}^{(l)}, r_{ij}^*), \quad (23)$$

where the distance measure  $\text{sm}(r_{ij}^{(l)}, r_{ij}^*)$  between  $r_{ij}^{(l)}$  and  $r_{ij}^*$  can be calculated by equation (6) and  $r_{ij}^{(*)} = (T_{ij}^{(*)}, I_{ij}^{(*)}, F_{ij}^{(*)})$  is the mean value of  $r_{ij}^{(l)} = (T_{ij}^{(l)}, I_{ij}^{(l)}, F_{ij}^{(l)})$  ( $l = 1, 2, \dots, t$ ) determined by the following formula:

$$T_{ij}^{(*)} = \frac{1}{t} \sum_{l=1}^t T_{ij}^{(l)}, I_{ij}^{(*)} = \frac{1}{t} \sum_{l=1}^t I_{ij}^{(l)}, F_{ij}^{(*)} = \frac{1}{t} \sum_{l=1}^t F_{ij}^{(l)}. \quad (24)$$

On the basis of the similar measures, the weight of expert  $e_l$  ( $l = 1, 2, \dots, t$ ) can be derived by the following equation:

$$\theta_l = \frac{\text{sm}(R^{(l)}, R^*)}{\sum_{l=1}^t \text{sm}(R^{(l)}, R^*)}, \quad (25)$$

where  $\theta_l \in [0, 1]$ , and  $\sum_{l=1}^t \theta_l = 1$ . Moreover, the weight of experts derived by this method has the desirable characteristic: the larger the similarity  $\text{sm}(R^{(l)}, R^*)$  is, the more closer the individual evaluation  $R^{(l)}$  to the overall evaluation  $R^*$  is and the larger the weight of expert  $e_l$  ( $l = 1, 2, \dots, t$ ) is.

**Step 3.** Calculate the collective decision matrix  $R = (r_{ij})_{m \times n}$  using the SN weighted averaging (SNWA) operator [21], where  $r_{ij} = (T_{ij}, I_{ij}, F_{ij}) = \sum_{l=1}^t \theta_l r_{ij}^{(l)}$ .

**Step 4.** Determine the weight vector of the attribute. It is often difficult to express the weight information of the attribute in advance due to time limited or experts' professional knowledge. Thus, we develop an entropy-based method to derive the importance of attribute  $C_j$  ( $j = 1, 2, \dots, n$ ):

$$\omega_j = \frac{1 - E_j}{n - \sum_{j=1}^n E_j}. \quad (26)$$

$\omega_i \in [0, 1]$  and  $\sum_{i=1}^n \omega_i = 1$ , and the entropy measure  $E_j$  introduced by Biswas et al. [54] can be calculated from the following equation 16:

$$E_j = \frac{1}{m} \sum_{i=1}^m \left( 1 - |2I_{ij} - 1| \times (T_{ij} + F_{ij}) \right). \quad (27)$$

*Step 5.* Set ideal scheme  $I = (I_1, I_2, \dots, I_n)$  utilizing the following formula:

$$I_j = (T_{I_j}, I_{I_j}, F_{I_j}) = \begin{cases} \left( \max_i T_{ij}, \min_i I_{ij}, \min_i F_{ij} \right), & \text{for the benefit attribute,} \\ \left( \min_i T_{ij}, \max_i I_{ij}, \max_i F_{ij} \right), & \text{for the cost attribute.} \end{cases} \quad (28)$$

*Step 6.* Apply the SNIWD measure to calculate the distances between alternative  $B_i (i = 1, 2, \dots, m)$  and ideal scheme  $I$ :

$$\text{SWIND}(B_i, I) = \left( \sum_{j=1}^m \psi_j d_{\text{SNN}}(r_{\sigma(ij)}, I_{\sigma(j)})^k \right)^{1/k}, \quad i = 1, 2, \dots, n. \quad (29)$$

*Step 7.* Rank the alternatives in accordance with the results obtained in the previous step, and hence, select the best choice.

## 5. Numerical Case of Investment Selection

In this section, we give a mathematical example of the investment selection problem [21] to verify the effectiveness and applicability of the presented method. A company would like to invest a sum of money to get a good return. Four possible alternatives are considered: (1)  $B_1$  is a computer company; (2)  $B_2$  is a food company; (3)  $B_3$  is a car company; and (4)  $B_4$  is an arms company. Three experts  $\{E_1, E_2, E_3\}$  are invited to assess the companies from the following attributes:  $C_1$  is the risk analysis;  $C_2$  is the environmental impact analysis, and  $C_3$  is the growth analysis, wherein  $C_1$  and  $C_3$  are of the benefit types, while  $C_2$  belongs to the cost type. Then, the decision procedures are illustrated as follows.

*Step 1.* The individual SN decision matrix provided by experts is listed in Tables 1–3.

*Step 2.* On the basis of the aforementioned decision matrix, the overall decision matrix  $R^* = (r_{ij}^{(*)})_{m \times n}$  is calculated by using equation (24), listed in Table 4.

Using equation (25), the similar measures between individual opinions  $R^{(l)} (l = 1, 2, 3)$  and the overall decision matrix  $R^*$  are calculated as

$$\begin{aligned} \text{sm}(R^{(1)}, R^*) &= 0.883, \\ \text{sm}(R^{(2)}, R^*) &= 0.903, \\ \text{sm}(R^{(3)}, R^*) &= 0.896. \end{aligned} \quad (30)$$

Thus, the weights of experts are derived as

$$\begin{aligned} \theta_1 &= 0.329, \\ \theta_2 &= 0.337, \\ \theta_3 &= 0.334. \end{aligned} \quad (31)$$

*Step 3.* According to the weights of the experts, the collective SN decision matrix can be calculated by using the SNWA operator, presented in Table 5.

*Step 4.* Applying equations (26) and (27), the weight vector of attributes is computed as  $\omega = (0.3634, 0.2862, 0.3504)$ .

*Step 5.* The results of the ideal scheme by applying equation (28) are calculated as given in Table 6.

*Step 6.* Without loss of generality, let the parameter and weight vector of the SNIWD measure be  $\varepsilon = 0.5$  and  $\omega = (0.3, 0.5, 0.2)$ , respectively. Then, based on the weights of attributes obtained in Step 5, the distances between each alternative  $B_i (i = 1, 2, 3, 4)$  and ideal scheme  $I$  are calculated by using equation (29):

$$\begin{aligned} \text{SNIWD}(B_1, I) &= 0.1526, \\ \text{SNIWD}(B_2, I) &= 0.0922, \\ \text{SNIWD}(B_3, I) &= 0.1070, \\ \text{SNIWD}(B_4, I) &= 0.0945. \end{aligned} \quad (32)$$

*Step 7.* Rank all the alternatives in accordance with the decreasing values of  $\text{SNIWD}(B_i, I)$ . The smaller the value of  $\text{SNIWD}(B_i, I)$ , the closest  $B_i$  to the ideal scheme, and thus the better alternative  $B_i$ . Therefore, the alternatives can be ranked as

$$B_2 > B_4 > B_3 > B_1. \quad (33)$$

Hence, the best alternative is  $B_2$ .

Moreover, we can apply some special cases of the SNWID mentioned in Section 4 to calculate the relative distances from the alternatives to the ideal scheme for obtaining a more comprehensive picture. The aggregation results are shown in Table 7, and the subsequent ranking order is listed in Table 8.

It can be seen in Table 8 that different ranking lists can be achieved from different cases of the SNIWD measures. Therefore, this method presents a more flexible mechanism for decision makers to choose different schemes according to their own needs or actual situations.

To perform the applicability of the presented method, we conduct a comparative research on some existing approaches for handling SN decision-making problems. We select the correlation coefficient method proposed by Ye [55], cross-entropy method by Ye [56], TOSIS method developed by Zeng et al., [27], SNWA method introduced by

TABLE 1: SN decision matrix  $R^{(1)}$ .

	$C_1$	$C_2$	$C_3$
$B_1$	(0.6, 0.2, 0.3)	(0.5, 0.1, 0.2)	(0.5, 0.1, 0.3)
$B_2$	(0.5, 0.3, 0.2)	(0.5, 0.3, 0.3)	(0.7, 0.1, 0.3)
$B_3$	(0.5, 0.1, 0.2)	(0.3, 0.1, 0.3)	(0.5, 0.2, 0.2)
$B_4$	(0.5, 0.3, 0.2)	(0.7, 0.2, 0.2)	(0.7, 0.2, 0.2)

TABLE 2: SN decision matrix  $R^{(2)}$ .

	$C_1$	$C_2$	$C_3$
$B_1$	(0.4, 0.1, 0.3)	(0.6, 0.2, 0.2)	(0.5, 0.3, 0.3)
$B_2$	(0.6, 0.1, 0.2)	(0.5, 0.2, 0.3)	(0.7, 0.2, 0.3)
$B_3$	(0.5, 0.2, 0.2)	(0.3, 0.2, 0.4)	(0.6, 0.2, 0.3)
$B_4$	(0.7, 0.3, 0.1)	(0.5, 0.1, 0.2)	(0.6, 0.3, 0.2)

TABLE 3: SN decision matrix  $R^{(3)}$ .

	$C_1$	$C_2$	$C_3$
$B_1$	(0.3, 0.2, 0.3)	(0.5, 0.3, 0.2)	(0.5, 0.2, 0.3)
$B_2$	(0.6, 0.1, 0.2)	(0.5, 0.2, 0.2)	(0.6, 0.1, 0.2)
$B_3$	(0.4, 0.2, 0.3)	(0.2, 0.2, 0.5)	(0.4, 0.2, 0.3)
$B_4$	(0.7, 0, 0.1)	(0.4, 0.3, 0.2)	(0.6, 0.1, 0.2)

TABLE 4: Overall decision matrix  $R^*$ .

	$C_1$	$C_2$	$C_3$
$B_1$	(0.448, 0.159, 0.262)	(0.552, 0.182, 0.200)	(0.500, 0.182, 0.300)
$B_2$	(0.569, 0.144, 0.200)	(0.500, 0.229, 0.262)	(0.670, 0.126, 0.262)
$B_3$	(0.469, 0.159, 0.229)	(0.268, 0.159, 0.391)	(0.507, 0.200, 0.262)
$B_4$	(0.644, 0.000, 0.126)	(0.552, 0.182, 0.200)	(0.637, 0.182, 0.200)

TABLE 5: Collective SN decision matrix  $R$ .

	$C_1$	$C_2$	$C_3$
$B_1$	(0.447, 0.158, 0.263)	(0.536, 0.182, 0.200)	(0.500, 0.182, 0.300)
$B_2$	(0.570, 0.144, 0.200)	(0.500, 0.229, 0.262)	(0.670, 0.126, 0.262)
$B_3$	(0.469, 0.159, 0.229)	(0.268, 0.159, 0.392)	(0.507, 0.200, 0.263)
$B_4$	(0.645, 0.000, 0.126)	(0.551, 0.190, 0.200)	(0.636, 0.182, 0.200)

TABLE 6: Ideal scheme.

	$C_1$	$C_2$	$C_3$
$I$	(0.645, 0.000, 0.126)	(0.268, 0.229, 0.392)	(0.670, 0.126, 0.200)

Peng et al. [21], ordered weighted SN cosine similarity measure [26], and power aggregation model provided by Liu and Luo [25]. All the ranking lists are illustrated in Table 9.

It is noted from Table 9 that the best choice is either  $B_2$  or  $B_4$ , and the ranking lists of all alternatives may vary

depending on the decision method used. The main reasons can be summarized as follows:

- (1) The proposed SNIWD and the entropy model can efficiently eliminate the large deviation opinions provided by experts through the ordered weighting mechanism, which widely exists in MAGDM problems.
- (2) An entropy model is put forward to derive the unknown weights' information of attributes in this paper. By contrast, the weights of attributes are determined by decision makers (experts) in advance in the aforementioned methods.

TABLE 7: Aggregated results rendered by particular cases of the SNIWD.

	Maximum	Minimum	SNWHD	SNWED	SNOWHD	SNOWED	SNIWHD
$B_1$	0.1643	0.1087	0.1462	0.1487	0.1546	0.1563	0.1504
$B_2$	0.1207	0.0207	0.0773	0.0883	0.0892	0.0961	0.0833
$B_3$	0.146	0.0233	0.0948	0.1068	0.0985	0.1073	0.0966
$B_4$	0.1713	0.0000	0.0595	0.0933	0.0633	0.0962	0.0630

TABLE 8: Ranking results obtained by particular cases of the SNIWD.

Method	Ranking
Maximum	$B_2 > B_3 > B_1 > B_4$
Minimum	$B_4 > B_1 > B_2 > B_3$
SNWHD	$B_2 > B_4 > B_3 > B_1$
SNWED	$B_2 > B_4 > B_3 > B_1$
SNOWHD	$B_4 > B_2 > B_3 > B_1$
SNOWED	$B_2 > B_4 > B_3 > B_1$
SNIWHD	$B_4 > B_2 > B_3 > B_1$

TABLE 9: Ranking results obtained by the existing decision-making method.

Method	Ranking
Correlation coefficient method [55]	$B_4 > B_1 > B_2 > B_3$
Cross-entropy method [56]	$B_4 > B_2 > B_3 > B_1$
TOSIS method [27]	$B_2 > B_4 > B_1 > B_3$
SNWA method [21]	$B_2 > B_4 > B_3 > B_1$
Ordered weighted cosine similarity measure method [26]	$B_2 > B_4 > B_3 > B_1$
Power aggregation method [25]	$B_4 > B_2 > B_3 > B_1$

## 6. Conclusions

In this study, we present a new approach based on the integrated distance measure and entropy weights for MAGDM with SN information. The SNIWD measure is proposed to improve the defects of the previous methods. The main advantage of the SNIWD is that it combines the ordered weighted and arithmetic weighted functions for reflecting the SN deviations. Moreover, it generalizes a great many of SN distance measures, including the SNOWD and the SNWD. Then, we develop a MAGDM approach based on the SNIWD and the entropy method within SN situations, wherein the entropy measure is utilized to determine the unknown weight information. A case study regarding selection of a suitable investment case is given to illustrate the efficiency of the proposed framework. The results and comparative study with other existing models test the advantages and effectiveness of our method. The preponderances of the proposed method based on the SNIWD measure and the entropy weight are summed up as follows: (1) the existing approaches based on the ordered weighted distance measures in decision-making areas only pay attention to the weights of the ordered deviation. They fail to account for the importance of attributes. By contrast, the introduced method based on the SNIWD can effectively fuse both importance of the ordered deviations and attributes; (2) the attribute weight is given by decision makers in advance in

the existing literature. However, we present an entropy measure method to derive the unknown attribute weight information, which helps to achieve a more objective result; and (3) the proposed method based on the SNIWD is more flexible as it provides a chance for the decision maker to select the appropriate parameters that are near to his or her interests or the needs of the decision-making problems.

In our subsequent study, we will consider some other applications of the proposed approach, such as education evaluation and social network. Some new extensions by using other variables are also considered in complex situations.

## Data Availability

No data were used to support this study.

## Conflicts of Interest

The authors declare no conflicts of interest.

## Acknowledgments

This paper was supported by Major Humanities and Social Sciences Research Projects in Zhejiang Universities (no. 2018QN058), the Zhejiang Natural Science Foundation (Project no. LY20G030006), and the Ningbo Natural Science Foundation (no. 2019A610037).

## References

- [1] L. A. Zadeh, "Fuzzy sets," *Information and Control*, vol. 8, no. 3, pp. 338–353, 1965.
- [2] K. T. Atanassov, "Intuitionistic fuzzy sets," *Fuzzy Sets and Systems*, vol. 20, no. 1, pp. 87–96, 1986.
- [3] R. R. Yager, "Pythagorean membership grades in multicriteria decision making," *IEEE Transactions on Fuzzy Systems*, vol. 22, no. 4, pp. 958–965, 2014.
- [4] T.-Y. Chen, "Remoteness index-based Pythagorean fuzzy VIKOR methods with a generalized distance measure for multiple criteria decision analysis," *Information Fusion*, vol. 41, pp. 129–150, 2018.
- [5] H. Garg, "New logarithmic operational laws and their aggregation operators for Pythagorean fuzzy set and their applications," *International Journal of Intelligent Systems*, vol. 34, pp. 82–106, 2019.
- [6] D. Liang, Z. Xu, D. Liu, and Y. Wu, "Method for three-way decisions using ideal TOPSIS solutions at Pythagorean fuzzy information," *Information Sciences*, vol. 435, pp. 282–295, 2018.
- [7] X. Peng and G. Selvachandran, "Pythagorean fuzzy set: state of the art and future directions," *Artificial Intelligence Review*, vol. 52, no. 3, pp. 1873–1927, 2019.



- [8] D. Yu, Z. Xu, and W. Wang, "Bibliometric analysis of fuzzy theory research in China: a 30-year perspective," *Knowledge-Based Systems*, vol. 141, pp. 188–199, 2018.
- [9] Z. Yang, T. Ouyang, X. Fu, and X. Peng, "A decision-making algorithm for online shopping using deep-learning-based opinion pairs mining and q-rung orthopair fuzzy interaction Heronian mean operators," *International Journal of Intelligent Systems*, vol. 35, no. 5, pp. 783–825, 2020.
- [10] Z. L. Peng, H. Garg, J. Li, G. Srivastava, and Z. Cao, "Investigation of multiple heterogeneous relationships using a q-rung orthopair fuzzy multi-criteria decision algorithm," *Neural Computing and Applications*, 2020.
- [11] G. W. Wei and M. Lu, "Pythagorean fuzzy power aggregation operators in multiple attribute decision making," *International Journal of Intelligent Systems*, vol. 33, pp. 169–186, 2018.
- [12] S. Zeng, Z. Mu, and T. Baležentis, "A novel aggregation method for pythagorean fuzzy multiple attribute group decision making," *International Journal of Intelligent Systems*, vol. 33, no. 3, pp. 573–585, 2018.
- [13] S. Zeng, X. Peng, T. Baležentis, and D. Streimikiene, "Prioritization of low-carbon suppliers based on Pythagorean fuzzy group decision making with self-confidence level," *Economic Research-Ekonomska Istraživanja*, vol. 32, no. 1, pp. 1073–1087, 2019.
- [14] C. Zhang, C. Chen, D. Streimikiene, and T. Baležentis, "Intuitionistic fuzzy MULTIMOORA approach for multi-criteria assessment of the energy storage technologies," *Applied Soft Computing*, vol. 79, pp. 410–423, 2019.
- [15] X. Zhang and Z. Xu, "Extension of TOPSIS to multiple criteria decision making with pythagorean fuzzy sets," *International Journal of Intelligent Systems*, vol. 29, no. 12, pp. 1061–1078, 2014.
- [16] F. Smarandache, *A Unifying Field in Logics. Neutrosophy: Neutrosophic Probability, Set and Logic*, American Research Press, Rehoboth, MA, USA, 1999.
- [17] H. Wang, F. Smarandache, Y. Q. Zhang, and R. Sunderraman, "Single valued neutrosophic sets," *Multispace Multistruct*, vol. 4, pp. 410–413, 2010.
- [18] J. Ye, "A multicriteria decision-making method using aggregation operators for simplified neutrosophic sets," *Journal of Intelligent & Fuzzy Systems*, vol. 26, no. 5, pp. 2459–2466, 2014a.
- [19] J. Ye, "An extended TOPSIS method for multiple attribute group decision making based on single valued neutrosophic linguistic numbers," *Journal of Intelligent & Fuzzy Systems*, vol. 28, no. 1, pp. 247–255, 2015.
- [20] J.-j. Peng, J.-q. Wang, H.-y. Zhang, and X.-h. Chen, "An outranking approach for multi-criteria decision-making problems with simplified neutrosophic sets," *Applied Soft Computing*, vol. 25, pp. 336–346, 2014.
- [21] J.-j. Peng, J.-q. Wang, J. Wang, H.-y. Zhang, and X.-h. Chen, "Simplified neutrosophic sets and their applications in multi-criteria group decision-making problems," *International Journal of Systems Science*, vol. 47, no. 10, pp. 2342–2358, 2015.
- [22] G. D. Küçük and R. Şahin, "A novel hybrid approach for simplified neutrosophic decision-making with completely unknown weight information," *International Journal for Uncertainty Quantification*, vol. 8, no. 2, pp. 161–173, 2018.
- [23] J. Ye, "A netting method for clustering-simplified neutrosophic information," *Soft Computing*, vol. 21, no. 24, pp. 7571–7577, 2017.
- [24] R. Şahin and P. D. Liu, "Possibility-induced simplified neutrosophic aggregation operators and their application to multi-criteria group decision-making," *Journal of Experimental & Theoretical Artificial Intelligence*, vol. 4, pp. 769–785, 2017.
- [25] C. Liu and Y. Luo, "Power aggregation operators of simplified neutrosophic sets and their use in multi-attribute group decision making," *IEEE/CAA Journal of Automatica Sinica*, vol. 6, no. 2, pp. 575–583, 2019.
- [26] J. Ye, "Generalized ordered weighted simplified neutrosophic cosine similarity measure for multiple attribute group decision making," *International Journal of Cognitive Informatics and Natural Intelligence*, vol. 14, no. 1, pp. 51–62, 2020.
- [27] S. Zeng, D. Luo, C. Zhang, and X. Li, "A correlation-based TOPSIS method for multiple attribute decision making with single-valued neutrosophic information," *International Journal of Information Technology & Decision Making*, vol. 19, no. 01, pp. 343–358, 2020.
- [28] X. D. Peng and J. G. Dai, "A bibliometric analysis of neutrosophic set: two decades review from 1998 to 2017," *Artificial Intelligence Review*, vol. 53, pp. 199–255, 2020.
- [29] A. Kaufmann, *Introduction to the Theory of Fuzzy Subsets*, Academic Press, New York, NY, USA, 1975.
- [30] R. R. Yager, "On ordered weighted averaging aggregation operators in multicriteria decisionmaking," *IEEE Transactions on Systems, Man, and Cybernetics*, vol. 18, no. 1, pp. 183–190, 1988.
- [31] Z. S. Xu and J. Chen, "An overview of distance and similarity measures of intuitionistic fuzzy sets," *International Journal of Uncertainty, Fuzziness and Knowledge-Based Systems*, vol. 16, no. 04, pp. 529–555, 2008.
- [32] J. M. Merigó and A. M. Gil-Lafuente, "New decision-making techniques and their application in the selection of financial products," *Information Sciences*, vol. 180, no. 11, pp. 2085–2094, 2010.
- [33] Z. Xu and M. Xia, "Distance and similarity measures for hesitant fuzzy sets," *Information Sciences*, vol. 181, no. 11, pp. 2128–2138, 2011.
- [34] S. Zeng and W. Su, "Intuitionistic fuzzy ordered weighted distance operator," *Knowledge-Based Systems*, vol. 24, no. 8, pp. 1224–1232, 2011.
- [35] S. Zeng, "Some intuitionistic fuzzy weighted distance measures and their application to group decision making," *Group Decision and Negotiation*, vol. 22, no. 2, pp. 281–298, 2013.
- [36] M. Shakeel, S. Abdullah, and R. Ahmed, "Cubic ordered weighted distance operator and application in group decision-making," *Journal of Intelligent Systems*, vol. 29, no. 1, pp. 440–458, 2020.
- [37] L. Zhou, H. Chen, and J. Liu, "Continuous ordered weighted distance measure and its application to multiple attribute group decision making," *Group Decision and Negotiation*, vol. 22, no. 4, pp. 739–758, 2013.
- [38] L. Zhou, J. Wu, and H. Chen, "Linguistic continuous ordered weighted distance measure and its application to multiple attributes group decision making," *Applied Soft Computing*, vol. 25, pp. 266–276, 2014.
- [39] V. G. Alfaro-García, J. M. Merigó, A. M. Gil-Lafuente, and J. Kacprzyk, "Logarithmic aggregation operators and distance measures," *International Journal of Intelligent Systems*, vol. 33, no. 7, pp. 1488–1506, 2018.
- [40] V. G. Alfaro-García, J. M. Merigó, L. Plata-Pérez, G. G. Alfaro-Calderon, and A. M. Gil-Lafuente, "Induced and logarithmic distances with multi-region aggregation operators," *Technological and Economic Development of Economy*, vol. 25, pp. 664–692, 2019.
- [41] J. M. Merigó and M. Casanovas, "Decision-making with distance measures and induced aggregation operators,"



- Computers & Industrial Engineering*, vol. 60, no. 1, pp. 66–76, 2011.
- [42] W. Xue, S. Xian, and Y. Dong, “A novel intuitionistic fuzzy induced ordered weighted euclidean distance operator and its application for group decision making,” *International Journal of Intelligent Systems*, vol. 32, no. 7, pp. 739–753, 2017.
  - [43] L. Yu, S. Zeng, J. M. Merigó, and C. Zhang, “A new distance measure based on the weighted induced method and its application to Pythagorean fuzzy multiple attribute group decision making,” *International Journal of Intelligent Systems*, vol. 34, no. 7, pp. 1440–1454, 2019.
  - [44] C. Cao, S. Zeng, and D. Luo, “A single-valued neutrosophic linguistic combined weighted distance measure and its application in multiple-attribute group decision-making,” *Symmetry*, vol. 11, no. 2, p. 275, 2019.
  - [45] J. M. Merigó, D. Palacios-Marqués, and P. Soto-Acosta, “Distance measures, weighted averages, OWA operators and Bonferroni means,” *Applied Soft Computing*, vol. 50, pp. 356–366, 2017.
  - [46] S. Zeng and Y. Xiao, “A method based on TOPSIS and distance measures for hesitant fuzzy multiple attribute decision making,” *Technological and Economic Development of Economy*, vol. 24, no. 3, pp. 969–983, 2018.
  - [47] R. Sahin and G. D. Kucuk, “Group decision making with simplified neutrosophic ordered weighted distance operator,” *Mathematical Methods in the Applied Sciences*, vol. 41, pp. 4795–4809, 2018.
  - [48] T. Balezentis, D. Streimikiene, R. Melnikienė, and S. Z. Zeng, “Prospects of green growth in the electricity sector in Baltic States: pinch analysis based on ecological footprint,” *Resources Conservation and Recycling*, vol. 142, pp. 37–48, 2019.
  - [49] S. D. Xian, Y. Xiao, L. Li, and D. X. Yu, “Trapezoidal Pythagorean fuzzy linguistic entropic combined ordered weighted Minkowski distance operator based on preference relations,” *International Journal of Intelligent Systems*, vol. 34, pp. 2196–2224, 2019.
  - [50] Z. Yang, X. Li, H. Garg, and M. Qi, “Decision support algorithm for selecting an antivirus mask over COVID-19 pandemic under spherical normal fuzzy environment,” *International Journal of Environmental Research and Public Health*, vol. 17, no. 10, p. 3407, 2020c.
  - [51] Z. Yang and J. Chang, “Interval-valued pythagorean normal fuzzy information aggregation operators for multi-attribute decision making,” *IEEE Access*, vol. 8, pp. 51295–51314, 2020d.
  - [52] D. Yu and Z. Xu, “Intuitionistic fuzzy two-sided matching model and its application to personnel-position matching problems,” *Journal of the Operational Research Society*, vol. 71, no. 2, pp. 312–321, 2020.
  - [53] S. Zeng, J. Chen, and X. Li, “A hybrid method for pythagorean fuzzy multiple-criteria decision making,” *International Journal of Information Technology & Decision Making*, vol. 15, no. 02, pp. 403–422, 2016.
  - [54] P. Biswas, S. Pramanik, and B. C. Giri, “Entropy based grey relational analysis method for multi-attribute decision making under single valued neutrosophic assessments,” *Neutrosophic Sets and Systems*, vol. 2, pp. 102–110, 2014.
  - [55] J. Ye, “Multicriteria decision-making method using the correlation coefficient under single-valued neutrosophic environment,” *International Journal of General Systems*, vol. 42, no. 4, pp. 386–394, 2013.
  - [56] J. Ye, “Single valued neutrosophic cross-entropy for multi-criteria decision making problems,” *Applied Mathematical Modelling*, vol. 38, no. 3, pp. 1170–1175, 2014b.

## Research Article

# Research on Probability Mean-Lower Semivariance-Entropy Portfolio Model with Background Risk

Qi Wu,<sup>1</sup> Yuelin Gao<sup>1,2</sup> and Ying Sun<sup>2</sup>

<sup>1</sup>Ningxia Province Key Laboratory of Intelligent Information and Data Processing, North Minzu University, Yinchuan 750021, China

<sup>2</sup>Ningxia Cooperative Innovation Center of Scientific Computing and Intelligent Information Processing, North Minzu University, Yinchuan 750021, China

Correspondence should be addressed to Yuelin Gao; [gaoyuelin@263.net](mailto:gaoyuelin@263.net)

Received 29 March 2020; Accepted 5 June 2020; Published 17 July 2020

Guest Editor: Zaoli Yang

Copyright © 2020 Qi Wu et al. This is an open access article distributed under the Creative Commons Attribution License, which permits unrestricted use, distribution, and reproduction in any medium, provided the original work is properly cited.

In the financial market, investors must deal with uncertain risk, and they also face background risk and many uncertain factors caused by their own characteristics. Considering the fuzzy nature of these factors as well as investors' risk preferences, transaction costs, and so on, in order to reduce investment risk, an improved probability entropy measure is introduced, and a probability mean-lower semivariance-entropy model with different risk attitudes is established by using fuzzy sets and probability theory. To solve the portfolio model, an improved differential evolution algorithm is proposed and a numerical example is given. The numerical results show that the proposed algorithm is effective and that the model can disperse the financial risk to a certain extent and reasonably solve the portfolio problem under many different conditions.

## 1. Introduction

The portfolio problem studies how to reasonably distribute the wealth in the hands of investors to different assets in order to realize the rapid growth of wealth and control investment risk. Markowitz [1] put forward the classical mean-variance (m-v) model in 1952, which provided the theoretical basis for the portfolio problem and introduced the era of quantitative analysis. The basic idea is to measure returns via the expected return of an asset, to measure the risk via the variance of the return of an asset, to minimize the risk when the expected return of a portfolio is certain, or to maximize the expected return of a portfolio when the risk taken by the investor is certain. Many researchers, such as Yu and Lee [2] and Shen et al. [3], have made many extensions to this. The models mentioned above measure the risk using the variance. Because the distribution of asset returns is asymmetrical, using the variance to measure risk may sacrifice too much of the expected returns in the process of eliminating the extreme low or high returns. To express or measure the real investment risk in financial market more

accurately, scholars have proposed new risk measurement indicators that can be used instead of the variance. For example, Petters and Dong [4] introduce the capital asset pricing model (CAPM), the linear factor model and the concepts of the value at risk, and the conditional value at risk and related risk measurements. Kang and Li [5] propose a unified framework to solve the distributed robust average risk optimization problem, which uses the variance, VaR, and CVaR as the three risk measures. Ma et al. [6] employ the Lagrange dual method and the BSDE theory to tackle a continuous-time m-v asset-liability management problem. To explore the multiple heterogeneous relationships among membership functions and criteria, a novel decision algorithm is based on q-ROF set in literature [7] to deal with these using interactive operators and Maclaurin symmetric mean (MSM) operators.

Financial market risk is considered to be uncertain, and Shape [8] is of the view that the uncertainty in financial markets cannot be predicted based on certainty. Risk, uncertainty, and randomness are equal to each other. Probability theory is used to describe random uncertainty. Qin [9]

first gives a measure of the variance of portfolio returns, verifies it based on uncertainty theory, and then introduces the corresponding mean-variance model. Zhang and Chen [10] study the mean-variance portfolio selection problem with system switching under the constraint of banning short selling. However, a financial market is an extremely complex system, and the influence of human factors on investors' decision-making in the investment process should not be underestimated. Investors will make different investment decisions under the influence of social factors, psychological factors, subjective will, and personal experience. In the light of these factors, in 1970, Bellman and Zadeh [11] put forward the theory of fuzzy decision-making. Tiryaki and Fang et al. [12] describe the investor's point of view with fuzzy sets; construct two fuzzy Black-Litterman models with the fuzzy view and the fuzzy random view, respectively; redefine the expected return and uncertainty matrix of view; and use fuzzy methods to appropriately represent the view. It is shown that the fuzzy method can better represent the information in the view and more accurately measure the uncertainty. Tsaur [13] develops a fuzzy portfolio model that focuses on different investor risk attitudes and thus enables fuzzy portfolio selection for investors with different risk attitudes. Yang et al. [14] proposed a deep-learning model, and the sentiment dictionary is used to calculate sentiment orientation, which is represented by the q-rung orthopair fuzzy set. Due to the uncertainty effects of COVID-19 and limits of human cognition, Yang et al. [15] proposed a decision support algorithm based on the novel concept of the spherical normal fuzzy (SpNoF) set.

In the investment process, people face not only financial risks but also background risks, including those related to labour income, proprietary income, real estate investment, unexpected expenses caused by health problems, health insurance, and so on. Different investors have different attitudes towards risk, and extremely rational investors are absolutely risk averse. How to diversify investment to reduce risk has become a hot issue that has been studied by researchers. As early as 1952, Markowitz put forward a view of the "Don't put your eggs in the same basket," which fully illustrates the importance of decentralized investment. At present, some scholars have used proportional entropy as a combined measure for decentralized portfolios. Huang [16] considers the credibility applying the mean-variance model and mean-semivariance model to proportional entropy fuzzy portfolios, as well as the clear form of the corresponding model. Lassance and Vrins [17] accurately quantify the uncertainty embedded in a distribution using a target function that depends on the R'enyi entropy index and considers the high-order moments. The portfolio generates a number of minimum variance combinations that are superior to the prior settings by minimizing the R'enyi entropy in terms of the risk-working capital trade closure. Fang et al. [18] consider the degree of diversification of a portfolio. Lee et al. [19] consider the limited control of total funds, such as the total, risk, and liquidity, to achieve a distributed strategic asset allocation with global constraints. Li et al. [20] discuss fuzzy multiobjective dynamic portfolio optimization for time-inconsistent investors, establish a model to

simultaneously maximize the cumulative combined objective function and minimize the cumulative portfolio variance, and design and propose a multiobjective dynamic evolutionary algorithm as a possible solution to the proposed model. A novel approach based on the genetic algorithm (GA) for feature selection and parameter optimization of support vector machine (SVM) is proposed in literature [21]. Yang and Chang [22] proposed the interval-valued Pythagorean normal fuzzy (IVPNF) sets by introducing the NFN into IVPF environment.

The structure of the remainder of this paper is as follows. In Section 2, the relevant concepts are given, including the membership function of the trapezoid fuzzy number, the mean probability value, the lower semivariance of the probability, and so on. In Section 3, the establishment process of the probability mean-lower semivariance-entropy model is given. In Section 4, an improved differential evolution algorithm is designed to solve the model. Section 5 uses Chinese stock market data to conduct the empirical analysis, including the investors with different risk attitudes. It contains the two aspects of background risk and transaction costs and discusses the portfolio problem of how risk attitudes and background risk affect investors' decision-making. Finally, some conclusions are given in Section 6.

## 2. Preliminaries

*Definition 1.* Li [23] defined a fuzzy set as  $\tilde{A} \in F(U)$ , for any  $\gamma \in [0, 1]$ . Then, fuzzy set  $\tilde{A}$  with a  $\gamma$ -level set  $[\tilde{A}]^\gamma$  is defined as

$$[\tilde{A}]^\gamma = \{x \mid x \in U, \mu_{\tilde{A}}(x) \geq \gamma\} = [\underline{a}(\gamma), \bar{a}(\gamma)], \quad (1)$$

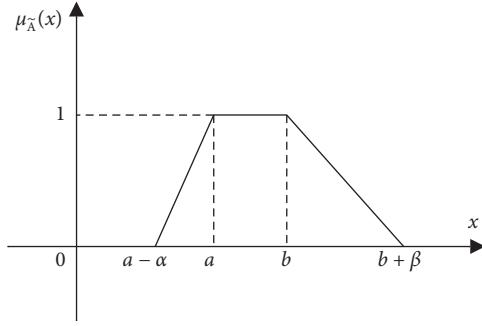
where  $\gamma$  is the confidence level.  $\underline{a}(\gamma)$  and  $\bar{a}(\gamma)$  are denoted as the left and right endpoints of the  $\gamma$  level set, respectively.

*Definition 2.* Li [23] defined  $\tilde{A} = (a, b, \alpha, \beta)$  is a trapezoidal fuzzy number. Then, the membership function of the trapezoidal fuzzy number with the risk attitude is defined as

$$\mu_{\tilde{A}}(x) = \begin{cases} 1 - \left(\frac{a-x}{\alpha}\right)^k, & a - \alpha \leq x \leq a, \\ 1, & a \leq x \leq b, \\ 1 - \left(\frac{x-b}{\beta}\right)^k, & b \leq x \leq b + \beta, \\ 0, & \text{otherwise,} \end{cases} \quad (2)$$

where  $k$  is a real number greater than 0, which is the fitness of the risk attitude. The  $[a, b]$  known as the trapezoidal fuzzy number of peak area,  $\alpha$  and  $\beta$ , respectively, is called  $\tilde{A}$  width of left and right, as shown in Figure 1. By finding the derivative of the above membership function, we can know that the smaller the  $k$  is, the more averse the investors are to risk.

In view of the above formula of (2) of the trapezoidal fuzzy number with the risk attitude and the definition of

FIGURE 1: Membership function of trapezoidal fuzzy number  $\tilde{A}$ .

$\gamma$ -level set, the  $\gamma$ -level set [23] of  $\tilde{A}$  can be obtained as follows:  $[\tilde{A}]^\gamma = [\underline{a}, \bar{a}] = [a - \alpha(1 - \gamma)^{1/k}, b + \beta(1 - \gamma)^{1/k}]$ .

The upper and lower mean probabilities of trapezoidal fuzzy number  $\tilde{A}$  with the risk attitude [23] are, respectively, denoted as

$$M^+(\tilde{A}) = 2 \int_0^1 \gamma [b + \beta(1 - \gamma)^{1/k}] d\gamma = b + \frac{2k^2\beta}{(2k+1)(k+1)}, \quad (3)$$

$$M^-(\tilde{A}) = 2 \int_0^1 \gamma [a - \alpha(1 - \gamma)^{1/k}] d\gamma = a - \frac{2k^2\alpha}{(2k+1)(k+1)}. \quad (4)$$

Via formulas (3) and (4), the mean value of the clear probability of trapezoidal fuzzy number  $\tilde{A}$  with the risk attitude [23] is denoted as

$$M(\tilde{A}) = \frac{1}{2} (M^-(\tilde{A}) + M^+(\tilde{A})) = \frac{a+b}{2} + \frac{k^2(\beta - \alpha)}{(2k+1)(k+1)}. \quad (5)$$

The upper and lower semivariances of the probability of trapezoidal fuzzy number  $\tilde{A}$  with the risk attitude are as follows:

$$\text{Var}^+(\tilde{A}) = 2 \int_0^1 \gamma (M(\tilde{A}) - \bar{a}(\gamma))^2 d\gamma, \quad (6)$$

$$\text{Var}^-(\tilde{A}) = 2 \int_0^1 \gamma (M(\tilde{A}) - \underline{a}(\gamma))^2 d\gamma. \quad (7)$$

From the above formulas (6) and (7), the clear variance of the probability of trapezoidal fuzzy number  $\tilde{A}$  with the risk attitude [23] is denoted as

$$\begin{aligned} \text{Var}(\tilde{A}) &= \frac{1}{2} \int_0^1 \gamma [\bar{a}(\gamma) - \underline{a}(\gamma)]^2 d\gamma \\ &= \frac{1}{2} \int_0^1 \gamma [b + \beta(1 - \gamma)^{1/k} - (a - \alpha(1 - \gamma)^{1/k})]^2 d\gamma \\ &= \frac{(b-a)^2}{4} + \frac{k^2(b-a)(\alpha+\beta)}{(2k+1)(k+1)} + \frac{k^2(\alpha+\beta)^2}{4(k+1)(k+2)}. \end{aligned} \quad (8)$$

### 3. Establishment of Model

The securities market is an extremely complex system. The returns and risk of securities are uncertain, and especially the influence of human factors on investment decisions cannot be ignored. In many cases, the returns and risks of securities can only be described in some vague languages, such as low risk and low return and high risk and high return. This makes investors make investment decisions in vague environments. For the convenience of the explanation, first of all, the relevant symbols involved in this paper are given as follows:

$\tilde{r}_i = (a_i, b_i, \alpha_i, \beta_i)$  represents the rate of return on financial risk asset  $i$

$\tilde{r}_b = (a_b, b_b, \alpha_b, \beta_b)$  represents the rate of return on background risk asset  $b$

$c_i$  represents the unit transaction cost of asset  $i$

$X = (x_1, x_2, \dots, x_n)$  represents the asset portfolio

$x_i$  represents the investment proportion of risk asset  $i$

$k$  represents the fitness value of the risk attitude, where  $k$  is a real number greater than 0

$\text{Cov}(\tilde{r}_i, \tilde{r}_j)$  represents the possible covariance between asset  $i$  and asset  $j$

$\text{Cov}(\tilde{r}_i, \tilde{r}_b)$  represents the possible covariance between financial risk asset  $i$  and background risk asset  $b$

$S(x)$  represents the likelihood entropy

Suppose there are  $n$  kinds of assets in the market, and the rate of return  $\tilde{r}_i$  of each asset is a trapezoidal fuzzy variable  $\tilde{r}_i = (a_i, b_i, \alpha_i, \beta_i)$ ,  $i = 1, 2, \dots, n$  with the risk attitude. The corresponding  $\gamma$  level set is denoted as  $[\tilde{r}_i] = [r_{i1}(\gamma), r_{i2}(\gamma)] = [a_i - \alpha_i(1 - \gamma)^{1/k}, b_i + \beta_i(1 - \gamma)^{1/k}]$ .

The membership function of financial risk assets with risk attitude [23] is as follows:

$$\mu_{\tilde{r}_i}(x) = \begin{cases} 1 - \left( \frac{a_i - x}{\alpha_i} \right)^k, & a_i - \alpha_i \leq x \leq a_i, \\ 1, & a_i \leq x \leq b_i, \\ 1 - \left( \frac{x - b_i}{\beta_i} \right)^k, & b_i \leq x \leq b_i + \beta_i, \\ 0, & \text{otherwise.} \end{cases} \quad (9)$$

It is assumed that the return of the asset with background risk  $\tilde{r}_b$  is also a trapezoidal fuzzy variable  $\tilde{r}_b = (a_b, b_b, \alpha_b, \beta_b)$  with the risk attitude and the corresponding  $\gamma$  level set is denoted as  $[\tilde{r}_b] = [r_{b1}(\gamma), r_{b2}(\gamma)] = [a_b - \alpha_b(1 - \gamma)^{1/k}, b_b + \beta_b(1 - \gamma)^{1/k}]$ . The membership function [18] of the asset with background risk is as follows:

$$\mu_{\tilde{r}_b}(x) = \begin{cases} 1 - \left(\frac{a_b - x}{\alpha_b}\right)^k, & a_b - \alpha_b \leq x \leq a_b, \\ 1, & a_b \leq x \leq b_b, \\ 1 - \left(\frac{x - b_b}{\beta_b}\right)^k, & b_b \leq x \leq b_b + \beta_b, \\ 0, & \text{otherwise.} \end{cases} \quad (10)$$

Suppose the investment strategy is self-financing; that is, no new funds are injected into the portfolio adjustment process. For the transaction cost function, we use the commonly used V-type function to represent it. Therefore, the total transaction cost of the portfolio is expressed as

$$C = \sum_{i=1}^n c_i |x_i - x_i^0|. \quad (11)$$

Thus, the equation containing background risks and transaction costs is expressed as follows:

$$\tilde{R} = \sum_{i=1}^n \tilde{r}_i x_i + \tilde{r}_b - C. \quad (12)$$

Because the linear combination of the trapezoidal fuzzy numbers is a trapezoidal fuzzy number,  $\sum_{i=1}^n \tilde{r}_i x_i + \tilde{r}_b = (\sum_{i=1}^n x_i \alpha_i + \alpha_b, \sum_{i=1}^n x_i b_i + b_b, \sum_{i=1}^n x_i \alpha_i + \alpha_b, \sum_{i=1}^n x_i \beta_i + \beta_b)$ .

Via formulas (3)–(5), the mean value of the clear probability of trapezoidal fuzzy number  $\tilde{R}$  with the risk attitude, background risk, and transaction cost is denoted as

$$\begin{aligned} M(\tilde{R}) &= M\left(\sum_{i=1}^n \tilde{r}_i x_i + \tilde{r}_b - C\right) \\ &= \sum_{i=1}^n x_i M(\tilde{r}_i) + M(\tilde{r}_b) - c_i |x_i - x_i^0| \\ &= \sum_{i=1}^n x_i \left( \frac{a_i + b_i}{2} + \frac{k^2(\beta_i - \alpha_i)}{(2k+1)(k+1)} \right) + \frac{a_b + b_b}{2} \\ &\quad + \frac{k^2(\beta_b - \alpha_b)}{(2k+1)(k+1)} - c_i |x_i - x_i^0|. \end{aligned} \quad (13)$$

From formula (7), the lower semivariance of the clear probability of the trapezoid fuzzy number  $\tilde{R}$  is expressed as

$$\begin{aligned} \text{Var}^-(\tilde{R}) &= \text{Var}^-\left(\sum_{i=1}^n \tilde{r}_i x_i + \tilde{r}_b - C\right) \\ &= \sum_{i=1}^n x_i^2 \text{Var}^-(\tilde{r}_i) + 2 \sum_{i < j=1}^n x_i x_j \text{Cov}^-(\tilde{r}_i, \tilde{r}_j) + \text{Var}^-(\tilde{r}_b) + 2 \sum_{i=1}^n x_i \text{Cov}^-(\tilde{r}_i, \tilde{r}_b) \\ &= \sum_{i=1}^n x_i^2 \left\{ \frac{(b_i - a_i)^2}{4} + \frac{k^2 \alpha_i^2}{(k+1)(k+2)} + \frac{k^2(b_i - a_i)(\alpha_i + \beta_i)}{(2k+1)(k+1)} + \frac{k^4(\beta_i - \alpha_i)(\beta_i + 3\alpha_i)}{[(2k+1)(k+1)]^2} \right\} \\ &\quad + \sum_{i < j=1}^n x_i x_j \left\{ \frac{(b_i - a_i)(b_j - a_j)}{2} + \frac{k^2[(b_i - a_i)(\alpha_j + \beta_j) + (b_j - a_j)(\alpha_i + \beta_i)]}{(2k+1)(k+1)} + \frac{2k^2 \alpha_i^2}{(k+2)(k+1)} \right. \\ &\quad \left. + \frac{2k^4[(\beta_i - \alpha_i)(\alpha_j + \beta_j) + 2\alpha_i(\beta_j - \alpha_j)]}{[(2k+1)(k+1)]^2} \right\} \\ &\quad + \frac{(b_b - a_b)^2}{4} + \frac{k^2 \alpha_b^2}{(k+1)(k+2)} + \frac{k^2(b_b - a_b)(\beta_b + \alpha_b)}{(2k+1)(k+1)} + \frac{k^4(\beta_b - \alpha_b)(\beta_b + 3\alpha_b)}{[(2k+1)(k+1)]^2} \\ &\quad + \sum_{i=1}^n x_i \left\{ \frac{(b_i - a_i)(b_b - a_b)}{2} + \frac{k^2[(b_i - a_i)(\alpha_b + \beta_b) + (b_b - a_b)(\alpha_i + \beta_i)]}{(2k+1)(k+1)} + \frac{2k^2 \alpha_i \alpha_b}{(k+2)(k+1)} \right. \\ &\quad \left. + \frac{2k^4[(\beta_i - \alpha_i)(\alpha_b + \beta_b) + 2\alpha_i(\beta_b - \alpha_b)]}{[(2k+1)(k+1)]^2} \right\}. \end{aligned} \quad (14)$$

In the traditional mean-variance model, the variance is usually used to measure the risk in a portfolio. In fact, it is

inappropriate to measure risk using the variance for the following reasons: (1) it only describes the degree of



deviation of the return, and it does not describe the direction of the deviation; and (2) the variance does not reflect the losses of the portfolio. Therefore, this paper measures the risk using the lower semivariance of the probability of the rate of return on assets and measures the return using the mean probability of the rate of return on assets from the above formulas (11), (12). Assuming that the investor is rational and short-selling is prohibited in the whole investment process, the following model is constructed:

$$\begin{aligned} \min \quad & \text{Var}^-(\bar{R}) = \text{Var}^-\left(\sum_{i=1}^n \tilde{r}_i x_i + \tilde{r}_b - C\right), \\ \text{s.t.} \quad & M\left(\sum_{i=1}^n \tilde{r}_i x_i + \tilde{r}_b\right) - \sum_{i=1}^n c_i |x_i - x_i^0| \geq r, \\ & \sum_{i=1}^n x_i = 1, \quad x_i \geq 0, \quad i = 1, 2, \dots, n, \end{aligned} \quad (15)$$

where  $r$  represents the minimum level of the investor's net return on the portfolio.

In recent years, according to information entropy theory, many scholars use the proportional entropy as an index to measure the degree of portfolio diversification. The concept of entropy was introduced by the German physicist Rudolph Clausius in 1850 and applied to thermodynamics to express the degree of confusion in the distribution of any kind of energy in space. The more chaotic an energy distribution is, the greater the entropy is. In 1948, Shannon [24] first introduced the concept of entropy into information theory, which is defined as follows.

It is assumed that a random test with  $n$  results is performed, and the discrete probability of each result is  $p_i$  ( $i = 1, 2, \dots, n$ ). The information entropy is

$$S(p_1, p_2, \dots, p_n) = -\sum_{i=1}^n p_i \ln(p_i), \quad (16)$$

where  $p_i$  ( $i = 1, 2, \dots, n$ ) represents the probability of a sample occurrence and it satisfies  $\sum_{i=1}^n p_i = 1$ .

As a measure of the degree of chaos, entropy has the following properties:

- (1) Nonnegative:  $S(p_1, p_2, \dots, p_n) = -\sum_{i=1}^n p_i \ln(p_i) \geq 0$
- (2) Additivity: for independent events, the sum of entropies is equal to the entropy of sum
- (3) Extremum property: when the probability of the occurrence of all samples is equal, that is,  $p_i = (1/n)$  ( $i = 1, 2, \dots, n$ ), its entropy reaches the maximum,  $S(p_1, p_2, \dots, p_n) \leq S((1/n), (1/n), \dots, (1/n)) = \ln n$
- (4) Asperity:  $S(p_1, p_2, \dots, p_n)$  is a symmetric concave function for all variables

From the above properties, it is not difficult to find that the information entropy measures the uncertainty of the information. When the information entropy is larger, the uncertainty of the information is greater, and the utility value is smaller. In contrast, the smaller the information entropy is, the smaller the uncertainty of the information is, and the greater the utility value is.

In the investment portfolio research, many researchers use the information entropy to measure the degree of risk diversification in the portfolio, replace the probability of the sample appearance with the investment proportion of the assets in the portfolio, and obtain the measurement index of the degree of decentralization. The proportional entropy can be expressed as

$$E_n(x) = -\sum_{i=1}^n x_i \ln x_i, \quad (17)$$

where  $x_i$  represents the investment proportion of asset  $i$  ( $i = 1, 2, \dots, n$ ). From equation (16), when  $x_i = 1/n$ , the value is the maximum; that is, the degree of decentralization of the portfolio of assets is the largest. In real life, however, investors will not allocate wealth to each asset in equal proportions, which does not meet the investors' investment behaviour and when the rate of return  $\tilde{r}_i$  of the assets is lower than the rate of return  $r_f$  of the risk-free assets, that is,  $\tilde{r}_i < r_f$  ( $i = 1, 2, \dots, n$ ); investors are not going to invest in such assets, and their purpose is to reduce risk and increase revenue through the moderate decentralization of their assets. Based on the above analysis, in order to overcome the deficiency of proportional entropy, Zhang et al. [25] construct the probability entropy based on a decentralized measurement index as follows:

$$\begin{aligned} S(x) = & -\sum_{i=1}^n \left[ \frac{x_i \theta(x_i)}{2} \ln \left( \varepsilon + \frac{x_i \theta(x_i)}{2} \right) \right. \\ & \left. + \left( 1 - \frac{x_i \theta(x_i)}{2} \right) \ln \left( 1 - \frac{x_i \theta(x_i)}{2} \right) \right], \end{aligned} \quad (18)$$

where  $\varepsilon > 0$  is a sufficiently small number, such as  $\varepsilon = 1.000e-7$ ;  $\max\{E(\tilde{r}_i - r_f), 0\} / \text{Var}(\tilde{r}_i)$  represents the proportion of remuneration fluctuations in asset  $i$ ;  $\theta(x_i) = \max\{E(\tilde{r}_i - r_f), 0\} / \text{Var}(\tilde{r}_i) / \{\sum_{i=1}^n \max\{E(\tilde{r}_i - r_f), 0\} / \text{Var}(\tilde{r}_i)\}$  is the compensation factor of the investment proportion of  $x_i$ ;  $E(\tilde{r}_i)$  and  $\text{Var}(\tilde{r}_i)$  represent the mean probability and variance of the probability of the  $i$ -th asset, respectively; and  $r_f$  represents the rate of return on risk-free assets. Based on the probability entropy of the above decentralization measurement index, it can be seen that the greater the proportion of the return fluctuation of asset  $i$  is, the greater the proportion of investment in asset  $i$  is. It is not difficult to find that when  $E(\tilde{r}_i) < r_f$ , the investment proportion  $x_i = 0$  ( $i = 1, 2, \dots, n$ ) of asset  $i$  is consistent with the investment decisions of investors in practice.

According to the above analysis, this paper considers investors' attitudes towards risk and their investment decisions on assets with background risk, takes the possible lower variance of the return on assets as the risk measure, measures the return on the basis of the mean probability of the return on assets, and uses the probability entropy as an effective tool for measuring the risk of the lower variance of the probability, which is all done to measure the degree of diversification of the asset portfolio. Therefore, the following probability mean-lower semivariance-entropy model with background risk and transaction costs considering the different risk attitudes of investors is established:



$$\begin{aligned}
\min \quad & \text{Var}^-(\tilde{R}) = \text{Var}^-\left(\sum_{i=1}^n \tilde{r}_i x_i + \tilde{r}_b - C\right), \\
\max \quad & S(x) = -\sum_{i=1}^n \left[ \frac{x_i \theta(x_i)}{2} \ln\left(\varepsilon + \frac{x_i \theta(x_i)}{2}\right) + \left(1 - \frac{x_i \theta(x_i)}{2}\right) \ln\left(1 - \frac{x_i \theta(x_i)}{2}\right) \right] \\
\text{s.t.} \quad & M\left(\sum_{i=1}^n \tilde{r}_i x_i + \tilde{r}_b\right) - \sum_{i=1}^n c_i |x_i - x_i^0| \geq r \\
& \sum_{i=1}^n x_i = 1, \quad x_i \geq 0, \quad i = 1, 2, \dots, n,
\end{aligned} \tag{19}$$

where  $r$  represents the minimum level of the investor's net return on the portfolio.

In the above two-objective programming problem (19), there is no optimal solution in the strictest sense, and thus, it

is usually transformed into a single objective problem by using the simple weighting method of the objective function. The model is as follows:

$$\begin{aligned}
\min \quad & \lambda \text{Var}^-\left(\sum_{i=1}^n \tilde{r}_i x_i + \tilde{r}_b - C\right) + (1 - \lambda) \sum_{i=1}^n \left[ \frac{x_i \theta(x_i)}{2} \ln\left(\varepsilon + \frac{x_i \theta(x_i)}{2}\right) + \left(1 - \frac{x_i \theta(x_i)}{2}\right) \ln\left(1 - \frac{x_i \theta(x_i)}{2}\right) \right], \\
\text{s.t.} \quad & M\left(\sum_{i=1}^n \tilde{r}_i x_i + \tilde{r}_b\right) - \sum_{i=1}^n c_i |x_i - x_i^0| \geq r, \\
& \sum_{i=1}^n x_i = 1, \quad x_i \geq 0, \quad i = 1, 2, \dots, n,
\end{aligned} \tag{20}$$

where  $\lambda \in [0, 1]$  represents the preference coefficient of the investor.  $\lambda \rightarrow 0$  indicates that investors pursue diverse asset portfolios and tend to diversify their investment strategies.  $\lambda \rightarrow 1$  indicates that investors dislike diverse asset portfolios.

Considering the conditional constraints of the model (19), the problem (19) is transformed into the following unconstrained optimization problem that is in the form of penalty function:

$$\min \quad \lambda \text{Var}^-\left(\sum_{i=1}^n \tilde{r}_i x_i + \tilde{r}_b - C\right) + (1 - \lambda) \sum_{i=1}^n \left[ \frac{x_i \theta(x_i)}{2} \ln\left(\varepsilon + \frac{x_i \theta(x_i)}{2}\right) + \left(1 - \frac{x_i \theta(x_i)}{2}\right) \ln\left(1 - \frac{x_i \theta(x_i)}{2}\right) \right] + Lp(x), \tag{21}$$

where  $L > 0$  is called the penalty factor and it is a preset large enough normal number.  $p(x) = (\max\{0, r - M(\tilde{r}_i x_i + \tilde{r}_b) + \sum_{i=1}^n c_i |x_i - x_i^0|\})^2 + (\sum_{i=1}^n x_i - 1)^2$  is called the constraint violation function, and it is easy to see that  $p(x) \geq 0$ .

#### 4. Differential Evolution Algorithm

**4.1. The Basic Principle of the Algorithm.** The differential evolution algorithm is similar to the genetic algorithm. Different from the genetic algorithm, it does not need to code and decode the feasible solutions. The initial population

of the differential evolution algorithm is randomly generated, and the evolutionary population is formed by mutating, crossing, and selecting each individual in the population until the termination condition is satisfied.

The number of objective function variables in the differential evolution algorithm is the dimension  $D$  of the algorithm's search space, and NP is the size of the initial intermediate population, which is generally set by scholars according to the actual situation. The evolution operation of the differential evolution algorithm is controlled by the fitness function. The fitness function can be used to evaluate

the relative value of the individual relative to the whole population, and the fitness function of this article is expressed as

$$\lambda \text{Var}^{-} \left( \sum_{i=1}^n \tilde{r}_i x_i + \tilde{r}_b - C \right) + (1 - \lambda) \sum_{i=1}^n \left[ \frac{x_i \theta(x_i)}{2} \ln \left( \varepsilon + \frac{x_i \theta(x_i)}{2} \right) + \left( 1 - \frac{x_i \theta(x_i)}{2} \right) \ln \left( 1 - \frac{x_i \theta(x_i)}{2} \right) \right] + Lp(x). \quad (22)$$

The evolution of the differential evolution algorithm [26] is as follows:

- (1) Mutation operation. The mutation operation is carried out on the basis of the difference vector between the parent individuals. Let the currently evolved individual be  $x_i^t$ , where  $i$  is the serial number of the current individual in the population and  $t$  is the number of iterations. Randomly select three individuals  $x_{r1}^t$ ,  $x_{r2}^t$ , and  $x_{r3}^t$  ( $r1 \neq r2 \neq r3 \neq i$ ) from the current population and add the vector difference  $x_{r2}^t - x_{r3}^t$  between two individuals to  $x_{r1}^t$  under the action of scaling factor  $F$ . Then, the individual  $v_i^{t+1}$  obtained from the mutation can be expressed as

$$v_i^{t+1} = x_{r1}^t + F(x_{r2}^t - x_{r3}^t). \quad (23)$$

- (2) Cross-operation. The mutated individual  $v_i^{t+1}$  and the current evolutionary individual  $x_i^t$  of the population intersect in a discrete crossing manner to generate individual  $u_i^{t+1}$  and the  $j$ -th component [26] of individual  $u_i^{t+1}$  is expressed as follows:

$$u_i^{t+1} = \begin{cases} v_{ij}^{t+1}, & \text{if } \text{rand} \leq \text{CR} \text{ or } j = \text{randi}(1, D), \\ x_{ij}^t, & \text{otherwise,} \end{cases} \quad (24)$$

where  $\text{rand}$  is the uniformly distributed random numbers over  $(0, 1)$  and  $\text{randi}(1, D)$  is a randomly selected integer in  $\{1, 2, 3, \dots, D\}$ . To ensure that at least one bit of  $u_i^{t+1}$  is contributed by  $v_i^{t+1}$  and  $\text{CR} \in [0, 1]$  is the cross-probability, it is used to control which variables in  $u_i^{t+1}$  are contributed by  $v_i^{t+1}$  and  $x_i^t$ . It can be seen that, with the increase in the cross-probability  $\text{CR}$ , the contribution of  $v_i^{t+1}$  to  $u_i^{t+1}$  is also increasing. When  $\text{CR} = 1$ ,  $u_i^{t+1} = v_i^{t+1}$ .

- (3) Selection operation [27]:

$$x_i^{t+1} = \begin{cases} u_i^{t+1}, & \text{if } f(u_i^{t+1}) < f(x_i^t), \\ x_i^t, & \text{otherwise.} \end{cases} \quad (25)$$

The greedy selection strategy is used to select between the parent individual  $x_i^t$  and the experimental individual  $u_i^{t+1}$ , in which  $f(x)$  is the fitness function, and the individual with the best fitness is selected. The selection strategy of the differential evolution algorithm is actually an elite reserve strategy.

## 4.2. Improvement of the Differential Evolutionary Algorithm

**4.2.1. Normalization.** To solve the above model, the differential evolution algorithm first generates the initial intermediate population. That is, it randomly initializes a group of intermediate particles in the feasible solution space and normalizes each intermediate particle to generate the initial population as follows:

$$x_i = \frac{y_i}{\sum_{i=1}^n y_i}, \quad (26)$$

where  $\sum_{i=1}^n x_i = 1$ ,  $i = 1, 2, \dots, n$ .

**4.2.2. Exponential Increment Crossover Operator.** The cross-probability is used to control individual  $u_i^{t+1}$ , which is provided by the mutated individual  $v_i^{t+1}$  and the current individual  $x_i^t$ . As the  $\text{CR}$  increases, the contribution of the mutated individual  $v_i^{t+1}$  to  $u_i^{t+1}$  is greater; and when  $\text{CR} = 1$ ,  $u_i^{t+1} = v_i^{t+1}$ . In this paper, the cross-probability factor with an exponential increase in random iterations is used, and the updated formula [27] is as follows:

$$\text{CR} = \text{CR}_{\min} + (\text{CR}_{\max} - \text{CR}_{\min}) * \exp \left( -a * \left( 1 - \frac{t}{T_{\max}} \right)^b \right), \quad (27)$$

where  $a = 40$ ,  $b = 4$ ,  $T_{\max}$  is the maximum number of iterations,  $t$  is the current number of iterations,  $\text{CR}_{\min} = 0.1$ , and  $\text{CR}_{\max} = 0.9$ . In this way, it can avoid the cross-factor is a fixed parameter that makes it fall into the local extreme value, and it can well balance the global and local search ability.

**4.2.3. New Mutation Operation.** If the mutated individual is considered to be composed of only the random individuals, although it is advantageous to maintain the diversity of the population, the global search capability is strong, but the convergence speed is slow; and if the mutated individual only considers the  $x_{\text{best}}^t$ , although the local search capability is strong and the accuracy is high, the algorithm will fall into the local optimum. Combined with the characteristics of these two methods, the effects of a random individual  $x_{r1}^t$  and the optimal individual  $x_{\text{best}}^t$  are simultaneously considered, the vector difference  $(x_{r2}^t - x_{r3}^t)$  of the two individuals is added to  $x_{r1}^t$  and  $x_{\text{best}}^t$  under the action of the

scaling factor  $F$ , and the mutated individual is obtained. The mutation equation [28] selected in this paper is as follows:

$$v_i^{t+1} = \eta x_{r_1}^t + (1 - \eta)x_{\text{best}}^t + F(x_{r_2}^t - x_{r_3}^t), \quad (28)$$

$$\eta = \frac{(T_{\max} - t)}{T_{\max}}, \quad (29)$$

$$F = \eta * 0.5 + 0.5, \quad (30)$$

where  $\eta \in [0, 1]$ ;  $T_{\max}$  is the maximum number of iterations;  $t$  is the current number of iterations; and  $F \in [0, 2]$  is a scaling factor, which is used to control the scaling degree of difference variables. It can be seen that  $F$  linearly decreases as  $t$  increases. In the search process,  $\eta$  gradually decreases from 1 to 0. That is, the weight of  $x_{r_1}^t$  to  $x_{\text{best}}^t$  gradually increases, which makes the population have better diversity in the early stage and can ensure faster convergence speed and better search accuracy in the later stage.

#### 4.3. Specific Steps of the Algorithm

Step 1. Set the basic parameters including the population size  $NP$ , the contraction factor  $F$ , the maximum number of iterations  $T_{\max}$ , the respective upper and lower bounds  $CR_{\max}$  and  $CR_{\min}$  of the cross-probability  $a$  and  $b$ , the penalty factor  $L$ , and the control error  $\varepsilon$ .

Step 2. Randomly generate the initial intermediate population for normalization operations and set the evolutionary algebra to  $t = 1$ .

Step 3. Use formula (22) to calculate the fitness value of each individual, and the optimal fitness value and the optimal individual are obtained.

Step 4. Judge whether the termination condition of the penalty function method is reached or the maximum number of iterations  $T_{\max}$  is reached. If so, exit the algorithm and output the optimal value; otherwise, the differential evolution algorithm starts to iterate, and the next step is carried out.

Step 5. The mutation operation, cross-operation, and selection operation are performed according to equations (24), (25), and (27)–(30).

Step 6. The evolutionary algebra to  $t = t + 1$  and return to step 3.

## 5. Empirical Analysis

The following examples will be used to illustrate the validity of the model. We assume that the return on assets of investors is a trapezoidal fuzzy number. Randomly select 5 stocks from the Shanghai Stock Exchange and estimate the probability distribution of trapezoidal fuzzy number of return on assets by analyzing the historical information of the relevant stocks [23]. The related information is shown in Table 1.

We use the proposed differential evolution (DE) algorithm with random mutation and exponential increments to solve the model. The specific parameters of the algorithm are

TABLE 1: The probability distribution of the rates of return of assets.

Assets	Trapezoidal fuzzy number
Stock 1	(0.0449, 0.0505, 0.0612, 0.0679)
Stock 2	(0.0447, 0.0502, 0.0608, 0.0675)
Stock 3	(0.1276, 0.1436, 0.1739, 0.1930)
Stock 4	(0.0466, 0.0524, 0.0635, 0.0705)
Stock 5	(0.0815, 0.0917, 0.1111, 0.1233)
Asset with background risk	(0.0400, 0.0450, 0.0545, 0.0605)

set as follows: a lot of experimental show that the population size  $NP = 30$  and the maximum number of iterations  $T_{\max} = 200$  can greatly reduce the running time of the algorithm. In addition, the parameter  $CR_{\min} = 0.1$ ,  $CR_{\max} = 0.9$ ,  $a = 40$ , and  $b = 4$  in literature [27] enable the algorithm to better balance the global and local search capability. Penalty factor  $L = 10^8$  and  $\varepsilon > 0$  is a sufficiently small number, such as  $\varepsilon = 1.000e - 7$ . All the tests are run in MATLAB 2015a, on an Intel (R) Celeron (R) CPU G3900 @ 2.80 GHz, Windows 7.

To solve this example, it is assumed that the return of the risk-free asset  $r_f$  is 0.007, the transaction cost ratio of the stock is 0.003, and the investors' minimum net return requirement for a portfolio is 0.085. Then, the above intelligent algorithm is used to solve the above model, and the investment strategy is obtained as follows.

From Tables 2–4, it can be seen that different risk attitudes result in different investment strategies. Investors invest in the five kinds of assets and one kind of background risk asset according to the risk attitude and the above five investment strategies. The investment proportions in these assets are also different under the different investment strategies. When the risk attitude adaptation value  $k = 0.5$ , the proportion of stock 1 in the five investment strategies is the smallest except for the fourth investment strategy, and the proportion of stock 1 in the fourth investment strategy is also very small. It can be seen that, regardless of the investment strategy, investors are very cautious about investing in stock 1. However, the investment proportions in the five investment strategies for stocks 1, 2, 4, and 5 are the largest. When the risk attitude  $k = 1.0$ , among the five investment strategies, stock 3 accounts for the largest investment proportion since investors prefer stock 3, and stock 1 accounts for the smallest proportion in investment strategies 1, 2, and 4. When the risk attitude  $k = 2.0$ , the proportion of stock 5 in investment strategies 2 and 4 is the largest, and compared with the other investment strategies, stock 5 is also welcome by investors.

According to Tables 2–4, we can get that, with the increase in the fitness value of risk attitude, that is, investors' attitude towards risk is changed from the aversion to seeking, the lower semivariance is also increased, that is, the risk is increasing, and the corresponding income is also increasing. Figures 2–4 show the effective frontiers of risk averse, risk neutral, and risk-seeking investors when background risk is involved, and Figure 5 shows the comparison diagram of the effective frontiers of investors under the different risk attitudes with background risk. From Figure 5, it can be intuitively seen that risk-averse investors avoid risk,

TABLE 2: Portfolios, returns, and lower semivariances of risk-averse investors.

Risk attitude	Portfolio strategies				
$k = 0.5$					
$x_1$	0.0405	0.0155	0.0025	0.0854	0.0969
$x_2$	0.1287	0.0914	0.1334	0.0762	0.1187
$x_3$	0.3133	0.3501	0.3662	0.3649	0.4062
$x_4$	0.2048	0.2128	0.0767	0.1789	0.1618
$x_5$	0.3126	0.3302	0.4212	0.2946	0.2163
Return	0.0953	0.1129	0.1198	0.1249	0.1260
Lower semivariance	0.0040	0.0053	0.0059	0.0063	0.0067

TABLE 3: Portfolios, returns, and lower semivariances of risk-neutral investors.

Risk attitude	Portfolio strategies				
$k = 1.0$					
$x_1$	0.0159	0.0186	0.0893	0.0343	0.0577
$x_2$	0.3018	0.1446	0.0560	0.1727	0.1087
$x_3$	0.3689	0.3907	0.5883	0.3916	0.4267
$x_4$	0.0372	0.1033	0.1900	0.1358	0.0333
$x_5$	0.2762	0.3428	0.0764	0.2655	0.3735
Return	0.1011	0.1100	0.1149	0.1267	0.1327
Lower semivariance	0.0144	0.0166	0.0182	0.0211	0.0233

TABLE 4: Portfolios, returns, and lower semivariances of venture-seeking investors.

Risk attitude	Portfolio strategies				
$k = 2.0$					
$x_1$	0.1610	0.2735	0.0042	0.0242	0.0254
$x_2$	0.1025	0.0116	0.2412	0.2319	0.0096
$x_3$	0.3431	0.3361	0.3619	0.2709	0.4505
$x_4$	0.1114	0.0343	0.1438	0.1271	0.1810
$x_5$	0.2819	0.3446	0.2490	0.3459	0.3335
Return	0.1219	0.1230	0.1261	0.1321	0.1470
Lower semivariance	0.0628	0.0647	0.0673	0.0735	0.0864

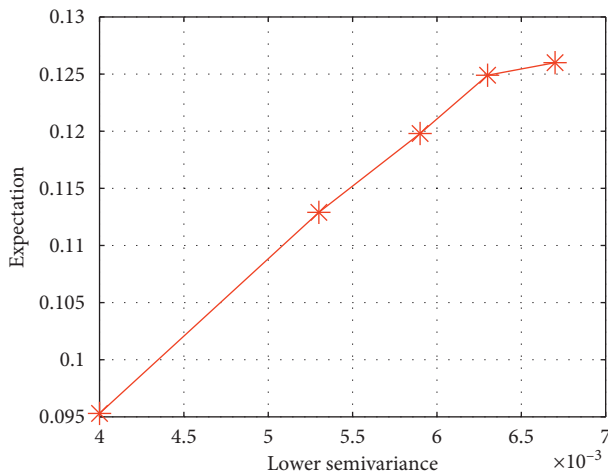


FIGURE 2: The effective frontier of risk-averse investors with background risk.

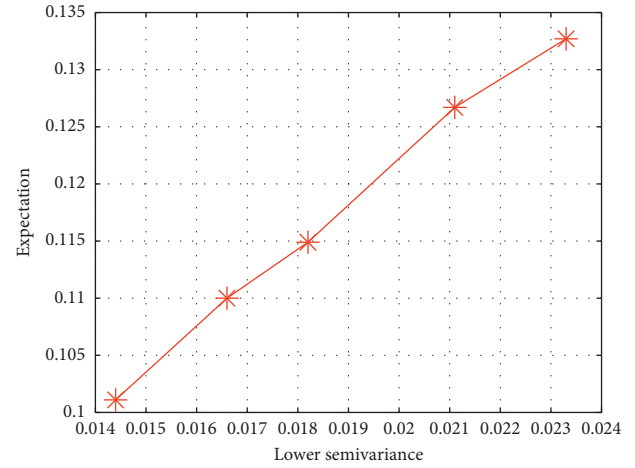


FIGURE 3: The effective frontier of risk-neutral investors with background risk.

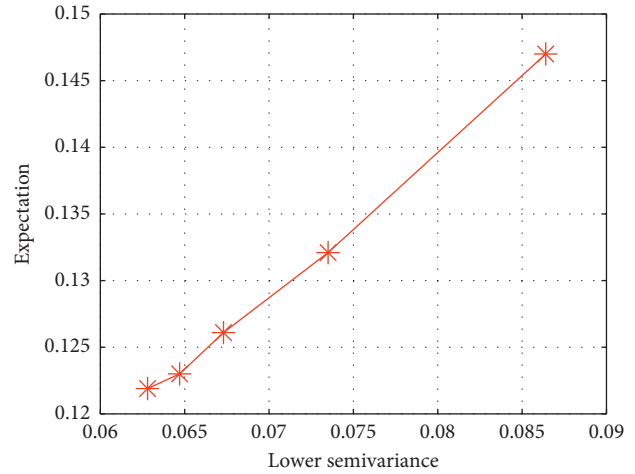


FIGURE 4: The effective frontier of risk-seeking investors with background risk.

and risk-loving investors seek risk because high risk is often accompanied by high returns.

As the risk attitude increases, so does the risk. Investors have different risk attitudes that affect their investment strategy choices. However, by comparing Tables 2–4, we can find that, under the same risk attitude, the lower semivariance without background risk is much smaller than that with background risk, and the corresponding return is much smaller. Furthermore, the greater the background risk is, the greater the risk that investors will bear, and so the impact of background risk in the investment process cannot be underestimated.

Table 5 shows the returns and lower semivariances of the portfolios without background risk under different risk attitudes. Figures 6–8 show the effective frontiers of risk averse, risk neutral, and risk-seeking investors without background risk under different risk attitudes. Figure 9 compares the effective frontiers of investors under different risk attitudes without background risk.

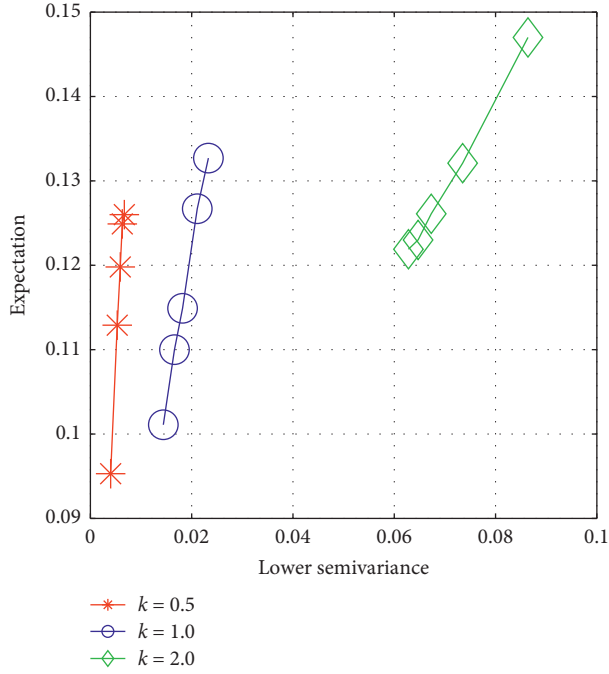


FIGURE 5: Comparison of effective frontiers of investors under different risk attitudes with background risk.

TABLE 5: Returns and lower semivariances of portfolios without background risk under different risk attitudes.

Risk attitude	Portfolio strategies				
$k = 0.5$					
$x_1$	0.1021	0.1458	0.3093	0.0159	0.2609
$x_2$	0.0208	0.0046	0.0587	0.3018	0.0162
$x_3$	0.5447	0.4091	0.4348	0.3689	0.3130
$x_4$	0.0349	0.2421	0.0172	0.0372	0.0347
$x_5$	0.2974	0.1985	0.1800	0.2762	0.3752
Return	0.0661	0.0768	0.0825	0.0860	0.0976
Lower semivariance	0.0007	0.0009	0.0010	0.0011	0.0014
$k = 1.0$					
$x_1$	0.0457	0.1792	0.0042	0.0343	0.0254
$x_2$	0.1327	0.0276	0.2412	0.1727	0.0096
$x_3$	0.3489	0.4417	0.3619	0.3916	0.4505
$x_4$	0.2678	0.1045	0.1438	0.1358	0.1810
$x_5$	0.2050	0.2469	0.2490	0.2655	0.3335
Return	0.0701	0.0723	0.0808	0.0832	0.1015
Lower semivariance	0.0017	0.0018	0.0023	0.0024	0.0036
$k = 2.0$					
$x_1$	0.1717	0.0594	0.1610	0.0242	0.0178
$x_2$	0.0862	0.0894	0.1025	0.2319	0.1987
$x_3$	0.3849	0.4446	0.3431	0.2709	0.1669
$x_4$	0.0204	0.0627	0.1114	0.1271	0.0398
$x_5$	0.3368	0.3440	0.2819	0.3459	0.5768
Return	0.0726	0.0777	0.0845	0.0880	0.0954
Lower semivariance	0.0035	0.0040	0.0049	0.0052	0.0060

Figure 10 shows the effective frontier comparison diagram with (without) background risk under different risk attitudes. It can be clearly and intuitively seen that the investment strategy with assets with background risk has high risk, but it is also accompanied by high returns.

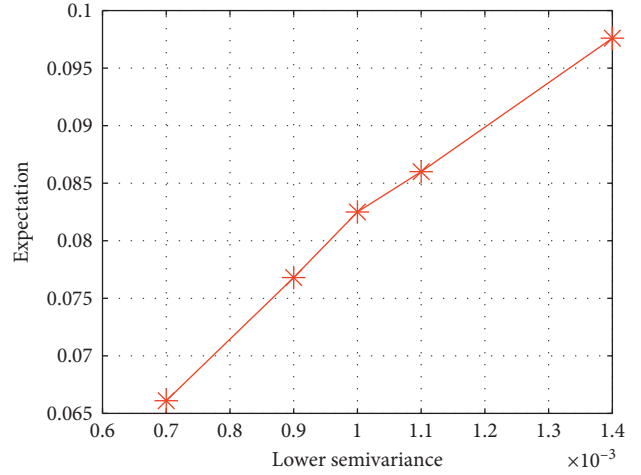


FIGURE 6: Effective frontier for risk-averse investors without background risk.

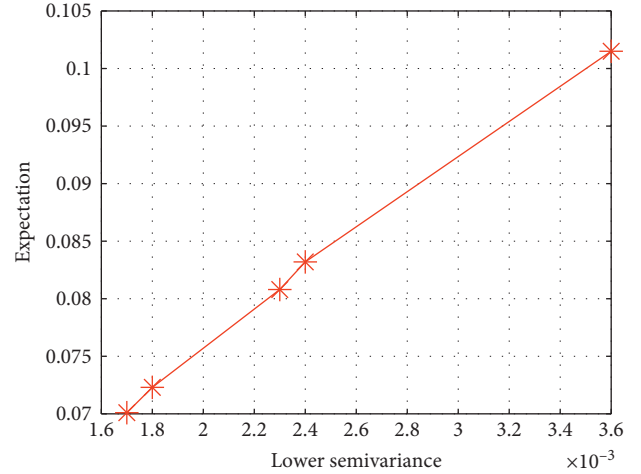


FIGURE 7: Effective frontier for risk-neutral investors without background risk.

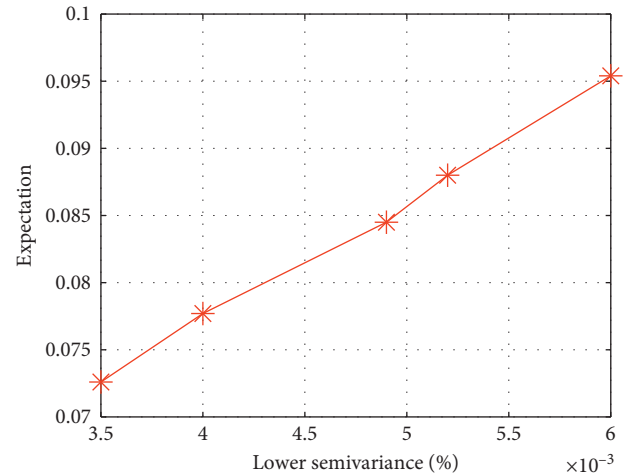


FIGURE 8: Effective frontier for risk-seeking investors without background risk.

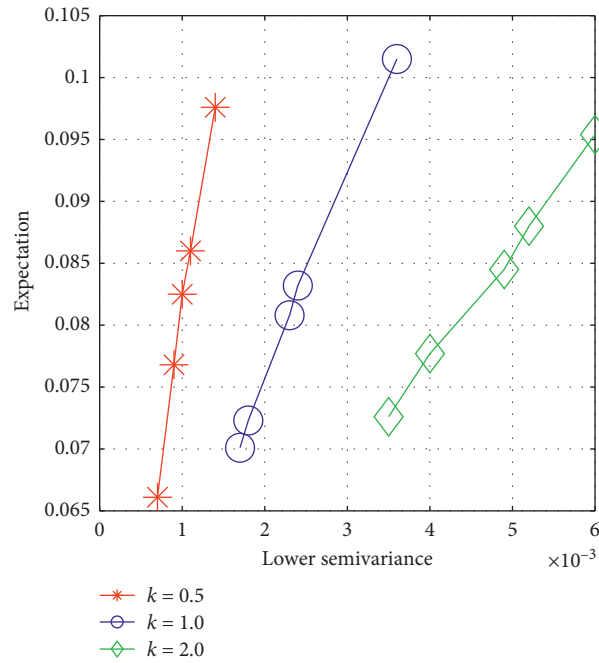


FIGURE 9: Effective frontier comparison of investors under different risk attitudes without background risk.

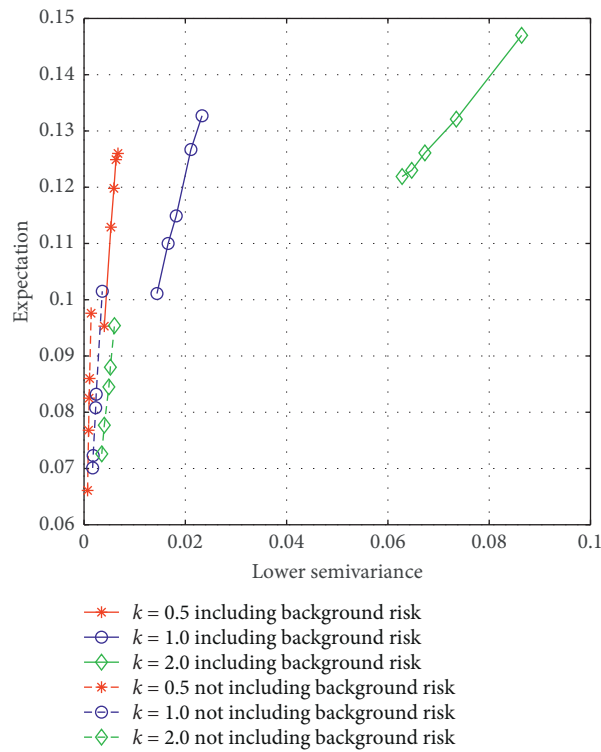


FIGURE 10: Comparison of the effective frontiers with background risks under different risk attitudes.

Table 6 shows the comparison of the returns and the lower semivariances under different risk attitudes. It can be seen that, under the same risk attitude, the lower semivariance of the portfolio without entropy is larger than the

lower semivariance of the portfolio with entropy, and the corresponding return is higher than that with entropy. However, when  $k = 0.5$ , the last investment strategy has a lower semivariance of entropy that is larger than the lower

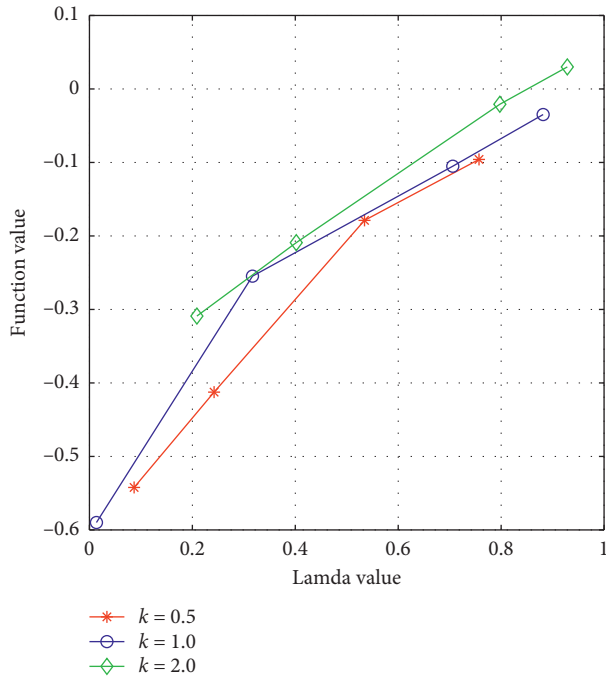


TABLE 6: Comparison of the entropy factors in portfolios under different risk attitudes.

Risk attitude			Investment portfolios				
$k = 0.5$	Entropy-containing	Return	0.0953	0.1129	0.1198	0.1249	0.1260
		Lower semivariance	0.0040	0.0053	0.0059	0.0063	<b>0.0067</b>
	No entropy	Return	0.1148	0.1212	0.1231	0.1257	0.1276
		Lower semivariance	0.0055	0.0060	0.0061	0.0065	<b>0.0066</b>
$k = 1.0$	Entropy-containing	Return	0.1011	0.1100	0.1149	0.1267	0.1327
		Lower semivariance	0.0144	0.0166	0.0182	0.0211	<b>0.0233</b>
	No entropy	Return	0.1145	0.1178	0.1179	0.1279	0.1283
		Lower semivariance	0.0178	0.0186	0.0189	0.0217	<b>0.0224</b>
$k = 2.0$	Entropy-containing	Return	0.1219	0.1230	0.1261	0.1321	0.1470
		Lower semivariance	0.0628	0.0647	0.0673	0.0735	0.0864
	No entropy	Return	0.1218	0.1245	0.1287	0.1485	0.1522
		Lower semivariance	0.0642	0.0653	0.0698	0.0865	0.0894

TABLE 7: Table of relationship between lambda value and function value under different risk attitudes.

Risk attitude	$\lambda$	Function value
$k = 0.5$	0.0868	-0.5422
	0.2422	-0.4125
	0.5345	-0.1788
	0.7570	-0.0959
$k = 1.0$	0.0136	-0.5899
	0.3168	-0.2547
	0.7060	-0.1051
	0.8816	-0.0348
$k = 2.0$	0.2088	-0.3090
	0.4019	-0.2091
	0.7975	-0.0208
	0.9286	0.0300

FIGURE 11:  $\lambda$  comparison chart under different risk attitudes.

semivariance without entropy; when  $k = 2.0$ , the return of the first investment strategy with entropy is also larger than that without entropy. Since the entropy is used to measure the degree of decentralization of the portfolio and reduce the risk, the entropy portfolio has a smaller risk.

For unconstrained optimization problem of the weight of  $\lambda$  values as shown in Table 7, we have done a lot of experiments, respectively, to get  $\lambda$  value and function value under different risk attitudes; it can be seen as the  $\lambda$  value increases, the function value will increase, under the condition of risk attitude to adapt to the same value, when  $\lambda \rightarrow 0$ , probability entropy contribution to the risk control; when  $\lambda \rightarrow 1$ , the risk of the lower semivariance measure of probability dominates.

Figure 11 more intuitively shows the changing trend of weighting with different values. When  $\lambda \rightarrow 0$ , investors pursue diversified investment strategies and invest more boldly. When  $\lambda \rightarrow 1$ , investors hate the diversity of portfolios and invest more cautiously, which is also consistent with the law of risk attitude.

## 6. Conclusions

In the financial market, investors have different perceptions of risk and different attitudes towards risk in the investment process. In this paper, the fuzzy portfolio problem under different risk attitudes is studied. We use the probability mean of the return on assets to measure the return and the lower semivariance to measure the risk. In addition, considering the different attitudes of investors to risk, background risk, and transaction costs, the probability entropy is used as an effective measure for the degree of diversification of an asset portfolio, and a probability mean-lower semivariance-entropy model is constructed. We use a differential evolution algorithm to solve the model and obtain five portfolio strategies under different risk attitudes. The effects of the risk attitude, background risk, and probability entropy on investors' investment decisions are analyzed. Through the experimental results, it is found that the risk-averse investors avoid the risk, and the investors who like the risk seek the risk. Furthermore, the investment in assets with background

risk will increase the total risk of the investors because the diversification effect of the entropy on the risk can make investors reduce the risks and improve the returns.

## Data Availability

Five stocks are randomly selected from the Shanghai Stock Exchange, and the probability distribution of trapezoidal fuzzy number of return on assets is estimated by analyzing the historical information of the relevant stocks. The data in Table 1 are selected from [23, 27]. All data and models generated or used during the study are available within the article.

## Conflicts of Interest

The authors declare that they have no conflicts of interest.

## Acknowledgments

This research was supported by the National Natural Science Foundation of China under Grant nos. 11961001 and 61561001, the Construction Project of First-Class Subjects in Ningxia Higher Education (NXYLXK2017B09), and the major proprietary funded project of North Minzu University (ZDZX201901).

## References

- [1] H. Markowitz, "Portfolio selection," *The Journal of Finance*, vol. 7, no. 1, pp. 77–91, 1952.
- [2] J.-R. Yu and W.-Y. Lee, "Portfolio rebalancing model using multiple criteria," *European Journal of Operational Research*, vol. 209, no. 2, pp. 166–175, 2011.
- [3] Y. Shen, X. Zhang, and T. K. Siu, "Mean-variance portfolio selection under a constant elasticity of variance model," *Operations Research Letters*, vol. 42, no. 5, pp. 337–342, 2014.
- [4] A. O. Petters and X. Dong, *Capital Market Theory and Portfolio Risk Measures. An Introduction to Mathematical Finance with Applications*, Springer, New York, NY, USA, 2016.
- [5] Z. Kang and Z. Li, "An exact solution to a robust portfolio choice problem with multiple risk measures under ambiguous distribution," *Mathematical Methods of Operations Research*, vol. 87, no. 2, pp. 169–195, 2018.
- [6] H. Ma, M. Wu, and N. Huang, "A random parameter model for continuous-time mean-variance asset-liability management," *Mathematical Problems in Engineering*, vol. 2015, no. 16, Article ID 687428, 2015.
- [7] Z. L. Yang, H. Garg, J. Li, G. Srivastavad, and Z. Cao, "Investigation of multiple heterogeneous relationships using a q-rung orthopair fuzzy multi-criteria decision algorithm," *Neural Computing and Applications*, pp. 1–16, 2020.
- [8] W. F. Shape, "Capital asset prices: a theory of market equilibrium under conditions of risk," *The Journal of Finance*, vol. 19, no. 3, pp. 425–442, 1964.
- [9] Z. Qin, "Mean-variance model for portfolio optimization problem in the simultaneous presence of random and uncertain returns," *European Journal of Operational Research*, vol. 245, no. 2, pp. 480–488, 2015.
- [10] M. Zhang and P. Chen, "Mean-variance portfolio selection with regime switching under shorting prohibition," *Operations Research Letters*, vol. 44, no. 5, pp. 658–662, 2016.
- [11] R. Bellman and L. A. Zadeh, "Decision making in a fuzzy environment," *Management Science*, vol. 17, no. 4, pp. 141–164, 1970.
- [12] Y. Fang, L. Bo, D. Zhao, and S. Wang, "Fuzzy views on black-litterman portfolio selection model," *Journal of Systems Science and Complexity*, vol. 31, no. 4, pp. 975–987, 2018.
- [13] R.-C. Tsaur, "Fuzzy portfolio model with different investor risk attitudes," *European Journal of Operational Research*, vol. 227, no. 2, pp. 385–390, 2013.
- [14] Z. Yang, T. Ouyang, X. Fu, and X. Peng, "A decision-making algorithm for online shopping using deep-learning-based opinion pairs mining and q-rung orthopair fuzzy interaction Heronian mean operators," *International Journal of Intelligent Systems*, vol. 35, no. 5, pp. 783–825, 2020.
- [15] Z. Yang, X. Li, H. Garg, and M. Qi, "Decision support algorithm for selecting an antivirus mask over COVID-19 pandemic under spherical normal fuzzy environment," *International Journal of Environmental Research and Public Health*, vol. 17, no. 10, p. 3407, 2020.
- [16] X. Huang, "An entropy method for diversified fuzzy portfolio selection," *International Journal of Fuzzy Systems*, vol. 14, no. 1, pp. 160–165, 2012.
- [17] N. Lassance and F. D. Vrins, "Minimum Rényi entropy portfolios," 2018, <https://arxiv.org/abs/1705.05666>.
- [18] S. C. Fang, J. R. Rajasekera, and H. S. J. Tsao, *Entropy Optimization and Mathematical Programming*, Springer Science & Business Media, Berlin, Germany, 2012.
- [19] M. Lee, R. H. Kwon, C.-G. Lee, and H. Anis, "Decentralized strategic asset allocation with global constraints," *Journal of Asset Management*, vol. 19, no. 1, pp. 13–26, 2018.
- [20] Y. Li, B. Wang, A. Fu et al., "Fuzzy portfolio optimization for time-inconsistent investors: a multi-objective dynamic approach," *Soft Computing*, vol. 24, no. 13, pp. 9927–9941, 2019.
- [21] Z. Tao, L. Huiling, W. Wenwen, and Y. Xia, "GA-SVM based feature selection and parameter optimization in hospitalization expense modeling," *Applied Soft Computing*, vol. 75, no. 2, pp. 323–332, 2019.
- [22] Z. L. Yang and J. P. Chang, "Interval-valued pythagorean normal fuzzy information aggregation operators for multi-attribute decision making," *IEEE Access*, vol. 8, pp. 51295–51314, 2020.
- [23] J. Li, *Research on Portfolio Model with Background Risk under Various Measures*, Institutes of Technology of South China, Guangzhou, China, 2017.
- [24] C. E. Shannon, "A mathematical theory of communication," *Bell System Technical Journal*, vol. 27, no. 3, pp. 379–423, 1948.
- [25] W.-G. Zhang, Y.-J. Liu, and W.-J. Xu, "A possibilistic mean-semivariance-entropy model for multi-period portfolio selection with transaction costs," *European Journal of Operational Research*, vol. 222, no. 2, pp. 341–349, 2012.
- [26] J. M. Liu and Y. L. Gao, "Differential evolutionary algorithm with adaptive mutation and exponential incremental crossing operator," *Journal of Henan Normal University*, vol. 37, no. 6, pp. 18–21, 2009.
- [27] Z. X. Deng, D. Q. Cao, X. J. Liu et al., "A new differential evolutionary algorithm," *Computer Engineering and Application*, vol. 44, no. 24, pp. 40–42, 2008.
- [28] H. L. Wu, Y. N. Wang, and Z. L. Chen, "An improved differential evolutionary algorithm for solving mixed integer nonlinear programming problems," *Small-scale Micro-computer System*, vol. 28, no. 4, pp. 666–669, 2007.

## Research Article

# A Neutrosophic-Based Approach in Data Envelopment Analysis with Undesirable Outputs

Xinna Mao,<sup>1</sup> Zhao Guoxi ,<sup>1</sup> Mohammad Fallah,<sup>2</sup> and S. A. Edalatpanah <sup>3</sup>

<sup>1</sup>Department of Mathematics and Information Science, Xinxiang University, Xinxiang 453003, China

<sup>2</sup>Department of Industrial Engineering, Islamic Azad University, Central Tehran Branch, Tehran, Iran

<sup>3</sup>Department of Applied Mathematics, Ayandegan Institute of Higher Education, Tonekabon, Iran

Correspondence should be addressed to S. A. Edalatpanah; [saedalatpanah@gmail.com](mailto:saedalatpanah@gmail.com)

Received 7 April 2020; Revised 26 May 2020; Accepted 3 June 2020; Published 13 July 2020

Academic Editor: Harish Garg

Copyright © 2020 Xinna Mao et al. This is an open access article distributed under the Creative Commons Attribution License, which permits unrestricted use, distribution, and reproduction in any medium, provided the original work is properly cited.

Data Envelopment Analysis is one of the paramount mathematical methods to compute the general performance of organizations, which utilizes similar sources to produce similar outputs. Original DEA schemes involve crisp information of inputs and outputs that may not always be accessible in real-world applications. Nevertheless, in some cases, the values of the data are information with indeterminacy, impreciseness, vagueness, inconsistent, and incompleteness. Furthermore, the conventional DEA models have been originally formulated solely for desirable outputs. However, undesirable outputs may additionally be present in the manufacturing system, which wishes to be minimized. To tackle the mentioned issues and in order to obtain a reliable measurement that keeps original advantage of DEA and considers the influence of undesirable factors under the indeterminate environments, this paper presents a neutrosophic DEA model with undesirable outputs. The recommended technique is based on the aggregation operator and has a simple construction. Finally, an example is given to illustrate the new model and ranking approach in details.

## 1. Introduction

All organizations, whether governmental or private, require an effective performance assessment for development, growth, and sustainability in the competitive world of today so that within this growth it can appraise the efficiency and effectiveness of its organizational programs and its human resources processes. In other words, senior executive managers have always been seeking for a solution to ensure that their strategies are executed and, hence, have selected performance assessment methods as tools to implement their strategies. We should be mindful that novel measurement systems have been developed to target the existing strategies, and in this system, the indexes could be viewed as a crucial factor, in the present and future successes of the company. If these factors are alleviated or improved, then the company has launched its strategy.

The Data Envelopment Analysis (DEA) is a nonparametric method to analyse and assess the performance of

decision-making units (DMUs), which converts several inputs into several outputs and considers the qualitative and quantitative criterions. Based on the work of [1], Charnes et al. [2] proposed this methodology that is called the CCR model. After that, Banker et al. [3] extended this model and established a new model to measure efficiency that is the so-called BBC model. With DEA, directors can achieve the relative efficiency of a set of DMUs. Note that the production function does not need to be known in this technique. In the recent years, an extensive application of DEA in numerous fields, such as banking institutions [4], insurance industry [5], financial services [6], education [7], sustainability [8], energy [9], and health-care services [10], has been observed. Furthermore, in the past four decades, numerous reports and articles have been published in esteemed global journals verifying that this method is operational, see [11–16].

However, in some cases, the values of the data are often information with indeterminacy, impreciseness, vagueness, inconsistent, and incompleteness. Inaccurate assessments

are mainly the outcome of information that is unquantifiable, incomplete, and unavailable. By fuzzy sets [17], it is possible to model the uncertainty in information. In addition, there are several models of DEA with the fuzzy set, see [17–19] and references therein. However, fuzzy sets (FSs) deliberate only the membership function and cannot arrange other parameters of vagueness. Therefore, intuitionistic fuzzy sets (IFSs) have been introduced in [20], see also the Pythagorean fuzzy sets [21–23].

Though IFSs is able to address incomplete data for numerous real-world topics, it cannot handle other natures of uncertainty such as indeterminate information. Hence, Smarandache [24] puts forward an indeterminacy degree of membership as an autonomous element and proposes the neutrosophic set (NS). Then, inspired by sports (winner, loser, and equal), voting (agree, disagree, and abstain), answering (yes, no, and I do not know), decision-making (decision, no decision, and doubt), and acceptance (accept, rejection, and suspension) and since the principle of excluded middle cannot be applied to new logic, he combines three-valued logic with nonstandard analysis. Since then, a series of subclasses of NS have emerged, mainly including interval neutrosophic set [25–27], bipolar neutrosophic set [28, 29], single-valued neutrosophic set [30–33], simplified neutrosophic sets [34–36], neutrosophic structured element [37], multivalued neutrosophic set [38, 39], and neutrosophic linguistic set [40, 41] which have been proposed. Moreover, these concepts utilized in several problems, see [42–51].

In the DEA literature, there are also some models of DEA with IFSs, see [52–60]. However, in actual activities, there are some indeterminate information. If the indeterminacy factors are ignored, the relative effectiveness of DMUs will still be evaluated using the DEA model established on the basis of determinate values and biased or even wrong information will be obtained, which will bring some errors to management decisions. Therefore, it seems convenient and necessary to consider the neutrosophic DEA model.

As far as we know, there are few studies concerning DEA with neutrosophic information. The utilization of neutrosophic set in DEA can be traced to Edalatpanah [61] and additional investigations have been accessible in [62–67]. However, these neutrosophic DEA methods are formulated solely for desirable outputs and cannot eliminate the influence of undesirable factors on the efficiency evaluation. We know that the undesirable outputs may additionally be present in the manufacturing system that needs to be minimized. For example, in banking industry nonperforming loans/assets and in manufacturing systems, the production of a variety of emissions, pollutions, and industrial waste gas are undesirable outputs [68–73]. Therefore, there is still a need from the neutrosophic DEA method to develop a new model that keeps original advantage and considers the influence of undesirable factors.

Consequently, in this study, we establish a novel method of DEA with undesirable outputs in which all data are single-valued neutrosophic sets (SVNSs). Furthermore, a competent algorithm for solving the new DEA model has been presented. The main contributions of this paper are four folds: (1) we model the indeterminacies in the input and output data using SVNSs; (2) the proposed approach considers the impact of undesirable outputs on the performance of DMUs; (3) we provide a theorem regarding the feasibility and boundedness of the solution of new model; (4) we determine the efficiency scores of the DMUs as crisp values.

The paper unfolds as follows. Some basic knowledge and concepts on DEA and its models are deliberated in Section 2. In Section 3, some knowledge and arithmetic operations on neutrosophic sets are discussed. In Section 4, we propose a new model of neutrosophic DEA with undesirable outputs and establish an algorithm to solve it. In Section 5, the proposed model and the related algorithm are illustrated with a numerical example to ensure their validity and usefulness over the existing models. Finally, conclusions and future direction are offered in Section 6.

## 2. The Basic Concepts of DEA and its Models

DEA is a mathematical programming methodology that allows performance measurement of homogeneous DMUs that have several inputs and outputs. In DEA approach, there is no need to determine the specific form of the production function, and linear programming is needed to construct a piecewise linear surface (frontier) to cover all data, and then the efficiency of each of the DMUs is calculated from this frontier. The frontier obtained is the efficiency boundary, where the points on it are efficient, and other DMUs that are inside the cover surface are inefficient.

Let DMUO be under consideration; then, the production possibility set of the BCC model proposed by Banker et al. [3] is as follows:

$$T_{\text{BCC}} = \left\{ (x, y) \left| \begin{array}{l} \sum_{q=1}^n \alpha_q x_q \leq x, \sum_{q=1}^n \alpha_q y_q \geq y, \sum_{q=1}^n \alpha_q = 1, \\ \alpha_q \geq 0, q = 1, \dots, n \end{array} \right. \right\}. \quad (1)$$

Therefore, the BCC model is as follows:

$$\begin{array}{ll} \text{Min} & \eta_o \\ & \sum_{q=1}^n \alpha_q x_{pq} \leq \eta_o x_p, \quad p = 1, \dots, m \\ \text{s.t.} & \sum_{q=1}^n \alpha_q y_{sq} \geq y_{so}, \quad s = 1, \dots, k \\ & \sum_{q=1}^n \alpha_q = 1, \quad \alpha_q \geq 0, q = 1, \dots, n. \end{array} \quad (2)$$



For the BCC model with undesirable outputs, Guo and Wu [68] proposed

$$\begin{aligned} \text{Min} \quad & \eta_o \\ \text{s.t.} \quad & \sum_{q=1}^n \alpha_q x_{pq} \leq \eta_o x_{p_o}, \quad p = 1, \dots, m \\ & \sum_{q=1}^n \alpha_j y_{sq}^g \geq y_{s_o}^g, \quad s = 1, \dots, k \\ & \sum_{q=1}^n \alpha_j y_{s'q}^b \leq \eta_o y_{s'o}^b, \quad s' = 1, \dots, k' \\ & \sum_{q=1}^n \alpha_q = 1, \quad \alpha_q \geq 0, \quad q = 1, \dots, n. \end{aligned} \quad (3)$$

In Model (3), we assume that there are  $n$  DMUs that use inputs  $x_{pq}$  ( $p = 1, \dots, m$ ), to achieve desirable outputs (good)  $y_{sq}^g$  ( $s = 1, \dots, k$ ) and undesirable outputs (bad)  $y_{s'q}^b$  ( $s' = 1, \dots, k'$ ). After calculation, if  $\eta_o = 1$ , then DMU<sub>o</sub> is efficient; else, it is inefficient.

### 3. Neutrosophic Sets

Smarandache has given a number of actual examples for potential applications of NS; nevertheless, usage of NSs in real applied problems is difficult. Hence, NSs reduced into a type of SVNNS that will preserve the processes of the NSs. Here, we will discuss some basic definitions related to neutrosophic sets and SVNNSs, respectively [30–33].

**Definition 1.** In universal  $U$ , a NS is distinct with truth, falsity, and indeterminacy membership functions of  $x$  in the real nonstandard  $]^-0, 1^+[$ , where the summation of them belong to  $[0, 3]$ . If these functions are singleton in the  $[0, 1]$ , then a SVNNS  $\psi$  is denoted by

$$\psi = \{(x, \tilde{h}_\psi(x), \tilde{\ell}_\psi(x), \tilde{\lambda}_\psi(x)) \mid x \in U\}. \quad (4)$$

Furthermore,  $\psi = \langle \tilde{h}_\psi, \tilde{\ell}_\psi, \tilde{\lambda}_\psi \rangle$  is called the single-valued neutrosophic number (SVNN) if  $U$  has just one component.

**Definition 2.** Suppose that  $C$  and  $D$  be two SVNNSs, then  $C \subseteq D$  if and only if  $\tilde{h}_C(x) \leq \tilde{h}_D(x)$ ,  $\tilde{\ell}_C(x) \geq \tilde{\ell}_D(x)$ , and  $\tilde{\lambda}_C(x) \geq \tilde{\lambda}_D(x)$ .

**Definition 3.** Let  $M$  and  $N$  be two SVNNSs. Then, equations (5) to (8) are true:

$$(i) \quad M \oplus N = \langle \tilde{h}_M + \tilde{h}_N - \tilde{h}_M \tilde{h}_N, \tilde{\ell}_M \tilde{\ell}_N, \tilde{\lambda}_M \tilde{\lambda}_N \rangle, \quad (5)$$

$$(ii) \quad M \otimes N = \langle \tilde{h}_M \tilde{h}_N, \tilde{\ell}_M + \tilde{\ell}_N - \tilde{\ell}_M \tilde{\ell}_N, \tilde{\lambda}_M + \tilde{\lambda}_N - \tilde{\lambda}_M \tilde{\lambda}_N \rangle, \quad (6)$$

$$(iii) \quad \alpha M = \langle 1 - (1 - \tilde{h}_M(x))^\alpha, (\tilde{\ell}_M(x))^\alpha, (\tilde{\lambda}_M(x))^\alpha \rangle, \quad \alpha > 0, \quad (7)$$

$$(iv) \quad M^\alpha = \langle (\tilde{h}_M(x))^\alpha, 1 - (1 - \tilde{\ell}_M(x))^\alpha, 1 - (1 - \tilde{\lambda}_M(x))^\alpha \rangle, \quad \alpha > 0. \quad (8)$$

**Definition 4.** Suppose that  $M_q = \langle \tilde{h}_{M_q}, \tilde{\ell}_{M_q}, \tilde{\lambda}_{M_q} \rangle$  ( $q = 1, \dots, n$ ) be a collection SVNNSs. Then, the related weighted arithmetic average operator is

$$F_W(M_1, \dots, M_n) = \sum_{q=1}^n \omega_q M_q, \quad (9)$$

and the aggregation operator is defined as follows:

$$F_W(M_1, \dots, M_n) = \left\langle 1 - \prod_{q=1}^n (1 - \tilde{h}_{M_q}(x))^{\omega_q}, \prod_{q=1}^n (\tilde{\ell}_{M_q}(x))^{\omega_q}, \prod_{q=1}^n (\tilde{\lambda}_{M_q}(x))^{\omega_q} \right\rangle, \quad (10)$$

where  $W = (\omega_1, \omega_2, \dots, \omega_n)$  is the weight vector of  $M_q$ ,  $\omega_q \in [0, 1]$  and  $\sum_{q=1}^n \omega_q = 1$ .

### 4. Proposed Model

In the DEA literature, there are some models of DEA with neutrosophic information, see [61–67]. Nevertheless, these models work solely for desirable outputs and cannot consider undesirable outputs. Hence, there is a requisite to develop a new model that keeps original advantage of neutrosophic DEA models and considers the influence of undesirable outputs. In this section, we propose an input-oriented BCC model with undesirable outputs in which all data are SVNNSs. Furthermore, we propose an algorithm for solving the new DEA model. Moreover, a theorem regarding the feasibility and boundedness of the solution of the new model has been provided. For the  $q$ th DMU, consider the input  $\tilde{x}_{pq} = \langle \tilde{h}_{x_{pq}}, \tilde{\ell}_{x_{pq}}, \tilde{\lambda}_{x_{pq}} \rangle$ , desirable outputs

$\tilde{y}_{sq}^g = \langle \tilde{h}_{y_{sq}^g}, \tilde{\ell}_{y_{sq}^g}, \tilde{\lambda}_{y_{sq}^g} \rangle$ , and undesirable outputs  $\tilde{y}_{sq}^b = \langle \tilde{h}_{y_{sq}^b}, \tilde{\ell}_{y_{sq}^b}, \tilde{\lambda}_{y_{sq}^b} \rangle$  which are the SVNNSs. Thus, by combinations of the BCC model under the single-valued neutrosophic environment with undesirable outputs, we have the following model:

$$\begin{aligned} \text{Min} \quad & \eta_o \\ \text{s.t.} \quad & \sum_{q=1}^n \alpha_q \tilde{x}_{pq} \leq \eta_o \tilde{x}_{p_o}, \quad p = 1, \dots, m \\ & \sum_{q=1}^n \alpha_j \tilde{y}_{sq}^g \geq \tilde{y}_{s_o}^g, \quad s = 1, \dots, k \\ & \sum_{q=1}^n \alpha_j \tilde{y}_{s'q}^b \leq \eta_o \tilde{y}_{s'o}^b, \quad s' = 1, \dots, k' \\ & \sum_{q=1}^n \alpha_q = 1, \quad \alpha_q \geq 0, \quad q = 1, \dots, n. \end{aligned} \quad (11)$$

Step 1. Construct the problem based on Model (10).

Step 2. According to Definitions 3 and 4, transform the SVNbcc-UO model of Step 1 into

$$\begin{aligned}
 \text{Min} \quad & \eta_o \\
 \text{S.t.} \quad & \left\langle 1 - \prod_{q=1}^n (1 - \tilde{h}_{x_{pq}})^{\alpha_q}, \prod_{q=1}^n (\ell_{x_{pq}})^{\alpha_q}, \prod_{q=1}^n (\tilde{\lambda}_{x_{pq}})^{\alpha_q} \right\rangle \leq \left\langle 1 - (1 - \tilde{h}_{x_{po}})^{\eta_o}, (\ell_{x_{po}})^{\eta_o}, (\tilde{\lambda}_{x_{po}})^{\eta_o} \right\rangle, \quad p = 1, \dots, m \\
 & \left\langle 1 - \prod_{q=1}^n (1 - \tilde{h}_{y_{sq}})^{\alpha_q}, \prod_{q=1}^n (\ell_{y_{sq}})^{\alpha_q}, \prod_{q=1}^n (\tilde{\lambda}_{y_{sq}})^{\alpha_q} \right\rangle \geq \left\langle \tilde{h}_{y_{so}}^g, \ell_{y_{so}}^g, \tilde{\lambda}_{y_{so}}^g \right\rangle, \quad s = 1, \dots, k \\
 & \left\langle 1 - \prod_{q=1}^n (1 - \tilde{h}_{y_{s'q}})^{\alpha_q}, \prod_{q=1}^n (\ell_{y_{s'q}})^{\alpha_q}, \prod_{q=1}^n (\tilde{\lambda}_{y_{s'q}})^{\alpha_q} \right\rangle \leq \left\langle 1 - (1 - \tilde{h}_{y_{s'o}})^{\eta_o}, (\ell_{y_{s'o}})^{\eta_o}, (\tilde{\lambda}_{y_{s'o}})^{\eta_o} \right\rangle, \quad s' = 1, \dots, k' \\
 & \sum_{q=1}^n \alpha_q = 1 \\
 & \alpha_q \geq 0, \quad q = 1, \dots, n.
 \end{aligned}$$

Step 3. By Definition 2, transform Step 2 into

$$\begin{aligned}
 \text{Min} \quad & \eta_o \\
 & \prod_{q=1}^n (1 - \tilde{h}_{x_{pq}})^{\alpha_q} \geq (1 - \tilde{h}_{x_{po}})^{\eta_o}, \quad p = 1, 2, \dots, m \\
 & \prod_{q=1}^n (\ell_{x_{pq}})^{\alpha_q} \geq (\ell_{x_{po}})^{\eta_o}, \quad p = 1, 2, \dots, m \\
 & \prod_{q=1}^n (\tilde{\lambda}_{x_{pq}})^{\alpha_q} \geq (\tilde{\lambda}_{x_{po}})^{\eta_o}, \quad p = 1, 2, \dots, m \\
 & \prod_{q=1}^n (1 - \tilde{h}_{y_{sq}})^{\alpha_q} \leq (1 - \tilde{h}_{y_{so}}^g), \quad s = 1, \dots, k \\
 & \prod_{q=1}^n (\ell_{y_{sq}})^{\alpha_q} \leq \ell_{y_{so}}^g, \quad s = 1, \dots, k \\
 \text{s.t.} \quad & \prod_{q=1}^n (\tilde{\lambda}_{y_{sq}})^{\alpha_q} \leq \tilde{\lambda}_{y_{so}}^g, \quad s = 1, \dots, k \\
 & \prod_{q=1}^n (1 - \tilde{h}_{y_{s'q}})^{\alpha_q} \geq (1 - \tilde{h}_{y_{s'o}})^{\eta_o}, \quad s' = 1, \dots, k' \\
 & \prod_{q=1}^n (\ell_{y_{s'q}})^{\alpha_q} \geq (\ell_{y_{s'o}})^{\eta_o}, \quad s' = 1, \dots, k' \\
 & \prod_{q=1}^n (\tilde{\lambda}_{y_{s'q}})^{\alpha_q} \geq (\tilde{\lambda}_{y_{s'o}})^{\eta_o}, \quad s' = 1, \dots, k' \\
 & \sum_{q=1}^n \alpha_q = 1, \\
 & \alpha_q \geq 0, \quad q = 1, \dots, n.
 \end{aligned}$$

Step 4. Convert Step 3 into the following linear model:

$$\begin{aligned}
 \text{Min} \quad & \eta_o \\
 & \sum_{q=1}^n \alpha_q \ln(1 - \tilde{h}_{x_{pq}}) \geq \eta_o \ln(1 - \tilde{h}_{x_{po}}), \quad p = 1, 2, \dots, m \\
 & \sum_{q=1}^n \alpha_q \ln(\ell_{x_{pq}}) \geq \eta_o \ln(\ell_{x_{po}}), \quad p = 1, 2, \dots, m \\
 & \sum_{q=1}^n \alpha_q \ln(\tilde{\lambda}_{x_{pq}}) \geq \eta_o \ln(\tilde{\lambda}_{x_{po}}), \quad p = 1, 2, \dots, m \\
 & \sum_{q=1}^n \alpha_q \ln(1 - \tilde{h}_{y_{sq}}) \leq \ln(1 - \tilde{h}_{y_{so}}^g), \quad s = 1, \dots, k \\
 & \sum_{q=1}^n \alpha_q \ln(\ell_{y_{sq}}) \leq \ln(\ell_{y_{so}}^g), \quad s = 1, \dots, k \\
 \text{s.t.} \quad & \sum_{q=1}^n \alpha_q \ln(\tilde{\lambda}_{y_{sq}}) \leq \ln(\tilde{\lambda}_{y_{so}}^g), \quad s = 1, \dots, k \\
 & \sum_{q=1}^n \alpha_j \ln(1 - \tilde{h}_{y_{s'q}}) \geq \eta_o \ln(1 - \tilde{h}_{y_{s'o}}), \quad s' = 1, \dots, k' \\
 & \sum_{q=1}^n \alpha_j \ln(\ell_{y_{s'q}}) \geq \eta_o \ln(\ell_{y_{s'o}}), \quad s' = 1, \dots, k' \\
 & \sum_{q=1}^n \alpha_j \ln(\tilde{\lambda}_{y_{s'q}}) \geq \eta_o \ln(\tilde{\lambda}_{y_{s'o}}), \quad s' = 1, \dots, k' \\
 & \sum_{q=1}^n \alpha_q = 1 \\
 & \alpha_q \geq 0, \quad q = 1, \dots, n.
 \end{aligned}$$

Step 5. Using Step 4, get the optimal efficiency of each DMU.

ALGORITHM 1: Solution of the SVNbcc-UO model.

We called this model as single-valued neutrosophic BCC with undesirable outputs (SVNBCC-UO). Now, we present an algorithm to solve Model (11).

In the following, we show that our model is feasible and bounded.

**Theorem 1.** *The model of SVNbcc-UO is feasible and bounded. Furthermore, its optimal objective function is 1.*

*Proof.* From Algorithm 1, we can transform the model SVNbcc-UO into Step 4 in Algorithm 1. So, with the so-

lution  $\alpha_q = \begin{cases} 1, & q = o, \\ 0, & \text{else,} \end{cases}$  and  $\eta_o = 1$ , it is easy to see that the

Step 4 in Algorithm 1 is always feasible. Thus, regardless of the values of inputs and outputs, there is always at least one feasible solution for Step 4 in Algorithm 1. Because the above solution is feasible along with the objective function of Step 4



TABLE 1: Input information of the 15 DMUs.

DMUS	Input 1	Input 2	Input 3
1	$\langle 0.6, 0.4, 0.3 \rangle$	$\langle 0.5, 0.4, 0.3 \rangle$	$\langle 0.7, 0.3, 0.4 \rangle$
2	$\langle 0.3, 0.1, 0.2 \rangle$	$\langle 0.6, 0.5, 0.1 \rangle$	$\langle 0.6, 0.4, 0.5 \rangle$
3	$\langle 0.4, 0.2, 0.1 \rangle$	$\langle 0.2, 0.6, 0.3 \rangle$	$\langle 0.8, 0.2, 0.1 \rangle$
4	$\langle 0.5, 0.5, 0.2 \rangle$	$\langle 0.2, 0.3, 0.1 \rangle$	$\langle 0.5, 0.2, 0.2 \rangle$
5	$\langle 0.3, 0.2, 0.4 \rangle$	$\langle 0.2, 0.8, 0.7 \rangle$	$\langle 0.7, 0.2, 0.7 \rangle$
6	$\langle 0.5, 0.2, 0.2 \rangle$	$\langle 0.7, 0.5, 0.1 \rangle$	$\langle 0.7, 0.3, 0.2 \rangle$
7	$\langle 0.7, 0.1, 0.2 \rangle$	$\langle 0.4, 0.4, 0.2 \rangle$	$\langle 0.7, 0.3, 0.2 \rangle$
8	$\langle 0.2, 0.6, 0.5 \rangle$	$\langle 0.1, 0.7, 0.2 \rangle$	$\langle 0.3, 0.9, 0.6 \rangle$
9	$\langle 0.6, 0.3, 0.3 \rangle$	$\langle 0.5, 0.2, 0.5 \rangle$	$\langle 0.9, 0.2, 0.3 \rangle$
10	$\langle 0.4, 0.7, 0.7 \rangle$	$\langle 0.8, 0.2, 0.6 \rangle$	$\langle 0.6, 0.2, 0.3 \rangle$
11	$\langle 0.7, 0.3, 0.3 \rangle$	$\langle 0.4, 0.1, 0.3 \rangle$	$\langle 0.5, 0.1, 0.4 \rangle$
12	$\langle 0.6, 0.3, 0.5 \rangle$	$\langle 0.5, 0.5, 0.3 \rangle$	$\langle 0.6, 0., 0.3 \rangle$
13	$\langle 0.5, 0.2, 0.4 \rangle$	$\langle 0.9, 0.3, 0.3 \rangle$	$\langle 0.8, 0.1, 0.4 \rangle$
14	$\langle 0.4, 0.3, 0.1 \rangle$	$\langle 0.8, 0.4, 0.1 \rangle$	$\langle 0.9, 0.2, 0.3 \rangle$
15	$\langle 0.6, 0.4, 0.3 \rangle$	$\langle 0.5, 0.1, 0.1 \rangle$	$\langle 0.6, 0.1, 0.1 \rangle$

TABLE 2: Output information of the 15 DMUs.

DMUS	Output 1(good)	Output 2 (good)	Output 3 (bad)
1	$\langle 0.5, 0.5, 0.7 \rangle$	$\langle 0.5, 0.4, 0.4 \rangle$	$\langle 0.5, 0.2, 0.1 \rangle$
2	$\langle 0.2, 0.7, 0.5 \rangle$	$\langle 0.7, 0.2, 0.5 \rangle$	$\langle 0.4, 0.1, 0.1 \rangle$
3	$\langle 0.3, 0.5, 0.8 \rangle$	$\langle 0.6, 0.7, 0.5 \rangle$	$\langle 0.6, 0.2, 0.1 \rangle$
4	$\langle 0.2, 0.5, 0.7 \rangle$	$\langle 0.3, 0.5, 0.6 \rangle$	$\langle 0.5, 0.2, 0.1 \rangle$
5	$\langle 0.8, 0.4, 0.3 \rangle$	$\langle 0.8, 0.5, 0.1 \rangle$	$\langle 0.3, 0.1, 0.6 \rangle$
6	$\langle 0.3, 0.6, 0.7 \rangle$	$\langle 0.1, 0.6, 0.7 \rangle$	$\langle 0.8, 0.1, 0.2 \rangle$
7	$\langle 0.5, 0.2, 0.6 \rangle$	$\langle 0.5, 0.5, 0.4 \rangle$	$\langle 0.9, 0.2, 0.3 \rangle$
8	$\langle 0.3, 0.3, 0.6 \rangle$	$\langle 0.7, 0.4, 0.7 \rangle$	$\langle 0.3, 0.3, 0.3 \rangle$
9	$\langle 0.6, 0.4, 0.4 \rangle$	$\langle 0.5, 0.5, 0.5 \rangle$	$\langle 0.4, 0.2, 0.1 \rangle$
10	$\langle 0.2, 0.3, 0.7 \rangle$	$\langle 0.5, 0.3, 0.3 \rangle$	$\langle 0.5, 0.4, 0.1 \rangle$
11	$\langle 0.3, 0.8, 0.5 \rangle$	$\langle 0.2, 0.7, 0.6 \rangle$	$\langle 0.5, 0.2, 0.2 \rangle$
12	$\langle 0.6, 0.1, 0.4 \rangle$	$\langle 0.2, 0.2, 0.3 \rangle$	$\langle 0.1, 0.5, 0.5 \rangle$
13	$\langle 0.4, 0.7, 0.8 \rangle$	$\langle 0.4, 0.8, 0.6 \rangle$	$\langle 0.7, 0.1, 0.1 \rangle$
14	$\langle 0.5, 0.5, 0.6 \rangle$	$\langle 0.5, 0.3, 0.5 \rangle$	$\langle 0.5, 0.2, 0.4 \rangle$
15	$\langle 0.2, 0.4, 0.8 \rangle$	$\langle 0.7, 0.4, 0.6 \rangle$	$\langle 0.4, 0.1, 0.1 \rangle$

TABLE 3: The efficiencies of the DMUs.

DMUS	Efficiency ( $\eta^*$ )	Rank
DMU1	0.8329	6
DMU2	0.7504	8
DMU3	0.9451	4
DMU4	0.8197	7
DMU5	1.0000	1
DMU6	0.5822	12
DMU7	0.7430	9
DMU8	1.0000	1
DMU9	0.9821	2
DMU10	1.0000	1
DMU11	0.9463	3
DMU12	1.0000	1
DMU13	0.7270	10
DMU14	0.8987	5
DMU15	0.6549	11

in Algorithm 1 is minimization, the best value regarding the objective function is certainly lower than or equal to 1.  $\square$

## 5. Numerical Experiment

In this section, the proposed SVNCCC-UO and the related algorithm are illustrated with a numerical example to ensure their validity and usefulness over the existing models.

*Example 1.* Consider an efficiency problem with 15 DMUs, three inputs, two desirable outputs, and one undesirable output that all information are presented as SVNNS (see Tables 1 and 2).

Here, we used Algorithm 1 for solving the SVNCCC-UO model. Suppose that DMU<sub>1</sub> is under consideration, so based on Algorithm 1 we have the following.

First, we construct the model using Steps 1–3. Then, by means of Step 4, we construct the  $\min \eta_1$  with the constraints of Step 4 in Algorithm 1. For example, by Step 4 in Algorithm 1 for Input 1, we have the following relation:

$$\begin{aligned}
& \alpha_1 \ln(1 - 0.6) + \alpha_2 \ln(1 - 0.3) + \alpha_3 \ln(1 - 0.4) + \alpha_4 \ln(1 - 0.5) \\
& + \alpha_5 \ln(1 - 0.3) + \alpha_6 \ln(1 - 0.5) + \alpha_7 \ln(1 - 0.7) + \alpha_8 \ln(1 - 0.2) \\
& + \alpha_9 \ln(1 - 0.6) + \alpha_{10} \ln(1 - 0.4) + \alpha_{11} \ln(1 - 0.7) + \alpha_{12} \ln(1 - 0.6) \\
& + \alpha_{13} \ln(1 - 0.5) + \alpha_{14} \ln(1 - 0.4) + \alpha_{15} \ln(1 - 0.6) \geq \eta_1 \ln(1 - 0.6).
\end{aligned} \tag{12}$$

So, after calculations with Matlab, we get  $\eta_1^* = 0.9068$  for DMU<sub>1</sub>. Correspondingly, the technical efficiencies of each DMU<sub>i</sub> are measured using the proposed algorithm and are presented in Table 3.

To validate the presented efficiencies, these efficiencies were compared with the efficiencies obtained by the existing neutrosophic DEA methods and are given in Figure 1. In this figure, we can see the impact of undesirable outputs on the performance of DMUs. From Figure 1, we can see that the efficiencies of DMUs are found to be smaller for SVNCCC-UO compared to the existing neutrosophic DEA methods. It is interesting that DMUs 1–4, 6–7, and 9 are efficient in the existing neutrosophic DEA methods; however, they are actually inefficient with the efficiency scores of 0.8329, 0.7504, 0.9451, 0.8197, 0.5822, 0.7430, and 0.9821 using

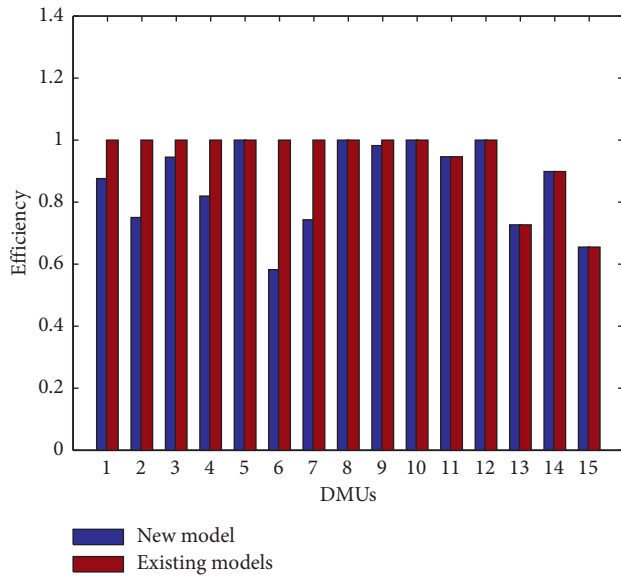


FIGURE 1: Comparison of the new model and the existing models.

SVNBCC-UO, respectively. Therefore, SVNBCC-UO is more *realistic* than the existing neutrosophic DEA methods. Therefore, if we solve the mentioned problem with the existing methods, we cannot get to a reliable evaluation.

## 6. Conclusions and Future Work

This paper, established a new strategy to solve a neutrosophic data envelopment analysis model with undesirable outputs. In comparison with the existing neutrosophic DEA methods, the significant characteristic of the new DEA method is that it can handle the undesirable outputs simply and effectively. A numerical experiment and comparison results with the existing models have been demonstrated to display the competence of the presented method. The proposed methodology has created hopeful consequences from computing and performance facets. It is worth mentioning that the uncertainty, ambiguity, and indeterminacy in this paper are limited to single-valued neutrosophic numbers. Nevertheless, the other types of numbers such as bipolar NSs and interval-valued neutrosophic numbers, Pythagorean fuzzy set, and  $q$ -rung orthopair fuzzy set can also be used to indicate variables characterizing the core in world-wide problems. As for future research, we intend to extend the proposed approach to these kinds of tools.

## Data Availability

The data used to support the findings of this study are included within the article.

## Conflicts of Interest

The authors declare no conflicts of interest.

## Acknowledgments

This work was supported by Xinxiang University.

## References

- [1] M. J. Farrell, "The measurement of productive efficiency," *Journal of the Royal Statistical Society. Series A (General)*, vol. 120, no. 3, p. 253, 1957.
- [2] A. Charnes, W. W. Cooper, and E. Rhodes, "Measuring the efficiency of decision making units," *European Journal of Operational Research*, vol. 2, no. 6, pp. 429–444, 1978.
- [3] R. D. Banker, A. Charnes, and W. W. Cooper, "Some models for estimating technical and scale inefficiencies in data envelopment analysis," *Management Science*, vol. 30, no. 9, pp. 1078–1092, 1984.
- [4] Y. J. Lee, S.-J. Joo, and H. G. Park, "An application of data envelopment analysis for Korean banks with negative data," *Benchmarking: An International Journal*, vol. 24, no. 4, pp. 1052–1064, 2017.
- [5] S. Kaffash, R. Azizi, Y. Huang, and J. Zhu, "A survey of data envelopment analysis applications in the insurance industry 1993-2018," *European Journal of Operational Research*, vol. 284, no. 3, pp. 801–813, 2020.
- [6] H. H. Liu, J. J. Huang, and Y. H. Chiu, "Integration of network data envelopment analysis and decision-making trial and evaluation laboratory for the performance evaluation of the financial holding companies in Taiwan," *Managerial and Decision Economics*, vol. 41, no. 1, pp. 64–78, 2020.
- [7] L. A. Moncayo-Martínez, A. Ramírez-Nafarrate, and M. G. Hernández-Balderama, "Evaluation of public HEI on teaching, research, and knowledge dissemination by Data Envelopment Analysis," *Socio-Economic Planning Sciences*, vol. 69, p. 100718, 2020.
- [8] N. Ai, M. Kjerland, C. Klein-Banai, and T. L. Theis, "Sustainability assessment of universities as small-scale urban systems: a comparative analysis using Fisher Information and Data Envelopment Analysis," *Journal of Cleaner Production*, vol. 212, pp. 1357–1367, 2019.
- [9] D. Fernández, C. Pozo, R. Folgado, L. Jiménez, and G. Guillén-Gosálbez, "Productivity and energy efficiency assessment of existing industrial gases facilities via data envelopment analysis and the Malmquist index," *Applied Energy*, vol. 212, pp. 1563–1577, 2018.
- [10] S. Kohl, J. Schoenfelder, A. Fügner, and J. O. Brunner, "The use of Data Envelopment Analysis (DEA) in healthcare with a focus on hospitals," *Health Care Management Science*, vol. 22, no. 2, pp. 245–286, 2019.
- [11] M. Shafiee, F. Hosseinzadeh Lotfi, and H. Saleh, "Supply chain performance evaluation with data envelopment analysis and balanced scorecard approach," *Applied Mathematical Modelling*, vol. 38, no. 21-22, pp. 5092–5112, 2014.
- [12] A. Emrouznejad and G.-I. Yang, "A survey and analysis of the first 40 years of scholarly literature in DEA: 1978-2016," *Socio-Economic Planning Sciences*, vol. 61, pp. 4–8, 2018.
- [13] H. Chen, J. Liu, Y. Li, Y.-H. Chiu, and T.-Y. Lin, "A two-stage dynamic undesirable data envelopment analysis model focused on media reports and the impact on energy and health efficiency," *International Journal of Environmental Research and Public Health*, vol. 16, no. 9, p. 1535, 2019.
- [14] S. Soheilrad, K. Govindan, A. Mardani, E. K. Zavadskas, M. Nilashi, and N. Zakuan, "Application of data envelopment analysis models in supply chain management: a systematic review and meta-analysis," *Annals of Operations Research*, vol. 271, no. 2, pp. 915–969, 2018.
- [15] R. Lacko, Z. Hajduová, and V. Gábor, "Data envelopment analysis of selected specialized health centres and possibilities of its application in the terms of Slovak republic health care

- system,” *Journal of Health Management*, vol. 19, no. 1, pp. 144–158, 2017.
- [16] E. Krmac and B. Djordjević, “A new DEA model for evaluation of supply chains: a case of selection and evaluation of environmental efficiency of suppliers,” *Symmetry*, vol. 11, no. 4, 2019.
  - [17] A. Hatami-Marbini, A. Emrouznejad, and M. Tavana, “A taxonomy and review of the fuzzy data envelopment analysis literature: two decades in the making,” *European Journal of Operational Research*, vol. 214, no. 3, pp. 457–472, 2011.
  - [18] A. Emrouznejad, M. Tavana, and A. Hatami-Marbini, “The state of the art in fuzzy data envelopment analysis,” *Performance Measurement with Fuzzy Data Envelopment Analysis*, vol. 309, pp. 1–45, 2014.
  - [19] F. Hosseinzadeh Lotfi, A. Ebrahimnejad, M. Vaez-Ghasemi, and Z. Moghaddas, *Data Envelopment Analysis with R*, Springer International Publishing, Cham, Switzerland, 2020.
  - [20] K. T. Atanassov, “Intuitionistic fuzzy sets,” *Fuzzy Sets and Systems*, vol. 20, no. 1, pp. 87–96, 1986.
  - [21] R. R. Yager, “Pythagorean fuzzy subsets,” in *Proceedings of the 2013 Joint IFSA World Congress and NAFIPS Annual Meeting*, pp. 57–61, IFSA/NAFIPS, Edmonton, Canada, 2013.
  - [22] L. Wang and N. Li, “Pythagorean fuzzy interaction power Bonferroni mean aggregation operators in multiple attribute decision making,” *International Journal of Intelligent Systems*, vol. 35, no. 1, pp. 150–183, 2020.
  - [23] R. Kumar, S. A. Edalatpanah, S. Jha, and R. Singh, “A Pythagorean fuzzy approach to the transportation problem,” *Complex & Intelligent Systems*, vol. 5, no. 2, pp. 255–263, 2019.
  - [24] F. Smarandache, *A Unifying Field in Logics. Neutrosophy: Neutrosophic Probability, Set and Logic*, American Research Press, Rehoboth, MA, USA, 1999.
  - [25] F. G. Lupiáñez, “Interval neutrosophic sets and topology,” *Kybernetes*, vol. 38, no. 3–4, pp. 621–624, 2009.
  - [26] H. Garg and Nancy, “Multiple attribute decision making based on immediate probabilities aggregation operators for single-valued and interval neutrosophic sets,” *Journal of Applied Mathematics and Computing*, vol. 63, no. 1–2, pp. 619–653, 2020.
  - [27] Y. Yuan, Y. Ren, Y. Ren, X. Liu, and J. Wang, “Approach to image segmentation based on interval neutrosophic set,” *Numerical Algebra, Control & Optimization*, vol. 10, no. 1, pp. 1–11, 2020.
  - [28] S. Broumi, A. Bakali, M. Talea, F. Smarandache, and M. Ali, “Shortest path problem under bipolar neutrosophic setting,” *Applied Mechanics and Materials*, vol. 859, pp. 59–66, 2016.
  - [29] V. Uluçay, I. Deli, and M. Şahin, “Similarity measures of bipolar neutrosophic sets and their application to multiple criteria decision making,” *Neural Computing and Applications*, vol. 29, no. 3, pp. 739–748, 2018.
  - [30] J. Ye, “Multicriteria decision-making method using the correlation coefficient under single-valued neutrosophic environment,” *International Journal of General Systems*, vol. 42, no. 4, pp. 386–394, 2013.
  - [31] S. Broumi, F. Smarandache, M. Talea, and A. Bakali, “Single valued neutrosophic graphs: degree, order and size,” in *Proceedings of the 2016 IEEE International Conference on Fuzzy Systems*, pp. 2444–2451, FUZZ-IEEE, New Orleans, LA, USA, 2016.
  - [32] X. Peng and J. Dai, “Approaches to single-valued neutrosophic MADM based on MABAC, TOPSIS and new similarity measure with score function,” *Neural Computing and Applications*, vol. 29, no. 10, pp. 939–954, 2018.
  - [33] H. Garg, “Novel neutrality aggregation operator-based multiattribute group decision-making method for single-valued neutrosophic numbers,” *Soft Computing*, vol. 24, no. 14, pp. 10327–10349, 2020.
  - [34] J. Ye, “A multicriteria decision-making method using aggregation operators for simplified neutrosophic sets,” *Journal of Intelligent & Fuzzy Systems*, vol. 26, no. 5, pp. 2459–2466, 2014.
  - [35] J.-J. Peng, J.-Q. Wang, H.-Y. Zhang, and X.-H. Chen, “An outranking approach for multi-criteria decision-making problems with simplified neutrosophic sets,” *Applied Soft Computing*, vol. 25, pp. 336–346, 2014.
  - [36] J. Ye, “Generalized ordered weighted simplified neutrosophic cosine similarity measure for multiple attribute group decision making,” *International Journal of Cognitive Informatics and Natural Intelligence*, vol. 14, no. 1, pp. 51–62, 2020.
  - [37] S. A. Edalatpanah, “Neutrosophic structured element,” *Expert Systems*, Article ID e12542, 2020.
  - [38] J.-J. Peng, J.-Q. Wang, X.-H. Wu, J. Wang, and X.-H. Chen, “Multi-valued neutrosophic sets and power aggregation operators with their applications in multi-criteria group decision-making problems,” *International Journal of Computational Intelligence Systems*, vol. 8, no. 2, pp. 345–363, 2015.
  - [39] N. L. A. M. Kamal, L. Abdullah, I. Abdullah, S. Alkhazaleh, and F. Karaaslan, “Multi-valued interval neutrosophic soft set: formulation and theory,” *Neutrosophic Sets and Systems*, vol. 30, pp. 149–170, 2019.
  - [40] J. Ye, “Some aggregation operators of interval neutrosophic linguistic numbers for multiple attribute decision making,” *Journal of Intelligent & Fuzzy Systems*, vol. 27, no. 5, pp. 2231–2241, 2014.
  - [41] J. Ye, “Hesitant interval neutrosophic linguistic set and its application in multiple attribute decision making,” *International Journal of Machine Learning and Cybernetics*, vol. 10, no. 4, pp. 667–678, 2019.
  - [42] S. A. Edalatpanah, “Systems of neutrosophic linear equations,” *Neutrosophic Sets and Systems*, vol. 33, pp. 92–104, 2020.
  - [43] S. A. Edalatpanah, “A nonlinear approach for neutrosophic linear programming,” *Journal of Applied Research on Industrial Engineering*, vol. 6, no. 4, pp. 367–373, 2019.
  - [44] S. K. Das and S. A. Edalatpanah, “A new ranking function of triangular neutrosophic number and its application in integer programming,” *International Journal of Neutrosophic Science*, vol. 4, no. 2, pp. 82–92, 2020.
  - [45] S. A. Edalatpanah, “A direct model for triangular neutrosophic linear programming,” *International Journal of Neutrosophic Science*, vol. 1, no. 1, pp. 19–28, 2020.
  - [46] R. Kumar, S. A. Edalatpanah, S. Jha, S. Broumi, and A. Dey, “Neutrosophic shortest path problem,” *Neutrosophic Sets and Systems*, vol. 23, pp. 5–15, 2018.
  - [47] H. Garg, “Algorithms for single-valued neutrosophic decision making based on topsis and clustering methods with new distance measure,” *AIMS Mathematics*, vol. 5, no. 3, pp. 2671–2693, 2020.
  - [48] U. Riveccio, “Neutrosophic logics: prospects and problems,” *Fuzzy Sets and Systems*, vol. 159, no. 14, pp. 1860–1868, 2008.
  - [49] X. Peng and J. Dai, “A bibliometric analysis of neutrosophic set: two decades review from 1998 to 2017,” *Artificial Intelligence Review*, vol. 53, no. 1, pp. 199–255, 2020.
  - [50] G. N. Nguyen, L. H. Son, A. S. Ashour, and N. Dey, “A survey of the state-of-the-arts on neutrosophic sets in biomedical

- diagnoses,” *International Journal of Machine Learning and Cybernetics*, vol. 10, no. 1, 2019.
- [51] M. Abdel-Basset, G. Manogaran, A. Gamal, and F. Smarandache, “A hybrid approach of neutrosophic sets and DEMATEL method for developing supplier selection criteria,” *Design Automation for Embedded Systems*, vol. 22, no. 3, pp. 257–278, 2018.
  - [52] S. A. Edalatpanah, “A data envelopment analysis model with triangular intuitionistic fuzzy numbers,” *International Journal of Data Envelopment Analysis*, vol. 7, no. 4, pp. 47–58, 2019.
  - [53] A. Arya and S. P. Yadav, “A new approach to rank the decision making units in presence of infeasibility in intuitionistic fuzzy environment,” *Iranian Journal of Fuzzy Systems*, vol. 17, no. 2, pp. 183–199, 2020.
  - [54] J. Puri and S. P. Yadav, “Intuitionistic fuzzy data envelopment analysis: an application to the banking sector in India,” *Expert Systems with Applications*, vol. 42, no. 11, pp. 4982–4998, 2015.
  - [55] B. D. Rouyendegh, A. Yildizbasi, and I. Yilmaz, “Evaluation of retail industry performance ability through integrated intuitionistic fuzzy TOPSIS and data envelopment analysis approach,” *Soft Computing*, vol. 24, no. 16, pp. 12255–12266, 2020.
  - [56] W. Zhou, J. Chen, B. Ding, and S. Meng, “Interval-valued intuitionistic fuzzy envelopment analysis and preference fusion,” *Computers & Industrial Engineering*, vol. 142, p. 106361, 2020.
  - [57] J. Liu, J. Song, Q. Xu, Z. Tao, and H. Chen, “Group decision making based on DEA cross-efficiency with intuitionistic fuzzy preference relations,” *Fuzzy Optimization and Decision Making*, vol. 18, no. 3, pp. 345–370, 2019.
  - [58] A. Arya and S. P. Yadav, “Development of intuitionistic fuzzy data envelopment analysis models and intuitionistic fuzzy input-output targets,” *Soft Computing*, vol. 23, no. 18, pp. 8975–8993, 2019.
  - [59] S. Singh, “Intuitionistic fuzzy dea/ar and its application to flexible manufacturing systems,” *RAIRO-Operations Research*, vol. 52, no. 1, pp. 241–257, 2018.
  - [60] S. H. R. Hajiagha, H. Akrami, E. Kazimieras Zavadskas, and S. S. Hashemi, “An intuitionistic fuzzy data envelopment analysis for efficiency evaluation under uncertainty: case of a finance and credit institution,” *E a M: Ekonomik a Management*, vol. 161, pp. 128–137, 2013.
  - [61] S. A. Edalatpanah, “Neutrosophic perspective on DEA,” *Journal of Applied Research on Industrial Engineering*, vol. 5, no. 4, pp. 339–345, 2018.
  - [62] W. Yang, L. Cai, S. A. Edalatpanah, and F. Smarandache, “Triangular single valued neutrosophic data envelopment analysis: application to hospital performance measurement,” *Symmetry*, vol. 12, no. 4, p. 588, 2020.
  - [63] W. Abdelfattah, “Data envelopment analysis with neutrosophic inputs and outputs,” *Expert Systems*, vol. 36, no. 6, Article ID e12453, 2019.
  - [64] C. Kahraman, İ. Otay, B. Öztay, and S. Ç. Onar, “An integrated AHP & DEA methodology with neutrosophic sets,” in *Studies in Fuzziness and Soft Computing*, pp. 623–645, Springer-Verlag, Berlin Germany, 2019.
  - [65] S. A. Edalatpanah, “Data envelopment analysis based on triangular neutrosophic numbers,” *CAAI Transactions on Intelligence Technology*, vol. 5, no. 2, pp. 94–98, 2020.
  - [66] S. A. Edalatpanah and F. Smarandache, “Data envelopment analysis for simplified neutrosophic Sets,” vol. 29, 2019.
  - [67] N. Nabeeh, “A hybrid neutrosophic approach of DEMATEL with AR-DEA in technology selection,” *Neutrosophic Sets and Systems*, vol. 31, pp. 17–30, 2020.
  - [68] D. Guo and J. Wu, “A complete ranking of DMUs with undesirable outputs using restrictions in DEA models,” *Mathematical and Computer Modelling*, vol. 58, no. 5–6, pp. 1102–1109, 2013.
  - [69] R. Färe and S. Grosskopf, “Modeling undesirable factors in efficiency evaluation: comment,” *European Journal of Operational Research*, vol. 157, no. 1, pp. 242–245, 2004.
  - [70] B. Walheer, “Output, input, and undesirable output interconnections in data envelopment analysis: convexity and returns-to-scale,” *Annals of Operations Research*, vol. 284, no. 1, pp. 447–467, 2020.
  - [71] S. Lozano, E. Gutiérrez, and P. Moreno, “Network DEA approach to airports performance assessment considering undesirable outputs,” *Applied Mathematical Modelling*, vol. 37, no. 4, pp. 1665–1676, 2013.
  - [72] A. Hadi Vencheh, R. Kazemi Matin, and M. Tavassoli Kajani, “Undesirable factors in efficiency measurement,” *Applied Mathematics and Computation*, vol. 163, no. 2, pp. 547–552, 2005.
  - [73] W. Zhu, M. Xu, and C.-P. Cheng, “Dealing with undesirable outputs in DEA: an aggregation method for a common set of weights,” *Journal of the Operational Research Society*, vol. 71, no. 4, pp. 579–588, 2020.



## Research Article

# A Novel Ensemble Credit Scoring Model Based on Extreme Learning Machine and Generalized Fuzzy Soft Sets

Dayu Xu <sup>1</sup>, Xuyao Zhang <sup>2</sup>, Junguo Hu,<sup>1</sup> and Jiahao Chen<sup>3</sup>

<sup>1</sup>College of Information Engineering, Zhejiang A&F University, Hangzhou, Zhejiang, China

<sup>2</sup>College of Economics and Management, Zhejiang A&F University, Hangzhou, Zhejiang, China

<sup>3</sup>Fuqua School of Business, Duke University, Durham, NC, USA

Correspondence should be addressed to Xuyao Zhang; [xyzafu@163.com](mailto:xyzafu@163.com)

Received 28 February 2020; Accepted 4 May 2020; Published 30 June 2020

Guest Editor: Zaoli Yang

Copyright © 2020 Dayu Xu et al. This is an open access article distributed under the Creative Commons Attribution License, which permits unrestricted use, distribution, and reproduction in any medium, provided the original work is properly cited.

This paper mainly discusses the hybrid application of ensemble learning, classification, and feature selection (FS) algorithms simultaneously based on training data balancing for helping the proposed credit scoring model perform more effectively, which comprises three major stages. Firstly, it conducts preprocessing for collected credit data. Then, an efficient feature selection algorithm based on adaptive elastic net is employed to reduce the weakly related or uncorrelated variables to get high-quality training data. Thirdly, a novel ensemble strategy is proposed to make the imbalanced training data set balanced for each extreme learning machine (ELM) classifier. Finally, a new weighting method for single ELM classifiers in the ensemble model is established with respect to their classification accuracy based on generalized fuzzy soft sets (GFSS) theory. A novel cosine-based distance measurement algorithm of GFSS is also proposed to calculate the weights of each ELM classifier. To confirm the efficiency of the proposed ensemble credit scoring model, we implemented experiments with real-world credit data sets for comparison. The process of analysis, outcomes, and mathematical tests proved that the proposed model is capable of improving the effectiveness of classification in average accuracy, area under the curve (AUC), H-measure, and Brier's score compared to all other single classifiers and ensemble approaches.

## 1. Introduction

Nowadays, financial institutions tend to adopt different risk assessment and credit scoring models to reduce potential risk to a certain extent [1]. By analyzing customer credit data to figure out the probability that potential borrowers will default on their loans, the evaluation approaches can be utilized to turn customer data into principle, which could support credit decisions [2]. In that way, an effective credit scoring model can be a reliable supporting system to help managers in making their financial decisions.

To handle the potential risk of financial services, in the past few years, increasingly financial institutions are moving from traditional manual methods to advanced approaches that require building various types of evaluation models. For credit evaluation, three main methods, which are statistical approaches, nonparametric approaches, and AI methods,

are being widely utilized [3–7]. These three methods work efficiently in various circumstances. Statistical methods consist of different models, which include discriminant analysis models, linear probability models, and probit and logit models. Yet nonparametric approaches tend to utilize the decision tree, *K*-nearest neighbor algorithm, fuzzy logic, Naïve Bayes, and so on. AI methods are more advanced and technology-dependent, such as artificial neural networks, support vector machines (SVM), particle swarm optimization (PSO), and genetic algorithm (GA).

Many researches also indicated that ensemble approaches show more effective performance in the evaluation of credit than single classifiers. To avoid the downsides of single classifiers, an increasing number of researchers have switched to using customized and combined various methods instead of using individual classification models separately. The principle of the hybrid approach is to

perform preprocessing on the data input to the classifiers. The focus is to gather information from group-based classifiers based on the same issue and then export these strengths to get valid credit scoring decisions [8, 9]. In recent years, the research of fuzzy soft sets theory has made great progress, especially in the application field of multiattribute decision making [10, 11]. The development of fuzzy soft sets theory can provide a new perspective for us to build more state-of-the-art ensemble data classification and credit evaluation models [12].

The motivation of our study is to construct a more reliable credit scoring model that can generate accurate outcomes within imbalanced data. Three main approaches will be addressed to achieve this goal: (1) improved elastic net-based feature selection, (2) novel ensemble strategy and learning algorithm for imbalanced credit data, and (3) dynamic weighting method for single ELM classifiers based on new proposed similarity measure of GFSS. Because in real applications of credit risk evaluation, especially in peer-to-peer lending, credit data could be gathered from many different channels, including social networking and judicial administration platforms. The data collected from these channels are usually very sparse, redundant, rough, and imbalanced (good customers generally outnumber bad customers) and often consist of various weakly related or even uncorrelated features [13, 14]. These data characteristics will make the commonly used credit scoring models unstable, which leads to the credit evaluation results become unreliable and inaccurate. Through the above three approaches proposed in this article, the problems arising in credit scoring for imbalanced data can be handled and solved effectively.

In Section 2, we will talk about the construction of a new ensemble credit scoring model. The experimental outcomes will be discussed in Section 3. Finally, Section 4 concludes the paper.

## 2. New Ensemble Credit Scoring Model

This section mainly talks about the construction of the ensemble classification model for credit scoring.

**2.1. Adaptive Elastic Net-Based Feature Selection.** A large number of researchers have studied the appropriate feature selection approaches for credit scoring, such as cost-sensitive [15], information gain ratio [16], and genetic algorithm [17]. The Lasso estimator can reduce the regression coefficients to zero in  $L_1$ -norm. This method can also reduce features (variables) as well as select the most important one to build simple but effective models while keeping the high efficiency. Denote historical credit scoring data as  $(x_i, y_i)$ ,  $i = 1, 2, \dots, N$ , where  $x_i = (x_{i1}, x_{i2}, \dots, x_{ip})$  are variables for customers and  $y_i$  are category tags (binary responses, denote 0 as default and 1 as nondefault). The regression model could be constructed as follows:

$$y_i = \beta_0 + \sum_{j=1}^p \beta_j x_{ij}, \quad (1)$$

where  $\beta_0$  and  $\beta_j$  are the intercept and regression coefficients, respectively. Suppose that every observation is not correlated

and that all the variables are normalized. The Lasso proper estimate of  $\hat{\beta}$  could be constructed as

$$\hat{\beta} = \arg \min \left\{ \sum_{i=1}^N \left( y_i - \sum_{j=1}^p \beta_j x_{ij} \right)^2 + \lambda \sum_{j=1}^p |\beta_j| \right\}. \quad (2)$$

Based on the information above, a large  $\lambda$  would reduce some coefficients in  $\beta_j$  to zero. That is, Lasso reduces the coefficients to zero while  $\lambda$  gradually increases. In addition, the Lasso model is able to hold any number of variables. Therefore, both the reduction of coefficients and the selection of features (variables) can be carried out at the same time.

Although Lasso has been proved to be easily interpretable and effective under various circumstances, it still has some shortcomings [18]. Zou and Hastie [19] put forward an expansion approach called elastic net to conduct selection. Similarly, the elastic net is also able to conduct automatic selection of variables and shrinkage of coefficient at the same time and select groups of correlated variables. For any constant and nonnegative  $\lambda_1$  and  $\lambda_2$ , the estimation of  $\hat{\beta}$  by the elastic net  $\hat{\beta}_{\text{Enet}}$  could be carried out as follows:

$$\hat{\beta}_{\text{Enet}} = \arg \min \left\{ \sum_{i=1}^N \left( y_i - \sum_{j=1}^p \beta_j x_{ij} \right)^2 + \lambda_1 \sum_{j=1}^p |\beta_j| + \lambda_2 \sum_{j=1}^p \beta_j^2 \right\}, \quad (3)$$

where  $\sum_{j=1}^p |\beta_j|$  is an element of  $L_1$ -norm and  $\lambda_2 \sum_{j=1}^p \beta_j^2$  is the  $L_2$ -norm element.

In addition, Zou and Zhang [20] also pointed out that the elastic net does not possess the oracle property. They then proposed a new adaptive elastic net which combines the  $L_2$  penalty with the weighted  $L_1$  penalty to penalize the squared error loss. Therefore, the adaptive elastic net could be treated as the package of the adaptive Lasso and elastic net. The valuation of  $\hat{\beta}$  by the adaptive elastic net  $\hat{\beta}_{\text{Enet}}$  could be calculated as

$$\hat{\beta}_{\text{Enet}} = \arg \min \left\{ \sum_{i=1}^N \left( y_i - \sum_{j=1}^p \beta_j x_{ij} \right)^2 + \lambda_1^* \sum_{j=1}^p \hat{\omega}_j |\beta_j| + \lambda_2 \sum_{j=1}^p \beta_j^2 \right\}, \quad (4)$$

where  $\hat{\omega}_j = (|\hat{\beta}_{\text{Enet}}|)^{-\gamma}$ ,  $\gamma$  is positive, while  $\lambda_1^*$  is fixed and nonnegative.

Using formula (4), we will be capable of obtaining the most significant attributes ("big fish") from the variable pool. Then, we can plug them into credit scoring models to get a more precise result but with minimum computational and operational cost.

**2.2. ELM-Based Classifier.** ELM model, as a single-hidden layer feedforward neural network (SLFN), can select the input weight and hidden biases randomly without any adjustment during its process. The Moore–Penrose generalized inverse matrices of the hidden-layer output matrix can be utilized to analyze and determine the output weights. ELM exhibits excellent performance of generalizing and the reduction in the iterative time of training process. Clearly, it is more effective than any other ANN-type machine learning algorithms [21].



For the historical training credit data set  $(x_i, y_i)$  that is mentioned above, the input vector  $x_i = (x_{i1}, x_{i2}, \dots, x_{ip})^T \in R^p$  is the  $i^{th}$  sample with  $p$ -dimensional features, and  $Y = [y_1, y_2, \dots, y_N]$ . Then,  $p$  is the amount of input neurons.  $p$  is also equivalent to the input features. Let  $L$  be the amount of hidden neurons. Denote  $C$  as the amount of output neurons, which is also equivalent to the category number. Denote the input weight matrix as  $K = [k_1, k_2, \dots, k_L]$ , where  $k_j = [k_{j1}, k_{j2}, \dots, k_{jp}]$  is the vector connecting the  $p$  input neurons with the  $j$ th hidden neuron.  $b = [b_1, b_2, \dots, b_j, \dots, b_L]^T$  is the bias value of the hidden neurons, where  $b_j$  is the bias value of the  $j$ th hidden neurons. The above parameters do not change during the whole process. The output could be computed by as follows:

$$h(x_i) = G(Kx_i + b), \quad (5)$$

where  $G(x)$  is the activation function. Let  $H$  be the output of all the samples. It can be calculated by using the following equation:

$$H = \begin{bmatrix} h_1(x_1) & h_2(x_1) & \cdots & h_L(x_1) \\ h_1(x_2) & h_2(x_2) & \cdots & h_L(x_2) \\ \vdots & \vdots & \cdots & \vdots \\ h_1(x_N) & h_2(x_N) & \cdots & h_L(x_N) \end{bmatrix}_{N \times L}. \quad (6)$$

The  $i$ th column represents the  $i$ th hidden nodes output vector relative to the inputs  $x_1$  to  $x_N$ . The  $j$ th row represents the output vector of the hidden layer relative to the input  $x_j$ . The output of ELM can be calculated by

$$f(x) = \sum_{i=1}^L \alpha_i G(Kx_i + b) = o_j, \quad j = 1, 2, \dots, N, \quad (7)$$

where  $\alpha_i = [\alpha_{i1}, \alpha_{i2}, \dots, \alpha_{iC}]^T$  is the weight vector that connects the  $i$ th hidden nodes with the output nodes. ELM is able to evaluate those  $N$  samples without any mistake. In other words,  $\sum_{j=1}^L \|o_j - y_j\| = 0$ . Then, the following equation can be obtained:

$$\sum_{i=1}^L \alpha_i G(Kx_i + b) = y_j, \quad j = 1, 2, \dots, N. \quad (8)$$

Equation (8) can also be rewritten as follows:

$$H\alpha = Y. \quad (9)$$

Based on (9), the value of output weight could be estimated using a least square solution as follows:

$$\hat{\alpha} = H^\dagger Y, \quad (10)$$

where  $H^\dagger$  stands for the Moore–Penrose generalized inverse of  $H$ . For credit scoring classification, the outcome of ELM is as follows:

$$f(x) = \text{sign} \left( \sum_{i=1}^L \hat{\alpha}_i G(Kx_i + b) \right) = \text{sign}(\hat{\alpha} \cdot h(x)). \quad (11)$$

**2.3. Ensemble Strategy for Imbalanced Data.** To better solve the classification of imbalanced data, a considerable number

of approaches have been used. They can be categorized into three types: preprocessing, cost-sensitive learning, and ensemble methodology. Preprocessing is able to decrease the classification bias based on the bias-variance decomposition to enhance the single classifier. Undersampling [22, 23], oversampling [24, 25], and strategic sampling are extensively utilized to offset imbalanced data.

Ensemble methodology can be viewed as a decision-making process that combines both individual learning algorithms and their outcomes in parallel to obtain the ultimate result. The basic idea behind the ensemble methodology is that the algorithm will get a number of single classifiers from the training set, and then it uses some ensemble strategies to integrate them to raise the accuracy and reliability of classification. Bagging [26], boosting [27], and stacking [28] are the most common ensemble approaches in credit scoring.

A novel ensemble strategy is planned for imbalanced data according to its imbalance ratio, which could determine the number of ELM classifiers that apply as single classifiers to predict credit scoring data, as well as the number of samples that feed into each ELM as training data.

For any given historical credit training data set that contains  $N$  samples, there are  $N^+$  “good applicants” and  $N^-$  “bad applicants,” such that  $N^+ + N^- = N$ . Then, the imbalance ratio is called IR, which can be calculated as follows:

$$IR = \frac{N^+}{N^-}. \quad (12)$$

After obtaining the IR, the amount of single ELM classifiers  $M$  in the ensemble model also can be calculated as follows:

$$M = \lceil IR \rceil = \left\lceil \frac{N^+}{N^-} \right\rceil, \quad (13)$$

where the symbol  $\lceil \cdot \rceil$  represents “ceiling” operation.

Equation (13) can help us to not only determine the number of ELM classifiers needed in the ensemble credit scoring model but will also guide us to make the imbalanced data become balanced for each classifier. Regarding the ensemble strategy for imbalanced data, we proposed  $M$ -based value. In the remainder of this subsection, we will elaborate the proposed strategy in detail.

Firstly, calculate the imbalance ratio  $IR$  for any given historical credit training data set on the basis of  $N^+$  and  $N^-$ . Secondly, determine the number of ELM classifiers  $M$  using (13).

Thirdly, for the first  $M-1$  ELM classifiers, we feed  $N^-$  “good applicants” samples and  $N^-$  “bad applicants” samples into the ELM classifiers to make sure that the training data sets of the first  $M-1$  classifiers are balanced, and random sampling without replacement method is employed to extract  $N^-$  samples from  $N^+$  “good applicants” samples for each classifier. After finishing the first  $M-1$  training data sets extraction, there are  $N^+ - (M-1) \cdot N^-$  “good applicants” sample that have not been extracted.

Finally, for the last ELM classifier, we let the remaining  $N^+ - (M-1) \cdot N^-$  “good applicants” samples into the training data sets. Considering that  $N^+ - (M-1) \cdot N^- < N^-$ , we will employ the SMOTE algorithm to create  $M \cdot N^- - N^+$  “good

applicants" samples from  $N^+$  "good applicants" samples. Thus, for the last ELM classifier, there are still  $N^-$  "good applicants" samples and  $N^-$  "bad applicants" samples fed into it as the training data set.

Through the described processes above, the ensemble strategy for the imbalanced data we proposed has been realized, and the training data for each classifier is balanced. In the next subsection, we will further introduce the GFSS theory-based ensemble credit scoring approach, which utilizes the results of each single ELM classifier.

**2.4. GFSS Theory-Based Ensemble Credit Scoring Model.** Since we have the results of each ELM classifier, we also need to figure out the weights with respect to their performance. The accuracy of classification is expected to be greatly improved. The theory of soft sets, which is firstly put forward by Molodtsov [29], can be regarded as a way for solving the uncertainties in imprecise environments (e.g., credit scoring area). Maji et al. [30] launched a research focusing on both fuzzy and soft sets. We will firstly introduce the principle of generalized fuzzy soft sets and then put forward a similarity measure of generalized fuzzy soft sets using angular cosine. After that, we can get the weights of each credit scoring model using similarity measure and the accuracy of classification. Finally, we are able to build the generalized fuzzy soft sets theory-based ensemble credit scoring model.

**2.4.1. GFSS Theory.** Based on the theories proposed by Molodtsov [29] and Maji et al. [30], we can make some definitions for fuzzy soft sets.

**Definition 1.** Denote  $U$  as the initial universal set. Denote  $P$  as a set of parameters.  $P(U)$  is the power set of  $U$ .  $(F, P)$  is a soft set over  $U$  if  $P$  is a mapping given by  $F: P \rightarrow P(U)$ .

**Definition 2.** Denote  $U$  as the initial universal set. Denote  $P$  as a set of parameters. The power set of all fuzzy subsets of  $U$  is  $I^U$ . Let  $A \subset P$ : A pair  $(F, P)$  be the fuzzy soft set over  $U$  if  $F$  is a mapping given by  $F: A \rightarrow I^U$ .

Then, Maji and Samanta's [31] definition of GFSS is as follows:

**Definition 3.** Denote  $U$  as the initial universal set. Denote  $P$  as a set of parameters. Let  $(U, P)$  be the soft universe. Denote  $F: P \rightarrow I^U$  and  $\mu$  as the fuzzy subset of  $P$ , i.e.,  $\mu: P \rightarrow I = [0, 1]$ , where  $I^U$  is all fuzzy subsets of  $U$ . Denote  $F_\mu$  as the mapping given by  $F_\mu: P \rightarrow I^U \times I$ , which can also be denoted as  $F_\mu(e) = (F(e), \mu(e))$ , where  $F(e) \in I^U$ . In this way,  $F_\mu$  can be viewed as a GFSS over the soft universe  $(U, P)$ .

For every  $e_i$ ,  $F_\mu(e_i) = (F(e_i), \mu(e_i))$  illustrates both the level of belonging of the subsets of  $U$  to  $F(e_i)$  and the possibility of belonging.

In this paper,  $U$  denotes the historical data of customer credit  $X = \{x_1, x_2, \dots, x_n\}$ , where  $x_i \in R^p$ , and  $F(e_i)$  represents the performance of the classification by a single customer from a single classifier and  $\mu(e_i)$  denotes the overall degree of classification of a certain single classifier.

TABLE 1: Confusion matrix.

Real class (%)	Projected class (%)	
	Good	Bad
Good	TP <sub>m</sub>	FN <sub>m</sub>
Bad	FP <sub>m</sub>	TN <sub>m</sub>

**2.4.2. Similarity Measure of GFSS.** It is important to address the similarity measurement of GFSS during the setting of GFSS and the establishment of our model. Thus, we establish a new approach for the similarity measure of GFSS for the scoring of credits.

**Definition 4.** For  $M$  single classifiers, denote  $\eta_t$  and  $\mu_m$  as the elements of  $F_\mu$ . The definition is as follows:

$$\eta_t^m = \frac{1 - |\hat{y}_t^m - y_t|}{1 + |\hat{y}_t^m - y_t|}, \quad (14)$$

where  $y_t$  ( $t = 1, 2, \dots, T$ ) is the category tag of the  $t$ th customer (binary responses denote 0 as default and 1 as nondefault);  $\hat{y}_t^m$  ( $m = 1, 2, \dots, M$ ) is the forecasting result of the  $t$ th customer predicted by the  $m$ th classifier and is between 0 and 1.  $\eta_t^m$  is the accuracy degree of classification of a single classifier for a single customer. This accuracy ranges between 0 and 1. This is in line with our initial intuition. In addition,  $\mu_m$  is the  $m$ th classifier's overall classification performance, which can be calculated as follows:

$$\mu_m = \sqrt{\frac{TP_m}{TP_m + FN_m} \cdot \frac{TN_m}{TN_m + FP_m}}, \quad (15)$$

where  $TP_m$ ,  $FN_m$ ,  $TN_m$ , and  $FP_m$  are elements of the confusion matrix (Table 1).  $TP_m$  is the amount of good customers accurately labeled as good,  $TN_m$  is the amount of bad customers accurately labeled as bad,  $FN_m$  is the amount of good customers falsely labeled as bad, and  $FP_m$  is the amount of bad customers falsely labeled as good. The greater the value of  $\mu_m$ , the more accurate the result is calculated by the  $m$ th classifier.

Based on the above discussion, it can be noted that  $\eta_{it}$  and  $\mu_m$  from Definition 4 are able to evaluate the performance of classification of every single model. Therefore, we can build the GFSS  $F_\mu^m(\eta, \mu)$  of the  $m$ th classifier as follows:

$$F_\mu^m(\eta, \mu) = \left( \left( \frac{y_1}{\eta_1^m}, \frac{y_2}{\eta_2^m}, \dots, \frac{y_t}{\eta_t^m}, \dots, \frac{y_T}{\eta_T^m} \right), \mu_m \right). \quad (16)$$

**Definition 5.** For two GFSS  $F_\mu^i$  and  $F_\mu^j$  over the universal set  $U$ , where  $i, j \in [1, M]$ , the similarity measurement of GFSS  $SG(F_\mu^i, F_\mu^j)$  can be calculated as follows:

$$SG(F_\mu^i, F_\mu^j) = \frac{\sum_{t=1}^T (\eta_{it}^i \mu_i) \times (\eta_{jt}^j \mu_j)}{\sqrt{\sum_{t=1}^T (\eta_{it}^i)^2} \sqrt{\sum_{t=1}^T (\eta_{jt}^j)^2}} \quad (17)$$

**2.4.3. Ensemble Credit Scoring Modeling.** The determination of the weight for every single model is the most important

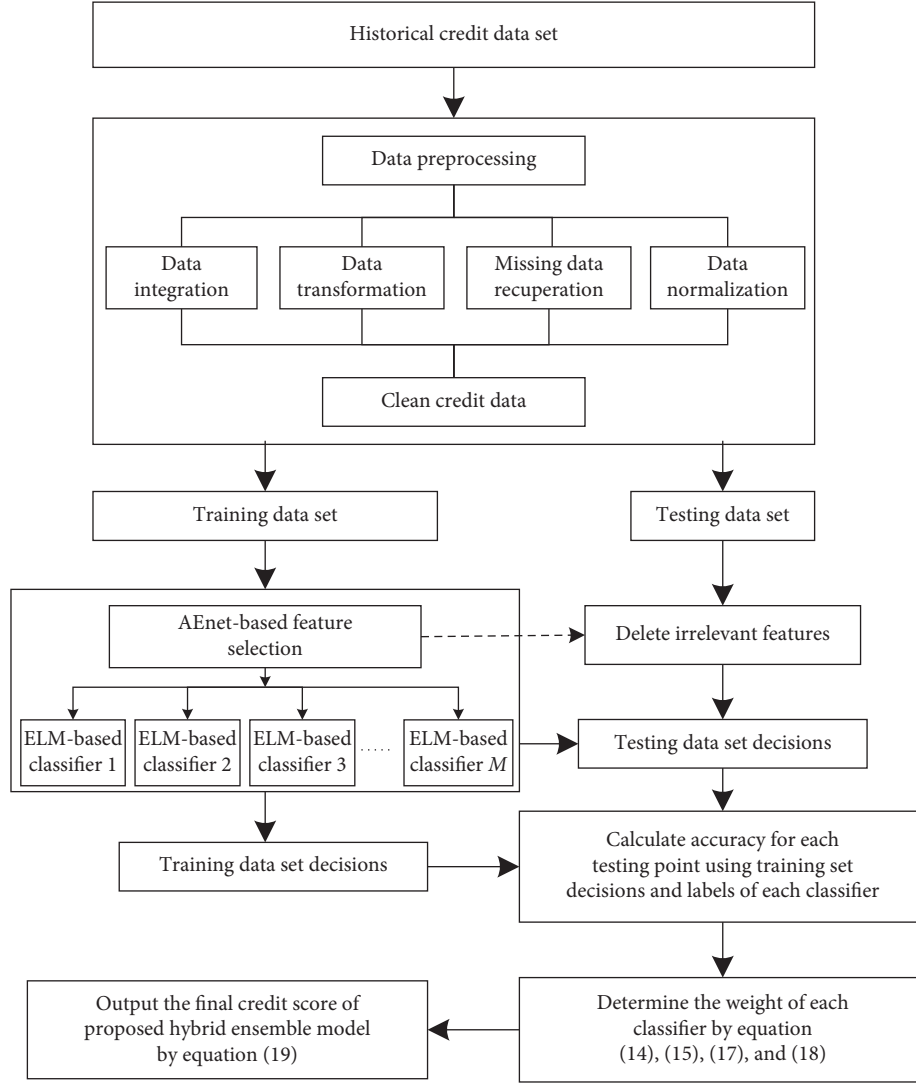


FIGURE 1: Flow diagram of the proposed EGHE model.

step in the establishment of the ensemble credit score modeling. The purpose of this determination is to compare the calculated credit score with the actual records.

The similarity measure of GFSS can be utilized to do the determination, i.e., the calculated  $SG(F_\mu^m, F_\mu^*)$  value, where  $F_\mu^*$  is the GFSS of the actual score of customers. In this way, the weight of  $m$ th classifier can be calculated by

$$\bar{\omega}^m = \frac{SG(F_\mu^m, F_\mu^*)}{\sum_{m=1}^M SG(F_\mu^m, F_\mu^*)}, \quad (18)$$

where  $0 \leq \bar{\omega}^m \leq 1$  and  $\sum_{m=1}^M \bar{\omega}^m = 1$ . Thus, the final score could be calculated as

$$\hat{y}_t = \sum_{m=1}^M \bar{\omega}^m \hat{y}_t^m. \quad (19)$$

Figure 1 presents the flow-process diagram of the ensemble model. The algorithm of “ELM and GFSS Theory-Based Hybrid Ensemble” model is described. We will call this EGHE in the following parts (Algorithm 1).

### 3. Results and Discussion

**3.1. Preparation of Dataset.** During the evaluation, we collected many different private and public data sets. We have collected a total of six credit data sets and four additional imbalanced data sets with different IR are obtained, i.e., three public and three private. The public sets can be obtained from the UCI Machine Learning Repository. They are real-world credit score data sets and are now widely used by researchers. The German, Australian, and Japanese data sets are used for extra verification. The private data sets consist of the Iranian data set that has also been widely used in many studies and the Bene 1 and 2 data sets, which can be obtained from two key financial institutions in Benelux et al. [32]. This Iranian set has various customer data of many small Iranian private banks [33, 34]. Four additional imbalanced datasets are also from the Machine Learning Repository, UCI. They are Shuttle, Skin\_segment, MiniBooNE, and LC2017Q1 which contains loan data of the first quarter in 2017 from Lending Club. The characteristics of all experimental data sets can be found in Table 2.

**Input:** Historical data of credit scoring  $(x_i, y_i)$ .  
**Output:** Score of every single customer  $\hat{y}_i$ .  
Step 1. Preprocessing of data.  
Step 2. Variables selection using AEnet.  
Step 3. Imbalanced data rebalancing by using the proposed ensemble strategy.  
Step 4. Credit scoring of every single ELM classifier.  
Step 5. Compute  $\eta_i$  and  $\mu_m$  using (14) and (15).  
Step 6. Calculate the SG  $(F_\mu^m, F_\mu^*)$  of single classifier using (17).  
Step 7. Calculate the weight of  $m$ th classifier using (18).  
Step 8. Get the final credit score of every customer  $\hat{y}_i$ .

ALGORITHM 1: EGHE algorithm.

TABLE 2: Characteristics of data sets.

Data sets	Size	Attributes	Good/bad	Imbalance ratio	Number of classifiers
<i>Credit scoring data sets</i>					
Germany	1000	25	700/300	2.33	3
Australia	690	14	307/383	0.80	1
Japan	690	15	296/357	0.83	1
Iran	1000	27	950/50	19	19
Bene 1	3,123	33	2,082/1,041	2	2
Bene 2	7,190	33	5,033/2,157	2.33	3
<i>Additional imbalanced data sets</i>					
Shuttle	12,380	9	11,428/952	12.004	13
Skin_segment	117,728	3	114,039/3,679	30.99	31
MiniBooNE	201,355	10	196,555/4,800	40.95	41
LC2017Q1	95,633	72	94,414/1,219	77.45	78

In this paper, we compared our proposed model with the other four state-of-the-art models, namely, C5.0 decision tree, SVM with Radial Basis Function, kernel SVM-R, Deep Belief Networks (DBN), and Bayes to validate the performance of our approaches. All the continuous attributes will be discretized into various intervals. Every single data set will be divided into a two-thirds training set and one-third testing set randomly. We use the open source platform *R-statistics* (version R-3.2.2.) to conduct our experiments.

**3.2. Experimental Results.** Different methods are utilized as comparison models to test the validity of the EGHE credit scoring model.

Firstly, the FS algorithm that is based on AEnet is used to obtain the highly correlated variables after initial data gathering and preprocessing. We could notice that after selection, the variables in these ten data sets are all decreased to various degrees (Table 3). In consideration of the complexity of computation, deleting irrelevant or weakly correlated variables is becoming increasingly important for big-data-oriented credit assessment issues.

After feature selection, we can perform two experiments to further see the effect of feature selection on the classification of each model: (1) all single classifiers with feature selection and (2) all single classifiers without feature selection. Tables 4 and 5 show in detail the AUC, H-measure (HM), Brier's score (BS), and accuracy (ACC) for all single classifiers with and without feature selection.

TABLE 3: Number of features before and after AEnet-based selection.

Data sets	Number of features	
	Before	After
Germany	25	21
Australia	14	10
Japan	15	12
Iran	27	22
Bene 1	33	15
Bene 2	33	20
Shuttle	16	13
Skin_segment	3	3
MiniBooNE	10	9
LC2017Q1	72	48

From the results of every single classifier in Tables 4 and 5, we can see that the feature selection helps enhance the effectiveness of classification of most single classifiers. After feature selection, C5.0 shows accuracy values that are 0.8%, 1.76%, 1.63%, 4.49%, 2.85%, 0.82%, 3.47%, 4.15%, 7.94%, and 4.12% greater than without feature selection for Germany, Australia, Japan, Iran, Bene 1, Bene 2, Shuttle, Skin\_segment, MiniBooNE, and LC2017Q1 data sets, respectively. In the same way, SVM-R increased the accuracy values by 0.93%, 1.08%, 0.67%, 4.53%,  $-0.4\%$ , 1.94%, 0.87%, 1.02%, 2.03%, and 2.54%, respectively, for ten experimental data sets. DBN and Naïve Bayes improve their effectiveness too after feature selection. Only SVM-R on Bene 1 reduced

TABLE 4: Results for all single classifiers without AEnet-based feature selection.

Data set	Performance measures	Single classifiers				
		C5.0	SVM-R	DBN	Bayes	ELM
Germany	AUC	0.680	0.732	0.753	0.761	0.764
	HM	0.336	0.362	0.399	0.338	0.379
	BS	0.251	0.167	0.173	0.199	0.172
	ACC	0.745	0.752	0.749	0.745	<b>0.762</b>
Australia	AUC	0.867	0.812	0.876	0.857	0.852
	HM	0.516	0.603	0.613	0.581	0.610
	BS	0.148	0.113	0.107	0.166	0.127
	ACC	0.736	0.742	<b>0.751</b>	0.734	0.735
Japan	AUC	0.857	0.908	0.911	0.888	0.882
	HM	0.689	0.608	0.608	0.667	0.618
	BS	0.156	0.120	0.138	0.176	0.142
	ACC	0.738	0.749	<b>0.757</b>	0.742	0.751
Iran	AUC	0.616	0.604	0.614	0.715	0.710
	HM	0.111	0.074	0.061	0.192	0.133
	BS	0.071	0.071	0.078	0.077	0.083
	ACC	0.623	0.617	0.640	0.627	<b>0.648</b>
Bene 1	AUC	0.728	0.821	0.767	0.740	0.752
	HM	0.310	0.366	0.250	0.335	0.351
	BS	0.267	0.176	0.168	0.297	0.199
	ACC	0.701	0.749	0.698	0.690	<b>0.753</b>
Bene 2	AUC	0.745	0.789	0.746	0.707	0.762
	HM	0.385	0.309	0.238	0.276	0.270
	BS	0.143	0.178	0.142	0.172	0.153
	ACC	0.728	0.720	0.715	0.711	<b>0.747</b>
Shuttle	AUC	0.604	0.675	0.693	0.714	0.722
	HM	0.299	0.334	0.367	0.317	0.358
	BS	0.224	0.153	0.158	0.186	0.163
	ACC	0.662	0.693	<b>0.740</b>	0.698	0.720
Skin_segment	AUC	0.770	0.749	0.804	0.802	0.805
	HM	0.458	0.556	0.564	0.543	0.576
	BS	0.131	0.105	0.099	0.156	0.119
	ACC	0.653	0.685	0.689	0.687	<b>0.695</b>
MiniBooNE	AUC	0.761	0.837	0.838	0.833	0.833
	HM	0.613	0.560	0.559	0.625	0.584
	BS	0.140	0.112	0.126	0.164	0.134
	ACC	0.655	0.690	0.696	0.695	<b>0.710</b>
LC2017Q1	AUC	0.547	0.557	0.563	0.669	0.671
	HM	0.099	0.067	0.057	0.181	0.126
	BS	0.062	0.066	0.072	0.071	0.078
	ACC	0.655	0.670	0.688	0.687	<b>0.712</b>

by 0.4%, but this does not contradict the improvement on the classification that our AEnet-based feature selection brings. Not only do outliers, redundant, and weakly or even unrelated variables help improve the effectiveness, but also affect the model establishment and cause great computation.

It is noteworthy that, compared with C5.0, SVM-R, DBN, and Bayes, ELM has manifested the superiority in accuracy on the vast majority of data sets. Table 6 reports the average running time (total time for training and testing) for all models. For these experiments, we use an Intel i5-8500 with CPU at 3.0 GHz and 16 GB of RAM.

From Table 6, we can see that ELM costs less time than other single models to carry out credit scoring activities. The efficiency of computing resources also makes ELM a great match for ensemble learning and modeling.

After implementing feature selection, completing the ensemble strategy, and individual model classification, the EGHE model can be achieved. Based on (14), (15), and (17)–(19), the weights of single ELM classifiers are calculated according to their efficiency, respectively. To validate the availability of EGHE, we employed several ensemble models in contrast with EGHE. These models were split into two parts. The first one contains four FS algorithms with GFSS-based combination. They are cost-sensitive, GA, information gain ratio (IGR), and elastic net (Enet). Cost-sensitive, GA, and IGR are popular feature selection approaches in the credit scoring area [16, 35, 36]. The second group applies four other approaches with AEnet-based feature selection, which were weighted average (WAVG) [37], majority voting (MajVot) [38], weighted voting (WVOT) [39], and fuzzy soft set (FSS). Those methods are frequently adopted in the



TABLE 5: Results for all single classifiers with AEnet-based feature selection.

Data set	Performance measurement	Single classifiers				
		C5.0	SVM-R	DBN	Bayes	ELM
Germany	AUC	0.690	0.756	0.762	0.774	0.768
	HM	0.181	0.295	0.248	0.267	0.268
	BS	0.230	0.163	0.172	0.192	0.173
	ACC	0.751	0.759	0.752	0.758	<b>0.765</b>
Australia	AUC	0.882	0.902	0.915	0.912	0.883
	HM	0.614	0.635	0.642	0.623	0.624
	BS	0.121	0.104	0.131	0.121	0.130
	ACC	0.749	0.750	<b>0.755</b>	0.741	0.748
Japan	AUC	0.861	0.910	0.919	0.910	0.878
	HM	0.608	0.621	0.631	0.622	0.622
	BS	0.116	0.112	0.126	0.113	0.119
	ACC	0.749	0.752	<b>0.766</b>	0.753	0.758
Iran	AUC	0.631	0.650	0.612	0.723	0.638
	HM	0.137	0.118	0.108	0.212	0.117
	BS	0.068	0.071	0.078	0.072	0.081
	ACC	0.652	0.645	0.650	0.652	<b>0.658</b>
Bene 1	AUC	0.770	0.810	0.806	0.773	0.798
	HM	0.312	0.345	0.336	0.302	0.320
	BS	0.233	0.177	0.184	0.264	0.241
	ACC	0.721	0.746	0.719	0.721	<b>0.753</b>
Bene 2	AUC	0.763	0.824	0.815	0.780	0.796
	HM	0.354	0.386	0.269	0.285	0.326
	BS	0.132	0.119	0.137	0.125	0.137
	ACC	0.734	0.734	0.715	0.723	<b>0.747</b>
Shuttle	AUC	0.652	0.682	0.686	0.723	0.729
	HM	0.323	0.337	0.363	0.321	0.362
	BS	0.242	0.155	0.156	0.188	0.165
	ACC	0.685	0.699	<b>0.743</b>	0.707	0.727
Skin_segment	AUC	0.832	0.756	0.796	0.812	0.813
	HM	0.495	0.562	0.558	0.550	0.582
	BS	0.141	0.106	0.098	0.158	0.120
	ACC	0.675	0.692	<b>0.712</b>	0.696	0.702
MiniBooNE	AUC	0.822	0.845	0.830	0.844	0.841
	HM	0.662	0.566	0.553	0.633	0.589
	BS	0.151	0.113	0.125	0.166	0.135
	ACC	0.707	0.704	0.689	0.704	<b>0.717</b>
LC2017Q1	AUC	0.591	0.563	0.557	0.678	0.678
	HM	0.107	0.068	0.056	0.183	0.125
	BS	0.067	0.067	0.071	0.072	0.079
	ACC	0.682	0.687	0.681	0.696	<b>0.719</b>

TABLE 6: Running time for all models with feature selection (seconds).

Data sets	Models				
	C5.0	SVM-R	DBN	Bayes	ELM
Germany	1.76	2.89	4.33	1.72	<b>1.38</b>
Australia	1.16	2.02	2.99	1.07	<b>0.97</b>
Japan	1.25	2.05	2.90	1.13	<b>0.94</b>
Iran	1.82	3.01	4.31	1.69	<b>1.44</b>
Bene 1	5.63	10.11	14.29	5.85	<b>4.62</b>
Bene 2	12.71	21.13	28.96	12.32	<b>10.01</b>
Shuttle	21.79	35.78	53.61	21.29	<b>17.11</b>
Skin_segment	207.20	340.24	509.76	202.49	<b>182.46</b>
MiniBooNE	354.38	581.92	871.87	346.33	<b>277.87</b>
LC2017Q1	591.26	970.78	1254.49	560.57	<b>436.04</b>

establishment and utilization of different combination models. They also employ ELM as the classifier but did not take the ensemble strategy that is proposed above, only using

random sampling methods to make all training data sets become balanced. Table 7 displays the results of AUC, H-measure, and Brier's score for all ensemble models.



TABLE 7: Classification outcomes from all data sets for different performance measures with various combinations.

Data set	Performance measurement	Other feature selection methods with GFSS-based combination				Traditional combination methods with AEnet-based feature selection				EGHE
		Cost-sensitive	GA	IGR	Enet	WAVG	MajVot	WVOT	FSS	
Germany	AUC	0.786	0.792	0.777	0.781	0.777	0.786	0.789	0.771	0.823
	HM	0.286	0.177	0.226	0.238	0.222	0.285	0.246	0.305	0.325
	BS	0.166	0.208	0.197	0.182	0.181	0.183	0.192	0.157	0.184
	ACC	0.842	0.862	0.833	0.827	0.845	0.859	0.836	0.844	<b>0.886</b>
Australia	AUC	0.921	0.927	0.933	0.928	0.921	0.922	0.932	0.928	0.945
	HM	0.667	0.519	0.573	0.628	0.637	0.637	0.632	0.653	0.659
	BS	0.092	0.145	0.173	0.103	0.101	0.112	0.107	0.097	0.095
	ACC	0.872	0.878	0.882	0.863	0.872	0.873	0.876	0.874	<b>0.895</b>
Japan	AUC	0.923	0.928	0.918	0.932	0.918	0.927	0.928	0.925	0.937
	HM	0.650	0.492	0.566	0.618	0.602	0.642	0.617	0.648	0.660
	BS	0.099	0.157	0.174	0.109	0.121	0.112	0.116	0.103	0.098
	ACC	0.871	0.862	0.861	0.868	0.853	0.864	0.873	0.868	<b>0.904</b>
Iran	AUC	0.791	0.778	0.781	0.767	0.777	0.779	0.783	0.778	0.802
	HM	0.279	0.150	0.217	0.162	0.283	0.108	0.107	0.294	0.303
	BS	0.042	0.069	0.056	0.049	0.044	0.048	0.049	0.044	0.059
	ACC	0.883	0.881	0.874	0.861	0.867	0.885	0.877	0.883	<b>0.915</b>
Bene 1	AUC	0.843	0.812	0.822	0.821	0.882	0.879	0.886	0.888	0.881
	HM	0.396	0.263	0.338	0.258	0.324	0.441	0.385	0.447	0.351
	BS	0.161	0.240	0.256	0.197	0.188	0.159	0.198	0.154	0.173
	ACC	0.881	0.872	0.864	0.872	0.872	0.872	0.865	0.876	<b>0.896</b>
Bene 2	AUC	0.921	0.838	0.858	0.868	0.878	0.844	0.876	0.883	0.888
	HM	0.537	0.401	0.478	0.489	0.505	0.436	0.432	0.496	0.506
	BS	0.091	0.136	0.168	0.122	0.102	0.115	0.112	0.103	0.114
	ACC	<b>0.878</b>	0.860	0.857	0.868	0.881	0.875	0.882	0.884	<b>0.898</b>
Shuttle	AUC	0.896	0.914	0.914	0.922	0.897	0.919	0.917	0.906	0.943
	HM	0.653	0.510	0.562	0.625	0.620	0.635	0.622	0.636	0.658
	BS	0.091	0.143	0.170	0.103	0.099	0.110	0.104	0.096	0.095
	ACC	0.852	0.866	0.862	0.858	0.849	0.870	0.862	0.851	<b>0.916</b>
Skin_segment	AUC	0.902	0.913	0.899	0.926	0.896	0.922	0.915	0.903	0.936
	HM	0.637	0.486	0.555	0.615	0.586	0.638	0.607	0.631	0.659
	BS	0.096	0.154	0.171	0.107	0.119	0.110	0.113	0.098	0.098
	ACC	0.853	0.849	0.844	0.863	0.833	0.862	0.859	0.845	<b>0.908</b>
MiniBooNE	AUC	0.773	0.767	0.764	0.763	0.757	0.775	0.770	0.758	0.800
	HM	0.272	0.149	0.213	0.159	0.277	0.109	0.104	0.286	0.302
	BS	0.042	0.067	0.054	0.048	0.0439	0.047	0.047	0.041	0.059
	ACC	0.875	0.877	0.885	0.876	0.884	0.880	0.893	0.890	<b>0.903</b>
LC2017Q1	AUC	0.823	0.801	0.804	0.816	0.859	0.874	0.872	0.867	0.879
	HM	0.386	0.260	0.332	0.257	0.315	0.440	0.378	0.435	0.350
	BS	0.158	0.237	0.252	0.195	0.182	0.157	0.196	0.149	0.203
	ACC	0.861	0.888	0.877	0.875	0.871	0.878	0.871	0.873	<b>0.912</b>

From Tables 7 and 5, we can see that, compared with the single classifiers, ensemble methods reveal significant advantages with regard to the accuracy of classification. Compared with other single classifiers and combined approaches in both groups, EGHE has an advantage in all metrics across all datasets. Experiments on several state-of-the-art ensemble models are performed to verify the effectiveness of the EGHE model. They are an EMPNGA-based multistage hybrid model put forward by Zhang and Xia [37]; the heterogeneous ensemble credit model put forward by Xia et al. [40]; EBCA-RF&XGB-PSO model that is put forward by He et al. [41]; heterogeneous ensemble learning-based two-stage credit risk model (TSHE) proposed by Papouskova and Hajek [42]; twin neural networks (TNN) proposed by Jayadeva et al. [43]; and a new rule-based knowledge extraction (RKE)

method proposed by Mahani and Baba [44] recently. Table 8 gives the results of ensemble models in different data sets.

From Table 8, we could tell that the results of these models are very close. The accuracy of EGHE model is better than most of the other models but Iranian. The EBCA-RF&XGB-PSO model achieved a high accuracy of 0.921 in the Iranian data set because it uses the Extended Balance Cascade method that can effectively solve the issue of class imbalance. However, the ensemble strategy and GFSS theory-based model EGHE can deal with the thorny problem of unbalanced data classification better in most experimental data sets; even in some severely skewed data sets, ideal outcomes have been achieved, such as in Shuttle, Skin\_segment, MiniBooNE, and LC2017Q1.

TABLE 8: Comparison results of ensemble models in different data sets.

Data set	Performance measurement	Ensemble models						
		EMPNGA-based model	Heterogeneous ensemble	EBCA-RF& XGB-PSO	TSHE	TNN	RKE	EGHE
Germany	AUC	0.802	0.795	0.798	0.775	0.811	0.790	0.823
	HM	0.400	0.386	0.397	0.376	0.320	0.376	0.325
	BS	0.158	0.164	0.163	0.184	0.181	0.158	0.184
	ACC	0.768	0.859	0.869	0.839	0.873	0.874	<b>0.886</b>
Australia	AUC	0.940	0.923	0.931	0.933	0.931	0.929	0.945
	HM	0.672	0.648	0.661	0.628	0.649	0.676	0.659
	BS	0.092	0.101	0.092	0.101	0.095	0.099	0.096
	ACC	0.875	0.842	0.861	0.852	0.882	0.877	<b>0.895</b>
Japan	AUC	0.932	0.925	0.919	0.935	0.923	0.921	0.937
	HM	0.665	0.651	0.636	0.649	0.650	0.649	0.660
	BS	0.095	0.091	0.097	0.090	0.097	0.090	0.098
	ACC	0.872	0.883	0.889	0.887	0.890	0.887	<b>0.904</b>
Iran	AUC	0.876	0.824	0.831	0.824	0.790	0.821	0.802
	HM	0.424	0.384	0.489	0.384	0.298	0.416	0.303
	BS	0.058	0.047	0.061	0.043	0.058	0.053	0.059
	ACC	0.907	0.908	<b>0.921</b>	0.902	0.911	0.910	0.915
Bene 1	AUC	0.824	0.821	0.818	0.821	0.868	0.819	0.881
	HM	0.376	0.383	0.442	0.423	0.346	0.384	0.351
	BS	0.152	0.147	0.147	0.150	0.169	0.139	0.173
	ACC	0.872	0.869	0.869	0.865	0.883	0.872	<b>0.896</b>
Bene 2	AUC	0.866	0.871	0.863	0.881	0.874	0.875	0.887
	HM	0.479	0.488	0.465	0.498	0.498	0.490	0.506
	BS	0.102	0.098	0.101	0.118	0.112	0.110	0.114
	ACC	0.871	0.867	0.875	0.887	0.885	0.882	<b>0.898</b>
Shuttle	AUC	0.913	0.870	0.850	0.865	0.929	0.850	0.943
	HM	0.442	0.405	0.500	0.403	0.648	0.431	0.658
	BS	0.060	0.050	0.062	0.045	0.095	0.055	0.096
	ACC	0.886	0.878	0.892	0.886	0.902	0.892	<b>0.916</b>
Skin_segment	AUC	0.859	0.867	0.837	0.862	0.921	0.848	0.935
	HM	0.392	0.404	0.452	0.444	0.649	0.397	0.659
	BS	0.158	0.155	0.150	0.158	0.096	0.143	0.098
	ACC	0.870	0.877	0.889	0.898	0.894	0.893	<b>0.908</b>
MiniBooNE	AUC	0.903	0.919	0.883	0.925	0.788	0.906	0.800
	HM	0.499	0.515	0.476	0.523	0.297	0.507	0.302
	BS	0.106	0.103	0.103	0.124	0.058	0.114	0.059
	ACC	0.890	0.895	0.901	0.897	0.889	0.901	<b>0.903</b>
LC2017Q1	AUC	0.858	0.846	0.822	0.923	0.866	0.845	0.879
	HM	0.402	0.274	0.340	0.368	0.345	0.266	0.350
	BS	0.165	0.250	0.258	0.213	0.199	0.202	0.203
	ACC	0.888	0.897	0.903	0.895	0.898	0.903	<b>0.912</b>

#### 4. Conclusion

In this paper, we proposed a novel ensemble credit scoring model called EGHE, which integrates efficient feature selection algorithm, novel ensemble strategy, and GFSS-based weighting method for single ELM classifiers. In the proposed model, the adaptive elastic net-based feature selection algorithm was firstly utilized to obtain high-quality training data to improve the evaluation efficiency without reducing the predictive precision. ELM model was employed as basic classifier, and a novel ensemble strategy was generated to make the imbalanced training data sets become balanced for each ELM classifier. Additionally, we proposed a new weighting method to build the GFSS theory-based ensemble credit scoring model. Dual-scale classification accuracy metric that is based on new similarity measurement of GFSS was constructed to compute the final weight of every

single classifier. The biggest contribution of this paper is that the proposed EGHE is able to predict credit risk reliably and accurately, especially for unbalanced credit data. Comparisons between EGHE and other credit scoring models were implemented on ten real-world datasets with four metrics (average accuracy, AUC, H-measure, and Brier's score). A variety of state-of-the-art ensemble models were employed to compare with EGHE to prove its validity. The experiments results demonstrated that the proposed EGHE model was robust and represented a positive development in credit scoring.

#### Data Availability

(1) The "Germany" data set used to support the findings of this study are included within the following URL: <http://archive.ics.uci.edu/ml/datasets/Statlog+%28German+Credit+Data%29>.

(2) The “Australia” data set used to support the findings of this study are included within the following URL: <http://archive.ics.uci.edu/ml/datasets/Statlog+%28Australian+Credit+Approval%29>. (3) The “Japan” data set used to support the findings of this study are included within the following URL: <https://archive.ics.uci.edu/ml/datasets/Japanese+Credit+Screening>. (4) The “Iran” data set used to support the findings of this study are included in [34, 45]. (5) The “Bene 1” and “Bene 2” data set used to support the findings of this study are included within the following article: [32]. (6) The “Shuttle” data set used to support the findings of this study are included within the following URL: [http://archive.ics.uci.edu/ml/datasets/statlog+\(shuttle\)](http://archive.ics.uci.edu/ml/datasets/statlog+(shuttle)). (7) The “Skin\_segment” data set used to support the findings of this study are included within the following URL: <http://archive.ics.uci.edu/ml/datasets/Skin+Segmentation>. (8) The “MiniBooNE” data set used to support the findings of this study are included within the following URL: <http://academictorrents.com/details/7fafb101f9c7961f9b840daeb4af43039107ddef>. (9) The “LC2017Q1” data set used to support the findings of this study are included within the following URL and article: [41] <http://www.lendingclub.com>.

## Disclosure

Dayu Xu and Xuyao Zhang are co-first authors.

## Conflicts of Interest

The authors declare that they have no conflicts of interest regarding the publication of this paper.

## Authors' Contributions

Dayu Xu and Xuyao Zhang contributed equally to this work.

## Acknowledgments

The authors acknowledge the support for the project (no. 20YJC630173) supported by the Ministry of Education of Humanities and Social Science Project, the project (no. 31971493) by the National Natural Science Foundation of China, the National Key Research and Development Program of China (no. 2018YFD0401403), the Zhejiang Province Key Science and Technology Projects (no. 2018C02050), the Hangzhou Agricultural and Social Development Project (no. 20190101A07), and the Zhejiang Education and Teaching Reform Project (no. jg20180175) supported by the Department of Education of Zhejiang Province.

## References

- [1] C. Serrano-Cinca and B. Gutiérrez-Nieto, “The use of profit scoring as an alternative to credit scoring systems in peer-to-peer (p2p) lending,” *Decision Support Systems*, vol. 89, pp. 113–122, 2016.
- [2] C. Liberati and F. Camillo, “Personal values and credit scoring: new insights in the financial prediction,” *Journal of the Operational Research Society*, vol. 69, no. 12, pp. 1–21, 2018.
- [3] J. Sun, H. Li, P.-C. Chang, and Q.-H. Huang, “Dynamic credit scoring using B & B with incremental-SVM-ensemble,” *Kybernetes*, vol. 44, no. 4, pp. 518–535, 2015.
- [4] A. Kammoun, “Credit scoring models for a Tunisian microfinance institution: comparison between artificial neural network and logistic regression,” *Review of Economics & Finance*, vol. 6, pp. 61–78, 2016.
- [5] Z. Zhao, S. Xu, B. H. Kang, M. M. J. Kabir, Y. Liu, and R. Wasinger, “Investigation and improvement of multi-layer perceptron neural networks for credit scoring,” *Expert Systems with Applications*, vol. 42, no. 7, pp. 3508–3516, 2015.
- [6] S. Y. Sohn, D. H. Kim, and J. H. Yoon, “Technology credit scoring model with fuzzy logistic regression,” *Applied Soft Computing*, vol. 43, pp. 150–158, 2016.
- [7] H. Xiao, Z. Xiao, and Y. Wang, “Ensemble classification based on supervised clustering for credit scoring,” *Applied Soft Computing*, vol. 43, pp. 73–86, 2016.
- [8] S. Oreski and G. Oreski, “Genetic algorithm-based heuristic for feature selection in credit risk assessment,” *Expert Systems with Applications*, vol. 41, no. 4, pp. 2052–2064, 2014.
- [9] D. Liang, C.-F. Tsai, and H.-T. Wu, “The effect of feature selection on financial distress prediction,” *Knowledge-Based Systems*, vol. 73, no. 1, pp. 289–297, 2015.
- [10] F. Feng, H. Fujita, M. I. Ali, R. R. Yager, and X. Liu, “Another view on generalized intuitionistic fuzzy soft sets and related multiattribute decision making methods,” *IEEE Transactions on Fuzzy Systems*, vol. 27, no. 3, pp. 474–488, 2019.
- [11] X. Peng and H. Garg, “Algorithms for interval-valued fuzzy soft sets in emergency decision making based on WDBA and CODAS with new information measure,” *Computers & Industrial Engineering*, vol. 119, pp. 439–452, 2018.
- [12] F. Feng, Z. Xu, H. Fujita, and M. Liang, “Enhancing promethee method with intuitionistic fuzzy soft sets,” *International Journal of Intelligent Systems*, vol. 35, no. 7, pp. 1071–1104, 2020.
- [13] R. Emekter, Y. Tu, B. Jirasakuldech, and M. Lu, “Evaluating credit risk and loan performance in online peer-to-peer (p2p) lending,” *Applied Economics*, vol. 47, no. 1, pp. 54–70, 2015.
- [14] Y. Guo, W. Zhou, C. Luo, C. Liu, and H. Xiong, “Instance-based credit risk assessment for investment decisions in p2p lending,” *European Journal of Operational Research*, vol. 249, no. 2, pp. 417–426, 2016.
- [15] S. Benítez-Peña, R. Blanquero, E. Carrizosa, and P. Ramírez-Cobo, “Cost-sensitive feature selection for support vector machines,” *Computers & Operations Research*, vol. 106, pp. 169–178, 2019.
- [16] S. Jadhav, H. He, and K. Jenkins, “Information gain directed genetic algorithm wrapper feature selection for credit rating,” *Applied Soft Computing*, vol. 69, pp. 541–553, 2018.
- [17] N. Kozodoi, S. Lessmann, K. Papakonstantinou, Y. Gatsoulis, and B. Baesens, “A multi-objective approach for profit-driven feature selection in credit scoring,” *Decision Support Systems*, vol. 120, pp. 106–117, 2019.
- [18] L. Cui, L. Bai, Z. Zhang, Y. Wang, and E. R. Hancock, “Identifying the most informative features using a structurally interacting elastic net,” *Neurocomputing*, vol. 336, pp. 13–26, 2018.
- [19] H. Zou and T. Hastie, “Regularization and variable selection via the elastic net,” *Journal of the Royal Statistical Society: Series B (Statistical Methodology)*, vol. 67, no. 2, pp. 301–320, 2005.
- [20] H. Zou and H. H. Zhang, “On the adaptive elastic-net with a diverging number of parameters,” *The Annals of Statistics*, vol. 37, no. 4, pp. 1733–1751, 2009.

- [21] A. Bequé and S. Lessmann, "Extreme learning machines for credit scoring: an empirical evaluation," *Expert Systems with Applications*, vol. 86, pp. 42–53, 2017.
- [22] W.-C. Lin, C.-F. Tsai, Y.-H. Hu, and J.-S. Jhang, "Clustering-based undersampling in class-imbalanced data," *Information Sciences*, vol. 409–410, pp. 17–26, 2017.
- [23] W. W. Y. Jhang, J. Hu, D. S. Yeung, S. Yin, and F. Roli, "Diversified sensitivity-based undersampling for imbalance classification problems," *IEEE Transactions on Cybernetics*, vol. 45, no. 11, pp. 2402–2412, 2017.
- [24] G. Douzas and F. Bacao, "Self-Organizing Map Oversampling (SOMO) for imbalanced data set learning," *Expert Systems with Applications*, vol. 82, pp. 40–52, 2017.
- [25] G. Douzas, F. Bacao, and F. Last, "Improving imbalanced learning through a heuristic oversampling method based on K-means and SMOTE," *Information Sciences*, vol. 465, pp. 1–20, 2018.
- [26] S. Dahiya, S. S. Handa, and N. P. Singh, "A feature selection enabled hybrid-bagging algorithm for credit risk evaluation," *Expert Systems*, vol. 34, no. 6, pp. 1–11, 2017.
- [27] Y. Xia, C. Liu, and N. Liu, "Cost-sensitive boosted tree for loan evaluation in peer-to-peer lending," *Electronic Commerce Research and Applications*, vol. 24, pp. 30–49, 2017.
- [28] M. Doumpos and C. Zopounidis, "Model combination for credit risk assessment: a stacked generalization approach," *Annals of Operations Research*, vol. 151, no. 1, pp. 289–306, 2007.
- [29] D. Molodtsov, "Soft set theory-first results," *Computers & Mathematics with Applications*, vol. 37, no. 4–5, pp. 19–31, 1999.
- [30] P. K. Maji, R. Biswas, and A. R. Roy, "Fuzzy soft sets," *Journal of Fuzzy Mathematics*, vol. 9, no. 3, pp. 589–602, 2001.
- [31] P. K. Maji and S. K. Samanta, "Generalised fuzzy soft sets," *Computers & Mathematics with Applications*, vol. 59, no. 4, pp. 1425–1432, 2010.
- [32] B. Baesens, R. Setiono, C. Mues, and J. Vanthienen, "Using neural network rule extraction and decision tables for credit-risk evaluation," *Management Science*, vol. 49, no. 3, pp. 312–329, 2003.
- [33] K. Setiono, B. Mac Namee, and S. J. Delany, "Using semi-supervised classifiers for credit scoring," *Journal of the Operational Research Society*, vol. 64, no. 4, pp. 513–529, 2012.
- [34] A. I. Marqués, V. García, and J. S. Sánchez, "Exploring the behaviour of base classifiers in credit scoring ensembles," *Expert Systems with Applications*, vol. 39, no. 11, pp. 10244–10250, 2012.
- [35] H. Zhao and S. Yu, "Cost-sensitive feature selection via the  $\ell_{2,1}$ -norm," *International Journal of Approximate Reasoning*, vol. 104, pp. 25–37, 2019.
- [36] D. Wang, Z. Zhang, R. Bai, and Y. Mao, "A hybrid system with filter approach and multiple population genetic algorithm for feature selection in credit scoring," *Journal of Computational and Applied Mathematics*, vol. 329, pp. 307–321, 2018.
- [37] D. Zhang and Z. Xia, "Weighted-averaging estimator for possible threshold in segmented linear regression model," *Journal of Statistical Planning and Inference*, vol. 200, pp. 102–118, 2019.
- [38] D. Tripathi, D. R. Edla, V. Kuppili, A. Bablani, and R. Dharavath, "Credit scoring model based on weighted voting and cluster based feature selection," *Procedia Computer Science*, vol. 132, pp. 22–31, 2018.
- [39] A. L. M. Vilela, C. Wang, K. P. Nelson, and H. E. Stanley, "Majority-vote model for financial markets," *Physica A: Statistical Mechanics and Its Applications*, vol. 515, pp. 762–770, 2019.
- [40] Y. Xia, C. Liu, B. Da, and F. Xie, "A novel heterogeneous ensemble credit scoring model based on bstacking approach," *Expert Systems with Applications*, vol. 93, pp. 182–199, 2018.
- [41] H. He, W. Zhang, and S. Zhang, "A novel ensemble method for credit scoring: adaption of different imbalance ratios," *Expert Systems with Applications*, vol. 98, pp. 105–117, 2018.
- [42] M. Papouskova and P. Hajek, "Two-stage consumer credit risk modelling using heterogeneous ensemble learning," *Decision Support Systems*, vol. 118, pp. 33–45, 2019.
- [43] Jayadeva, H. Pant, M. Sharma, and S. Soman, "Twin Neural Networks for the classification of large unbalanced datasets," *Neurocomputing*, vol. 343, pp. 34–49, 2019.
- [44] A. Mahani and A. R. Baba-Ali, "A new rule-based knowledge extraction approach for imbalanced datasets," *Knowledge and Information Systems*, pp. 1–27, 2019.
- [45] A. Marqués, V. García, and J. S. Sánchez, "Two-level classifier ensembles for credit risk assessment," *Expert Systems with Applications*, vol. 39, pp. 10916–10922, 2012.



## Research Article

# Some T-Spherical Fuzzy Einstein Interactive Aggregation Operators and Their Application to Selection of Photovoltaic Cells

Shouzhen Zeng<sup>1,2,3</sup>, Muhammad Munir<sup>4</sup>, Tahir Mahmood<sup>4</sup>, and Muhammad Naeem<sup>4</sup>

<sup>1</sup>School of Business, Ningbo University, Ningbo 315211, China

<sup>2</sup>College of Statistics and Mathematics, Zhejiang Gongshang University, Hangzhou 310018, China

<sup>3</sup>School of Management, Fudan University, Shanghai 200433, China

<sup>4</sup>Department of Mathematics and Statistics, International Islamic University, Islamabad, Pakistan

Correspondence should be addressed to Tahir Mahmood; [tahirbakhata@iiu.edu.pk](mailto:tahirbakhata@iiu.edu.pk)

Received 12 April 2020; Accepted 11 May 2020; Published 9 June 2020

Guest Editor: Zaoli Yang

Copyright © 2020 Shouzhen Zeng et al. This is an open access article distributed under the Creative Commons Attribution License, which permits unrestricted use, distribution, and reproduction in any medium, provided the original work is properly cited.

In this article, it is pointed out that the existing intuitionistic fuzzy and T-spherical fuzzy Einstein averaging and geometric operators have some limitations. To overcome these limitations, we proposed some new averaging and geometric operators in the T-spherical fuzzy environment instead of the intuitionistic fuzzy environment because the T-spherical fuzzy set is the most generalized form and the proposed operators can be particularized to the intuitionistic fuzzy environment. First, new operational laws for T-spherical fuzzy information are defined, on the basis of which Einstein geometric interaction operators and Einstein averaging interactive aggregation operators are then proposed. Some basic properties and advantages of proposed aggregation operators are also discussed. Moreover, the proposed operators are applied to the MADM problem to check their reliability. The superiority of the proposed operators over existing work is checked with the help of an example.

## 1. Introduction

To deal with uncertainty, a tool called fuzzy set (FS) was introduced by Zadeh [1]. FS tells the degree of membership (MD) of an object. Intuitionistic fuzzy set (IFS), a generalization of FS, was introduced by Atanassov [2, 3]. IFS has two functions, a membership and a nonmembership function, and both functions map on a closed unit interval from a nonempty set. As the name indicates that they tell the MD and nonmembership degree (NMD) of an object, respectively, the IFS has a condition that the sum of both degrees must belong to  $[0, 1]$ . Whenever the sum of both degrees exceeds from 1, IFS fails to handle that information. To overcome this issue, Yager [4, 5] relaxed the condition that the square sum of both degrees must belong to  $[0, 1]$  and named that structure as Pythagorean fuzzy set (PyFS). In PyFS, the decision maker has more options for giving values to an object but the decision maker is not free to give any value because there are some limitations. To overcome this problem, Yager [6] proposed an improved fuzzy structure called q-rung orthopair fuzzy set (q-ROPFS) in which there is no limitation overall.

The notion picture fuzzy set (PFS) was introduced by Coung [7]. In PFS, there are four functions which express the MD, NMD, abstinence (AD), and refusal with a condition that the sum of MD, AD, and NMD must belong to  $[0, 1]$ . PFS fails when their sum exceeds one. Mahmood et al. [8] overcame this problem by introducing the concept of spherical fuzzy set in which they relaxed the condition that the square sum of MD, AD, and NMD must belong to  $[0, 1]$ . In [8], they also proposed the concept of a T-spherical fuzzy set in which the decision makers have to find the power for which the sum lies in the unit's closed interval.

All the fuzzy structures discussed above are used to solve many problems in the field of decision making, similarity measures, etc. Xu and Yager [9] proposed weighted geometric operators for IFS. Zeng et al. [10] proposed some probabilistic averaging operators for IFS and studied their application to group decision making. Garg [11] investigated the MADM problem using interval-valued IF robust geometric aggregation operators. Zhang et al. [12] discussed the IF MULTI-MOORA approach for the MADM problem. He et al. [13] investigated the MADM problem using interactive geometric

aggregation operators for IFS. Zhao and Wei [14] used Einstein t-norm and t-conorm to introduce IF Einstein geometric aggregation (IFEWA) operators and IF Einstein averaging aggregation (IFEWG) operators to solve the MADM problem. Mu et al. [15] investigated the MADM problem using Zhenyuan aggregation operators for interval-valued IFSs. Some MADM problems are solved for IFSs in [16–18]. Garg [19] investigated the MADM problem using Einstein norms for PyFSs. Wei and Lu [20] used power operators for PyFSs to solve the MADM problem. Yang and Chang [21] solved the MADM problem using interval-valued Pythagorean normal fuzzy aggregation operators. Zeng et al. [22] investigated the MADM problem using the novel aggregation method for PyFS. Zeng et al. [23] investigated the MADM problem using PyF confidence aggregation operators. By using PyFSs, some problems are solved in [24, 25]. Peng et al. [26] investigated the MADM problem by using exponential aggregation operators for q-ROPFS. Yang et al. [27] solved the MADM problem using q-ROPF interaction Heronian mean operators. Yang et al. [28] proposed the q-ROPF multicriteria decision algorithm and used it to investigate multiple heterogeneous relationships. Hussain et al. [29] investigated the MADM problem using a covering-based q-ROPF rough set model. Hussain et al. [30] used q-ROPF soft averaging operators to solve the MADM problem. Some MADM problems are studied using q-ROPFSs in [31–33].

Wei [34] proposed picture fuzzy Hamacher aggregation operators and studied their application in the MADM problem. Khan et al. [35] investigated the MADM problem using some logarithmic aggregation operators for PFS. Some MADM problems for PFS are studied in [36–38]. Quek et al. [39] studied the MADM problem using T-spherical fuzzy weighted aggregation operators. Garg [40] proposed interactive aggregation operators for T-spherical fuzzy sets and solved the MADM problem using the proposed operators. Zeng et al. [41] proposed immediate probabilistic averaging aggregation operators for T-spherical fuzzy sets and investigated their application in the selection of solar cells. Munir et al. [42] solved the MADM problem using Einstein aggregation operators for T-spherical fuzzy set. By using spherical fuzzy sets and T-spherical fuzzy sets, some MADM problems are studied in [43–46].

The existing Einstein operations [14, 42] fail under some circumstances, e.g., if  $I_1 = (m_A, 0)$  and  $I_2 = (0, n_A)$  are intuitionistic fuzzy numbers (IFNs), then IFEWA operators aggregate these IFNs as (some value, 0) and IFEWG operators aggregates these IFNs as (0, some value). From the above example, it is easy to notice that the IFEWA operator cannot aggregate the nonmembership value when nonmembership value of anyone IFN becomes zero and similarly the IFEWG operator cannot aggregate the membership value when nonmembership value of anyone IFN becomes zero. This issue motivates us to propose some improved Einstein aggregation operators which will overcome these problems.

The purposes of this manuscript are as follows:

- (1) To develop some new interactive Einstein operational laws

- (2) To develop new T-spherical fuzzy Einstein weighted geometric interaction operators using the new proposed interactive operational laws
- (3) To develop new T-spherical fuzzy Einstein weighted averaging interaction operators based on the new proposed interactive operations
- (4) To present an algorithm for solving the MADM problem
- (5) To check the applicability of the proposed operators through a numerical example

To achieve these aims, the rest of the article is summarized as follows. Section 2 has some notions that will be helpful for the readers in further sections. In Section 3, new operational laws are proposed for T-spherical fuzzy sets, and in Section 4, T-spherical fuzzy Einstein interaction geometric operators are proposed and some basic properties are also proved. In Section 5, T-spherical fuzzy Einstein interaction averaging operators are defined and some of their basic properties are also discussed. The advantages of the proposed work and comparative analysis between the existing and proposed operators are developed in Section 6. In Section 7, an algorithm for solving a MADM problem is developed and also applied in an example. A brief conclusion of the manuscript is included in Section 8.

## 2. Preliminaries

Some basic definitions over the set  $X$  are defined in this section. These basic notions will help the readers to understand the proposed work.

*Definition 1* (see [8]). A T-spherical fuzzy set on  $X$  is defined as

$$P = \{(x, m(x), i(x), n(x)) \mid x \in X\}, \quad (1)$$

where  $m, i, n: X \rightarrow [0, 1]$  are a membership, abstinence, and nonmembership function, respectively, with the condition  $0 \leq m^t(x) + i^t(x) + n^t(x) \leq 1, \forall x \in X, t \in \mathbb{N}$ .

$r(x) = \sqrt[t]{1 - (m^t(x) + i^t(x) + n^t(x))}$  is called the refusal degree of  $x$  in  $P$ , and  $(m, i, n)$  is known as T-spherical fuzzy number (T-SFN).

*Definition 2* (see [8]). Let  $P = (m, i, n) \in$  T-spherical fuzzy set. Then, the score value of  $P$  is defined as  $SC(P) = m^t(x) - n^t(x)$ , and the accuracy value of  $P$  is defined as  $AC(P) = m^t(x) + i^t(x) + n^t(x)$ . A T-SFN with a greater score is superior to others. If the score of any two T-SFNs becomes equal, then their superiority will be checked with the help of their accuracy values. The number which has greater accuracy value will be superior as compared to the others. If accuracy values also become equal, then both numbers are considered similar.

*Remark 1*

- (1) Definitions 1 and 2 can be reduced for spherical fuzzy set if we consider  $t = 2$



- (2) Definitions 1 and 2 can be reduced for PFS if we consider  $t = 1$
- (3) Definitions 1 and 2 can be reduced for q-ROFS if we consider  $i = 0$
- (4) Definitions 1 and 2 can be reduced for PyFS if we consider  $t = 2$  and  $i = 0$

- (5) Definitions 1 and 2 can be reduced for IFS if we consider  $t = 1$  and  $i = 0$
- (6) Definition 1 can be reduced for FS if we consider  $t = 1$ ,  $i = 0$ , and  $n = 0$

**Definition 3** (see [14]). Some operations for any two IFNs  $I_1 = (m_1, n_1)$  and  $I_2 = (m_2, n_2)$  are defined as

$$\begin{aligned}
 I_1 \otimes I_2 &= \left( \frac{m_1 m_2}{1 + (1 - m_1)(1 - m_2)}, \frac{n_1 + n_2}{1 + n_1 n_2} \right), \\
 I_1 \oplus I_2 &= \left( \frac{m_1 + m_2}{1 + m_1 m_2}, \frac{n_1 n_2}{1 + (1 + n_1)(1 - n_2)} \right), \\
 \tau I_1 &= \left( \frac{(1 + m_1)^\tau + (1 - m_1)^\tau}{(1 + m_1)^\tau - (1 - m_1)^\tau}, \frac{2n_1^\tau}{(2 - n_1)^\tau + n_1^\tau} \right), \quad \tau > 0, \\
 I_1^\tau &= \left( \frac{2m_1^\tau}{(2 - m_1)^\tau + m_1^\tau}, \frac{(1 + n_1)^\tau + (1 - n_1)^\tau}{(1 + n_1)^\tau - (1 - n_1)^\tau} \right), \quad \tau > 0.
 \end{aligned} \tag{2}$$

### 3. Einstein Interaction Operations for T-Spherical Fuzzy Set

Existing Einstein operations have some limitations that they fail under some conditions. So, we proposed some new

Einstein operations on which we define some new aggregation operators. Let  $P_1 = (m_1, i_1, n_1)$  and  $P_2 = (m_2, i_2, n_2)$  be two T-spherical fuzzy sets; then, their Einstein operations are as follows:

$$\begin{aligned}
 P_1 \otimes P_2 &= \left( \sqrt[2]{\frac{2((1 - n_1^t - i_1^t)(1 - n_2^t - i_2^t) - (1 - m_1^t - i_1^t - n_1^t)(1 - m_2^t - i_2^t - n_2^t))}{(1 + n_1^t)(1 + n_2^t) + (1 - n_1^t)(1 - n_2^t)}}, \sqrt[2]{\frac{(1 + i_1^t)(1 + i_2^t) - (1 - i_1^t)(1 - i_2^t)}{(1 + i_1^t)(1 + i_2^t) + (1 - i_1^t)(1 - i_2^t)}}, \sqrt[2]{\frac{(1 + n_1^t)(1 + n_2^t) - (1 - n_1^t)(1 - n_2^t)}{(1 + n_1^t)(1 + n_2^t) + (1 - n_1^t)(1 - n_2^t)}} \right), \\
 P_1 \oplus P_2 &= \left( \sqrt[2]{\frac{(1 + m_1^t)(1 + m_2^t) - (1 - m_1^t)(1 - m_2^t)}{(1 + m_1^t)(1 + m_2^t) + (1 - m_1^t)(1 - m_2^t)}}, \sqrt[2]{\frac{(1 + i_1^t)(1 + i_2^t) - (1 - i_1^t)(1 - i_2^t)}{(1 + i_1^t)(1 + i_2^t) + (1 - i_1^t)(1 - i_2^t)}}, \sqrt[2]{\frac{2((1 - m_1^t - i_1^t)(1 - m_2^t - i_2^t) - (1 - m_1^t - i_1^t - n_1^t)(1 - m_2^t - i_2^t - n_2^t))}{(1 + m_1^t)(1 + m_2^t) + (1 - m_1^t)(1 - m_2^t)}} \right), \\
 \tau P_1 &= \left( \sqrt[2]{\frac{(1 + m_1^t)^\tau - (1 - m_1^t)^\tau}{(1 + m_1^t)^\tau + (1 - m_1^t)^\tau}}, \sqrt[2]{\frac{(1 + i_1^t)^\tau - (1 - i_1^t)^\tau}{(1 + i_1^t)^\tau + (1 - i_1^t)^\tau}}, \sqrt[2]{\frac{2((1 - m_1^t - i_1^t)^\tau - (1 - m_1^t - i_1^t - n_1^t)^\tau)}{(1 + m_1^t)^\tau + (1 - m_1^t)^\tau}} \right), \quad \tau > 0, \\
 (P_1)^\tau &= \left( \sqrt[2]{\frac{2((1 - n_1^t - i_1^t)^\tau - (1 - m_1^t - i_1^t - n_1^t)^\tau)}{(1 + n_1^t)^\tau + (1 - n_1^t)^\tau}}, \sqrt[2]{\frac{(1 + i_1^t)^\tau - (1 - i_1^t)^\tau}{(1 + i_1^t)^\tau + (1 - i_1^t)^\tau}}, \sqrt[2]{\frac{(1 + n_1^t)^\tau - (1 - n_1^t)^\tau}{(1 + n_1^t)^\tau + (1 - n_1^t)^\tau}} \right), \quad \tau > 0.
 \end{aligned} \tag{3}$$

**Remark 2**

- (1) The defined operations will be reduced to spherical fuzzy sets for  $t = 2$
- (2) The defined operations will be reduced to PFSs for  $t = 1$

- (3) The defined operations will be reduced to q-ROFSs for  $i = 0$
- (4) The defined operations will be reduced to PyFSs for  $t = 2$  and  $i = 0$
- (5) The defined operations will be reduced to IFSs for  $t = 1$  and  $i = 0$

- (6) The defined operations will be reduced to FSs for  $t = 1$ ,  $i = 0$ , and  $n = 0$

#### 4. T-Spherical Fuzzy Einstein Geometric Interaction Operators

In this section, on the basis of new proposed Einstein operations, we defined geometric interaction operators in the

environment of T-spherical fuzzy set and some of its basic properties such as monotonicity, boundedness, and idempotency are also discussed. The validity of the proposed work is checked with the help of an example.

**Definition 4.** For any collection of T-SFNs,  $P_j = (m_j, i_j, n_j)$  ( $j = 1, 2, 3, \dots, k$ ). The mapping

$$T-SFEWIG_w(P_1, P_2, \dots, P_k) = \otimes_{j=1}^k P_j^{w_j}$$

$$= \left( \sqrt[t]{\frac{2(\prod_{j=1}^k (1 - n_j^t - i_j^t)^{w_j} - \prod_{j=1}^k (1 - m_j^t - i_j^t - n_j^t)^{w_j}}{\prod_{j=1}^k (1 + n_j^t)^{w_j} + \prod_{j=1}^k (1 - n_j^t)^{w_j}}}, \sqrt[t]{\frac{\prod_{j=1}^k (1 + i_j^t)^{w_j} - \prod_{j=1}^k (1 - i_j^t)^{w_j}}{\prod_{j=1}^k (1 + i_j^t)^{w_j} + \prod_{j=1}^k (1 - i_j^t)^{w_j}}}, \sqrt[t]{\frac{\prod_{j=1}^k (1 + n_j^t)^{w_j} - \prod_{j=1}^k (1 - n_j^t)^{w_j}}{\prod_{j=1}^k (1 + n_j^t)^{w_j} + \prod_{j=1}^k (1 - n_j^t)^{w_j}}} \right), \quad (4)$$

is called the T-spherical fuzzy Einstein weighted interactive geometric (T-SFEWIG) operator, where  $w = (w_1, \dots, w_k)^T$  is the weight vector of  $P_j$  with  $w_j \in [0, 1]$  and  $\sum_{j=1}^k w_j = 1$ .

**Theorem 1.** If all  $P_j = P_0$ , then  $T-SFEWIG_w(P_1, P_2, \dots, P_k) = P_0$ .

*Proof.* Let  $P_j = P_0 = (m_0, i_0, n_0)$  for all  $j$ ; then,

$$T-SFEWIG_w(P_1, P_2, \dots, P_k) = \left( \sqrt[t]{\frac{2(\prod_{j=1}^k (1 - n_j^t - i_j^t)^{w_j} - \prod_{j=1}^k (1 - m_j^t - i_j^t - n_j^t)^{w_j}}{\prod_{j=1}^k (1 + n_j^t)^{w_j} + \prod_{j=1}^k (1 - n_j^t)^{w_j}}}, \sqrt[t]{\frac{\prod_{j=1}^k (1 + i_j^t)^{w_j} - \prod_{j=1}^k (1 - i_j^t)^{w_j}}{\prod_{j=1}^k (1 + i_j^t)^{w_j} + \prod_{j=1}^k (1 - i_j^t)^{w_j}}}, \sqrt[t]{\frac{\prod_{j=1}^k (1 + n_j^t)^{w_j} - \prod_{j=1}^k (1 - n_j^t)^{w_j}}{\prod_{j=1}^k (1 + n_j^t)^{w_j} + \prod_{j=1}^k (1 - n_j^t)^{w_j}}} \right)$$

$$= \left( \sqrt[t]{\frac{2((1 - n_j^t - i_j^t)^{\sum_{j=1}^k w_j} - (1 - m_j^t - i_j^t - n_j^t)^{\sum_{j=1}^k w_j})}{(1 + n_j^t)^{\sum_{j=1}^k w_j} + (1 - n_j^t)^{\sum_{j=1}^k w_j}}}, \sqrt[t]{\frac{(1 + i_j^t)^{\sum_{j=1}^k w_j} - (1 - i_j^t)^{\sum_{j=1}^k w_j}}{(1 + i_j^t)^{\sum_{j=1}^k w_j} + (1 - i_j^t)^{\sum_{j=1}^k w_j}}}, \sqrt[t]{\frac{(1 + n_j^t)^{\sum_{j=1}^k w_j} - (1 - n_j^t)^{\sum_{j=1}^k w_j}}{(1 + n_j^t)^{\sum_{j=1}^k w_j} + (1 - n_j^t)^{\sum_{j=1}^k w_j}}} \right)$$

$$= (m_0, i_0, n_0) = P_0. \quad (5)$$

**Theorem 2.** Consider a collection of T-SFNs  $P_j$  ( $j = 1, 2, \dots, k$ ) with  $P^L = \min_j P_j$  and  $P^U = \max_j P_j$ . Then,

$$P^L \leq T-SFEWIG_w(P_1, P_2, \dots, P_k) \leq P^U. \quad (6)$$

*Proof.* Straightforward.  $\square$

**Theorem 3.** Consider any two T-SFNs  $P_j = (m_j, i_j, n_j)$  and  $P'_j = (m'_j, i'_j, n'_j)$  ( $j = 1, 2, \dots, k$ ) such that  $P_j \leq P'_j$  for all  $j$ . Then,

$$T - \text{SFEWIG}_w(P_1, P_2, \dots, P_k) \leq T - \text{SFEWIG}_w(P'_1, P'_2, \dots, P'_k). \quad (7)$$

*Proof.* Let  $P_j \leq P'_j$ ; then,  $m_j \leq m'_j$ ,  $i_j \leq i'_j$ , and  $n_j \geq n'_j$ . Then, by using basic information,

$$\begin{aligned} & \sqrt[t]{\frac{2\left(\prod_{j=1}^k (1 - n_j^t - i_j^t)^{w_j} - \prod_{j=1}^k (1 - m_j^t - i_j^t - n_j^t)^{w_j}\right)}{\prod_{j=1}^k (1 + n_j^t)^{w_j} + \prod_{j=1}^k (1 - n_j^t)^{w_j}}} \\ & \leq \sqrt[t]{\frac{2\left(\prod_{j=1}^k (1 - (n'_j)^t - (i'_j)^t)^{w_j} - \prod_{j=1}^k (1 - (m'_j)^t - (i'_j)^t - (n'_j)^t)^{w_j}\right)}{\prod_{j=1}^k (1 + (n'_j)^t)^{w_j} + \prod_{j=1}^k (1 - (n'_j)^t)^{w_j}}} \\ & \sqrt[t]{\frac{\prod_{j=1}^k (1 + i_j^t)^{w_j} - \prod_{j=1}^k (1 - i_j^t)^{w_j}}{\prod_{j=1}^k (1 + i_j^t)^{w_j} + \prod_{j=1}^k (1 - i_j^t)^{w_j}}} \leq \sqrt[t]{\frac{\prod_{j=1}^k (1 + (i'_j)^t)^{w_j} - \prod_{j=1}^k (1 - (i'_j)^t)^{w_j}}{\prod_{j=1}^k (1 + (i'_j)^t)^{w_j} + \prod_{j=1}^k (1 - (i'_j)^t)^{w_j}}} \\ & \sqrt[t]{\frac{\prod_{j=1}^k (1 + n_j^t)^{w_j} - \prod_{j=1}^k (1 - n_j^t)^{w_j}}{\prod_{j=1}^k (1 + n_j^t)^{w_j} + \prod_{j=1}^k (1 - n_j^t)^{w_j}}} \geq \sqrt[t]{\frac{\prod_{j=1}^k (1 + (n'_j)^t)^{w_j} - \prod_{j=1}^k (1 - (n'_j)^t)^{w_j}}{\prod_{j=1}^k (1 + (n'_j)^t)^{w_j} + \prod_{j=1}^k (1 - (n'_j)^t)^{w_j}}}. \end{aligned} \quad (8)$$

This shows that

$$T - \text{SFEWIG}_w(P_1, P_2, \dots, P_k) \leq T - \text{SFEWIG}_w(P'_1, P'_2, \dots, P'_k). \quad (9)$$

□

**Definition 5.** For any collection of T-SFNs,  $P_j = (m_j, i_j, n_j)$  ( $j = 1, 2, 3, \dots, k$ ). The mapping

$$T - \text{SFEOWIG}_w(P_1, P_2, \dots, P_k) = \otimes_{j=1}^k P_{\sigma(j)}^{\omega_j}$$

$$= \left( \sqrt[t]{\frac{2\left(\prod_{j=1}^k (1 - n_{\sigma(j)}^t - i_{\sigma(j)}^t)^{w_j} - \prod_{j=1}^k (1 - m_{\sigma(j)}^t - i_{\sigma(j)}^t - n_{\sigma(j)}^t)^{w_j}\right)}{\prod_{j=1}^k (1 + n_{\sigma(j)}^t)^{w_j} + \prod_{j=1}^k (1 - n_{\sigma(j)}^t)^{w_j}}}, \sqrt[t]{\frac{\prod_{j=1}^k (1 + i_{\sigma(j)}^t)^{w_j} - \prod_{j=1}^k (1 - i_{\sigma(j)}^t)^{w_j}}{\prod_{j=1}^k (1 + i_{\sigma(j)}^t)^{w_j} + \prod_{j=1}^k (1 - i_{\sigma(j)}^t)^{w_j}}}, \sqrt[t]{\frac{\prod_{j=1}^k (1 + n_{\sigma(j)}^t)^{w_j} - \prod_{j=1}^k (1 - n_{\sigma(j)}^t)^{w_j}}{\prod_{j=1}^k (1 + n_{\sigma(j)}^t)^{w_j} + \prod_{j=1}^k (1 - n_{\sigma(j)}^t)^{w_j}}} \right), \quad (10)$$

$T - \text{SFEOWIG}_w$  is called the T-spherical fuzzy Einstein ordered weighted interactive geometric (T-SFEOWIG) operator, where  $\omega = (\omega_1, \dots, \omega_k)^T$  is the associated weight vector of  $P_j$  with  $\omega_j \in [0, 1]$  and  $\sum_{j=1}^k \omega_j = 1$  and  $\sigma(j)$  is any permutation of  $(1, 2, \dots, k)$  such that  $\tilde{P}_{\sigma(j-1)} \geq \tilde{P}_{\sigma(j)}$ .

**Theorem 4.** If all  $P_j = P_0$ , then  $T - \text{SFEOWIG}_w(P_1, P_2, \dots, P_k) = P_0$ .

*Proof.* Same as in Theorem 1. □

**Theorem 5.** Consider a collection of T-SFNs  $P_j$  ( $j = 1, 2, \dots, k$ ) with  $P^L = \min_j P_j$  and  $P^U = \max_j P_j$ . Then,

$$P^L \leq T - \text{SFEOWIG}_w(P_1, P_2, \dots, P_k) \leq P^U. \quad (11)$$

*Proof.* Straightforward. □

**Theorem 6.** For any two T-SFNs,  $P_j = (m_j, i_j, n_j)$  and  $P'_j = (m'_j, i'_j, n'_j)$  for all  $(j = 1, 2, \dots, k)$  such that  $P_j \leq P'_j$  for all  $j$ . Then,

$$\begin{aligned} T-SFEOWIG_{\omega}(P_1, P_2, \dots, P_k) &\leq T-SFEOWIG_{\omega} \\ &\cdot (P'_1, P'_2, \dots, P'_k). \end{aligned} \quad (12)$$

*Proof.* Directly follows from the proof of Theorem 3.  $\square$

**Definition 6.** For any collection of T-SFNs,  $P_j = (m_j, i_j, n_j)$  ( $j = 1, 2, 3, \dots, k$ ). The mapping

$$\begin{aligned} T-SFEHIG_{w,\omega}(\tilde{P}_1, \tilde{P}_2, \dots, \tilde{P}_k) &= \otimes_{j=1}^k \tilde{P}_{\sigma(j)}^{\omega_j} \\ &= \left( \sqrt[t]{\frac{2 \left( \prod_{j=1}^k (1 - \tilde{n}_{\sigma(j)}^t - \tilde{i}_{\sigma(j)}^t)^{\omega_j} - \prod_{j=1}^k (1 - \tilde{m}_{\sigma(j)}^t - \tilde{i}_{\sigma(j)}^t - \tilde{n}_{\sigma(j)}^t)^{\omega_j} \right)}{\prod_{j=1}^k (1 + n_{\sigma(j)}^t)^{\omega_j} + \prod_{j=1}^k (1 - n_{\sigma(j)}^t)^{\omega_j}}}, \sqrt[t]{\frac{\prod_{j=1}^k (1 + \tilde{i}_{\sigma(j)}^t)^{\omega_j} - \prod_{j=1}^k (1 - \tilde{i}_{\sigma(j)}^t)^{\omega_j}}{\prod_{j=1}^k (1 + \tilde{i}_{\sigma(j)}^t)^{\omega_j} + \prod_{j=1}^k (1 - \tilde{i}_{\sigma(j)}^t)^{\omega_j}}}, \right. \\ &\quad \left. \sqrt[t]{\frac{\prod_{j=1}^k (1 + \tilde{n}_{\sigma(j)}^t)^{\omega_j} - \prod_{j=1}^k (1 - \tilde{n}_{\sigma(j)}^t)^{\omega_j}}{\prod_{j=1}^k (1 + \tilde{n}_{\sigma(j)}^t)^{\omega_j} + \prod_{j=1}^k (1 - \tilde{n}_{\sigma(j)}^t)^{\omega_j}}} \right), \end{aligned} \quad (13)$$

$T-SFEHIG_{w,\omega}$  is called the T-spherical fuzzy Einstein hybrid interactive geometric (T-SFEHIG) operator, where  $\tilde{P}_j = (P_j)^{k\omega_j}$ . Let  $w = (w_1, \dots, w_k)^T$  is the weight vector and  $\omega = (\omega_1, \dots, \omega_k)^T$  is the associated weight vector of  $P_j$  with a condition that both weight and associated weight vectors belong to closed unit interval and their sum is equal to 1.

Hybrid aggregation operators first aggregate the given data considering their attributes and then rearrange them in a specific order. After that, they aggregate the data considering their order. This means that hybrid operators are a generalization of weighted and ordered weighted operators. So, the T-SFEHIG operator will satisfy idempotency, monotonicity, and bounded property.

**Example 1.** Consider T-SFNs  $P_1 = (0.7, 0.3, 0.2)$ ,  $P_2 = (0.9, 0.1, 0.6)$ ,  $P_3 = (0.4, 0.6, 0.8)$ ,  $P_4 = (0.1, 0.5, 0.7)$ , and  $P_5 = (0.0, 0.0, 0.8)$  with a weight vector  $w = (0.25, 0.20, 0.15, 0.18, 0.22)^T$ .

**Solution 1.** First of all, we find the aggregated value of these T-SFNs by using the T-spherical fuzzy Einstein hybrid geometric aggregation (T-SFEHG) operator [42] to find out the drawbacks of the given operators. For this purpose, first, we have to calculate the value of  $t$  for which the given data lie in T-SF information.

As  $0.9 + 0.1 + 0.6 = 1.6$ ,

For  $t = 2$ ,  $0.9^2 + 0.1^2 + 0.6^2 = 1.18$

$t = 3$ ,  $0.9^3 + 0.1^3 + 0.6^3 = 0.946$

Similarly, for  $t = 3$ , all the given data lie in the T-spherical fuzzy information.

By using T-spherical fuzzy Einstein weighted geometric operator, we shall be able to find these values:

$$\begin{aligned} P_1 &= (0.6388, 0.3232, 0.5381), \\ P_2 &= (0.9, 0.1, 0.6), \\ P_3 &= (0.4163, 0.5464, 0.7370), \\ P_4 &= (0.1050, 0.4829, 0.6776), \\ P_5 &= (0.0, 0.0, 0.8206). \end{aligned} \quad (14)$$

Their scores values will be

$$\begin{aligned} SC(P_1) &= 0.1048, \\ SC(P_2) &= 0.5130, \\ SC(P_3) &= -0.3282, \\ SC(P_4) &= -0.3099, \\ SC(P_5) &= -0.5525. \end{aligned} \quad (15)$$

Now using the score value, the aggregated values obtained by using T-SFEWG operators are rearranged in descending order. Then, these ordered values are again aggregated by using the T-SFEHG operator with associated weight vector being  $\omega = (0.112, 0.236, 0.304, 0.236, 0.112)$ :

$$\begin{aligned} \tilde{P}_{\sigma(1)} &= (0.9, 0.1, 0.6), \\ \tilde{P}_{\sigma(2)} &= (0.6388, 0.3232, 0.5381), \\ \tilde{P}_{\sigma(3)} &= (0.1050, 0.4829, 0.6776), \\ \tilde{P}_{\sigma(4)} &= (0.4163, 0.5464, 0.7370), \\ \tilde{P}_{\sigma(5)} &= (0.0, 0.0, 0.8206). \end{aligned} \quad (16)$$

Now, employ the T-SFEHG operator as follows:

$$T-SFEHG_{w,\omega}(P_1, \dots, P_5) = (0.0, 0.8525, 0.9882). \quad (17)$$

From the above result, it is noticed that when abstinence or nonmembership value of one T-SFN is zero, then the T-SFEHG operator cannot aggregate the whole membership value. This shows a big flaw in the T-SFEHG operator. This means that the results obtained from T-SFEHG operators are not reliable. Now, by using the T-SFEHG operator, we shall show that the proposed operator will overcome this drawback.

By using the T-SFEWIG operator, we shall be able to find

$$\begin{aligned} P_1 &= (0.7393, 0.3232, 0.2154), \\ P_2 &= (0.9, 0.1, 0.6), \\ P_3 &= (0.4131, 0.5464, 0.7370), \\ P_4 &= (0.0988, 0.4829, 0.6776), \\ P_5 &= (0.0, 0.0, 0.8206). \end{aligned} \quad (18)$$

Their scores values will be

$$\begin{aligned} SC(P_1) &= 0.3941, \\ SC(P_2) &= 0.5130, \\ SC(P_3) &= -0.3299, \\ SC(P_4) &= -0.3101, \\ SC(P_5) &= -0.5525. \end{aligned} \quad (19)$$

Now using the score value, the aggregated values obtained by using T-SFEWIG operators are rearranged in descending order. Then, these ordered values are again

aggregated by using the T-SFEHG operator with the associated weight vector being  $\omega = (0.112, 0.236, 0.304, 0.236, 0.112)$ :

$$\begin{aligned} \tilde{P}_{\sigma(1)} &= (0.9, 0.1, 0.6), \\ \tilde{P}_{\sigma(2)} &= (0.7393, 0.3232, 0.2154), \\ \tilde{P}_{\sigma(3)} &= (0.0988, 0.4829, 0.6776), \\ \tilde{P}_{\sigma(4)} &= (0.4131, 0.5464, 0.7370), \\ \tilde{P}_{\sigma(5)} &= (0.0, 0.0, 0.8206). \end{aligned} \quad (20)$$

Now, employ the T-SFEHG operator as follows:

$$T-SFEHG_{\omega, w}(\tilde{P}_1, \dots, \tilde{P}_5) = (0.6878, 0.4329, 0.6591). \quad (21)$$

This shows that the T-SFEIG operator aggregates the membership value.

## 5. T-Spherical Fuzzy Einstein Hybrid Interaction Averaging Operators

In this section, on the basis of new proposed Einstein operations, we define averaging interaction operators in T-spherical fuzzy environment and some basic properties are also discussed.

**Definition 7.** Consider a collection of T-SFN  $P_j = (m_j, i_j, n_j)$  ( $j = 1, 2, 3, \dots, k$ ). Then,

$$T-SFEWIA_w(P_1, P_2, \dots, P_k) = \oplus_{j=1}^k w_j P_j$$

$$= \left( \sqrt[t]{\frac{\prod_{j=1}^k (1 + m_j^t)^{w_j} - \prod_{j=1}^k (1 - m_j^t)^{w_j}}{\prod_{j=1}^k (1 + m_j^t)^{w_j} + \prod_{j=1}^k (1 - m_j^t)^{w_j}}}, \sqrt[t]{\frac{\prod_{j=1}^k (1 + i_j^t)^{w_j} - \prod_{j=1}^k (1 - i_j^t)^{w_j}}{\prod_{j=1}^k (1 + i_j^t)^{w_j} + \prod_{j=1}^k (1 - i_j^t)^{w_j}}}, \sqrt[t]{\frac{2(\prod_{j=1}^k (1 - m_j^t - i_j^t)^{w_j} - \prod_{j=1}^k (1 - m_j^t - i_j^t - n_j^t)^{w_j})}{\prod_{j=1}^k (1 + m_j^t)^{w_j} + \prod_{j=1}^k (1 - m_j^t)^{w_j}}} \right), \quad (22)$$

$T-SFEWIA_w$  is called T-spherical fuzzy Einstein weighted interactive averaging (T-SFEWIA) operator with weight vector  $w = (w_1, w_2, \dots, w_k)^T$  of  $P_j$  with  $w_j \in [0, 1]$  and  $\sum_{j=1}^k w_j = 1$ .

**Theorem 7.** If all  $P_j = P_0$ , then  $T-SFEWIA_w(P_1, P_2, \dots, P_k) = P_0$ .

**Proof.** Let  $P_j = P_0 = (m_0, i_0, n_0)$  for all  $j$ ; then,

$$\begin{aligned}
T - \text{SFEWIA}_w(P_1, P_2, \dots, P_k) &= \left( \sqrt[t]{\frac{\prod_{j=1}^k (1 + m_j^t)^{w_j} - \prod_{j=1}^k (1 - m_j^t)^{w_j}}{\prod_{j=1}^k (1 + m_j^t)^{w_j} + \prod_{j=1}^k (1 - m_j^t)^{w_j}}}, \sqrt[t]{\frac{\prod_{j=1}^k (1 + i_j^t)^{w_j} - \prod_{j=1}^k (1 - i_j^t)^{w_j}}{\prod_{j=1}^k (1 + i_j^t)^{w_j} + \prod_{j=1}^k (1 - i_j^t)^{w_j}}}, \right. \\
&\quad \left. \sqrt[t]{\frac{2(\prod_{j=1}^k (1 - m_j^t - i_j^t)^{w_j} - \prod_{j=1}^k (1 - m_j^t - i_j^t - n_j^t)^{w_j})}{\prod_{j=1}^k (1 + m_j^t)^{w_j} + \prod_{j=1}^k (1 - m_j^t)^{w_j}}} \right) \\
T - \text{SFEWIA}_w(P_1, P_2, \dots, P_k) &= \left( \sqrt[t]{\frac{(1 + m_j^t)^{\sum_{j=1}^k w_j} - (1 - m_j^t)^{\sum_{j=1}^k w_j}}{(1 + m_j^t)^{\sum_{j=1}^k w_j} + (1 - m_j^t)^{\sum_{j=1}^k w_j}}}, \sqrt[t]{\frac{(1 + i_j^t)^{\sum_{j=1}^k w_j} - (1 - i_j^t)^{\sum_{j=1}^k w_j}}{(1 + i_j^t)^{\sum_{j=1}^k w_j} + (1 - i_j^t)^{\sum_{j=1}^k w_j}}}, \right. \\
&\quad \left. \sqrt[t]{\frac{2\left((1 - m_j^t - i_j^t)^{\sum_{j=1}^k w_j} - (1 - m_j^t - i_j^t - n_j^t)^{\sum_{j=1}^k w_j}\right)}{(1 + m_j^t)^{\sum_{j=1}^k w_j} + (1 - m_j^t)^{\sum_{j=1}^k w_j}}} \right) \quad (23) \\
&= (m_0, i_0, n_0) = P_0.
\end{aligned}$$

**Theorem 8.** Consider a collection of T-SFNs  $P_j$  ( $j = 1, 2, \dots, k$ ) with  $P^L = \min_j P_j$  and  $P^U = \max_j P_j$ . Then,

$$P^L \leq T - \text{SFEWIA}_w(P_1, P_2, \dots, P_k) \leq P^U. \quad (24)$$

**Theorem 9.** For any two T-SFNs,  $P_j = (m_j, i_j, n_j)$  and  $P'_j = (m'_j, i'_j, n'_j)$  such that  $P_j \leq P'_j$  for all  $j$ . Then,

$$T - \text{SFEWIA}_w(P_1, P_2, \dots, P_k) \leq T - \text{SFEWIA}_w(P'_1, P'_2, \dots, P'_k). \quad (25)$$

*Proof.* Straightforward.  $\square$

*Proof.* Let  $P_j \leq P'_j$ ; then,  $m_j \leq m'_j$ ,  $i_j \leq i'_j$ , and  $n_j \geq n'_j$ . Then, by using this basic information,

$$\begin{aligned}
&\sqrt[t]{\frac{2(\prod_{j=1}^k (1 - m_j^t - i_j^t)^{w_j} - \prod_{j=1}^k (1 - m_j^t - i_j^t - n_j^t)^{w_j})}{\prod_{j=1}^k (1 + m_j^t)^{w_j} + \prod_{j=1}^k (1 - m_j^t)^{w_j}}} \\
&\leq \sqrt[t]{\frac{2\left(\prod_{j=1}^k (1 - (m'_j)^t - (i'_j)^t)^{w_j} - \prod_{j=1}^k (1 - (m'_j)^t - (i'_j)^t - (n'_j)^t)^{w_j}\right)}{\prod_{j=1}^k (1 + (m'_j)^t)^{w_j} + \prod_{j=1}^k (1 - (m'_j)^t)^{w_j}}}, \\
&\sqrt[t]{\frac{\prod_{j=1}^k (1 + i_j^t)^{w_j} - \prod_{j=1}^k (1 - i_j^t)^{w_j}}{\prod_{j=1}^k (1 + i_j^t)^{w_j} + \prod_{j=1}^k (1 - i_j^t)^{w_j}}} \leq \sqrt[t]{\frac{\prod_{j=1}^k (1 + (i'_j)^t)^{w_j} - \prod_{j=1}^k (1 - (i'_j)^t)^{w_j}}{\prod_{j=1}^k (1 + (i'_j)^t)^{w_j} + \prod_{j=1}^k (1 - (i'_j)^t)^{w_j}}}, \\
&\sqrt[t]{\frac{\prod_{j=1}^k (1 + m_j^t)^{w_j} - \prod_{j=1}^k (1 - m_j^t)^{w_j}}{\prod_{j=1}^k (1 + m_j^t)^{w_j} + \prod_{j=1}^k (1 - m_j^t)^{w_j}}} \geq \sqrt[t]{\frac{\prod_{j=1}^k (1 + (m'_j)^t)^{w_j} - \prod_{j=1}^k (1 - (m'_j)^t)^{w_j}}{\prod_{j=1}^k (1 + (m'_j)^t)^{w_j} + \prod_{j=1}^k (1 - (m'_j)^t)^{w_j}}}. \quad (26)
\end{aligned}$$



This shows that

$$T - SFEWIA_w(P_1, P_2, \dots, P_k) \leq T - SFEWIA_w(P'_1, P'_2, \dots, P'_k). \quad (27)$$

□

**Definition 8.** Consider a collection of T-SFNs  $P_j = (m_j, i_j, n_j)$  ( $j = 1, 2, 3, \dots, k$ ). Then,

$$T - SFEOWIA_w(P_1, P_2, \dots, P_k) = \bigoplus_{j=1}^k \omega_j P_{\sigma(j)}$$

$$= \left( \sqrt[t]{\frac{\prod_{j=1}^k (1 + m_{\sigma(j)}^t)^{\omega_j} - \prod_{j=1}^k (1 - m_{\sigma(j)}^t)^{\omega_j}}{\prod_{j=1}^k (1 + m_{\sigma(j)}^t)^{\omega_j} + \prod_{j=1}^k (1 - m_{\sigma(j)}^t)^{\omega_j}}}, \sqrt[t]{\frac{\prod_{j=1}^k (1 + i_{\sigma(j)}^t)^{\omega_j} - \prod_{j=1}^k (1 - i_{\sigma(j)}^t)^{\omega_j}}{\prod_{j=1}^k (1 + i_{\sigma(j)}^t)^{\omega_j} + \prod_{j=1}^k (1 - i_{\sigma(j)}^t)^{\omega_j}}}, \sqrt[t]{\frac{2 \left[ \prod_{j=1}^k (1 - m_{\sigma(j)}^t - i_{\sigma(j)}^t)^{\omega_j} - \prod_{j=1}^k (1 - m_{\sigma(j)}^t - i_{\sigma(j)}^t - n_{\sigma(j)}^t)^{\omega_j} \right]}{\prod_{j=1}^k (1 + m_{\sigma(j)}^t)^{\omega_j} + \prod_{j=1}^k (1 - m_{\sigma(j)}^t)^{\omega_j}}} \right) \quad (28)$$

$T - SFEOWIA_w$  is called the T-spherical fuzzy Einstein ordered weighted interactive averaging (T-SFEOWIA) operator with associated weight vector  $\omega = (\omega_1, \omega_2, \dots, \omega_k)^T$  of  $P_j$  with  $\omega_j \in [0, 1]$  and  $\sum_{j=1}^k \omega_j = 1$ . Here,  $\sigma(j)$  is any permutation of  $(1, 2, \dots, k)$  such that  $\tilde{P}_{\sigma(j-1)} \geq \tilde{P}_{\sigma(j)}$ .

**Theorem 10.** If for all  $P_j = P_0$ , then  $T - SFEOWIA_w(P_1, P_2, \dots, P_k) = P_0$ .

*Proof.* Same as in Theorem 7. □

**Theorem 11.** Consider a collection of T-SFNs  $P_j$  ( $j = 1, 2, \dots, k$ ) with  $P^L = \min_j P_j$  and  $P^U = \max_j P_j$ . Then,

$$P^L \leq T - SFEOWIA_w(P_1, P_2, \dots, P_k) \leq P^U. \quad (29)$$

*Proof.* Straightforward. □

**Theorem 12.** Consider any two T-SFNs  $P_j = (m_j, i_j, n_j)$  and  $P'_j = (m'_j, i'_j, n'_j)$  such that  $P_j \leq P'_j$  for all  $j$ . Then,

$$T - SFEOWIA_w(P_1, P_2, \dots, P_k) \leq T - SFEOWIA_w(P'_1, P'_2, \dots, P'_k). \quad (30)$$

*Proof.* Same as in Theorem 9. □

**Definition 9.** Consider a collection of T-SFNs  $P_j = (m_j, i_j, n_j)$  ( $j = 1, 2, 3, \dots, k$ ). The mapping

$$T - SFEHIA_{w,\omega}(\tilde{P}_1, \tilde{P}_2, \dots, \tilde{P}_k) = \bigoplus_{j=1}^k \omega_j \tilde{P}_{\sigma(j)}$$

$$= \left( \sqrt[t]{\frac{\prod_{j=1}^k (1 + \tilde{m}_{\sigma(j)}^t)^{\omega_j} - \prod_{j=1}^k (1 - \tilde{m}_{\sigma(j)}^t)^{\omega_j}}{\prod_{j=1}^k (1 + \tilde{m}_{\sigma(j)}^t)^{\omega_j} + \prod_{j=1}^k (1 - \tilde{m}_{\sigma(j)}^t)^{\omega_j}}}, \sqrt[t]{\frac{\prod_{j=1}^k (1 + \tilde{i}_{\sigma(j)}^t)^{\omega_j} - \prod_{j=1}^k (1 - \tilde{i}_{\sigma(j)}^t)^{\omega_j}}{\prod_{j=1}^k (1 + \tilde{i}_{\sigma(j)}^t)^{\omega_j} + \prod_{j=1}^k (1 - \tilde{i}_{\sigma(j)}^t)^{\omega_j}}}, \sqrt[t]{\frac{2 \left( \prod_{j=1}^k (1 - \tilde{m}_{\sigma(j)}^t - \tilde{i}_{\sigma(j)}^t)^{\omega_j} - \prod_{j=1}^k (1 - \tilde{m}_{\sigma(j)}^t - \tilde{i}_{\sigma(j)}^t - \tilde{n}_{\sigma(j)}^t)^{\omega_j} \right)}{\prod_{j=1}^k (1 + \tilde{m}_{\sigma(j)}^t)^{\omega_j} + \prod_{j=1}^k (1 - \tilde{m}_{\sigma(j)}^t)^{\omega_j}}} \right), \quad (31)$$

is called the T-spherical fuzzy Einstein hybrid interactive averaging (T-SFEHIA) operator, where  $\tilde{P}_j = k\omega_j P_j$  and  $\omega_j, \omega_j \in [0, 1]$ , and  $\sum_{j=1}^k \omega_j = 1$  and  $\sum_{j=1}^k \omega_j = 1$ .

Hybrid aggregation operators first aggregate the given data considering their attributes and then rearrange them in

a specific order. After that, they aggregate the data considering their order. This means that hybrid operators are a generalization of weighted and ordered weighted operators. So, the T-SFEHIA operator will satisfy idempotency, monotonicity, and bounded property.

**Example 2.** Consider five T-SFNs  $P_1 = (0.9, 0.3, 0.4)$ ,  $P_2 = (0.6, 0.3, 0.2)$ ,  $P_3 = (0.3, 0.8, 0.6)$ ,  $P_4 = (0.4, 0.5, 0.8)$ , and  $P_5 = (0.6, 0.0, 0.0)$  with a weight vector  $\omega = (0.25, 0.20, 0.15, 0.18, 0.22)^T$ .

**solution 1.** First of all, we find the aggregated value of these T-SFNs by using the T-spherical fuzzy Einstein hybrid averaging aggregation (T-SFEHA) operator [42] to find out the drawbacks of given operators. For this purpose, first, we have to find the value of  $t$  for which the given data lie in T-spherical fuzzy environment.

As  $0.3 + 0.8 + 0.6 = 1.7$ ,

For  $t = 2$ ,  $0.3^2 + 0.8^2 + 0.6^2 = 1.09$

For  $t = 3$ ,  $0.3^3 + 0.8^3 + 0.6^3 = 0.755$

Similarly, for  $t = 3$ , all the given data lie in the T-spherical fuzzy environment.

By using T-spherical fuzzy Einstein weighted averaging operator, we shall be able to find these values:

$$\begin{aligned} P_1 &= (0.9362, 0.2104, 0.3029), \\ P_2 &= (0.6, 0.3, 0.2), \\ P_3 &= (0.2726, 0.8527, 0.6984), \\ P_4 &= (0.3862, 0.5437, 0.8211), \\ P_5 &= (0.6187, 0.0, 0.0). \end{aligned} \quad (32)$$

Their scores values will be

$$\begin{aligned} SC(P_1) &= 0.7927, \\ SC(P_2) &= 0.2080, \\ SC(P_3) &= -0.3203, \\ SC(P_4) &= -0.4961, \\ SC(P_5) &= 0.2368. \end{aligned} \quad (33)$$

Now using the score value, the aggregated values obtained by using T-SFEWA operators are rearranged in descending order. Then, these ordered values are again aggregated by using the T-SFEHA operator with associated weight vector being  $\omega = (0.112, 0.236, 0.304, 0.236, 0.112)$ :

$$\begin{aligned} \tilde{P}_{\sigma(1)} &= (0.9362, 0.2104, 0.3029), \\ \tilde{P}_{\sigma(2)} &= (0.6187, 0.0, 0.0), \\ \tilde{P}_{\sigma(3)} &= (0.6, 0.3, 0.2), \\ \tilde{P}_{\sigma(4)} &= (0.2726, 0.8527, 0.6984), \\ \tilde{P}_{\sigma(5)} &= (0.3862, 0.5437, 0.8211). \end{aligned} \quad (34)$$

Now, employ the T-SFEHA operator as follows:

$$T-SFEHA_{w,\omega}(\tilde{P}_1, \dots, \tilde{P}_5) = (0.6187, 0.0, 0.0). \quad (35)$$

From the above result, it is noticed that when abstinence or nonmembership value of one T-SFN is zero, then the T-SFEHA operator cannot aggregate the whole abstinence and nonmembership value. This shows a big flaw in the T-SFEHA operator. This means that the results obtained

from T-SFEHA operators are not reliable. Now, by using the T-SFEIA operator, we shall show that the proposed operator will overcome this drawback.

By using T-SFEIA operator, we shall be able to find

$$\begin{aligned} P_1 &= (0.9362, 0.4308, 0.2739), \\ P_2 &= (0.6, 0.3, 0.2), \\ P_3 &= (0.2726, 0.7370, 0.5956), \\ P_4 &= (0.3862, 0.4829, 0.7888), \\ P_5 &= (0.6187, 0.0, 0.0). \end{aligned} \quad (36)$$

Their scores values will be

$$\begin{aligned} SC(P_1) &= 0.7999, \\ SC(P_2) &= 0.2080, \\ SC(P_3) &= -0.1910, \\ SC(P_4) &= -0.4333, \\ SC(P_5) &= 0.2368. \end{aligned} \quad (37)$$

Now using the score value, the aggregated values obtained by using T-SFEWIA operators are rearranged in descending order. Then, these ordered values are again aggregated by using the T-SFEHIA operator, with associated weight vector being  $\omega = (0.112, 0.236, 0.304, 0.236, 0.112)$ :

$$\begin{aligned} \tilde{P}_{\sigma(1)} &= (0.9362, 0.4308, 0.2739), \\ \tilde{P}_{\sigma(2)} &= (0.6187, 0.0, 0.0), \\ \tilde{P}_{\sigma(3)} &= (0.6, 0.3, 0.2), \\ \tilde{P}_{\sigma(4)} &= (0.2726, 0.7370, 0.5956), \\ \tilde{P}_{\sigma(5)} &= (0.3862, 0.4829, 0.7888). \end{aligned} \quad (38)$$

Now, employ the T-SFEHIA operator as follows:

$$T-SFEHIA_{w,\omega}(\tilde{P}_1, \dots, \tilde{P}_5) = (0.6372, 0.5055, 0.3978). \quad (39)$$

This shows that the T-SFEIA operator aggregates the membership value.

## 6. Advantages

In this section, we prove that our work is more generalized than the existing work. In our proposed work, experts are free in giving the values to alternatives according to the given attributes. Not only this, the proposed work is also valid under those conditions where the existing work fails. Here, we reduced the proposed work to intuitionistic, Pythagorean, q-rung orthopair, picture, and spherical fuzzy environments. This proves that the proposed work is valid for all those environments.

Consider the T-SFEHIA defined as follows:

- (1) For  $t = 2$ , equation (31) reduces to SF Einstein hybrid interaction averaging operators (SFEHIA operators), i.e.,

$$T - SFEHIA_{w,\omega}(\tilde{P}_1, \tilde{P}_2, \dots, \tilde{P}_k) = \left( \sqrt{\frac{\prod_{j=1}^k (1 + \tilde{m}_{\sigma(j)}^2)^{\omega_j} - \prod_{j=1}^k (1 - \tilde{m}_{\sigma(j)}^2)^{\omega_j}}{\prod_{j=1}^k (1 + \tilde{m}_{\sigma(j)}^2)^{\omega_j} + \prod_{j=1}^k (1 - \tilde{m}_{\sigma(j)}^2)^{\omega_j}}}, \sqrt{\frac{\prod_{j=1}^k (1 + \tilde{i}_{\sigma(j)}^2)^{\omega_j} - \prod_{j=1}^k (1 - \tilde{i}_{\sigma(j)}^2)^{\omega_j}}{\prod_{j=1}^k (1 + \tilde{i}_{\sigma(j)}^2)^{\omega_j} + \prod_{j=1}^k (1 - \tilde{i}_{\sigma(j)}^2)^{\omega_j}}}, \sqrt{\frac{2 \left( \prod_{j=1}^k (1 - \tilde{m}_{\sigma(j)}^2 - \tilde{i}_{\sigma(j)}^2)^{\omega_j} - \prod_{j=1}^k (1 - \tilde{m}_{\sigma(j)}^2 - \tilde{i}_{\sigma(j)}^2 - n_{\sigma(j)}^t)^{\omega_j} \right)}{\prod_{j=1}^k (1 + \tilde{m}_{\sigma(j)}^2)^{\omega_j} + \prod_{j=1}^k (1 - \tilde{m}_{\sigma(j)}^2)^{\omega_j}}} \right). \quad (40)$$

- (2) For  $t = 1$ , equation (31) reduces to PF Einstein hybrid interaction averaging operators (PFEHIA operators), i.e.,

$$PFEHIA_{w,\omega}(\tilde{P}_1, \tilde{P}_2, \dots, \tilde{P}_k) = \left( \frac{\prod_{j=1}^k (1 + \tilde{m}_{\sigma(j)})^{\omega_j} - \prod_{j=1}^k (1 - \tilde{m}_{\sigma(j)})^{\omega_j}}{\prod_{j=1}^k (1 + \tilde{m}_{\sigma(j)})^{\omega_j} + \prod_{j=1}^k (1 - \tilde{m}_{\sigma(j)})^{\omega_j}}, \frac{\prod_{j=1}^k (1 + \tilde{i}_{\sigma(j)})^{\omega_j} - \prod_{j=1}^k (1 - \tilde{i}_{\sigma(j)})^{\omega_j}}{\prod_{j=1}^k (1 + \tilde{i}_{\sigma(j)})^{\omega_j} + \prod_{j=1}^k (1 - \tilde{i}_{\sigma(j)})^{\omega_j}}, \frac{2 \left( \prod_{j=1}^k (1 - \tilde{m}_{\sigma(j)})^{\omega_j} - \prod_{j=1}^k (1 - \tilde{m}_{\sigma(j)} - \tilde{i}_{\sigma(j)} n_{\sigma(j)})^{\omega_j} \right)}{\prod_{j=1}^k (1 + \tilde{m}_{\sigma(j)})^{\omega_j} + \prod_{j=1}^k (1 - \tilde{m}_{\sigma(j)})^{\omega_j}} \right). \quad (41)$$

- (3) For  $i = 0$ , equation (31) reduces to q-ROPF Einstein hybrid interaction averaging operators (q-ROFEHIA operators), i.e.,

$$q - ROFEHIA_{w,\omega}(\tilde{P}_1, \tilde{P}_2, \dots, \tilde{P}_k) = \left( \sqrt[t]{\frac{\prod_{j=1}^k (1 + \tilde{m}_{\sigma(j)}^t)^{\omega_j} - \prod_{j=1}^k (1 - \tilde{m}_{\sigma(j)}^t)^{\omega_j}}{\prod_{j=1}^k (1 + \tilde{m}_{\sigma(j)}^t)^{\omega_j} + \prod_{j=1}^k (1 - \tilde{m}_{\sigma(j)}^t)^{\omega_j}}}, \sqrt[t]{\frac{2 \left( \prod_{j=1}^k (1 - \tilde{m}_{\sigma(j)}^t)^{\omega_j} - \prod_{j=1}^k (1 - \tilde{m}_{\sigma(j)}^t - n_{\sigma(j)}^t)^{\omega_j} \right)}{\prod_{j=1}^k (1 + \tilde{m}_{\sigma(j)}^t)^{\omega_j} + \prod_{j=1}^k (1 - \tilde{m}_{\sigma(j)}^t)^{\omega_j}}} \right). \quad (42)$$

- (4) For  $t = 2$  and  $i = 0$ , equation (31) reduces to PyF Einstein hybrid interaction averaging operators (PyFEHIA operators), i.e.,

$$PyFEHIA_{w,\omega}(\tilde{P}_1, \tilde{P}_2, \dots, \tilde{P}_k) = \left( \sqrt{\frac{\prod_{j=1}^k (1 + \tilde{m}_{\sigma(j)}^2)^{\omega_j} - \prod_{j=1}^k (1 - \tilde{m}_{\sigma(j)}^2)^{\omega_j}}{\prod_{j=1}^k (1 + \tilde{m}_{\sigma(j)}^2)^{\omega_j} + \prod_{j=1}^k (1 - \tilde{m}_{\sigma(j)}^2)^{\omega_j}}}, \sqrt{\frac{2 \left( \prod_{j=1}^k (1 - \tilde{m}_{\sigma(j)}^2)^{\omega_j} - \prod_{j=1}^k (1 - \tilde{m}_{\sigma(j)}^2 - \tilde{n}_{\sigma(j)}^2)^{\omega_j} \right)}{\prod_{j=1}^k (1 + \tilde{m}_{\sigma(j)}^2)^{\omega_j} + \prod_{j=1}^k (1 - \tilde{m}_{\sigma(j)}^2)^{\omega_j}}} \right). \quad (43)$$

- (5) For  $t = 1$  and  $i = 0$ , equation (31) reduces to IF Einstein hybrid interaction averaging operators (IFEHA operators), i.e.,

$$\text{IFEHA}_{w,\omega}(\tilde{P}_1, \tilde{P}_2, \dots, \tilde{P}_k) = \left( \frac{\prod_{j=1}^k (1 + \tilde{m}_{\sigma(j)})^{\omega_j} - \prod_{j=1}^k (1 - \tilde{m}_{\sigma(j)})^{\omega_j}}{\prod_{j=1}^k (1 + \tilde{m}_{\sigma(j)})^{\omega_j} + \prod_{j=1}^k (1 - \tilde{m}_{\sigma(j)})^{\omega_j}}, \frac{2(\prod_{j=1}^k (1 - \tilde{m}_{\sigma(j)})^{\omega_j} - \prod_{j=1}^k (1 - \tilde{m}_{\sigma(j)} - \tilde{n}_{\sigma(j)})^{\omega_j})}{\prod_{j=1}^k (1 + \tilde{m}_{\sigma(j)})^{\omega_j} + \prod_{j=1}^k (1 - \tilde{m}_{\sigma(j)})^{\omega_j}} \right). \quad (44)$$

Similarly, we can reduce T-SFEWIA operator, T-SFEOWIA operator, T-SFEWIG operator, T-SFEOWIG operator, and T-SFEHIG operator.

The proposed aggregation operators can aggregate the data given in FS, IFS, PyFS, q-ROPFS, PFS, and spherical fuzzy set environments, but the converse is not possible. Here, with the help of an example, it is proved that the proposed aggregation operator can aggregate the data given in IFSs.

**Example 4.** Let IFNs  $P_1 = (0.2, 0.5)$ ,  $P_2 = (0.7, 0.1)$ ,  $P_3 = (0.3, 0.4)$ ,  $P_4 = (0.6, 0.2)$ , and  $P_5 = (0.5, 0.5)$  with a weight vector  $w = (0.25, 0.20, 0.15, 0.18, 0.22)^T$ .

**Solution 1.** We can write these IFNs in the form of T-SFNs as  $P_1 = (0.2, 0, 0.5)$ ,  $P_2 = (0.7, 0, 0.1)$ ,  $P_3 = (0.3, 0, 0.4)$ ,  $P_4 = (0.6, 0, 0.2)$ , and  $P_5 = (0.5, 0, 0.5)$ . Then, by using the T-SFEWIA operator, we shall be able to find these values:

$$\begin{aligned} P_1 &= (0.2481, 0, 0.5312), \\ P_2 &= (0.7, 0, 0.1), \\ P_3 &= (0.2281, 0, 0.3630), \\ P_4 &= (0.5538, 0, 0.2071), \\ P_5 &= (0.5401, 0, 0.4599). \end{aligned} \quad (45)$$

Their scores values will be

$$\begin{aligned} SC(P_1) &= -0.2831, \\ SC(P_2) &= 0.6, \\ SC(P_3) &= -0.1350, \\ SC(P_4) &= 0.3467, \\ SC(P_5) &= 0.0801. \end{aligned} \quad (46)$$

Now, using the score value, the aggregated values obtained by using T-SFEWIA operators are rearranged in descending order. Then, these ordered values are again aggregated by using the T-SFEHIA operator with the associated weight vector being  $\omega = (0.112, 0.236, 0.304, 0.236, 0.112)$ :

$$\begin{aligned} \tilde{P}_{\sigma(1)} &= (0.7, 0, 0.1), \\ \tilde{P}_{\sigma(2)} &= (0.5538, 0, 0.2071), \\ \tilde{P}_{\sigma(3)} &= (0.5401, 0, 0.4599), \\ \tilde{P}_{\sigma(4)} &= (0.2281, 0, 0.3630), \\ \tilde{P}_{\sigma(5)} &= (0.2481, 0, 0.5312). \end{aligned} \quad (47)$$

Now, utilize the T-SFEHIA operator as follows:

$$T-SFEHIA_{w,\omega}(\tilde{P}_1, \tilde{P}_2, \dots, \tilde{P}_5) = (0.4709, 0, 0.2645). \quad (48)$$

Here, it is proved that the information given in IFNs can be solved by using the T-SFEHIA operator. Similarly, we can solve the information given in IFNs by using the T-SEHIG operator and the information given in any other fuzzy structure can also be aggregated using the proposed operators.

## 7. An Algorithm for MADM with T-Spherical Fuzzy Information

Consider a set of alternatives  $D = \{d_1, d_2, d_3, \dots, d_l\}$  and a set of attributes  $M = \{m_1, m_2, m_3, \dots, m_k\}$  having a weight vector  $w = \{w_1, w_2, w_3, \dots, w_l\}$ , where  $w_j \in [0, 1]$  and  $\sum_{m=1}^l w_m = 1$ . For making a decision, we have to follow these steps:

**Step 1.** Calculate  $t$  for which the values lie in T-spherical information

**Step 2.** Aggregate the given alternatives according to attributes by T-SFEWIA (or T-SFEWIG) operators using some weight vectors

**Step 3.** Find scores values and with the help of score value, we reorder them in descending order

**Step 4.** Aggregate these ordered values using T-SFEHIA (or T-SFEHIG) operator

**Step 5.** Using score values find out the best option

**Example 3.** The board of governors of a company decided to reduce their expenses for maximizing the profit. They observe that the cost of electricity is one of the major expense and they can reduce it if they started to generate electricity using solar energy. They have three options of photovoltaic cells that they may use in their solar plant:

TABLE 1: Decision matrix.

	$M_1$	$M_2$	$M_3$	$M_4$	$M_5$
$d_1$	(0.4, 0.1, 0.7)	(0.5, 0.2, 0.4)	(0.8, 0.3, 0.7)	(0.4, 0.8, 0.5)	(0.9, 0.5, 0.2)
$d_2$	(0.7, 0.4, 0.3)	(0.2, 0.4, 0.7)	(0.9, 0.3, 0.6)	(0.3, 0.2, 0.8)	(0.4, 0.7, 0.5)
$d_3$	(0.4, 0.7, 0.5)	(0.6, 0.6, 0.1)	(0.6, 0.9, 0.2)	(0.8, 0.1, 0.1)	(0.5, 0.6, 0.2)

TABLE 2: Aggregated values.

	$M_1$	$M_2$	$M_3$	$M_4$	$M_5$
$d_1$	$\begin{pmatrix} 0.4308, \\ 0.1077, \\ 0.7367 \end{pmatrix}$	$\begin{pmatrix} 0.5, \\ 0.2, \\ 0.4 \end{pmatrix}$	$\begin{pmatrix} 0.7370, \\ 0.2726, \\ 0.7172 \end{pmatrix}$	$\begin{pmatrix} 0.3862, \\ 0.7770, \\ 0.5022 \end{pmatrix}$	$\begin{pmatrix} 0.9164, \\ 0.5160, \\ 0.1906 \end{pmatrix}$
$d_2$	$\begin{pmatrix} 0.4308, \\ 0.4308, \\ 0.3061 \end{pmatrix}$	$\begin{pmatrix} 0.2, \\ 0.4, \\ 0.7 \end{pmatrix}$	$\begin{pmatrix} 0.8440, \\ 0.2726, \\ 0.6677 \end{pmatrix}$	$\begin{pmatrix} 0.2896, \\ 0.1931, \\ 0.7820 \end{pmatrix}$	$\begin{pmatrix} 0.4129, \\ 0.7206, \\ 0.5037 \end{pmatrix}$
$d_3$	$\begin{pmatrix} 0.4308, \\ 0.7485, \\ 0.5064 \end{pmatrix}$	$\begin{pmatrix} 0.6, \\ 0.6, \\ 0.1 \end{pmatrix}$	$\begin{pmatrix} 0.5464, \\ 0.8440, \\ 0.2430 \end{pmatrix}$	$\begin{pmatrix} 0.7770, \\ 0.0965, \\ 0.0829 \end{pmatrix}$	$\begin{pmatrix} 0.5160, \\ 0.6187, \\ 0.2031 \end{pmatrix}$

- (i)  $d_1$ : monocrystalline photovoltaic cell
- (ii)  $d_2$ : polycrystalline photovoltaic cell
- (iii)  $d_3$ : thin Film photovoltaic cell

They assess the given photovoltaic cell on the basis of the following attributes.

- (i)  $M_1$ : heat tolerance
- (ii)  $M_2$ : cost
- (iii)  $M_3$ : reliability
- (iv)  $M_4$ : efficiency
- (v)  $M_5$ : ability of charge separation

*Step 1.* As  $0.8 + 0.3 + 0.7 = 1.8 \notin [0, 1]$ ,  $0.8^2 + 0.3^2 + 0.7^2 = 1.22 \notin [0, 1]$  and  $0.8^3 + 0.3^3 + 0.7^3 = 0.882 \in [0, 1]$ . Similarly, we found that all values in Table 1 belong to  $[0, 1]$  for  $t = 3$ .

*Step 2.* By taking  $w = (0.25, 0.20, 0.15, 0.18, 0.22)^T$ , we find T-SFEWIA values of given data, as listed in Table 2.

*Step 3.* Scores of each alternative with respect to all attributes are shown in Table 3.

By comparing the score values, we have

$$\begin{aligned}
 &SC(P_{15}) > SC(P_{12}) > SC(P_{13}) > SC(P_{14}) > SC(P_{11}), \\
 &SC(P_{21}) > SC(P_{23}) > SC(P_{25}) > SC(P_{22}) > SC(P_{24}), \\
 &SC(P_{34}) > SC(P_{32}) > SC(P_{33}) > SC(P_{35}) > SC(P_{31}).
 \end{aligned} \tag{49}$$

Based on above score analysis, the data are arranged in descending order and the aggregated values of ordered data are as listed in Table 4.

*Step 4.* The associated weight vector will be  $\omega = (0.112, 0.236, 0.304, 0.236, 0.112)^T$ , and by using T-SFEHA operators, we have

$$\begin{aligned}
 \tilde{P}_1 &= (0.6596, 0.5227, 0.4668), \\
 \tilde{P}_2 &= (0.6176, 0.5291, 0.5276), \\
 \tilde{P}_3 &= (0.5826, 0.7075, 0.2290).
 \end{aligned} \tag{50}$$

*Step 5.* Now, we have to find the score values:

$$\begin{aligned}
 SC(\tilde{P}_1) &= 0.1853, \\
 SC(\tilde{P}_2) &= 0.0887, \\
 SC(\tilde{P}_3) &= 0.1858, \\
 SC(\tilde{P}_3) &> SC(\tilde{P}_1) > SC(\tilde{P}_2).
 \end{aligned} \tag{51}$$

Since the score value of  $d_3$  is highest, the thin film photovoltaic cell is the best option.

Now, we check their validity by using Einstein hybrid geometric interaction operators.

By taking  $w = (0.25, 0.20, 0.15, 0.18, 0.22)^T$ , we find T-SFEWG values of given data, as listed in Table 5.

Scores of each alternative with respect to all attributes are shown in Table 6.

By comparing the score values, we have

$$\begin{aligned}
 &SC(P_{15}) > SC(P_{13}) > SC(P_{12}) > SC(P_{14}) > SC(P_{11}), \\
 &SC(P_{23}) > SC(P_{21}) > SC(P_{25}) > SC(P_{22}) > SC(P_{24}), \\
 &SC(P_{34}) > SC(P_{33}) > SC(P_{32}) > SC(P_{35}) > SC(P_{31}).
 \end{aligned} \tag{52}$$

TABLE 3: Score values.

	$M_1$	$M_2$	$M_3$	$M_4$	$M_5$
$d_1$	-0.3199	0.0610	0.0314	-0.0690	0.7626
$d_2$	0.3906	-0.3350	0.3035	-0.4538	-0.0574
$d_3$	-0.0499	0.2150	0.1488	0.4685	0.1290

TABLE 4: Ordered aggregated values.

	$M_1$	$M_2$	$M_3$	$M_4$	$M_5$
$d_1$	$\begin{pmatrix} 0.9164, \\ 0.5160, \\ 0.1906 \end{pmatrix}$	$\begin{pmatrix} 0.5, \\ 0.2, \\ 0.4 \end{pmatrix}$	$\begin{pmatrix} 0.7370, \\ 0.2726, \\ 0.7172 \end{pmatrix}$	$\begin{pmatrix} 0.3862, \\ 0.7770, \\ 0.5022 \end{pmatrix}$	$\begin{pmatrix} 0.4308, \\ 0.1077, \\ 0.7367 \end{pmatrix}$
$d_2$	$\begin{pmatrix} 0.7485, \\ 0.4308, \\ 0.3061 \end{pmatrix}$	$\begin{pmatrix} 0.8440, \\ 0.2726, \\ 0.6677 \end{pmatrix}$	$\begin{pmatrix} 0.4129, \\ 0.7206, \\ 0.5037 \end{pmatrix}$	$\begin{pmatrix} 0.2, \\ 0.4, \\ 0.7 \end{pmatrix}$	$\begin{pmatrix} 0.2896, \\ 0.1931, \\ 0.7820 \end{pmatrix}$
$d_3$	$\begin{pmatrix} 0.7770, \\ 0.0965, \\ 0.0829 \end{pmatrix}$	$\begin{pmatrix} 0.6, \\ 0.6, \\ 0.1 \end{pmatrix}$	$\begin{pmatrix} 0.5464, \\ 0.8440, \\ 0.2430 \end{pmatrix}$	$\begin{pmatrix} 0.5160, \\ 0.6187, \\ 0.2031 \end{pmatrix}$	$\begin{pmatrix} 0.4308, \\ 0.7485, \\ 0.5064 \end{pmatrix}$

TABLE 5: Aggregated values.

	$M_1$	$M_2$	$M_3$	$M_4$	$M_5$
$d_1$	$\begin{pmatrix} 0.4117, \\ 0.1077, \\ 0.7485 \end{pmatrix}$	$\begin{pmatrix} 0.5, \\ 0.2, \\ 0.4 \end{pmatrix}$	$\begin{pmatrix} 0.7998, \\ 0.2726, \\ 0.6398 \end{pmatrix}$	$\begin{pmatrix} 0.4008, \\ 0.7770, \\ 0.4829 \end{pmatrix}$	$\begin{pmatrix} 0.9051, \\ 0.5160, \\ 0.2064 \end{pmatrix}$
$d_2$	$\begin{pmatrix} 0.7347, \\ 0.4308, \\ 0.3232 \end{pmatrix}$	$\begin{pmatrix} 0.2, \\ 0.4, \\ 0.7 \end{pmatrix}$	$\begin{pmatrix} 0.9071, \\ 0.2726, \\ 0.5464 \end{pmatrix}$	$\begin{pmatrix} 0.2984, \\ 0.1931, \\ 0.7770 \end{pmatrix}$	$\begin{pmatrix} 0.4034, \\ 0.7206, \\ 0.5160 \end{pmatrix}$
$d_3$	$\begin{pmatrix} 0.4064, \\ 0.7485, \\ 0.5381 \end{pmatrix}$	$\begin{pmatrix} 0.6, \\ 0.6, \\ 0.1 \end{pmatrix}$	$\begin{pmatrix} 0.6434, \\ 0.8440, \\ 0.1817 \end{pmatrix}$	$\begin{pmatrix} 0.7807, \\ 0.0965, \\ 0.0965 \end{pmatrix}$	$\begin{pmatrix} 0.5103, \\ 0.6187, \\ 0.2064 \end{pmatrix}$

TABLE 6: Score values.

	$M_1$	$M_2$	$M_3$	$M_4$	$M_5$
$d_1$	-0.3495	0.0610	0.2497	-0.0482	0.7327
$d_2$	0.3628	-0.3350	0.5833	-0.4425	-0.0717
$d_3$	-0.0887	0.2150	0.2603	0.4749	0.1241

TABLE 7: Ordered aggregated values.

	$M_1$	$M_2$	$M_3$	$M_4$	$M_5$
$d_1$	$\begin{pmatrix} 0.9051, \\ 0.5160, \\ 0.2064 \end{pmatrix}$	$\begin{pmatrix} 0.7998, \\ 0.2726, \\ 0.6398 \end{pmatrix}$	$\begin{pmatrix} 0.5, \\ 0.2, \\ 0.4 \end{pmatrix}$	$\begin{pmatrix} 0.4008, \\ 0.7770, \\ 0.4829 \end{pmatrix}$	$\begin{pmatrix} 0.4117, \\ 0.1077, \\ 0.7485 \end{pmatrix}$
$d_2$	$\begin{pmatrix} 0.9071, \\ 0.2726, \\ 0.5464 \end{pmatrix}$	$\begin{pmatrix} 0.7347, \\ 0.4308, \\ 0.3232 \end{pmatrix}$	$\begin{pmatrix} 0.4034, \\ 0.7206, \\ 0.5160 \end{pmatrix}$	$\begin{pmatrix} 0.2, \\ 0.4, \\ 0.7 \end{pmatrix}$	$\begin{pmatrix} 0.2984, \\ 0.1931, \\ 0.7770 \end{pmatrix}$
$d_3$	$\begin{pmatrix} 0.7807, \\ 0.0965, \\ 0.0965 \end{pmatrix}$	$\begin{pmatrix} 0.6434, \\ 0.8440, \\ 0.1817 \end{pmatrix}$	$\begin{pmatrix} 0.6, \\ 0.6, \\ 0.1 \end{pmatrix}$	$\begin{pmatrix} 0.5103, \\ 0.6187, \\ 0.2064 \end{pmatrix}$	$\begin{pmatrix} 0.4064, \\ 0.7485, \\ 0.5381 \end{pmatrix}$



Based on the above score analysis, the data are arranged in descending order and the aggregated values of ordered data are as listed in Table 7.

Associated weight vector will be  $\omega = (0.112, 0.236, 0.304, 0.236, 0.112)^T$ , and by using T-SFEHG operators, we have

$$\begin{aligned}\tilde{P}_1 &= (0.5445, 0.5217, 0.5419), \\ \tilde{P}_2 &= (0.6830, 0.5376, 0.5913), \\ \tilde{P}_3 &= (0.7556, 0.6879, 0.2780).\end{aligned}\quad (53)$$

Step 6. Now, we have to find the score values:

$$\begin{aligned}SC(\tilde{P}_1) &= 0.0023, \\ SC(\tilde{P}_2) &= 0.1080, \\ SC(\tilde{P}_3) &= 0.4099, \\ SC(\tilde{P}_3) &> SC(\tilde{P}_2) > SC(\tilde{P}_1).\end{aligned}\quad (54)$$

Here again, the score value of alternative  $d_3$  is high. So, the thin film photovoltaic cell is the best option.

## 8. Conclusion

In this paper, it is pointed out that the existing work [14, 42] fails under some conditions such as in Einstein averaging operators, if one nonmembership value of an IFN is zero, then the NMD of aggregated value will also become zero and neglect the other nonmembership values. Similarly, if the membership value of one IFN becomes zero, then the MD of the aggregated value of the Einstein geometric operator will also become zero and neglect the other membership values. So, new interactive operational laws are proposed in this article. On the basis of these operational laws, T-spherical Einstein interactive geometric operators and T-spherical Einstein interactive averaging operators are proposed. After that, some conditions are discussed under which the proposed operators can reduce to other fuzzy frameworks. A comparison of proposed and existing work is also established and explained using an example. We validate the proposed operators with the help of an application in MADM. In the future, we have a plan to propose some power aggregation operations for T-spherical fuzzy sets and try to use them in the MADM process.

## Data Availability

The data used in this article are artificial and hypothetical, and anyone can use these data before prior permission by just citing this article.

## Conflicts of Interest

The authors declare that they have no conflicts of interest.

## Acknowledgments

This paper was supported by Major Humanities and Social Sciences Research Projects in Zhejiang Universities (no. 2018QN058), China Postdoctoral Science Foundation (no. 2019M651403), Zhejiang Province Natural Science Foundation (no. LY18G010007), and Ningbo Province Natural Science Foundation (no. 2019A610037) and the Fundamental Research Funds for the Provincial Universities of Zhejiang.

## References

- [1] L. A. Zadeh, "Fuzzy sets," *Information and Control*, vol. 8, no. 3, pp. 338–353, 1965.
- [2] K. T. Atanassov, "Intuitionistic fuzzy sets," *Fuzzy Sets and Systems*, vol. 20, no. 1, pp. 87–96, 1986.
- [3] K. T. Atanassov, *Intuitionistic Fuzzy Sets*, Springer-Verlag, Heidelberg, Germany, 1999.
- [4] R. R. Yager, "Pythagorean fuzzy subsets," in *Proceedings of the 2013 Joint IFSA World Congress and NAFIPS Annual Meeting (IFSA/NAFIPS)*, Edmonton, AB, Canada, June 2013.
- [5] R. R. Yager, "Pythagorean membership grades in multicriteria decision making," *IEEE Transactions on Fuzzy Systems*, vol. 22, no. 4, pp. 958–965, 2014.
- [6] R. R. Yager, "Generalized orthopair fuzzy sets," *IEEE Transactions on Fuzzy Systems*, vol. 25, no. 5, pp. 1222–1230, 2017.
- [7] B. C. Cùròng, "Picture fuzzy sets," *Journal of Computer Science and Cybernetics*, vol. 30, no. 4, p. 409, 2015.
- [8] T. Mahmood, K. Ullah, Q. Khan, and N. Jan, "An approach toward decision-making and medical diagnosis problems using the concept of spherical fuzzy sets," *Neural Computing and Applications*, vol. 31, no. 11, pp. 7041–7053, 2018.
- [9] Z. Xu and R. R. Yager, "Some geometric aggregation operators based on intuitionistic fuzzy sets," *International Journal of General Systems*, vol. 35, no. 4, pp. 417–433, 2006.
- [10] S. Zeng, W. Su, and C. Zhang, "Intuitionistic fuzzy generalized probabilistic ordered weighted averaging operator and its application to group decision making," *Technological and Economic Development of Economy*, vol. 22, no. 2, pp. 177–193, 2015.
- [11] H. Garg, "Some robust improved geometric aggregation operators under interval-valued intuitionistic fuzzy environment for multi-criteria decision-making process," *Journal of Industrial & Management Optimization*, vol. 14, no. 1, pp. 283–308, 2018.
- [12] C. Zhang, C. Chen, D. Streimikiene, and T. Balezentis, "Intuitionistic fuzzy MULTIMOORA approach for multi-criteria assessment of the energy storage technologies," *Applied Soft Computing*, vol. 79, pp. 410–423, 2019.
- [13] Y. He, H. Chen, L. Zhou, J. Liu, and Z. Tao, "Intuitionistic fuzzy geometric interaction averaging operators and their application to multi-criteria decision making," *Information Sciences*, vol. 259, pp. 142–159, 2014.
- [14] X. Zhao and G. Wei, "Some intuitionistic fuzzy Einstein hybrid aggregation operators and their application to multiple attribute decision making," *Knowledge-Based Systems*, vol. 37, pp. 472–479, 2013.
- [15] Z. Mu, S. Zeng, and Q. Liu, "Some interval-valued intuitionistic fuzzy Zhenyuan aggregation operators and their application to multi-attribute decision making," *International*

- Journal of Uncertainty, Fuzziness and Knowledge-Based Systems*, vol. 26, no. 4, pp. 633–653, 2018.
- [16] S. Zeng, S.-M. Chen, and K.-Y. Fan, "Interval-valued intuitionistic fuzzy multiple attribute decision making based on nonlinear programming methodology and TOPSIS method," *Information Sciences*, vol. 506, pp. 424–442, 2020.
  - [17] S. Zeng, S.-M. Chen, and L.-W. Kuo, "Multiattribute decision making based on novel score function of intuitionistic fuzzy values and modified VIKOR method," *Information Sciences*, vol. 488, pp. 76–92, 2019.
  - [18] P. Wang and P. Liu, "Some Maclaurin symmetric mean aggregation operators based on Schweizer-Sklar operations for intuitionistic fuzzy numbers and their application to decision making," *Journal of Intelligent & Fuzzy Systems*, vol. 36, no. 4, pp. 3801–3824, 2019.
  - [19] H. Garg, "A new generalized Pythagorean fuzzy information aggregation using Einstein operations and its application to decision making," *International Journal of Intelligent Systems*, vol. 31, no. 9, pp. 886–920, 2016.
  - [20] G. Wei and M. Lu, "Pythagorean fuzzy power aggregation operators in multiple attribute decision making," *International Journal of Intelligent Systems*, vol. 33, no. 1, pp. 169–186, 2018.
  - [21] Z. Yang and J. Chang, "Interval-valued Pythagorean normal fuzzy information aggregation operators for multi-attribute decision making," *IEEE Access*, vol. 8, pp. 51295–51314, 2020.
  - [22] S. Zeng, Z. Mu, and T. Baležentis, "A novel aggregation method for Pythagorean fuzzy multiple attribute group decision making," *International Journal of Intelligent Systems*, vol. 33, no. 3, pp. 573–585, 2018.
  - [23] S. Zeng, X. Peng, T. Baležentis, and D. Streimikiene, "Prioritization of low-carbon suppliers based on Pythagorean fuzzy group decision making with self-confidence level," *Economic Research-Ekonomska Istraživanja*, vol. 32, no. 1, pp. 1073–1087, 2019.
  - [24] S. Zeng, "Pythagorean fuzzy multiattribute group decision making with probabilistic information and OWA approach," *International Journal of Intelligent Systems*, vol. 32, no. 11, pp. 1136–1150, 2017.
  - [25] K. Ullah, T. Mahmood, Z. Ali, and N. Jan, "On some distance measures of complex Pythagorean fuzzy sets and their applications in pattern recognition," *Complex and Intelligent Systems*, vol. 6, no. 1, pp. 15–27, 2020.
  - [26] X. Peng, J. Dai, and H. Garg, "Exponential operation and aggregation operator for q-rung orthopair fuzzy set and their decision-making method with a new score function," *International Journal of Intelligent Systems*, vol. 33, no. 11, pp. 2255–2282, 2018.
  - [27] Z. Yang, T. Ouyang, X. Fu, and X. Peng, "A decision-making algorithm for online shopping using deep-learning-based opinion pairs mining and q-rung orthopair fuzzy interaction Heronian mean operators," *International Journal of Intelligent Systems*, vol. 35, no. 5, pp. 783–825, 2020.
  - [28] Z. L. Yang, H. Garg, J. Li, G. Srivastava, and Z. Cao, "Investigation of multiple heterogeneous relationships using a q-rung orthopair fuzzy multi-criteria decision algorithm," *Neural Computing and Applications*, pp. 1–22. In press, 2020.
  - [29] A. Hussain, A. M. Irfan, and T. Mahmood, "Covering based q-rung orthopair fuzzy rough set model hybrid with TOPSIS for multi-attribute decision making," *Journal of Intelligent and Fuzzy Systems*, vol. 37, no. 1, pp. 981–993, 2019.
  - [30] A. Hussain, M. I. Ali, T. Mahmood, and M. Munir, "q-Rung orthopair fuzzy soft average aggregation operators and their application in multicriteria decision-making," *International Journal of Intelligent Systems*, vol. 35, no. 4, pp. 571–599, 2020.
  - [31] Z. Yang, X. Li, Z. Cao, and J. Li, "q-Rung orthopair normal fuzzy aggregation operators and their application in multi-attribute decision-making," *Mathematics*, vol. 7, no. 12, p. 1142, 2019.
  - [32] H. Garg, J. Gwak, T. Mahmood, and Z. Ali, "Power aggregation operators and VIKOR methods for complex q-rung orthopair fuzzy sets and their applications," *Mathematics*, vol. 8, no. 4, p. 538, 2020.
  - [33] P. Liu, Z. Ali, and T. Mahmood, "A method to multi-attribute group decision-making problem with complex q-rung orthopair linguistic information based on heronian mean operators," *International Journal of Computational Intelligence Systems*, vol. 12, no. 2, pp. 1465–1496, 2019.
  - [34] G. Wei, "Picture fuzzy Hamacher aggregation operators and their application to multiple attribute decision making," *Fundamenta Informaticae*, vol. 157, no. 3, pp. 271–320, 2018.
  - [35] S. Khan, S. Abdullah, L. Abdullah, and S. Ashraf, "Logarithmic aggregation operators of picture fuzzy numbers for multi-attribute decision making problems," *Mathematics*, vol. 7, no. 7, p. 608, 2019.
  - [36] P. Liu, M. Munir, T. Mahmood, and K. Ullah, "Some similarity measures for interval-valued picture fuzzy sets and their applications in decision making," *Information*, vol. 10, no. 12, p. 369, 2019.
  - [37] S. Zeng, S. Ashraf, M. Arif, and S. Abdullah, "Application of exponential jensen picture fuzzy divergence measure in multi-criteria group decision making," *Mathematics*, vol. 7, no. 2, p. 191, 2019.
  - [38] S. Zeng, D. Luo, C. Zhang, and X. Li, "A correlation-based TOPSIS method for multiple attribute decision making with single-valued neutrosophic information," *International Journal of Information Technology & Decision Making*, vol. 19, no. 1, pp. 343–358, 2020.
  - [39] S. G. Quek, G. Selvachandran, M. Munir et al., "Multi-attribute multi-perception decision-making based on generalized T-spherical fuzzy weighted aggregation operators on neutrosophic sets," *Mathematics*, vol. 7, no. 9, p. 780, 2019.
  - [40] H. Garg, M. Munir, K. Ullah, T. Mahmood, and N. Jan, "Algorithm for T-spherical fuzzy multi-attribute decision making based on improved interactive aggregation operators," *Symmetry*, vol. 10, no. 12, p. 670, 2018.
  - [41] S. Zeng, H. Garg, M. Munir, T. Mahmood, and A. Hussain, "A multi-attribute decision making process with immediate probabilistic interactive averaging aggregation operators of T-spherical fuzzy sets and its application in the selection of solar cells," *Energies*, vol. 12, no. 23, p. 4436, 2019.
  - [42] M. Munir, H. Kalsoom, K. Ullah, T. Mahmood, and Y.-M. Chu, "T-spherical fuzzy Einstein hybrid aggregation operators and their applications in multi-attribute decision making problems," *Symmetry*, vol. 12, no. 3, p. 365, 2020.
  - [43] S. Zeng, A. Hussain, T. Mahmood, M. Irfan Ali, S. Ashraf, and M. Munir, "Covering-based spherical fuzzy rough set model hybrid with TOPSIS for multi-attribute decision-making," *Symmetry*, vol. 11, no. 4, p. 547, 2019.
  - [44] P. Liu, Q. Khan, T. Mahmood, and N. Hassan, "T-spherical fuzzy power Muirhead mean operator based on novel operational laws and their application in multi-attribute group decision making," *IEEE Access*, vol. 7, pp. 22613–22632, 2019.
  - [45] M. Q. Wu, T. Y. Chen, and J. P. Fan, "Divergence measure of T-spherical fuzzy sets and its applications in pattern recognition," *IEEE Access*, vol. 8, pp. 10208–10221, 2020.
  - [46] K. Ullah, H. Garg, T. Mahmood, N. Jan, and Z. Ali, "Correlation coefficients for T-spherical fuzzy sets and their applications in clustering and multi-attribute decision making," *Soft Computing*, vol. 24, no. 3, pp. 1647–1659, 2020.

## Research Article

# A Model of High-Dimensional Feature Reduction Based on Variable Precision Rough Set and Genetic Algorithm in Medical Image

Zhou Tao <sup>1,2</sup>, Lu Huiling <sup>2</sup>, Fuyuan Hu <sup>3</sup>, Shi Qiu <sup>4</sup>, and Wu Cuiying<sup>5</sup>

<sup>1</sup>School of Computer Science and Engineering, North Minzu University, Yinchuan 750021, China

<sup>2</sup>School of Science, Ningxia Medical University, Yinchuan 750004, China

<sup>3</sup>School of Electronic & Information Engineering, Suzhou University of Science and Technology, Suzhou 215009, China

<sup>4</sup>Key Laboratory of Spectral Imaging Technology CAS, Xi'an Institute of Optics and Precision Mechanics, Chinese Academy of Sciences, Xi'an 710119, China

<sup>5</sup>Human Resources Department, The Second Affiliated Hospital of Xiamen Medical College, Xiamen 361021, China

Correspondence should be addressed to Lu Huiling; [lu\\_huiling@163.com](mailto:lu_huiling@163.com)

Received 29 March 2020; Accepted 20 April 2020; Published 30 May 2020

Guest Editor: Zaoli Yang

Copyright © 2020 Zhou Tao et al. This is an open access article distributed under the Creative Commons Attribution License, which permits unrestricted use, distribution, and reproduction in any medium, provided the original work is properly cited.

Aiming at the shortcomings of high feature reduction using traditional rough sets, such as insensitivity with noise data and easy loss of potentially useful information, combining with genetic algorithm, in this paper, a VPRS-GA (Variable Precision Rough Set--Genetic Algorithm) model for high-dimensional feature reduction of medical image is proposed. Firstly, rigid inclusion of the lower approximation is extended to partial inclusion by classification error rate  $\beta$  in the traditional rough set model, and the ability dealing with noise data is improved. Secondly, some factors of feature reduction are considered, such as attribute dependency, attributes reduction length, and gene coding weight. A general framework of fitness function is put forward, and different fitness functions are constructed by using different factors such as weight and classification error rate  $\beta$ . Finally, 98 dimensional features of PET/CT lung tumor ROI are extracted to build decision information table of lung tumor patients. Three kinds of experiments in high-dimensional feature reduction are carried out, using support vector machine to verify the influence of recognition accuracy in different fitness function parameters and classification error rate. Experimental results show that classification accuracy is affected deeply by different weight values under the invariable classification error rate condition and by increasing classification error rate under the invariable weigh value condition. Hence, in order to achieve better recognition accuracy, different problems use suitable parameter combination.

## 1. Introduction

Rough set theory was developed by Pawlak in 1982 [1], and it is a mathematical tool to deal with vagueness and uncertainty. The classification ability unchanged in its main idea, decision or classification rules of problem are derived by knowledge reduction [2]. The Variable Precision Rough Set (VPRS) theory, proposed by Ziarko, and is an extension of original rough set model. For inconsistent information system, the VPRS model allows a flexible approximation boundary region by a precision variable  $\beta$  [3]. When  $\beta = 0$ , Pawlak rough set model is a special case of variable precision

rough set model. The main task of variable precision rough set model is to solve the problem of data classification with no function or uncertainty. The hierarchical model of attribute reduction for variable precision rough set is studied by Xiaowei [4]. There is abnormal phenomenon in existing attribute reduction models; therefore, a variable precision rough set attribute reduction algorithm with the property of interval is proposed, and the reduction abnormal problem is transformed into a hierarchical model representation, and the reduction anomaly is gradually eliminated by the layer-by-layer reduction model; Jie and Jiayang [5] puts forward that there may be a reduction



jump phenomenon in variable precision rough set feature reduction, which affects the quality of reduction and brings the problem of attribute reduction of variable precision rough set; Pei and Qinghua [6] proposes an FCM clustering algorithm based on variable precision rough set; according to the threshold characteristics of the variable precision rough set model, the algorithm divides the objects in the edge of the cluster into the positive, negative, and boundary regions, to improve the accuracy of clustering. Two different solutions of variable precision rough set attribute reduction algorithm are proposed by Hao and Junan [7]; based on tolerance matrix and minimal reduction of attribute core, the attribute kernel idea of variable precision rough set is proposed. The experimental results show that the two algorithms can reduce the search space and improve the efficiency of the algorithm.

Feature reduction is one of the core contents of rough set theory; in the condition of keeping the classification ability for knowledge base unchanged, we delete irrelevant or unimportant knowledge, which can reduce the dimension of the decision system, reduce the time complexity, and improve the efficiency of the algorithm [8]. People want to find the minimum reduction, but it has been proved to be an NP-Hard problem [9]; the main research is how to find the second optimal solution. Genetic algorithm is a computational model which is based on the natural selection and evolution mechanism; its core idea is inspired by the natural selection rule of the survival of the fittest, can achieve a highly parallel, random, and adaptive search, is not easy to fall into local optimal [10], can find the global optimal solution with high probability, and has great advantage in solving the NP-Hard problem.

In this paper, a new algorithm of PET/CT high-dimensional feature selection is proposed based on genetic algorithm and variable precision rough set model. On one hand, the algorithm considers the value of chromosome coding, the minimum number of attributes, and the dependency of attributes to construct a general fitness function framework and adjusting weight coefficient of each factor to achieve different fitness function; on the other hand, aiming at the limitation of Pawlak rough set model, introducing the classification error rate of  $\beta$ , it extends rigid inclusion of the lower approximation for traditional rough set to partial inclusion, not only improving the concept of approximate space, but also enhancing the ability to deal with noise data and changing the range of  $\beta$  to achieve different fitness function. Finally, through extracting PET/CT lung cancer ROI 98-dimensional feature to construct the information decision table of lung cancer patients, 8 group experiments of high-dimensional features selection are done by using support vector machine to classify and recognize reduction subsets, to verify the degree of influence on the different weights and different classification error rate, and find a set of parameters suitable for this problem ( $\omega_1 = 1, \omega_2 = 1, \omega_3 = 0; \beta = 0.6$ ). The experimental results show that different parameters can be used to get different experimental results, so we should choose the appropriate parameter combination according to different problems so as to get better recognition accuracy.

## 2. Materials and Methods

**2.1. PET/CT.** PET/CT is a kind of advanced medical imaging technology, which is a combination of the good performance of PET and CT on the same device, and provides the anatomical and functional metabolism of the subjects under the same conditions [11]. PET is a functional image; it can provide metabolic information of tissue and organ and reflect functional changes of the human body from the molecular level, such as the physiological, pathological, biochemical, and metabolic, but has poor spatial resolution, cannot be accurately located, and cannot display the anatomical information of the lesions [12]. CT belongs to the anatomical structure of images, with high spatial resolution and density resolution; it has unique advantages in displaying the anatomical structure and density of the body [13], it also can provide detailed anatomical information of human organs and tissues, but can not reflect the functional information of tissues and organs [14] (Figure 1).

**2.2. Genetic Algorithm.** Genetic algorithm is a computational model which is based on the natural selection and evolution mechanism; its core idea is inspired by the natural selection rule of the survival of the fitness, so the search algorithm is an iterative process of survival and detection, is a very effective search and optimization technique, can achieve a highly parallel, random, and adaptive search, cannot easily fall into local optimum, and can find the global optimal solution with high probability and its robustness is good [15]. General use of genetic algorithm for reduction is achieved by a binary coding, 1 indicates that the position selects the corresponding attribute, while 0 indicates that the corresponding attribute is not selected. Genetic algorithm consists of four parts: encoding and decoding, fitness function, genetic operator, and control parameters, genetic operators include selection operator, crossover operator, and mutation operator, The selection operator is generally selected by roulette wheel selection method, according to the selection probability  $p_i = (f_i / \sum_{i=1}^M f_i)$ , crossover operator is a single point crossover, with a certain probability  $p$  to select individuals to participate in crossover, mutation operator selects the individual with the probability  $p$  and randomly selects the corresponding gene of the variant individuals to operate [16]. The general steps are as follows: determining the initial population and calculating the target value of each individual in the population and the corresponding value of the fitness function, choosing the chromosomes with high fitness value, and forming a matching set (selection), according to certain rules of reproduction (crossover and mutation), to meet the conditions to stop the genetic iteration, or return to step 3 (Figure 2).

**2.3. Variable Precision Rough Set.** Ziarko proposed the variable precision rough set model in 1993, he first proposed the concept of classification error rate; in the case of a given classification error rate, the objects with the same attributes can be classified into classes as many as possible [17].

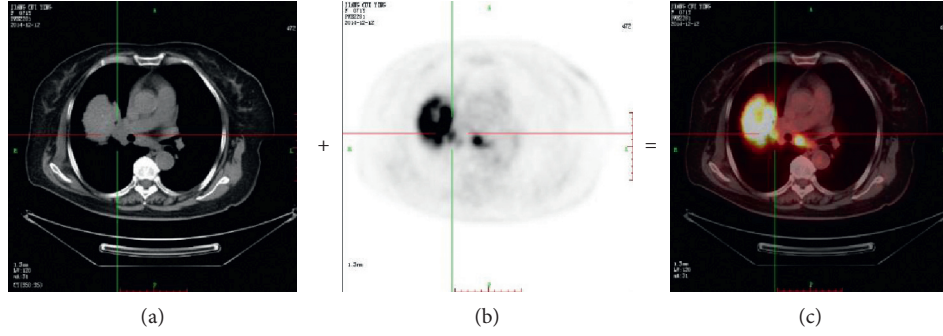


FIGURE 1: The source image of CT, PET, PET/CT.

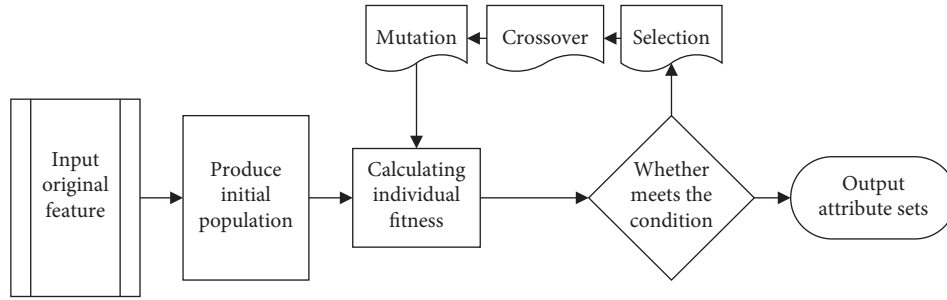


FIGURE 2: Flow chart of knowledge reduction method based on genetic algorithm.

**Definition 1** (equivalence class). Assuming that  $R$  is an equivalence relation on  $K$ , a collection of all elements equivalent to an element  $k$  in  $K$  is called an equivalence class of  $k$ , denoted as  $[k]$ .

**Definition 2** (indiscernibility relation). If  $P \subseteq R$  and  $P \neq \phi$ , then  $\cap P$  is also an equivalence relation, it is called the indiscernibility relation on  $P$ , denoted as  $\text{ind}[P]$ .

**Definition 3** (upper approximation and lower approximation). The knowledge base of  $K = (U, R)$ ,  $X \subseteq U$ ,  $R$  is equivalent to the relationship between  $U$ . The lower approximation of  $X$  can be understood as all of the classification errors that are not greater than  $\beta$  are included in the  $R$  equivalence class in  $X$ . The upper approximation of  $X$  can be understood as the intersection of all those with classification error not greater than  $\beta$  and equivalence classes with  $X$  is not empty [18]. Expressions are as follows:

$$\begin{aligned} \underline{RX}_\beta &= \cup \left\{ Y \in \frac{U}{R} \mid Y \subseteq X \right\}, \\ \overline{RX}_\beta &= \cup \left\{ Y \in \frac{U}{R} \mid Y \cap X \neq \emptyset \right\}. \end{aligned} \quad (1)$$

Assume that the decision information table  $S = (U, A, V, f)$ , where  $U$  is a sample of the universe and a nonempty finite sample set,  $U = \{x_1, x_2, x_3, \dots, x_n\}$ , and  $x_i$  represents each sample.  $A = P \cup Q$ ,  $P$  represents a collection of conditional attributes,  $Q$  represents a set of decision attributes.  $V$  represents the range of attribute.  $f: U \times A \rightarrow V$  is an information function that gives an attribute value for each attribute of each  $x_i$ , that is,  $\forall_a \in A, x \in U, f(x, a) \in V_a$ .  $X$

and  $Y$  represent nonempty set in finite field  $U$ .  $P, Q \subseteq A$  represents the condition attribute set and decision attribute set;  $\text{ind}(P)$ ,  $\text{ind}(Q)$  is an indiscernibility relation determined by  $P, Q$ ;  $\text{ind}(P)$  is a collection of equivalence classes called condition class, expressed in  $U/P$ , i.e.,  $U/\text{ind}(P) = \{P_1, P_2, P_3, \dots, P_n\}$ ;  $\text{ind}(Q)$  is a collection of equivalence classes called decision class, expressed in  $U/Q$ , that is  $U/\text{ind}(Q) = \{Q_1, Q_2, Q_3, \dots, Q_n\}$ .

**Definition 4** (majority inclusion relation). If there is a  $e \in Y$  for each  $e \in X$ , then  $Y$  contains  $X$ , denoted as  $Y \supseteq X$ , then

$$c(X, Y) = \begin{cases} 1 - |X \cap Y|/|X|, & |X| > 0, \\ 0, & |X| = 0, \end{cases} \quad (2)$$

where  $|X|$  represents the cardinality of the set  $X$  and  $c(X, Y)$  is the relative classification error rate of set  $X$  on set  $Y$ .

Make  $(0 \leq \beta < 0.5)$ ; the majority inclusion relation is defined as  $Y \supseteq_\beta X \iff c(X, Y) \leq \beta$ ; the “majority” requirement implies that the number of common elements in  $X$  and  $Y$  is greater than 50% of the number of elements in  $X$ .

**Definition 5** ( $\beta$ -reduction). Conditional attribute set  $P$  is a subset of  $P$  for  $\beta$ -reduction or approximate reduction of decision attribute set  $Q$ , and the subset is  $\text{red}(P, Q, \beta)$  and meets the following two conditions [19]:

- (1)  $\gamma(P, Q, \beta) = \gamma(\text{red}(P, Q, \beta), Q, \beta)$
- (2) To remove any attribute from  $\text{red}(P, Q, \beta)$ , condition (1) is not valid

### 2.3.1. Attribute Dependency

**Definition 6.** The dependency of the decision attribute set  $Q$  and the conditional attribute set  $P$  is defined as

$$\gamma(P, Q, \beta) = \frac{|\text{pos}(P, Q, \beta)|}{|U|}. \quad (3)$$

$\text{pos}(P, Q, \beta) = \cup_{Y \in U/Q_{\text{ind}(P)_\beta}} Q$ ,  $|U|$  is the number of objects contained in the domain,  $|\text{pos}(P, Q, \beta)|$  is the number of objects contained in the positive domain of all equivalence classes that are not greater than the  $\beta$  classification error, which indicates that the conditional attributes can correctly divide the object to  $U/Q$ .  $\gamma$  ( $0 \leq \gamma \leq 1$ ) is the  $\beta$  dependency of the decision attribute  $Q$  to the conditional attribute  $P$  and is an evaluation of the ability to classify objects with the classification error  $\beta$ .  $\gamma=0$  means that  $P$  cannot be used to divide objects into equivalence classes in  $Q$ ,  $\gamma=1$  means that  $P$  can be used to divide objects into equivalence classes in  $Q$  completely,  $0 < \gamma < 1$  means that  $P$  can be used to divide objects into equivalence classes in  $Q$  partly.

### 2.3.2. Attribute Importance

**Definition 7.** Assume that the decision information table is  $S = (U, A, V, f)$ ,  $A = P \cup Q$ ,  $s \in h$ , the relative importance of attribute  $s$  is

$$Z(s) = \frac{\gamma(P, Q, \beta) - \gamma(P - \{s\}, Q, \beta)}{\gamma(P, Q, \beta)} = 1 - \frac{\gamma(P - \{s\}, Q, \beta)}{\gamma(P, Q, \beta)}. \quad (4)$$

An attribute is able to distinguish an object; the greater the value, the stronger the ability.

The selection of threshold  $\beta$  for variable precision rough set needs to meet the following requirements.

The choice of  $\beta$  to make the classification accuracy as high as possible:

- (1)  $0 \leq \beta < 0.5$
- (2)  $\beta$  makes the attributes contained in the reduction results as little as possible

**2.4. SVM.** Support vector machine (SVM) is a supervised learning model for data analysis, pattern recognition, and regression analysis in the field of machine learning. The best compromise between model complexity (the learning accuracy of a particular training sample) and learning ability (ability to identify an arbitrary sample without error) should be found based on limited sample information. In order to obtain the best generalization ability, the basic idea is to use the structural risk minimization principle to construct the optimal classification hyperplane in the attribute space. SVM has some advantages such as good generalization ability, simple data structure, low computational complexity, short training time, few parameters selection, high fitting precision, strong robustness, and so on [20, 21]. It has great advantages in dealing with small sample, nonlinear, and

high-dimensional pattern recognition. It is often used in pattern recognition [12, 22], regression estimation, and so on.

- (1) After the introduction of kernel function and penalty parameter by SVM, the optimal discriminant function model is

$$f(x) = \text{sgn} \left( \sum_{i=1}^n a_i y_i k(x_i, x) + b \right). \quad (5)$$

Among it,  $0 < a < C$ ,  $y_i \in \{1, -1\}$ .

- (2) The optimization function of SVM is

$$Q(a) = \sum_{i=1}^n a_i - \frac{1}{2} \sum_{i,j=1}^n a_i a_j y_i y_j k(x_i, x_j). \quad (6)$$

- (3) The radial basis kernel function is a widely used kernel function; the kernel function is used in this paper:

$$k(x, y) = \exp(-g\|x - y\|^2). \quad (7)$$

Among them,  $g > 0$ ,  $g$  is an important parameter in the kernel function, which affects the complexity of SVM classification algorithm.

The kernel function parameter  $g$  and penalty coefficient  $C$  of support vector machine (SVM) is an important parameter which affects the performance of SVM classification, so  $(C, g)$  is used as the optimization variable. In the process of learning SVM, 5-fold cross validation is used to calculate the optimal classification performance of kernel function parameter and penalty coefficient, and then the diagnosis result of optimization is applied to the SVM classifier for lung cancer, the final selection of the sensitivity, specificity, accuracy, and computation time as the evaluation indexes of related experiments.

## 3. Results and Discussion

**3.1. Main Idea.** The main idea of the model is as follows.

**3.1.1. Parameters.** Population size  $M$ , chromosome length  $N$  (the number of condition attributes), crossover probability  $P_c$ , mutation probability  $P_m$ , fitness function  $F(x)$ , and the maximum number of iterations  $K$  are the parameters.

**3.1.2. Coding.** The binary coding method is used, which is represented by a binary string whose length is equal to the number of condition attributes; each bit corresponds to a condition attribute, a bit of 1 indicates that the corresponding condition attribute is selected, 0 indicates that the condition attribute is not selected, e.g., {00110101} represents a chromosome with a length of 8, and it is known that the corresponding 1, 2, 5, 7 of 0 indicates that the corresponding condition attribute is not selected, then {c3, C4, C6, c8} is the last individual to choose the attributes set.



**3.1.3. The Initial Population.** Assuming the population size  $M$  (the number of chromosomes in the population is  $M$ ),  $M$  length of  $Lr$  chromosome (0, 1) is the randomly generated as the initial population.

**3.1.4. Genetic Operators.** Genetic operators include selection operator, crossover operator, and mutation operator. The selection operator generally uses the roulette wheel selection method, according to the selection probability  $p_i = (f_i / \sum_{i=1}^M f_i)$  to select. Crossover operator uses a single-point crossover, with a certain probability  $P_c$  to select the individual uniform crossover. The mutation operator selects the individuals with the probability  $P_m$  to carry on the variation, and randomly selects the corresponding bit of the nonnuclear attribute.

**3.1.5. Fitness Function.** The fitness function is the core of the genetic algorithm, the fitness value is the only index to evaluate the fitness function; this paper from the gene encoding value, the minimum number of attributes reduction, attribute dependency, and other aspects constructs a fitness function framework, by adjusting the weights of various factors and changing the classification error rate to achieve different fitness function. The fitness function is set as follows:

target1. Attribute dependency:  $\gamma(P, Q, \beta) = (|\text{pos}_P^\beta(Q)|/|U|)$ , it represents the  $\beta$  dependency of decision attribute  $Q$  for conditional attribute  $P$ .

target2. Attributes reduction Length:  $|C\_reduct| = ((|P| - |Lr|)/|P|)$ ,  $|P|$  is the number of condition attributes represented by 0, 1.  $|Lr|$  represents the number of 1 in attribute  $P$ , the shorter the better results.

target3. Gene coding weight function: i.e., Penalty function,  $\text{target3} = \sum \text{abs}(r \times (r - 1))/|r|$ . Gene values can only take 0 and 1, but the chromosome will show not 1 and not 0, such that the value is less than 0 or greater than 1. The value must be punished; therefore, the gene coding weight function is constructed. If the gene is 0,  $r \times (r - 1) = 0$ , but the gene is 1,  $r \times (r - 1) = 0$ . So do not punish the genes of 0 or 1, but if there is a chromosome with a length of 6:  $r = [0 \ 0 \ -2 \ -1 \ 2 \ 1]$ ,  $(r - 1) = [-1 \ -1 \ -3 \ -2 \ 1 \ 0]$ ,  $r \times (r - 1) = [0 \ 0 \ 6 \ 2 \ 2 \ 0]$ , then  $\sum \text{abs}(r \times (r - 1)) = 10$ , length is 6, so  $\text{target3} = 10/6 = 1.67$ .

Therefore, the fitness function constructed in this paper is

$$F(x) = -\omega_1 \times \text{target1} - \omega_2 \times \text{target2} + \omega_3 \times \text{target3}, \quad (8)$$

where  $\omega$  is the weight coefficient of fitness function,  $\omega = (0, 1, 2, 3)$ , because the genetic algorithm can only find the minimum value, and the bigger the fitness value, the better it is, so the objective function is minus and the penalty function is plus.

Flow chart about this model is given in Figure 3.

### 3.2. Model Concrete Steps

Input: A decision information table  $S = (U, A, V, f)$

Output: red  $(P, Q, \beta)$

generate  $(M)$ ,  $Lr = 98$ //Initial population  $M$ , 01 sequence of Chromosome length 98

Setting  $\beta$ ,  $\omega$ , crossover probability  $P_c$ , mutation probability  $P_m$ , iteration number  $K$

Begin

for  $i = 1 : K$

target1 =  $(|\text{pos}_P^\beta(Q)|/|U|)$

target2 =  $((|P| - |Lr|)/|P|)$

target3 =  $(\sum \text{abs}(r \times (r - 1))/|r|)$

Fitness

function =  $-\omega_1 \times \text{target1} - \omega_2 \times \text{target2} + \omega_3 \times \text{target3}$ ;  
//Fitness function

$P = \text{Select}(M, 2, P_c)$ ;//Crossover probability  $P_c$

$Q = \text{Crossover}(P, 2, P_c)$ ;//Crossover algorithm

$Q' = \text{Mutation}(Q, P_m)$ ;//Mutation algorithm

End

### 3.3. Experimental Environment and Data

**3.3.1. Hardware Environment.** Intel Core i5 4670-3.4 GHz with 8.0 GB memory and 500 GB hard disk were used.

**3.3.2. Software Environment.** Matlab R2012b, LibSVM, and Windows 7 operating system were used.

**3.3.3. Experimental Data.** The PET/CT images of 2000 lung cancer patients were collected as the study samples (1000 cases of benign lung tumor, 1000 cases of malignant lung tumor). Firstly, ROI was extracted from the lung tumor and pretreated; then 8-dimensional shape features, 7-dimensional gray features, 3-dimensional Tamura features, 56-dimensional GLCM features, and the 24-dimensional frequency domain features were extracted from the lung tumor ROI, and 98-dimensional feature vectors are discretized and normalized. In the decision attribute, 1 represents the lung malignant tumor and -1 represents the lung benign tumor. Figure 4(a) shows four PET/CT images, ROI of Lung malignant tumor, and Figure 4(b) shows four PET/CT images' ROI of lung benign tumor. Table 1 gives the feature values of two patients with lung cancer (one patient was a malignant tumor and the other was a benign tumor).

**3.4. Analysis of Experimental Results.** In this paper, 3 kinds of experiments are designed according to the weight value  $\omega = (0, 1, 2, 3)$  of the fitness function and the classification error rate  $\beta = \{0.4, 0.2, 0\}$  (namely, the inclusion degree  $1 - \beta = \{0.6, 0.8, 1\}$ ). For first type of experiments,  $1 - \beta = 0.6$ , according to the different values of  $\omega$  to do the three groups of experiments totally. For second type of experiments,  $\omega_1 = 1, \omega_2 = 1, \omega_3 = 0$ , according to the different values of  $\beta$  to do three groups of experiments. For third type of experiments,  $1 - \beta = 0.6$ , by increasing the  $\omega$

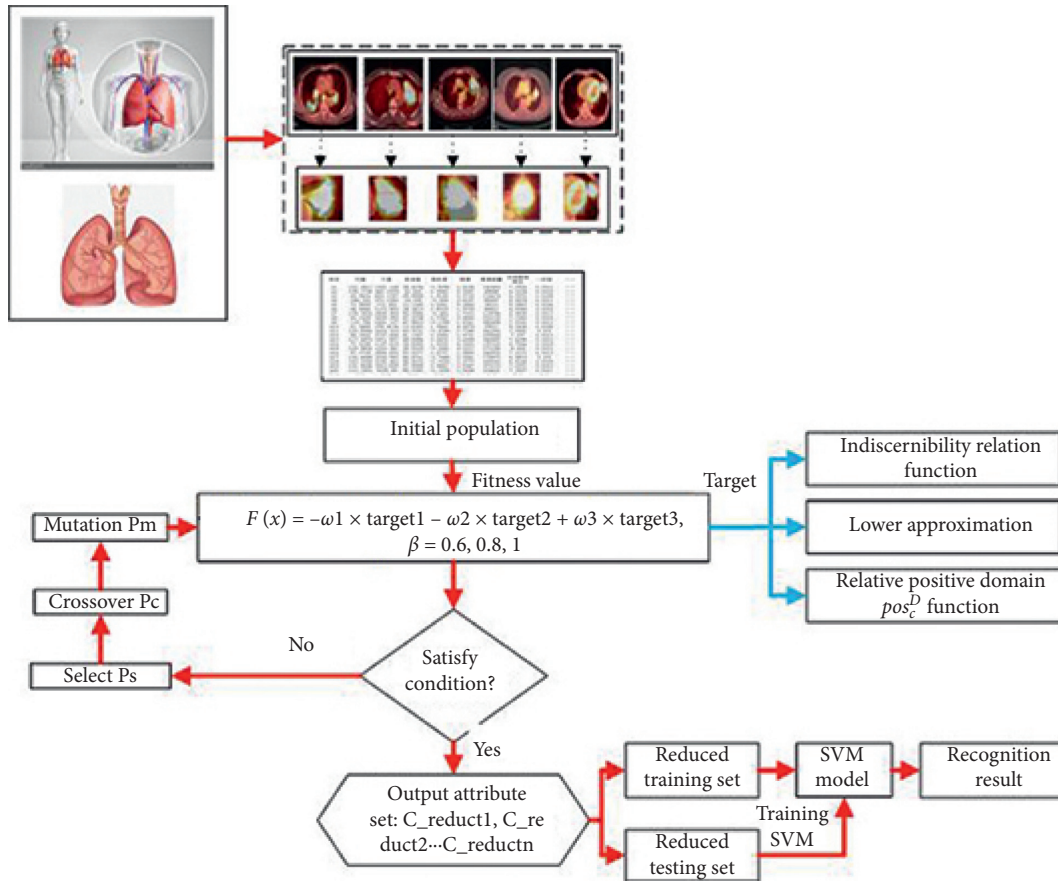


FIGURE 3: Flow chart of high-dimensional feature selection based on genetic algorithm and variable precision rough set.

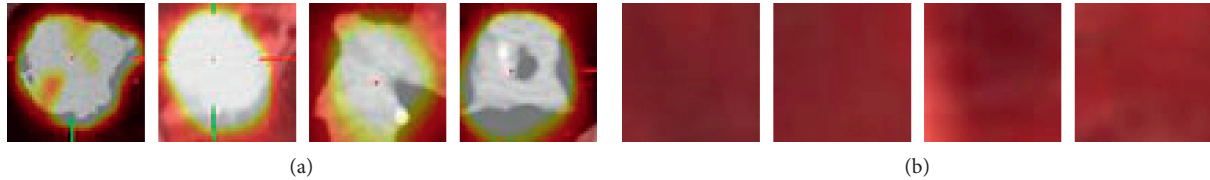


FIGURE 4: Part of lung tumor PET/CT image ROI. (a) Part of the lung malignant tumor PET/CT-ROI. (b) Part of the lung benign tumor PET/CT-ROI.

value to achieve the best fitness function, to achieve the best results.

**3.4.1. Experiment 1—Research on Different Weight Coefficients under the Condition in the Same Classification Error Rate.**  $\omega$  values and  $\beta$  values of experiment 1 are shown in Table 2, and  $1 - \beta = 0.6$ .

**(1) 1st Group Experiment.**  $\{\omega_1, \omega_2, \omega_3\} = \{1, 0, 0\}$ : The algorithm is run 5 times according to this group weights; the results of the 5 groups are given in Table 3, including the reduction of the conditional attributes, the length of reduction, the optimal fitness value, the attribute dependency degree, and the time. The convergence of VPRS-GA under

the variation for fitness function value in one time is shown in Figure 5.

Each reduction is classified by SVM classifier, using the method of 5-fold cross validation, through changing the training samples and test samples; the results of the five groups were obtained, including accuracy, sensitivity, specificity, and time (training samples are constructed by 800 malignant samples and 800 benign samples; testing samples are constructed by 200 malignant samples and 200 benign samples; the experiment is repeated 5 times by changing training samples and testing samples). Finally, the average values of these five groups are obtained as the final result of the reduction and shown in Table 4.

The weight value in this group experiment is  $\{\omega_1, \omega_2, \omega_3\} = \{1, 0, 0\}$ , attribute dependency degree are

TABLE 1: ROI feature values of lung tumor PET/CT image.

Types of disease	Shape feature	Gray feature	Tamura texture	Texture features of GLCM				Texture feature of wavelet		
				0 degree	45 degrees	90 degrees	135 degrees	Norm	Standard deviation	Energy
Lung malignant tumor	6.0000	122.2810	14.7000	0.0808	0.0779	0.0790	0.0611	649.2580	37.1752	1.0000
	0.0012	1491.1500	30.9650	2.8937	2.9067	2.8989	3.1284	26.9473	3.8486	0.0017
	0.0000	38.6154	0.2326	0.2576	0.2820	0.2653	0.4490	9.3520	1.3355	0.0002
	0.0000	-0.5056		0.1668	0.1676	0.1659	0.1649	16.8200	2.4025	0.0007
	0.0000	2.4166		0.0792	0.0759	0.0772	0.0566	27.1143	3.8693	0.0017
	0.0000	140453		0.2576	0.2820	0.2653	0.4490	20.3163	2.9020	0.0010
	0.0000	7.0524		16.4110	16.4469	16.3584	16.4431	13.1755	1.8818	0.0004
	0.0000			2.7089	2.7072	2.7100	2.8066	18.3441	2.6199	0.0008
				0.5755	0.6007	0.5810	0.7345			
				210.9390	211.7900	209.5780	208.8250			
				0.3064	0.3351	0.3135	0.3950			
				-0.6779	-0.6708	-0.6775	-0.5696			
				0.0000	0.0000	0.0000	0.0000			
				0.7625	0.7802	0.7658	0.8001			
	4.0000	50.3912	10.1616	0.8087	0.7915	0.8077	0.7864	379.9170	2.6741	1.0000
Lung benign tumor	0.0033	6.0006	1.8835	0.4324	0.4732	0.4370	0.4840	5.7551	0.8211	0.0002
	0.0000	2.4496	2.6329	0.0433	0.0621	0.0469	0.0679	1.1745	0.1677	0.0000
	0.0000	0.5649		9.4899	7.8127	9.2429	9.2429	3.4684	0.4955	0.0001
	0.0000	2.8589		0.8082	0.7905	0.8072	0.7853	2.0823	0.2972	0.0000
	0.0000	3283		0.0433	0.0621	0.0469	0.0679	2.1821	0.3117	0.0000
	0.0000	3.2559		7.8367	7.8363	7.8396	7.8363	0.8937	0.1276	0.0000
	0.0000			0.4024	0.4301	0.4045	0.4370	2.2387	0.3197	0.0000
				0.1782	0.2326	0.1894	0.2481			
				55.5257	55.0899	55.5291	54.9831			
				0.0596	0.0873	0.0650	0.0958			
				-0.4707	-0.3295	-0.4351	-0.2911			
				0.0000	0.0000	0.0000	0.0000			
				2.0429	2.1172	2.0651	2.1394			

TABLE 2: Fitness function weight proportion and  $\beta$  value.

Experiment times	$1 - \beta = 0.6$		
	$\omega 1$	$\omega 2$	$\omega 3$
First group experiment	1	0	0
Second group experiment	1	1	0
Third group experiment	1	1	1

TABLE 3: Results of VPRS-GA running 5 times when  $1 - \beta = 0.6$ ,  $\{\omega 1 = 1, \omega 2 = 0, \omega 3 = 0\}$ .

Experiment times	C_ reduction	Reduction length	Optimal fitness value	Attribute dependency degree	Time (s)
1	{4 5 8 9 11 12 13 17 20 22 23 24 27 30 32 33 35 38 42 48 49 52 57 59 61 62 63 64 65 68 70 72 73 75 77 78 80 87 88 91 92}	41	-0.9705	0.9705	971.9144
2	{1 2 3 4 5 8 11 12 13 14 16 17 19 23 24 25 26 27 28 30 32 36 38 39 40 42 43 44 46 47 52 53 55 61 63 66 67 69 71 72 73 77 79 80 82 84 85 87 92}	49	-0.9685	0.9685	1007.6907
3	{4 6 11 12 15 17 18 24 25 26 28 29 31 36 38 39 42 43 45 47 49 53 56 65 68 69 72 76 77 79 80 81 83 85 88 91 92}	37	-0.9695	0.9695	1043.2000
4	{4 8 9 11 12 13 14 15 17 23 29 34 35 39 40 43 47 48 50 53 55 56 60 61 64 68 70 75 80 81 82 83 84 86}	34	-0.9790	0.9790	947.3111
5	{3 4 6 8 10 11 12 13 15 17 19 20 21 24 26 29 31 39 42 44 45 48 50 53 54 56 59 64 68 77 83 84 87 89 92}	35	-0.9775	0.9775	964.5092
	Average value	39.2	-0.9730	0.9730	986.9251

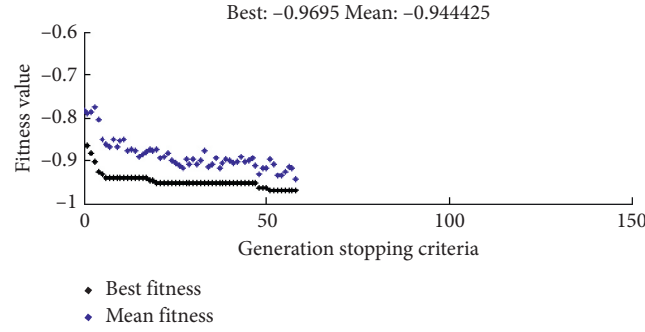


FIGURE 5: The variation of fitness function value in a running process for Experiment 1-first group.

TABLE 4: The statistical results of the first group for experiment 1 with the SVM classifier.

Experiment times		Accuracy (%)	Sensitivity (%)	Specificity (%)	Time (s)
Reduction 1	1	92.50	86.00	99.00	33.2607
	2	97.25	97.50	97.00	34.5051
	3	99.00	99.00	99.00	35.8677
	4	98.00	99.50	96.50	35.1075
	5	99.25	100.00	98.50	35.5948
	Average value	97.20	96.40	98.00	34.8672
Reduction 2	1	93.25	87.00	99.50	43.6533
	2	97.25	98.00	96.50	44.5900
	3	98.75	98.50	99.00	43.9506
	4	97.50	99.00	96.00	44.5064
	5	99.25	100.00	98.50	44.8513
	Average value	97.20	96.50	97.90	44.3103
Reduction 3	1	92.75	87.50	98.00	32.6916
	2	95.75	97.50	94.00	33.7209
	3	98.00	98.00	98.00	34.0701
	4	97.00	98.50	95.50	33.3174
	5	98.50	99.50	97.50	33.3257
	Average value	96.40	96.20	96.60	33.4251
Reduction 4	1	93.75	88.50	99.00	30.6485
	2	96.50	97.50	95.50	31.9240
	3	97.50	97.00	98.00	32.4082
	4	97.75	99.00	96.50	32.5419
	5	99.00	100.00	98.00	36.1516
	Average value	96.90	96.40	97.40	31.8806
Reduction 5	1	94.00	89.00	99.00	31.9557
	2	96.50	97.50	95.50	33.6909
	3	97.25	97.00	97.50	33.0159
	4	97.75	99.00	96.50	39.9980
	5	99.00	100.00	98.00	32.5692
	Average value	96.90	96.50	97.30	34.2459

regarded as fitness function. The average attribute dependency degree is 0.973, the average length of reduction is 39.2, and the average optimal fitness value is  $-0.973$ . The average recognition accuracy of the experiment is 96.92%. The premature phenomena are shown in Figure 5, and evolution progress is terminated early.

(2) *2nd Group Experiment.*  $\{\omega_1, \omega_2, \omega_3\} = \{1, 1, 0\}$ : This experiment introduces an objective function to control the length of reduction (the shorter the length of reduction, the better it is), the influence degree of the objective function which controls the reduction on the fitness function and the

final recognition accuracy is verified. The algorithm is run 5 times according to this group weights, and the results of the 5 groups are given in Table 5, including the reduction of the conditional attributes, the length of reduction, the optimal fitness value, the attribute dependency, and the time. The convergence of VPRS-GA under the variation for fitness function value in one time is shown in Figure 6.

Each reduction is classified by SVM classifier, using the method of 5-fold cross validation, through changing the training samples and test samples, the results of the five groups were obtained, including accuracy, sensitivity, specificity, and time (training samples are constructed by

TABLE 5: Results of VPRS-GA running 5 times when  $1 - \beta = 0.6$ ,  $\{\omega_1 = 1, \omega_2 = 1, \omega_3 = 0\}$ .

Experiment times	C_ reduction	Reduction length	Optimal fitness value	Attribute dependency degree	Time (s)
1	{5 9 14 20 26 41 43 46 48 54 55 57 64 66 74 79 86 90}	18	-4.6487	0.9965	1072.4072
2	{1 4 11 12 14 24 34 40 42 43 56 60 61 65 67 68 71 72 85}	19	-4.0109	1	632.8122
3	{2 13 27 29 39 42 45 56 59 63 68 70 75}	13	-4.6512	0.9990	1102.3967
4	{1 3 4 7 9 11 12 15 30 34 38 42 46 48 55 62 65 77 79}	19	-4.9674	1	879.4670
5	{3 9 11 13 29 39 41 42 43 46 50 55 65 67 77 85 86}	16	-4.4114	0.9815	1507.5539
	Average value	17	-4.5379	0.9954	1038.9274

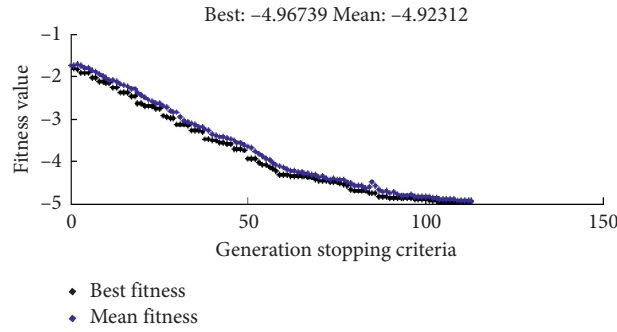


FIGURE 6: The variation of fitness function value in a running process for experiment 1-second group.

800 malignant samples and 800 benign samples; testing samples are constructed by 200 malignant samples and 200 benign samples; the experiment is repeated 5 times by changing training samples and testing samples). Finally, the average values of these five groups are obtained as the final result of the reduction and shown in Table 6.

The experimental weight of this group is  $\{\omega_1, \omega_2, \omega_3\} = \{1, 1, 0\}$ ; attribute dependency degree and the length of reduction are regarded as fitness function. As can be seen from Table 5, the reduction length is 13, 17, and so on. The average length of reduction was 17, which was significantly reduced compared with the average length of the reduction in Table 3 in the experiment of the first groups, which reduced the time, improved the efficiency of the algorithm, and increased the attribute dependency of the algorithm, even up to 1. The average recognition accuracy of the experimental group was 96.98%, which was increased by 0.06% compared with that in the first groups.

(3) *3rd Group Experiment.*  $\{\omega_1, \omega_2, \omega_3\} = \{1, 1, 1\}$ : On the basis of attribute dependency degree and attribute reduction length, this experiment introduces gene coding weight function, in order to verify the effect of gene coding weight function on fitness function and the final recognition accuracy. The algorithm are run 5 times according to this group weights, the results of the 5 groups are given in Table 7, including the reduction of the conditional attributes, the length of reduction, the optimal fitness value, the attribute dependency, and the time. The convergence of VPRS-GA under the variation for fitness function value in one time is shown in Figure 7.

Each reduction is classified by SVM classifier, using the method of 5-fold cross validation, through changing the training samples and test samples; the results of the five groups were obtained, including accuracy, sensitivity, specificity, and time (training samples are constructed by 800 malignant samples and 800 benign samples; testing samples are constructed by 200 malignant samples and 200 benign samples; the experiment is repeated 5 times by changing training samples and testing samples). Finally, the average values of these five groups are obtained as the final result of the reduction and shown in Table 8.

The experimental weight of this group is  $\{\omega_1, \omega_2, \omega_3\} = \{1, 1, 1\}$ ; attribute dependency degree, the length of reduction, and gene coding weight value are regarded as fitness function. However, the premature phenomena are shown in Figure 7, and evolution progress is terminated early. From Table 7, we can see that the attribute dependency decreases gradually and even the attribute dependency of Reduction 1 is reduced to 0.759. The average recognition accuracy of the experimental group was 96.85%. The accuracy of recognition was decreased compared with the second groups, and hence, using gene encoding weight function in the fitness function to improve recognition accuracy is useless, only for the samples with different results, to analyze specific issues. The 3 experiment runs of experiment 1 verified the necessity of the fitness function, by continuously introducing fitness objective function, such as target1, target2, and target3, the conclusion is that the fitness function is better when it is not bigger, but after the introduction of target3, the accuracy declines; therefore, the introduction of target1 and target2 in this algorithm can get better results.



TABLE 6: The statistical results of the second group for experiment 1 with the SVM classifier.

Experiment times		Accuracy (%)	Sensitivity (%)	Specificity (%)	Time (s)
Reduction 1	1	93.00	86.00	100.00	11.6488
	2	96.25	96.00	96.50	12.5511
	3	98.50	99.00	98.00	13.1509
	4	97.25	98.50	96.00	13.4468
	5	99.25	100.00	98.50	14.4839
	Average value	96.85	95.90	97.80	13.0563
Reduction 2	1	94.25	89.00	99.50	12.1096
	2	97.25	97.00	97.50	12.8636
	3	98.00	98.00	98.00	13.5677
	4	97.50	98.00	97.00	13.8196
	5	98.75	99.00	98.50	13.6691
	Average value	97.15	96.20	98.10	13.2059
Reduction 3	1	93.00	87.50	98.50	8.7757
	2	97.25	97.50	97.00	10.3424
	3	97.75	98.00	97.50	10.7411
	4	97.75	98.50	97.00	11.2344
	5	99.00	100.00	98.00	11.3006
	Average value	96.95	96.30	97.60	10.4788
Reduction 4	1	93.75	87.50	100.00	14.6417
	2	96.50	97.50	95.50	15.4736
	3	97.50	97.00	98.00	15.7621
	4	98.00	99.00	97.00	16.1355
	5	99.25	100.00	98.50	16.3381
	Average value	97.00	96.20	97.80	15.6702
Reduction 5	1	92.50	86.50	98.50	12.4933
	2	96.75	98.00	95.50	14.0057
	3	98.00	98.00	98.00	14.5194
	4	98.00	99.00	97.00	14.5792
	5	99.50	99.50	99.50	15.0400
	Average value	96.95	96.20	97.70	14.1275

TABLE 7: Results of VPRS-GA running 5 times when  $1 - \beta = 0.6$ ,  $\{\omega_1 = 1, \omega_2 = 1, \omega_3 = 1\}$ .

Experiment times	C_ reduction	Reduction length	Optimal fitness value	Attribute dependency degree	Time (s)
1	{4 5 7 26 27 34 35 41 47 54 55 71 74 75 78 80 83 90}	18	-1.4192	0.7590	688.8635
2	{4 15 16 19 22 27 28 29 30 35 38 42 45 50 52 53 59 61 62 64 65 70 71 72 77 87 88}	27	-1.5232	0.8640	812.4857
3	{6 17 19 24 28 31 33 34 38 39 43 45 47 48 49 51 55 56 66 67 69 70 71 72 76 77 78 80 81 84 87 89 91 92}	34	-1.3545	0.7950	952.1511
4	{3 6 8 9 16 17 19 20 24 25 28 35 37 39 41 42 46 49 51 52 54 59 63 65 66 74 83 86}	28	-1.4703	0.8365	871.4839
5	{1 7 8 15 17 19 20 23 29 37 45 48 54 60 62 70 73 75 77 78 79 86}	22	-1.4990	0.7995	779.7617
	Average value	25.8	-1.4532	0.8108	820.9492

3.4.2. *Experiment 2—Research on Different Classification Error Rates under the Condition in the Same Weight Coefficient.* According to experiment 1, we can see that when  $\omega_1 = 1$ ,  $\omega_2 = 1$ ,  $\omega_3 = 0$ , the experimental results are the best, so in experiment 2, the case of the weight value of was unchanged,  $\omega_1 = 1$ ,  $\omega_2 = 1$ ,  $\omega_3 = 0$ , and the  $\beta$  value was changed, and they are shown in Table 9.

(1) *1st Group Experiment.*  $1 - \beta = 0.6$ : The algorithm is run 5 times according to this group weights; the results of the 5 groups are shown in Table 5, including the reduction of the

conditional attributes, the length of reduction, the optimal fitness value, the attribute dependency, and the time. The convergence of VPRS-GA under the variation for fitness function value for one time is shown in Figure 6 (i.e., not repeated in the second group of experiment 1).

(2) *2nd Group Experiment.*  $1 - \beta = 0.8$ : The algorithm are is 5 times according to this group weights, the results of the 5 groups are given in Table 10, including the reduction of the conditional attributes, the length of reduction, the optimal fitness value, the attribute dependency, and the time. The



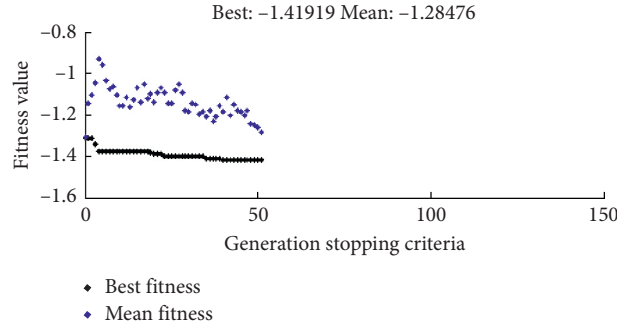


FIGURE 7: The variation of fitness function value in a running process for experiment 1-third group.

TABLE 8: The statistical results of the third group for experiment 1 with the SVM classifier.

Experiment times		Accuracy (%)	Sensitivity (%)	Specificity (%)	Time (s)
Reduction 1	1	92.75	86.00	99.50	9.2492
	2	97.25	97.50	97.00	10.7461
	3	98.50	98.50	98.50	11.3811
	4	97.75	99.00	96.50	11.5560
	5	98.75	100.00	97.50	11.7022
	Average value	97.00	96.20	97.80	10.9269
Reduction 2	1	93.50	87.50	99.50	14.8245
	2	97.00	96.50	97.50	16.1535
	3	97.75	98.50	97.00	16.6452
	4	98.00	98.50	97.50	17.5450
	5	98.75	99.50	98.00	17.2348
	Average value	97.00	96.10	97.90	16.4806
Reduction 3	1	91.25	83.00	99.50	20.1904
	2	96.50	97.00	96.00	21.8535
	3	98.00	98.00	98.00	21.9605
	4	96.25	99.00	93.50	22.3091
	5	98.25	100.00	96.50	23.6896
	Average value	96.05	95.40	96.70	22.0006
Reduction 4	1	93.00	87.00	99.00	16.5454
	2	96.75	96.00	97.50	17.2432
	3	98.75	98.50	99.00	17.9301
	4	98.00	99.00	97.00	18.9560
	5	99.00	99.50	98.50	18.5249
	Average value	97.10	96.00	98.20	17.8399
Reduction 5	1	92.75	86.00	99.50	14.1173
	2	97.25	98.00	96.50	16.1295
	3	99.00	99.50	98.50	15.8992
	4	97.75	99.50	96.00	16.4876
	5	98.75	100.00	97.50	16.6070
	Average value	97.10	96.60	97.60	15.8481

TABLE 9: Fitness function weight proportion and  $\beta$  value.

Experiment times	$\omega_1 = 1, \omega_2 = 1, \omega_3 = 0$		
	$1 - \beta = 0.6$	$1 - \beta = 0.8$	$1 - \beta = 1$
First group experiment	○		
Second group experiment		○	
Third group experiment			○

convergence of VPRS-GA under the variation for fitness function value for one time is shown in Figure 8.

Each reduction is classified by SVM classifier, using the method of 5-fold cross validation, through changing the training samples and test samples; the results of the five

groups were obtained, including accuracy, sensitivity, specificity, and time (training samples are constructed by 800 malignant samples and 800 benign samples; testing samples are constructed by 200 malignant samples and 200 benign samples; the experiment is repeated 5 times by

TABLE 10: Results of VPRS-GA running 5 times when  $1 - \beta = 0.8$ ,  $\{\omega_1 = 1, \omega_2 = 1, \omega_3 = 0\}$ .

Experiment times	C_ reduction	Reduction length	Optimal fitness value	Attribute dependency degree	Time (s)
1	{8 9 11 12 15 16 17 18 25 26 29 31 35 39 40 41 42 48 58 65 67 68 70 83 84 91}	26	-6.7816	0.9490	1000.2827
2	{1 6 8 9 11 12 15 17 21 23 26 28 30 31 34 44 50 56 58 59 62 63 64 68 71 75 77 82 89 92}	30	-6.7797	0.9615	947.7387
3	{6 8 12 14 15 16 17 21 28 35 38 39 45 49 55 58 61 62 64 65 77 82 85}	23	-6.8694	0.9070	1286.6181
4	{4 6 7 8 11 12 13 16 17 20 25 26 31 32 34 35 41 42 44 49 50 55 58 68 72 74 76 78 79 85 89 92}	32	-6.7225	0.9540	1051.0220
5	{3 6 8 9 10 16 17 26 27 34 36 37 38 40 42 44 46 51 52 62 66 67 84 86 87}	25	-6.5892	0.8405	846.9324
Average value		27.2	-6.7484	0.9224	1026.5188

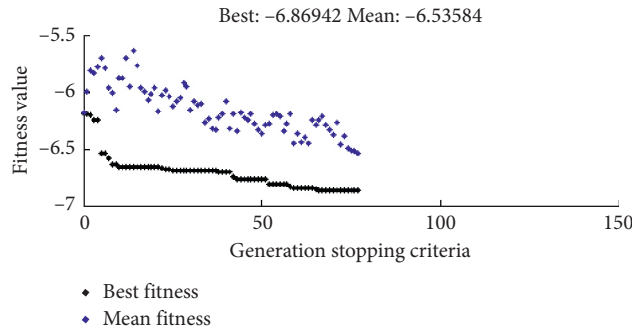


FIGURE 8: The variation of fitness function value in a running process for experiment 2-second group.

changing training samples and testing samples). Finally, the average values of these five groups are obtained as the final result of the reduction and shown in Table 11.

In the case of constant weight  $\omega$  and classification error rate of  $\beta = 0.2$  (which contains  $1 - \beta = 0.8$ ), the classification error rate is changed on the basis of the attribute dependency and the length of control reduction. The premature phenomena are shown in Figure 8, and evolution progress is terminated early, such that the attribute dependency of reduction 5 was 0.8405, appeared in attribute dependency on less than 0.9, compared with first groups of experiment 2 attribute dependency declined. The average recognition accuracy of the experimental group was 96.74%. Compared with the classification error rate of 0.4 and inclusion degree of 0.6, the accuracy was decreased by 0.24%.

(3) *3rd Group Experiment*.  $1 - \beta = 1$ : The algorithm is run 5 times according to the group weights, and the results of the 5 groups are shown in Table 12, including the reduction of the conditional attributes, the length of reduction, the optimal fitness value, the attribute dependency, and the time. The convergence of VPRS-GA under the variation for fitness function value for one time is shown in Figure 9.

Each reduction is classified by SVM classifier, using the method of 5-fold cross validation, through changing the training samples and test samples, the results of the five groups were obtained, including accuracy, sensitivity, specificity, and time (training samples are constructed by 800 malignant samples and 800 benign samples; testing samples are constructed by 200 malignant samples and 200

benign samples; the experiment is repeated 5 times by changing training samples and testing samples). Finally, the average values of these five groups are obtained as the final result of the reduction and shown in Table 13.

In the case of constant weight  $\omega$  and classification error rate of  $\beta = 0$  (which contains  $1 - \beta = 1$ ), the classification error rate is reduced and the inclusion degree is improved on the basis of the attribute dependency and the length of control reduction. The premature phenomena are shown in Figure 9, and evolution progress is terminated early. The average recognition accuracy of the experimental group was 95.73%, which was decreased by 0.06% compared with that in the second group. In experiment 2, the effect of changing the classification error rate on the recognition accuracy was verified by the 3 groups of experiments. By continually reducing the classification error rate, the final recognition accuracy has been declining, when inclusion degree is 1,  $\beta = 0$ ; variable precision rough set becomes Pawlak rough set, the recognition accuracy of the recognition accuracy of is minimum, which was verified the advantages of variable precision rough set.

3.4.3. *Experiment 3—Research on Increasing the Weight Coefficient under the Condition in the Same Classification Error Rate*. According to experiment 1 and experiment 2, we can know that when  $\beta = 0.6$ ,  $\omega_1 = 1$ ,  $\omega_2 = 1$ ,  $\omega_3 = 0$ , the recognition accuracy is the best; therefore, in the third experiment, by increasing the weight of  $\omega$ , 3 groups of experiments are performed, fitness goals: target 1 (attribute

TABLE 11: The statistical results of the second group for experiment 2 with the SVM classifier.

Experiment times		Accuracy (%)	Sensitivity (%)	Specificity (%)	Time (s)
Reduction 1	1	93.00	86.50	99.50	22.8007
	2	95.75	97.00	94.50	23.7646
	3	97.00	96.00	98.00	23.3250
	4	97.50	98.50	96.50	24.4491
	5	99.25	100.00	98.50	24.4816
	Average value	96.50	95.60	97.40	23.7642
Reduction 2	1	93.75	88.00	99.50	25.2403
	2	96.25	97.50	95.00	26.5289
	3	98.00	97.00	99.00	26.5523
	4	98.00	99.00	97.00	26.8212
	5	99.50	100.00	99.00	27.5880
	Average value	97.10	96.30	97.90	26.5461
Reduction 3	1	92.75	87.50	98.00	18.0780
	2	96.75	97.50	96.00	19.2992
	3	97.00	96.00	98.00	18.7243
	4	97.75	99.50	96.00	20.8482
	5	98.75	100.00	97.50	20.3507
	Average value	96.60	96.10	97.10	19.4601
Reduction 4	1	92.00	86.50	97.50	25.7260
	2	97.00	97.50	96.50	27.3024
	3	97.75	96.50	99.00	27.2316
	4	97.50	99.00	96.00	28.1554
	5	99.00	100.00	98.00	29.1471
	Average value	96.65	95.90	97.40	27.5125
Reduction 5	1	92.75	87.50	98.00	14.3715
	2	96.75	96.00	97.50	15.2637
	3	97.50	98.00	97.00	15.8929
	4	97.75	99.00	96.50	16.2997
	5	99.50	100.00	99.00	16.6792
	Average value	96.85	96.10	97.60	15.7014

TABLE 12: Results of VPRS-GA running 5 times when  $1 - \beta = 1$ ,  $\{\omega_1 = 1, \omega_2 = 1, \omega_3 = 0\}$ .

Experiment times	C_ reduction	Reduction length	Optimal fitness value	Attribute dependency degree	Time (s)
1	{15 44 68 73 79 84}	6	-2.7313	0.7965	1144.9901
2	{34 51 54 75 80 90}	6	-2.7047	0.8460	969.9391
3	{2 34 49 70 71 72 76 81}	8	-3.4057	0.7535	1123.3489
4	{12 25 78 85}	4	-2.2872	0.9285	1166.8133
5	{6 7 12 13 42 44 55 57 65 66 69 77 81 86 87}	15	-3.3230	0.8665	1323.6077
Average value		7.8	-2.8903	0.8382	1145.7398

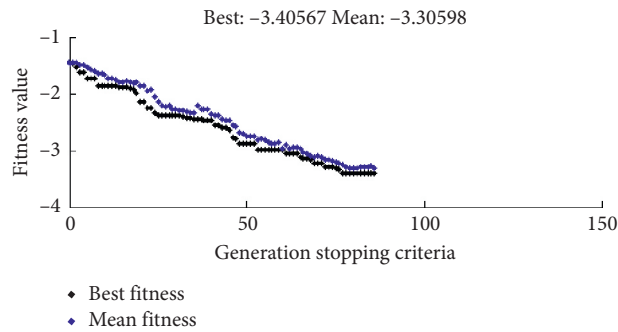


FIGURE 9: The variation of fitness function value in a running process for experiment 2-third group.

TABLE 13: The statistical results of the third group for experiment 2 with the SVM classifier.

Experiment times		Accuracy (%)	Sensitivity (%)	Specificity (%)	Time (s)
Reduction 1	1	92.25	84.50	100.00	8.1271
	2	95.50	97.00	94.00	9.4583
	3	95.75	94.00	97.50	8.8198
	4	96.00	98.00	94.00	9.3754
	5	97.25	99.00	95.50	9.8691
	Average value	95.35	94.50	96.20	9.1299
Reduction 2	1	92.00	84.50	99.50	6.4894
	2	96.25	95.50	97.00	8.0198
	3	95.25	93.00	97.50	7.7337
	4	96.00	97.50	94.50	7.6012
	5	98.00	100.00	96.00	8.2763
	Average value	95.50	94.10	96.90	7.6241
Reduction 3	1	92.00	84.50	99.50	6.4894
	2	96.25	95.50	97.00	8.0198
	3	95.25	93.00	97.50	7.7337
	4	96.00	97.50	94.50	7.6012
	5	98.00	100.00	96.00	8.2763
	Average value	95.50	94.10	96.90	7.6241
Reduction 4	1	92.75	85.50	100.00	6.7264
	2	96.75	96.00	97.50	7.8467
	3	96.00	94.50	97.50	7.3022
	4	95.75	97.50	94.00	7.9460
	5	98.00	100.00	96.00	8.4184
	Average value	95.85	94.70	97.00	7.6479
Reduction 5	1	92.00	84.50	99.50	11.4719
	2	96.25	97.50	95.00	12.8705
	3	98.50	99.00	98.00	13.2049
	4	97.75	99.50	96.00	13.3513
	5	98.50	100.00	97.00	13.3144
	Average value	96.60	96.10	97.10	12.8426

dependency), target 2 (the minimum number of attributes reduction), and target 3 (gene encoding weight function), the three objective functions play an important role in the evaluation of fitness function. However, the importance of fitness function is reduced in these three objectives. Therefore, in this experiment, when the other conditions are unchanged, the weight coefficient of the target 1 is increased, to verify the influence of the change in the weight coefficient on the experimental results, and they are shown in Table 14.

(1) *1st Group Experiment.*  $\omega_1 = 1$ ,  $\omega_2 = 1$ ,  $\omega_3 = 0$ : The algorithm are run 5 times according to this group weights, the results of the 5 groups are given in Table 5, including the reduction of the conditional attributes, the length of reduction, the optimal fitness value, the attribute dependency and the time. The convergence of VPRS-GA under the variation for fitness function value in one time is shown in Figure 6 (i.e., not repeated for the second group of experiment 1).

(2) *2nd Group Experiment.*  $\omega_1 = 2$ ,  $\omega_2 = 1$ ,  $\omega_3 = 0$ : The algorithm is run 5 times according to this group weights, the results of the 5 groups are given in Table 15, including the reduction of the conditional attributes, the length of reduction, the optimal fitness value, the attribute dependency, and the time. The convergence of VPRS-GA under the variation for fitness function value in one time is shown in Figure 10.

TABLE 14: Fitness function weight proportion and  $\beta$  value.

Experiment times	$1 - \beta = 0.6$		
	$\omega_1$	$\omega_2$	$\omega_3$
First group experiment	1	1	0
Second group experiment	2	1	0
Third group experiment	3	1	0

Each reduction is classified by SVM classifier, using the method of 5-fold cross validation, through changing the training samples and test samples, the results of the five groups were obtained, including accuracy, sensitivity, specificity, and time (training samples are constructed by 800 malignant samples and 800 benign samples; testing samples are constructed by 200 malignant samples and 200 benign samples; the experiment is repeated 5 times by changing training samples and testing samples). Finally, the average values of these five groups are obtained as the final result of the reduction and shown in Table 16.

The experimental group in the case of  $1 - \beta = 0.6$  unchanged, the weight of  $\omega_1$  was increased. The attribute dependency and the optimal fitness function are relatively high; the average precision of reduction 1, reduction 2, and reduction 3 in Table 16 is more than 97% and that of reduction 2 is even up to 97.25%. The average recognition accuracy of the experimental group is 97.03%, which is higher than that of the first group.

TABLE 15: Results of VPRS-GA running 5 times when  $1 - \beta = 0.6$ ,  $\{\omega_1 = 2, \omega_2 = 1, \omega_3 = 0\}$ .

Experiment times	C_ reduction	Reduction length	Optimal fitness value	Attribute dependency degree	Time (s)
1	{2 3 4 5 11 13 16 18 24 30 34 37 39 41 42 51 55 64 70 77 78 82}	22	-3.4859	0.9060	2151.5464
2	{8 9 11 12 14 15 23 25 26 29 30 33 37 42 43 45 46 50 60 61 69 74 80 87 89}	25	-3.0845	0.9390	4276.1634
3	{8 11 12 13 16 18 19 24 29 36 37 43 64 65 68 71 86 91 92}	19	-3.5039	0.9150	2619.7164
4	{2 3 4 8 10 11 12 13 15 16 19 23 25 30 48 55 64 65 68 74 77 80 81 83 84 86 89}	27	-2.9150	0.9575	4427.1631
5	{5 8 9 11 12 15 17 23 25 29 31 36 39 41 48 54 59 63 80 83 86 89}	22	-2.9920	0.9525	4316.1464
Average value		23	-3.1962	0.9340	3558.1471

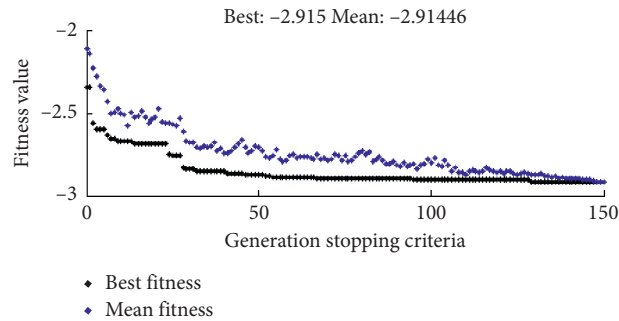


FIGURE 10: The variation of fitness function value in a running process for experiment 3-second group.

TABLE 16: The statistical results of the second group for experiment 3 with the SVM classifier.

Experiment times		Accuracy (%)	Sensitivity (%)	Specificity (%)	Time (s)
Reduction 1	1	92.75	86.00	99.50	18.8497
	2	97.25	98.00	96.50	15.7162
	3	98.50	99.00	98.00	15.8691
	4	98.00	99.00	97.00	16.4603
	5	99.50	100.00	99.00	16.1914
	Average value	97.20	96.40	98.00	16.6173
Reduction 2	1	94.50	89.50	99.50	19.0813
	2	96.75	98.00	95.50	20.0251
	3	97.75	98.00	97.50	19.7008
	4	98.50	99.00	98.00	20.0924
	5	98.75	99.00	98.50	20.9245
	Average value	97.25	96.70	97.80	19.9648
Reduction 3	1	94.00	88.00	100.00	13.1369
	2	97.25	98.00	96.50	14.4797
	3	98.00	98.00	98.00	14.2662
	4	97.25	98.50	96.00	14.7190
	5	99.25	100.00	98.50	14.8799
	Average value	97.15	96.50	97.80	14.2963
Reduction 4	1	93.50	87.50	99.50	24.0456
	2	97.00	97.50	96.50	25.2082
	3	98.00	98.00	98.00	25.1175
	4	97.75	99.50	96.00	27.0188
	5	98.25	100.00	96.50	26.7471
	Average value	96.90	96.50	97.30	25.6274
Reduction 5	1	93.25	88.00	98.50	18.0959
	2	96.00	98.00	94.00	19.6563
	3	97.50	97.50	97.50	19.6723
	4	98.00	99.00	97.00	20.7829
	5	98.50	99.50	97.50	21.9703
	Average value	96.65	96.40	96.90	20.0355

TABLE 17: Results of VPRS-GA running 5 times when  $1 - \beta = 1$ ,  $\{\omega_1 = 1, \omega_2 = 1, \omega_3 = 0\}$ .

Experiment times	C_ reduction	Reduction length	Optimal fitness value	Attribute dependency degree	Time (s)
1	{3 4 5 8 9 11 12 17 19 29 34 35 38 46 52 53 55 59 63 66 72 75 77 78 79 87 92}	27	-3.8867	0.9550	2898.1789
2	{4 8 9 11 12 15 17 29 33 37 38 39 42 43 48 55 67 73 78 81 83 84 88 89 90}	25	-3.8167	0.9715	5578.3772
3	{2 3 4 8 9 10 11 12 13 15 16 19 24 25 30 36 49 54 55 60 64 67 68 70 74 77 83 85 86 91}	30	-3.8807	0.9530	3483.1096
4	{4 5 7 11 12 14 15 17 25 29 33 36 39 41 42 47 48 50 55 56 58 62 67 69 72 74 77 84 86 90 91}	31	-3.9430	0.9665	3574.2822
5	{3 4 5 8 9 11 12 17 19 29 34 35 38 46 52 53 55 59 63 66 72 75 77 78 79 87 92}	27	-3.8867	0.9550	2791.9582
Average value		28	-3.8827	0.9602	3665.1812

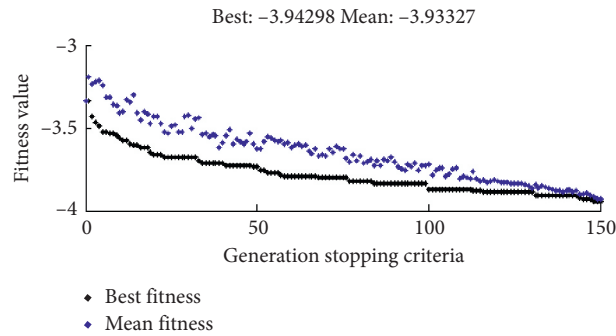


FIGURE 11: The variation of fitness function value in a running process for experiment 3-third group.

TABLE 18: The statistical results of the Second group for experiment 3 with the SVM classifier.

Experiment times		Accuracy (%)	Sensitivity (%)	Specificity (%)	Time (s)
Reduction 1	1	92.00	87.00	97.00	21.8717
	2	97.50	97.50	97.50	21.0550
	3	98.50	98.50	98.50	20.3206
	4	98.00	99.00	97.00	22.1164
	5	99.25	100.00	98.50	27.2536
	Average value	97.05	96.40	97.70	22.5235
Reduction 2	1	94.00	88.50	99.50	23.3123
	2	95.75	97.50	94.00	24.3349
	3	97.50	97.00	98.00	24.4202
	4	97.75	99.00	96.50	25.6607
	5	99.00	99.50	98.50	25.9071
	Average value	96.80	96.30	97.30	24.7270
Reduction 3	1	92.75	86.50	99.00	25.2584
	2	96.25	97.50	95.00	26.2412
	3	97.75	98.00	97.50	26.0127
	4	97.75	99.00	96.50	26.8670
	5	98.75	100.00	97.50	26.5387
	Average value	96.65	96.20	97.10	26.1836
Reduction 4	1	91.50	85.50	97.50	25.3231
	2	96.25	97.50	95.00	26.4943
	3	97.50	97.00	98.00	27.5283
	4	98.00	99.50	96.50	32.2954
	5	98.25	99.50	97.00	27.7432
	Average value	96.30	95.80	96.80	27.8769
Reduction 5	1	92.00	88.00	96.00	19.5196
	2	97.00	97.00	97.00	21.4889
	3	98.25	98.00	98.50	20.3612
	4	98.50	100.00	97.00	21.3361
	5	99.00	99.00	99.00	22.5526
	Average value	96.95	96.40	97.50	21.0517



(3) *3rd Group Experiment*.  $\omega_1 = 3$ ,  $\omega_2 = 1$ ,  $\omega_3 = 0$ : The algorithm is run 5 times according to the group weights, and the results of the 5 groups are given in Table 17, including the reduction of the conditional attributes, the length of reduction, the optimal fitness value, the attribute dependency, and the time. The convergence of VPRS-GA under the variation for fitness function value for one time is shown in Figure 11.

Each reduction is classified by SVM classifier, using the method of 5-fold cross validation, through changing the training samples and test samples; the results of the five groups were obtained, including accuracy, sensitivity, specificity, and time (training samples are constructed by 800 malignant samples and 800 benign samples; testing samples are constructed by 200 malignant samples and 200 benign samples; the experiment is repeated 5 times by changing training samples and testing samples). Finally, the average values of these five groups are obtained as the final result of the reduction and shown in Table 18.

The experiment in the case of  $1 - \beta = 0.6$  unchanged, increase the weight of the  $\omega_1$ .  $\omega_1 = 3$ ,  $\omega_2 = 1$ ,  $\omega_3 = 0$ . In Table 18, the recognition accuracy of reduction 1 is over 97% only. The average recognition accuracy of the experimental group is 96.75%, and the accuracy is decreased by 0.28% compared with that in the other second groups. The three groups of experiment 3, the purpose is to verify whether the experimental accuracy is influenced by increasing the weight. The experimental results show that the accuracy of second group for experimental weight  $\{2, 1, 0\}$  compared with first group experiment when  $\{1, 1, 0\}$  is high, but the third groups of experimental weight was  $\{3, 1, 0\}$ , and the accuracy declined; therefore, the weight of  $\{2, 1, 0\}$  is the best choice for this experiment.

## 4. Conclusions

Aiming at the deficiency of the traditional rough set model, this paper proposes a new feature selection model based on genetic algorithm and variable precision rough set; by introducing the  $\beta$  value, the rigid inclusion of the approximation for the traditional rough set is relaxed, and then we design the 3 kinds of experiments by constructing the decision information table of the PET/CT feature for lung tumor ROI. The first type of experiment is the inclusion of  $1 - \beta = 0.6$ , and different values of  $\omega$  made a total of three groups of experiments; the experimental results show that the better recognition accuracy can be obtained when the weight is  $\{1, 1, 0\}$ , and the results show that the gene coding weight function has no effect on the fitness function. For the second type of experiments,  $\omega_1 = 1$ ,  $\omega_2 = 1$ ,  $\omega_3 = 0$ , according to the different values of  $\beta$  to do three groups of experiments, the results show that the recognition accuracy of  $1 - \beta = 0.6$  is the best, which shows that the larger the  $\beta$  value is, the lower approximate cardinality will be larger, then the relative accuracy will increase. For the third type of experiments,  $1 - \beta = 0.6$ ,  $\omega$  value is increased to achieve the best fitness function, in order to achieve the best results. The experimental results show that the recognition accuracy is better than the others when the weight value is  $\{2, 1, 0\}$ , so it

is better to solve the problem by increasing the proportion of attribute dependency. Through the above experiments, it is shown that the high-dimensional feature selection algorithm based on genetic algorithm and variable precision rough set can solve the multiobjective optimization problem well. However, when the fitness function and its parameters are applied in the specific application, it is necessary to analyze the specific problems.

## Data Availability

The data used to support the findings of this study are available from the corresponding author upon request.

## Conflicts of Interest

The authors declare no conflicts of interest.

## Acknowledgments

This work was supported by National Natural Science Foundation of China (Grant nos. 61561040 and 61876121), First-Class Disciplines Foundation of Ningxia (No. NXYLXK2017B09).

## References

- [1] S. Luo, D. Miao, Z. Zhang, Y. Zhang, and S. Hu, "A neighborhood rough set model with nominal metric embedding," *Information Sciences*, vol. 520, pp. 373–388, 2020.
- [2] B. Barman and S. Patra, "Variable precision rough set based unsupervised band selection technique for hyperspectral image classification," *Knowledge-Based Systems*, vol. 1936, Article ID 105414, 2020.
- [3] Y. Chenyi and L. Jinjin, "Approximate attribute reduction under variable precision rough set  $\beta$ ," *Journal of Shandong University*, vol. 11, pp. 17–21, 2011.
- [4] S. Xiaowei, *Research on Hierarchical Model of Attribute Reduction in Variable Precision Rough Set*, Central South University, Changsha, China, 2013.
- [5] Z. Jie and W. Jiayang, "Analysis of reduction feature of variable precision rough set model," *Computer Application Research*, vol. 7, pp. 12–15, 2007.
- [6] Z. Pei and Z. Qinghua, "FCM clustering algorithm based on variable precision rough set," *Journal of Shanxi University*, vol. 3, pp. 342–348, 2016.
- [7] C. Hao and Y. Junan, "Attribute kernel and minimum attribute reduction algorithm of variable precision rough set," *Acta Sinica Sinica*, vol. 5, pp. 1011–1017, 2012.
- [8] S. Xu, X. Yang, H. Yu, D.-J. Yu, J. Yang, and E. C.C. Tsang, "Multi-label learning with label-specific feature reduction," *Knowledge-Based Systems*, vol. 104, pp. 52–61, 2016.
- [9] I. Maryam and G. Hassan, "Feature space discriminant analysis for hyperspectral data feature reduction," *ISPRS Journal of Photogrammetry and Remote Sensing*, vol. 102, pp. 1–13, 2015.
- [10] S. Q. Wang, C. Y. Gao, C. Luo, G. M. Zheng, and Y. N. Zhou, "Research on feature selection/attribute reduction method based on rough set theory," *Procedia Computer Science*, vol. 154, pp. 194–198e, 2019.
- [11] A. W. Omar, M. Azzam, O. Hadi, and B. Jamal, "CEAP: SVM-based intelligent detection model for clustered vehicular ad

- hoc networks,” *Expert Systems with Applications*, vol. 50, pp. 40–54, 2016.
- [12] H. Lee and Y.-P. P. Chen, “Image based computer aided diagnosis system for cancer detection,” *Expert Systems with Applications*, vol. 42, no. 12, pp. 5356–5365, 2015.
  - [13] J. A. Guy and P. L. Harold, “After detection: the improved accuracy of lung cancer assessment using radiologic computer-aided diagnosis,” *Academic Radiology*, vol. 23, no. 2, pp. 186–191, 2016.
  - [14] E. Kiyonori, T. Shodayu, J. Binghu et al., “Pleural invasion by peripheral lung cancer: prediction with three-dimensional CT,” *Academic Radiology*, vol. 3, pp. 310–319, 2015.
  - [15] B. Koohestani, “A crossover operator for improving the efficiency of permutation-based genetic algorithms,” *Expert Systems with Applications*, vol. 1511, Article ID 113381, 2020.
  - [16] N. K. Lee, X. Li, and D. Wang, “A comprehensive survey on genetic algorithms for DNA motif prediction,” *Information Sciences*, vol. 466, pp. 25–43, 2018.
  - [17] S. Shibao and Y. Leilei, “Research on variable precision rough set model and its application,” *Computer Engineering and Application*, vol. 07, pp. 10–13, 2009.
  - [18] T. Xiaolong, *Several Problems of Multi Granularity Variable Precision Rough Set*, Guangxi University For Nationalities, Nanning, China, 2015.
  - [19] W. Xueming, *Research on Several Rough Set Models and Neural Network*, University of Electronic Science and Technology of China, Chengdu, China, 2013.
  - [20] T. Sun, J. Wang, X. Li et al., “Comparative evaluation of support vector machines for computer aided diagnosis of lung cancer in CT based on a multi-dimensional data set,” *Computer Methods and Programs in Biomedicine*, vol. 111, no. 2, pp. 519–524, 2013.
  - [21] Z. Yang, T. Ouyang, X. Fu, and X. Peng, “A decision-making algorithm for online shopping using deep-learning-based opinion pairs mining and q -rung orthopair fuzzy interaction Heronian mean operators,” *International Journal of Intelligent Systems*, vol. 35, no. 5, pp. 783–825, 2020.
  - [22] W. Chen, C. Lin, C. Li et al., “Tracing the evolution of 3D printing technology in China using LDA-based patent abstract mining,” *IEEE Transactions on Engineering Management*, vol. 36, pp. 1–11, 2020.

## Research Article

# Reactive Strategies in the Multiproject Scheduling with Multifactor Disruptions

Weixin Wang <sup>1</sup>, Jiafu Su <sup>2</sup>, Jin Xu <sup>1</sup> and Xianlong Ge <sup>3</sup>

<sup>1</sup>Research Centre for International Business and Economics, International Business School, Sichuan International Studies University, Chongqing 400031, China

<sup>2</sup>National Research Base of Intelligent Manufacturing Service, Chongqing Technology and Business University, Chongqing 400067, China

<sup>3</sup>Economics and Management School, Chongqing Jiaotong University, Chongqing 400074, China

Correspondence should be addressed to Jiafu Su; [jiafu.su@hotmail.com](mailto:jiafu.su@hotmail.com)

Received 3 February 2020; Accepted 29 April 2020; Published 30 May 2020

Guest Editor: Yi Su

Copyright © 2020 Weixin Wang et al. This is an open access article distributed under the Creative Commons Attribution License, which permits unrestricted use, distribution, and reproduction in any medium, provided the original work is properly cited.

Multiproject scheduling aims at the generation of the baseline schedules, which has been studied for several years with the goal of minimizing the total cost of the project. In this paper, we analyzed the impact of network structure disruption, activity disruption, and resource disruption on scheduling scheme, respectively; this problem is related to the disruptions in scheduling process, which leads to a deviation between actual scheduling and baseline scheduling. The mode of the related activities is changed and the start time is reset. Because it is a NP-hard problem and involves a large number of activities, the dual population genetic algorithm is designed to solve this problem. From the results of case analysis, we find that single disruption on scheduling was local, when there was no resource conflict. While multifactor disruptions have greater effect on duration and total cost, multifactor disruptions would affect each other, so it was more complicated.

## 1. Introduction

During the execution of a project, disruptions can occur, which cause the delay of activities or change of resource extent. Examples of such disruptions are bad weather, equipment failure, etc. In view of these problems, scholars analyzed influences of interference factors on project scheduling problem. Zhao et al. [1] studied the flow-shop scheduling problem with random machine breakdowns by using the proactive scheduling theory. Chu et al. [2] studied the proactive scheduling problem of emergency response in mass casualty incident, and the objective is fatality minimization. Flexible job shop scheduling problems were transformed into the proactive scheduling problem and a genetic algorithm (GA) was designed to solve the problem. Ferrucci and Bock [3] studied the proactive real-time routing problem that applies multiple profiles, and request profiles were automatically identified. Lamas and Demeulemeester [4] developed a new procedure for proactive

project scheduling problem under resource-constrained condition, and the reactive policy was designed which considers stochastic activity duration. Davari and Demeulemeester [5] studied proactive and reactive project scheduling problem that considers selection-based reactions and buffer-based reactions and indicated that the contribution of other reactions is limited. Ning et al. [6] analyzed the effects of key parameters such as the activity duration variability, the deadline, and so on. A comprehensive optimization model is proposed in order to analyze cash flow gap of contractors. In the stage of proactive scheduling, the time buffers are added to the baseline scheme, and when the disruption occurred, the reactive scheduling is constructed. Shen et al. [7] analyzed dynamic software project scheduling problem by using the proactive rescheduling method, a dynamic scheduling model was established, which considers cost, duration, and robustness, and a multiobjective evolutionary algorithm was designed. Li et al. [8] proposed robust proactive project scheduling with uncertain activity

time and cost and then proposed to minimize the expected total construction time by control activity's starting time and mode. They studied the stochastic discrete time-cost trade-off project scheduling problem, and a proactive scheduling model was proposed for the SDTCTP-B based on robust optimization theory. Ivanov and Sokolov [9] proposed a new approach to supply chain scheduling in order to answer the uncertainty, and the adaptive scheduling was designed in order to feed dynamic changes back into the scheduling process. Liu et al. [10] analyzed a hybrid rescheduling technique in the supply chain environment, and a new strategy with event and periodic driven methods was proposed in order to improve the stability and robustness in the supply chain. Xia et al. [11] studied the project scheduling problem of speed optimization and cargo allocation, which considered maximizing total profits. Wang et al. [12] analyzed multiproject scheduling problem with disruptions and proposed proactive and reactive scheduling strategies. Servranckx and Vanhoucke [13] introduced a new method for the reactive project scheduling, and several revision plans indicate that a series of decisions are created for coping with unexpected changes; we can choose an optimal revision plan at the decision point so that it minimizes the cost. Davari and Demeulemeester [14] proposed the proactive and reactive resource-constrained project scheduling problem with stochastic durations, the baseline schedule cost and a series of reactions costs are considered, and proactive and reactive policies are introduced to solve the integrated problems. Proactive and reactive project scheduling to minimize cash flow gap was proposed by Ning et al. [6], and two hybrid metaheuristic algorithms were developed to solve this problem. Two reactive scheduling models with different objectives were designed by Zheng et al. [15], and three heuristic algorithms were developed. Lamas and Demeulemeester [4] introduced a new procedure for generating a baseline schedule for the proactive resource-constrained project scheduling problem, a new robustness measure was defined, and a branch-and-cut method was proposed to solve this problem. The main principles of proactive and reactive scheduling were analyzed by Vonder et al. [16], in order to revise the baseline scheduling. Lambrechts et al. [17] considered the uncertainty of resource availability, targeting the minimization of the absolute difference of the sum of the start times of each activity in actual scheduling and baseline scheduling, and the RCPSP proactive and reactive scheduling strategy was proposed. Above research on scheduling methods indicates that scheduling stability is enhanced by a setting time buffer or resource buffer because of the constraints concerning resource availability and the time window during the scheduling process. But it will lead to a longer duration or excessive occupancy of resources. When an interruption occurs, the baseline scheme will be infeasible or lead to resource conflicts between activities, and then a reactive scheduling strategy is designed to solve this problem.

Some previous research showed that the project activity is interrupted, and the reactive strategies are put into service, in order to recover the project operation as soon as possible. Therefore, the efficiency and the cost of the scheduling

process had been affected by the optimal and worst reactive scheduling. In the actual project execution, reactive scheduling strategy performs better than proactive scheduling strategy, so the reactive scheduling strategy is more practical [18]. Various types of disruptions are the main factors, which affect the project progress [19]. Domestic and foreign scholars have studied the interference management problems in different scenarios. Sawik [20] proposed a novel two-period modeling approach for supply chain disruption mitigation and a multiperiod approach is compared. Philip [21] and Hong-Minh et al. [22] analyzed the dynamical supply chain scheduling problem, and coping strategy was proposed to recover normal operation. Li et al. [23] and Hishamuddin et al. [24] analyzed real-time recovery in vehicle scheduling problem; the final goal is to recover the negative effects of uncertain events. Hur et al. [25] analyzed project scheduling problem under uncertain environment, which can be solved through real-time adjustment in the start time of interrelated activities. Al-Fawzan and Haouari [26] analyzed the influence of schedule robustness on resource-constrained project scheduling, and a biobjective optimization model was established, which considers robustness maximization and makespan minimization. Zhu et al. [27] analyzed the types of disruptions, and the classification scheme was proposed; the aim is to minimize the deviation between actual scheduling and baseline scheduling at minimum cost. Jian et al. [28] and Su and Sun [29] investigated the uncertainty of demand in a closed-loop supply chain, and the proposed mathematical model helps maximize total profit.

Although there has been great progress in the research of interference-facing RCPSPs (resource-constrained project scheduling problems), there are still many practical problems needed to be further studied by experts and scholars. Most of them considered single goal such as minimal cost or robustness [12, 30–32]; this paper comprehensively considered the above problems and found that identifying and quantifying the disruptions of multiproject scheduling is important to the problems. The interruption of multiproject scheduling comes from the internal and external of the scheduling system, which may be caused by many factors. Interruption of the disturbing incident led to the implementation of multiproject scheduling which deviated from the baseline scheduling scheme; in order to reduce the impact of disruptions on multiproject scheduling, we analyze the impact of network structure disruption, activity disruption, and resource disruption on scheduling system, respectively. Multiple execution modes of activities are set. When a disruption occurred, related activities are disturbed and the baseline scheduling scheme becomes unavailable, so the project cannot be finished on time, and the reactive strategy is a way to solve this problem. In reactive strategies, the optimization model is established in order to minimize the deviation between actual scheduling and baseline scheduling. When the interference occurs, the disturbed activities set is constructed by the unexecuted and ongoing activities, the execution modes are changed, and the start times are reset for these activities. The structure of this article is as follows. In Section 2, we introduce multiproject



scheduling with multifactor disruptions, and the optimization model for the scheduling with disruptions is established. Section 3 designs dual population genetic algorithm to solve this problem. In Section 4, case analysis of the model and algorithm was carried out, and dual genetic algorithm was tested from different aspects. In Section 5, the conclusions of this paper are presented.

## 2. Problem Description

We may encounter different disruptions in the execution, such as project network disruption, resource disruption, and activity disruption. For project network disruption, the predecessor and successor relationship of network activity determines the order of activities, and the original project network structure will be changed by new activity added or original activity reduced [12, 33]. Resource disruption implies that the shortage of resources will affect the duration of all subsequent activities. Activity disruption occurs mainly due to the shortage of resources and excess resources. The multiproject scheduling with multifactor disruptions is complicated, and according to the impact of disruptions, the baseline scheduling scheme is adjusted. At normal state, the objective of the reactive scheduling scheme is to minimize the negative impact of the disruptions. Because this paper analyzes the influence of disruptions, project duration deviation and the cost of changed execution mode are considered. When the disruption occurs, our research object is unexecuted activities or ongoing activities. An activity set is composed of unexecuted activities and ongoing activities. The baseline scheme is not feasible or there is an obvious deviation between the baseline scheme and the actual scheme, which had been affected by disruptions. We not only need to make a new scheduling scheme as soon as possible but also need to consider the optimization goal. In this paper, we used a research method based on activity, and the multiproject is expressed as an AoN (activity-on-node) network. A project contains  $N$  subprojects, and the duration and resource requirements of each activity and precedence relation are known. The symbols used in this article are defined as follows.

Because each objective function value has different units and dimensions, these targets need to make indexes dimensionless. The value in the formula is obtained by the dimensionless method for each objective function; the specific formula is as follows:

$$\begin{aligned} f_1^* &= \frac{(f_1 - f_1^{\min})}{(f_1^{\max} - f_1^{\min})}, \\ f_2^* &= \frac{(f_2 - f_2^{\min})}{(f_2^{\max} - f_2^{\min})}. \end{aligned} \quad (1)$$

In order to simplify this problem, so that it is easier to build the model, we proposed the following assumptions.

*Hypothesis 1.* The optimization goal is the shortest duration limit in the benchmark multiproject scheduling.

*Hypothesis 2.* The precedence relationship between the activities is “end start.”

**2.1. Disruption Recovery Model.** When a certain activity of the project is delayed, the benchmark schedule and resource are all changed, which initiate additional cost or loss. The goal of this paper is to minimize the deviation between new scheduling plan and baseline scheduling plan, so the reactive strategies in the multiproject scheduling are proposed. In order to minimize the loss by multifactor disruptions, the disruption recovery model is established.

$$\text{Min } \omega_1 f_1^* + \omega_2 f_2^*, \quad (2)$$

$$\omega_1 + \omega_2 = 1, \quad (3)$$

$$f_1 = \sum_k r_{ijk} c_k \times y_k + \sum_j \sum_m m c_{ijm} \cdot \sum_t x_{ijmt}, \quad (4)$$

$$f_2 = \sum_{m \in M} \sum_{t \in T} t \cdot x_{ijmt}, \quad (5)$$

$$\text{s.t. } \sum_i \sum_j \sum_{EF_{jm}}^{LF_{jm}} x_{ijmt} = 1, \quad (6)$$

$$\sum_i \sum_j \sum_{EF_{jm}}^{LF_{jm}} t \cdot x_{ijmt} \leq \sum_i \sum_j \sum_{EF_{jm}}^{LF_{jm}} t \cdot x_{i(j+1)mt} - t d_{ijm}, \quad (7)$$

$$\sum_i \sum_{m=1}^M \sum_{EF_{jm}}^{LF_{jm}} r_{ijmk} \cdot x_{ijmk} \leq R_k, \quad (8)$$

$$\sum_i \sum_{m=1}^M \sum_{EF_{jm}}^{LF_{jm}} r_{ijmn} \cdot x_{ijmn} \leq R_n. \quad (9)$$

Equation (2) represents the objective function, that is, the sum of the duration deviation and cost deviation was minimized, equation (3) indicates the sum of weights, equation (4) indicates the sum of the cost of increased resource and the cost of changed mode, equation (5) indicates the duration deviation between new schedule planning and baseline schedule planning after the disruption, equation (6) indicates that each activity has only one completion time, equation (7) represents the predecessor and successor relationship constraint of activities in the model, equation (8) represents the constraint of renewable resources, and equation (9) shows the constraint of nonrenewable resources.

## 3. Designing Double Population Genetic Algorithm

The basic idea of a genetic algorithm (GA) comes from the fact that evolutionary biology was pioneered by Professor Holland and used to solve complex optimization problems.

We design the appropriate selection mechanism, such as replication, crossover, and mutation, to get the optimal or near-optimal solution. However, the genetic algorithm has some shortcomings such as slow convergence rate or falling into local convergence, which affects the effect of solution of the algorithm [34]. In order to maintain the diversity of the population, a two-population genetic algorithm is proposed, and the two populations have the same population size POP. Population  $POP_L$  and population  $POP_R$  adopt the parallel operation mechanism. The two populations carry out operations such as duplication, crossover, and mutation, respectively. When the operation is completed, the individuals in both populations are randomly exchanged. In order to improve the search ability of the two-population genetic algorithm, the population  $POP_L$  is made responsible for the local search, setting a smaller crossover probability to avoid the elite individuals being destroyed. The population  $POP_R$  is mainly responsible for the global search, setting a large crossover probability to avoid the early convergence. Two populations evolved according to the unused evolutionary rules and strategies, and the parallel evolution of population  $POP_L$  and population  $POP_R$  increased the rate of evolution. The random exchanging process of the individuals of two populations improves the search performance of the algorithm. Figure 1 shows the two-population genetic algorithm flowchart.

**3.1. Coding Design.** The expression of individual performance in genetic algorithms is crucial. Among several representations, activity list notation (AL) and random key notation (RK) are widely used. These two methods embed the priority structure into the activity. In the AL method, the location of an activity determines the relative priority of the activity to others, while in the RK method, the sequence of activity scheduling is determined by the priority value of each activity. This article uses the RK notation. Vector  $\lambda$  represents the individual priority value, and  $\mu$  represents the mode list. The same encoding and decoding methods are used both in population  $POP_L$  and population  $POP_R$ . Execution mode list  $\mu$  represents individual populations of vector  $\lambda$ , and the activity's schedule is assigned in sequence. In this execution list, every activity  $i (i \in \{1, \dots, N\})$  is assigned one mode  $m_i$  and decides whether the scheduling scheme is viable relative to nonrenewable resources. The coding structure is represented as  $I = \begin{bmatrix} \lambda \\ \mu \end{bmatrix} = \begin{bmatrix} j_1, j_2, \dots, j_J \\ m_1, m_2, \dots, m_i \end{bmatrix}$ .  $ERR(\mu)$  is used to express additional resource requirement; in this algorithm, the influence of disruptions on the scheduling scheme is represented by additional resource requirement change.  $ERR(\mu) = 0$  indicates that the scheduling scheme is feasible. If  $ERR(\mu)$  is greater than 0, the scheduling scheme is not feasible.

$$ERR(u) = \sum_{j=1}^I \left( \max \left( 0, \sum_{i=1}^N (r_{ijm}^v - R^p(\eta)) \right) \right). \quad (10)$$

**3.2. Initial Population.** The first step of dual population genetic algorithm is to design a left-justified scheduling scheme  $POP_L$ . Random key  $\lambda$  is generated randomly, and execution mode  $m_i$  for each activity  $i$  is generated by using random selection. In order to minimize the number of unenforceable solutions in the initial population, the non-executable solutions are converted to executable solutions in the process of local search. If the values of  $ERR(\mu)$  are still the same or similar, then we change the execution mode of this activity. This step is repeatedly executed until the assigned mode is feasible, that is,  $ERR(\mu) = 0$ , or reaches the maximum number of tests.

**3.3. Fitness Function.** Fitness function is the basis to evaluate the merits of chromosome. It is important to the convergence speed and the quality of solution of the two-population genetic algorithm. The original intention of the algorithm design is to minimize the deviation between the newly generated scheduling scheme and the benchmark scheme, that is, minimize the influence of disruptions on the project scheduling. Because the population contains unenforceable programs, the unenforceable programs must be penalized or they will be replaced in the population as feasible implementation program. Therefore, the fitness function which has the penalty function is better. In the dual population genetic algorithm, excellent fitness function can improve the performance of the algorithm. If the scheduling scheme is feasible, the fitness function is equal to the objective function, that is,  $fit(t) = Z(t)$ , and then the list of vector  $\lambda$  and mode  $\mu$  will be obtained. If the mode is infeasible, the fitness function is equal to the objective function plus the  $ERR(\mu)$  value of the mode list  $\mu$ . The bigger the fitness is, the better the quality of the scheduling scheme is. The fitness function of dual population genetic algorithm is as follows:

$$f(t) = \begin{cases} z(t), & ERR(\mu) = 0, \\ z(t) + ERR(\mu), & ERR(\mu) \neq 0. \end{cases} \quad (11)$$

**3.4. Selection Operator.** The population  $POP_L$  is mainly responsible for the local search, while the population  $POP_R$  is mainly responsible for the global search; therefore, the two populations use different selection methods to perform the selection operation, respectively. The league selection mechanism is adopted by the high individuals that have been selected, which enter the next generation. This operation is repeatedly executed until the number of individuals entering the next generation meets the required number. The population  $POP_L$  is generated by using the roulette wheel selection mechanism; the roulette wheel selection mechanism is closely related to the value of the individual fitness, and high individuals are selected with high probability, while low individuals are selected with low probability.

**3.5. Crossover Operator.** The sequence cross-operation mode is adopted by the population  $POP_R$ , two gene points are selected from its parents randomly, the gene string between



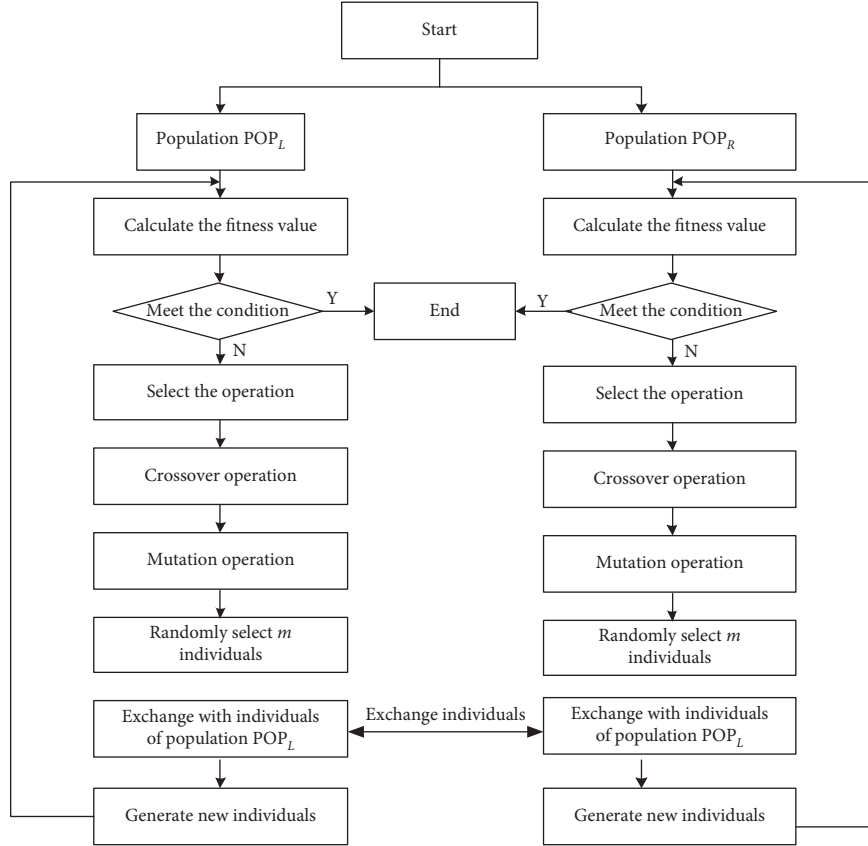


FIGURE 1: Flowchart of dual population genetic algorithm.

these two gene points is copied to progeny chromosome 1, and the corresponding gene is removed from parent 2 at the same time. The retained genes are filled in the corresponding positions of chromosome 1. The cross-operation mode is adopted by the population  $POP_L$ . Several genes are selected from parent 1 randomly, which is treated as the corresponding gene of the progeny chromosome, while the selected gene coding of parent 2 is deleted at the same time. The retained genes are filled in the corresponding positions, and then a new chromosome is generated.

**3.6. Mutation Operator.** Mutation method of the population  $POP_L$  is different from the mutation method of population  $POP_R$ . Mutation operations are performed separately. Inversion mutation is adopted by the population  $POP_R$ . This gene fragment of the chromosome is selected randomly, and the gene string is inverted. The mutation operation of population  $POP_R$  is shown in Figure 2.

Two gene sites are selected randomly from the population  $POP_L$  by using exchange mutation mode, and the value of gene coding is exchanged, in order to generate a new chromosome.

**3.7. Termination Conditions.** In dual population genetic algorithm, parent population is replaced by the progeny population. The size of population will remain unchanged. The principle of the survival of the fittest is followed in

replacement stage. For each individual  $i$ , who is already replaced from population, the parent is selected and a new individual is generated. Even if there is a deteriorating outcome, offspring with the highest fitness value is selected in the population, who will replace individual  $i$ . However, for the high-quality scheduling scheme to be selected, an individual corresponds to the best completion time of a scheduling scheme, that means it does not execute the replacement operation. When dual population genetic algorithm has been executed until a specified evolutionary generation, we need to stop operating and output the corresponding result.

## 4. Case Analysis and Results

This paper analyzed the impact of dynamic changes in customer needs (such as temporary increase orders) on multiproject scheduling, established an optimized model, and used two-population genetic algorithm for simulation test. In this case, each activity represents the corresponding process, and there are total twenty-eight activities including virtual start activities and virtual end activities, and three kinds of resources are needed. The predecessor and successor relationship is shown in Figure 3. Indirect cost of unit duration  $c = 4$ , and the unit prices of the three kinds of resources are, respectively, 3, 3, and 5. Table 1 shows the relevant information for each activity in the baseline scenario, including the execution pattern of the 28 activities

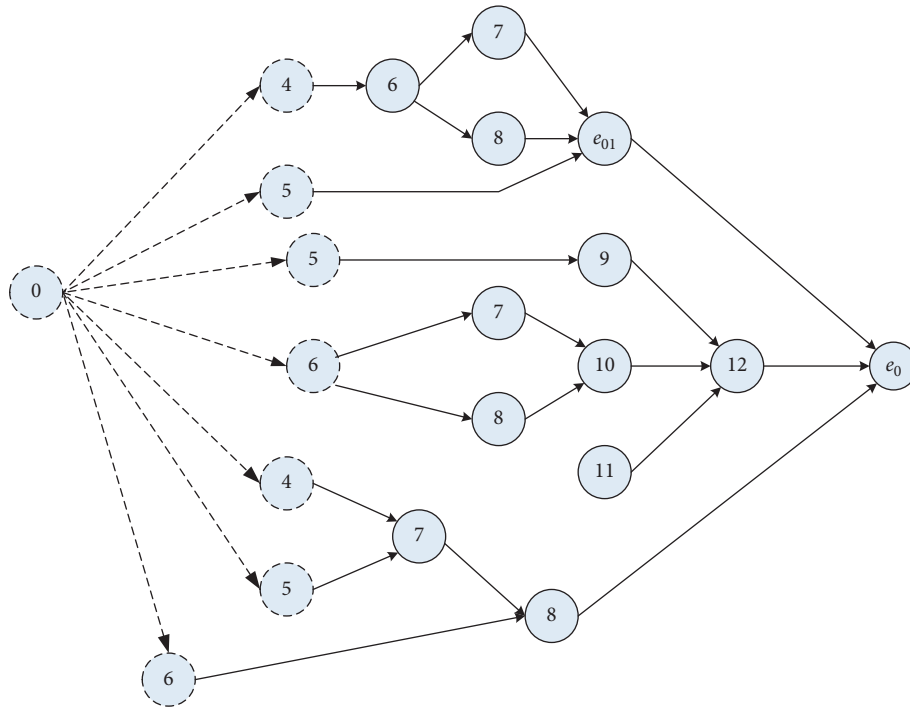


FIGURE 2: The new network structure after disruptions.

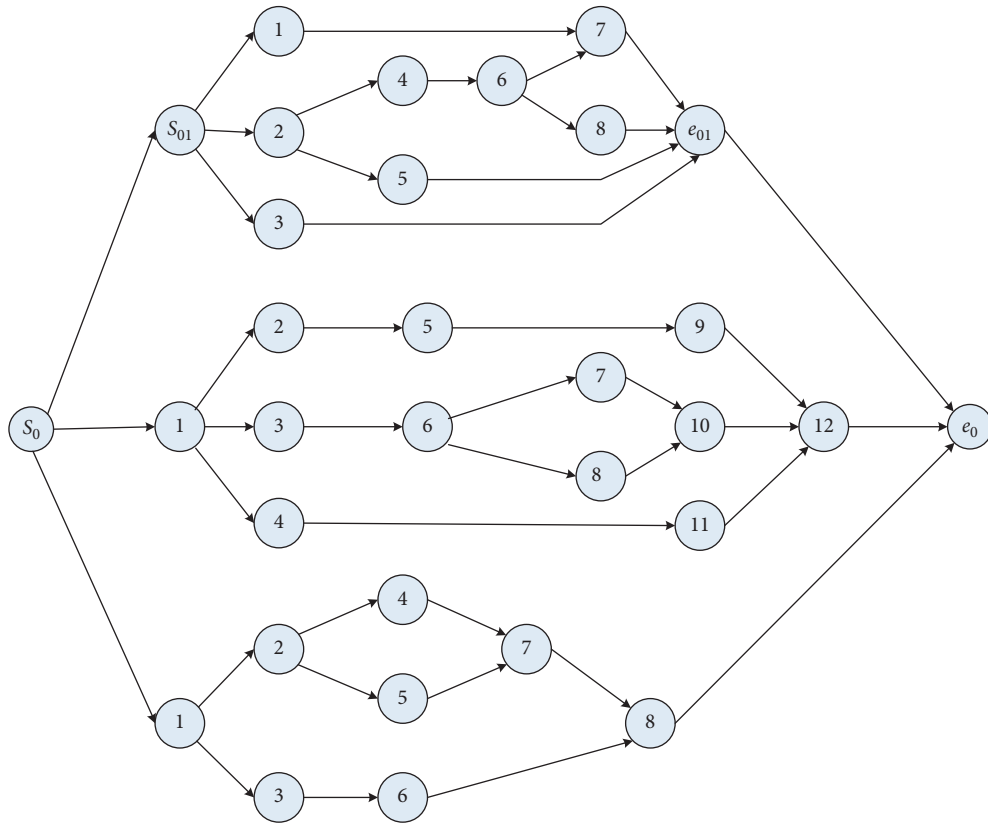


FIGURE 3: The network structure of baseline schedule plan.

(three execution modes per activity), the duration of the project, and the type and amount of resources used. According to the project activity relation in Figure 3, the network

structure diagram of the project can be determined. The resources in multiproject baseline scheduling scheme are, respectively,  $R_1 = 63$ ,  $R_2 = 58$ , and  $R_3 = 52$ . The baseline scheduling

TABLE 1: The symbols used in this article.

---

$i$	indicates that there are $i$ subprojects in multiple projects
$j$	indicates the number of activities in each subproject
$f_1$	indicates the cost of changed mode
$f_2$	indicates the duration deviation
$\omega_1$	represents the weight of project change cost
$\omega_2$	represents the weight of the duration deviation
$r_{ijm}$	represents the demand amount of renewable resources of the activity $j$ in the subproject $i$
$y_k = 1$	represents resource $k$ is selected; $y_k = 0$ represents others
$m$	represents the execution mode
$mc_{ijm}$	indicates the cost of changed execution model of the activity $j$ in the subproject $i$
$x_{ijmt} = 1$	represents the activity is completed at time $t$ of the activity $j$ in the subproject $i$
$x_{ijmt} = 0$	represents others
$r_{ijnm}$	indicates the demand amount of renewable resources $n$ of the activity $j$ in the subproject $i$
$r_{ijnk}$	indicates the total amount of nonrenewable resources $k$ of the activity $j$ in the subproject $i$
$d_{ijm}$	indicates the duration of the activity $j$ of the subproject $i$ under the execution mode $m$
$EF_{jm}$	represents the earliest start time of the activity $j$ of the subproject $i$ under the execution mode $m$
$LF_{jm}$	represents the latest start time of the activity $j$ of the subproject $i$ under the execution mode $m$
$R_k$	indicates the total quantity of nonrenewable resource $k$
$R_n$	indicates the total quantity of renewable resource $n$

---

is  $\prod^b = (S^b, X^b)$ , the planned start time of the project is  $S^b = \begin{pmatrix} 0, 0, 0, 20, 20, 36, 48, 48, 0, 11, 11, 11, 27, 24, 31 \\ 31, 48, 46, 20, 59, 0, 12, 12, 31, 31, 24, 44, 55 \end{pmatrix}$ , and the execution mode is  $X^b = \begin{pmatrix} 1, 2, 2, 2, 1, 1, 1, 2, 1, 1, 2, 1, 2, 2 \\ 1, 1, 1, 2, 2, 2, 1, 2, 2, 1, 1, 1, 2 \end{pmatrix}$ .

#### 4.1. Case Analysis of Single Disruption

**4.1.1. Single Disruption of Project Network.** During the execution of the project, due to the changing requirements of the customer, we need to adjust the baseline schedule. The activity A is added between the activity 4 and activity 6 in subproject1, the duration of the activity A is 9, and the resource demand amount of the three kinds of resources is, respectively, 8, 6, and 7. The new project network after disruption is shown in Figure 4.

According to the logical constraint relationship of activity A, it cannot be started before activity 4 is completed. A new network structure is formed by unexecuted activities and ongoing activities. The start time of activity A is 41. By assigning constraints (3)–(9) to objective function (2), the multiproject scheduling model is established, and then MATLAB is invoked by Java to solve the problem. Assume the population size  $\text{Popsiz} = 50$  and let evolution algebra  $\text{Maxgen} = 50$ ; according to the optimal result obtained after 50 times of operation, the comparative results are obtained as shown in Table 2.

The new inserted activity A has no influence on other subprojects, but it affects subsequent activities. We compare the new schedule with the baseline schedule in Table 3. In new schedule, three activities of scheduling mode are adjusted. The total duration is extended by 5, while the total cost increased by 162.

**4.1.2. Single Disruption of Activity.** In the process of project scheduling, the delay of one or more activities leads to the delay of the entire project. Activity 6 in subproject3 needs rework. When the delayed interference occurs in activity 6, all subsequent activities are affected. So after activity

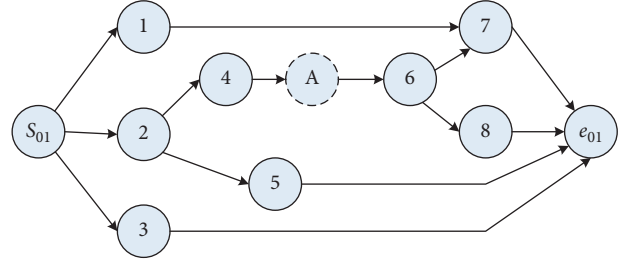


FIGURE 4: The new network structure after adding activity A.

TABLE 2: Comparative results of baseline scheduling scheme and new scheduling scheme.

---

Subproject1	Baseline scheduling scheme					New scheduling scheme				
	$M$	Duration	$R_1$	$R_2$	$R_3$	$M$	Duration	$R_1$	$R_2$	$R_3$
1	1	13	6	7	9	1	13	6	7	9
2	2	20	12	11	4	2	20	12	11	4
3	2	12	7	0	15	2	12	7	0	15
4	2	16	8	2	12	2	16	8	2	12
5	1	12	13	13	12	1	12	13	13	12
6	1	12	13	2	12	3	7	15	11	17
7	1	8	7	12	6	2	6	9	12	9
8	1	11	6	6	4	2	9	12	11	12

---

disruption, activity  $6^\#$  is added behind activity 6. This is similar to the disruption caused by adding an activity in network structure in the previous section, while the difference is that the priority of activity  $6^\#$  is higher than all unexecuted activities. The new network structure is shown in Figure 5. The completion time of activity 6 is used as the starting point, and a new network structure is formed by unexecuted activities and ongoing activity  $2^\#$ . Activity 0 is a virtual start activity, its duration and resource amount are 0, and its start time is 25. The parameter setting of the dual population algorithm is the same as that in Section 4.2.1.

TABLE 3: The information of baseline scheduling scheme.

	$M$	Duration	$R_1$	$R_2$	$R_3$	$M$	Duration	$R_1$	$R_2$	$R_3$	$M$	Duration	$R_1$	$R_2$	$R_3$
<i>Subproject1</i>															
1	1	13	6	7	9	2	8	11	10	12	3	7	15	10	14
2	1	22	6	11	4	2	20	12	11	4	3	13	12	13	4
3	1	15	7	0	8	2	12	7	0	15	3	9	9	5	15
4	1	19	8	2	5	2	16	8	2	12	3	13	13	6	12
5	1	12	13	13	12	2	9	16	20	11	3	5	18	23	12
6	1	12	13	2	12	2	8	13	9	15	3	7	15	11	17
7	1	8	7	12	6	2	6	9	12	9	3	7	9	14	10
8	1	11	6	6	4	2	9	12	11	12	3	6	15	14	14
<i>Subproject2</i>															
1	1	11	12	2	11	2	7	12	12	11	3	6	14	15	11
2	1	16	12	7	13	2	11	13	12	12	3	9	13	16	12
3	1	17	2	6	4	2	13	2	12	11	3	11	7	12	11
4	1	9	15	12	10	2	5	15	12	15	3	5	16	15	15
5	1	23	7	10	9	2	21	10	12	9	3	17	11	16	11
6	1	10	6	6	12	2	7	12	13	12	3	6	15	13	13
7	1	15	13	13	12	2	8	13	13	16	3	7	16	13	18
8	1	13	13	13	11	2	10	15	15	11	3	8	15	16	19
9	1	11	12	12	12	2	7	15	12	14	3	5	18	15	16
10	1	15	6	6	12	2	10	12	12	13	3	9	13	13	14
11	1	11	10	12	10	2	9	13	12	10	3	9	15	16	12
12	1	19	11	10	11	2	17	11	13	11	3	12	13	15	13
<i>Subproject3</i>															
1	1	12	12	13	12	2	7	20	17	12	3	6	20	19	16
2	1	22	10	10	11	2	19	12	12	11	3	14	16	12	14
3	1	15	9	6	11	2	12	14	6	11	3	11	17	8	13
4	1	13	13	13	12	2	11	16	18	12	3	10	19	19	19
5	1	9	13	11	12	2	8	17	11	15	3	7	19	17	16
6	1	11	12	12	7	2	6	18	18	9	3	4	19	20	15
7	1	11	12	2	8	2	10	19	5	13	3	6	19	9	16
8	1	10	5	8	10	2	9	5	11	13	3	8	9	16	17

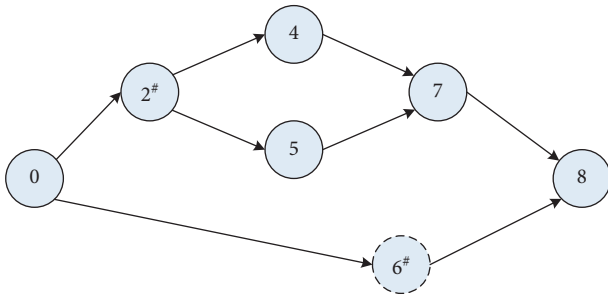


FIGURE 5: The new network structure after single disruption.

According to the optimal result obtained after 50 times of operation, the relevant data are summarized, and the information of the new schedule scheme is shown in Table 4.

Activity 6<sup>#</sup> has no influence on other subprojects, but it affects subsequent activities. We compare the new schedule with the baseline schedule in Table 4. In new schedule, four activities of scheduling mode are adjusted. The total duration is unchanged, while the total cost increased by 197.

**4.1.3. Single Disruption of Resource.** In this section, we analyze the influence of resource reduction on the scheduling process. Suppose that at  $t = 30$ , the total amount of resource  $R_1$  in the project has been reduced by 20. The

TABLE 4: Comparative results of baseline scheduling scheme and new scheduling scheme.

Subproject3	Baseline scheduling scheme					New scheduling scheme				
	$M$	Duration	$R_1$	$R_2$	$R_3$	$M$	Duration	$R_1$	$R_2$	$R_3$
1	1	12	12	13	12	1	12	12	13	12
2	2	19	12	12	11	2	19	12	12	11
3	2	12	14	6	11	2	12	14	6	11
4	1	13	13	13	12	3	7	19	19	19
5	1	9	13	11	12	2	6	17	11	15
6(6#)	1	11	12	12	7	3	5	19	17	16
7	1	11	12	2	8	2	8	19	5	13
8	2	7	5	11	13	3	6	9	16	17

reduction resource amount may affect activities 7, 8, 9, 10, 11, and 12 in subproject2 and other subprojects. A new network structure is formed by unexecuted activities and ongoing activities 5 and 6. The priority of activities 5 and 6 are higher than all unexecuted activities. The parameter setting of the dual population algorithm is the same as that in Section 4.2.1. According to the optimal result obtained after 50 times of operation, the relevant data are summarized, the information of the new schedule scheme is shown in Table 5.

In new schedule, due to the shortage of resource  $R_1$ , the duration of activities 5 and 6 is delayed, and four activities of

TABLE 5: Comparative results of baseline scheduling scheme and new scheduling scheme.

	Baseline scheduling scheme					New scheduling scheme				
	M	Duration	R <sub>1</sub>	R <sub>2</sub>	R <sub>3</sub>	M	Duration	R <sub>1</sub>	R <sub>2</sub>	R <sub>3</sub>
<i>Subproject2</i>										
1	1	11	12	2	11	1	11	12	2	11
2	1	16	12	7	13	1	19	12	12	11
3	2	13	2	12	11	2	13	2	12	11
4	1	9	15	12	10	1	9	15	12	10
5	2	21	10	12	9	1	23	7	10	9
6	2	7	12	13	12	1	10	6	6	12
7	1	15	13	13	12	2	13	13	13	12
8	1	13	13	13	11	2	13	13	13	11
9	1	11	12	12	12	1	11	12	12	12
10	2	10	12	12	13	3	9	13	13	14
11	2	9	13	12	10	3	9	15	16	12
12	2	17	11	13	11	2	17	11	13	11
<i>Subproject2</i>										
4	1	13	13	13	12	1	16	13	13	12
7	1	11	12	2	8	1	14	12	2	8

scheduling mode are adjusted. And there are resource conflicts between subprojects; activities 4 and 7 are delayed because of the shortage of resource  $R_1$ . The total duration is extended by 2, while the total cost increased by 17. For most of the unexecuted activities, the scheduling time and mode have to be adjusted. When the interference occurs, it will be more complicated to formulate a new scheduling scheme based on the baseline scheduling scheme.

**4.2. Case Analysis of Multifactor Disruptions.** During project execution, resource disruption occurs at  $t = 30$ , the total amount of resource  $R_2$  in the project is reduced by 15, and activities 4 and 5 in subproject1 are interrupted and postponed. Because of the resource contest caused by the previous disruptions, later activities will be affected and the completion time will be postponed. An activity disruption occurs at  $t = 33$ , and activity 5 in subproject3 has to be reworked. Then, activity 7 in subproject3 is postponed. A new network structure is formed by unexecuted activities and ongoing activities in multiproject. The parameter setting of the dual population algorithm is the same as that in Section 4.2.1. According to the optimal result obtained after 50 times of operation, the new project network after disruption is shown in Figure 2, and the relevant data are summarized; the information of the new schedule scheme is shown in Table 6.

In new schedule, due to the shortage of resource  $R_2$ , the duration of activities 4–8 and 6 are all delayed, there are resource conflicts between subprojects, and activity 10 has to change the scheduling mode because of the shortage of resource  $R_2$ . The duration of subproject1 is extended by 6. Because activity 5 in subproject3 is reworked, activity 7 has to change the scheduling mode. The duration of subproject3 is extended by 3, while the total cost increased by 168. From the above analysis, it can be concluded that the multifactor disruptions have a greater impact on

TABLE 6: Comparative results of baseline scheduling scheme and new scheduling scheme.

	Baseline scheduling scheme					New scheduling scheme				
	M	Duration	R <sub>1</sub>	R <sub>2</sub>	R <sub>3</sub>	M	Duration	R <sub>1</sub>	R <sub>2</sub>	R <sub>3</sub>
<i>Subproject1</i>										
1	1	13	6	7	9	1	13	6	7	9
2	2	20	12	11	4	2	20	12	11	4
3	2	12	7	0	15	2	12	7	0	15
4	2	16	8	2	12	2	18	8	2	12
5	1	12	13	13	12	1	15	13	13	12
6	1	12	13	2	12	1	13	13	2	12
7	1	8	7	12	6	1	11	7	12	6
8	2	9	12	11	12	1	11	6	6	4
<i>Subproject2</i>										
1	1	11	12	2	11	1	11	12	2	11
2	1	16	12	7	13	1	16	12	7	13
3	2	13	2	12	11	2	13	2	12	11
4	1	9	15	12	10	1	9	15	12	10
5	2	21	10	12	9	2	21	10	12	9
6	2	7	12	13	12	2	7	12	13	12
7	1	15	13	13	12	1	15	13	13	12
8	1	13	13	13	11	1	13	13	13	11
9	1	11	12	12	12	1	11	12	12	12
10	2	10	12	12	13	1	15	6	6	12
11	2	9	13	12	10	2	9	13	12	10
12	2	17	11	13	11	2	17	11	13	11
<i>Subproject3</i>										
1	1	12	12	13	12	1	12	12	13	12
2	2	19	12	12	11	2	19	12	12	11
3	2	12	14	6	11	2	12	14	6	11
4	1	13	13	13	12	1	13	13	13	12
5(5#)	1	9	13	11	12	2	8	17	11	15
6	1	11	12	12	7	1	11	12	12	7
7	1	11	12	2	8	3	6	19	9	16
8	2	9	5	11	13	2	9	5	11	13

scheduling and resource disruption causes later activities to change the scheduling strategy.

**4.3. Comparative Analysis of Algorithms.** In this paper, we download the standard study from the website of project scheduling problem, <http://129.187.106.231/psplib/>, and take PSPLIB data, J10, J20, J30, J40, J60, and J90, as examples; dual population genetic algorithm, Tabu search algorithm, and genetic algorithm are tested to analyze the performance of the three algorithms. The convergence of the calculation results is shown in Table 7.

From the satisfactory solution quality (quality for short), dual population genetic algorithm was the best, genetic algorithm was better, and Tabu search algorithm was the worst. When the number of activities was small, dual population genetic algorithm and genetic algorithm were not much different, but the quality of Tabu search algorithm was worse. With the number of activities increased, the advantage of dual population genetic algorithm became obvious. So, dual population genetic algorithm is more suitable for solving multiproject reactive scheduling problems.

TABLE 7: The results of tests.

N	DGA		GA		TB	
	Cost	Time	Cost	Time	Cost	Time
J10	191.25	0.06	182.73	0.02	291.41	0.02
J20	1037.54	0.21	1027.96	0.06	2006.86	0.07
J30	2688.65	0.39	2700.44	0.14	4671.3	0.18
J40	5271.65	0.56	5329.7	0.33	9755.49	0.38
J60	12763.8	3.96	13124.6	0.72	21874.4	1.25
J90	32549.2	5.67	32718.4	2.09	49765.7	3.61

From the calculation time (time for short), the calculation time of genetic algorithm was the least. For Tabu search algorithm, with the number of activities increased, the number of the neighborhood solutions increased, so the calculation time was longer than the time of genetic algorithm. The dual population genetic algorithm had the longest calculation time; however, it was in acceptable limit. Above all, from the satisfactory solution quality and the calculation time, we know that dual population genetic algorithm was a better algorithm.

## 5. Conclusions

In this paper, the multiproject scheduling problem with disruptions was proposed. First, we analyzed the impact of network structure disruption, activity disruption, and resource disruption, respectively. The optimization model was established, and a dual population genetic algorithm was designed to solve this problem, and the following conclusions were drawn:

- (i) Based on the characteristics of multiproject scheduling problem with disruptions, we analyzed the impact of network structure disruption, activity disruption, and resource disruption on scheduling system. Dual population algorithm was designed to solve this problem, and the scheduling scheme with minimum interference was formulated. When the scheduling scheme deviated from the baseline scheduling scheme, the modes of the related activities were changed and the start time was reset, and then the best adjustment cost and project completion time were obtained.
- (ii) The impact of single disruption on scheduling was local, which often caused the duration to be extended and the total cost to be increased. If there was no resource conflict, the effect was local to subproject. While resource disruption would caused resource conflicts between subprojects, so later activities have to change scheduling mode. Multifactor disruptions have greater effect on duration and total cost, and multifactor disruptions would affect each other, so it was more complicated.
- (iii) The dual population genetic algorithm was designed to solve the problem. The performance of dual population genetic algorithm was superior when there were a large number of activities in the project. Dual population genetic algorithm improved the

evolution speed and improved the search performance of the algorithm. The global optimization ability was enhanced, and the performance of the algorithm was improved.

## Data Availability

The data used to support the findings of this study are included within the article.

## Conflicts of Interest

The authors declare that they have no conflicts of interest.

## Acknowledgments

This research was funded by Chongqing Social Science Planning Project, grant number 2016BS080, Chongqing Humanities and Social Science Research Projects, grant number 20SKGH130 and Sichuan International Studies University Scientific Research Project, grant number sisu2019044.

## References

- [1] C. Y. Zhao, Z. Q. Lu, and W. W. Cui, "Proactive and reactive scheduling optimization on flow shops with random machine breakdowns," *Journal of Zhejiang University (Engineering Science)*, vol. 50, no. 4, pp. 641–649, 2016.
- [2] X. Chu, Q. Y. Zhong, and Y. Qu, "Proactive and reactive scheduling optimization of emergency response in mass casualty incident," *Operations Research and Management Science*, vol. 25, no. 5, pp. 7–11, 2014.
- [3] F. Ferrucci and S. Bock, "Pro-active real-time routing in applications with multiple request patterns," *European Journal of Operational Research*, vol. 253, no. 2, pp. 356–371, 2016.
- [4] P. Lamas and E. Demeulemeester, "A purely proactive scheduling procedure for the resource-constrained project scheduling problem with stochastic activity durations," *Journal of Scheduling*, vol. 19, no. 4, pp. 409–428, 2016.
- [5] M. Davari and E. Demeulemeester, "Important classes of reactions for the proactive and reactive resource-constrained project scheduling problem," *Annals of Operations Research*, vol. 274, no. 1-2, pp. 187–210, 2019.
- [6] M. Ning, Z. He, N. Wang, and R. Liu, "Metaheuristic algorithms for proactive and reactive project scheduling to minimize contractor's cash flow gap under random activity duration," *IEEE Access*, vol. 6, pp. 30547–30558, 2018.
- [7] X. N. Shen, L. L. Minku, R. Bahsoon, and X. Yao, "Dynamic software project scheduling through a proactive and reactive-rescheduling method," *IEEE Transaction on Software Engineering*, vol. 42, no. 7, pp. 658–686, 2016.
- [8] H. B. Li, Z. Xu, L. Xiong, and Y. B. Liu, "Robust proactive and reactive project scheduling model for the stochastic discrete time/cost trade-off problem," *Discrete Dynamics in Nature and Society*, vol. 2015, Article ID 586087, 10 pages, 2015.
- [9] D. Ivanov and B. Sokolov, "Dynamic supply chain scheduling," *Journal of Scheduling*, vol. 15, no. 2, pp. 201–216, 2012.
- [10] A. Liu, J. Fowler, and M. Pfund, "Dynamic co-ordinated scheduling in the supply chain considering flexible routes," *International Journal of Production Research*, vol. 54, no. 1, pp. 322–335, 2016.



- [11] J. Xia, K. X. Li, H. Ma, and Z. Xu, "Joint planning of fleet deployment, speed optimization, and cargo allocation for liner shipping," *Transportation Science*, vol. 49, no. 4, pp. 922–938, 2015.
- [12] W. Wang, X. Ge, L. Li, and J. Su, "Proactive and reactive multi-project scheduling in uncertain environment," *IEEE Access*, vol. 7, pp. 88986–88997, 2019.
- [13] T. Servranckx and M. Vanhoucke, "Strategies for project scheduling with alternative subgraphs under uncertainty: similar and dissimilar sets of schedules," *European Journal of Operational Research*, vol. 279, no. 1, pp. 38–53, 2019.
- [14] M. Davari and E. Demeulemeester, "The proactive and reactive resource-constrained project scheduling problem," *Journal of Scheduling*, vol. 21, no. 2, pp. 211–237, 2019.
- [15] W. Zheng, Z. He, N. Wang, and T. Jia, "Proactive and reactive resource-constrained max-NPV project scheduling with random activity duration," *Journal of the Operational Research Society*, vol. 69, no. 1, pp. 115–126, 2018.
- [16] S. V. D. Vonder, E. Demeulemeester, R. Leus, and W. Herroelen, "Proactive-reactive project scheduling trade-offs and procedures," *International Series in Operations Research and Management Science*, vol. 92, pp. 25–51, 2006.
- [17] O. Lambrechts, E. Demeulemeester, and W. Herroelen, "Proactive and reactive strategies for resource-constrained project scheduling with uncertain resource availabilities," *Journal of Scheduling*, vol. 11, no. 2, pp. 121–136, 2008.
- [18] C. Artigues, R. Leus, and F. T. Nobibon, "Robust optimization for resource-constrained project scheduling with uncertain activity durations," *Flexible Services and Manufacturing Journal*, vol. 5, no. 1-2, pp. 175–205, 2013.
- [19] S. Jiafu, Y. Yu, and Y. Tao, "Measuring knowledge diffusion efficiency in R&D networks," *Knowledge Management Research and Practice*, vol. 16, no. 2, pp. 208–219, 2018.
- [20] T. Sawik, "Two-period vs. multi-period model for supply chain disruption management," *International Journal of Production Research*, vol. 57, no. 14, pp. 4502–4518, 2019.
- [21] T. Philip, "Filling customer orders from multiple locations: a comparison of pooling methods," *Journal of Business Logistics*, vol. 20, no. 1, pp. 121–140, 1999.
- [22] S. M. Hong-Minh, S. M. Disney, and M. M. Naim, "The dynamics of emergency transshipment supply chains," *International Journal of Physical Distribution & Logistics Management*, vol. 30, no. 9, pp. 788–817, 2000.
- [23] C. Li, X. Qi, and D. Song, "Real-time schedule recovery in liner shipping service with regular uncertainties and disruption events," *Transportation Research Part B: Methodological*, vol. 93, pp. 762–788, 2016.
- [24] H. Hishamuddin, R. A. Sarker, and D. Essam, "A recovery model for a two-echelon serial supply chain with consideration of transportation disruption," *Computers & Industrial Engineering*, vol. 64, no. 2, pp. 552–561, 2013.
- [25] D. Hur, V. A. Mabert, and K. M. Bretthauer, "Real-time schedule adjustment decisions: a case study," *Omega*, vol. 32, no. 5, pp. 333–344, 2004.
- [26] M. A. Al-Fawzan and M. Haouari, "A bi-objective model for robust resource-constrained project scheduling," *International Journal of Production Economics*, vol. 96, no. 2, pp. 175–187, 2005.
- [27] G. Zhu, J. F. Bard, and G. Yu, "Disruption management for resource-constrained project scheduling," *Journal of the Operational Research Society*, vol. 56, no. 4, pp. 365–381, 2005.
- [28] J. Jian, Y. Zhang, L. Jiang et al., "Coordination of supply chains with competing manufacturers considering fairness concerns," *Complexity*, vol. 2020, Article ID 4372603, 15 pages, 2020.
- [29] Y. Su and W. Sun, "Analyzing a closed-loop supply chain considering environmental pollution using the NSGA-II," *IEEE Transactions on Fuzzy Systems*, vol. 27, no. 5, pp. 1066–1074, 2019.
- [30] X. L. Ge, X. B. Ge, and W. X. Wang, "A path-based selection solution approach for the low carbon vehicle routing problem with time window constraint," *Applied Sciences-Basel*, vol. 10, no. 4, 2020.
- [31] J. Su, Q. Bai, and S. Sindakis, "Vulnerability of multinational corporation knowledge network facing resource loss: a super-network perspective," *Management Decision*, 2020.
- [32] Y. Su and W. Sun, "Sustainability evaluation of the supply chain with undesired outputs and dual-role factors based on double frontier network DEA," *Soft Computing*, vol. 22, no. 16, pp. 5525–5533, 2018.
- [33] J. F. Su, Y. Yang, and X. Zhang, "Knowledge transfer efficiency measurement with applications for open innovation networks," *International Journal of Technology Management*, vol. 81, no. 1-2, pp. 118–142, 2019.
- [34] F. Arıkan and Z. Güngör, "An application of fuzzy goal programming to a multi-objective project network problem," *Fuzzy Sets & Systems*, vol. 119, no. 1, pp. 49–58, 2001.

## Research Article

# Restoration Methods Selection for Wood Components of Chinese Ancient Architectures Based on TODIM with Single-Valued Neutrosophic Sets

Xiaolu. Long,<sup>1</sup> Lizhi. Liu,<sup>2</sup> Can. Xiao <sup>1</sup>, Pengfei. Cheng <sup>3,4</sup> and Chengxun. Fu<sup>4,5</sup>

<sup>1</sup>College of Architecture, Hunan University, Changsha 410082, China

<sup>2</sup>Management Committee of Xiangtan Economic and Technological Development Zone, Xiangtan 411201, China

<sup>3</sup>School of Business, Hunan University of Science and Technology, Xiangtan 411201, China

<sup>4</sup>Hunan Engineering Research Center for Intelligent Decision Making and Big Data on Industrial Development, Xiangtan 411201, China

<sup>5</sup>Hunan Valin Xiangtan Iron and Steel Co. Ltd., Xiangtan 411101, China

Correspondence should be addressed to Can. Xiao; [xiaocan@hnu.edu.cn](mailto:xiaocan@hnu.edu.cn) and Pengfei. Cheng; [1180033@hnust.edu.cn](mailto:1180033@hnust.edu.cn)

Received 19 March 2020; Accepted 27 April 2020; Published 13 May 2020

Guest Editor: Zaoli Yang

Copyright © 2020 Xiaolu. Long et al. This is an open access article distributed under the Creative Commons Attribution License, which permits unrestricted use, distribution, and reproduction in any medium, provided the original work is properly cited.

The selection of restoration methods for ancient architectures is of great significance for the protection of human cultural heritage. This paper proposes a novel restoration methods selection approach for wood components of Chinese ancient architectures, in which a multicriteria group decision-making (MCGDM) method with decision-making information is in the form of single-valued neutrosophic sets (SNNs). Firstly, it establishes an index system by comprehensively considering subjective and objective criteria. In addition, the best-worst method (BWM) and the entropy weight method are combined to produce index weights. Furthermore, the TODIM method is utilized by the single-valued neutrosophic sets to prioritize restoration methods. Finally, a specific case of wood component restoration is conducted to demonstrate the practicability of the proposed model. The robustness and effectiveness of the proposed method is verified by sensitivity analysis and comparison analysis.

## 1. Introduction

There are a large number of ancient architectural heritages with high historical, scientific, and artistic values in China. However, many of them are suffering not only from natural damage such as storms, fires, or insects but also from societal damage by rapid urbanization or inappropriate protective measures. Ancient architectures are nonrenewable, so it is important to choose appropriate restoration measures to reduce damage. The restoration for Chinese ancient architectures is a rather complex task. As the selection of restoration method is usually determined by a group of experts, it is a group decision-making problem affected by several factors such as situation of components, restoration process, restoration outcomes, and situation of commissioned restoration company.

With the development in architectural heritage protection practices, the restoration technologies have achieved rich achievements which have provided more options for the restoration of wood components of Chinese ancient architectures [1]. Although some progress has been made, there are still some issues to be addressed. Firstly, the common principles of restoration for ancient architectures include authenticity, reversibility, and minimal intervention. At present, the restoration technology of ancient buildings continues to advance, but it has not been applied scientifically and reasonably. If the repair method is not adopted properly, it will not only fail to effectively restore the ancient buildings but also cause irreversible secondary damage. Secondly, the evaluation information is usually partially. There is a lack of research on the standardization of selection process of restoration methods. Thirdly, in practice, the

restoration methods selection is often determined based on experts' own knowledge and experience, which might lead to information insufficiency. Relevant research rarely uses quantitative methods to assess the decision-making process of Chinese ancient architectures' restoration.

In summary, the motivation of this paper is to propose a novel model of restoration methods selection for wood components of Chinese ancient architectures, which should improve the scientificity and standardization of decision-making during restoration methods selection and be conducive to the protection of ancient architectures. The rest of the paper is organized as follows. In Section 2, previous studies are reviewed in brief. In Section 3, some basic concepts and definitions about neutrosophic sets are introduced. Subsequently, a restoration methods selection model for wood components of Chinese ancient architectures based on MCGDM is developed in Section 4. In Section 5, a case study is operated concretely, sensitivity analysis and comparative analysis are illustrated to verify the proposed model. Finally, Section 6 summarizes the content of the article and provides some possible directions of future study.

## 2. Literature Review

At present, a lot of restoration technologies for wood components of ancient architectures have been developed. The progress of modern technologies is mainly reflected in the use of new technical methods and new materials. For instance, Zaboklicki and Gebiski [2] generalized that polymer composite inserts (such as epoxy resin, glass, and carbon fiber) enhance the continuity of wooden beams and expand their carrying capacity. Orlando et al. [3] focused on how to repair the ends of wooden beams, which decay easily. The study of Koike [4] reviews the development of wood biomass-sourced epoxy resin systems in Japan over the years. Dourado et al. [5] and Casals et al. [6] studied repaired wood structure adopting epoxy composites. Khelifa and Celzard [7] and Baratta and Corbi [8] recommended applying carbon fibre-reinforced polymer (CFRP) or fibre-reinforced polymer (FRP) to increase the bending capacity of timber structure. In real case, different technologies have different degrees of intervention on ancient architectures, and inappropriate technological advances might lead to negative effects; therefore, the choice of restoration methods must take the nonrenewability of Chinese ancient architectures into account. Therefore, we need to develop a scientific and reasonable measure to choose the restoration method.

Recently, some related indices affecting the restoration of Chinese ancient architectures have been discussed. Existing maintenance theory believes that the best protection and maintenance method would be a combination of active and passive maintenance; however, a lack of skilled operators is an obstacle to protect ancient architectures [9]. Fregonese et al. [10] believed that monitoring the condition of ancient building structures would be helpful in finding suitable restoration schemes. Gao et al. [11] even proposed an ancient timber buildings structural health assessment method based on fuzzy-element theory improved by asymmetric proximity. Lourenço [12] mentioned the importance of

architectural characteristics such as structure and materials for the restoration of ancient architectures and pointed out that the value and authenticity of the building should be taken into consideration. By establishing the economic evaluation index system considering the cost, effect, technical, and other index for the ancient architecture protection scheme, Wang et al. [13] tried to choose a more economical ancient architecture protection scheme. Based on existing studies discussed above, they only focused on objective criteria such as component's conditions and technical methods. There are no studies considering both subjective and objective factors simultaneously, and the situation of restoration company has not been considered in the evaluation; no comprehensive index system has been established for the restoration of ancient architectures.

Neutrosophy has been introduced by Smarandache [14], whose fundamental proposition is that each concept has not only a certain degree of truth but also a degree of falsity and indeterminacy that must be considered independently from each other [15]. The neutrosophic set is similar to human thinking, reflecting the uncertainty caused by incomplete knowledge, incorrect knowledge acquisition, or random guessing [16]. Zhang et al. [17, 18] considered that the neutrosophic set is an effective tool for evaluating vague information. In the process of decision-making on the restoration methods of wood components, due to the uncertainty of actual restoration cases, experts' evaluation information is usually vague, and experts' evaluation information often represents emotional preference, which makes it difficult to be stated in an accurate quantitative form. We would better use neutrosophic numbers to describe the results of assessments [19, 20].

Methods for determining weights usually include subjective weighting methods and objective ones. In order to rank unknown weights, Rezaei [21] proposed the best-worst method (BWM) for multicriteria decision-making problem to calculate subjective weights. Compared with other methods to determine subjective weights (such as AHP), the BWM method has advantages in lesser data comparison and more consistent comparisons. However, the single use of subjective weights cannot guarantee the objectivity of evaluation results, and it will increase the difficulty in decision-makers' analysis and the possibility of errors. Hence, we shall use the entropy weight method. According to the characteristics of entropy, the entropy value shows the randomness and disorder of an index, and then, we can determine the degree of discreteness of the index. Therefore, a combination of BWM method with entropy weight method to compute index weights is necessary, which is not only based on the inherent laws of the index data but also expert experience. Thus, the result of index weights is more reliable [22].

TODIM (an acronym in Portuguese for interactive and multicriteria decision-making model) is based on the prospect theory [23]. Prospect theory [24] is considered to be the most typical behavioral decision theory and has been widely used in multicriteria decision problems [25–27]. TODIM method describes the dominance of each alternative over others fully considered the psychological behavior of decision-makers under risk [28, 29]. In order to depict the

psychological behavior of decision-makers, it is possible to modify parameters to reflect the preferences of decision-makers [30–32]. To prioritize restoration methods, we shall use the TODIM method.

From the discussion above, the purpose of this study is to design a restoration methods selection model based on TODIM with single-valued neutrosophic sets for wood components of Chinese ancient architectures. This model is designed to help experts select the most appropriate restoration method. The contributions of this research are summarized as follows: (1) developing an index system for the restoration of wood components of Chinese ancient architectures; (2) using single-valued neutrosophic weighted average operator to aggregate experts' evaluation results, which make them more comprehensive and reliable; (3) applying the BWM method and entropy weight method to determine the index weights in case of unknown criteria and index weights; (4) introducing the TODIM method to obtain the ranking orders of alternatives; and (5) demonstrating the process of the proposed model by presenting an empirical study of a particular case. Also, to verify the validity and reliability of the model, sensitivity analysis and comparison analysis are conducted.

### 3. Preliminaries

In this section, we introduce some concepts and definitions, which will be useful in developing the wood components restoration methods selection model.

**Definition 1** (neutrosophic set) (see [33]). Let  $X$  be a space of points (objects), with a generic element in  $X$  denoted by  $x$ . Then, a neutrosophic set  $A$  in  $X$  is characterized by three membership functions, including a truth-membership function  $T_A$ , an indeterminacy-membership function  $I_A$ , and

a falsity-membership function  $F_A$  and is defined as  $A = \{ \langle x, T_A(x), I_A(x), F_A(x) \rangle \mid x \in X \}$ , where  $T_A(x)$ ,  $I_A(x)$ , and  $F_A(x)$  are real standard or nonstandard subsets of  $]0^-, 1^+[$ , that is,  $T_A(x): X \longrightarrow ]0^-, 1^+[$ ,  $I_A(x): X \longrightarrow ]0^-, 1^+[$ , and  $F_A(x): X \longrightarrow ]0^-, 1^+[$ . The sum of  $T_A(x)$ ,  $I_A(x)$ , and  $F_A(x)$  is unrestricted and  $0^- \leq T_A(x) + I_A(x) + F_A(x) \leq 3^+$ .

**Definition 2** (single-valued neutrosophic set) (see [34]). Let  $X$  be a space of points (objects), with a generic element in  $X$  denoted by  $x$ . A single-valued neutrosophic set (SVNS)  $A$  in  $X$  is characterized by truth-membership function  $T_A$ , indeterminacy-membership function  $I_A$ , and falsity-membership function  $F_A$  with  $T_A, I_A, F_A \in [0, 1]$  for all  $x$  in  $X$ . The sum of three memberships of a SVNS  $A$ , for all  $x \in X$ ,  $0 \leq T_A(x) + I_A(x) + F_A(x) \leq 3$ .

**Definition 3** (see [35]). Let  $A$  and  $B$  be two single-valued neutrosophic numbers, and then the operations can be defined as follows:

- (1)  $\lambda A = \langle 1 - (1 - T_A)^\lambda, (I_A)^\lambda, (F_A)^\lambda \rangle, \lambda > 0$
- (2)  $A^\lambda = \langle (T_A)^\lambda, 1 - (1 - I_A)^\lambda, 1 - (1 - F_A)^\lambda \rangle, \lambda > 0$
- (3)  $A + B = \langle T_A + T_B - T_A \cdot T_B, I_A \cdot I_B, F_A \cdot F_B \rangle$
- (4)  $A \cdot B = \langle T_A \cdot T_B, I_A + I_B - I_A \cdot I_B, F_A + F_B - F_A \cdot F_B \rangle$
- (5)  $A^C = \langle F_A, 1 - I_A, 1 - T_A \rangle$

**Definition 4** (see [36]). Let  $A = \{ \langle x_i | \langle T_A(x_i), I_A(x_i), F_A(x_i) \rangle \rangle, \dots, \langle x_n | \langle T_A(x_n), I_A(x_n), F_A(x_n) \rangle \rangle \}$  and  $B = \{ \langle x_i | \langle T_B(x_i), I_B(x_i), F_B(x_i) \rangle \rangle, \dots, \langle x_n | \langle T_B(x_n), I_B(x_n), F_B(x_n) \rangle \rangle \}$  be two SVNSs for  $x_i \in X (i = 1, 2, \dots, n)$ . Then, the normalized Euclidean distance between  $A$  and  $B$  can be defined as follows:

$$D(A, B) = \sqrt{\frac{1}{3n} \sum_{i=1}^n \{ (T_A(x_i) - T_B(x_i))^2 + (I_A(x_i) - I_B(x_i))^2 + (F_A(x_i) - F_B(x_i))^2 \}}. \quad (1)$$

**Definition 5** (see [36]). According to Majumdar et al.'s study, for single-valued neutrosophic set  $A = \{ \langle x, T_A(x), I_A(x), F_A(x) \rangle \mid x \in X \}$ , an entropy on neutrosophic set  $A$  is computed as follows:

$$E(A) = 1 - \frac{1}{n} \sum_{x_i} (T_A(x_i) + F_A(x_i)) \otimes |I_A(x_i) - I_{Ac}(x_i)|. \quad (2)$$

**Definition 6.** (see [37]). The entropy weight of a neutrosophic set in a study by Tan et al. is shown as follows:

$$W_j = \frac{(1 - E(x_j))}{\sum_{j=1}^n (1 - E(x_j))}. \quad (3)$$

**Definition 7.** In the literature of Biswas et al. [38], fuzzification of SVNS  $N(\sim) = \{ \langle x | \langle TN(\sim)(x), IN(\sim)(x), FN(\sim)(x) \rangle \mid x \in X \}$  is defined as follows:

$$\mu_F^-(x) = 1 - \sqrt{\frac{1}{3} \left\{ (1 - T_N^-(x))^2 + I_N^-(x)^2 + F_N^-(x)^2 \right\}}. \quad (4)$$

**Definition 8** (see [39]). The single-valued neutrosophic weighted averaging (SVNWA) aggregation operator proposed by Ye's research can be shown as follows:

$$F_{A_i} = \psi_1 A_1 \otimes \psi_2 A_2 \otimes \dots \otimes \psi_n A_n \\ = \langle \langle 1 - \prod_{i=1}^n (1 - T_{A_i})^{\psi_i}, \prod_{k=1}^n (I_{A_i})^{\psi_i}, \prod_{k=1}^n (F_{A_i})^{\psi_i} \rangle \rangle, \quad (5)$$



where  $\Psi = (\Psi_1, \Psi_2, \dots, \Psi_n)$  is the weight vector of  $A_i (i = 1, 2, \dots, n)$ ,  $\Psi_i \in [0, 1]$ , and  $\sum_{i=1}^n \Psi_i = 1$ .

#### 4. The Proposed Selection Model for Wood Components Restoration Methods

The selection of restoration methods for wood components of Chinese ancient architectures stands for a group decision-making problem seeking to find the best option. In actual cases, many indices could not be evaluated with accurate values in the decision-making process. Thus, the proposed model adopts single-valued neutrosophic sets to describe the characteristics of each index. The general process of the proposed model is shown in Figure 1. Details of the model will be explained in the rest of this section.

**4.1. The Establishment of Index System.** The restoration methods selection for wood components is generally decided by a group of  $k$  experts. Based on analysis proposed in literature and experts' opinion, the evaluation of restoration for wood components of Chinese ancient architectures can be mainly measured by four categories, denoted by four criteria  $A_i (i = 1, 2, \dots, 4)$ : basic situation of components ( $A_1$ ), restoration process ( $A_2$ ), restoration outcomes ( $A_3$ ), and situation of commissioned restoration company ( $A_4$ ). Moreover, under each criterion, there are several subcriteria, which influence the selection of restoration methods. Hence, an index system is established, as shown in Table 1.

**4.2. The Acquisition of Evaluation Matrix.** The aspects to be considered in evaluating wood components restoration of Chinese ancient architectures include practical cases, experts, wood components to be repaired, and diverse evaluation indices. Different experts may make different assessments based on their education background, distinct experiences, different assessment criteria, and different restoration methods suitable for different wood component's conditions. Because of the ambiguity and complexity of information, the evaluation values of indices often cannot be expressed in clear numbers. Decision-makers are more inclined to use fuzzy numbers such as linguistic terms with multiple granularities to evaluate indices. Thus, in this section, the evaluation results obtained from experts can be transformed into single-valued neutrosophic numbers. Hence, we can get the evaluation matrix  $R = (r_{ij})$ . The specific process is as follows:

Step 1. Obtaining linguistic terms with multigranularity.

In practical cases, experts may choose linguistic terms based on their preferences. Therefore, due to semantic differences in linguistic terms, different experts may have different evaluation values. Evaluation values of indices are given in the form of multigranularity linguistic terms [40] by an expert group consisting of different experts. Therefore, a linguistic term set containing ordered linguistic terms needs to be set in advance. Different linguistic term sets show different

characteristics of membership function. For example, linguistic term set  $\{m_0, m_1, m_2, m_3, m_4, m_5, m_6, m_7, m_8\}$  can be donated in linguistic terms as {extremely bad, very bad, bad, medium bad, medium, medium good, good, very good, extremely good}, while linguistic term set  $\{l_0, l_1, l_2, l_3, l_4, l_5, l_6\}$  can be donated in linguistic terms as {very bad, bad, medium bad, medium, medium good, good, very good}, but different experts may have different understanding of these terms [41]. Hence, it would be better that experts provide evaluation values for different restoration methods according to a preset linguistic term set.

Step 2. Transforming the evaluation information from experts' questionnaire according to the symmetric linguistic evaluation scale into single-valued neutrosophic numbers with truth, indeterminacy, and falsity.

The linguistic term set in this study is {extremely high, very high, high, medium high, medium, medium low, low, very low, extremely low}, including nine granular linguistic terms. The linguistic terms along with SVNns are defined in Table 2 as given in the literature [38] to rate each alternative with respect to each index.

Step 3. Determining the weights of experts.

In accordance with the different backgrounds and experiences of different experts, the importance of decision-making experts differs. In this paper, experts' decision power can be expressed in the linguistic terms set {very important, important, medium, unimportant, very unimportant}, and the corresponding single-valued neutrosophic numbers are shown in Table 3. The weight of expert is donated as  $e_k (k = 1, 2, \dots, n)$ ; according to equation (4), the weights of experts can be computed by the following equation [38]:

$$e_k = \frac{u_k}{\sum_{k=1}^l u_k} = \frac{1 - \sqrt{\frac{(1 - T^k)^2 + (I^k)^2 + (F^k)^2}{3}}}{\sum_{k=1}^l \left(1 - \sqrt{\frac{(1 - T^k)^2 + (I^k)^2 + (F^k)^2}{3}}\right)}. \quad (6)$$

Step 4. Aggregating the neutrosophic numbers into  $R = (r_{ij})$ .

We use the single-valued neutrosophic weighted averaging (SVNWA) aggregation operator described by equation (5) introduced in Section 2 to aggregate the neutrosophic numbers. Then, we shall get the evaluation matrix  $R = (r_{ij})$ .

**4.3. The Assignment of Index Weights.** In this section, we employ a combination of subjective and objective weights to determine the index weights. To begin with, we utilize an efficient method called BWM to calculate subjective weights of four criteria. Then, we adopt the principle of objectivity to calculate the entropy weight of each index. Based on the subjective-objective method to determine the synthetic weight of each index, the detailed procedures are as follows.

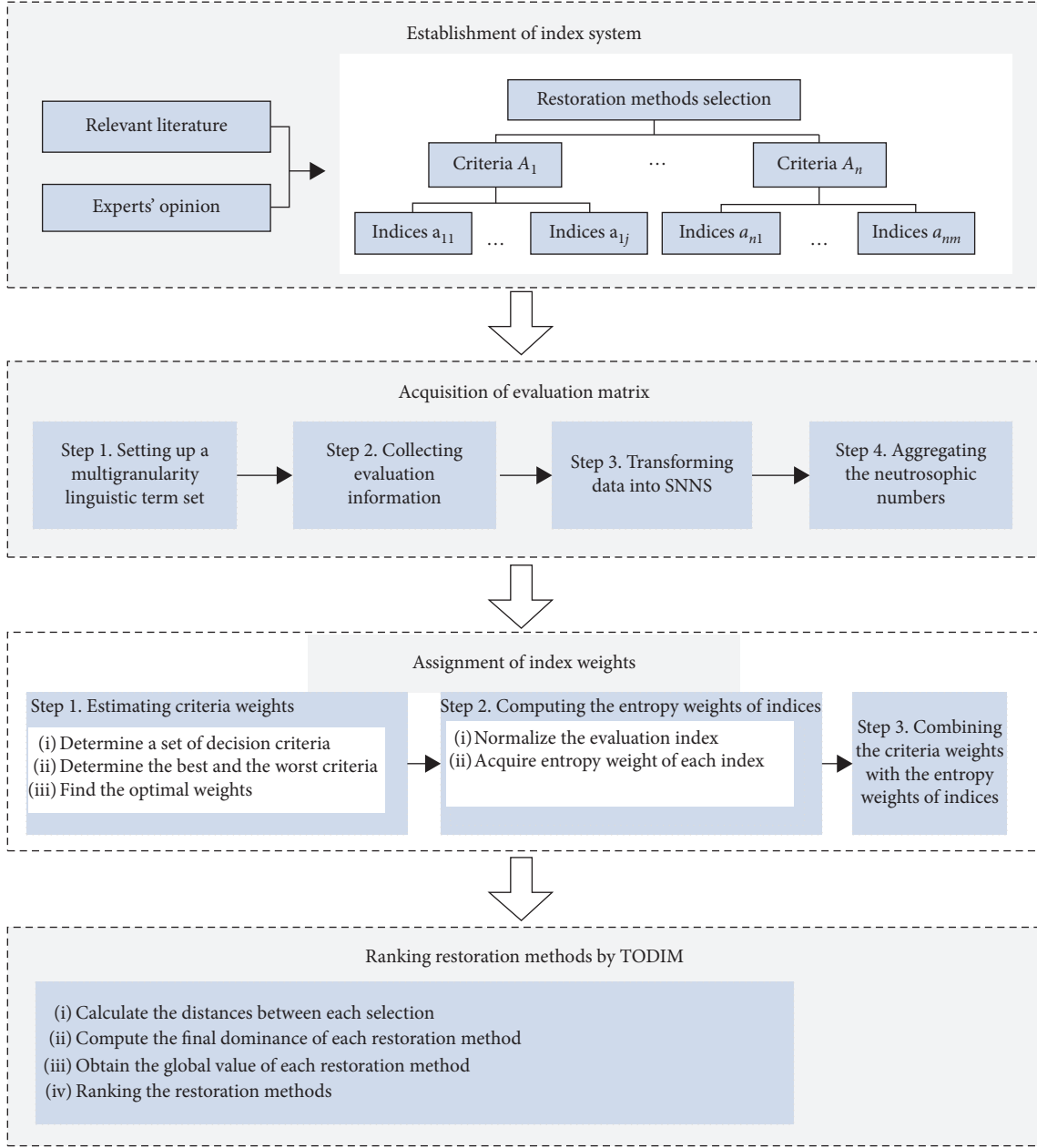


FIGURE 1: Summary of the process of the proposed model.

**4.3.1. Estimating Criteria Weights.** BWM method, introduced by Raize, is the newest method to solve multicriteria decision-making problems [42]. In this section, we apply it to calculate the weights of four criteria [43]:

Step 1. Determining a set of decision criteria. We should consider the criteria  $\{A_1, A_2, \dots, A_n\}$  that should be used to make a decision.

Step 2. The best (e.g., most desirable and most important) and the worst (e.g., least desirable and least important) criteria are determined by decision-maker in general.

Step 3. In the light of the BWM questionnaire, the preference of the best criterion over all the other criteria

using a number between 1 and 9 should be determined. The resulting best-to-others vector would be  $A_B = (a_{B1}, a_{B2}, \dots, a_{Bn})$ , where  $a_{Bj}$  indicates the preference of the best criterion  $B$  over criterion  $j$ . It is clear that  $a_{BB} = 1$ .

Step 4. According to the BWM questionnaire, the preference of all the criteria over the worst criterion, using a number between 1 and 9, should be determined. The resulting others-to-worst vector would be  $A_W = (a_{1W}, a_{2W}, \dots, a_{nW})$ , where  $a_{jW}$  indicates the preference of the criterion  $j$  over the worst criterion  $W$ . It is clear that  $a_{WW} = 1$ .

Step 5. Finding the optimal weights  $\{w_1^*, w_2^*, \dots, w_n^*\}$  by solving (7). The optimal weight for the criterion is the one where for each pair of  $w_B/w_j$  and  $w_j/w_W$ , we



TABLE 1: Index system of restoration methods selection for wood components of Chinese ancient architectures.

Criteria	Index	Definition	Index type
Basic situation of components ( $A_1$ )	Used years ( $a_{11}$ )	The degree that the used years of the component is suitable for these restoration methods	Benefit
	Material properties ( $a_{12}$ )	The degree that the material properties of the component is suitable for these restoration methods	Benefit
	Structural rationality ( $a_{13}$ )	The degree of rationality that the structure of the component is suitable for these restoration methods	Benefit
	Cause of damage ( $a_{14}$ )	The cause of damage of the component is suitable for these restoration methods	Benefit
	Severity of damage ( $a_{15}$ )	The degree of severity that the damage of the component is suitable for these restoration methods	Benefit
	Impact on neighboring components ( $a_{16}$ )	The degree of impact on neighboring components using these restoration methods	Cost
Restoration process ( $A_2$ )	Restoration expense ( $a_{21}$ )	The cost spent for the restoration	Cost
	Material acquisition ( $a_{22}$ )	The degree of difficulty in obtaining materials for the restoration	Cost
	Process complexity ( $a_{23}$ )	The degree of process complexity in the restoration	Cost
	Requirements for equipment ( $a_{24}$ )	The level of requirements for equipment in the restoration	Cost
Restoration outcomes ( $A_3$ )	Probability of authenticity restoration ( $a_{31}$ )	The probability of fixing the components without changing the original materials and processing methods of the component	Benefit
	Degree of preservation of historical information ( $a_{32}$ )	The probability that historical information shall not be destroyed during restoration	Benefit
	Probability of irreversible effects on the original component ( $a_{33}$ )	The probability that the original component could not be returned to the prerepair state after restoration if an error occurred during the repair process	Cost
	Possibility of reversible effects on the original component ( $a_{34}$ )	The possibility that the original component could be returned to the prerepair state after restoration if an error occurred during the repair process	Benefit
	Service life after restoration ( $a_{35}$ )	The length of time that the component may be used after restoration	Benefit
	Difficulty of maintenance ( $a_{36}$ )	The difficulty in maintenance of the component after restoration	Cost
Situation of commissioned restoration company ( $A_4$ )	Teamwork capacity ( $a_{41}$ )	The cooperation efficiency of the restoration team	Benefit
	Proficiency ( $a_{42}$ )	Restoration team professionals' degree of skills	Benefit
	Advanced restoration equipment ( $a_{43}$ )	The performance of the restoration equipment	Benefit

TABLE 2: Linguistic terms for rating the alternatives with SVNNS.

Linguistic terms	SVNNS
Extremely good/high	<1.00, 0.00, 0.00>
Very good/high	<0.90, 0.10, 0.05>
Good/high	<0.80, 0.20, 0.15>
Medium good/high	<0.65, 0.35, 0.30>
Medium/fair	<0.50, 0.50, 0.45>
Medium bad/medium low	<0.35, 0.65, 0.60>
Bad/low	<0.20, 0.75, 0.80>
Very bad/low	<0.10, 0.85, 0.90>
Extremely bad/low	<0.05, 0.90, 0.95>

TABLE 3: Linguistic terms for rating the importance of experts with SVNNS.

Linguistic terms	SVNNS
Very important (VI)	<0.90, 0.10, 0.05>
Important (I)	<0.80, 0.20, 0.15>
Medium (M)	<0.50, 0.40, 0.45>
Unimportant (UI)	<0.35, 0.60, 0.70>
Very unimportant (VUI)	<0.10, 0.80, 0.90>

have  $w_B/w_j = a_{Bj}$  and  $w_j/w_W = a_{jW}$ . In order to meet these conditions for all  $j$ , we should find a solving method where the maximum absolute differences  $|(w_B/w_j) - a_{Bj}|$  and  $|(w_j/w_W) - a_{jW}|$  for all  $j$  are minimized. Considering the nonnegativity and condition for the weights, the following problem results:

$$\min \max_j \left\{ \left| \frac{w_B}{w_j} - a_{Bj} \right|, \left| \frac{w_j}{w_W} - a_{jW} \right| \right\}$$

s.t.

$$\sum_j w_j = 1$$

$$w_j \geq 0, \quad \text{for all } j.$$

(7)

Equation (7) is equivalent to the following equation:

$$\begin{aligned}
& \min \quad \xi \\
& \text{s.t.} \\
& \left| \frac{w_B}{w_j} - a_{Bj} \right| \leq \xi, \quad \text{for all } j \\
& \left| \frac{w_j}{w_w} - a_{jw} \right| \leq \xi, \quad \text{for all } j \\
& \sum_j w_j = 1 \\
& w_j \geq 0, \quad \text{for all } j.
\end{aligned} \tag{8}$$

Solving equation (8), the optimal weights  $(w_1^*, w_2^*, \dots, w_n^*)$  and  $\xi^*$  can be obtained.

Then, the consistency ratio using  $\xi^*$  and the corresponding consistency index can be calculated using the following formula:

$$\text{consistency ratio} = \frac{\xi^*}{\text{consistency index}}. \tag{9}$$

The maximum values of  $\xi$  (consistency index) for different values of  $a_{Bw}$  are shown in Table 4.

Consistency ratio  $\in [0, 1]$ : the value approaching 0 proved more consistency; instead, the value close to 1 shows less consistency. If the consistency ratio is  $\leq 0.1$ , it indicates a very good consistency. If not, we should revise  $a_{Bj}$  and  $a_{jw}$  to make the solution more consistent.

In the case when the number of criteria exceeds three, the BWM introduced above is limited in deriving the unique optimal weight vector. This leads to multiple optimal solutions. The improved method presented in the study of Rezaei [21] is used to acquire optimal weights with  $n$  criteria. If we use  $\{|w_B - a_{Bj}w_j|, |w_j - a_{jw}w_w|\}$  instead of  $\{|(w_B/w_j) - a_{Bj}|, |(w_j/w_w) - a_{jw}|\}$ , the problem can be solved as follows:

$$\begin{aligned}
& \min \max_j \quad \left\{ |w_B - a_{Bj}w_j|, |w_j - a_{jw}w_w| \right\}, \\
& \text{s.t.} \quad \sum_j w_j = 1 \\
& w_j \geq 0, \quad \text{for all } j.
\end{aligned} \tag{10}$$

Equation (10) can be transferred to a linear programming problem as follows:

$$\begin{aligned}
& \min \quad \xi^L \\
& \text{s.t.} \\
& |w_B - a_{Bj}w_j| \leq \xi^L, \quad \text{for all } j \\
& |w_j - a_{jw}w_w| \leq \xi^L, \quad \text{for all } j \\
& \sum_j w_j = 1 \\
& w_j \geq 0, \quad \text{for all } j.
\end{aligned} \tag{11}$$

Equation (11) is a linear program problem, which can compute the unique optimal weight  $\{w_1^*, w_2^*, \dots, w_n^*\}$ .

Therefore, we can obtain the weight vector  $\{w_1, w_2, w_3, w_4\}$  of basic situation of components  $A_1$ , restoration process  $A_2$ , restoration outcomes  $A_3$ , and situation of commissioned restoration company  $A_4$ .

**4.3.2. Calculating Index Weights.** In this section, we follow the combination of subjective and objective principles to compute the index weights. Firstly, we use entropy weight method to compute the entropy weight of each index. Then, we obtain synthesized weight of each index by combining criteria weights with entropy weights. The detailed processes are as follows:

Step 1. Normalizing the evaluation index.

The normalization equation [35] for neutrosophic numbers is as in the following equation. Then, we obtain the normalization matrix  $R = (\beta_{ij})$ :

$$r_{ij} = \begin{cases} T_{ij}, I_{ij}, F_{ij}, & \text{if } j \text{ is benefit index,} \\ 1 - T_{ij}, 1 - I_{ij}, 1 - F_{ij}, & \text{if } j \text{ is cost index.} \end{cases} \tag{12}$$

Step 2. Computing the entropy weights of indices.

According to equations (2) and (3) introduced in Section 2, first, we shall compute the entropy value of each index  $E(x_j)$ . Then, we can acquire the entropy weight  $w_j$  of each index based on the evaluation matrix.

Step 3. Calculating combination weights.

It is important to confirm the weights of the evaluation indicators of the restoration methods, which affects the accuracy of the evaluation results. Subjective weight method relies on knowledge and experience of the experts, and the evaluation results are usually arbitrary. The objective weighting method is based on objective actual conditions and can reduce subjective arbitrariness. So, a combination of subjective and objective methods is necessary. The optimal weight vector of criteria is  $w_i^*$  according to the explanation of BWM in Section 4.3.1. Then, we compute a comprehensive index weight  $H_{ij}$  which combines the subjective weights of criteria with the entropy weights of indices according to the following equation [44]:

$$H_{ij} = \frac{w_i^* \times w_j}{\sum_{i=1}^n w_i^* \times w_j}. \tag{13}$$

**4.4. The Process of Decision-Making Based on TODIM.** To solve multicriteria decision-making problems, Gomes and Lima [45] proposed the TODIM method based on prospect theory. Lourenzutti and Krohling [46] introduced the primary principle of the TODIM method. Recently, an unexpected initiative of the TODIM method was pointed out by Lourenzutti et al., which states that both the losses and the gains should be amplified proportionally by the criterion weight, and then applied to prospect function. The suggested modification in the  $\phi_c$  function is as follows:

TABLE 4: Consistency index (CI) table.

$a_{Bw}$	1	2	3	4	5	6	7	8	9
Consistency index (max $\xi$ )	0.00	0.44	1.00	1.63	2.30	3.00	3.73	4.47	5.23

$$\phi_c(X_i, X_j) = \begin{cases} \sqrt{w_c(s_{ic} - s_{jc})}, & \text{if } s_{ic} \geq s_{jc}, \\ -\frac{1}{\theta} \sqrt{w_c(s_{jc} - s_{ic})}, & \text{otherwise.} \end{cases} \quad (14)$$

The selection of restoration methods for wood components of Chinese ancient architectures is a multicriteria group decision-making (MCGDM) problem consisting of expert  $e_k (k = 1, 2, \dots, n)$ , denoted by  $\omega = \{e_1, e_2, \dots, e_k\}$ . Suppose that there exist  $n$  restoration methods  $X_i (i = 1, 2, 3, \dots, n)$ , denoted by  $X = \{X_1, X_2, \dots, X_n\}$ . In this part, we use the TODIM method to solve the restoration methods selection problem. The main procedure is generalized as follows:

Step 1. Calculating the distances  $d_{ij}$  between each selection based on equation (1).

Step 2. Computing the final dominance of restoration method  $X_i$  over each restoration method  $X_k$  under each criterion  $A_j$  as follows [23]:

$$\delta(X_i, X_k) = \sum_{j=1}^n \phi_j(X_i, X_k), \quad \forall (i, k) \text{ where}$$

$$\phi_j(X_i, X_k) = \begin{cases} \sqrt{w_j d(b_{ij}, b_{kj})}, & \text{if } b_{ij} > b_{kj}, \\ 0, & \text{if } b_{ij} = b_{kj}, \\ -\frac{1}{\theta} \sqrt{w_j d(b_{ij}, b_{kj})}, & \text{otherwise,} \end{cases} \quad (15)$$

where  $d(b_{ij}, b_{kj})$  is the distance between  $b_{ij}$  and  $b_{kj}$ . The  $w_j$  is the weight of the  $j$  criterion calculated by the BWM method. In this paper, we use comprehensive index weight  $H_{ij}$  instead of  $w_j$ , where  $H_{ij}$  is the index weight calculated by a combination of the criteria weights calculated by BWM and the indices weights obtained by the entropy weight method. So, we shall apply equation (16) to acquire the final dominance of restoration method  $X_i$  over each restoration method  $X_k$  under each index  $a_{ij}$ :

$$\delta(X_i, X_k) = \sum_{j=1}^n \phi_j(X_i, X_k), \quad \forall (i, k) \text{ where}$$

$$\phi_j(X_i, X_k) = \begin{cases} \sqrt{H_{ij} d(b_{ij}, b_{kj})}, & \text{if } b_{ij} > b_{kj}, \\ 0, & \text{if } b_{ij} = b_{kj}, \\ -\frac{1}{\theta} \sqrt{H_{ij} d(b_{ij}, b_{kj})}, & \text{otherwise.} \end{cases} \quad (16)$$

Step 3. The global value of restoration method  $X_i$  is obtained as follows [23]:

$$\varepsilon_i = \frac{\sum_j \delta(X_i, X_k) - \min_i \sum_j \delta(X_i, X_k)}{\max_i \sum_j \delta(X_i, X_k) - \min_i \sum_j \delta(X_i, X_k)}. \quad (17)$$

Step 4. Ranking the restoration methods  $X_i$  by their value  $\varepsilon_i$ .

According to the value  $\varepsilon_i$ , we could select restoration method  $X_i$ . The higher the value  $\varepsilon_i$ , the better the restoration method  $X_i$ .

## 5. Empirical Study

The proposed model is applied to solve the selection problem of restoration methods for wood components of Chinese ancient architectures. A Chinese ancient architecture called “Fuhoutang” needed to be restored. Fuhoutang is a state-level cultural legacy, which was constructed during the Xianfeng period of Qing Dynasty. The management authority of Fuhoutang commissioned company  $R$  to restore it. One of the components to be restored is a beam at the bottom of the wooden frame in the hall, donated by  $C_1$ . The original information of  $C_1$  is outlined in Table 5. Four experts, donated by  $DM_1$ ,  $DM_2$ ,  $DM_3$ , and  $DM_4$ , respectively, studied the condition of  $C_1$  and then provided four possible restoration methods, including stabilizing by outer iron hoop, inserting internal steel, filling with epoxy, and replacing the component, which are denoted by  $X_1$ ,  $X_2$ ,  $X_3$ , and  $X_4$  (shown in Figure 2). These four restoration methods are evaluated by experts through several evaluation indices to determine the advantages and disadvantages of each method, and the evaluation index system is listed in Table 1.

According to the selection model presented in Section 3, first, we get the evaluation matrix through the conditions of the wood component to be restored, restoration process, the possible outcomes, and restoration company's conditions. Then, the index weights are calculated by a combination of criteria weights and entropy weights. Finally, the ranking order of the four restoration methods can be acquired by using the TODIM method. Furthermore, the effectiveness and reliability of the proposed model are verified by sensitivity analysis and comparison analysis.

**5.1. Evaluation Matrix.** The evaluation matrix is obtained from experts according to the evaluation index system. In the light of the evaluation method proposed in Section 4.2, experts evaluate the four methods, and the index evaluation value is represented by linguistic terms with multi-granularity. We transform the linguistic terms into single-valued neutrosophic numbers (SVNNs) according to Table 2. Based on experts' distinct experience, the importance of four experts differs from each other, as shown in Table 6. According to Table 3, the importance of each expert could be

TABLE 5: The information of the condition of the specific component to be repaired.

$C_1$	Component's condition
Used years	About 150 years
Original material	Chinese fir
The cause of damage	Crack, decay
Damage situation	The beam is 35 cm in diameter and 4.2 meters long. The crack is about 80 cm long, about 4 cm wide, and about 5 cm deep, which is caused by material properties. Near the crack, a decay of about 8 cm in width, 20 cm in length, and 3 cm in depth was eroded by bugs

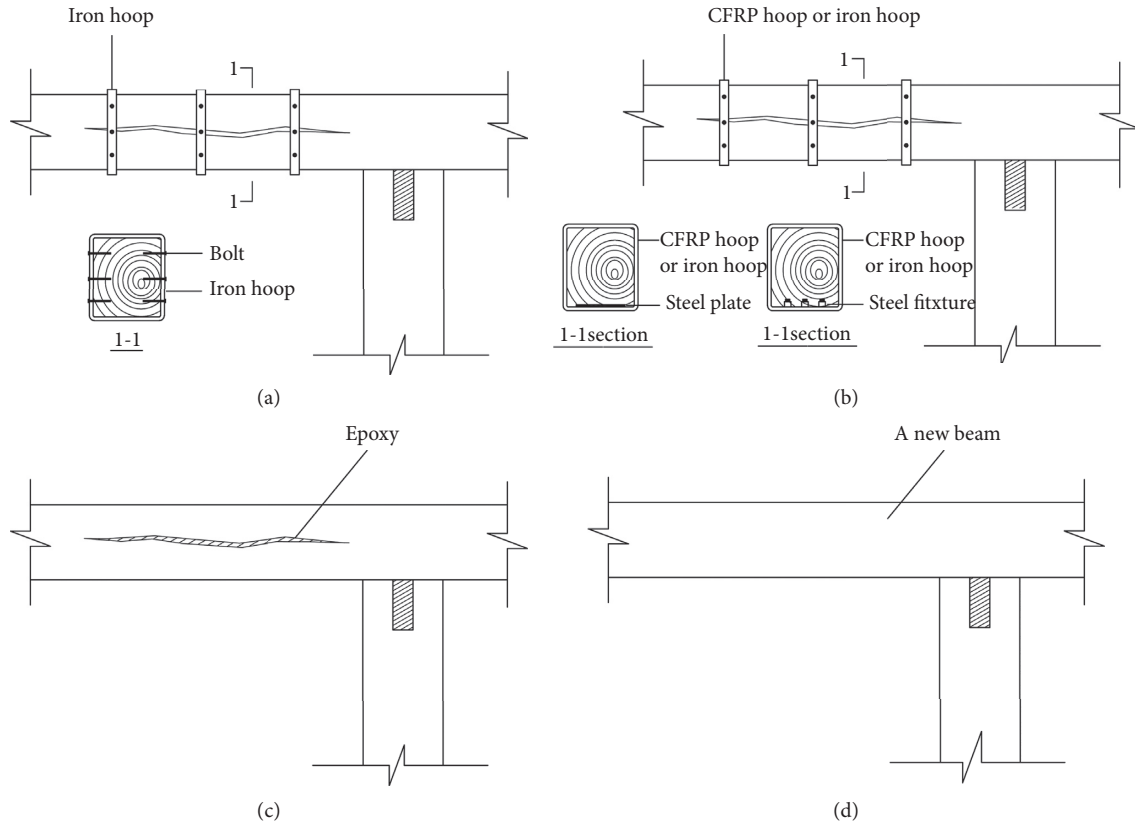
FIGURE 2: Four alternative restoration methods for  $C_1$ : (a) stabilizing by outer iron hoop; (b) inserting internal steel (CFRP stands for carbon fibre-reinforced polymer); (c) filling with epoxy; (d) replacing the component.

TABLE 6: Importance of experts expressed with SVNNS.

	$DM_1$	$DM_2$	$DM_3$	$DM_4$
Linguistic terms	M	M	I	VI
SVNNs	$\langle 0.50, 0.40, 0.45 \rangle$	$\langle 0.50, 0.40, 0.45 \rangle$	$\langle 0.80, 0.20, 0.15 \rangle$	$\langle 0.90, 0.10, 0.05 \rangle$

described by linguistic terms with its relevant SVNNS. Therefore, the weights of experts ( $e_k$ ) are determined by using equation (6):  $e_1 = 0.1950$ ,  $e_2 = 0.1950$ ,  $e_3 = 0.2899$ , and  $e_4 = 0.3201$ . Then, the evaluation values of these indices do need to be aggregated. We shall use equation (4), the single-valued neutrosophic weighted averaging (SVNWA) aggregation operator to aggregate these indices. Finally, we obtain the evaluation matrix  $R = (r_{ij})$  based on single-valued neutrosophic sets outlined in Table 7.

**5.2. The Calculation of Index Weights.** According to the BWM method introduced in Section 4.3.1, we calculate the subjective weights of four criteria. Firstly, the criteria shown in Table 1 are denoted by  $A_1$  to  $A_4$ ; among them, basic situation of components ( $A_1$ ) is the most important criterion, and restoration process ( $A_2$ ) is the least important criterion, which is confirmed by experts. Secondly, the pairwise comparison vectors for the best and the worst criteria are outlined in Tables 8 and 9. Table 8 represents that

TABLE 7: The aggregated SVNNS-based decision matrix.

Criteria	Index	Alternatives			
		$X_1$	$X_2$	$X_3$	$X_4$
$A_1$	$a_{11}$	<0.719, 0.281, 0.229>	<0.5, 0.5, 0.45>	<0.777, 0.223, 0.172>	<0.465, 0.525, 0.491>
	$a_{12}$	<0.761, 0.239, 0.187>	<0.506, 0.494, 0.442>	<0.8, 0.2, 0.15>	<0.545, 0.455, 0.398>
	$a_{13}$	<0.704, 0.296, 0.240>	<0.648, 0.352, 0.298>	<0.733, 0.267, 0.214>	<0.262, 0.709, 0.715>
	$a_{14}$	<0.625, 0.375, 0.325>	<0.473, 0.526, 0.476>	<0.777, 0.223, 0.172>	<0.453, 0.547, 0.496>
	$a_{15}$	<0.625, 0.375, 0.325>	<0.579, 0.421, 0.370>	<0.8, 0.2, 0.15>	<0.159, 0.791, 0.841>
	$a_{16}$	<0.191, 0.776, 0.790>	<0.492, 0.507, 0.456>	<0.186, 0.782, 0.796>	<1, 0, 0>
$A_2$	$a_{21}$	<0.281, 0.697, 0.690>	<0.765, 0.235, 0.183>	<0.534, 0.466, 0.416>	<0.714, 0.286, 0.232>
	$a_{22}$	<0.181, 0.769, 0.819>	<0.565, 0.435, 0.384>	<0.413, 0.587, 0.536>	<0.765, 0.235, 0.183>
	$a_{23}$	<0.35, 0.65, 0.6>	<0.825, 0.175, 0.121>	<0.456, 0.544, 0.493>	<0.766, 0.234, 0.169>
	$a_{24}$	<0.305, 0.680, 0.658>	<0.8, 0.2, 0.15>	<0.5, 0.5, 0.45>	<0.738, 0.263, 0.210>
$A_3$	$a_{31}$	<0.205, 0.756, 0.783>	<0.627, 0.373, 0.319>	<0.534, 0.466, 0.416>	<0.081, 0.869, 0.919>
	$a_{32}$	<0.761, 0.239, 0.187>	<0.623, 0.377, 0.323>	<0.534, 0.466, 0.416>	<0.133, 0.817, 0.867>
	$a_{33}$	<0.247, 0.720, 0.736>	<0.707, 0.293, 0.240>	<0.554, 0.446, 0.395>	<1, 0, 0>
	$a_{34}$	<0.836, 0.164, 0.109>	<0.589, 0.410, 0.354>	<0.534, 0.466, 0.416>	<0.1, 0.85, 0.9>
	$a_{35}$	<0.474, 0.526, 0.476>	<0.579, 0.421, 0.370>	<0.65, 0.35, 0.3>	<0.860, 0.140, 0.085>
	$a_{36}$	<0.576, 0.424, 0.364>	<0.612, 0.388, 0.337>	<0.474, 0.526, 0.476>	<0.2, 0.75, 0.8>
$A_4$	$a_{41}$	<0.825, 0.175, 0.121>	<0.533, 0.466, 0.416>	<0.777, 0.223, 0.172>	<0.701, 0.299, 0.244>
	$a_{42}$	<0.857, 0.143, 0.088>	<0.5, 0.5, 0.45>	<0.8, 0.2, 0.15>	<0.608, 0.392, 0.342>
	$a_{43}$	<0.886, 0.114, 0.062>	<0.530, 0.469, 0.418>	<0.8, 0.2, 0.15>	<0.625, 0.375, 0.325>

TABLE 8: Pairwise comparison vector of the most important criterion.

Criteria	$A_1$	$A_2$	$A_3$	$A_4$
Best criterion: $A_1$	1	6	2	4

TABLE 9: Pairwise comparison vector of the least important criterion.

Criteria	$A_1$	$A_2$	$A_3$	$A_4$
Worst criterion: $A_2$	6	1	4	2

the preference values of the best criteria ( $A_1$ ) over criterion ( $A_2$ ), criterion ( $A_3$ ), and criterion ( $A_4$ ) are 6, 2, and 4, respectively. The preference values of criteria ( $A_1$ ), criterion ( $A_3$ ), and criterion ( $A_4$ ) over the worst criterion ( $A_2$ ) are 6, 4, and 2, respectively, as shown in Table 9. Finally, the weight vector of criteria  $w^* = \{w_1^*, w_2^*, w_3^*, w_4^*\}$  is calculated by Equation (11), and we can get  $w_1^* = 0.5098$ ,  $w_2^* = 0.0784$ ,  $w_3^* = 0.2745$ ,  $w_4^* = 0.1373$ , and  $\xi^* = 0.0392$ . For the consistency ratio based on the BWM method, as  $a_{BW} = a_{12} = 6$ , the consistency index for this problem is 3.00 (shown in Table 4), and the consistency ratio according to equation (9) is  $0.0392/3.00 \approx 0.0131$ , which illustrates a very good consistency.

Afterwards, the weights of indices can be computed by applying the entropy weight method outlined in Section 4.3.2. First, by normalizing the evaluation indices by utilizing equation (12), we shall get the evaluation matrix  $R = (\beta_{ij})$ , which is shown in Table 10. Then, we can obtain the entropy weight of each index based on the normalized evaluation matrix.

At last, index weights can be acquired by combining the subjective weights of criteria with the entropy weights of indices, which is obtained as in Table 11.

**5.3. The Sequence of Restoration Methods.** We use the TODIM method based on MCGDM introduced in Section 4.4 to solve the restoration methods selection problem. First, we calculate the final dominance of restoration methods  $X_i$  over each other plan  $X_k$  under each index  $a_{ij}$  by using equation (16), and the parameter  $\theta$  is usually 1; the result can be shown in Table 12. Then, the global value of each restoration method is obtained by equation (17). Finally, according to value  $\varepsilon_i$ , we could sort out restoration methods selection  $X_i$ , which is obtained as in Table 13. Hence, the most appropriate restoration method for  $C_1$  is " $X_1$ ," namely, stabilizing by outer iron hoop.

**5.4. Sensitivity Analysis.** The parameter  $\theta$  in TODIM is the loss attenuation coefficient that controls the influence caused when a loss occurs. We believe that if  $\theta < 1$ , the loss is amplified; if  $\theta > 1$ , the loss is attenuated. The prospect theory states that, in general, individuals are more sensitive to losses than gains, which suggests that  $\theta < 1$ . Therefore, the value of this parameter greatly affects the ranking order of the alternatives. Choosing a small  $\theta$  means we are looking for an alternative which provides less loss under all conditions; on the contrary, if we choose a big  $\theta$ , then we are looking for an alternative which provide greater benefits, even if we have losses on certain criteria [46]. For the purpose of analyzing the influence of different values of  $\theta$  on the final ranking orders, we take different  $\theta$  values to calculate the examples for restoration methods to check the stability of the ranking results. The results are outlined in Table 14 and Figure 3. We can see the different ranking orders calculated by different  $\theta$  clearly. When  $\theta \geq 0.8$ , the ranking order is the same as in the previous example, and the ranking order is  $X_1 > X_3 > X_2 > X_4$ ; when the loss attenuation coefficient becomes smaller,  $\theta \leq 0.5$ ,  $X_3$  and  $X_1$  are replaced, and the ranking result becomes  $X_3 > X_1 > X_2 > X_4$ . This proves that when the loss is



TABLE 10: The normalized evaluation matrix.

Criteria	Index	Alternatives			
		$X_1$	$X_2$	$X_3$	$X_4$
$A_1$	$a_{11}$	<0.719, 0.281, 0.229>	<0.5, 0.5, 0.45>	<0.777, 0.223, 0.172>	<0.465, 0.525, 0.491>
	$a_{12}$	<0.761, 0.239, 0.187>	<0.506, 0.494, 0.442>	<0.8, 0.2, 0.15>	<0.545, 0.455, 0.398>
	$a_{13}$	<0.704, 0.296, 0.240>	<0.648, 0.352, 0.298>	<0.733, 0.267, 0.214>	<0.262, 0.709, 0.715>
	$a_{14}$	<0.625, 0.375, 0.325>	<0.473, 0.526, 0.476>	<0.777, 0.223, 0.172>	<0.453, 0.547, 0.496>
	$a_{15}$	<0.625, 0.375, 0.325>	<0.579, 0.421, 0.370>	<0.8, 0.2, 0.15>	<0.159, 0.791, 0.841>
	$a_{16}$	<0.809, 0.224, 0.210>	<0.508, 0.493, 0.544>	<0.814, 0.218, 0.204>	<0, 1, 1>
$A_2$	$a_{21}$	<0.719, 0.303, 0.310>	<0.235, 0.765, 0.817>	<0.466, 0.534, 0.584>	<0.286, 0.714, 0.768>
	$a_{22}$	<0.819, 0.231, 0.181>	<0.435, 0.565, 0.616>	<0.587, 0.413, 0.464>	<0.235, 0.765, 0.817>
	$a_{23}$	<0.65, 0.35, 0.4>	<0.175, 0.825, 0.879>	<0.544, 0.456, 0.507>	<0.234, 0.766, 0.831>
	$a_{24}$	<0.695, 0.320, 0.342>	<0.2, 0.8, 0.85>	<0.5, 0.5, 0.55>	<0.262, 0.738, 0.790>
$A_3$	$a_{31}$	<0.205, 0.756, 0.783>	<0.627, 0.373, 0.319>	<0.534, 0.466, 0.416>	<0.081, 0.869, 0.919>
	$a_{32}$	<0.761, 0.239, 0.187>	<0.623, 0.377, 0.323>	<0.534, 0.466, 0.416>	<0.133, 0.817, 0.867>
	$a_{33}$	<0.753, 0.280, 0.264>	<0.293, 0.707, 0.760>	<0.446, 0.554, 0.605>	<0, 1, 1>
	$a_{34}$	<0.836, 0.164, 0.109>	<0.589, 0.410, 0.354>	<0.534, 0.466, 0.416>	<0.1, 0.85, 0.9>
	$a_{35}$	<0.474, 0.526, 0.476>	<0.579, 0.421, 0.370>	<0.65, 0.35, 0.3>	<0.860, 0.140, 0.085>
	$a_{36}$	<0.424, 0.576, 0.636>	<0.388, 0.612, 0.663>	<0.526, 0.474, 0.524>	<0.8, 0.25, 0.2>
$A_4$	$a_{41}$	<0.825, 0.175, 0.121>	<0.533, 0.466, 0.416>	<0.777, 0.223, 0.172>	<0.701, 0.299, 0.244>
	$a_{42}$	<0.857, 0.143, 0.088>	<0.5, 0.5, 0.45>	<0.8, 0.2, 0.15>	<0.608, 0.392, 0.342>
	$a_{43}$	<0.886, 0.114, 0.062>	<0.530, 0.469, 0.418>	<0.8, 0.2, 0.15>	<0.625, 0.375, 0.325>

TABLE 11: The weights of criteria and index for restoration methods selection.

Criteria	Weight	Index	Weight
$A_1$	0.5098	$a_{11}$	0.0705
		$a_{12}$	0.0882
		$a_{13}$	0.1025
		$a_{14}$	0.0570
		$a_{15}$	0.1050
		$a_{16}$	0.1232
$A_2$	0.0784	$a_{21}$	0.0142
		$a_{22}$	0.0132
		$a_{23}$	0.0135
		$a_{24}$	0.0140
$A_3$	0.2745	$a_{31}$	0.0539
		$a_{32}$	0.0532
		$a_{33}$	0.0640
		$a_{34}$	0.0578
		$a_{35}$	0.0444
		$a_{36}$	0.0368
$A_4$	0.1373	$a_{41}$	0.0302
		$a_{42}$	0.0280
		$a_{43}$	0.0302

TABLE 12: The final dominance of restoration methods alternatives ( $\theta = 1$ ).

	$X_1$	$X_2$	$X_3$	$X_4$
$X_1$	0	-1.5129	-0.0042	-2.1098
$X_2$	1.5129	0	1.4057	-0.9879
$X_3$	0.0042	-1.4057	0	-2.0915
$X_4$	2.0081	0.8676	2.0915	0

magnified, the decision-makers tend to choose  $X_3$ . When the loss is reduced, that is, the larger the loss attenuation coefficient, the lower the degree of evasion by the decision-

TABLE 13: Ranking order of restoration methods by  $\varepsilon_i$ .

Alternatives	Values $\varepsilon_i$	Ranking orders
$X_1$	1	1
$X_2$	0.3601	3
$X_3$	0.9963	2
$X_4$	0	4

TABLE 14: Ranking order of restoration methods with different  $\theta$ .

Different values of $\theta$	Values $\varepsilon_i$				Ranking orders
	$X_1$	$X_2$	$X_3$	$X_4$	
$\theta = 2.25$	1	0.2803	0.9464	0	$X_1 > X_3 > X_2 > X_4$
$\theta = 2.0$	1	0.3246	0.9893	0	$X_1 > X_3 > X_2 > X_4$
$\theta = 1.5$	1	0.3386	0.9922	0	$X_1 > X_3 > X_2 > X_4$
$\theta = 1.0$	1	0.3601	0.9963	0	$X_1 > X_3 > X_2 > X_4$
$\theta = 0.8$	1	0.3716	0.9985	0	$X_1 > X_3 > X_2 > X_4$
$\theta = 0.5$	0.9973	0.3925	1	0	$X_3 > X_1 > X_2 > X_4$
$\theta = 0.3$	0.9937	0.4101	1	0	$X_3 > X_1 > X_2 > X_4$

maker, the decision-makers tend to choose  $X_1$ . It means that adjusting the decision-maker's risk aversion tendency will affect the ranking results, and it also indicates that the psychological behavior of the decision-maker will affect one's decision-making. The results of sensitivity analysis show that the proposed method can well express the cognition of decision-makers, quantify the uncertainty to a certain extent, and avoid the loss and distortion of information as much as possible. Therefore, to an extent, the feasibility and robustness of the proposed model is verified.

**5.5. Comparison Analysis.** As explained in Section 2, the model is proposed to select restoration methods for wood components of Chinese architectures. In order to verify that



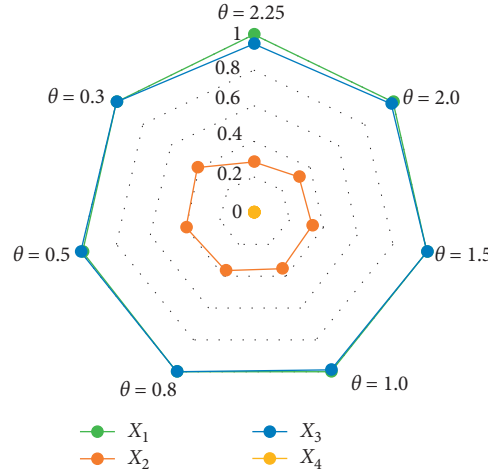


FIGURE 3: The radar chart displaying the result of sensitivity analysis.

TABLE 15: The comparison of different ranking methods.

Alternatives	TOPSIS		VIKOR			
	Close degree	Ranking orders	$S_i$	$R_i$	$Q_i$	Ranking orders
$X_1$	0.6666	$X_3 > X_1 > X_2 > X_4$	0.3119	0.0531	0.0099	$X_1 > X_3 > X_2 > X_4$
$X_2$	0.4413		0.5142	0.0843	0.4615	
$X_3$	0.7533		0.3276	0.0508	0.0244	
$X_4$	0.3655		0.6328	0.0244	1.0000	

the proposed model can be validly and practically used to identify the most suitable restoration method for specific wood components, we employ the TOPSIS [47] and VIKOR [48] to make comparative analysis of the above empirical study. The ranking order of the four restoration methods obtained by TOPSIS and VIKOR is outlined in Table 15. From Table 15, the ranking result of the proposed model is consistent with those computed by the TOPSIS when  $\theta \leq 0.5$ . And the ranking order of the case study is the same as those computed by VIKOR. But in the calculation of the VIKOR method,  $Q(X_1) - Q(X_3) < 0.25$ , it means the ranking results of  $X_1$  and  $X_3$  are similar, so both  $X_1$  and  $X_3$  are close to the ideal restoration method. It can be seen that TODIM can better reflect the psychological behavior of the decision-makers and can flexibly respond to the trend of risk aversion. Therefore, the validity of the proposed model can be verified. Compared with the existing approaches for restoration methods selection for wood components of Chinese architectures, the advantages of the model proposed can be summarized as follows:

- (i) The model comprehensively considers the subjective and objective criteria in the index system. According to the index system, the evaluation information characterized by multigranularity linguistic terms is obtained from the experts, and the single-valued neutrosophic set is used to quantify the expert evaluation information. Therefore, this makes the selection of restoration methods more realistic.

- (ii) In order to solve the ranking problem with unknown criteria weights and index weights in the TODIM scheme, combine BWM method and entropy weight method to calculate the criteria and index weights, respectively. As a result, index weights are reliable and more accurate.
- (iii) The proposed model employs TODIM prioritized alternative restoration methods. The TODIM method fully considers the risk aversion of decision-makers and reflects the preferences of decision-makers by adjusting parameter  $\theta$ . Hence, the proposed restoration methods selection model based on TODIM with single-valued neutrosophic sets is a suitable method to solve multicriteria group decision-making problems considering the psychological behavior of decision-makers.

## 6. Conclusion

A selection model of restoration methods for wood components of Chinese ancient architectures has been developed in this paper, which is helpful to assisting experts to solve the problem of selecting appropriate restoration methods. Subjective and objective criteria have been simultaneously utilized in the establishment of index system. Moreover, single-valued neutrosophic sets are employed to characterize the evaluation information given by experts in multigranularity language terms and to quantify the assessment information. In addition, the BWM method and entropy

weight method are used to obtain the criteria and index weights. Finally, the TODIM method has been used to get the prioritization of restoration methods. The proposed model has been conducted to an empirical study in Fuhoutang for restoration methods selection of a specific wood component. The detailed process of the model has been illustrated in this paper. Furthermore, the sensitivity analysis and comparison analysis proved the reliability and effectiveness of the proposed selection model.

In conclusion, the proposed model not only improves extant approaches in the field of restoration methods decision-making for Chinese ancient architectures but also gives rational support to experts in the process of decision-making. So, both theoretical development and practical application are reflected in this work. There are several implications for possible directions of further study. First, more types of information of restoration methods selection should be taken into consideration in the proposed model in future studies. Second, the model can be extended to apply other decision methods, such as TOPSIS and VIKOR. Finally, the proposed selection model can also be applied to other kinds of components of Chinese ancient architectures besides wood components.

## Data Availability

The data used to support the findings of this study are included within the article.

## Conflicts of Interest

The authors declare that there are no conflicts of interest.

## Acknowledgments

The authors would like to thank the experts who participated in the survey. This work was supported by the Human Philosophy Social Science Fund Projects (no. 18YBA150), the Later Support from National Social Science Fund (no. 19FGLB011), the Key Project of Hunan Education Department (no. 18A201), the Think Tank Project of Hunan Social Sciences Federation (no. ZK2019006), and the Hunan Provincial Natural Science Fund (nos. 2019JJ40088 and 2019JJ40479).

## References

- [1] M. Yu, Y. Oda, D. Fang, and J. Zhao, "Advances in structural mechanics of Chinese ancient architectures," *Frontiers of Architecture and Civil Engineering in China*, vol. 2, no. 1, pp. 1–25, 2008.
- [2] A. Zaboklicki and M. Gebiski, "Continuity of wooden beams as a method of reinforcement and preservation of timber structures at monumental buildings," *Transaction on the Built Environment*, vol. 26, pp. 541–546, 1997.
- [3] N. Orlando, Y. Taddia, E. Benvenuti, B. Pizzo, and C. Alessandri, "End-repair of timber beams with laterally-loaded glued-in rods: experimental trials and failure prediction through modelling," *Construction and Building Materials*, vol. 195, pp. 623–637, 2019.
- [4] T. Koike, "Progress in development of epoxy resin systems based on wood biomass in Japan," *Polymer Engineering & Science*, vol. 52, no. 4, pp. 701–717, 2012.
- [5] N. Dourado, F. A. M. Pereira, M. F. S. F. de Moura, and J. J. L. Morais, "Repairing wood beams under bending using carbon-epoxy composites," *Engineering Structures*, vol. 34, pp. 342–350, 2012.
- [6] M. V. Casals, V. R. Rodríguez, and C. L. Badia, "Timber structure repair of an emblematic catalan industrial building with wood grafts and epoxy resins," *Advanced Materials Research*, vol. 778, pp. 998–1005, 2013.
- [7] M. Khelifa and A. Celzard, "Numerical analysis of flexural strengthening of timber beams reinforced with CFRP strips," *Composite Structures*, vol. 111, pp. 393–400, 2014.
- [8] A. Baratta and I. Corbi, "FRP composites retrofitting for protection of monumental and ancient constructions," *The Open Construction and Building Technology Journal*, vol. 6, no. 1, pp. 361–367, 2012.
- [9] A. M. Forster and B. Kayan, "Maintenance for historic buildings: a current perspective," *Structural Survey*, vol. 27, no. 3, pp. 210–229, 2009.
- [10] L. Fregonese, G. Barbieri, L. Biolzi, M. Bocciarelli, A. Frigeri, and L. Taffurelli, "Surveying and monitoring for vulnerability assessment of an ancient building," *Sensors*, vol. 13, no. 8, pp. 9747–9773, 2013.
- [11] Z. Gao, D. Ma, W. Wang, X. Guo, and Q. Ge, "Development and application of ancient timber buildings structural condition assessment model based on a fuzzy matter-element model that includes asymmetric proximity," *Mathematical Problems in Engineering*, vol. 2018, Article ID 7426915, 12 pages, 2018.
- [12] P. B. Lourenço, "Recommendations for restoration of ancient buildings and the survival of a masonry chimney," *Construction and Building Materials*, vol. 20, no. 4, pp. 239–251, 2006.
- [13] R. Wang, X. Zhang, and T. T. Han, "Economic comparison for the protection scheme of ancient building based on BIM," *Applied Mechanics and Materials*, vol. 496–500, pp. 2553–2556, 2014.
- [14] F. Smarandache, "A Unifying Field in Logics: Neutrosophic Logic. Neutrosophy," *Neutrosophic Set, Neutrosophic Probability*, American Research Press, Rehoboth, NM, USA, 1999.
- [15] S.-Z. Luo, P.-F. Cheng, J.-Q. Wang, and Y.-J. Huang, "Selecting project delivery systems based on simplified neutrosophic linguistic preference relations," *Symmetry*, vol. 9, no. 8, p. 151, 2017.
- [16] P. Liu, P. Wang, and J. Liu, "Normal neutrosophic frank aggregation operators and their application in multi-attribute group decision making," *International Journal of Machine Learning and Cybernetics*, vol. 10, no. 5, pp. 833–852, 2019.
- [17] H.-Y. Zhang, P. Ji, J.-Q. Wang, and X.-H. Chen, "A novel decision support model for satisfactory restaurants utilizing social information: a case study of tripadvisor.com," *Tourism Management*, vol. 59, pp. 281–297, 2017.
- [18] D.-P. Li, J.-Q. He, P.-F. Cheng, J.-Q. Wang, and H.-Y. Zhang, "A novel selection model of surgical treatments for early gastric cancer patients based on heterogeneous multicriteria group decision-making," *Symmetry*, vol. 10, no. 6, pp. 223–252, 2018.
- [19] Z.-P. Tian, R.-X. Nie, and J.-Q. Wang, "Probabilistic linguistic multi-criteria decision-making based on evidential reasoning and combined ranking methods considering decision-makers' psychological preferences," *Journal of the Operational Research Society*, vol. 71, no. 5, pp. 700–717, 2019.

- [20] P. Liu, S. Cheng, and Y. Zhang, "An extended multi-criteria group decision-making PROMETHEE method based on probability multi-valued neutrosophic sets," *International Journal of Fuzzy Systems*, vol. 21, no. 2, pp. 388–406, 2019.
- [21] J. Rezaei, "Best-worst multi-criteria decision-making method," *Omega*, vol. 53, pp. 49–57, 2015.
- [22] X. S. You, T. Chen, and Q. Yang, "Approach to multi-criteria group decision-making problems based on the best-worst-method and ELECTRE method," *Symmetry*, vol. 8, no. 9, pp. 1–16, 2016.
- [23] R. Lourenzutti and R. A. Krohling, "A study of TODIM in a intuitionistic fuzzy and random environment," *Expert Systems with Applications*, vol. 40, no. 16, pp. 6459–6468, 2013.
- [24] D. Kahneman and A. Tversky, "Prospect theory: an analysis of decision under risk," *Econometrica*, vol. 47, no. 2, pp. 263–292, 1979.
- [25] H.-G. Peng, J.-Q. Wang, and H.-Y. Zhang, "Multi-criteria outranking method based on probability distribution with probabilistic linguistic information," *Computers & Industrial Engineering*, vol. 141, Article ID 106318, 2020.
- [26] R.-X. Nie and J.-Q. Wang, "Prospect theory-based consistency recovery strategies with multiplicative probabilistic linguistic preference relations in managing group decision making," *Arabian Journal for Science and Engineering*, vol. 45, no. 3, pp. 2113–2130, 2020.
- [27] P. Liu and F. Teng, "Probabilistic linguistic TODIM method for selecting products through online product reviews," *Information Sciences*, vol. 485, pp. 441–455, 2019.
- [28] P. Ren, Z. Xu, and X. Gou, "Pythagorean fuzzy TODIM approach to multi-criteria decision making," *Applied Soft Computing*, vol. 42, pp. 246–259, 2015.
- [29] P. Liu, L. Rong, and F. Teng, "The evaluation of ecosystem health based on hybrid TODIM method for Chinese case," *Technological and Economic Development of Economy*, vol. 25, no. 3, pp. 542–570, 2019.
- [30] G. Zhang, J. Q. Wang, and T. L. Wang, "Multi-criteria group decision-making method based on TODIM with probabilistic interval-valued hesitant fuzzy information," *Expert Systems*, vol. 36, no. 4, 2019.
- [31] L. Xie, J. He, P. Cheng, R. Xiao, and X. Zhou, "A multi-criteria 2-tuple linguistic group decision-making method based on TODIM for cholecystitis treatments selection," *IEEE Access*, vol. 7, pp. 127967–127986, 2019.
- [32] P. Liu and X. You, "Improved TODIM method based on linguistic neutrosophic numbers for multicriteria group decision-making," *International Journal of Computational Intelligence Systems*, vol. 12, no. 2, pp. 544–556, 2019.
- [33] A. Kharal, "A neutrosophic multi-criteria decision making method," *New Mathematics and Natural Computation*, vol. 10, no. 2, pp. 143–162, 2014.
- [34] H. B. Wang, Y. Q. Zhang, R. Sunderraman, and F. Smarandache, "Single valued neutrosophic sets," *Fuzzy Sets, Rough Sets and Multivalued Operations and Applications*, vol. 3, pp. 33–39, 2011.
- [35] J.-J. Peng, J.-Q. Wang, H.-Y. Zhang, and X.-H. Chen, "An outranking approach for multi-criteria decision-making problems with simplified neutrosophic sets," *Applied Soft Computing*, vol. 25, pp. 336–346, 2014.
- [36] P. Majumdar and S. K. Samanta, "On similarity and entropy of neutrosophic sets," *Journal of Intelligent & Fuzzy Systems*, vol. 26, no. 3, pp. 1245–1252, 2014.
- [37] R. P. Tan, W. D. Zhang, and L. L. Chen, "Study on emergency group decision making method based on VIKOR with single valued neutrosophic sets," *Journal of Safety Science and Technology*, vol. 13, no. 2, pp. 79–84, 2017.
- [38] P. Biswas, S. Pramanik, and B. C. Giri, "TOPSIS method for multi-attribute group decision-making under single-valued neutrosophic environment," *Neural Computing and Applications*, vol. 27, no. 3, pp. 727–737, 2015.
- [39] J. Ye, "A multicriteria decision-making method using aggregation operators for simplified neutrosophic sets," *Journal of Intelligent & Fuzzy Systems*, vol. 26, no. 5, pp. 2459–2466, 2014.
- [40] X.-Y. Zhang, H.-Y. Zhang, and J.-Q. Wang, "Discussing incomplete 2-tuple fuzzy linguistic preference relations in multi-granular linguistic MCGDM with unknown weight information," *Soft Computing*, vol. 23, no. 6, pp. 2015–2032, 2017.
- [41] C. Song, X.-K. Wang, P.-F. Cheng, J.-Q. Wang, and L. Li, "SACPC: a framework based on probabilistic linguistic terms for short text sentiment analysis," *Knowledge-Based Systems*, 2020.
- [42] J. Rezaei, "Best-worst multi-criteria decision-making method: some properties and a linear model," *Omega*, vol. 64, pp. 126–130, 2016.
- [43] H. A. Mahdiraji, S. Arzaghi, G. Stauskis, and E. K. Zavadskas, "A hybrid fuzzy BWM-COPRAS method for analyzing key factors of sustainable architecture," *Sustainability*, vol. 10, no. 5, p. 1626, 2018.
- [44] F.-c. Yu, G.-h. Fang, and R. Shen, "Study on comprehensive early warning of drinking water sources for the Gucheng lake in China," *Environmental Earth Sciences*, vol. 72, no. 9, pp. 3401–3408, 2014.
- [45] L. Gomes and M. Lima, "TODIM: basics and application on multicriteria ranking of projects with environmental impacts," *Foundations of Computing and Decision Sciences*, vol. 16, pp. 113–127, 1992.
- [46] R. Lourenzutti and R. A. Krohling, "TODIM based method to process heterogeneous information," *Procedia Computer Science*, vol. 55, pp. 318–327, 2015.
- [47] D. H. Liu, Y. Y. Liu, and L. Z. Wang, "Distance measure for fermatean fuzzy linguistic term sets based on linguistic scale function: an illustration of the TODIM and TOPSIS methods," *International Journal of Intelligent Systems*, vol. 34, no. 2, pp. 2807–2834, 2019.
- [48] L. Lei and W. F. Zhang, "Extended VIKOR method for multi-level hybrid multi-attribute group decision making," in *Proceedings of the 25th Chinese Control and Decision Conference (CCDC)*, pp. 1718–1722, Guiyang, China, May 2013.

## Research Article

# Decision Support Methodology Based on Covering-Based Interval-Valued Pythagorean Fuzzy Rough Set Model and Its Application to Hospital Open-Source EHRs System Selection

Fang Liu,<sup>1</sup> Ju Wu,<sup>2</sup> Lianming Mou,<sup>2</sup> and Yi Liu <sup>1,2,3</sup>

<sup>1</sup>Data Recovery Key Laboratory of Sichuan Province, Neijiang Normal University, Neijiang 641000, Sichuan, China

<sup>2</sup>School of Mathematics and Information Sciences, Neijiang Normal University, Neijiang 641000, Sichuan, China

<sup>3</sup>Numerical Simulation Key Laboratory of Sichuan Province, Neijiang Normal University, Neijiang 641000, Sichuan, China

Correspondence should be addressed to Yi Liu; [liuyi1@126.com](mailto:liuyi1@126.com)

Received 18 March 2020; Revised 17 April 2020; Accepted 22 April 2020; Published 11 May 2020

Guest Editor: Zaoli Yang

Copyright © 2020 Fang Liu et al. This is an open access article distributed under the Creative Commons Attribution License, which permits unrestricted use, distribution, and reproduction in any medium, provided the original work is properly cited.

The target of current work is to propose a new approach to deal with multiattribute decision-making (MADM) problems with interval-valued Pythagorean fuzzy set (IVPFS) based on the concepts of covering-based rough set (CRS) and TOPSIS and give its application in MADM problems. To begin with, we integrate the fuzzy rough set (FRS), IVPFS and CRS and define the covering-based interval-valued Pythagorean fuzzy rough set (CIVPFRS). Firstly, the relative notions of the CIVPFRS model are introduced. In addition, the distance measure of interval-valued Pythagorean fuzzy numbers (IVPFNs) is defined; based on the proposed distance, the rough and precision degrees of CIVPFRS are discussed. Thirdly, on the basis of the theoretical analysis for CIVPFRS models, an interval-valued Pythagorean fuzzy TOPSIS method is designed to deal with the MADM problems with interval-valued Pythagorean fuzzy information (IVPFI). Last of all, the validity and merits of the proposed approach are illustrated by an example, and the sensitivity analysis of the parameters and the comparison with the existing related methods are carried out.<sup>β</sup>

## 1. Introduction

Fuzzy set theory (FS) [1] and rough set theory (RS) [2] are both used to address some problems with uncertainty. RS describes the target set by two definite sets, which are upper approximation set and lower approximation set. The description process does not need any prior knowledge, it is completely based on the given data for analysis and judgment, so RS has been employed in many fields, for instance, data mining, artificial intelligence, decision analysis, and many other fields. Different from RS, FS needs prior knowledge to describe the object, such as expert experience, which has better applicability. There is a strong complementarity between RS and FS. Therefore, the integration of the two has become a new research hotspot, which has aroused the research interest of scholars [1, 3–6].

Intuitionistic fuzzy sets (IFSs) [7] are an effective extension of FSs, which can describe the fuzziness of the

objective world from three aspects: support, opposition, and neutrality. As an IFS can consider both the membership degree (MD) and nonmembership degree (NMD) of elements belonging to the set at the same time, therefore, IFS is widely concerned by decision makers and fruitful results have been achieved. Wan and Dong [8] studied the theory and method of decision-making based on interval-valued intuitionistic fuzzy sets. However, IFSs have some limitations in the application of MADM. For example, it can only describe the fuzzy phenomenon that the sum of MD and NMD is not more than one, but it cannot do anything to the phenomenon that the sum of MD and NMD is more than one. For this reason, Yager and Abbasov [9] put forward the Pythagorean fuzzy set (PFS) to solve the abovementioned limitations. The main difference between IFS and PFS is that, in PFS the sum of squares of MD and NMD are real numbers between zero and one. Based on Yager's research, many scholars have studied the PFS and obtained some research



results. Among them, Garg [10] developed some new operational laws and their corresponding weighted geometric aggregation operators. Garg [11] extended the traditional Maclaurin symmetric mean operator to hesitant Pythagorean fuzzy environment. Liu et al. [12] constructed the multiattribute group decision-making (MAGDM) approach with linguistic Pythagorean fuzzy (LPF) information based on generalized LPF aggregation operators. Then, Liu et al. [13] investigated MADM problems with Pythagorean linguistic information based on some new aggregation operators. Zhang and Xu [14] studied the TOPSIS method under PFS environment; Akram et al. [15] extended the TOPSIS method to solve MCGDM problems with Pythagorean fuzzy data. Wan et al. [16] developed a three-phase method for solving MAGDM using PFNs. Wan et al. [17] also developed a PF mathematical programming method to solve the MAGDM problem in the PF environment. Then, Wan et al. [18] proposed a new order relation for PFNs and applies to MAGDM. In order to express the more complicated uncertainty information, Peng and Yang [19] extended the PFS to the IVPFS and built decision approach for MADM problems with IVPFI based on some proposed aggregation operators. After that, some research studies on IVPFS have emerged in succession. Such as Wei et al. [20] established some MADM methods based on proposed interval-valued Pythagorean fuzzy (IVPF) Maclaurin symmetric average operator and IVPF-weighted Maclaurin symmetric average operator. Garg [21] presented the mean and geometric aggregation operators in interval-valued Pythagorean fuzzy environment. Khan and Abdullah [22] introduced the concept of IVPF Choquet integral average operator. Wang et al. [23] proposed interval-valued hesitant Pythagorean fuzzy sets (IVHPFSs) and investigated some properties of IVHPFSs.

Zakowski's [24] CRS is a generalization model of the classical RS. It is an extension of the partition of Pawlak RS to the covering of RS. On this basis, two rough approximation operators are constructed and many conclusions are obtained. After that many scholars investigated many kinds of RS models based on covering from different angles. In 2003, Zhu and Wang [25] put forward the generalized rough set model of covering and studied the reduction and axiomatic properties of the model. Then, they put forward three different types of CRS models based on the known models and described many important properties. In 2016, Safari and Hooshmandasl [26] introduced twelve kinds of coverage approximation operators and studied the structural properties and interrelations of these twelve types of CRS models. Furthermore, Ma [27] replaces the classical equivalence relation with the general binary relation (neighborhood relation), thus generalizes the CRS. In recent years, many scholars have extended the classical CRS to the fuzzy environment. Dubios and Prade [28] presented the rough fuzzy set (RFS) and fuzzy rough set (FRS). Researchers have carried out some research studies on CFRS. Ma [29] introduced the generalized structure of CFRS. Deer et al. [30, 31] presented the concept of fuzzy  $\beta$ -neighborhoods and fuzzy neighborhoods. Hussain et al. [32] presented q-rung orthopair fuzzy TOPSIS (q-ROF-TOPSIS) methodology for

the MADM problem which depends on the covering-based q-rung orthopair fuzzy sets (Cq-ROFRSs) model. Zeng et al. [33] proposed a method to solve MADM problem based on covering-based spherical fuzzy rough set (CSFRS) models and built TOPSIS method to deal with MADM problem. Hussain et al. [34] presented the notions of rough Pythagorean fuzzy ideals in semigroups. Zheng et al. [4] put forward the extended uncertainty measurement criterion of CRIFSs and introduced an improved roughness method. By combining PFS and FRS, Zhang and Li [5] put forth the concept of Pythagorean fuzzy rough set (PFRS).

As can be seen from the latest hot research directions, the CIVPFS model is an important tool for dealing with uncertainty in the real world. Therefore, it is necessary to build the CIVPFRS model by integrating the IVPFS and CFRS in order to deal with some information with more complicated uncertainty. As far as we know, there is no concept of IVPF rough set in IVPF  $\beta$ -neighborhood systems. In order to fill this research space, this paper attempts to study CIVPFRS model through IVPF  $\beta$ -neighborhood systems. This paper proposes a new approach to deal with MADM problems with IVPFS information based on the concepts of CRS and TOPSIS and gives its application in MADM problem. In real life, CIVPFRS model is a vital tool to handle complexity and uncertainty. Based on the concept of CRS, IVPFS, and FRS, the idea of building CIVPFRS model by IVPF  $\beta$ -neighborhoods is studied. In addition, by adjusting the value of  $0 \leq (\mu_U(x)) + (\nu_U(x)) \leq 1$ , it is found that CIVPFRS is an important extension of cover-based interval-valued intuitionistic fuzzy rough set (CIVIFRS). By adjusting the value of  $\mu_L = \mu_U$  and  $\nu_L = \nu_U$ , it is an important extension of cover-based Pythagorean fuzzy rough set (CPFRS). By adjusting  $\mu_L = \mu_U$ ,  $\nu_L = \nu_U$ , and  $0 \leq (\mu_U(x)) + (\nu_U(x)) \leq 1$ , it is an important extension of cover-based intuitionistic fuzzy rough set (CIFRS). This shows that CIVPFRS model has stronger ability to deal with uncertainty than IFS, interval-valued intuitionistic fuzzy set (IVIFS), and PFS.

Based on the abovementioned ideas, the present paper introduces the CIVPFRS model based on IVPF  $\beta$ -neighborhoods and its utilizations in MADM problem. The rest of this paper is arranged as follows: the basic concepts of PFS and IVPFS and their generalization are introduced in Section 2. In Section 3, the concept of CIVPFRS model based on IVPF  $\beta$ -neighborhoods is proposed along with the corresponding axiomatic system. Apart from these, the roughness and precision degrees of CIVPFRS model are also mainly discussed in this section. In Section 4, based on the analysis of CIVPFRS model, we introduce the interval-valued Pythagorean fuzzy TOPSIS (IVPF-TOPSIS) method to solve the MADM problem with IVPFI. Furthermore, we also construct a method based on CIVPFRS model to solve the MADM problem with IVPFI and design the corresponding algorithm. In Section 5, an example of practical application is provided to show how IVPF-TOPSIS can deal with MADM problems by using the concept of CIVPFRS model based on IVPF  $\beta$ -neighborhoods. Moreover, the sensitivity analysis of the parameters and the correctness analysis of the results are carried out and the conclusion will be obtained in Section 6.

## 2. Preliminaries

Basic concepts and notations of PFS and IVPFS are outlined in this section.

**Definition 1** (see [9]). Let  $U$  be a finite universe set. The PFS  $P$  of  $U$  is defined as follows:

$$P = \{\langle y, \mu_P(y), \nu_P(y) \rangle \mid y \in U\}, \quad (1)$$

where  $0 \leq \mu_P \leq 1$  and  $0 \leq \nu_P \leq 1$  denote the MD and NMD of  $y \in U$  to the set  $P$ , which satisfy  $0 \leq \mu_P^2(y) + \nu_P^2(y) \leq 1$  for all  $y \in U$ .  $\pi_P(y) = \sqrt{1 - \mu_P^2(y) - \nu_P^2(y)}$  represents the degree of indeterminacy of  $y$  to  $P$  and called the indeterminacy degree.

**Definition 2** (see [19]). Let  $U$  be a finite universe set. For every  $y \in U$ ,  $\mu_P(y)$  and  $\nu_P(y)$  are closed intervals, that is,  $\mu_P(y) = [\mu_L(y), \mu_U(y)]$  and  $\nu_P(y) = [\nu_L(y), \nu_U(y)]$ . Then, an IVPFS IVP in  $U$  is defined as follows:

$$\text{IVP} = \{\langle y, ([\mu_L(y), \mu_U(y)], [\nu_L(y), \nu_U(y)]) \rangle \mid y \in U\}, \quad (2)$$

where  $0 \leq (\mu_U(y))^2 + (\nu_U(y))^2 \leq 1$ . Then, the degree of indeterminacy is defined as  $\pi_{\text{IVP}}(y) = [\pi_L(y), \pi_U(y)] = [\sqrt{1 - \mu_U^2(y) - \nu_U^2(y)}, \sqrt{1 - \mu_L^2(y) - \nu_L^2(y)}]$ . Denoted  $\text{IVP} = \text{IVP}([\mu_L, \mu_U], [\nu_L, \nu_U])$  as an IVPFN, where  $[\mu_L, \mu_U] \subseteq [0, 1]$  and  $[\nu_L, \nu_U] \subseteq [0, 1]$ . In the following, we use  $\text{IVPF}(U)$  to denote all IVPFSs on  $U$ .

The score function and accuracy function used to compare two IVPFNs are defined as follows:

**Definition 3** (see [19]). For an IVPFN  $\text{IVP} = \text{IVP}([\mu_L, \mu_U], [\nu_L, \nu_U])$ , the score function of IVP is defined as follows:

$$s(\text{IVP}) = \frac{1}{2}(\mu_L^2 + \mu_U^2 - \nu_L^2 - \nu_U^2), \quad (3)$$

where  $-1 \leq s(\text{IVP}) \leq 1$ . The accuracy function of  $\text{IVP} = \text{IVP}([\mu_L, \mu_U], [\nu_L, \nu_U])$  can be defined as follows:

$$a(\text{IVP}) = \frac{1}{2}(\mu_L^2 + \mu_U^2 + \nu_L^2 + \nu_U^2), \quad (4)$$

where  $0 \leq a(\text{IVP}) \leq 1$ .

For any IVPFN  $P_A, P_B$  of  $U$ , we can compare two IVPFNs by the following rules:

- (1) If  $s(P_A) > s(P_B)$ , then  $P_A$  is bigger than  $P_B$  and is denoted by  $P_A > P_B$ .
- (2) If  $s(P_A) = s(P_B)$ , then
  - (i) If  $a(P_A) > a(P_B)$ , then  $P_A > P_B$ .
  - (ii) If  $a(P_A) = a(P_B)$ , then  $P_A \sim P_B$ .

## 3. CIVPFRS Model

In this section, we introduce the concept of CIVPFRS.

**Definition 4.** (1) Assume  $U$  is an universe set,  $\tilde{E} = \{\tilde{E}_1, \tilde{E}_2, \dots, \tilde{E}_n\}$ , where  $\tilde{E} \in \text{IVPF}(U)$  and  $k = 1, \dots, n$ . For any IVPFN  $\beta = \langle [s_L, s_U], [t_L, t_U] \rangle$ , then  $\tilde{E}$  is called an interval-valued Pythagorean fuzzy  $\beta$ -covering (IVPF  $\beta$ -covering) of  $U$  if

$$\left( \bigcup_{k=1}^n \tilde{E}_k \right)(y) \geq \beta, \quad (5)$$

for all  $y \in U$ . The  $(U, \tilde{E})$  is called an interval-valued Pythagorean fuzzy covering approximation space (IVPFCAS).

(2) Let  $(U, \tilde{E})$  be an IVPFCAS and  $\tilde{E} = \{\tilde{E}_1, \tilde{E}_2, \dots, \tilde{E}_n\}$  be an IVPF  $\beta$ -covering of  $U$  for some  $\beta = \langle [s_L, s_U], [t_L, t_U] \rangle$ . Then,

$$\tilde{N}_{E(y)}^\beta = \bigcap \{\tilde{E}_k \in \tilde{E} \mid \tilde{E}_k(y) \geq \beta, k = 1, \dots, n\} \quad (6)$$

is called an IVPF  $\beta$ -neighborhood of  $y$  in  $U$ .

Let  $\tilde{N}_E^\beta = \{\tilde{N}_{E(y)}^\beta \mid y \in U\}$  represent IVPF  $\beta$ -neighborhood system induced by IVPF  $\beta$ -covering  $\tilde{E}$ . The IVPF  $\beta$ -neighborhood system is represented by the IVPF matrix as follows:

$$\tilde{M}_E^\beta = \left[ \tilde{N}_{E(y)}^\beta(z) \right]_{(y,z) \in U \times U}. \quad (7)$$

**Example 1.** Suppose that  $(U, \tilde{E})$  is an IVPFCAS and  $\tilde{E} = \{\tilde{E}_1, \tilde{E}_2, \dots, \tilde{E}_5\}$  is a set of IVPFS, where  $U = \{y_1, y_2, \dots, y_6\}$ ,  $\beta = \langle [0.3, 0.5], [0.3, 0.4] \rangle$ . Details are shown in Table 1.

Therefore,  $\tilde{E}$  is an IVPF  $\beta$ -covering of  $U$ . Then,

$$\begin{aligned} \tilde{N}_{\tilde{E}(y_1)}^{\langle [0.3, 0.5], [0.3, 0.4] \rangle} &= \tilde{E}_1 \cap \tilde{E}_4, \\ \tilde{N}_{\tilde{E}(y_2)}^{\langle [0.3, 0.5], [0.3, 0.4] \rangle} &= \tilde{E}_1 \cap \tilde{E}_3, \\ \tilde{N}_{\tilde{E}(y_3)}^{\langle [0.3, 0.5], [0.3, 0.4] \rangle} &= \tilde{E}_1 \cap \tilde{E}_5, \\ \tilde{N}_{\tilde{E}(y_4)}^{\langle [0.3, 0.5], [0.3, 0.4] \rangle} &= \tilde{E}_1 \cap \tilde{E}_5, \\ \tilde{N}_{\tilde{E}(y_5)}^{\langle [0.3, 0.5], [0.3, 0.4] \rangle} &= \tilde{E}_2 \cap \tilde{E}_3, \\ \tilde{N}_{\tilde{E}(y_6)}^{\langle [0.3, 0.5], [0.3, 0.4] \rangle} &= \tilde{E}_2 \cap \tilde{E}_4. \end{aligned} \quad (8)$$

By calculations, we have the  $\tilde{N}_E^{\langle [0.3, 0.5], [0.3, 0.4] \rangle}$ , as shown in Table 2. Then, we get the IVPF matrix and listed as follows. That is,



TABLE 1: IVPF  $\beta$ -covering  $\tilde{E}$  in Example 1.

$U/\tilde{E}$	$\tilde{E}_1$	$\tilde{E}_2$	$\tilde{E}_3$	$\tilde{E}_4$	$\tilde{E}_5$
$y_1$	$\langle [0.6, 0.8], [0.1, 0.2] \rangle$	$\langle [0.5, 0.7], [0.5, 0.6] \rangle$	$\langle [0.3, 0.5], [0.7, 0.8] \rangle$	$\langle [0.6, 0.9], [0.1, 0.3] \rangle$	$\langle [0.3, 0.4], [0.3, 0.6] \rangle$
$y_2$	$\langle [0.4, 0.7], [0.2, 0.3] \rangle$	$\langle [0.2, 0.4], [0.1, 0.5] \rangle$	$\langle [0.4, 0.8], [0.1, 0.4] \rangle$	$\langle [0.5, 0.6], [0.4, 0.7] \rangle$	$\langle [0.2, 0.7], [0.1, 0.2] \rangle$
$y_3$	$\langle [0.3, 0.6], [0.3, 0.4] \rangle$	$\langle [0.7, 0.8], [0.4, 0.6] \rangle$	$\langle [0.2, 0.8], [0.2, 0.3] \rangle$	$\langle [0.1, 0.3], [0.6, 0.9] \rangle$	$\langle [0.6, 0.7], [0.1, 0.2] \rangle$
$y_4$	$\langle [0.5, 0.8], [0.1, 0.3] \rangle$	$\langle [0.2, 0.3], [0.6, 0.9] \rangle$	$\langle [0.1, 0.4], [0.1, 0.3] \rangle$	$\langle [0.4, 0.7], [0.3, 0.6] \rangle$	$\langle [0.4, 0.8], [0.1, 0.4] \rangle$
$y_5$	$\langle [0.1, 0.2], [0.5, 0.7] \rangle$	$\langle [0.3, 0.7], [0.1, 0.3] \rangle$	$\langle [0.8, 0.9], [0.1, 0.2] \rangle$	$\langle [0.6, 0.7], [0.2, 0.5] \rangle$	$\langle [0.1, 0.8], [0.2, 0.3] \rangle$
$y_6$	$\langle [0.4, 0.6], [0.4, 0.6] \rangle$	$\langle [0.3, 0.7], [0.1, 0.2] \rangle$	$\langle [0.5, 0.6], [0.3, 0.5] \rangle$	$\langle [0.7, 0.8], [0.1, 0.3] \rangle$	$\langle [0.1, 0.4], [0.1, 0.2] \rangle$

TABLE 2:  $\tilde{N}_E^{\langle [0.3, 0.5], [0.3, 0.4] \rangle}$  in Example 1.

$\tilde{N}_E^\beta$	$y_1$	$y_2$	$y_3$	$y_4$	$y_5$	$y_6$
$y_1$	$\langle [0.6, 0.8], [0.1, 0.3] \rangle$	$\langle [0.4, 0.6], [0.4, 0.7] \rangle$	$\langle [0.1, 0.3], [0.6, 0.9] \rangle$	$\langle [0.4, 0.7], [0.3, 0.6] \rangle$	$\langle [0.1, 0.2], [0.5, 0.7] \rangle$	$\langle [0.4, 0.6], [0.4, 0.6] \rangle$
$y_2$	$\langle [0.3, 0.5], [0.7, 0.8] \rangle$	$\langle [0.4, 0.7], [0.2, 0.4] \rangle$	$\langle [0.2, 0.6], [0.3, 0.4] \rangle$	$\langle [0.1, 0.4], [0.1, 0.3] \rangle$	$\langle [0.1, 0.2], [0.5, 0.7] \rangle$	$\langle [0.4, 0.6], [0.4, 0.6] \rangle$
$y_3$	$\langle [0.3, 0.4], [0.3, 0.6] \rangle$	$\langle [0.2, 0.7], [0.2, 0.3] \rangle$	$\langle [0.3, 0.6], [0.3, 0.4] \rangle$	$\langle [0.4, 0.8], [0.1, 0.4] \rangle$	$\langle [0.1, 0.2], [0.5, 0.7] \rangle$	$\langle [0.1, 0.4], [0.4, 0.6] \rangle$
$y_4$	$\langle [0.3, 0.4], [0.3, 0.6] \rangle$	$\langle [0.2, 0.7], [0.2, 0.3] \rangle$	$\langle [0.3, 0.6], [0.3, 0.4] \rangle$	$\langle [0.4, 0.8], [0.1, 0.4] \rangle$	$\langle [0.1, 0.2], [0.5, 0.7] \rangle$	$\langle [0.1, 0.4], [0.4, 0.6] \rangle$
$y_5$	$\langle [0.3, 0.5], [0.7, 0.8] \rangle$	$\langle [0.2, 0.4], [0.1, 0.5] \rangle$	$\langle [0.2, 0.8], [0.4, 0.6] \rangle$	$\langle [0.1, 0.3], [0.6, 0.9] \rangle$	$\langle [0.3, 0.7], [0.1, 0.3] \rangle$	$\langle [0.3, 0.6], [0.3, 0.5] \rangle$
$y_6$	$\langle [0.5, 0.7], [0.5, 0.6] \rangle$	$\langle [0.2, 0.4], [0.4, 0.7] \rangle$	$\langle [0.1, 0.3], [0.6, 0.9] \rangle$	$\langle [0.2, 0.3], [0.6, 0.9] \rangle$	$\langle [0.3, 0.7], [0.2, 0.5] \rangle$	$\langle [0.3, 0.7], [0.1, 0.3] \rangle$

$$M_E^{\langle [0.3, 0.5], [0.3, 0.4] \rangle} = \begin{pmatrix} \langle [0.6, 0.8], [0.1, 0.3] \rangle & \langle [0.4, 0.6], [0.4, 0.7] \rangle & \langle [0.1, 0.3], [0.6, 0.9] \rangle & \langle [0.4, 0.7], [0.3, 0.6] \rangle & \langle [0.1, 0.2], [0.5, 0.7] \rangle & \langle [0.4, 0.6], [0.4, 0.6] \rangle \\ \langle [0.3, 0.5], [0.7, 0.8] \rangle & \langle [0.4, 0.7], [0.2, 0.4] \rangle & \langle [0.2, 0.6], [0.3, 0.4] \rangle & \langle [0.1, 0.4], [0.1, 0.3] \rangle & \langle [0.1, 0.2], [0.5, 0.7] \rangle & \langle [0.4, 0.6], [0.4, 0.6] \rangle \\ \langle [0.3, 0.4], [0.3, 0.6] \rangle & \langle [0.2, 0.7], [0.2, 0.3] \rangle & \langle [0.3, 0.6], [0.3, 0.4] \rangle & \langle [0.4, 0.8], [0.1, 0.4] \rangle & \langle [0.1, 0.2], [0.5, 0.7] \rangle & \langle [0.1, 0.4], [0.4, 0.6] \rangle \\ \langle [0.3, 0.4], [0.3, 0.6] \rangle & \langle [0.2, 0.7], [0.2, 0.3] \rangle & \langle [0.3, 0.6], [0.3, 0.4] \rangle & \langle [0.4, 0.8], [0.1, 0.4] \rangle & \langle [0.1, 0.2], [0.5, 0.7] \rangle & \langle [0.1, 0.4], [0.4, 0.6] \rangle \\ \langle [0.3, 0.5], [0.7, 0.8] \rangle & \langle [0.2, 0.4], [0.1, 0.5] \rangle & \langle [0.2, 0.8], [0.4, 0.6] \rangle & \langle [0.1, 0.3], [0.6, 0.9] \rangle & \langle [0.3, 0.7], [0.1, 0.3] \rangle & \langle [0.3, 0.6], [0.3, 0.5] \rangle \\ \langle [0.5, 0.7], [0.5, 0.6] \rangle & \langle [0.2, 0.4], [0.4, 0.7] \rangle & \langle [0.1, 0.3], [0.6, 0.9] \rangle & \langle [0.2, 0.3], [0.6, 0.9] \rangle & \langle [0.3, 0.7], [0.2, 0.5] \rangle & \langle [0.3, 0.7], [0.1, 0.3] \rangle \end{pmatrix}. \quad (9)$$

**Definition 5.** Assume that  $(U, \tilde{E})$  is an IVPFCAS and  $\tilde{E} = \{\tilde{E}_1, \tilde{E}_2, \dots, \tilde{E}_n\}$  is an IVPF  $\beta$ -covering of  $U$  for some  $\beta = \langle [s_L, s_U], [t_L, t_U] \rangle$  and  $U = \{y_1, y_2, \dots, y_m\}$ . Suppose that  $\tilde{N}_E^\beta = \{\tilde{N}_{\tilde{E}(y)}^\beta \mid y \in U\}$  is an IVPF  $\beta$ -neighborhood system, where

$$\tilde{N}_{\tilde{E}(y_i)}^\beta = \left\{ \langle y_j, [\mu_{\tilde{N}_{\tilde{E}(y_i)}^\beta}(y_j), \mu_{\tilde{N}_{\tilde{E}(y_i)}^\beta}(y_j)] \rangle, \right. \\ \left. [\nu_{\tilde{N}_{\tilde{E}(y_i)}^\beta}(y_j), \nu_{\tilde{N}_{\tilde{E}(y_i)}^\beta}(y_j)] \rangle \mid j = 1, \dots, m \right\}, \quad (10)$$

for all  $i = 1, \dots, m$ .

Then, for any  $A \in \text{IVPF}(U)$ ,

$$A = \left\{ \langle y_j, [\mu_{LA}(y_j), \mu_{UA}(y_j)] \rangle, \right. \\ \left. [\nu_{LA}(y_j), \nu_{UA}(y_j)] \rangle \mid j = 1, \dots, m \right\}, \quad (11)$$

and the upper and lower approximations of  $A$  with respect to  $\tilde{N}_E^\beta$ , denoted by  $\tilde{N}_E^\beta(A)$  and  $\underline{\tilde{N}}_E^\beta(A)$ , are two IVPFSs; they are defined as follows:

$$\tilde{N}_E^\beta(A) = \left\{ \langle y_i, [\mu_{\tilde{N}_E^\beta(A)}(y_i), \mu_{\tilde{N}_E^\beta(A)}(y_i)] \rangle, \right. \\ \left. [\nu_{\tilde{N}_E^\beta(A)}(y_i), \nu_{\tilde{N}_E^\beta(A)}(y_i)] \rangle \mid i = 1, \dots, m \right\}, \quad (12)$$

$$\underline{\tilde{N}}_E^\beta(A) = \left\{ \langle y_i, [\mu_{\underline{\tilde{N}}_E^\beta(A)}(y_i), \mu_{\underline{\tilde{N}}_E^\beta(A)}(y_i)] \rangle, \right. \\ \left. [\nu_{\underline{\tilde{N}}_E^\beta(A)}(y_i), \nu_{\underline{\tilde{N}}_E^\beta(A)}(y_i)] \rangle \mid i = 1, \dots, m \right\}, \quad (13)$$

where

$$\begin{aligned}
\mu_{\widetilde{LN}_E^\beta(A)}(y_i) &= \bigvee_{j=1}^m \left\{ \mu_{\widetilde{LN}_E^\beta(y_i)}^\beta(y_j) \wedge \mu_{LA}(y_j) \right\}, \\
\mu_{\widetilde{UN}_E^\beta(A)}(y_i) &= \bigvee_{j=1}^m \left\{ \mu_{\widetilde{UN}_E^\beta(y_i)}^\beta(y_j) \wedge \mu_{UA}(y_j) \right\}, \\
\nu_{\widetilde{LN}_E^\beta(A)}(y_i) &= \bigwedge_{j=1}^m \left\{ \nu_{\widetilde{LN}_E^\beta(y_i)}^\beta(y_j) \vee \nu_{LA}(y_j) \right\}, \\
\nu_{\widetilde{UN}_E^\beta(A)}(y_i) &= \bigwedge_{j=1}^m \left\{ \nu_{\widetilde{UN}_E^\beta(y_i)}^\beta(y_j) \vee \nu_{UA}(y_j) \right\}, \\
\mu_{\widetilde{LN}_E^\beta(A)}(y_i) &= \bigwedge_{j=1}^m \left\{ \nu_{\widetilde{LN}_E^\beta(y_i)}^\beta(y_j) \vee \mu_{LA}(y_j) \right\}, \\
\mu_{\widetilde{UN}_E^\beta(A)}(y_i) &= \bigwedge_{j=1}^m \left\{ \nu_{\widetilde{UN}_E^\beta(y_i)}^\beta(y_j) \vee \mu_{UA}(y_j) \right\}, \\
\nu_{\widetilde{LN}_E^\beta(A)}(y_i) &= \bigvee_{j=1}^m \left\{ \mu_{\widetilde{LN}_E^\beta(y_i)}^\beta(y_j) \wedge \nu_{LA}(y_j) \right\}, \\
\nu_{\widetilde{UN}_E^\beta(A)}(y_i) &= \bigvee_{j=1}^m \left\{ \mu_{\widetilde{UN}_E^\beta(y_i)}^\beta(y_j) \wedge \nu_{UA}(y_j) \right\}.
\end{aligned} \tag{14}$$

The operators  $\widetilde{N}_E^\beta(A)$  and  $\widetilde{N}_E^\beta(A)$  are called the upper and lower interval-valued Pythagorean fuzzy rough approximation operators (IVPFRAOs) with respect to  $\widetilde{N}_E^\beta$ , respectively.

*Example 2* (continued from Example 1). Let an IVPFS

$$\begin{aligned}
A = \{ & \langle y_1, [0.5, 0.7], [0.3, 0.4] \rangle, \langle y_2, [0.1, 0.4], [0.6, 0.7] \rangle, \\
& \langle y_3, [0.2, 0.8], [0.4, 0.6] \rangle, \langle y_4, [0.6, 0.8], [0.1, 0.3] \rangle, \\
& \langle y_5, [0.3, 0.6], [0.3, 0.5] \rangle, \langle y_6, [0.7, 0.9], [0.1, 0.2] \rangle \}.
\end{aligned} \tag{15}$$

Then,

$$\begin{aligned}
\widetilde{N}_E^\beta(A) = \{ & \langle y_1, [0.5, 0.7], [0.3, 0.4] \rangle, \langle y_2, [0.1, 0.4], [0.4, 0.7] \rangle, \\
& \langle y_3, [0.2, 0.8], [0.4, 0.6] \rangle, \langle y_4, [0.6, 0.8], [0.1, 0.3] \rangle, \\
& \langle y_5, [0.3, 0.6], [0.3, 0.5] \rangle, \langle y_6, [0.7, 0.9], [0.1, 0.2] \rangle \}, \\
\widetilde{N}_E^\beta(A) = \{ & \langle y_1, [0.5, 0.7], [0.3, 0.4] \rangle, \langle y_2, [0.1, 0.4], [0.6, 0.7] \rangle, \\
& \langle y_3, [0.2, 0.8], [0.4, 0.6] \rangle, \langle y_4, [0.4, 0.8], [0.1, 0.3] \rangle, \\
& \langle y_5, [0.3, 0.6], [0.3, 0.5] \rangle, \langle y_6, [0.5, 0.7], [0.2, 0.5] \rangle \}.
\end{aligned} \tag{16}$$

**Definition 6.** Let  $P_1 = \langle [\mu_{LA}, \mu_{UA}], [\nu_{LA}, \nu_{UA}] \rangle$  and  $P_2 = \langle [\mu_{LA}, \mu_{UA}], [\nu_{LA}, \nu_{UA}] \rangle$  be two IVPFNs, and the generalized distance between  $P_1$  and  $P_2$  is defined as follows:

$$\begin{aligned}
d(P_1, P_2) = & \left\{ \frac{1}{4} (1-p) \left[ |\mu_{LA}^2 - \mu_{LB}^2|^\lambda + |\mu_{UA}^2 - \mu_{UB}^2|^\lambda \right. \right. \\
& \left. \left. + |\nu_{LA}^2 - \nu_{LB}^2|^\lambda + |\nu_{UA}^2 - \nu_{UB}^2|^\lambda \right] \right. \\
& \left. + p \left[ |\pi_{LA}^2 - \pi_{LB}^2|^\lambda + |\pi_{UA}^2 - \pi_{UB}^2|^\lambda \right] \right\}^{1/\lambda},
\end{aligned} \tag{17}$$

where  $\pi_{LA} = \sqrt{1 - \mu_{UA}^2 - \nu_{UA}^2}$ ,  $\pi_{LB} = \sqrt{1 - \mu_{UB}^2 - \nu_{UB}^2}$ ,  $\pi_{UA} = \sqrt{1 - \mu_{LA}^2 - \nu_{LA}^2}$ ,  $\pi_{UB} = \sqrt{1 - \mu_{LB}^2 - \nu_{LB}^2}$ ,  $\lambda > 0$ , and  $p \in [0, 1]$ .

When the parameters  $\lambda$  and  $p$  take different values, we will get some different distance measures.

*Case 1.* When  $\lambda = 1$ , the distance will be reduced to Hamming-indeterminacy degree-preference distance:

$$\begin{aligned}
d(P_1, P_2) = & \frac{1}{4} (1-p) \left[ |\mu_{LA}^2 - \mu_{LB}^2| + |\mu_{UA}^2 - \mu_{UB}^2| \right. \\
& \left. + |\nu_{LA}^2 - \nu_{LB}^2| + |\nu_{UA}^2 - \nu_{UB}^2| \right] \\
& + p \left[ |\pi_{LA}^2 - \pi_{LB}^2| + |\pi_{UA}^2 - \pi_{UB}^2| \right].
\end{aligned} \tag{18}$$

In Case 1, if  $p = 0$ , the effect of the indeterminacy degree is not considered. The distance will be reduced to metric distance:

$$\begin{aligned}
d(P_1, P_2) = & \frac{1}{4} \left[ |\mu_{LA}^2 - \mu_{LB}^2| + |\mu_{UA}^2 - \mu_{UB}^2| \right. \\
& \left. + |\nu_{LA}^2 - \nu_{LB}^2| + |\nu_{UA}^2 - \nu_{UB}^2| \right].
\end{aligned} \tag{19}$$

*Case 2.* When  $\lambda = 2$ , the distance will be reduced to Euclidean-indeterminacy degree-preference distance:

$$\begin{aligned}
d(P_1, P_2) = & \left\{ \frac{1}{4} (1-p) \left[ |\mu_{LA}^2 - \mu_{LB}^2|^2 + |\mu_{UA}^2 - \mu_{UB}^2|^2 \right. \right. \\
& \left. \left. + |\nu_{LA}^2 - \nu_{LB}^2|^2 + |\nu_{UA}^2 - \nu_{UB}^2|^2 \right] \right. \\
& \left. + p \left[ |\pi_{LA}^2 - \pi_{LB}^2|^2 + |\pi_{UA}^2 - \pi_{UB}^2|^2 \right] \right\}^{1/2}.
\end{aligned} \tag{20}$$

In Case 2, if  $p = 0$ , the distance will be reduced to Euclidean distance:

$$\begin{aligned}
d(P_1, P_2) = & \left\{ \frac{1}{4} \left[ |\mu_{LA}^2 - \mu_{LB}^2|^2 + |\mu_{UA}^2 - \mu_{UB}^2|^2 \right. \right. \\
& \left. \left. + |\nu_{LA}^2 - \nu_{LB}^2|^2 + |\nu_{UA}^2 - \nu_{UB}^2|^2 \right] \right\}^{1/2}.
\end{aligned} \tag{21}$$

Let  $P_1$  and  $P_2$  be two IVPFNs, and it is easy to verify that the distance  $d$  satisfied the following properties:

- (1)  $d(P_1, P_2) \geq 0$
- (2)  $d(P_1, P_2) = d(P_2, P_1)$
- (3)  $d(P_1, P_2) = 0 \iff A = B$

**Definition 7.** Let  $A$  and  $B$  be two IVPFSs. The distance  $D(A, B)$  of  $A$  and  $B$  is defined as follows:

$$D(A, B) = \frac{1}{|U|} \sum_{y \in U} \left\{ \frac{1}{4} (1-p) \left[ |\mu_{LA}^2(y) - \mu_{LB}^2(y)|^\lambda + |\mu_{UA}^2(y) - \mu_{UB}^2(y)|^\lambda + |\nu_{LA}^2(y) - \nu_{LB}^2(y)|^\lambda + |\nu_{UA}^2(y) - \nu_{UB}^2(y)|^\lambda \right] + p \left[ |\pi_{LA}^2(y) - \pi_{LB}^2(y)|^\lambda + |\pi_{UA}^2(y) - \pi_{UB}^2(y)|^\lambda \right] \right\}^{1/\lambda}, \quad (22)$$

where  $\lambda > 0$  and  $p \in [0, 1]$ .

**Definition 8.** Suppose that  $(U, \tilde{E})$  is an IVPFCAS and  $\tilde{E} = \{\tilde{E}_1, \tilde{E}_2, \dots, \tilde{E}_n\}$  is an IVPF  $\beta$ -covering of  $U$  for some  $\beta = \langle [s_L, s_U], [t_L, t_U] \rangle$ . Suppose that  $\tilde{N}_E^\beta = \{\tilde{N}_{E(y)}^\beta \mid y \in U\}$  is an IVPF  $\beta$ -neighborhood system. For any  $A \in \text{IVPF}(U)$ ,  $\tilde{N}_E^\beta(A)$  and  $\overline{\tilde{N}_E^\beta}(A)$  are the lower and upper approximations of  $A$ . The rough degree and precision degree of  $A$  are defined as follows:

$$\begin{aligned} R_{\tilde{N}_E^\beta(A)}^\beta &= D\left(\tilde{N}_E^\beta(A), \overline{\tilde{N}_E^\beta}(A)\right), \\ P_{\tilde{N}_E^\beta(A)}^\beta &= 1 - R_{\tilde{N}_E^\beta(A)}^\beta. \end{aligned} \quad (23)$$

**Example 3.** (continued from Example 2). Let  $\lambda = 4$  and  $p = 0.5$ . According to Definitions 6 and 7, the rough degree and precision degree of  $A$  with respect to  $\tilde{N}_E^\beta$  can be calculated as follows:

$$\begin{aligned} R_{\tilde{N}_E^\beta(A)}^\beta &= 0.1188, \\ P_{\tilde{N}_E^\beta(A)}^\beta &= 0.8812. \end{aligned} \quad (24)$$

## 4. A Novel Method to Solve MADM Problems with IVPFI

In Section 3, we established the CIVPFRS. Based on this, we will construct a model and method for a class of MADM problems with IVPFI in this section. In addition, we will propose a decision-making algorithm to solve the MADM problems.

**4.1. Decision-Making Method.** We will propose the model and method, which is used to solve the MADM problems with IVPFI based on CIVPFRS.

**4.1.1. The Form Descriptions of Problem of MADM Problem with IVPFI.** Assume that  $U = \{y_1, y_2, \dots, y_m\}$  is a set of alternatives and  $\tilde{E} = \{\tilde{E}_1, \tilde{E}_2, \dots, \tilde{E}_n\}$  is the set of attributes.

Let  $W = (w_1, w_2, \dots, w_n)^T$  be the weight vector of the attributes, where  $0 \leq w_j \leq 1, j = 1, 2, \dots, n$ , which satisfies  $\sum_{j=1}^n w_j = 1$ . Let the decision maker  $D$  present the evaluation values of the attributes  $y_i, i = 1, \dots, m$  with respect to the attribute set  $\tilde{E}_j (j = 1, \dots, n)$  by  $\tilde{E}_j(y_i) = \langle [\mu_L, \mu_U], [\nu_L, \nu_U] \rangle_{ij}$ . It means, the MD to which  $y_i$  satisfies  $\tilde{E}_j$  is interval-valued  $[\mu_L, \mu_U]$ , and the NMD to which  $y_i$  dissatisfies  $\tilde{E}_j$  is interval-valued  $[\nu_L, \nu_U]$ . By using IVPF-TOPSIS method, we establish IVPF-PIS  $\text{IVP}^+ = \{\tilde{E}_j, \max\{s(\tilde{E}_j(y_i)) \mid j = 1, \dots, n\}\}$  and IVPF-NIS  $\text{IVP}^- = \{\tilde{E}_j, \min\{s(\tilde{E}_j(y_i)) \mid j = 1, \dots, n\}\}$ , where  $s$  is the score function, which is defined in Definition 3. After that we calculate the distances  $D^+$  and  $D^-$  between each alternative  $y_i$  and  $\text{IVP}^+$  and  $\text{IVP}^-$ , respectively, according to Definition 6. Therefore, we construct a new IVPFS  $D = \langle [\mu_{DL}, \mu_{DU}], [\nu_{DL}, \nu_{DU}] \rangle = \langle [D^+, D^+], [D^-, D^-] \rangle$ .

In this section, a new method is proposed to solve the MADM problem by using the CIVPFRS established in Section 3.

**4.1.2. Decision-Making Method and Process.** Considering the characteristics of MADM problems, we will present a decision-making model and its algorithm steps based on CIVPFRS. This model consists of three parts. In the first part, we will determine IVPF decision objectives for all alternatives. In the second part, we will use the precision parameter  $\beta (0 < \beta \leq 1)$  to calculate the upper and lower approximations of the IVPF decision-making object for all alternatives. In the third part, on the basis of the first two steps, we use the decision-making principle to rank all alternatives and then give the optimal object of the MADM problem.

Next, we will introduce in detail the model and method for solving the MADM problem based on CIVPFRS.

First, we will propose the IVPF-TOPSIS method. This method takes into account the following principles. The optimal alternative should be the one with the shortest distance from IVPF-PIS and the longest distance from IVPF-NIS.

IVPF-PIS and IVPF-NIS are calculated using the score function, which is defined in Definition 3:

$$\begin{aligned} \text{IVP}^+ &= \{\tilde{E}_j, \max\{s(\tilde{E}_j(y_i)) \mid j = 1, \dots, n\} \mid (i = 1, \dots, m) \\ &= \left\{ \langle \tilde{E}_1, [\mu_{1L}^+, \mu_{1U}^+], [\nu_{1L}^+, \nu_{1U}^+] \rangle, \dots, \langle \tilde{E}_n, [\mu_{nL}^+, \mu_{nU}^+], [\nu_{nL}^+, \nu_{nU}^+] \rangle \right\}, \end{aligned} \quad (25)$$

$$\begin{aligned} \text{IVP}^- &= \{\tilde{E}_j, \min\{s(\tilde{E}_j(y_i)) \mid j = 1, \dots, n\} \mid (i = 1, \dots, m) \\ &= \left\{ \langle \tilde{E}_1, [\mu_{1L}^-, \mu_{1U}^-], [\nu_{1L}^-, \nu_{1U}^-] \rangle, \dots, \langle \tilde{E}_n, [\mu_{nL}^-, \mu_{nU}^-], [\nu_{nL}^-, \nu_{nU}^-] \rangle \right\}. \end{aligned} \quad (26)$$

Next, according to Definition 6, we calculate  $D^+$  and  $D^-$  between each alternative  $y_i$  and  $\text{IVP}^+$  and  $\text{IVP}^-$ , respectively, for all  $i = 1, 2, \dots, m$ , as follows:

$$\begin{aligned}
D^+ &= \sum_{j=1}^n w_j \cdot d((\tilde{E}_j(y_i)), (\tilde{E}_j(\text{IVP}^+))) \\
&= \sum_{j=1}^n w_j \cdot \left\{ \frac{1}{4} (1-p) \left[ |\mu_{L_{ij}}^2 - \mu_{jL}^{+2}|^\lambda + |\mu_{U_{ij}}^2 - \mu_{jU}^{+2}|^\lambda + |\nu_{L_{ij}}^2 - \nu_{jL}^{+2}|^\lambda + |\nu_{U_{ij}}^2 - \nu_{jU}^{+2}|^\lambda \right] \right. \\
&\quad \left. + p \left[ |\pi_{L_{ij}}^2 - \pi_{jL}^{+2}|^\lambda + |\pi_{U_{ij}}^2 - \pi_{jU}^{+2}|^\lambda \right] \right\}^{1/\lambda},
\end{aligned} \tag{27}$$

$$\begin{aligned}
D^- &= \sum_{j=1}^n w_j \cdot d((\tilde{E}_j(y_i)), (\tilde{E}_j(\text{IVP}^-))) \\
&= \sum_{j=1}^n w_j \cdot \left\{ \frac{1}{4} (1-p) \left[ |\mu_{L_{ij}}^2 - \mu_{jL}^{-2}|^\lambda + |\mu_{U_{ij}}^2 - \mu_{jU}^{-2}|^\lambda + |\nu_{L_{ij}}^2 - \nu_{jL}^{-2}|^\lambda \right. \right. \\
&\quad \left. \left. + |\nu_{U_{ij}}^2 - \nu_{jU}^{-2}|^\lambda \right] + p \left[ |\pi_{L_{ij}}^2 - \pi_{jL}^{-2}|^\lambda + |\pi_{U_{ij}}^2 - \pi_{jU}^{-2}|^\lambda \right] \right\}^{1/\lambda}.
\end{aligned} \tag{28}$$

Here, we construct a new IVPFS  $D = \langle [\mu_{DL}, \mu_{DU}], [\nu_{DL}, \nu_{DU}] \rangle = \langle [D^+, D^-], [D^-, D^+] \rangle$ . In order to fuse all preference information in the framework of CIVPFRS, we introduced the fuzzy logical operators [35] and then propose another method to fuse fuzzy preference information of MADM problems.

Triangular norms ( $t$ -norms) were first proposed in the framework of probabilistic metric spaces [35]. In some contexts,  $t$ -norms have been proved to be an appropriate tool for information fusion of the upper and lower approximations of interval-valued Pythagorean fuzzy decision-making object.

**Definition 9** (see [35]).  $t$ -norm is an associative, increasing and commutative mapping function  $\mathcal{T}: [0, 1]^2 \longrightarrow [0, 1]$ , which satisfies the boundary condition, for any  $(x \in [0, 1], \mathcal{T}(x, 1) = x)$ . Moreover, the triangular conorm ( $t$ -conorm) is an associative, increasing and commutative mapping function  $\mathcal{S}: [0, 1]^2 \longrightarrow [0, 1]$ , which satisfies the boundary condition, for any  $(x \in [0, 1], \mathcal{S}(x, 0) = x)$ .

In the current work, we consider the following the  $t$ -norms and  $t$ -conorms for MADM problems:

$$\begin{aligned}
\mathcal{T}_p(x, y) &= \frac{xy}{\sqrt{1 + (1-x^2)(1-y^2)}}, \\
\mathcal{S}_p(x, y) &= \sqrt{\frac{(x^2 + y^2)}{(1 + x^2 y^2)}}.
\end{aligned} \tag{29}$$

Secondly, based on the precision parameter  $\beta$ , we calculate the upper and lower approximations of the best and worst interval-valued Pythagorean fuzzy decision-making objects by Definition 5, respectively:

$$\begin{aligned}
\mu_{\underline{LN}_{\tilde{E}}(D)}^{\sim\beta}(y_i) &= \bigvee_{j=1}^m \left\{ \mu_{\underline{LN}_{\tilde{E}(y_i)}}^{\sim\beta}(y_j) \wedge \mu_{LD}(y_j) \right\}, \\
\mu_{\underline{UN}_{\tilde{E}}(D)}^{\sim\beta}(y_i) &= \bigvee_{j=1}^m \left\{ \mu_{\underline{UN}_{\tilde{E}(y_i)}}^{\sim\beta}(y_j) \wedge \mu_{UD}(y_j) \right\}, \\
\nu_{\underline{LN}_{\tilde{E}}(D)}^{\sim\beta}(y_i) &= \bigwedge_{j=1}^m \left\{ \nu_{\underline{LN}_{\tilde{E}(y_i)}}^{\sim\beta}(y_j) \vee \nu_{LD}(y_j) \right\}, \\
\nu_{\underline{UN}_{\tilde{E}}(D)}^{\sim\beta}(y_i) &= \bigwedge_{j=1}^m \left\{ \nu_{\underline{UN}_{\tilde{E}(y_i)}}^{\sim\beta}(y_j) \vee \nu_{UD}(y_j) \right\}, \\
\mu_{\underline{LN}_{\tilde{E}}(D)}^{\sim\beta}(y_i) &= \bigwedge_{j=1}^m \left\{ \nu_{\underline{LN}_{\tilde{E}(y_i)}}^{\sim\beta}(y_j) \vee \mu_{LD}(y_j) \right\}, \\
\mu_{\underline{UN}_{\tilde{E}}(D)}^{\sim\beta}(y_i) &= \bigwedge_{j=1}^m \left\{ \nu_{\underline{UN}_{\tilde{E}(y_i)}}^{\sim\beta}(y_j) \vee \mu_{UD}(y_j) \right\}, \\
\nu_{\underline{LN}_{\tilde{E}}(D)}^{\sim\beta}(y_i) &= \bigvee_{j=1}^m \left\{ \mu_{\underline{LN}_{\tilde{E}(y_i)}}^{\sim\beta}(y_j) \wedge \nu_{LD}(y_j) \right\}, \\
\nu_{\underline{UN}_{\tilde{E}}(D)}^{\sim\beta}(y_i) &= \bigvee_{j=1}^m \left\{ \mu_{\underline{UN}_{\tilde{E}(y_i)}}^{\sim\beta}(y_j) \wedge \nu_{UD}(y_j) \right\}.
\end{aligned} \tag{30}$$

Then, according to the upper and lower approximations of the IVPF decision-making object with the consistency consensus threshold  $\beta$ , we define a ranking function to solve the MADM problem.

**Definition 10.** For the IVPF decision-making object,  $D = \langle [D^+, D^-], [D^-, D^+] \rangle \in \text{IVPF}(U)$ , and the preference threshold is  $\alpha$  ( $0 < \alpha \leq 1$ ). The ranking functions of the lower and upper boundaries of MD and NMD of each alternative  $y_i$ , ( $i = 1, \dots, m$ ) with respect to IVPF( $U$ ) are defined as follows, respectively:

$$\delta_L(y_i) = \alpha \cdot \mathcal{T}_P \left( \mu_{\underline{LN}_E^\beta(D)}(y_i), \nu_{\underline{LN}_E^\beta(D)}(y_i) \right) + (1 - \alpha) \cdot \mathcal{T}_P \left( \mu_{\overline{LN}_E^\beta(D)}(y_i), \nu_{\overline{LN}_E^\beta(D)}(y_i) \right), \quad (31)$$

$$\delta_U(y_i) = \alpha \cdot \mathcal{T}_P \left( \mu_{\underline{UN}_E^\beta(D)}(y_i), \nu_{\underline{UN}_E^\beta(D)}(y_i) \right) + (1 - \alpha) \cdot \mathcal{T}_P \left( \mu_{\overline{UN}_E^\beta(D)}(y_i), \nu_{\overline{UN}_E^\beta(D)}(y_i) \right). \quad (32)$$

With the definitions of ranking functions of the MADM problem, the following conclusion is obvious, that is,

$$\begin{aligned} 0 &\leq \delta_L(y_i), \\ \delta_U(y_i) &\leq 1, \\ \forall y_i &\in U, \\ i &= 1, \dots, m. \end{aligned} \quad (33)$$

Finally, we construct the ranking function of  $\delta(y)$  for all  $y \in U$ :

$$\delta(y_i) = \frac{1}{2} (\delta_L(y_i) + \delta_U(y_i)) \quad (i = 1, 2, \dots, m). \quad (34)$$

Therefore, we can use the ranking function  $\delta(y)$  to get the final optimal object of all  $y \in U$  for MADM problems.

**4.2. Algorithm for the MADM.** In this section, we present the algorithm flow of solving the MADM problem based on CIVPFRS as shown in Algorithm 1.

## 5. An Illustrative Example

Electronic health records (EHRs) technology is beneficial to medical service providers because it can improve service levels and ensure better medical quality. However, the wide variety of open-source EHRs systems makes it difficult for the hospital administrator to decide which system to use. In Ref [36], six popular and active open-source EHRs systems were selected:  $U = \{\text{FreeMED}(y_1), \text{GNUmed}(y_2), \text{GNU Health}(y_3), \text{Hospital}(y_4), \text{HOSxP}(y_5), \text{and OpenEMR}(y_6)\}$ .

The set of evaluation criteria is  $\tilde{E} = \{\text{Usability}(\tilde{E}_1), \text{Functionality and features}(\tilde{E}_2), \text{Customisation}(\tilde{E}_3), \text{Ease of installation}(\tilde{E}_4), \text{Risk}(\tilde{E}_5), \text{and Staff Training}(\tilde{E}_6)\}$  (please refer to Ref [36] for detailed description and definition of attribute set).

Due to the uncertainty, imprecision, and hesitancy of the selection problem, decision maker uses IVPFNs to evaluate various open-source EHRs systems. The evaluation results are shown in Table 3. The weight information of each evaluation criteria is as follows:  $w_1 = 0.24, w_2 = 0.20, w_3 = 0.15, w_4 = 0.10, w_5 = 0.18$ , and  $w_6 = 0.13$ .

Here, we will use the method based on CIVPFRS to solve the problem of selecting open-source EHRs systems in hospitals. The selection problem of hospital open-source EHRs systems is cited from [36] and makes some improvement under the environment of MADM. Then, we will illustrate the principle and steps of the model and IVPF-TOPSIS in solving the MADM problem through the example.

We calculate IVPF-PIS IVP<sup>+</sup> and IVPF-NIS IVP<sup>-</sup> as follows, by using formulas (25) and (26):

$$\begin{aligned} \text{IVP}^+ &= \{ \langle \tilde{E}_1, [0.5, 0.8], [0.4, 0.5] \rangle, \langle \tilde{E}_2, [0.8, 0.9], [0.2, 0.4] \rangle, \langle \tilde{E}_3, [0.8, 0.9], [0.2, 0.3] \rangle, \\ &\quad \langle \tilde{E}_4, [0.8, 0.9], [0.4, 0.4] \rangle, \langle \tilde{E}_5, [0.6, 0.9], [0.2, 0.4] \rangle, \langle \tilde{E}_6, [0.7, 0.9], [0.1, 0.3] \rangle \}, \\ \text{IVP}^- &= \{ \langle \tilde{E}_1, [0.2, 0.3], [0.8, 0.9] \rangle, \langle \tilde{E}_2, [0.2, 0.5], [0.7, 0.8] \rangle, \langle \tilde{E}_3, [0.1, 0.2], [0.5, 0.8] \rangle, \\ &\quad \langle \tilde{E}_4, [0.3, 0.4], [0.7, 0.8] \rangle, \langle \tilde{E}_5, [0.1, 0.3], [0.5, 0.6] \rangle, \langle \tilde{E}_6, [0.2, 0.3], [0.8, 0.9] \rangle \}. \end{aligned} \quad (35)$$

Then, we calculate the distances  $\mu_D = D^+$  and  $\nu_D = D^-$ , according to formulas (27) and (28). Let  $\lambda = 120$  and  $p = 0.5$ . The calculation results are shown in Table 4.

Let the threshold IVPFN be  $\beta = \langle [0.1, 0.2], [0.5, 0.8] \rangle$ ; therefore,

$$\tilde{N}_{\tilde{E}(y_1)}^\beta = \tilde{E}_2 \cap \tilde{E}_3 \cap \tilde{E}_4 \cap \tilde{E}_5 \cap \tilde{E}_6,$$

$$\tilde{N}_{\tilde{E}(y_2)}^\beta = \tilde{E}_1 \cap \tilde{E}_2 \cap \tilde{E}_3 \cap \tilde{E}_4 \cap \tilde{E}_5 \cap \tilde{E}_6,$$

$$\tilde{N}_{\tilde{E}(y_3)}^\beta = \tilde{E}_2 \cap \tilde{E}_3 \cap \tilde{E}_4 \cap \tilde{E}_5 \cap \tilde{E}_6,$$

$$\tilde{N}_{\tilde{E}(y_4)}^\beta = \tilde{E}_1 \cap \tilde{E}_3 \cap \tilde{E}_5 \cap \tilde{E}_6,$$

$$\tilde{N}_{\tilde{E}(y_5)}^\beta = \tilde{E}_2 \cap \tilde{E}_3 \cap \tilde{E}_4 \cap \tilde{E}_5,$$

$$\tilde{N}_{\tilde{E}(y_6)}^\beta = \tilde{E}_1 \cap \tilde{E}_2 \cap \tilde{E}_3 \cap \tilde{E}_5 \cap \tilde{E}_6. \quad (36)$$

By calculation, we can obtain Table 5.

We calculate the lower and upper approximations, according to formulas (12) and (13). The results are shown in Table 6.

Input IVPFCAS  $(U, \tilde{E})$ ;  
Output Ranking results of all alternatives;  
Step 1. Construct IVPF-PIS  $IVP^+$  and IVPF-NIS  $IVP^-$  by formulas (25) and (26);  
Step 2. Calculate the distances  $\mu_D = D^+$  and  $\nu_D = D^-$  by using formulas (27) and (28), respectively.  
Step 3. Calculating the upper and lower approximations  $\mu_{\tilde{LN}_c^\beta(D)}^\beta(y_i)$ ,  $\nu_{\tilde{LN}_c^\beta(D)}^\beta(y_i)$ ,  $\mu_{\tilde{LN}_c^\beta(D)}^\beta(y_i)$ ,  $\nu_{\tilde{LN}_c^\beta(D)}^\beta(y_i)$ ,  $\mu_{\tilde{UN}_c^\beta(D)}^\beta(y_i)$ ,  $\nu_{\tilde{UN}_c^\beta(D)}^\beta(y_i)$  according to formulas (12) and (13).  
Step 4. Determine risk preference threshold  $\alpha$  ( $0 < \alpha \leq 1$ ) and calculate those ranking functions  $\delta_L(y_i)$  and  $\delta_U(y_i)$  by using formulas (31) and (32).  
Step 5. Calculate the ranking function  $\delta(y_i)$  according to formula (34).  
Step 6. List the ranking results of all alternatives.

ALGORITHM 1: Algorithm for MADM with CIVPFRS.

TABLE 3: IVPF  $\beta$ -covering  $\tilde{E}$ .

$U/\tilde{E}$	$\tilde{E}_1$	$\tilde{E}_2$	$\tilde{E}_3$	$\tilde{E}_4$	$\tilde{E}_5$	$\tilde{E}_6$
$y_1$	$\langle [0.2, 0.3], [0.8, 0.9] \rangle$	$\langle [0.5, 0.7], [0.3, 0.4] \rangle$	$\langle [0.4, 0.5], [0.5, 0.8] \rangle$	$\langle [0.2, 0.5], [0.5, 0.8] \rangle$	$\langle [0.6, 0.9], [0.2, 0.4] \rangle$	$\langle [0.7, 0.9], [0.1, 0.3] \rangle$
$y_2$	$\langle [0.6, 0.7], [0.3, 0.8] \rangle$	$\langle [0.4, 0.6], [0.1, 0.5] \rangle$	$\langle [0.4, 0.6], [0.3, 0.5] \rangle$	$\langle [0.8, 0.9], [0.4, 0.4] \rangle$	$\langle [0.1, 0.3], [0.5, 0.6] \rangle$	$\langle [0.4, 0.5], [0.5, 0.5] \rangle$
$y_3$	$\langle [0.4, 0.5], [0.6, 0.7] \rangle$	$\langle [0.8, 0.9], [0.2, 0.4] \rangle$	$\langle [0.7, 0.9], [0.3, 0.4] \rangle$	$\langle [0.5, 0.6], [0.1, 0.2] \rangle$	$\langle [0.6, 0.7], [0.2, 0.3] \rangle$	$\langle [0.6, 0.8], [0.2, 0.4] \rangle$
$y_4$	$\langle [0.4, 0.6], [0.1, 0.3] \rangle$	$\langle [0.2, 0.5], [0.7, 0.8] \rangle$	$\langle [0.1, 0.2], [0.5, 0.8] \rangle$	$\langle [0.3, 0.4], [0.7, 0.8] \rangle$	$\langle [0.4, 0.7], [0.1, 0.4] \rangle$	$\langle [0.4, 0.7], [0.1, 0.5] \rangle$
$y_5$	$\langle [0.2, 0.3], [0.6, 0.8] \rangle$	$\langle [0.6, 0.7], [0.4, 0.5] \rangle$	$\langle [0.6, 0.7], [0.4, 0.5] \rangle$	$\langle [0.6, 0.8], [0.3, 0.5] \rangle$	$\langle [0.6, 0.8], [0.4, 0.5] \rangle$	$\langle [0.2, 0.3], [0.8, 0.9] \rangle$
$y_6$	$\langle [0.5, 0.8], [0.4, 0.5] \rangle$	$\langle [0.7, 0.5], [0.1, 0.5] \rangle$	$\langle [0.8, 0.9], [0.2, 0.3] \rangle$	$\langle [0.2, 0.5], [0.7, 0.8] \rangle$	$\langle [0.7, 0.8], [0.2, 0.4] \rangle$	$\langle [0.5, 0.6], [0.4, 0.5] \rangle$

TABLE 4: Calculation results of distance  $D^+$  and  $D^-$ .

$U$	$y_1$	$y_2$	$y_3$	$y_4$	$y_5$	$y_6$
$D^+$	0.3505	0.4631	0.2623	0.5004	0.3972	0.2570
$D^-$	0.3745	0.4170	0.5197	0.3211	0.3544	0.5179

TABLE 5: Tabular representation of  $\tilde{N}_{\tilde{E}}^\beta$ .

$\tilde{N}_{\tilde{E}}^\beta$	$y_1$	$y_2$	$y_3$	$y_4$	$y_5$	$y_6$
$y_1$	$\langle [0.2, 0.5], [0.5, 0.8] \rangle$	$\langle [0.1, 0.3], [0.5, 0.6] \rangle$	$\langle [0.5, 0.6], [0.3, 0.4] \rangle$	$\langle [0.1, 0.2], [0.7, 0.8] \rangle$	$\langle [0.2, 0.3], [0.8, 0.9] \rangle$	$\langle [0.2, 0.5], [0.7, 0.8] \rangle$
$y_2$	$\langle [0.2, 0.3], [0.8, 0.9] \rangle$	$\langle [0.1, 0.3], [0.5, 0.8] \rangle$	$\langle [0.4, 0.5], [0.6, 0.7] \rangle$	$\langle [0.1, 0.2], [0.7, 0.8] \rangle$	$\langle [0.2, 0.3], [0.8, 0.9] \rangle$	$\langle [0.2, 0.5], [0.7, 0.8] \rangle$
$y_3$	$\langle [0.2, 0.5], [0.5, 0.8] \rangle$	$\langle [0.1, 0.3], [0.5, 0.6] \rangle$	$\langle [0.5, 0.6], [0.3, 0.4] \rangle$	$\langle [0.1, 0.2], [0.7, 0.8] \rangle$	$\langle [0.2, 0.3], [0.8, 0.9] \rangle$	$\langle [0.2, 0.5], [0.7, 0.8] \rangle$
$y_4$	$\langle [0.2, 0.3], [0.8, 0.9] \rangle$	$\langle [0.1, 0.3], [0.5, 0.8] \rangle$	$\langle [0.4, 0.5], [0.6, 0.7] \rangle$	$\langle [0.1, 0.2], [0.5, 0.8] \rangle$	$\langle [0.2, 0.3], [0.8, 0.9] \rangle$	$\langle [0.5, 0.6], [0.4, 0.5] \rangle$
$y_5$	$\langle [0.2, 0.5], [0.5, 0.8] \rangle$	$\langle [0.1, 0.3], [0.5, 0.6] \rangle$	$\langle [0.5, 0.6], [0.3, 0.4] \rangle$	$\langle [0.1, 0.2], [0.7, 0.8] \rangle$	$\langle [0.6, 0.7], [0.4, 0.5] \rangle$	$\langle [0.2, 0.5], [0.7, 0.8] \rangle$
$y_6$	$\langle [0.2, 0.3], [0.8, 0.9] \rangle$	$\langle [0.1, 0.3], [0.5, 0.8] \rangle$	$\langle [0.4, 0.5], [0.6, 0.7] \rangle$	$\langle [0.1, 0.2], [0.7, 0.8] \rangle$	$\langle [0.2, 0.3], [0.8, 0.9] \rangle$	$\langle [0.5, 0.5], [0.4, 0.5] \rangle$

TABLE 6: The lower and upper approximations.

$U$	$y_1$	$y_2$	$y_3$	$y_4$	$y_5$	$y_6$
$\mu_{\tilde{LN}_c^\beta(D)}^\beta(y_i)$	0.3	0.5	0.3	0.4	0.3	0.4
$\mu_{\tilde{UN}_c^\beta(D)}^\beta(y_i)$	0.4	0.7	0.4	0.5	0.4	0.5
$\nu_{\tilde{LN}_c^\beta(D)}^\beta(y_i)$	0.5	0.4	0.5	0.5	0.5	0.5
$\nu_{\tilde{UN}_c^\beta(D)}^\beta(y_i)$	0.5197	0.5	0.5197	0.5179	0.5197	0.5
$\mu_{\tilde{LN}_c^\beta(D)}^\beta(y_i)$	0.2623	0.2623	0.2623	0.2623	0.3972	0.2623
$\mu_{\tilde{UN}_c^\beta(D)}^\beta(y_i)$	0.3505	0.3	0.3505	0.3	0.3972	0.3
$\nu_{\tilde{LN}_c^\beta(D)}^\beta(y_i)$	0.5	0.5	0.5	0.5	0.4	0.5
$\nu_{\tilde{UN}_c^\beta(D)}^\beta(y_i)$	0.5197	0.7	0.5197	0.5179	0.5	0.5179

TABLE 7: The result of ranking functions.

$U$	$y_1$	$y_2$	$y_3$	$y_4$	$y_5$	$y_6$
$\delta_L(y_i)$	0.1119	0.1426	0.1119	0.1426	0.1171	0.1426
$\delta_U(y_i)$	0.1583	0.2666	0.1583	0.1861	0.1616	0.1801
$\delta(y_i)$	0.1351	0.2046	0.1351	0.1644	0.1394	0.1614

Consider the risk preference threshold  $\alpha = 0.75$ . Then, according to equations (31)–(34), we calculate the ranking functions. The results are shown in Table 7.

Finally, based on the values of the ranking function  $\delta(y_i)$  ( $i = 1, 2, \dots, 6$ ), we present the optimal ranking of all hospital open-source EHRs systems as follows:

$$y_2 \succ y_4 \succ y_6 \succ y_5 \succ y_3 = y_1. \quad (37)$$



TABLE 8: The effect of parameter  $\lambda$  changes.

Parameter	Ordering index of $y_i (i = 1, 2, \dots, 6)$	Ranking order
$\lambda = 1$	$\delta(y_1) = 0.0985, \delta(y_2) = 0.1783, \delta(y_3) = 0.0985, \delta(y_4) = 0.1297, \delta(y_5) = 0.1007, \delta(y_6) = 0.1297$	$y_2 \succ y_4 = y_6 \succ y_5 \succ y_3 = y_1$
$\lambda = 2$	$\delta(y_1) = 0.0917, \delta(y_2) = 0.1673, \delta(y_3) = 0.0917, \delta(y_4) = 0.1222, \delta(y_5) = 0.0939, \delta(y_6) = 0.1222$	$y_2 \succ y_4 = y_6 \succ y_5 \succ y_3 = y_1$
$\lambda = 12$	$\delta(y_1) = 0.1161, \delta(y_2) = 0.1933, \delta(y_3) = 0.1161, \delta(y_4) = 0.1460, \delta(y_5) = 0.1206, \delta(y_6) = 0.1460$	$y_2 \succ y_4 = y_6 \succ y_5 \succ y_3 = y_1$
$\lambda = 120$	$\delta(y_1) = 0.1351, \delta(y_2) = 0.2046, \delta(y_3) = 0.1351, \delta(y_4) = 0.1644, \delta(y_5) = 0.1394, \delta(y_6) = 0.1614$	$y_2 \succ y_4 \succ y_6 \succ y_5 \succ y_3 = y_1$
$\lambda = 1200$	$\delta(y_1) = 0.0980, \delta(y_2) = 0.1778, \delta(y_3) = 0.0980, \delta(y_4) = 0.1318, \delta(y_5) = 0.0989, \delta(y_6) = 0.1318$	$y_2 \succ y_4 = y_6 \succ y_5 \succ y_3 = y_1$

TABLE 9: The effect of parameter  $p$  changes.

Parameter	Ordering index of $y_i (i = 1, 2, \dots, 6)$	Ranking order
$p = 0.1$	$\delta(y_1) = 0.1356, \delta(y_2) = 0.2046, \delta(y_3) = 0.1356, \delta(y_4) = 0.1648, \delta(y_5) = 0.1398, \delta(y_6) = 0.1614$	$y_2 \succ y_4 \succ y_6 \succ y_5 \succ y_3 = y_1$
$p = 0.3$	$\delta(y_1) = 0.1354, \delta(y_2) = 0.2046, \delta(y_3) = 0.1354, \delta(y_4) = 0.1647, \delta(y_5) = 0.1397, \delta(y_6) = 0.1614$	$y_2 \succ y_4 \succ y_6 \succ y_5 \succ y_3 = y_1$
$p = 0.5$	$\delta(y_1) = 0.1351, \delta(y_2) = 0.2046, \delta(y_3) = 0.1351, \delta(y_4) = 0.1644, \delta(y_5) = 0.1394, \delta(y_6) = 0.1614$	$y_2 \succ y_4 \succ y_6 \succ y_5 \succ y_3 = y_1$
$p = 0.7$	$\delta(y_1) = 0.1346, \delta(y_2) = 0.2046, \delta(y_3) = 0.1346, \delta(y_4) = 0.1639, \delta(y_5) = 0.1389, \delta(y_6) = 0.1613$	$y_2 \succ y_4 \succ y_6 \succ y_5 \succ y_3 = y_1$
$p = 0.9$	$\delta(y_1) = 0.1336, \delta(y_2) = 0.2046, \delta(y_3) = 0.1336, \delta(y_4) = 0.1630, \delta(y_5) = 0.1380, \delta(y_6) = 0.1611$	$y_2 \succ y_4 \succ y_6 \succ y_5 \succ y_3 = y_1$

TABLE 10: The effect of parameter  $\alpha$  changes.

Parameter	Ordering index of $y_i (i = 1, 2, \dots, 6)$	Ranking order
$\alpha = 0.1$	$\delta(y_1) = 0.1233, \delta(y_2) = 0.1461, \delta(y_3) = 0.1233, \delta(y_4) = 0.1177, \delta(y_5) = 0.1386, \delta(y_6) = 0.1173$	$y_2 \succ y_5 \succ y_3 = y_1 \succ y_4 \succ y_6$
$\alpha = 0.3$	$\delta(y_1) = 0.1269, \delta(y_2) = 0.1641, \delta(y_3) = 0.1269, \delta(y_4) = 0.1321, \delta(y_5) = 0.1389, \delta(y_6) = 0.1309$	$y_2 \succ y_5 \succ y_4 \succ y_6 \succ y_3 = y_1$
$\alpha = 0.5$	$\delta(y_1) = 0.1305, \delta(y_2) = 0.1821, \delta(y_3) = 0.1305, \delta(y_4) = 0.1464, \delta(y_5) = 0.1391, \delta(y_6) = 0.1444$	$y_2 \succ y_4 \succ y_6 \succ y_5 \succ y_3 = y_1$
$\alpha = 0.7$	$\delta(y_1) = 0.1342, \delta(y_2) = 0.2001, \delta(y_3) = 0.1342, \delta(y_4) = 0.1608, \delta(y_5) = 0.1393, \delta(y_6) = 0.1580$	$y_2 \succ y_4 \succ y_6 \succ y_5 \succ y_3 = y_1$
$\alpha = 0.9$	$\delta(y_1) = 0.1378, \delta(y_2) = 0.2182, \delta(y_3) = 0.1378, \delta(y_4) = 0.1752, \delta(y_5) = 0.1395, \delta(y_6) = 0.1715$	$y_2 \succ y_4 \succ y_6 \succ y_5 \succ y_3 = y_1$

TABLE 11: The effect of parameter  $\beta$  changes.

Parameter	Ordering index of $y_i (i = 1, 2, \dots, 6)$	Ranking order
$\beta = \langle [0.1, 0.2], [0.5, 0.8] \rangle$	$\delta(y_1) = 0.1351, \delta(y_2) = 0.2046, \delta(y_3) = 0.1351, \delta(y_4) = 0.1644, \delta(y_5) = 0.1394, \delta(y_6) = 0.1614$	$y_2 \succ y_4 \succ y_6 \succ y_5 \succ y_3 = y_1$
$\beta = \langle [0.2, 0.3], [0.5, 0.8] \rangle$	$\delta(y_1) = 0.1351, \delta(y_2) = 0.2242, \delta(y_3) = 0.1351, \delta(y_4) = 0.1739, \delta(y_5) = 0.1394, \delta(y_6) = 0.1614$	$y_2 \succ y_4 \succ y_6 \succ y_5 \succ y_3 = y_1$
$\beta = \langle [0.3, 0.4], [0.5, 0.8] \rangle$	$\delta(y_1) = 0.1414, \delta(y_2) = 0.2242, \delta(y_3) = 0.1351, \delta(y_4) = 0.1739, \delta(y_5) = 0.1394, \delta(y_6) = 0.1614$	$y_2 \succ y_4 \succ y_6 \succ y_5 \succ y_1 \succ y_3$
$\beta = \langle [0.5, 0.5], [0.1, 0.8] \rangle$	$\delta(y_1) = 0.1234, \delta(y_2) = 0.1083, \delta(y_3) = 0.1118, \delta(y_4) = 0.1083, \delta(y_5) = 0.1083, \delta(y_6) = 0.1339$	$y_6 \succ y_1 \succ y_3 \succ y_4 = y_5 = y_2$
$\beta = \langle [0.5, 0.5], [0.5, 0.5] \rangle$	$\delta(y_1) = 0.1328, \delta(y_2) = 0.1118, \delta(y_3) = 0.1351, \delta(y_4) = 0.1083, \delta(y_5) = 0.1394, \delta(y_6) = 0.1614$	$y_6 \succ y_5 \succ y_3 \succ y_1 \succ y_2 \succ y_4$
$\beta = \langle [0.1, 0.2], [0.5, 0.5] \rangle$	$\delta(y_1) = 0.1328, \delta(y_2) = 0.1473, \delta(y_3) = 0.1351, \delta(y_4) = 0.1739, \delta(y_5) = 0.1394, \delta(y_6) = 0.1614$	$y_4 \succ y_6 \succ y_2 \succ y_5 \succ y_3 \succ y_1$
$\beta = \langle [0.1, 0.2], [0.3, 0.4] \rangle$	$\delta(y_1) = 0.1328, \delta(y_2) = 0.1083, \delta(y_3) = 0.1351, \delta(y_4) = 0.1685, \delta(y_5) = 0.1083, \delta(y_6) = 0.1346$	$y_4 \succ y_3 \succ y_6 \succ y_1 \succ y_2 = y_5$
$\beta = \langle [0.1, 0.2], [0.3, 0.5] \rangle$	$\delta(y_1) = 0.1328, \delta(y_2) = 0.1383, \delta(y_3) = 0.1351, \delta(y_4) = 0.1739, \delta(y_5) = 0.1118, \delta(y_6) = 0.1346$	$y_4 \succ y_2 \succ y_3 \succ y_6 \succ y_1 \succ y_5$

Hence, the best open-source EHRs system for the hospital is GNUMed.

**5.1. Discussion on Parameters.** In this section, we will discuss the effect on the sorting result when each parameter changes independently.

- (1) There are two parameters in the distance formula for calculating two IVPFNs; they are parameters  $\lambda > 0$  and  $0 \leq p \leq 1$ . First, we discuss the effect of parameter  $\lambda$  changes in distance on the results under  $p = 0.5$  and  $\alpha = 0.75$  and the consistency consensus threshold IVPFN  $\beta = \langle [0.1, 0.2], [0.5, 0.8] \rangle$ . When parameter  $\lambda$  changes, the ranking order changes, as shown in Table 8.

Although the values of ranking function will change as  $\lambda (\lambda > 0)$  change, the ranking order of alternatives will basically remain unchanged.

- (2) Then, we discuss the influence of parameter  $p (0 \leq p \leq 1)$  changes in distance on the results under  $\lambda = 120$  and  $\alpha = 0.75$  and the consistency consensus threshold IVPFN  $\beta = \langle [0.1, 0.2], [0.5, 0.8] \rangle$ . When

TABLE 12: Ranking orders from different methods.

Method	Ranking order
IVPFA-MULTIMOORA	$y_2 \succ y_3 \succ y_6 \succ y_5 \succ y_4 \succ y_1$
The method of this paper	$y_2 \succ y_4 \succ y_6 \succ y_5 \succ y_3 = y_1$

parameter  $p$  changes, the ranking order changes, as shown in Table 9.

Although the values of ranking function will have very small changes as  $p (0 \leq p \leq 1)$  change, the ranking order of alternatives will remain unchanged.

As can be seen from the above two points, the values of parameter  $\lambda$  and parameter  $p$  will not affect the final ranking order of alternatives, but will affect the value of the ranking function. When the value of  $\lambda$  is larger, the difference between the values of the ranking function may become larger; that is, as the value of parameter  $\lambda$  becomes larger, the value of the same ranking function may become different.

- (3) Influence of parameter  $\alpha (0 < \alpha \leq 1)$  on the ranking function changes on the results under  $\lambda = 120$  and  $p = 0.5$  and the consistency consensus

TABLE 13: The comparative analysis of the proposed method with the existing literature.

Methods	Score values	Ranking order
CIFRS [6]	Failed to handle	×
CPFRS [32]	Failed to handle	×
CIVIFRS	Failed to handle	×
CIVPFRS	$\delta(y_1) = 0.1351, \delta(y_2) = 0.2046, \delta(y_3) = 0.1351,$ $\delta(y_4) = 0.1644, \delta(y_5) = 0.1394, \delta(y_6) = 0.1614$	$y_2 > y_4 > y_6 > y_5 > y_3 = y_1$

threshold IVPFN  $\beta = \langle [0.1, 0.2], [0.5, 0.8] \rangle$ . When parameter  $\alpha$  changes, the ranking order changes, as shown in Table 10.

Although the values of ranking function will have very small changes as  $\alpha (0 < \alpha \leq 1)$  change, the ranking order of alternatives will basically remain unchanged.

- (4) Influence of the consistency consensus threshold IVPFN  $\beta = \langle [s_L, s_U], [t_L, t_U] \rangle$  on the IVPF  $\beta$ -neighborhood system changes on the results under  $\lambda = 120, p = 0.5$ , and  $\alpha = 0.75$ . When parameter  $\beta$  changes, the ranking order changes, as shown in Table 11.

From Table 11, we can get that the values of ranking function will great influence as the consistency consensus threshold IVPFN  $\beta = \langle [s_L, s_U], [t_L, t_U] \rangle$  change.

The value of  $\beta$  must meet the definition of IVPF  $\beta$ -covering. When the value of  $\beta$  is different, the IVPF  $\beta$ -neighborhood of each alternative will be different. It will directly affect the calculation results of the upper and lower approximations of IVPF decision-making objects, thus affecting the final decision result.

**5.2. Comparisons and Analyses.** In this section, the proposed method will be analyzed and compared with other existing method.

Firstly, with respect to the MADM, Liang et al. [36] proposed a method called IVPFA-MULTIMOORA. We apply IVPFA-MULTIMOORA to solve the EHRs systems selection problem and compare the result with our proposed method. When the  $\beta = \langle [0.1, 0.2], [0.5, 0.8] \rangle$ ,  $\lambda = 120$ ,  $p = 0.5$ ,  $\alpha = 0.75$ , and  $w = \{0.24, 0.20, 0.15, 0.10, 0.18, 0.13\}$ . The ranking results of the alternatives using two methods are shown in Table 12.

As can be seen from Table 12, the method proposed in this paper can choose the same best alternative as IVPFA-MULTIMOORA. This shows that the method proposed in this paper can solve MADM problems reasonably and effectively.

Secondly, according to the abovementioned analysis, the method proposed in this paper is obviously superior to IFSS and PFSSs. The advantages of the proposed method with the existing literatures are given below:

- (a) If  $\mu_L = \mu_U$  and  $\nu_L = \nu_U$ , the CIVPFRS model is reduced to the CPFRS model proposed in Reference [32]

- (b) If  $0 \leq (\mu_U(x)) + (\nu_U(x)) \leq 1$ , the CIVPFRS model is reduced to the CIVIFRS model

- (c) If  $\mu_L = \mu_U$ ,  $\nu_L = \nu_U$ , and  $0 \leq (\mu_U(x)) + (\nu_U(x)) \leq 1$ , then the CIVPFRS model is reduced to the CIFRS model presented in Reference [6]

From the abovementioned conclusion, CIFRS, CPFRS, and CIVIFRS models are special cases of CIVPFRS.

Now, by considering the above illustrative example in Section 5, the comparative study of the proposed method and the existing literature is given in Table 13.

Therefore, the method presented in this paper is more suitable because it provides more space to the decision maker in decision-making problems.

## 6. Conclusions

The CIVPFS model is an important tool for dealing with uncertainty in the real world. In this paper, the concept of CIVPFS via Pythagorean fuzzy  $\beta$ -neighborhood has been proposed by combining CRSs, IVPFS, and FRSSs. The rough degree and precision degree of CIVPFRS are mainly discussed. From the analysis of Section 3, we observe that CIVPFS is an important generalization of CIFRS. Then, we put forward an IVPF-TOPSIS methodologies to solve MADM problems. The CIVPFRS enriches the theory of CPFRS and granular computing and provides a new perspective for MADM problems with uncertainty. The following are the main contributions of this article:

- (1) Through IVPF  $\beta$ -covering and IVPF  $\beta$ -neighborhood, we construct the CIVPFS model.
- (2) We apply the CIVPFRS model to the MADM problem with IVPF information evaluation. The CIVPFRS model provides a new perspective for MADM with uncertain IVPF information evaluation and enriches the theory of granular computing.
- (3) The decision process and new algorithm are given.
- (4) Through comparative analysis, we can get that the MADM problem using IVPF information evaluation based on the CIVPFRS model is more effective than the fuzzy information evaluation based on the CIFRS model.

In the next research studies, we mainly focus on the following topics:

- (1) Discussion on other application methods in information systems

- (2) The study of knowledge reductions of the CIVPFRS model
- (3) The application of CIVPFRS in big data processing and analysis

## Data Availability

Data used to support the findings of this study are included within the article.

## Conflicts of Interest

There are no any conflicts of interest regarding the publication of the article.

## Acknowledgments

This research was funded by the Sichuan Province Youth Science and Technology Innovation Team (Grant no. 2019JDTD0015); Scientific Research Project of Education Department of Sichuan Province (Grant nos. 18ZA0273 and 15TD0027); and Scientific Research Project of Neijiang Normal University (Grant nos. 18TD08, 16JC10, and 2019YZ06).

## References

- [1] L. A. Zadeh, "Fuzzy sets," *Information and Control*, vol. 8, no. 3, pp. 338–353, 1965.
- [2] Z. a. Pawlak, "Rough sets," *International Journal of Computer & Information Sciences*, vol. 11, no. 5, pp. 341–356, 1982.
- [3] D. Meng, X. Zhang, and K. Qin, "Soft rough fuzzy sets and soft fuzzy rough sets," *Computers & Mathematics with Applications*, vol. 62, no. 12, pp. 4635–4645, 2011.
- [4] T. Zheng, M. Zhang, W. Zheng, and L. Zhou, "A new uncertainty measure of covering-based rough interval-valued intuitionistic fuzzy sets," *IEEE Access*, vol. 7, pp. 53213–53224, 2019.
- [5] C. Zhang and D.-Y. Li, "Pythagorean fuzzy rough sets and its applications in multi-attribute decision making," *Journal of Chinese Computer Systems*, vol. 37, pp. 1531–1535, 2016.
- [6] J. Zhan and B. Sun, "Covering-based intuitionistic fuzzy rough sets and applications in multi-attribute decision-making," *Artificial Intelligence Review*, vol. 53, no. 1, pp. 671–701, 2018.
- [7] K. T. Atanassov, "Intuitionistic fuzzy sets," *Fuzzy Sets and Systems*, vol. 20, no. 1, pp. 87–96, 1986.
- [8] S. P. Wan and J. Y. Dong, *Decision Making Theories and Methods Based on Interval-Valued Intuitionistic Fuzzy Set*, Springer, Singapore, 2020.
- [9] R. R. Yager and A. M. Abbasov, "Pythagorean membership grades, complex numbers, and decision making," *International Journal of Intelligent Systems*, vol. 28, no. 5, pp. 436–452, 2013.
- [10] H. Garg, "Novel neutrality operation-based Pythagorean fuzzy geometric aggregation operators for multiple attribute group decision analysis," *International Journal of Intelligent Systems*, vol. 34, no. 10, pp. 2459–2489, 2019.
- [11] H. Garg, "Hesitant Pythagorean fuzzy Maclaurin symmetric mean operators and its applications to multiattribute decision-making process," *International Journal of Intelligent Systems*, vol. 34, no. 4, pp. 601–626, 2019.
- [12] Y. Liu, Y. Qin, L. Xu, H.-B. Liu, and J. Liu, "Multiattribute group decision-making approach with linguistic pythagorean fuzzy information," *IEEE Access*, vol. 7, pp. 143412–143430, 2019.
- [13] Y. Liu, J. Liu, and Y. Qin, "Pythagorean fuzzy linguistic Muirhead mean operators and their applications to multi-attribute decision-making," *International Journal of Intelligent Systems*, vol. 35, no. 2, pp. 300–332, 2020.
- [14] X. Zhang and Z. Xu, "Extension of TOPSIS to multiple criteria decision making with pythagorean fuzzy sets," *International Journal of Intelligent Systems*, vol. 29, no. 12, pp. 1061–1078, 2014.
- [15] M. Akram, W. A. Dudek, and F. Ilyas, "Group decision-making based on pythagorean fuzzy TOPSIS method," *International Journal of Intelligent Systems*, vol. 34, no. 7, pp. 1455–1475, 2019.
- [16] S.-P. Wan, S.-Q. Li, and J.-Y. Dong, "A three-phase method for Pythagorean fuzzy multi-attribute group decision making and application to haze management," *Computers & Industrial Engineering*, vol. 123, pp. 348–363, 2018.
- [17] S.-P. Wan, Z. Jin, and J.-Y. Dong, "Pythagorean fuzzy mathematical programming method for multi-attribute group decision making with Pythagorean fuzzy truth degrees," *Knowledge and Information Systems*, vol. 55, no. 2, pp. 437–466, 2018.
- [18] S.-P. Wan, Z. Jin, and J.-Y. Dong, "A new order relation for Pythagorean fuzzy numbers and application to multi-attribute group decision making," *Knowledge and Information Systems*, vol. 62, no. 2, pp. 751–785, 2020.
- [19] X. Peng and Y. Yang, "Fundamental properties of interval-valued pythagorean fuzzy aggregation operators," *International Journal of Intelligent Systems*, vol. 31, no. 5, pp. 444–487, 2016.
- [20] G. Wei, H. Garg, H. Gao, and C. Wei, "Interval-valued pythagorean fuzzy Maclaurin symmetric mean operators in multiple attribute decision making," *IEEE Access*, vol. 6, pp. 67866–67884, 2018.
- [21] H. Garg, "A novel accuracy function under interval-valued Pythagorean fuzzy environment for solving multicriteria decision making problem," *Journal of Intelligent & Fuzzy Systems*, vol. 31, no. 1, pp. 529–540, 2016.
- [22] M. S. A. Khan and S. Abdullah, "Interval-valued Pythagorean fuzzy GRA method for multiple-attribute decision making with incomplete weight information," *International Journal of Intelligent Systems*, vol. 33, no. 8, pp. 1689–1716, 2018.
- [23] L. Wang, H. Wang, Z. Xu, and Z. Ren, "The interval-valued hesitant Pythagorean fuzzy set and its applications with extended TOPSIS and Choquet integral-based method," *International Journal of Intelligent Systems*, vol. 34, no. 6, pp. 1063–1085, 2019.
- [24] W. Zakowski, "Approximations in the space  $(U, \pi)$ ," *Demon and Stration Mathematica*, vol. 16, p. 761C769, 1983.
- [25] W. Zhu and F.-Y. Wang, "Reduction and axiomization of covering generalized rough sets," *Information Sciences*, vol. 152, pp. 217–230, 2003.
- [26] S. Safari and M. R. Hooshmandasl, "On twelve types of covering-based rough sets," *SpringerPlus*, vol. 5, no. 1, p. 1003, 2016.
- [27] L. Ma, "On some types of neighborhood-related covering rough sets," *International Journal of Approximate Reasoning*, vol. 53, no. 6, pp. 901–911, 2012.
- [28] D. Dubois and H. Prade, "Rough fuzzy sets and fuzzy rough sets," *International Journal of General System*, vol. 17, Article ID 191C209, 1989.

- [29] L. Ma, "Two fuzzy covering rough set models and their generalizations over fuzzy lattices," *Fuzzy Sets and Systems*, vol. 294, pp. 1–17, 2016.
- [30] L. D'eer, M. Restrepo, C. Cornelis, and J. Gómez, "Neighborhood operators for covering-based rough sets," *Information Sciences*, vol. 336, pp. 21–44, 2016.
- [31] L. D'eer, C. Cornelis, and L. Godo, "Fuzzy neighborhood operators based on fuzzy coverings," *Fuzzy Sets and Systems*, vol. 312, pp. 17–35, 2017.
- [32] A. Hussain, M. Irfan Ali, and T. Mahmood, "Covering based q-rung orthopair fuzzy rough set model hybrid with TOPSIS for multi-attribute decision making," *Journal of Intelligent & Fuzzy Systems*, vol. 37, no. 1, pp. 981–993, 2019.
- [33] S. Zeng, A. Hussain, T. Mahmood, M. Irfan Ali, S. Ashraf, and M. Munir, "Covering-based spherical fuzzy rough set model hybrid with TOPSIS for multi-attribute decision-making," *Symmetry*, vol. 11, no. 4, p. 547, 2019.
- [34] A. Hussain, T. Mahmood, and M. I. Ali, "Rough Pythagorean fuzzy ideals in semigroups," *Computational and Applied Mathematics*, vol. 38, no. 2, 2019.
- [35] A. M. Radzikowska and E. E. Kerre, "A comparative study of fuzzy rough sets," *Fuzzy Sets and Systems*, vol. 126, no. 2, pp. 137–155, 2002.
- [36] D. Liang, A. P. Darko, and J. Zeng, "Interval-valued pythagorean fuzzy power average-based MULTIMOORA method for multi-criteria decision-making," *Journal of Experimental & Theoretical Artificial Intelligence*, pp. 1–30, 2019.